

Borshkov Institute of Catalysis, Novosibirsk, Russia  
N.D. Zelinsky Institute of Organic Chemistry RAS, Moscow, Russia  
Lomonosov Moscow State University, Moscow, Russia  
Russian Mendeleev Chemical Society, Novosibirsk Department  
Siberian Branch of the Russian Academy of Sciences



# XI International Conference

# MECHANISMS of CATALYTIC

# REACTIONS

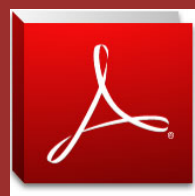
---

*Sochi, Krasnodar region, Russia*  
*October 7-11, 2019*

# ABSTRACTS



Novosibirsk-2019



Boreskov Institute of Catalysis, Novosibirsk, Russia  
N.D. Zelinsky Institute of Organic Chemistry RAS, Moscow, Russia  
Lomonosov Moscow State University, Moscow, Russia  
Russian Mendeleev Chemical Society, Novosibirsk Department  
Siberian Branch of the Russian Academy of Sciences

# **XI International Conference MECHANISMS of CATALYTIC REACTIONS**

*Sochi, Krasnodar region, Russia*

*October 7-11, 2019*

# **ABSTRACTS**

УДК 544.47+66.09  
ББК Г544  
М45

**M45 Mechanisms of Catalytic Reactions (MCR-XI).** XI International Conference. / October 7-11, 2019, Sochi, Krasnodar region, Russia [Electronic resource]: Abstracts / eds.: Prof. V.I. Bukhtiyarov, Prof. K.P. Bryliakov, Prof. E.A. Kozlova, Dr. Kaichev V.V. – Novosibirsk: BIC, 2019. URL:

- [http://catalysis.ru/resources/institute/Publishing/Report/2019/Abstracts-MCR-XI\\_2019.pdf](http://catalysis.ru/resources/institute/Publishing/Report/2019/Abstracts-MCR-XI_2019.pdf)
- ISBN 978-5-906376-25-1

**В надзаг.:** Boreskov Institute of Catalysis, Novosibirsk, Russia  
N.D. Zelinsky Institute of Organic Chemistry RAS, Moscow, Russia  
Lomonosov Moscow State University, Moscow, Russia  
Russian Mendeleev Chemical Society, Novosibirsk Department  
Siberian Branch of the Russian Academy of Sciences

The main topics are:

- Basic concepts, theory and modeling in catalysis
- Physical methods, including in situ and operando techniques, in catalysis
- Kinetics and mechanisms of catalyzed processes
- Advanced catalyst systems addressing current challenges: energy, materials, sustainability

The Conference is accompanied by the School-Conference for young scientists  
"Catalysis for energy, fuels, renewables"

УДК 544.47+66.09  
ББК Г544

ISBN 978-5-906376-25-1

© Boreskov Institute of Catalysis, 2019

## CONFERENCE ORGANIZERS

- Boreskov Institute of Catalysis, Novosibirsk, Russia
- N.D. Zelinsky Institute of Organic Chemistry RAS, Moscow, Russia
- Lomonosov Moscow State University, Moscow, Russia
- Russian Mendeleev Chemical Society, Novosibirsk Department
- Siberian Branch of the Russian Academy of Sciences



## UNDER THE AUSPICES OF



European Federation of Catalysis Societies



National Catalytic Society of Russia

## FINANCIAL SUPPORT



Russian Foundation for Basic Research

Российский фонд фундаментальных исследований  
Грант 19-03-20035

## HONORARY CONFERENCE PARTNERS



SPECS-TII RUS

SPECS™

SPECS Surface  
Nano Analysis GmbH

## CONFERENCE PARTNERS



Company "Soctrade"



Company "Kreator"



LLC "Merck"

## INFORMATION PARTNERS

KINETICS AND  
CATALYSIS

Journal "Kinetics and Catalysis"

TOPICS in  
CATALYSIS

Journal "Topics in Catalysis"

## Scientific Committee

**Valentin Ananikov**, N.D. Zelinsky Institute of Organic Chemistry RAS, Moscow, Russia

**Konstantin Bryliakov**, Boreskov Institute of Catalysis, Novosibirsk, Russia

**Valerii Bukhtiyarov**, Boreskov Institute of Catalysis, Novosibirsk, Russia

**Irina Ivanova**, Topchiev Institute of Petrochemical Synthesis RAS, Moscow, Russia

**Vasily Kaichev**, Boreskov Institute of Catalysis, Novosibirsk, Russia

**Ekaterina Kozlova**, Boreskov Institute of Catalysis, Novosibirsk, Russia

**Ekaterina Lokteva**, Lomonosov Moscow State University, Moscow, Russia

**Valery Lunin**, Lomonosov Moscow State University, Moscow, Russia

**Dmitry Murzin**, Åbo Akademi University, Turku, Finland

**Konstantin Neyman**, ICREA & University of Barcelona, Barcelona, Spain

**Valentin Parmon**, Boreskov Institute of Catalysis, Novosibirsk, Russia

**Günther Rupprechter**, Vienna University of Technology, Vienna, Austria

**Robert Schlögl**, Fritz Haber Institute of the Max Planck Society, Germany

Max Planck Institute for Chemical Energy Conversion, Germany

**Mikhail Sinev**, Semenov Institute of Chemical Physics RAS, Moscow, Russia

**Aleksander Stakheev**, N.D. Zelinsky Institute of Organic Chemistry RAS, Moscow, Russia

**Evgenii Talsi**, Boreskov Institute of Catalysis, Novosibirsk, Russia

**Malgorzata Witko**, Institute of Catalysis and Surface Chemistry, Krakow, Poland

## Organizing Committee

**Chairman:** **Valerii Bukhtiyarov**, Boreskov Institute of Catalysis, Novosibirsk, Russia

### Members:

**Konstantin Bryliakov**, Boreskov Institute of Catalysis, Novosibirsk, Russia

**Marina Bukhtiyarova**, Boreskov Institute of Catalysis, Novosibirsk, Russia

**Vasily Kaichev**, Boreskov Institute of Catalysis, Novosibirsk, Russia

**Ekaterina Kozlova**, Boreskov Institute of Catalysis, Novosibirsk, Russia

### Secretariat:

**Marina Klyusa**, Boreskov Institute of Catalysis, Novosibirsk, Russia

**Svetlana Logunova**, Boreskov Institute of Catalysis, Novosibirsk, Russia

**Secretary:** **Marina Suvorova**, Boreskov Institute of Catalysis, Novosibirsk, Russia



# PLENARY LECTURES

PL-2 ÷ PL-6



## PL-2

### Mechanisms of Hydrogen Peroxide Activation over Ti(IV) and Nb(V) Single Sites

Kholdeeva O.A.

*Boreskov Institute of Catalysis, Novosibirsk, Russia*

*Novosibirsk State University, Novosibirsk, Russia*

*khold@catalysis.ru*

Ti(IV) and Nb(V) single site catalysts have attracted much recent attention due to their ability to catalyze selective oxidations with the green oxidant hydrogen peroxide. However, their catalytic performance differs significantly in terms of activity, chemo- and regioselectivity [1-3]. In this lecture, we present our recent works directed toward understanding the mechanisms of H<sub>2</sub>O<sub>2</sub> activation over Ti(IV) and Nb(V). Ti- and Nb-substituted tungstates of the Lindqvist structure [MW<sub>5</sub>O<sub>18</sub>]<sup>n-</sup> (MW<sub>5</sub>, M = Ti and Nb) mimic well the catalytic performance of heterogeneous M-silicates. These compounds have been employed as tractable molecular models to gain insights into the structure and reactivity of Ti and Nb peroxo species using UV-vis, FT-IR, Raman, <sup>93</sup>Nb, <sup>17</sup>O and <sup>183</sup>W NMR spectroscopic techniques and DFT calculations [4,5]. For both metals, peroxo form 'HMO<sub>2</sub>' is more stable than hydroperoxo form 'MOOH', but 'MOOH' is more reactive than 'HMO<sub>2</sub>' toward epoxidation of alkenes. The superior heterolytic pathway selectivity observed for Nb catalysts can be explained by a combination of two main factors: 1) a lower energy barrier for the oxygen atom transfer from 'NbOOH' to the C=C bond leading to epoxide and 2) a higher energy cost of homolytic O–O bond breaking in the 'NbOOH' intermediate. The size of M and the flexibility of its coordination environment affect the oxygen transfer mechanism. For a rigid Ti(IV) environment, β-oxygen transfer from Ti(η<sup>1</sup>-OOH) is favored over α-oxygen transfer. The larger size of Nb(V) enables formation of a 7-coordinated Nb(η<sup>2</sup>-OOH) species for which α-oxygen transfer is energetically preferable over β-oxygen transfer. The different oxygen transfer mechanisms may account for different regioselectivities observed in heterogeneous Ti- and Nb-catalyzed epoxidations.

**Acknowledgement.** This work was supported by RFBR, grant 16-03-00827.

#### References:

- [1] I.D. Ivanchikova, N.V. Maksimchuk, I.Y. Skobelev, V.V. Kaichev, O.A. Kholdeeva, *J. Catal.* 332 (2015) 138.
- [2] I.D. Ivanchikova, I.Y. Skobelev, N.V. Maksimchuk, E.A. Paukshtis, M.V. Shashkov, O.A. Kholdeeva, *J. Catal.* 356C (2017) 85.
- [3] O.A. Kholdeeva, I.D. Ivanchikova, N.V. Maksimchuk, I.Y. Skobelev, *Catal. Today*, DOI: 10.1016/j.cattod.2018.04.002.
- [4] N.V. Maksimchuk, G.M. Maksimov, V.Yu. Evtushok, I.D. Ivanchikova, Yu.A. Chesalov, R.I. Maksimovskaya, O.A. Kholdeeva, A. Solé-Daura, J. M. Poblet, J. J. Carbó, *ACS Catal.*, 8 (2018) 9722.
- [5] N.V. Maksimchuk, I.D. Ivanchikova, G.M. Maksimov, I.V. Eltsov, V.Yu. Evtushok, O.A. Kholdeeva, D. Lebbie, R.J. Errington, A. Solé-Daura, J.M. Poblet, J.J. Carbó, *ACS Catal.*, 2019, *in press*.

## PL-3

### Catalysis Using Nanomaterials

Hutchings G.J.

*Cardiff Catalysis Institute, School of Chemistry, Cardiff University, Cardiff, UK*  
*hutch@cf.ac.uk*

Catalysis is of crucial importance for the manufacture of the goods and infrastructure necessary for the effective wellbeing of society. Catalysis continues to play a key role in the manufacture of chemical intermediates and there is a continuing requirement to design new effective catalysts. The identification that gold in nanoparticulate form is an exceptionally effective catalyst has paved the way for a new class of active catalysts. Gold is the most active catalyst for the oxidation of carbon monoxide at ambient temperature. It is also the most effective catalyst for the synthesis of vinyl chloride by acetylene hydrochlorination. Gold is now being commercialized in China for this reaction. In this presentation the synthesis of active catalysts will be described as well as their characterization for this important reaction. Aspects of the latest research on this topic will be presented together with examples of catalysis with gold palladium alloys and also new nanomaterials.

## Smart Catalysts and Today's Energy and Environmental Challenges

Fornasiero P.

*Department of Chemical and Pharmaceutical Sciences, ICCOM-CNR and INSTM,  
University of Trieste, Trieste, Italy  
pfornasiero@units.it*

The study of catalytic processes starting from well- defined materials that are tuned in morphology, composition and shape is offering new perspectives for catalyst design. CO oxidation turned out to be crucially dependent on the interfacial contact of the support (ceria) with the metal nanocrystal active sites [1]. Pt and PtCo nanocrystals supported on carbon were effectively employed in selective biomass conversion [2]. Brookite nanorods showed that anisotropy is important to promote photocatalytic hydrogen evolution [3]. Core-shell nanostructures have proved to be superior catalysts in several catalytic reactions, such as methane combustion [4], electrocatalytic water electrolysis [5] and CO<sub>2</sub> conversion [6]. Single Atom Catalysts [8], metal free nanocatalysts [9] and “intelligent” catalysts [10, 11] are now at the frontier of heterogeneous catalysts for sustainable industrial applications.

**Acknowledgement.** This work was supported by University of Trieste, INSTM and ICCOM-CNR.

### References:

- [1] M. Cargnello, V. V.T. Doan-Nguyen, T.R. Gordon, R.E. Diaz, E.A. Stach, R.J. Gorte, P. Fornasiero, C.B. Murray, *Science* 2013, 341, 771.
- [2] J. Luo, H. Yun, A.V. Mironenko, K.A. Goulas, J.D. Lee, M. Monai, C. Wang, V. Vorotnikov, C.B. Murray, D.G. Vlachos, P. Fornasiero, R.J. Gorte, *ACS Catal.* 2016, 6, 4095.
- [3] M. Cargnello, T. Montini, S.Y. Smolin, J.B. Priebe, J. J. Delgado, V.V.T Doan-Nguyen, I.S. McKay, J.A. Schwalbe, M.M. Pohl, R.T. Gordon, Y. Lu, J.B. Baxter, A. Brückner, P. Fornasiero, C.B. Murray, *PNAS* 2016, 113, 3966
- [4] M. Cargnello, J.J. Delgado Jaén, J.C. Hernández Garrido, K. Bakhmutsky, T. Montini, J.J. Calvino Gámez, R.J., Gorte, P. Fornasiero P. *Science* 2012, 337, 713.
- [5] G. Valenti, A. Boni, M. Melchionna, M. Cargnello, L. Nasi, G. Bertoni, R.J. Gorte, M. Marcaccio, S. Rapino, M. Bonchio, P. Fornasiero, M. Prato, F. Paolucci, *Nature Commun.* (2016) article number: 13549.
- [6] M. Melchionna, V. Bracamonte, A. Giuliani, L. Nasi, T. Montini, C. Tavagnacco, M. Bonchio, P. Fornasiero, M. Prato, *Energ. Environ. Sci.*, 2018, 11, 1571-1580.
- [7] A. Bakandritsos, R.G. Kadam, P. Kumar, G. Zoppellaro, M. Medved', J. Tuček, T. Montini, O. Tomanec, P. Andrýšková, B. Drahoš, R.S. Varma, M. Otyepka, M.B. Gawande, P. Fornasiero, R. Zbořil, *Adv. Mater.*, 2019, 31, n° 1900323.
- [8] D. Iglesias, A. Giuliani, M. Melchionna, S. Marchesan, A. Criado, L. Nasi, M. Bevilacqua, C. Tavagnacco, F. Vizza, M. Prato, P. Fornasiero, *Chem* 2018, 4, 106.
- [9] T. M. Onn, M. Monai, S. Dai, E. Fonda, T. Montini, X. Pan, G.W. Graham, P. Fornasiero, R.J. Gorte, *JACS*, 2018, 140, 4841-4848.
- [10] N. Luo, T. Montini, J. Zhang, P. Fornasiero, E. Fonda, T. Hou, W. Nie, J. Lu, J. Liu, M. Heggen, L. Lin, C. Ma, M. Wang, F. Fan, S. Jin, F. Wang, *Nature Energy*, 2019, DOI: 10.1038/s41560-019-0403-5

## PL-5

### Heterogeneous Chemistry at Liquid/Vapor Interfaces Investigated with Photoelectron Spectroscopy

Bluhm H.

*Fritz Haber Institute of the Max Planck Society, Department of Inorganic Chemistry, Berlin;  
Germany*

*bluhm@fhi-berlin.mpg.de*

Aqueous solution/vapor interfaces govern important phenomena in the environment and atmosphere, including the uptake and release of trace gases by aerosols and CO<sub>2</sub> sequestration by the oceans.[1] A detailed understanding of these processes requires the investigation of liquid/vapor interfaces with chemical sensitivity and interface specificity under ambient conditions, *i.e.*, temperatures above 200 K and water vapour pressures in the millibar to tens of millibar pressure range. This talk will discuss opportunities and challenges for investigations of liquid/vapor interfaces using X-ray photoelectron spectroscopy and describe some recent experiments that have focused on the propensity of certain ions and the role of surfactants at the liquid/vapor interface.

#### References:

[1] O. Björneholm et al., Chem. Rev. **116**, 7698 (2016).

## Nano-Catalysis vs. Dynamic Single-Atom Catalysis: Insights from Computational Modelling

Li J.

*Theoretical Chemistry Center, Department of Chemistry, Tsinghua University, Beijing, China  
junli@tsinghua.edu.cn*

Catalysis science is essential for chemical industries, biological transformation, atmospheric processes, environment, energy, and human health. In recent years, heterogeneous single-atom catalysts (SAC) have aroused significant interest in the catalysis community [1-3]. Based on recent *ab initio* molecular dynamics simulations of Au<sub>20</sub>/TiO<sub>2</sub> and Au<sub>20</sub>/CeO<sub>2</sub> nanocatalysts, we have revealed that the microscopic mechanisms of a series of nano-scale catalytic reactions involve *dynamic* single-atom catalysts (DSAC), which account for the activity and size-effect of gold catalysis [4-7]. In this talk, we will discuss our recent theoretical results on the computational studies relevant to DSAC and provide an overview of SACs and surface single-cluster catalysts (SCC) [8-10].

**Acknowledgement.** This work was supported by the National Natural Science Foundation of China, grant nos. 21433005, 91645203, and 21590792.

### References:

- [1] B.-T. Qiao, A.-Q. Wang, X.-F. Yang, L. F. Allard, Z. Jiang, Y.-T. Cui, J.-Y. Liu, J. Li, T. Zhang, "Single-Atom Catalysis of CO Oxidation Using Pt<sub>1</sub>/FeO<sub>x</sub>", *Nature Chem.* 3 (2011) 634.
- [2] X.-F. Yang, A.-Q. Wang, B.-T. Qiao, J. Li, J.-Y. Liu, T. Zhang, "Single-Atom Catalysts: A New Frontier in Heterogeneous Catalysis", *Acc. Chem. Res.* 46 (2013) 1740.
- [3] A. Wang, J. Li, T. Zhang, "Heterogeneous Single-Atom Catalysis", *Nat. Rev. Chem.* 2 (2018) 65.
- [4] Y.-G. Wang, Y. Yoon, V.A. Glezakou, J. Li, R. Rousseau, "The Role of Reducible Oxide-Metal Cluster Charge Transfer in Catalytic Processes: New Insights on the Catalytic Mechanism of CO Oxidation on Au/TiO<sub>2</sub> from Ab Initio Molecular Dynamics", *J. Am. Chem. Soc.* 135 (2013) 10673.
- [5] Y.-G. Wang, D.-H. Mei, V.-A. Glezakou, J. Li, R. Rousseau, "Dynamic Formation of Single-Atom Catalytic Active Sites on Ceria-Supported Gold Nanoparticles", *Nature Commun.* 6 (2015) 6511.
- [6] J.-C. Liu, Y.-G. Wang, J. Li, "Toward Rational Design of Oxide-Supported Single Atom Catalysts: Atomic Dispersion of Gold on Ceria", *J. Am. Chem. Soc.* 139 (2017) 6190.
- [7] Y. He, J.-C. Liu, L. Luo, Y.-G. Wang, J. Zhu, Y. Du, J. Li, S. X. Mao, C. Wang, "Size-Dependent Dynamic Structures of Supported Gold Nanoparticles in CO Oxidation Reaction Condition", *Proc. Natl. Acad. Sci. USA.* 115 (2018) 7700.
- [8] S.-R. Zhang, L. Nguyen, J.-X. Liang, J.-J. Shan, J.-Y. Liu, A. I. Frenkel, A. Patlolla, W.-X. Huang, J. Li, F. Tao, "Catalysis on Singly Dispersed Bimetallic Sites", *Nature Commun.* 6 (2015) 7938.
- [9] X.-L. Ma, J.-C. Liu, H. Xiao, J. Li, "Surface Single-Cluster Catalyst for N<sub>2</sub>-to-NH<sub>3</sub> Thermal Conversion", *J. Am. Chem. Soc.* 140 (2018) 46.
- [10] J.-C. Liu, X.-L. Ma, Y. Li, Y.-G. Wang, H. Xiao, J. Li, "Heterogeneous Fe<sub>3</sub> Single-Cluster Catalyst for Ammonia Synthesis via an Associative Mechanism", *Nature Commun.* 9 (2018) 1610.





# **KEYNOTE LECTURES**

**KL-1 ÷ KL-4, KLS-1**



## KL-1

### Molecular Aluminium and Iron Siloxide Compounds as Models for Active Sites in the Pores of Zeolites

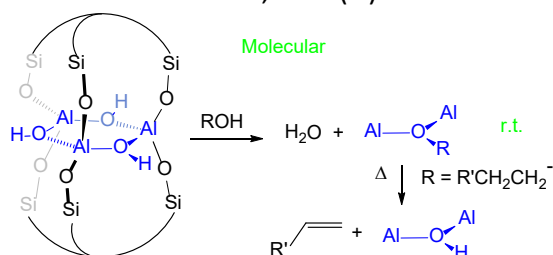
Lokare K.S.<sup>1</sup>, Frank N.<sup>1</sup>, Manicke N.<sup>1</sup>, Pinkert D.<sup>1</sup>, Braun-Cula B.<sup>1</sup>, Goikoetxea I.<sup>1</sup>, Jorewitz M.<sup>2</sup>, Kelly J.T.<sup>2</sup>, Herwig C.<sup>1</sup>, Leach S.<sup>1</sup>, Baldauf C.<sup>3</sup>, Asmis K.<sup>2</sup>, Sauer J.<sup>1</sup>, Limberg C.<sup>1</sup>

1 – Humboldt-Universität zu Berlin, Institut für Chemie, Berlin, Germany

2 – Wilhelm-Ostwald-Institut für Physikalische und Theoretische Chemie, Universität Leipzig, Leipzig, Germany

3 – Fritz-Haber-Institut der Max-Planck Gesellschaft, Berlin, Germany  
christian.limberg@chemie.hu-berlin.de

To gain insights into the properties of certain functions and units of extended oxides/hydroxides on the molecular level suitable molecular model compounds are needed. We have accessed models of aluminosilicates by trapping of intermediates occurring during the hydrolysis of suitable aluminium precursor compounds with the aid of stabilizing tripodal trisilanol ligands.[1a] *Tri-* and *octanuclear* aluminium hydroxide cluster complexes  $[Al_3(\mu_2-OH)_3(THF)_3(PhSi(OSiPh_2O)_3)_2]$ , **1** and  $[Al_8(\mu_3-OH)_2(\mu_2-OH)_{10}(THF)_3(p\text{-anisylSi(OSiPh}_2O)_3)_4]$ , **2**, could be isolated. **1** can be regarded as the  $Al(OH)_3$  cyclic trimer, where six protons have been replaced by silyl residues, while **2** features a unique  $[Al_8(\mu_3-OH)_2(\mu_2-OH)_{10}]^{12+}$  core. In contrast to most other known aggregates of that type **1** and **2** (i) can be readily prepared at reasonable scales, (ii) dissolve in common solvents, and (iii) retain their framework intact even in the presence of excessive



amounts of water. This paves the way for reactivity studies in solution addressing the individual functions.[1] The  $-Al-O(H)-Al-$  units in **1** proved far more acidic than should be assumed intuitively and catalytically competent in olefin isomerisations and alcohol dehydrations, which

sheds some light on the properties of such entities as part of amorphous alumina/silica materials or extraframework aluminium species in the pores of zeolites.[1b]

Moreover, access to novel polynuclear iron(II) siloxide complexes is presented, featuring rare high-spin, square planar  $FeO_4$  structural motifs,[2] that recently have been shown to be responsible for the catalytic activity of iron-modified zeolites.[2, 3]

**Acknowledgement.** This work was supported by the DFG. Grant Number: CRC 1109.

## KL-1

### References:

- [1] a) K. S. Lokare, N. Frank, B. Braun-Cula, I. Goikoetxea, J. Sauer, C. Limberg, *Angew. Chem. Int. Ed.* **2016**, *55*, 12325; b) K. S. Lokare, B. Braun-Cula, C. Limberg, M. Jorewitz, J. T. Kelly, K. R. Asmis, S. Leach, C. Baldauf, I. Goikoetxea, J. Sauer, *Angew. Chem. Int. Ed.* **2019**, *58*, 902-906.
- [2] D. Pinkert, S. Demeshko, F. Schax, B. Braun, F. Meyer, C. Limberg, *Angew. Chem. Int. Ed.* **2013**, *52*, 5155-5158; D. Pinkert, M. Keck, S. Ghassemi Tabrizi, C. Herwig, F. Beckmann, B. Braun-Cula, M. Kaupp, C. Limberg, *Chem. Commun.* **2017**, *53*, 8081-8084.
- [3] B. E. R. Snyder, P. Vanelderden, M. L. Bols, S. D. Hallaert, L. H. Böttger, L. Ungur, K. Pierloot, R. A. Schoonheydt, B. F. Sels, E. I. Solomon *Nature* **2016**, *536*, 317–321.

## In Situ Surface Spectroscopy and Microscopy of Reactions on Zirconia Based Model Catalysts

Rupprechter G.

*Institute of Materials Chemistry, Technische Universität Wien, Vienna, Austria  
guenther.rupprechter@tuwien.ac.at*

My group's philosophy is to study catalytic surface reactions on heterogeneous catalysts via a three-fold approach, employing surface science based planar model catalysts, atomically precise clusters and industrial-grade catalysts. The focus is on examining active functioning catalysts at (near) atmospheric pressure and at elevated temperature.

For ultrahigh vacuum (UHV) based model catalysts this requires in situ surface spectroscopy, such as sum frequency generation (SFG) laser spectroscopy, polarization-modulation infrared reflection absorption spectroscopy (PM-IRAS) and near atmospheric pressure X-ray photoelectron spectroscopy (NAP-XPS). To image ongoing surface reactions by in situ surface microscopy, photoemission electron microscopy (PEEM) was applied.

For technological catalysts, analogous operando studies were performed by Fourier transform infrared spectroscopy (FTIR), X-ray absorption spectroscopy (XAS), NAP-XPS, and X-ray diffraction (XRD). Most operando studies were performed at synchrotron sources (BESSY (DE), MaxLab (SE), SLS (CH), Diamond (UK), ALBA (ES)), in lock-step with theory.

This three-pronged approach yields a detailed view of the catalytically relevant atomic and electronic surface structure of catalysts, as well as of molecular details that steer reaction activity and selectivity.

Recently, we have studied ZrO<sub>2</sub> based reforming catalysts, using both model and technological catalysts:

- i) CO<sub>2</sub> activation by H<sub>2</sub>O on ultrathin ZrO<sub>2</sub> trilayer (O-Zr-O) film on Pt<sub>3</sub>Zr(0001) (NAP-XPS, PM-IRAS) Surf. Sci. 679 (2019) 139–146,
- ii) methane dry reforming on ZrO<sub>2</sub>/Pt(111) inverse model catalysts (NAP-XPS, IRAS, TPD) J. Phys.: Cond. Matt. 30 (2018) 264007 (1-12) and technological Ni/ZrO<sub>2</sub>-CeO<sub>2</sub> catalysts (FTIR, NAP-XPS, XAS, DFT) Catalysis Today, 283 (2017) 134-143, Catalysis Today 277 (2016) 234-245,
- iii) CO oxidation and H<sub>2</sub> oxidation on polycrystalline Pt, Pd and Rh surfaces, as well as ZrO<sub>2</sub> supported Pd and Rh particles (PEEM, MS, XPS, AFM, EBSD) Nat. Mat. 17 (2018) 519-522; Nat. Comms 9 (2018) 600; Catal. Lett. 148 (2018) 2947-2956, Surf. Sci. 679 (2019) 163–168.

I will discuss how in situ surface spectroscopy/microscopy studies enabled to observe novel phenomena (OH assisted CO<sub>2</sub> activation, details of SMSI, suppression of coke formation, local kinetics and long-range metal/oxide interface effects).

**Acknowledgement.** This work was supported by the Austrian Science Fund (SFB F4502 FOXSI).

## KL-3

### Dynamic Nonlinear Effects in Asymmetric Catalysis

Ottenbacher R.V.<sup>1,2</sup>, Talsi E.P.<sup>1,2</sup>, Bryliakov K.P.<sup>1,2</sup>

1 – Boreskov Institute of Catalysis, Novosibirsk, Russia

2 – Novosibirsk State University, Novosibirsk, Russia

bryliako@catalysis.ru

For three decades, “conventional” nonlinear effects (NLEs) in asymmetric catalysis, commonly becoming apparent as nonproportional relationship between the optical purity of the chiral catalyst and that of the chiral reaction product, have been extensively studied from both fundamental and practical perspectives [1]. On the contrary, this lecture is focused on *dynamic nonlinear effects* (DNLEs) [2], with the catalyst systems exhibiting variation of enantioselectivity over the reaction course; this variation is caused by the interactions of the catalyst with the chiral product or substrate, whose concentrations change as the reaction proceeds (Figure 1). Namely, such phenomena as *asymmetric autoinduction* [3], *asymmetric autocatalysis* [4], and *asymmetric autoamplification* [5] are considered, and examples of reactions exhibiting such effects, are presented. Whenever available, key details of the molecular mechanisms responsible for the observed nonlinearities are provided. Possible implications of dynamic nonlinear effects in asymmetric catalysis into the problem of prebiotic emergence of chirality on Earth are discussed.

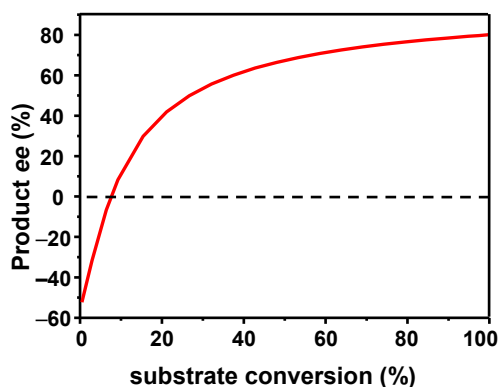


**Figure 1.** Example of enantioselectivity variation in a catalytic reaction, caused by asymmetric autoinduction [2].

**Acknowledgement.** This work was supported by the Russian Science Foundation, grant 17-13-01117.

#### References:

- [1] T. Satyanarayana, S. Abraham, H. B. Kagan, *Angew. Chem. Int. Ed.* 48 (2009) 456-494.
- [2] K. P. Bryliakov, *ACS Catalysis Submitted*.
- [3] A. H. Alberts, J. Wynberg, *J. Am. Chem. Soc.* 111 (1989) 7265-7266.
- [4] K. Soai, Y. Shibata, H. Morioka, K. Choji, *Nature* 378 (1995) 767-768.
- [5] E. P. Talsi, D. G. Samsonenko, K. P. Bryliakov, *ChemCatChem* 9 (2017) 2599-2607.

## Mechanistic Considerations Related to Ammonia Synthesis

Hargreaves J.S.J.

*School of Chemistry, Joseph Black Building, University of Glasgow, Glasgow, UK  
justinh@chem.gla.ac.uk*

The development of the Haber Bosch Process was a landmark achievement of the 20<sup>th</sup> Century. It can be directly credited with the sustainment of a significant proportion of the global population through access to synthetic fertiliser. On a global scale, the process produces ca 174 million tonnes of ammonia per annum with an annual projected growth rate of around 1.5% to meet growing demand. The entire process, including the generation of feedstock, is responsible for ca. 2% of global energy demand and ca 1.6% of anthropogenic CO<sub>2</sub> emissions. There is therefore great interest, and potential, in the identification of novel, more sustainable, strategies towards ammonia synthesis – these are directed towards the development of smaller scale and more localised, reduced scale processes. Such processes could be achieved through the development of electrocatalytic routes to take advantage of sustainable electricity production, photocatalytic routes and the development of more conventional heterogeneous catalytic approaches operational under less severe process conditions (the Haber Bosch Process currently operates at ca 400°C and > 100 atmospheres pressure with a promoted iron catalyst – the conditions applied are dictated by the requirement to achieve acceptable process conditions, with the reaction being favoured thermodynamically at lower reaction temperatures).

In this presentation, the possibility of the development of metal nitride based catalysts operational through the Mars - van Krevelen mechanism wherein the lattice nitrogen is reactive will be outlined and considered in the context of limiting scaling relationships which have been proposed elsewhere. Particular attention will be directed towards the role of structure and composition for a range of ternary and quaternary interstitial metal nitrides. A combination of experimental and computational modelling data will be presented to support this suggested pathway.

## **KLS-1**

# **Multi-Scale Engineering of Catalytic Systems for the Hydrogenation of Carbon Dioxide**

Gascon J.

*King Abdullah University of Science and Technology, KAUST Catalysis Center (KCC), Advanced Catalytic Materials, Thuwal, Saudi Arabia  
jorge.gascon@kaust.edu.sa*

Carbon dioxide levels today are higher than at any point in the past 800,000 years, exceeding 400 ppm in 2016 and leading to a dangerous temperature increase of the Earth's surface. Along with the necessity to develop efficient capture technologies, advances in the catalytic transformation of CO<sub>2</sub> to base chemicals would add an additional economic incentive to empower initiatives into CO<sub>2</sub> capture. In a potential (and feasible) scenario of cheap hydrogen produced via electrolysis, the formation of methanol and/or light olefins, some of the most demanded base chemicals, from CO<sub>2</sub> may become a very attractive technology. However, efficient catalysts for this process are still to be developed.

In this presentation we will report our last advances in the development of new catalysts and catalytic processes for the direct hydrogenation of CO<sub>2</sub>, under mild conditions, to methanol, short chain olefins, and aromatics.



# **ORAL PRESENTATIONS**

**Section I. Basic concepts, theory and modeling in catalysis**  
**IOP-I-1, OP-I-2 ÷ OP-I-11**

**Section II. Physical methods, including in situ and operando techniques, in catalysis**  
**IOP-II-1, OP-II-2 ÷ OP-II-14**

**Section III. Kinetics and mechanisms of catalyzed processes**  
**IOP-III-1, OP-III-2 ÷ OP-III-18**

**Section IV. Advanced catalyst systems addressing current challenges: energy, materials, sustainability**  
**IOP-IV-1, OP-IV-2 ÷ OP-IV-15**



## IOP-I-1

### Robust In Situ Investigation of Heterogeneous Hydrogenation Mechanisms with Parahydrogen

Kovtunov K.V., Koptyug I.V.

*International Tomography Centre SB RAS, Novosibirsk, Russia*

*kovtunov@tomo.nsc.ru*

Parahydrogen-induced polarization (PHIP) is a powerful technique for studying hydrogenation reactions in gas and liquid phases. Pairwise addition of parahydrogen to the hydrogenation substrate imparts nuclear spin order to reaction products, manifested as enhanced  $^1\text{H}$  NMR signals from the nascent proton sites. Nanoscale metal catalysts immobilized on supports comprise a promising class of catalysts for producing PHIP effects; however, on such catalysts the percentage of substrates undergoing the pairwise addition route—a necessary condition for observing PHIP—is usually low. PHIP effects are observed predominantly in the case of pairwise addition, i.e., both H atoms on the product must originate from the same  $\text{H}_2$  molecule. In theory, nuclear spin hyperpolarization can result in NMR signal enhancements of up to 5 orders of magnitude at high magnetic fields. Originally, this effect was first demonstrated for homogeneous catalysts where an isolated metal center provides the required pairwise addition of hydrogen. Later, PHIP approach has been mainly utilized for the mechanistic and kinetic studies of homogeneous hydrogenation reactions catalyzed by transition-metal complexes in solution. Therefore, PHIP effects were successfully observed over immobilized Ir, Rh, V, Co, Cr and Au complexes. The immobilization approach has shown its worth in PHIP experiments – the utilization of the Wilkinson’s catalyst immobilized on silica made it possible to produce a continuous flow of hyperpolarized gas, which was used for visualization of model objects, microreactors, and microfluidic devices. The antiphase multiplets in the  $^1\text{H}$  NMR spectra unambiguously testify to the presence of the pairwise hydrogen addition to the substrate, and the preservation of hydrogenation mechanism inherent for homogeneous precursor during immobilization is confirmed. The main shortcoming of immobilized catalysts is the lack of stability under reaction conditions associated with the favorable reduction to metal particles and leaching into solution.

Supported metal nanoparticles also demonstrated the ability to produce pronounced PHIP effects, which significantly expanded the scope of potential applicability of PHIP. Moreover, it was shown that the highest intensities of PHIP signals were obtained over  $\text{TiO}_2$ -supported metal catalysts. The attempts to explain this fact led to investigation of the strong metal-support interaction (SMSI) effect in the context of PHIP. Metal nanoparticle catalysts are attractive in view of the PHIP applications; for instance, MR imaging of model catalytic systems was demonstrated.

**Acknowledgement.** This work was supported by the RFBR (grant # 19-53-12013).

**Synergistic Effect of Multi Active Sites with Low-Coordination Lattice Oxygen on Catalytic Combustion of Methane over  $\text{Co}_3\text{O}_4(110)$**

Xiao-Ming Cao<sup>1</sup>, Wende Hu<sup>1</sup>, P. Hu<sup>2</sup>

*1 – Center for Computational Chemistry and Research Institute of Industrial Catalysis, East China University of Science and Technology, Shanghai, China*

*2 – School of Chemistry and Chemical Engineering, The Queen's University of Belfast, Belfast, UK  
xmcao@ecust.edu.cn*

The lower level of methane emission for natural gas vehicles is required to meet the increasing demands of stricter environmental standards. Cobalt-based spinel oxides as a kind of earth-abundant materials exhibit high activities for the catalytic combustion of methane. To understand the key factors governing the catalytic activities, on-site Coulomb repulsion corrected density functional theory calculations have been carried out to investigate the complete catalytic cycle of complex methane combustion on the active  $\text{Co}_3\text{O}_4(110)$  surface at the molecular level.

It is found that the two-fold coordinated lattice oxygen ( $\text{O}_{2c}$ ) and the hydrogen and the intermediate migration between multi Co-O sites would be of vital importance for methane combustion over  $\text{Co}_3\text{O}_4$  surfaces, especially for the deep C-H bond activation and the C-O bond coupling. It could explain the reason why the  $\text{Co}_3\text{O}_4(110)$  surface significantly outperforms the  $\text{Co}_3\text{O}_4(100)$  surface without exposed  $\text{O}_{2c}$  for methane combustion which has been verified by experimental results. More importantly, it is found that the cooperation of homogeneous multi-sites would improve the activity of the complex reaction like methane combustion. It not only facilitates the hydrogen transfer between different sites for the swift formation of  $\text{H}_2\text{O}$  to effectively avoid the passivation of the active low-coordinated  $\text{O}_{2c}$  site but also stabilizes produced surface intermediates, optimizing the reaction channel.

The understanding of this synergistic effect of multi active sites might not only be beneficial to develop the improved catalysts for methane combustion but also shed light on one advantage of heterogeneous catalysts with multi-sites compared to single-site catalysts for the complex catalytic progress with multi elementary steps.

## OP-I-2

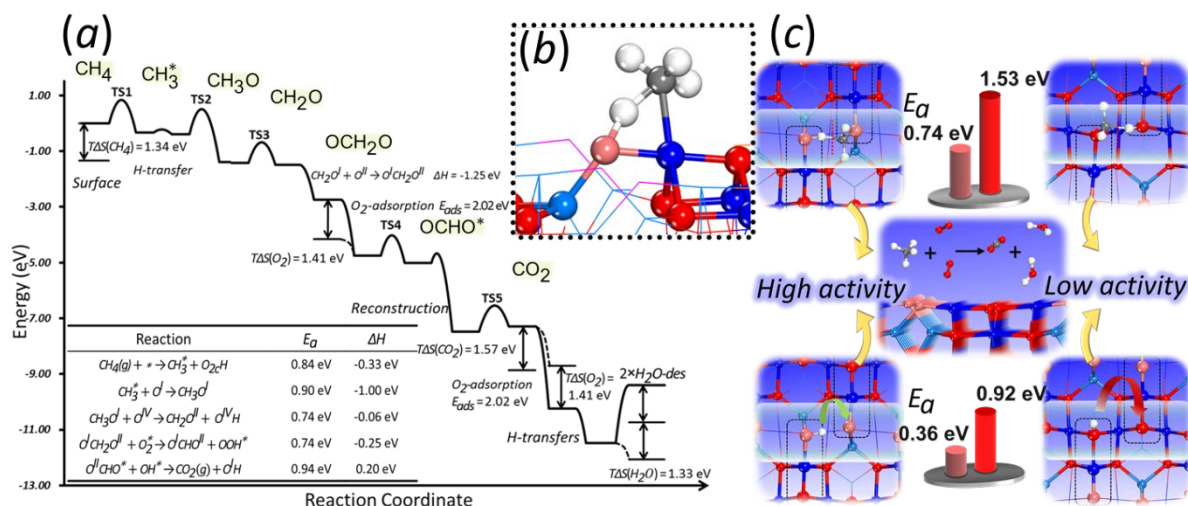


**Figure 1.** (a) The energy profile of the minimum energy path. TS1, TS2, TS3, TS4, and TS5 are the TSs for the elementary reactions of the 1<sup>st</sup> C-H bond activation, the 1<sup>st</sup> C-O coupling, 2<sup>nd</sup> C-H bond activation, 3<sup>rd</sup> C-H bond activation and 4<sup>th</sup> C-H activation of which the reaction formulae are listed, respectively. (b) the optimized structure of the transition states for the 1<sup>st</sup> C-H bond activation. (c) the comparison between O<sub>2c</sub> and O<sub>3c</sub> in 2<sup>nd</sup> C-H activation and H transfer.

**Acknowledgement.** This work was supported by National Natural Science Foundation of China (21673072 and 21333003).

### References:

- [1] W. Hu, X.-M. Cao, and P. Hu, ACS Catal. 6(2016) 5508.
- [2] W. Hu, X.-M. Cao, and P. Hu, J. Phys. Chem. C 122(2018) 19593.

## OP-I-3

### **Interrelations between Apparent Kinetics and Mechanism in Catalytic Processes of Redox Type: Oxygen Activation and Pathways in Light Alkane Oxidation**

Sinev M.Yu.

*Semenov Institute of Chemical Physics RAS, Moscow, Russia  
mysinev@yandex.ru*

The kinetic features of catalytic oxidation processes that proceed via a staged redox mechanism are considered. The main assumptions of the Mars-van-Krevelen model, widely used in describing processes of this kind, their correspondence to real catalytic systems – typical catalysts for the partial oxidation of light alkanes (oxidative coupling of methane, oxidative dehydration of  $C_{2+}$  and oxidative cracking of  $C_{3+}$  alkanes) – are analyzed.

Unlike total and partial oxidation catalysts of unsaturated hydrocarbons and functionalized organic compounds, typical catalysts used for the oxidation of light alkanes do not contain noble and transition metals. This requires some revision of existing notions about the activation of molecular oxygen, including the key factors that determine its interaction with active surface sites and participation in the catalytic cycle. Special attention is paid to

- thermodynamic and kinetic conditions for the applicability of the redox mechanism to particular catalytic processes (thermochemistry of oxide systems, lifetime of oxygen in a bound state);
- realization of the redox mechanism in the presence of non-redox oxides characterized by a very high energy of the formation of anion (oxygen) vacancies;
- chemical and phase transformations that determine the course and efficiency of the catalytic redox cycle;
- interpretation of the results of kinetic experiment in the case of heterogeneous-homogeneous processes and the influence of elementary reactions of free radicals on the empirically determined values of kinetic parameters.

The case studies described include the oxidative coupling of methane and oxidative dehydrogenation of ethane over rare-earth oxides and complex supported NaWMn/SiO<sub>2</sub> oxide.

The Interrelations between the apparent kinetics and the mechanism in catalytic processes of redox type is analyzed from the standpoint of solving the inverse kinetic problem in the case of complex multistep processes.

## Resonance-Coordinated Active Sites in the Catalytic Synthesis of Ammonia

Cholach A.R., Bryliakova A.A.

*Boreskov Institute of Catalysis, Novosibirsk, Russia*

*cholach@catalysis.ru*

The sites  $M_n$  ( $M = \text{Pt, Rh, Ir, Fe, Co, Ru, Re, Mo}$ ;  $n = 2, 3, 4$ ) consisting of  $n$  surface atoms  $M$  are sorted out by their undercoordination  $\Sigma$  as compared with the bulk atoms. The highest activities of sites  $^{\Sigma}M_n$  in the catalytic synthesis of ammonia were found to require the specific “resonant”  $\Sigma_{res}$  values, which are mainly inaccessible at perfect planes due to steric reasons [1]. The convergence of  $\Sigma$  and  $\Sigma_{res}$  is adopted as a strategy for tailoring the advanced catalytic sites. The shift of the  $\Sigma$  and  $\Sigma_{res}$  meaning was performed by variation the size of clusters and the content of binary alloys, respectively [2]. The model of the resonance-coordinated active sites has been verified by comparison of the calculated and literature data on the specific catalytic activities of metals, individual single crystals, and special centers Fe-C<sub>7</sub> and Ru-B<sub>5</sub>.

The volcano dependence of the catalytic activity on the heat of N<sub>2</sub> adsorption for various metals conforms to the reference data. A quantitative agreement between the experimental catalytic activities of Fe and Re single crystals and the calculated activities of the same planes is obtained. The model gives a clear picture of the Fe-C<sub>7</sub> center on planes (111) and (211), whose extraordinary catalytic activity is enabled by their distinctive geometry. In particular, the site  $^{12}\text{Fe}_4$  determines completely the total activity of the plane Fe(211) and the specific activity of Fe(111) is provided by the sites  $^{12}\text{Fe}_3$  and  $^{13}\text{Fe}_4$ , contributing 42.7% and 57.2% to the overall activity of that plane, respectively, through the closeness of their  $\Sigma$  to  $\Sigma_{res} = 12.3$ .

The similar sites at 4-, 5-, and 11- atomic clusters of the noble metals, due to their larger  $\Sigma$  values, are  $\sim 10$ - $10^3$  times more active than at perfect planes. The same Ru and Re clusters show the opposite behaviour that is in a qualitative agreement with the experimental data on the catalytic activity vs. the size of the supported Ru particles [3].

The synergetic effect for sites  $M_3$  and  $M_4$  of the Ru-, Re- and Mo-based alloys has been developed. This suggests that an active catalyst (Ru, Re, Mo) can be improved by its alloying with an inactive one (Pt, Rh, Ir) due to optimal combination between the content and atomic coordination of the active sites of a particular alloy. A correlation between local structure, thermodynamics, and activity of a site is likely valid for other catalytic systems.

**Acknowledgements.** This work was supported by the Russian Foundation for Basic Research (Grant №17-03-00049), and performed within the RFBR and Novosibirsk region Project №19-43-540012 and budget Project №AAAA-A17-117041710078-1 for Boreskov Institute of Catalysis.

### References:

- [1] A. Cholach, A. Bryliakova, A. Matveev, N. Bulgakov, Surf. Sci. 645 (2016) 41.
- [2] A. Cholach, Appl. Catal., A 562 (2018) 223.
- [3] W. Raróg-Pilecka, E. Miśkiewicz, D. Szmigiel, Z. Kowalczyk, J. Catal. 231 (2005) 11.

**“Mercury Test” and Fundamental Problems of Catalyst Poisoning in the Studies of Reaction Mechanisms**

Chernyshev V.M.<sup>1</sup>, Astakhov A.V.<sup>1</sup>, Chikunov I.E.<sup>1</sup>, Tyurin R.V.<sup>1</sup>, Eremin D.B.<sup>2</sup>, Ranny G.S.<sup>1</sup>,  
Khrustalev V.N.<sup>3</sup>, Ananikov V.P.<sup>1,2</sup>

*1 – Platov South-Russian State Polytechnic University (NPI), Novocherkassk, Russia*

*2 – Zelinsky Institute of Organic Chemistry, RAS, Moscow, Russia*

*3 – National Research Center «Kurchatov Institute», Moscow, Russia*

*chern13@yandex.ru*

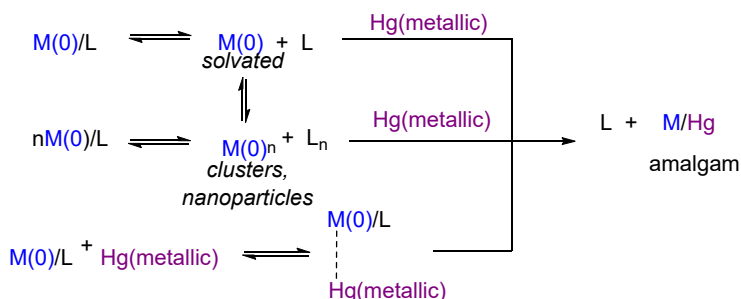
“Mercury test” (“Hg test”, “mercury poisoning test”, “Hg poisoning test”, and “Hg drop test”) is one of the oldest but frequently used methods for distinguishing truly homogeneous molecular catalysis from nanoparticle metal catalysis [1]. The method is based on the postulate that metallic mercury poisons M(0) clusters/nanoparticles but has no effect on molecular metal complexes. Inhibition of a catalytic reaction by metallic mercury is considered as the evidence of a cluster/nanoparticle catalysis, while the absence of a significant effect of mercury on a metal-catalyzed reaction is accepted as an attribute of a truly homogeneous catalysis. It should be noted that mercury test was subjected to criticism in several articles due to the revealed significant reactivity of some types of molecular metal complexes toward metallic mercury (see [1] and literature cited there). Nevertheless, despite the critical reports, the appropriateness and applicability of the mercury test as an universal method for the study of catalysis mechanisms has not been thoroughly examined.

In our study [1], on examples of various M(0) and M(II) complexes of palladium and platinum widely used in homogeneous catalysis, we have demonstrated general incorrectness of the mercury test as the method for distinguishing between homogeneous and cluster/nanoparticle catalysis mechanisms due to the next reasons: (i) the general and facile reactivity of molecular M(0) and M(II) complexes toward metallic mercury, (ii) the very high and oftentimes unpredictable dependence of the test results from operational conditions like mercury loading and agitation intensity for different catalysts.

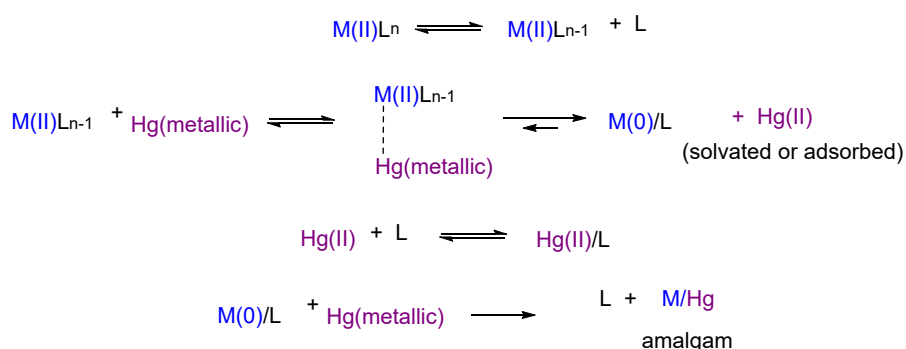
Two main types of mercury induced transformations, the cleavage of M(0) complexes and the oxidative-reductive transmetalation of M(II) complexes, including a new reaction of highly stable M(II)/NHC complexes (NHC – N-heterocyclic carbene ligand) [2-4], were elucidated using NMR, ESI-MS and EDXRF techniques. In most cases, the reaction products were isolated and characterized. A mechanistic picture for the reactions of metal complexes with mercury in conditions of mercury test was proposed (Scheme 1).

## OP-I-5

### Reactions of mercury with M(0) complexes:



### Reactions of mercury with M(II) complexes:



Scheme 1. Proposed mechanisms for the reactions of metallic mercury with M(0) and M(II) complexes

As an additional outcome, fundamental limitations of the concept of catalyst poisoning for distinguishing reaction mechanisms in dynamic catalytic systems were considered and mandatory conditions required for reliable implementation of catalyst poisons in the studies of metal-catalyzed reaction mechanisms have been formulated [1].

**Acknowledgement.** This work was supported by the Russian Foundation for basic Research, grant 16-29-10786.

### References:

- [1] V.M. Chernyshev, A.V. Astakhov, I.E. Chikunov, R.V. Tyurin, D.B. Eremin, G.S. Ranny, V.N. Khrustalev, V.P. Ananikov, *ACS Catal.*, 9 (2019) 2984. Doi: 10.1021/acscatal.8b03683.
- [2] V.M. Chernyshev, O.V. Khazipov, M.A. Shevchenko, A.Y. Chernenko, A.V. Astakhov, D.B. Eremin, D.V. Pasyukov, A.S. Kashin, V.P. Ananikov, *Chem. Sci.* 9 (2018) 5564. Doi: 10.1039/c8sc01353e.
- [3] O.V. Khazipov, M.A. Shevchenko, A.Y. Chernenko, A.V. Astakhov, D.V. Pasyukov, D.B. Eremin, Y.V. Zubavichus, V.N. Khrustalev, V.M. Chernyshev, V.P. Ananikov, *Organometallics* 37 (2018) 1483. Doi: 10.1021/acs.organomet.8b00124.
- [4] E.G. Gordeev, D.B. Eremin, V.M. Chernyshev, V.P. Ananikov *Organometallics* 37 (2018) 787. Doi: 10.1021/acs.organomet.7b00669.

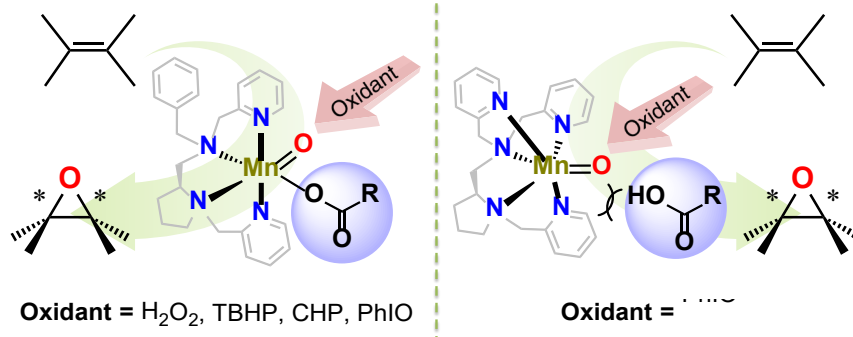
## Mechanistic Insights into the Enantioselective Oxidation Reactions Catalyzed by Chiral Manganese Catalysts

Sun W., Du J.Y., Sun Q.S.

State Key Laboratory for Oxo Synthesis and Selective Oxidation, Center for Excellence in Molecular Synthesis, Lanzhou Institute of Chemical Physics, Chinese Academy of Sciences, Lanzhou, P. R. China  
wsun@licp.cas.cn

The selective oxidation of hydrocarbons under mild conditions is of great current interest in enzymatic reactions as well as in synthetic organic chemistry [1]. In enzymatic reactions, metalloenzymes, such as heme and nonheme iron enzymes, catalyze a diverse array of important oxidative transformations, including olefin epoxidation and alkane hydroxylation reactions. Inspired by the high reactivity and selectivity shown by iron enzymes, in particular, synthetic nonheme iron complexes, and related manganese complexes have emerged as promising catalysts in the oxidation of organic substrates [2].

Over recent years our research groups have focused on the development of aminopyridine or aminobenzimidazole N4 ligands and manganese, iron complexes toward the asymmetric oxidation of C=C and C-H bonds [3,4]. Also, we have performed mechanistic studies to understand the nature of the active intermediates in the manganese complex-catalyzed enantioselective oxidations with N4 ligands [5].



**Acknowledgement.** This work was supported by the National Natural Science Foundation of China (21473226 and 21773237).

### References:

- [1] C. Sarantes, M. Stoikides, *J. Catal.* 93 (1985) 417. (a) L. Que, Jr., W. B. Tolman, *Nature* 455 (2008) 333.
- [2] K. P. Bryliakov, *Chem. Rev.* 117, (2017) 11406.
- [3] M. Wu, B. Wang, S. Wang, C. Xia, W. Sun, *Org. Lett.* 11 (2009) 3622.
- [4] B. Qiu, D. Xu, Q. Sun, C. Miao, Y.-M. Lee, X.-X. Li, W. Nam, W. Sun, *ACS Catal.* 8 (2018) 2479.
- [5] J. Y. Du, C. Miao, C. Xia, Y.-M. Lee, W. Nam, W. Sun, *ACS Catal.* 8 (2018) 4528.

## Metal/Metal-Oxide Interface Effects in Catalytic Materials: Theory Versus Experiment

Neyman K.M.

ICREA (Institució Catalana de Recerca i Estudis Avançats), Barcelona, Spain  
 Dept. de Ciència dels Materials i Química Física, Universitat de Barcelona, Barcelona, Spain  
 konstantin.neyman@icrea.cat

Active metal components are commonly present in technical catalysts as nanoparticles of many thousands of atoms. Due to their sizes, these species remain inaccessible for calculations based on density functional theory. However, they can be quite realistically represented by computationally tractable smaller model metal nanoparticles, whose surface sites marginally change the reactivity with increasing particle size. We developed this computational approach [1] and successfully applied it to describe various metal particles [2-6], including bimetallic ones [7], in catalytic materials. Our nanoparticle models expose a variety of active sites, whose structure and geometric flexibility notably better match those of the sites in catalysts under experimental conditions than still common slab models.

This talk will focus on how calculations of model metal particles supported on regular and nanostructured oxide surfaces allow us to delineate elusive interface effects on the structure and reactivity of catalysts [8-13]. Such effects determined in our simulations will be discussed in relation with the experimental observations of our co-authors.

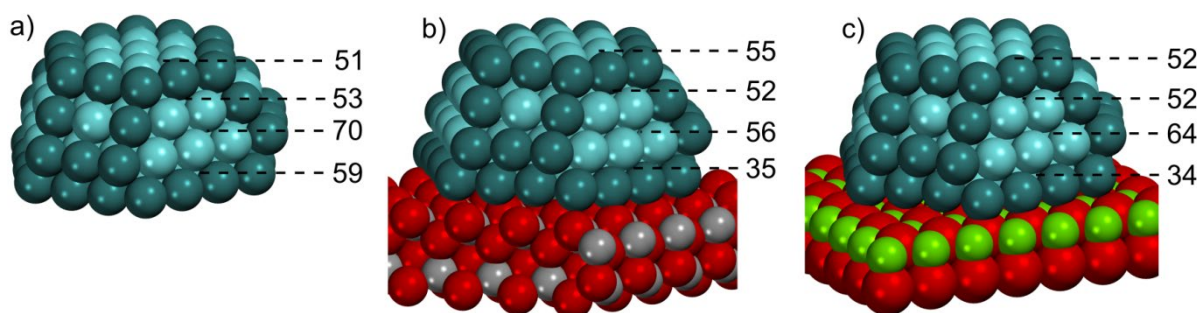


**Figure.** Difference between CO and O adsorption energies  $\Delta E$  (kJ/mol) =  $E_{\text{ads}}(\text{CO}) - E_{\text{ads}}(\text{O})$  on a) unsupported, b) cubic  $\text{ZrO}_2(111)$ -supported and c)  $\text{MgO}(100)$ -supported  $\text{Pd}_{119}$  particles. Smaller  $\Delta E$  values at the perimeter of oxide-supported Pd (due to somewhat stronger O bonding there) explain observed substantially enhanced CO tolerance [13].

### References:

- [1] I.V. Yudanov, K.M. Neyman, N. Rösch et al. Metal nanoparticles as models of single crystal surfaces and supported catalysts: Density functional study of size effects for CO on Pd(111). *J. Chem. Phys.* 117 (2002) 9887.  
 [2] F. Viñes, Y. Lykhach, H.-P. Steinrück, J. Libuda, K.M. Neyman et al. Methane activation by platinum: Critical role of edge and corner sites of metal nanoparticles. *Chem. - Eur. J.* 16 (2010) 6530.

## OP-I-7

- [3] F. Viñes, C. Loschen, F. Illas, K.M. Neyman. Edge sites as a gate for subsurface carbon in palladium nanoparticles. *J. Catal.* 266 (2009) 59.
- [4] K.M. Neyman, S. Schaueremann. Hydrogen diffusion into Pd nanoparticles: Pivotal promotion by carbon. *Angew. Chem. Int. Ed.* 49 (2010) 4743.
- [5] H.A. Aleksandrov, S.M. Kozlov, S. Schaueremann, G.N. Vayssilov, K.M. Neyman. How absorbed hydrogen affects catalytic activity of transition metals. *Angew. Chem. Int. Ed.* 53 (2014) 13371.
- [6] S.M. Kozlov, K.M. Neyman. Insights from CH<sub>4</sub> decomposition on nanostructured Pd. *J. Catal.* 337 (2016) 111.
- [7] S.M. Kozlov, G. Kovács, R. Ferrando, K.M. Neyman. How to determine accurate chemical ordering in several nanometer large bimetallic crystallites from electronic structure calculations. *Chem. Sci.* 6 (2015) 3868.
- [8] G.N. Vayssilov, Y. Lykhach, A. Bruix, F. Illas, K.M. Neyman, J. Libuda et al. Support nanostructure boosts oxygen transfer to catalytically active platinum nanoparticles. *Nature Mater.* 10 (2011) 310.
- [9] S.M. Kozlov, H.A. Aleksandrov, J. Goniakowski, K.M. Neyman. Effect of MgO(100) support on structure and properties of Pd and Pt nanoparticles with 49-155 atoms. *J. Chem. Phys.* 139 (2013) 084701.
- [10] A. Bruix, Y. Lykhach, V. Matolín, J. Libuda, K. M. Neyman et al. Maximum noble metal efficiency in catalytic materials: Atomically dispersed surface platinum. *Angew. Chem. Int. Ed.* 53 (2014) 10525.
- [11] S.M. Kozlov, H.A. Aleksandrov, K.M. Neyman. Energetic stability of absorbed H in Pd and Pt nanoparticles in a more realistic environment. *J. Phys. Chem. C* 119 (2015) 5180.
- [12] Y. Lykhach, S.M. Kozlov, T. Skála, V. Johánek, A. Neitzel, J. Mysliveček, S. Fabris, V. Matolín, K.M. Neyman, J. Libuda et al. Counting electrons on supported nanoparticles. *Nature Mater.* 15 (2016) 284.
- [13] Y. Suchorski, S.M. Kozlov, K.M. Neyman, G. Rupprechter et al. The role of metal/oxide interfaces for long-range metal particle activation during CO oxidation. *Nature Mater.* 17 (2018) 519.

## Theoretical Study of Chemical Ordering in Pd-Au Nanoparticles and Palladium Surface Segregation in Reactive Environment

Mamatkulov M.<sup>1</sup>, Yudanov I.<sup>1,2</sup>, Neyman K.<sup>3,4</sup>

*1 – Boreskov Institute of Catalysis, Novosibirsk, Russia*

*2 – Institute of Chemistry and Chemical Technology SB RAS, Krasnoyarsk, Russia*

*3 – Universitat de Barcelona, Barcelona, Spain*

*4 – Institució Catalana de Recerca i Estudis Avançats, Barcelona, Spain*

*mikhail@catalysis.ru*

Bimetallic nanoparticles (nanoalloys) are of great interest to catalysis research. Adding a second metal to a metallic particle can improve its catalytic efficiency by, among others, synergetic effects. Acting on composition of nanoalloys, it is possible to tune their catalytic activity. Pd-Au nanoalloys are example of systems with such properties: their catalytic activity and selectivity depend on Pd/Au ratio. Furthermore adding palladium to gold increases its melting temperature, this helps to rise longevity of gold-based catalysts. Since the way a catalyst functions is closely related to its structure, knowledge of atomic arrangement is essential for design of nanoalloy-based catalysts. However, determining atomic ordering in nanoalloys is a serious challenge due to the fact that atoms of two species may arrange in many different ways. Additionally, reactive environment may also affect the atomic arrangement. In a recent XPS study of CO oxidation over Pd-Au catalyst it was shown that the catalytic activity depends on temperature: the reaction occurred only at temperature over 150 °C. The authors suggested that this was due to palladium surface segregation induced by CO adsorption [1].

Our goal was to shed light on these results from theoretical point of view. In this work we have studied atomic ordering in Au<sub>145</sub>Pd<sub>56</sub> nanoparticle in vacuum and in the presence of CO molecules. To find an atomic arrangement in nanoparticles, we used recently developed TOP method [2, 3] combining nanoalloys topological description with quantum chemical calculations.

We found that structures close to global energy minimum possess two features: *i)* Au atoms are preferentially localised on the surface of the nanoparticle, *ii)* in the core of the nanoparticle Au and Pd atoms tend to mix. The energy of palladium segregation towards the nanoalloy surface was calculated. We found that structures with palladium atoms occupying surface centers become favorable in the presence of adsorbed CO molecules due to strong interaction of CO molecules with palladium atoms, indicating that reactive environment may favor palladium segregation towards the surface. Furthermore, we were able to estimate the energy cost of palladium segregation for a nanoparticle composed of 1289 atoms whose diameter is close to those of experimentally observed nanoparticles.

The results of our calculations are consistent with experiments on carbon monoxide oxidation in the presence of Pd-Au nanoalloy [4].

## OP-I-8

**Acknowledgement.** Calculations were performed using equipment of Siberian Supercomputer Center of Russian academy of Sciences, HPC computing resources at Lomonosov Moscow State University [5] and Red Española de Supercomputación.

### References:

- [1] Bukhtiyarov, A. V.; Prosvirin, I. P.; Saraev, A. A.; Klyushin, A. Y.; Knop-Gericke, A.; Bukhtiyarov, V. I. In situ formation of the active sites in Pd–Au bimetallic nanocatalysts for CO oxidation: NAP (near ambient pressure) XPS and MS study. *Faraday Discuss.* 2018, 208, 255-268.
- [2] Kozlov, S. M.; Kovács, G.; Ferrando, R.; Neyman, K. M. How to determine accurate chemical ordering in several nanometer large bimetallic crystallites from electronic structure calculations. *Chemical Science* 2015, 6, 3868—3880.
- [3] Kovács, G.; Kozlov, S. M.; Neyman, K. M. Versatile Optimization of Chemical Ordering in Bimetallic Nanoparticles. *The Journal of Physical Chemistry C* 2017, 121, 10803—10808.
- [4] Mamatkulov M.; Yudanov I.; Bukhtiyarov A.; Prosvirin I.; Bukhtiyarov V. and Neyman K. Pd Segregation on the Surface of Bimetallic PdAu Nanoparticles Induced by Low Coverage of Adsorbed CO. *The Journal of Physical Chemistry C* 2018, DOI: 10.1021/acs.jpcc.8b07402.
- [5] V. Sadovnichy, A. Tikhonravov, Vl. Voevodin, and V. Opanasenko "Lomonosov": Supercomputing at Moscow State University. In *Contemporary High Performance Computing: From Petascale toward Exascale* (Chapman & Hall/CRC Computational Science), pp.283-307, Boca Raton, USA, CRC Press, 2013.

## Structure, Stability and Catalytic Properties of Gold Protected Nanoclusters from DFT Calculation

Pichugina D.A., Nikitina N.A., Kuz'menko N.E.

*Department of Chemistry, M.V. Lomonosov Moscow State University, Moscow, Russia  
daria@phys.chem.msu.ru*

Protected gold nanoclusters are popular objects due to beneficial applications in heterogeneous catalysis. In spite of properties of atomic gold clusters have been study extensively, some points have remained under debate including (i) structure change of protected clusters after deposition on support, (ii) mechanism of small molecules activation on protected clusters, and (iii) ligand effect on the cluster activity and stability in solution or on support. These points and others will be discussed during the presentation. It will be shown that quantum chemical simulation of any processes involving gold nanoclusters has great prospect and provides new thermodynamic and kinetic data, as well as theoretical information concerning the ligand effect and the mechanism of reactions involving metal nanoparticles at atomic level.

The structures of  $\text{Au}_{20}(\text{SR})_{16-y}$  ( $\text{R}=\text{CH}_3, \text{Ph}$ ;  $y=0, 1, 2, 3$ ) were studied in gas phase and on  $\text{CeO}_x$  surface using DFT. Due to Au-S bonds are strong, cluster's activation by removing of one, two or three ligands were taken into account. The  $\text{O}_2$  and CO adsorption on the clusters, and further CO oxidation was simulated to understand the active site of supported gold nanoparticles in oxidation catalytic reactions. The structure and energies of five  $\text{Au}_{20}(\text{SR})_{16}$  isomers have been calculated. The most stable one corresponds to X-ray structure. The Au7 cluster's core consists of two tetrahedrons united by a common vertex; it is protected by an octameric ring, one triple and two monomeric staple motifs  $\text{SR}(\text{AuSR})_x$ . The interaction of  $\text{Au}_{20}(\text{SCH}_3)_{16}$  with regular  $\text{CeO}_2$  is weak. One, two, and three  $\text{SCH}_3$  groups of the protected cluster were removed to obtain  $\text{Au}_{20}(\text{SR})_{16-y}$ , which is a model of the cluster with broken ligand shell. The calculation reveals the formation of different catalytic sites, when  $\text{SCH}_3$  ligands are removed.

The  $\text{O}_2$  and CO activation on  $\text{Au}_{20}(\text{SR})_{16-y}$ ,  $\text{Au}_{20}(\text{SR})_{16-y}/\text{CeO}_x$  was simulated. According to calculation, oxygen can dissociate on  $\text{Au}_{20}(\text{SR})_{14}/\text{CeO}_x$ . It is activated in super-oxide state on clusters without one and three  $\text{SCH}_3$  ligands. Various scenarios of CO oxidation on protected Au clusters are considered. According to calculation cluster can be a catalyst in CO oxidation. It should be mentioned that the calculated activation energies of the corresponding steps of CO oxidation on the cluster's fragments ( $\text{Au}_2(\text{SR})_3$ ,  $(\text{AuSR})_4$ ,  $\text{Au}(\text{AuSR})_4$ ) are less than on the clusters. So, the atomic fragments of the ligand-protected gold clusters can be involved in catalytic reactions.

**Acknowledgement.** This work was supported by the Russian Science Foundation, grant 17-03-00962.

## Self-Sustained Oscillations in Oxidation of CH<sub>4</sub>, C<sub>2</sub>H<sub>6</sub> and C<sub>3</sub>H<sub>8</sub> over Metallic Catalysts: Mathematical Modelling Using the Quasi-Steady-State Approximations

Lashina E.A.<sup>1,3</sup>, Chumakova N.A.<sup>1,3</sup>, Chumakov G.A.<sup>2,3</sup>, Kaichev V.V.<sup>1,3</sup>

*1 – Boreskov Institute of Catalysis, Novosibirsk, Russia*

*2 – Sobolev Institute of Mathematics SB RAS, Novosibirsk, Russia*

*3 – Novosibirsk State University, Novosibirsk, Russia*

*lashina@catalysis.ru*

Self-sustained reaction-rate oscillations in various heterogeneous catalytic reactions have been actively studied for many years. For the first time, the oscillations were observed in the catalytic oxidation of CO on Pt-based catalysts at atmospheric pressure more than 40 years ago. Afterwards, the oscillations have been also discovered in other catalytic reactions such as the oxidation of H<sub>2</sub>, the oxidation of organic compounds, the hydrogenation of CO and hydrocarbons, NO reduction, N<sub>2</sub>O decomposition, etc. [1,2]. Numerous theoretical and experimental studies have been devoted to the investigation of reaction-rate oscillations and several oscillatory mechanisms were developed. However, it should be noted that mainly self-sustained oscillations in the oxidation of CO over Pt- and Pd-based catalysts were studied. This is a simple reaction and the reaction mechanism contains several elementary steps only. From this point of view the oscillatory mechanisms cannot be applied directly to the oxidation of light alkanes over transition metals. For example, the microkinetics scheme of the methane oxidation contained 18 steps [3,4], and more simple oscillatory mechanisms should be developed.

Experimentally, the self-sustained oscillations were observed in the catalytic oxidation of light hydrocarbons (methane, ethane, propane, etc.) over Ni, Pd, Co, Pt, and Ru. This is relaxation-type oscillations which can be described as fast evolution (jump up and jump down) between “low-active” and “high-active” states. The period of oscillations varied from several to tens of minutes, the main products are CO, CO<sub>2</sub>, H<sub>2</sub>, and H<sub>2</sub>O. The oscillations of products and reagents in the gas phase are accompanied with oscillations in the catalyst temperature and the reversible oxidation of the catalyst surface is observed [5-7]. The mechanisms of these reactions contain the numbers of steps and intermediates. For example, the oxidation of ethane is described by 36 elementary reactions [8]. It is very complicated to analyse corresponding kinetic models and find the values of the parameters, at which the limit cycle exists in the model. To describe the oscillatory dynamics we consider the quasi-steady-state approach, which help us to simplify the model. The simplified model is the system of two or three differential equations, studied numerically and using the methods of qualitative theory of dynamical systems.

## OP-I-10

In our previous work [3] we considered the kinetic model, predicted the isothermal oscillations in the oxidation of methane over Ni. Considering the quasi-steady-state approximations we showed that in some neighbourhood of the limit cycle the reaction mechanism and the kinetic model can be simplified. The resulted kinetic model is the system of only three ordinary differential equations [4]. This approach we also used to describe the self-sustained oscillations in the oxidation of ethane and propane over Ni. Using the quasi-steady-state approximations allowed us to significantly reduce the number of differential equations in the kinetic model. Taking into account both initial and simplified kinetic models we developed the mathematical models, described dynamics of the partial pressures as well as the catalyst temperature in CSTR reactor. The results of mathematic modelling of the oscillatory behaviour in the oxidation of propane over Ni are presented in Fig. 1. We believe that this approach can be used in the study of the self-sustained oscillations in the oxidation of the light hydrocarbons over other transitional metals including Pt and Pd.

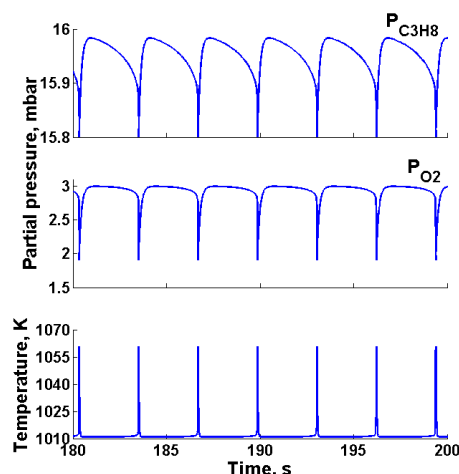


Fig. 1. Self-sustained oscillations in the oxidation of  $C_3H_8$  by  $O_2$  over Ni.

**Acknowledgement.** This work was supported by the RFBR, grant 19-03-00419.

### References:

- [1] G. Ertl. *Adv. Catal.* 37 (1990) 213.
- [2] M.M. Slinko, N.I. Jaeger. *Stud. Surf. Sci. Catal.* 86 (1994) 1.
- [3] E.A. Lashina, V.V. Kaichev, N.A. Chumakova, G.A. Chumakov, V.I. Bukhtiyarov. *Kin. Catal.* 53 (2012) 374-383.
- [4] E.A. Lashina, V.V. Kaichev, A.A. Saraev, Z.S. Vinokurov, N.A. Chumakova, G.A. Chumakov, V.I. Bukhtiyarov. *J. Phys. Chem. A* 121 (2017) 6874-6886.
- [5] V.V. Kaichev, D. Teschner, A.A. Saraev, et al. *J. Catal.* 334 (2016) 23-33.
- [6] V.V. Kaichev, A.A. Saraev, A.Yu. Gladky, I.P. Prosvirin, A. Knop-Gerike, V.I. Bukhtiyarov. *Catal. Lett.* 149 (2019) 313-321.
- [7] A.A. Saraev, Z.S. Vinokurov, V.V. Kaichev, A.N. Shmakov, V.I. Bukhtiyarov. *Catal. Sci. Technol.* 7 (2017) 1646-1649.
- [8] V.V. Ustyugov, V.V. Kaichev, E.A. Lashina, N.A. Chumakova, V.I. Bukhtiyarov. *Kin. Catal.* 57 (2016) 113-124.

## Spatial and Temporal Self-Organization during CO Oxidation over Ni

Makeev A.G., Peskov N.V., Slinko M.M., Bychkov V.Yu., Haritonov V.A., Korchak V.N.  
*Semenov Institute of Chemical Physics RAS, Moscow, Russia*  
*Faculty of Comput. Math. and Cybernet., Lomonosov Moscow State University, Moscow,*  
*Russia*  
*slinko@polymer.chph.ras.ru*

CO oxidation on transition-metal surfaces is one of the most extensively studied reactions because of its technological importance. This work is devoted to the study of the dynamic behaviour of CO oxidation over a Ni foil using on-line mass-spectrometry and visual observations of a catalyst surface. Over Ni the oscillatory behaviour was discovered only in CO excess [1] in contradiction with the oscillations during CO oxidation over Pt-group metals, which were observed in oxygen excess. The typical example of the oscillatory behaviour, observed during CO oxidation over the Ni foil is shown below. It can be seen, that CO<sub>2</sub> and temperature oscillate in phase with similar waveforms, while CO and O<sub>2</sub> produce out-of-phase oscillations with CO<sub>2</sub> and temperature.

The periodic deviation of oxygen imbalance together with the variations of catalyst colour changes indicated that the reversible oxidation of Ni to NiO occurred during the oscillations. Moreover the oscillations were accompanied by the distinct pattern formation. A series of photos show the movement of the dark boundary (the oxidation wave) from the top to the bottom of the foil coinciding with the direction of the gas flow in the reactor at 570 °C. During the oxidation process the activity of the catalyst is gradually decreasing. The wave of NiO reduction propagates from downstream to the uppermost part of the foil and causes the increase of the catalyst activity. The propagation rate of the oxidation wave is nearly 10 times lower than the rate of the reduction wave. Moreover, the reduction wave propagation rate tends to increase with temperature, while the front forward motion of the oxidation wave decreases with the temperature increase.

Mathematical modelling of the observed experimental data will be presented. It was shown that to obtain oscillations during CO oxidation under reducing conditions the kinetics of CO precursor-mediated adsorption must be included. Simulated oscillations occur due to periodic formation and reduction of the surface oxide. The introduction of the possibility of oxygen diffusion into the subsurface layer and formation of the subsurface oxygen allows mathematical modelling of the variation of Ni colour changes and wave phenomena during oscillating CO oxidation observed experimentally.

## OP-I-11

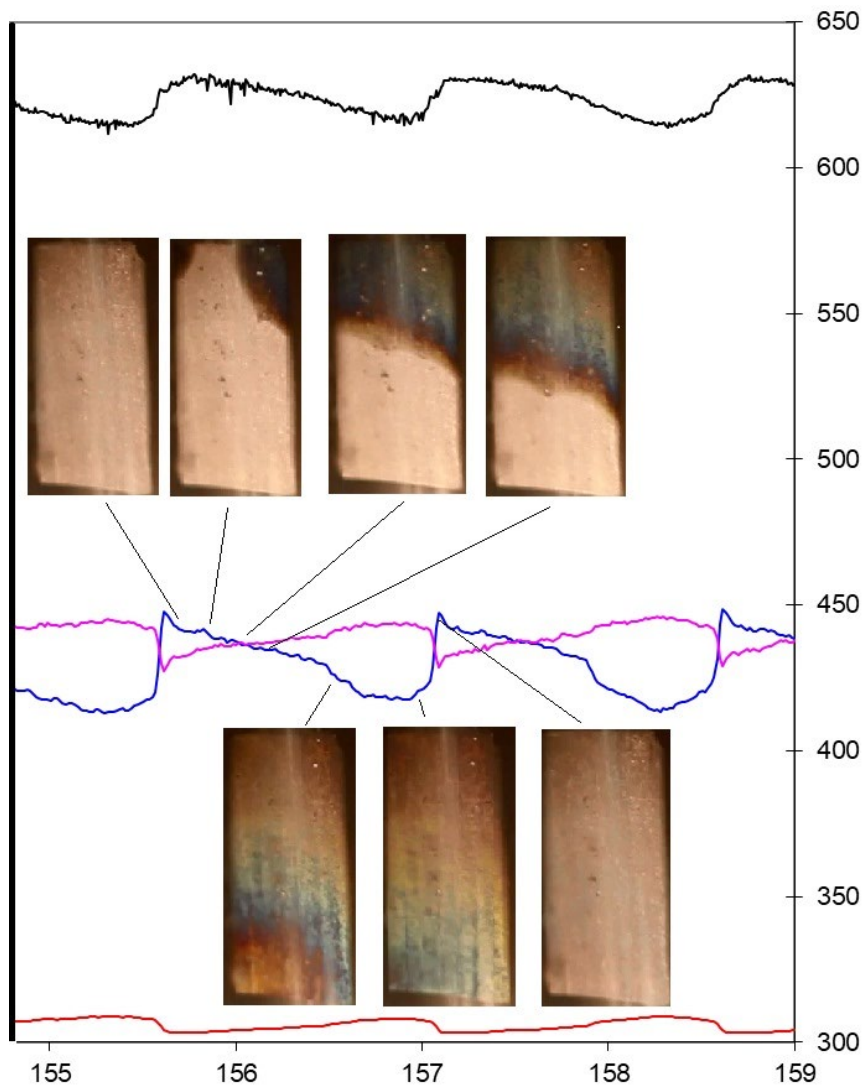


Fig.1

**Acknowledgement.** This work was supported by the Russian Science Foundation (grant N 17-13-01057).

### References:

[1] Bychkov, V. Yu.; Tulenin, Yu. P.; Slinko, M. M.; Gordienko, Yu. A.; Korchak, V. N. New Oscillating System: CO Oxidation over Ni. *Catal. Lett.* 2018, 148, 653-659.

### The Potential of Time-Resolved Operando UV-Vis Spectroscopy for Deriving Insights into Coke Formation and Removal in Propane Dehydrogenation

Zhang Ya.<sup>1,2</sup>, Otroshchenko T.<sup>1</sup>, Han Sh.<sup>1,2</sup>, Rodemerck U.<sup>1</sup>, Linke D. <sup>1</sup>, Jiang G.<sup>2</sup>,  
Kondratenko E.V.<sup>1</sup>

1 – Leibniz-Institut für Katalyse e.V. an der Universität Rostock, Rostock, Germany

2 – State Key Laboratory of Heavy Oil Processing, China University of Petroleum Beijing,  
Beijing, China

*evgenii.kondratenko@catalysis.de*

Propylene is an important building block of the chemical industry and finds its application in production of polymers, fibres, resins and solvents. To fill the supply gap for this olefin, non-oxidative dehydrogenation (DH) of propane has been commercialized [1]. Although the applied catalysts with supported Pt or CrO<sub>x</sub> species are highly active and selective, there are a number of issues associated with their usage, which are high price of the noble metal and toxicity of Cr(VI)-based compounds. Against this background, we focused on the development of alternative catalysts free of such limitations. Recently, we have introduced a concept for preparation of alternative-type catalysts that explores the idea of using lattice defects in ZrO<sub>2</sub>[2-5]. Structural defects, i.e. Zr<sub>cus</sub> (cus means coordinatively unsaturated) cations, were identified to be the PDH active sites. In addition to identifying the kind of active sites, we also focus on understanding factors affecting coke deposition, which is one of the major problems in the PDH reaction. The present contribution will demonstrate the potential of time-resolved operando UV-Vis spectroscopic experiments combined with steady-state catalytic tests and ex situ temperature-programed oxidation of spent catalysts for deriving mechanistic and kinetic insights into coke formation and oxidation in the course of the PDH reaction.

**Acknowledgement.** Financial support by Deutsche Forschungsgemeinschaft (KO 2261/8-1), National Natural Science Foundation of China (Grants 21878331, 91645108, U1162117), Science Foundation of China University of Petroleum, Beijing (C201604) and the State of Mecklenburg-Vorpommern are gratefully acknowledged.

#### References:

- [1] J.J.H.B. Sattler, J. Ruiz-Martinez, E. Santillan-Jimenez, B.M. Weckhuysen, *Chem Rev*, 114 (2014) 1061.
- [2] T. Otroshchenko, S. Sokolov, M. Stoyanova, V.A. Kondratenko, U. Rodemerck, D. Linke, E.V. Kondratenko, *Angew. Chem. Int. Ed.*, 54 (2015) 15880.
- [3] T. Otroshchenko, V. A. Kondratenko, U. Rodemerck, D. Linke, E. V. Kondratenko, *J. Catal.* 348 (2017) 282.
- [4] Y. Zhang, Y. Zhao, T. Otroshchenko, H. Lund, M.-M. Pohl, U. Rodemerck, D. Linke, H. Jiao, G. Jiang, E.V. Kondratenko, *Nature Communications*, 9:3794, DOI: 10.1038/s41467-018-06174-5.
- [5] Y. Zhang, Y. Zhao, T. Otroshchenko, Sh. Han, H. Lund, U. Rodemerck, D. Linke, H. Jiao, G. Jiang, E.V. Kondratenko, *J. Catalysis*, 371 (2019) 313

## Impact of V and M on Mechanism and Performance of V/Ce<sub>1-x</sub>M<sub>x</sub>O<sub>2-δ</sub> (M=Fe, Bi, Sb) Catalysts in NH<sub>3</sub>-SCR of NO<sub>x</sub> Assessed by *Operando* Spectroscopy

Keller S., Rabeah J., Bentrup U., Brückner A.

Leibniz-Institut für Katalyse an der Universität Rostock (LIKAT), Rostock, Germany

Sonja.Keller@catalysis.de

Vanadia-containing catalysts with ceria-based supports belong to the most efficient materials for the selective catalytic reduction of NO<sub>x</sub> by NH<sub>3</sub> at low temperature. Thus, we could obtain almost complete NO<sub>x</sub> conversion and N<sub>2</sub> selectivity at T ≤ 200°C at high flow rates with series of V/Ce<sub>1-x</sub>M<sub>x</sub>O<sub>2-δ</sub> (M = Zr, Ti, Mn) catalysts in which isovalent M<sup>4+</sup> ions form solid solutions with CeO<sub>2</sub> by replacing Ce<sup>4+</sup> in its lattice sites [1-2]. The high activity has been related to the unique oxygen transport ability of such Ce<sub>1-x</sub>M<sub>x</sub>O<sub>2-δ</sub> solid solutions which was shown to govern the redox activity of the highly dispersed VO<sub>x</sub> species deposited on their surface. It is the aim of this work to test the influence of trivalent ions such as Fe<sup>3+</sup>, Bi<sup>3+</sup> or Sb<sup>3+</sup> to prepare Ce<sub>1-x</sub>M<sub>x</sub>O<sub>2-δ</sub> supports, since this creates O vacancies expected to promote oxygen transport and storage capacity even more than with M<sup>4+</sup> ions. Moreover, the different ionic radii and reduction potentials of these M<sup>3+</sup> ions should have an additional impact on the performance of the corresponding V/Ce<sub>1-x</sub>M<sub>x</sub>O<sub>2-δ</sub> catalysts. For mechanistic investigations, DRIFT, EPR, and XANES/EXAFS spectroscopy were applied in *operando* or *in situ* mode, besides different *ex situ* characterization methods (Raman, XRD, XPS).

Ce<sub>1-x</sub>M<sub>x</sub>O<sub>2-δ</sub> samples (x = 0.01; 0.03; 0.05, M = Fe; Sb; Bi) were prepared by co-precipitation and subsequently impregnated with 5 wt.% V<sub>2</sub>O<sub>5</sub>. Catalytic tests were performed in a fixed-bed quartz flow reactor from 100 to 300°C with a feed consisting of 0.1% NH<sub>3</sub>, 0.1% NO, 5% O<sub>2</sub>/He and a GHSV of 70 000 h<sup>-1</sup>. *Operando* DRIFTS measurements were performed at 200°C using a commercial Harrick-cell connected to a mass spectrometer for product analysis. *Operando* EPR spectra were recorded in X-band using a homemade flow reactor connected to a gas dosing device and a mass spectrometer.

Introduction of Fe or Sb improved the performance of the V-free supports while Bi has a detrimental effect (Fig. 1a). In general, deposition of surface VO<sub>x</sub> improved the catalytic performance of all V/Ce<sub>1-x</sub>M<sub>x</sub>O<sub>2-δ</sub> catalysts in comparison to the corresponding bare supports. However, only in the case of V/Ce<sub>1-x</sub>Sb<sub>x</sub>O<sub>2-δ</sub> higher activity than with V/CeO<sub>2</sub> was obtained, while Fe and Bi in V/Ce<sub>1-x</sub>M<sub>x</sub>O<sub>2-δ</sub> had a detrimental effect.

On V-free supports, the SCR reaction follows a Langmuir-Hinshelwood-mechanism in which NO<sub>x</sub> is adsorbed as surface nitrates (NO<sub>y</sub>) which are reduced by gaseous NH<sub>3</sub>. Therefore, the ability to form reducible NO<sub>y</sub> species is related to catalytic activity. *Operando* DRIFTS experiments showed a facilitated reduction of adsorbed NO<sub>y</sub> in particular on Fe-doped catalysts (Fig. 1b), while bismuth doping hinders this ability. Therefore, increased activity of

## OP-II-2

iron-doped ceria is due to iron acting as an active centre itself by the  $\text{Fe}^{3+}/\text{Fe}^{2+}$  redox swing, as well as providing active surface oxygen to the reaction site.

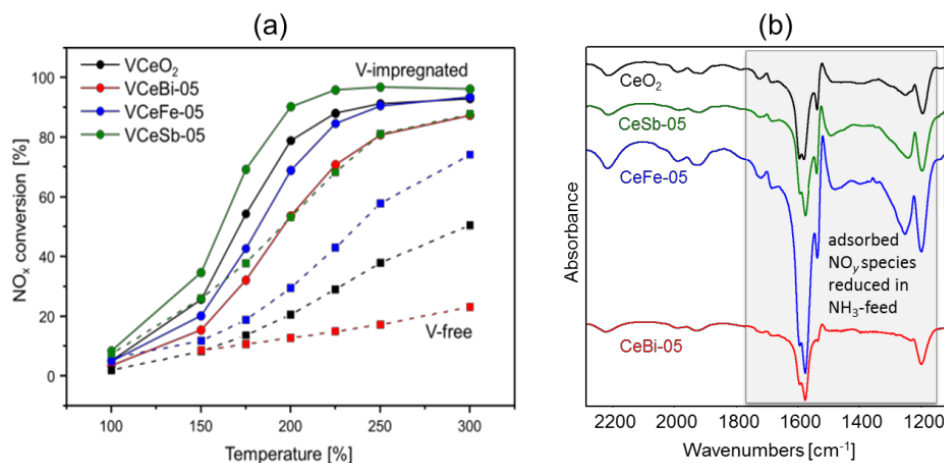


**Figure 1: NO<sub>x</sub> conversion of supports and V-impregnated catalysts (a) and subtracted DRIFT spectra (b) showing the effect of dopants on the reduction of adsorbed NO<sub>y</sub> by ammonia.**

The effect of the dopant on the catalytically important  $\text{V}^{5+}/\text{V}^{4+}$  swing was studied by *operando* EPR spectroscopy. The amount of  $\text{V}^{4+}$  formed in reaction feed was not affected by bismuth-doping, however, introducing antimony leads to a decrease in detectable  $\text{V}^{4+}$ . This is due to close contact of V and Sb and thereby antimony facilitates the reoxidation of  $\text{V}^{4+}$  to  $\text{V}^{5+}$ . In iron-doped samples,  $\text{V}^{4+}$  was detected, however due to the superposition of the  $\text{V}^{4+}$  with the  $\text{Fe}^{3+}$  signal the amount of  $\text{V}^{4+}$  is not quantifiable. During exposure to the reaction feed, the reduction of  $\text{Fe}^{3+}$  to  $\text{Fe}^{2+}$  was detected, which is further facilitated by contact between Fe and V. Therefore we propose, that close proximity of V and Fe leads to preferentially reducing  $\text{Fe}^{3+}$  and not  $\text{V}^{5+}$ , thereby decreasing catalytic activity.

Although for all dopants the formation of solid solutions with ceria was found, the effects in terms of OSC are different. Bi doping leads to an increase of oxygen vacancies, which is not accompanied by an increase of active surface oxygen, most probably due to the similar ionic radii of  $\text{Bi}^{3+}$  and  $\text{Ce}^{3+}$ . Here, static disorder is favoured, diminishing OSC and therefore reactivity. Iron increases the catalytic activity of the pure support significantly by increasing the OSC and acting as catalytic active centre itself. However, this beneficial effect is suppressed when the catalyst is impregnated with  $\text{VO}_x$ . Antimony increases the catalytic activity by impacting the catalytic cycle of vanadium. Close contact of Sb and V diminishes the amount of  $\text{V}^{4+}$  under reaction conditions, implying the facilitated reoxidation to  $\text{V}^{5+}$ .

**Acknowledgement.** This work was supported by the DFG, Project No. BR 1380/18-2.

### References:

- [1] T.H. Vuong, J. Radnik, E. Kondratenko, M. Schneider, U. Armbruster, A. Brückner, Appl. Catal., B 197 (2016) 159.
- [2] T.H. Vuong, S. Bartling, U. Bentrup, H. Lund, J. Rabeah, H. Atia, U. Armbruster, A. Brückner, Catal. Sci. Technol. 24 (2018) 6360.

## Dehydrogenation of Propane over Vanadia-Titania Catalysts: Active Sites and Reaction Mechanism

Kaichev V.V.<sup>1,2</sup>, Chesalov Yu.A.<sup>1,2</sup>, Saraev A.A.<sup>1,2</sup>, Tsapina A.M.<sup>1</sup>

*1 – Boreskov Institute of Catalysis, Novosibirsk, Russia*

*2 – Novosibirsk State University, Novosibirsk, Russia*

*vvk@catalysis.ru*

The oxidative and non-oxidative dehydrogenation of propane over a monolayer  $V_2O_5/TiO_2$  catalyst was examined using in situ Fourier-transform infrared spectroscopy (FTIR) and pseudo in situ X-ray photoelectron spectroscopy (XPS). According to FTIR, the catalyst surface contains isopropoxide, acetone, formate, acetate, and carbonate species in both cases. The fresh calcined catalyst contains vanadium in the  $V^{5+}$  state; however, its treatment in the propane flow leads to the reduction of  $V^{5+}$  to  $V^{3+}$ . Simultaneously, the catalyst treatment in propane leads to the formation of Ti–O–H groups, the removal of vanadyl oxygen species, and accumulation of carbonaceous deposits. Besides, XPS data indicate that the reduction of catalyst is accompanied by reversible destruction of the vanadia monolayer and formation of 3D clusters or nanoparticles on the titania surface, which leads to catalyst deactivation. In contrast, under the action of a propane/oxygen mixture flow, the accumulation of carbonaceous deposits and the destruction of the vanadia monolayer do not proceed;  $V^{5+}$  cations are partially reduced to  $V^{4+}$ . We suggest that the oxidative dehydrogenation of propane to propylene over vanadium oxide-based catalysts proceeds via the redox mechanism, where the oxidized catalyst surface oxidizes propane and is reoxidized by gas-phase oxygen. The active sites contain  $V^{5+}$  cations, and the C–H bond of propane is activated mainly on the vanadyl oxygen species. The key intermediate is isopropoxide, which can transform to propylene or acetone. Adsorbed acetone is unstable and is oxidized further to formate and acetate species, which could be oxidized to CO and  $CO_2$ . In contrast, the non-oxidative dehydrogenation of propane proceeds over the reduced catalyst. In this case, active sites contain coordinatively unsaturated  $V^{3+}$  cations. The mechanisms of both reactions are discussed.

## Enhancing Catalytic Activity of Perovskites by Tailored Exsolution

Rameshan R.<sup>1</sup>, Lindenthal L.<sup>1</sup>, Ruh T.<sup>1</sup>, Raschhofer<sup>1</sup>, Nening A.<sup>2</sup>, Opitz A.<sup>2</sup>, Rameshan C.<sup>1</sup>

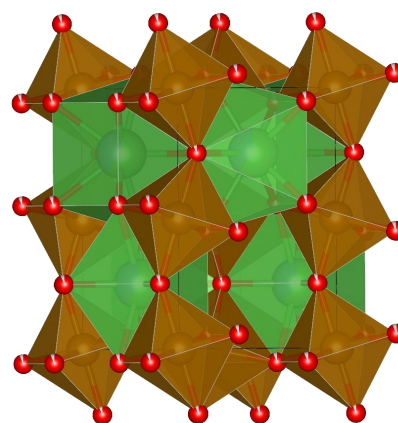
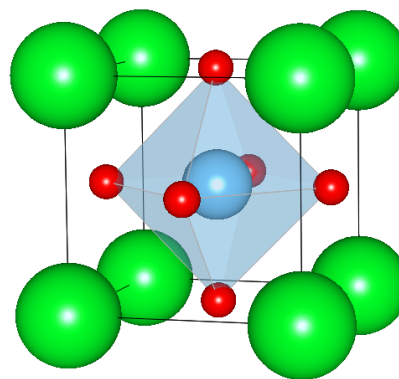
1 – Technische Universität Wien, Institute of Materials Chemistry, Vienna, Austria

2 – Technische Universität Wien, Institute of Chemical Technologies and Analytics, Vienna, Austria

raffael.rameshan@tuwien.ac.at

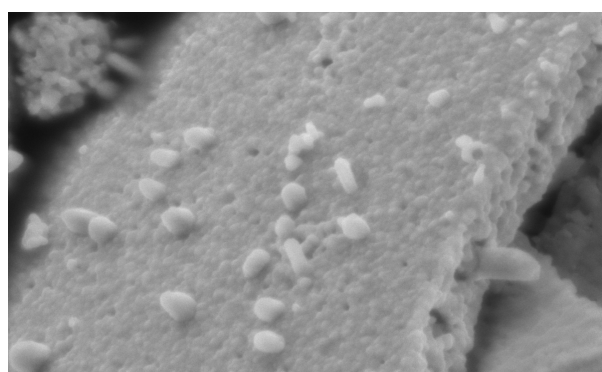
Perovskites provide a dynamic structure, where induced oxygen vacancies can trigger the formation of nanoparticles on the surface. The process of nanoparticle formation can thus be controlled and reversed by choosing a suitable chemical potential of the gas phase or by polarization (i.e. applying voltage to the system) of the perovskite.

Using a lab-based near ambient pressure X-ray photoelectron spectrometer (NAP-XPS) that is specially designed for investigations of electro-catalytic systems under realistic operating conditions combined with in-situ X-ray diffraction spectroscopy (XRD), scanning electron microscopy (SEM) and energy dispersive X-ray spectroscopy (EDX) we provide first results on the effect of exsolution on water gas shift (WGS) and reverse WGS reaction.



**Figures: Top:** Perovskite structure. **Middle:** Rietveld refinement of XRD data supported by DFT. Figures were generated by VESTA [1]. **Bottom:** Exsolved Particles on Nd<sub>0.9</sub>Ca<sub>0.1</sub>FeO<sub>3</sub>

**Acknowledgement.** This work has received funding from the European Research Council (ERC) under the European Union's Horizon 2020 research and innovation programme (grant agreement n° 755744 / ERC - Starting Grant TUCAS).



### References:

[1] Momma, Koichi, and Fujio Izumi. "VESTA 3 for three-dimensional visualization of crystal, volumetric and morphology data." *Journal of applied crystallography* 44.6 (2011): 1272-1276.

**Bi-Modified MoVNbTeO Catalysts for Oxidative Dehydrogenation of Ethane:  
NAP-XPS and In Situ XRD Study**

Svintsitskiy D.A.<sup>1,2</sup>, Kardash T.Yu.<sup>1,2</sup>, Lazareva E.V.<sup>1</sup>, Saraev A.A.<sup>1</sup>, Derevyannikova E.A.<sup>1</sup>,  
Vorokhta M.<sup>3</sup>, Šmíd B.<sup>3</sup>, Bondareva V.M.<sup>1</sup>

*1 – Boreskov Institute of Catalysis, Novosibirsk, Russia*

*2 – Novosibirsk State University, Novosibirsk, Russia*

*3 – Charles University, Department of Surface and Plasma Science, Faculty of Mathematics  
and Physics, Prague, Czech Republic  
sad@catalysis.ru*

The development of novel technologies for oxidative dehydrogenation of cheap and widely available light C<sub>2</sub>-C<sub>3</sub> alkanes is great challenge in terms of cooperation between industry and scientific community. The one of most effective catalysts for C<sub>2</sub>-C<sub>3</sub> hydrocarbons transformation are Mo-V-Nb-Te oxide compositions [1,2].

It was established that the modification of MoVNbTeO mixed oxide by Bi resulted in the improvement of its catalytic properties in oxidative dehydrogenation of ethane (ODE). The investigation of Bi-modified MoVNbTeO catalysts was carried out with the purpose to establish the influence of introduced Bi on the surface dynamics and structural features of MoVNbTeO catalysts under reducing ODE conditions (C<sub>2</sub>H<sub>6</sub>/O<sub>2</sub> > 1). The application of NAP-XPS and in situ XRD methods provided the reliable experimental data about surface and bulk transformations, respectively.

NAP-XPS study showed that Bi-modified catalysts were characterized by enhanced surface/subsurface Te concentration under reducing ODE conditions while compared with unmodified catalyst. EXAFS spectroscopy revealed that the local environment of Bi within MoVNbTeO particles corresponded to positions within extended six-membered channels of the M1 structure, which are similar to Te sites. The increase in the temperature of M1 phase destruction in ethane flow for Bi-modified catalysts was revealed using in situ XRD. The crystal lattice of the modified M1 phase did not undergo compression along the c-axis during heating in C<sub>2</sub>H<sub>6</sub>/He flow, in contrast to the unmodified catalyst, indicating the influence of Bi on Te mobility within the extended channels of the M1 structure.

Incorporation of Bi caused the limitation of Te mobility within channels, preventing its reduction and removal resulting in a significant decrease in the degree of deactivation for Bi-modified ODE catalysts at high temperature under reducing ODE conditions

**Acknowledgement.** This work was supported by the Russian Science Foundation, grant 17-73-20073. The authors acknowledge the CERIC-ERIC Consortium for the access to experimental facilities.

**References:**

[1] J. M. Lopez Nieto, *Top. Catal.* 41 (2006) 3–15.

[2] R.K. Grasselli, C.G. Lugmair, A.F. Volpe Jr, *Top. Catal.* 50 (2008) 66–73.

**Determination of Active Species in Pd Catalysts by Time-Resolved X-ray Absorption Spectroscopy**

Bugaev A.L.<sup>1</sup>, Guda A.A.<sup>1</sup>, Lomachenko K.A.<sup>2</sup>, Usoltsev O.A.<sup>1</sup>, Skorynina A.A.<sup>1</sup>, Groppo E.<sup>3</sup>,  
Safonova O.<sup>4</sup>, van Bokhoven J.<sup>4</sup>

*1 – The Smart Materials Research Institute, Southern Federal University, Rostov-on-Don, Russia*

*2 – European Synchrotron Radiation Facility, Grenoble, France*

*3 – University of Turin, Turin, Italy*

*4 – Paul Scherrer Institute, Villigen, Switzerland*

*abugaev@sfedu.ru*

Time-resolved X-ray absorption spectroscopy (XAS) provides a unique opportunity to determine the structure of short-living active states and discriminate them from spectator species. In this work, two recent successful examples of time-resolved operando XAS application to industrial palladium catalysts are summarized.

Formation of hydride and carbide phases in palladium nanoparticles (NPs) during hydrogenation of hydrocarbons is a critical process that governs catalytic activity and selectivity in hydrogenation reactions. To highlight the role of each of these phases, we designed an experiment where the two reagents, hydrogen and ethylene, were never directly mixed together but were fluxed through the catalysts alternatively. Although avoiding direct mixing of the reactants, such setup allowed reaction to proceed via two mechanisms: (i) hydrogenation of ethylene molecules adsorbed on the surface of Pd NPs using hydrogen from the gas phase, and (ii) hydrogenation of ethylene from the gas phase using hydrogen atoms accumulated in the bulk of NPs. The atomic structure of Pd NPs were monitored by XAS spectra collected with 0.5 s time resolution at SuperXAS beamline of SLS. The observed results are staggering: the amount of ethane produced during the switch of the flow from hydrogen to ethylene was unexpectedly decreasing with the increase of temperature. This fact was explained by analysis of XAS spectra, which evidenced that the amount of hydride phase is much less at high temperatures than at lower ones, proving the involvement of bulk dissolved hydrogen in the hydrogenation reaction. For the opposite direction of the switch (from ethylene to hydrogen), the amount of the formed ethane was almost independent on the temperature, explained by the fact that the number of surface adsorbed ethylene molecules is determined by the surface area of the catalyst and do not change with temperature, which was also proved by XAS data.

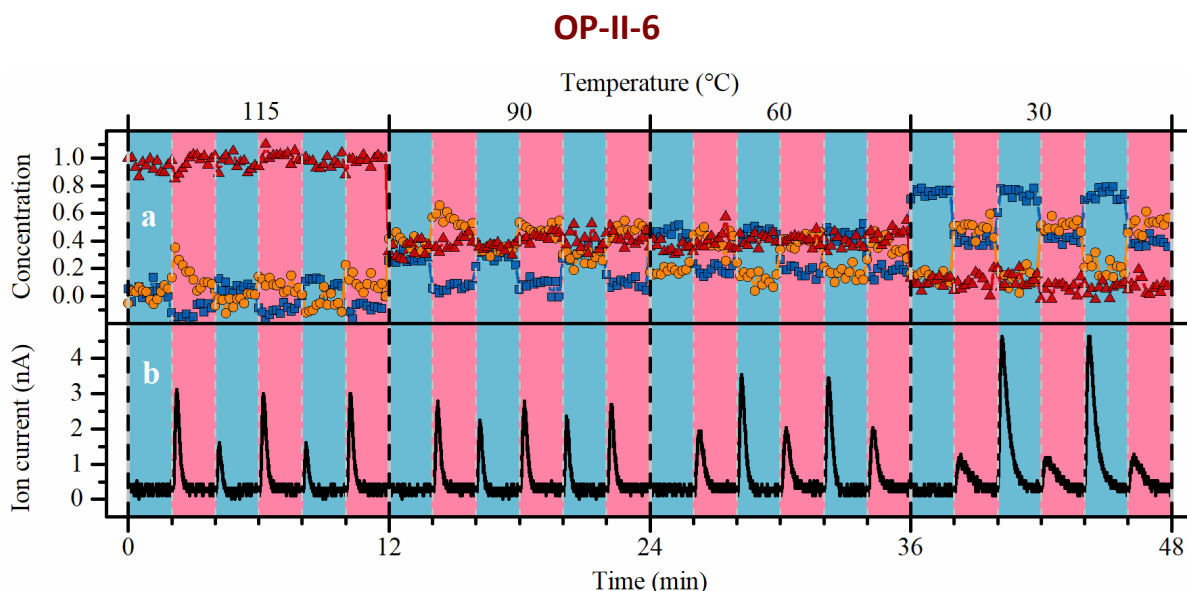


Figure 1. Time- and temperature-evolution of mixed hydride (blue squares), surface carbide (orange circles) and bulk carbide (red triangles) components determined from XANES (a) and  $m/Z = 30$  signal of ethane (b). The regions when the sample was exposed to hydrogen and ethylene are highlighted by light blue and light red background, respectively.

Another field of extensive application of Pd catalysts is the combustion of methane in the exhaust gases from natural gas engines. The Pd oxide is generally supposed to be the active phase, however the role of metallic Pd and surface to bulk distribution of Pd and PdO in the oxidation process is still under debate. We have performed a modulation excitation experiment where oxygen was periodically added to and removed from the constant flow of methane. The atomic and electronic structure of the sample was monitored by operando energy-dispersive XAS with 50 ms time resolution at ID24 beamline of ESRF. The suggested experimental design allowed us to observe for the first time several intermediate phases exhibiting higher activity than that of Pd oxide formed in the steady-state reaction conditions.

The reported material contains a considerable fraction of unpublished data.

**Acknowledgement.** This work was supported by the Ministry of Science and Higher Education of the Russian Federation (Project RFMEFI58417X0029, Agreement 14.584.21.0029).

## X-ray Absorption Spectroscopy Studies of Catalysts at P64/P65 Beamlines

Murzin V.<sup>1,2</sup>, Caliebe W.<sup>1</sup>, Welter E.<sup>1</sup>

1 – Deutsches Elektronen-Synchrotron DESY, Hamburg, Germany

2 – University of Wuppertal, Wuppertal, Germany

[vadim.murzin@desy.de](mailto:vadim.murzin@desy.de)

X-ray absorption spectroscopy (XAS) is a very powerful technique and can give an extensive amount of information about oxidation state, local coordination and geometry of a specific element. Recent developments in synchrotron X-ray instruments allowed to reduce the time for acquisition of one XAS spectrum down to several ms [1, 2]. That is very useful for *in situ* and *operando* studies of different physical and chemical processes including catalytic reactions.

P64/P65 XAS beamlines [1,3] were recently built at PETRA III ring (DESY, Hamburg). These beamlines were especially designed for *in situ* and *operando* studies and have a convenient gas infrastructure, a sample preparation lab with a glove-box and a fume hood. There is also a catalytic setup with mass-flow controllers, a capillary cell, a heating system (from RT to 700°C) and a mass-spectrometer, which can be used at both beamlines. User-provided sample cells for special applications can also be accommodated at the beamlines.

The XAS user community is constantly growing, and we have already attracted a lot of users who study homogeneous/heterogeneous catalysts, photocatalysts, electrocatalysts and many other systems [4-7]. We will present recent advances from users in research of catalytic systems and discuss possible experiments, which can be done at P64/P65.

**Acknowledgement.** This work was supported by BMBF MatDynamics project 05K16PX1

### References:

- [1] W. Caliebe, V. Murzin, A. Kalinko, M. Görlitz, **AIP Conf. Proc.** 2054 (2019) 060031.
- [2] B. Bornmann, J. Kläs, O. Müller, et al., **AIP Conf. Proc.** 2054 (2019) 040008.
- [3] E. Welter, R. Chernikov, M. Herrmann, and R. Nemausat, **AIP Conf. Proc.** 2054 (2019) 040002.
- [4] A. Gänzler, M. Casapu, F. Maurer, et al., **ACS Catal.** 8(6) (2018) 4800 – 4811.
- [5] M. Chen, W. Hua, J. Xiao., et al., **Nat. Commun.** 10(1) (2019) 1480.
- [6] O. Pliekhova, O. Pliekhov, M. Fanetti, et al., **Catal. Today** 328 (2019)105 – 110.
- [7] S. Preiß; C. Förster, S. Otto, et al., **Nat. Chem.** 9(12) (2017) 1249 – 1255.

**CuFeAl Nanocomposite Catalysts of CO Oxidation: *Operando* XAS Study**

Saraev A.A.<sup>1</sup>, Tsapina A.M.<sup>1</sup>, Fedorov A.V.<sup>1</sup>, Trigub A.L.<sup>2</sup>, Murzin V.Yu.<sup>3</sup>, Kaichev V.V.<sup>1</sup>

1 – Boreskov Institute of Catalysis, Novosibirsk, Russia

2 – National Research Centre Kurchatov Institute, Moscow, Russia

3 – Deutsche Elektronen-Synchrotron, Hamburg, Germany

asaraev@catalysis.ru

Gasification of solid fuels and following catalytic combustion of the resultant gas is allows utilizing low-grade fuels such as lignite, peat, and firewood as well as various industrial wastes. Besides, catalytic combustion produces a significantly lower amount of harmful emissions than “traditional combustion” of fuels. The application of this technology is limited by the absence of the effective and low cost catalysts. One of the promising catalysts for this process is CuFeAl nanocomposite which demonstrates high activity and stability in the oxidation of CO containing mainly in the resultant gas of solid fuel gasification [1,2]. Moreover, the CuFeAl-based catalysts are inexpensive and ecologically clean. To develop the catalysts with highest possible activity and stability, the origin the active species and the mechanism of the oxidation of CO over CuFeAl nanocomposite should be investigated. Here we present the first results of *operando* studies of the catalyst state in the oxidation of CO. *Operando* XAS experiments were performed at the Structural Materials Science station at Kurchatov Center for Synchrotron Radiation (Moscow, Russia) and P64/P65 stations at PETRA III (Hamburg, Germany). XANES is very useful for identification of different chemical states of copper and iron and allows us to study the chemistry of the catalysts under reaction conditions. EXAFS may clarify the structure of local environment of copper and iron atoms.

The catalysts were prepared as follows: the salts of the precursors ( $\text{Fe}(\text{NO}_3)_3 \cdot 9\text{H}_2\text{O}$ ,  $\text{Al}(\text{NO}_3)_3 \cdot 9\text{H}_2\text{O}$ , and  $\text{Cu}(\text{NO}_3)_2 \cdot 3\text{H}_2\text{O}$ ) were mixed in the required ratios, then the mixture was heated to give a homogeneous melt of crystal hydrate salts and was kept at a temperature of 200°C until water was completely removed; finally, the solid residue was calcined at 700°C for 1 h in air. It was found that the catalytic activity of FeAl nanocomposite catalysts depends on the Fe concentration and the maximum is achieved when the  $\text{Fe}_2\text{O}_3$  content is approximately 82 wt%. The promotion by copper leads to an increase of the catalytic activity of the nanocomposites. To compare the catalytic activity of synthesized catalysts we used the light-off temperature (the temperature of reaching 50% of the CO conversion). The light-off temperature in the oxidation of CO over the nanocomposite catalysts containing 3%, 5%, and 8% of CuO ( $\text{Cu}_3\text{Fe}_{79}\text{Al}_{18}$ ,  $\text{Cu}_5\text{Fe}_{78}\text{Al}_{17}$ , and  $\text{Cu}_8\text{Fe}_{76}\text{Al}_{16}$ ) is 205, 190, and 199°C, which is significantly lower than that observed over the best FeAl nanocomposite catalyst, where the light-off temperature over  $\text{Fe}_{82}\text{Al}_{18}$  is approximately 275°C. The catalyst of optimal composition (5% of CuO, 78% of  $\text{Fe}_2\text{O}_3$ , and 17% of  $\text{Al}_2\text{O}_3$ ) was the subject of *operando* XAS investigations.

## OP-II-8

We found that the fresh CuFeAl-composite catalysts consist of  $\text{CuFe}_2\text{O}_4$ ,  $\text{CuO}$ , and  $\text{Fe}_2\text{O}_3$ . According to the linear combination fitting method of Cu K-edge XANES spectrum the copper presents in two phases:  $\text{CuO}$  (25%) and  $\text{CuFe}_2\text{O}_4$  (75%). To obtain information about the catalytic process  $\text{Cu}_5\text{Fe}_{78}\text{Al}_{17}$  was studied by XANES and EXAFS directly during heating in the CO flow and  $\text{CO}:\text{O}_2 = 2:1$  mixture. In a CO flow, the reduction of copper from  $\text{Cu}^{2+}$  to  $\text{Cu}^{1+}$  and  $\text{Cu}^0$  started at temperature about  $200^\circ\text{C}$ ; at  $600^\circ\text{C}$  copper is mainly in the metallic state. At the same time the reduction of iron started at temperature about  $400^\circ\text{C}$ , and at  $600^\circ\text{C}$  about 20% of iron is in the metallic state. In  $\text{CO}:\text{O}_2 = 2:1$  mixture, the reduction of copper from  $\text{Cu}^{2+}$  to  $\text{Cu}^{1+}$  started at temperature about  $400^\circ\text{C}$ . And it should be stressed that no copper in the metallic state was observed, moreover, at  $600^\circ\text{C}$  approximately 50% of copper is in the  $\text{Cu}^{1+}$  state. At the same time,  $\text{Fe}^{3+}$  cations were slightly reduced to  $\text{Fe}^{2+}$  at  $600^\circ\text{C}$ . Thus, in the presence of oxygen the reoxidation of copper and iron cations take place. The following increase the partial pressure of  $\text{O}_2$  leads to shift initial reduction temperature to high temperature range, to decrease a part of  $\text{Cu}^{1+}$  state at  $600^\circ\text{C}$ , and no changing the oxidation state of iron. We believe that the lattice oxygen in the copper oxide has more lability then one in the iron oxides that leads to increase the activity of catalysts with additive of copper.

Hence, the obtained results allow us to speculate that the oxidation of CO over the CuFeAl-composite catalysts proceeds via the redox mechanism: CO oxidizes by oxygen from the lattices of iron and copper oxides to produce  $\text{CO}_2$  and oxygen from the gas phase oxidizes the reduced oxides.

**Acknowledgement.** This work was supported by the Russian Science Foundation, grant 17-73-20157.

### References:

- [1] A.V. Fedorov, A.M. Tsapina, O.A. Bulavchenko, A.A. Saraev, G.V. Odegova, D.Yu. Ermakov, Y.V. Zubavichus, V.A. Yakovlev, V.V. Kaichev, *Catal. Lett.* 148 (2018) 3715.
- [2] O.A. Bulavchenko, Z.S. Vinokurov, A.A. Saraev, A.M. Tsapina, A.L. Trigub, E.Yu. Gerasimov, A.Yu. Gladky, A.V. Fedorov, V.A. Yakovlev, V.V. Kaichev, *Inorg. Chem.* (2019) in press.

## Au Activation via Strong Metal Support Interaction in CO oxidation

Klyushin A.Yu.<sup>1,2</sup>, Jones T.<sup>2</sup>, Li X.<sup>2</sup>, Timpe O.<sup>2</sup>, Huang X.<sup>2</sup>, Lunkenbein T.<sup>2</sup>, Bukhtiyarov A.V.<sup>3</sup>,  
Prosvirin I.P.<sup>3</sup>, Bukhtiyarov V.I.<sup>3</sup>, Hävecker M.<sup>4</sup>, Knop-Gericke A.<sup>2,4</sup>, Schlögl R.<sup>1,2,4</sup>

*1 – Helmholtz-Zentrum Berlin/BESSY II, Berlin, Germany*

*2 – Fritz Haber Institute of the Max Planck Society, Department of Inorganic Chemistry,  
Berlin, Germany*

*3 – Boreskov Institute of Catalysis, Novosibirsk, Russia*

*4 – Max Planck Institute for Chemical Energy Conversion, Department of Heterogeneous  
Reactions, Mülheim an der Ruhr, Germany  
alexander.klyushin@helmholtz-berlin.de*

The discovery that gold nanoparticles (Au NPs) supported on metal oxides are active in low-temperature CO oxidation<sup>1</sup> has inspired a considerable amount of research directed toward the understanding of the activity of Au catalysts. Interestingly, the activity in CO oxidation of Au supported on a metal oxide is sensitive to the gold particle size distribution. This observation raises the question why small-sized gold is active whereas extended Au surfaces, e.g., single crystals, are not. The complexity of the gold catalytic system introduces many possible factors that can contribute to the catalytic activity of gold.<sup>2</sup> The possible contributions to the activity of Au can be divided into two broad categories: factors related to the gold particle itself (size, shape and surface chemistry) and factors related to the oxide support (charge transfer from/to the gold particle, supply of adsorption sites for reactants, formation of a reactive gold-oxide interface).

Thus, a systematic study of each separate factor is required. Since the active site is a transient state, present only under reaction conditions, it is important to characterize the Au samples in equilibrium with a gas phase environment. In this work near-ambient pressure X-ray photoelectron spectroscopy (NAP-XPS) was used to probe the surface composition, oxidation states and electronic structure, while the surface morphology was investigated by scanning and transmission electron microscopies (SEM and TEM).

First, the oxidation of extended surfaces was studied using a gold foil and ozone (O<sub>3</sub>) as an oxidant.<sup>3</sup> NAP-XPS showed surface core-level shifts after O<sub>3</sub> treatment due to a surface restructuring. SEM images revealed the presence of surface restructuring only in the regions exposed to O<sub>3</sub>. A surface oxide phase is formed during the activation of extended Au surfaces by O<sub>3</sub> treatment. However, this phase decomposes both in vacuum and under reaction conditions and is not likely to participate directly in CO oxidation on Au catalysts.

The next step was the investigation of Au NPs deposited on oxygen free-supports like highly oriented pyrolytic graphite, functionalized carbon nanotubes and Au foil.<sup>4</sup> The catalytic performance in the mbar pressure range, as well as at ambient pressure, was monitored with mass-spectrometry and correlated with the surface composition measured by NAP-XPS and the morphological changes monitored by electron microscopy. Au NPs on oxygen-free

## OP-II-9

supports do not show any catalytic activity, regardless of the type of the support and the method of synthesis.

Finally, the Au NPs supported on transition metal oxides show high catalytic activity.<sup>5</sup> But the catalytic performance depends on the method of preparation, and only the samples prepared by deposition-precipitation methods showed significant CO conversion at low temperature. XPS revealed the presence of two Au species ( $\text{Au}_{\text{metallic}}$  and  $\text{Au}_{\text{ionic}}$ ) on the surface of active samples. The binding energy shift of the  $\text{Au}_{\text{ionic}}$  peak, relative to bulk gold ( $\text{Au}_{\text{metallic}}$ ), depends on the support. TEM images indicate the formation of overlayer on the Au particles. Electron energy-loss spectra confirm the formation of a metal oxide overlayer on top of the Au NPs. DFT calculations performed on the Au/TiO<sub>2</sub> show that oxidized TiO<sub>2</sub> and Au interact weakly, with calculated work of adhesion ( $W_{\infty}$ ) < 0.1 J/m<sup>2</sup>, whereas reduced and defective TiO<sub>2</sub> supports show a strong metal-support interaction, increasing  $W_{\infty}$  to  $\geq 1.0$  J/m<sup>2</sup>. DFT predicts the Au 4f shifts of the ionic Au mirror these changes in adhesion and are 0.0 eV, 0.2 eV, and 0.7 eV for oxidized, reduced, and defected TiO<sub>2</sub>, respectively.<sup>6</sup>

Therefore, size reduction or oxidation strategies are not sufficient to activate Au. Our results suggest a mechanism of Au activation via a Strong Metal Support Interaction (SMSI), assuming a strong influence of the support on the electronic structure of the gold through charge transfer and stabilization of low-coordinated Au atoms. Therefore SMSI plays the key role in Au activation.

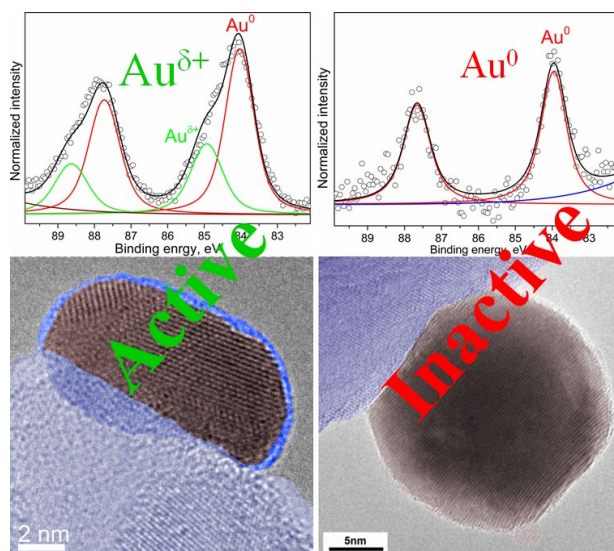


Figure 1. Au 4f XP spectrum and TEM image of sample synthesized by deposition-precipitation (left) and photochemical decomposition of intermediate gold-azido complex (right).

### References:

- [1] M. Haruta et al., *J. Catal.* 1989, 115, 301-309.
- [2] B.K. Min, C.M. Friend, *Chem. Rev.* 2007, 107, 2709-2724.
- [3] A.Yu. Klyushin, et al., *Phys. Chem. Chem. Phys.* 2014, 16, 7881-7886.
- [4] A.Yu. Klyushin, et al., *Topics in Catalysis* 2016, 59, 469-477.
- [5] A.Yu. Klyushin, et al. *ACS Catalysis* 2016, 6, 3372-3380.
- [6] A.Yu. Klyushin, et al., *ChemCatChem* 2018, 10, 3985-3989.

**CO Oxidation on the Model Pd-Au/HOPG Catalysts: NAP XPS and MS Study**

Bukhtiyarov A.V.<sup>1</sup>, Prosvirin I.P.<sup>1</sup>, Mamatkulov M.<sup>1</sup>, Yudanov I.V.<sup>1</sup>, Klyushin A.Yu.<sup>2</sup>,  
Knop-Gericke A.<sup>2</sup>, Neyman K.M.<sup>3,4</sup>, Bukhtiyarov V.I.<sup>1</sup>

*1 – Boreskov Institute of Catalysis, Novosibirsk, Russia*

*2 – Fritz-Haber-Institute der Max Planck Society, Berlin, Germany*

*3 – Departament de Ciència de Materials i Química Física and Institut de Química Teòrica i Computacional, Universitat de Barcelona, Barcelona, Spain*

*4 – ICREA (Institució Catalana de Recerca i Estudis Avançats), Barcelona, Spain  
avb@catalysis.ru*

Bimetallic systems attract the great interest of many scientific groups due to its ability to improve significantly catalytic properties in comparison with monometallic catalysts [1-2]. Good example proving this statement is the bimetallic Pd-Au catalysts, which exhibit extremely high activity in a number of industrially important reactions. This motivated researchers on numerous investigations of Pd-Au systems, which have shown that not only the ratio of the introduced metals, but also temperature of calcination will affect the surface composition causing the essential difference between Au/Pd atomic ratios in the bulk and surface [1-2]. Furthermore, surface composition can be varied under the influence of reaction mixture due to enrichment of the surface with one of the metals. It is evident that to clarify the influence of the above-mentioned effects on catalytic properties, the detailed in situ study of surface structure and composition of bimetallic Pd-Au catalysts is necessary to understand the nature of active sites and help to optimize the catalyst composition for the best activity, selectivity and stability.

Preparation of the model bimetallic Pd-Au/HOPG (highly oriented pyrolytic graphite) catalysts has been investigated with XPS and STM [3]. Initially, model “core-shell” type Pd-Au/HOPG catalysts with similar particle size distribution (5–8 nm) were prepared. Subsequent annealing of these samples in temperature range of 300–400°C leads to formation of Pd-Au alloyed particles.

Treatment of the alloyed Pd-Au/HOPG model catalysts under CO oxidation conditions destroys the alloy structure due to segregation of Pd over Pd-Au particle surface via formation of Pd-COads bonds. Heating the samples restores the alloy structure due to CO desorption even under the reaction conditions. All these changes in the particle structure were identified using NAP XPS technique.

Density functional calculations combined with calculations using topological energy expression method (TOP method) were applied to reveal the mechanism of this phenomenon and to quantify the stability of different arrangements of metal atoms in bimetallic PdAu nanoparticles in the presence of CO adsorbate. According to results of this computational approach, adsorption of CO already at a rather moderate coverage

## OP-II-10

is sufficient to make energetically feasible segregation of Pd at terraces of PdAu nanoparticles similar in size with experimentally studied ones.

**Acknowledgement.** This work was supported by the Russian Science Foundation, grant 19-13-00285.

### References:

- [1] C.W. Yi, K. Luo, T. Wei, D.W. Goodman, J. Phys. Chem. B. 109. (2005) 18535.
- [2] A. Wang, X.Y. Liu, C.-Y. Mou, T. Zhang, J. Catal. 308. (2013) 258.
- [3] A.V. Bukhtiyarov, I.P. Prosvirin, V.I. Bukhtiyarov, Appl. Surf. Sci. 367. (2016) 214.

## In Situ XRD and XPS Study of the Reduction of Mixed Mn-Zr and Mn-Co Oxide Catalysts of CO Oxidation

Bulavchenko O.A.<sup>1,2</sup>, Vinokurov Z.S.<sup>1,2</sup>, Afonasenko T.N.<sup>1</sup>, Tsyrl'nikov P.G.<sup>3</sup>, Ivanchikova A.V.<sup>2</sup>, Gerasimov E.Y.<sup>1,2</sup>, Saraev A.A.<sup>1,2</sup>, Kaichev V.V.<sup>1,2</sup>, Tsybulya S.V.<sup>1,2</sup>

1 – Boreskov Institute of Catalysis, Novosibirsk, Russia

2 – Novosibirsk State University, Novosibirsk, Russia

3 – Center of New Chemical Technologies BIC, Omsk, Russia

isizy@catalysis.ru

The reducibility of oxides is an essential characteristic of catalyst of different reactions. First of all, it is important for oxidation reactions following the Mars-van Krevelen mechanism. In this mechanism, a weakly bound surface oxygen atom is added to forming the oxygenated compound, leaving behind an oxygen vacancy on the surface. Then, the molecular oxygen react with the surface, dissociate and refill the vacancy. In this case, reducibility of oxide catalyst measures the tendency of oxide to lose oxygen or to donate it to an adsorbed species. Secondly, reduction can be an activation stage of Fischer-Tropsch synthesis, steam reforming and water-gas shift reaction. The catalysts activation leads to transformation from oxide state to metallic, depending on the reductive conditions the state of active sites can be changed significantly. Mn-containing oxides can effectively catalyze the oxidation of hydrocarbons, CO and chlorocarbons. Cooperative utilize of Mn and another oxide leads to synergetic effect – increase in catalytic activity as compared with simple oxides. In double metal oxide catalysts, the formation of mixed oxides is possible. The purpose of this work was to elucidate influence of redox properties of solid solutions on the catalytic performance. A series of catalysts based on mixed Mn-Zr and Mn-Co oxides with different molar ratios of cations have been prepared by coprecipitation. Reduction mechanism of Mn-containing catalysts with hydrogen was studied by a TPR-H<sub>2</sub>, in situ XRD, and XPS. There are differences in redox properties of Mn cations in Mn-Co and Mn-Zr oxide matrix. The reduction of the solid solutions Mn<sub>x</sub>Zr<sub>1-x</sub>O<sub>2-δ</sub> proceeds via two stages: Mn cations incorporated into the solid solutions undergo partial reduction; then Mn cations segregate on the surface of oxide. It was shown that the mechanism of reduction of Mn-Co oxides with hydrogen differs significantly from the processes occurring on simple oxides. The reduction of Mn-Co oxides occurs in two steps: (Mn,Co)<sub>3</sub>O<sub>4</sub> transforms to (Mn,Co)O solid solutions, then the reduction of solid solutions (Mn,Co)O to metallic cobalt Co and MnO proceeds. Correlations between the redox properties and the catalytic activity in the CO oxidation reaction have been found.

**Acknowledgement.** The reported study was funded by RFBR according to the research project № 18-33-00542 and the framework of the budget project for Boreskov Institute of Catalysis.

### References:

[1] O.A. Bulavchenko, Z.S. Vinokurov et al, Dalton Trans, 44 (2015) 15499

[2] O.A Bulavchenko., E.Y. Gerasimov, T.N. Afonasenko, Dalton Trans, 47 (2018) 17153.

**Deactivation Study of Pt/WO<sub>3</sub>–Al<sub>2</sub>O<sub>3</sub> Catalysts for Vegetable Oil Hydrodeoxygenation by EPR Spectroscopy and Thermal Analysis**

Yurpalov V.L., Drozdov V.A., Nepomnyashchiy A.A., Buluchevskiy E.A., Lavrenov A.V.  
*Center of New Chemical Technologies BIC, Omsk, Russia*  
*yurpalovv@mail.ru*

Electron paramagnetic resonance (EPR) spectroscopy may be efficiently used in the study of materials with paramagnetic centers, including carbon and carbon–metal oxide systems. For example, theoretical basis of EPR spectroscopy for carbon materials was used in the investigation of coked heterogeneous catalysts in combination with other research methods (thermal, magnetic, etc.) [1, 2]. However, these studies are quite rare and usually cannot definitely determine preferential mechanism of deactivation of the systems studied in a particular reaction.

In the previous work [3] we've demonstrated some advantages of using probe EPR in the acidic properties investigation of NiMo/WO<sub>3</sub>-Al<sub>2</sub>O<sub>3</sub> (NiMo/WA-*x*, *x* = 0–30 % wt of WO<sub>3</sub>) catalysts and also the application of classical EPR for deactivated catalysts. All the results were improved by the thermal analysis data. In current research the same approach was used for the supported Pt/WA-*x* catalysts which in fact possess much higher acidity than NiMo/WA-*x* catalytic systems.

EPR measurements were performed on Bruker EMXplus X-band (~9.74 GHz) spectrometer at 25°C. Each sample of 0.5Pt/WA-*x* (*x* = 0–30 % wt of WO<sub>3</sub>) catalyst (synthesis and composition of the support are reported in [3]) were activated at 500°C and treated by probe solution with further radical cation registration. As for deactivated catalysts, each one was placed directly into quartz tube and EPR spectrum was recorded without any treatment to characterize the surface carbon deposits (coke). The thermal analysis of the deactivated catalysts samples was performed in the range of 20–750°C using Netzch STA-449C Jupiter instrument.

The EPR signal in deactivated (coked) catalyst is a typical spectrum of paramagnetic species (PS) observed in carbon materials, and EPR spectra are similar for all the studied Pt/WA-*x* catalysts series. All the spectra are well described by the superposition of PS (defects) with *g* ~ 2.002 Lorentzian line, due to the presence of delocalized or partially delocalized π-electrons in graphene layers of small length, as well as edge defects in such layers [4]. The intensity of EPR signal in Pt/WA-*x* series is changing significantly depending on the composition of the catalyst: with an increase in the WO<sub>3</sub> modifier content to 15–25 % wt, it sharply increases by 8–10 times (Figure 1). According to TGA, the amount of carbon deposits with a decomposition temperature of 300-500°C also increases, as well as the total coke content in the samples series. Comparing the TGA and EPR results, we found a similar trend in the concentration of PS in the coked samples and the amount of carbon deposits formed on the support surface (Figure 1) depending on the support composition.

## OP-II-12

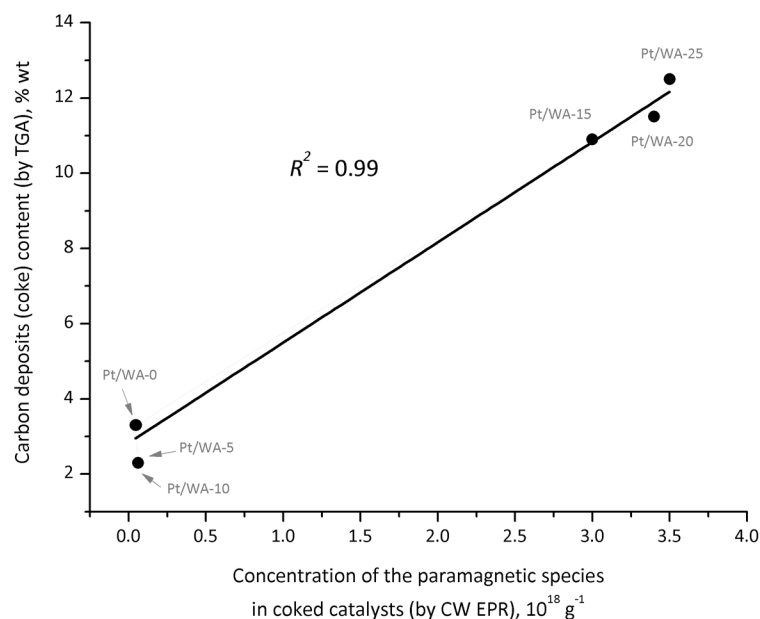


**Figure 1.** The relation of carbon deposits (coke) content formed on the support surface of Pt/WA-x (by TGA) with the PS concentration in coked Pt/WA-x catalysts (by CW EPR).

Coked catalysts with low concentration of PS (Pt/WA-0; 5; 10) have lower amount of carbon deposits, which are mainly located on the metal, while highly coked samples (Pt/WA-15; 20; 25) give a much intense EPR signal due to the presence of large PS number. This fact may be caused by the significant increase in acidity of the samples during the transition from the catalysts with low content of  $\text{WO}_3$  modifier to higher one. In our case this assumption agrees well with the results of BAS concentration determined by probe EPR spectroscopy.

Thereby, these results can help determine the preferential mechanism of coke formation in bi- and poly-functional catalysts, what in turn is important for the development of approaches to their regeneration.

**Acknowledgement.** The work was supported by the Ministry of Science and Higher Education of the Russian Federation in accordance with the Fundamental Research Program of State Academies of Sciences for 2013–2020 direction V.47, project № V.47.1.3 (No. AAAA-A17-117021450099-9). Physicochemical studies were carried out using the instrument base of the Omsk Research Collaboration Centre SB RAS, Omsk. The authors express gratitude to Antonicheva N. V. for providing thermal analysis experiments.

### References:

- [1] H. G. Karge, J.-P. Lange, A. Gutsze, et al. *J. Catal.* 114 (1988) 144.
- [2] C. L. Li, O. Novaro, E. Muñoz, et al. *Appl. Catal. A.* 199 (2000) 211.
- [3] V. L. Yurpalov, V. A. Drozdov, N. V. Antonicheva, et al. *Kinet. Catal.* 60 (2019) 257.
- [4] S. Łoś, L. Duclaux, W. Kempieński, *Curr. Top. Biophys.* 33 (2010) 147.

## Tandem Operando FTIR with GCMS Analysis for Evaluation Chlorosilanes Disproportionation Mechanism on the Supported Ionic Liquids Like Phase (SILLPs) Catalysts

Vorotyntsev A.V., Petukhov A.N., Markov A.N.

Nizhny Novgorod State Technical University n.a. R.E. Alekseev, Nizhny Novgorod, Russia  
dm.makarov.lmcp@gmail.com

It will be redundantly to mention the great role of silicon it plays in almost all spheres of our life. Nowadays, there are several different methods of polycrystalline silicon synthesis. The most common way is called Siemens process. It based on trichlorosilane thermal decomposition which yields in silicon, hydrogen, and hydrochloric acid. The most of polycrystalline silicon is obtained by this method in the world. But it has certain disadvantages, such as high cost and energy consumption, impurities, big amount of toxic side products. The main idea of the other way is thermal decomposition of silane which yields in target polycrystalline silicon. This process doesn't require high temperatures and toxic reagents. The low temperature of synthesis and absence of highly corrosive side products allow producing electronic-grade purity silicon. So, it becomes more and more attractive in terms of product quality, economics, and environment friendliness.

In this work, we continue our research for the efficient and stable catalyst of TCS dismutation [1, 2]. This work is demanded to investigate properties of imidazolium-based SILLPs catalysts (fig. 1) from point of view Tandem Operando DRIFTS technique with GCMS quantitative analysis for evaluation active sites and its role in chlorosilanes disproportionation.

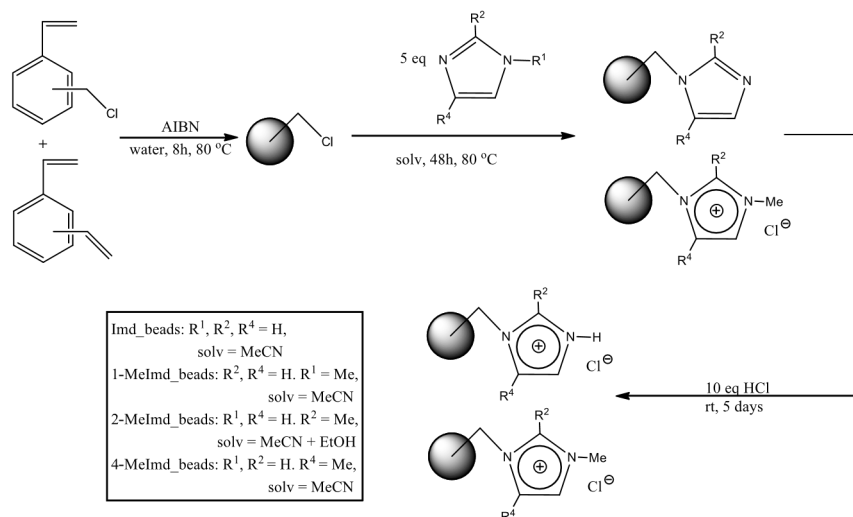


Fig 1. The scheme of the synthesis route from monomers to imidazole derivative functionalized SILLPs.

## OP-II-13

The size distribution of the obtained polymer beads has maximum between 0.2 and 0.5 mm. They have porous structure with incorporated hollow bubbles which have a diameter of 2-4 micrometers as can be seen on obtained SEM images (Fig. 1).

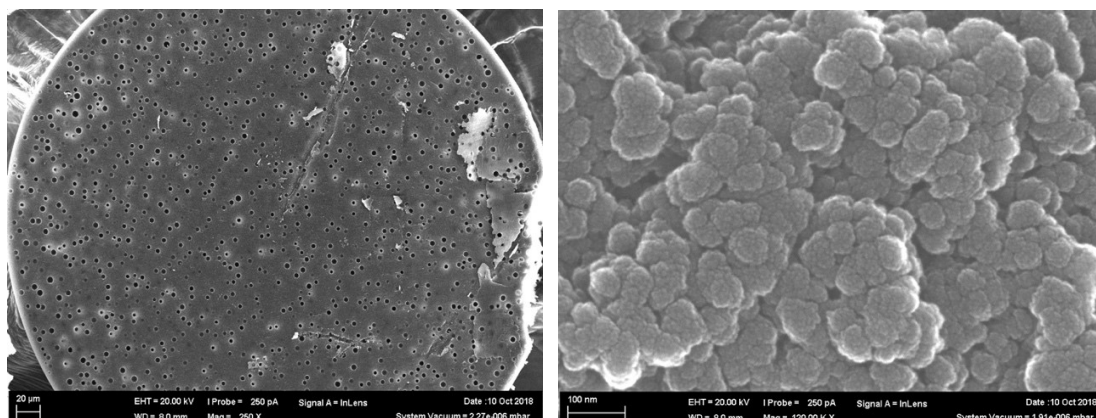


Fig. 2. SEM images of SILLPs catalyst (internal structure)

In order to obtain catalytic systems, such as SILLPs (fig. 1), imidazole derivatives were obtained and functionalized on the porous polymeric supports based on copolymers of divinylbenzene (DVB) and chloromethylstyrene (CMS). The choice of the initial matrix was due to their good physicochemical characteristics, cheapness and the possibility of varying structure (obtaining micro-, meso- and macroporous polymeric carriers) over a wide range, by changing the synthesis conditions.

In this work, a complete physicochemical characterization (AFM, SEM, EDS Mapping, TPD, EGA, BET, BJH, SAXS, MS, GCMS, FTIR) of the obtained catalyst was carried out and the catalytic activity was evaluated by the various techniques. Based on Operando FTIR and GCMS analysis reaction mechanism was proposed and determined the structure of the transition state (fig. 3).

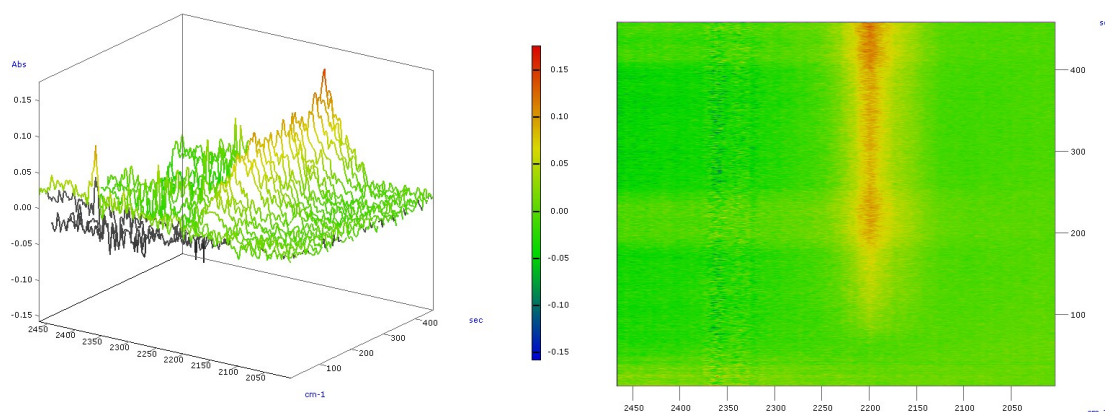


Fig. 3. Interaction between Chlorosilanes and catalyst on the active sites in 3D and 2D views by Operando FTIR.

## OP-II-13

**Acknowledgment.** This work was financially supported by the Russian Science Foundation, grant No. 17-73-20275.

### References:

- [1] A.V.Vorotyntsev, A.N. Petukhov, D.A. Makarov, T.S. Sazanova, T.N. Razov, A.V. Nyuchev, L.A. Mochalov, A.N. Markov, A.D. Kulikov, V.M. Vorotyntsev, *AppCatB: Env.* 239 (2018) 102-112.
- [2] A.V. Vorotyntsev, A.N. Petukhov, D.A. Makarov, E.N. Razov, I.V. Vorotyntsev, A.V. Nyuchev, N.I. Kirillova, V.M. Vorotyntsev, *AppCatB: Env.* 224 (2018) 621-633.

## Application of Isotopic Substitution in the IR Studies of Catalysts

Tsyganenko A.A.

*V.A.Fock Institute of Physics, St.Petersburg State University, St.Petersburg, Russia*  
*atsyg@yandex.ru or a.tsyganenko@spbu.ru*

The paper summarizes the authors experience in the use of isotopic substitution for the studies of catalysts, structure of intermediates and the mechanisms of catalytic reactions. Deuteration provides means to choose between the assignment of the bands to H-containing species or other vibrations and to find out the role of resonance in the formation of band contours. Different ability for H-D exchange enables us to differentiate the H-containing species, e.g. to distinguish surface OH groups from those of the bulk of catalysts. The structure of bands of partially substituted adsorbate isotopic mixtures allows to count the number of certain atoms in the structure of surface species and to distinguish equivalent atom in symmetrical molecules from the others, as it was done for dioxygen or ozone adsorbed on different oxides or CO on basic sites. Comparison of the observed and calculated isotopic shift values for different hypothetical structures facilitates the assignment of the spectra of reaction intermediates. The method of isotopic dilution is used in the studies of lateral interactions between the adsorbed molecules and helps us to separate the static and dynamic interaction, which affect the strength of surface sites or account for the vibrational energy transfer over the surface layer. The phenomenon of linkage isomerism on adsorption, recently established for CO, is of a great interest for catalysis. Accurate measurements of isotopic shifts on  $^{13}\text{C}$  substitution enable us to attribute unequivocally the bands to C- or O- bonded adsorbed CO species. Analysis of isotopic composition of gas provides information about the rate of isotopic scrambling reactions of CO or thiophene and to estimate the concentration of exchangeable surface oxygen sites or their proton-accepting properties. Temperature dependence of dissociative HD adsorption on ZnO illustrates the importance of atom mobility and the effect of the energy of zero vibrations upon the mechanism of reaction and product distribution. This reaction can be considered as a case of 'isotopic isomerism'. Another very recent example of such a phenomenon, when the adsorbed species can be different for isotopically mixed products is surface dicarbonyls of transition metal ions, when two CO molecules with different isotopic composition are not equivalent and form two kinds of species with the same formula, but different spectra. The problem and perspectives of isotope separation by resonance IR laser excitation of adsorbed molecules is discussed.

**Acknowledgement.** This work was supported by the Russian Science Foundation, grant 17-03-01372.

***In situ* - Determined Structural Dynamics as a Mechanistic Key Parameter in the Reactivity of LaNiO<sub>3</sub>-based Methane Dry Reforming Catalysts**

Bonmassar N.<sup>1</sup>, Schlicker L.<sup>2</sup>, Gili A.<sup>2</sup>, Gurlo A.<sup>2</sup>, Heggen M.<sup>3</sup>, Yunxua G.<sup>3</sup>, Doran A.<sup>4</sup>, Bernardi J.<sup>5</sup>, Penner S.<sup>1</sup>

1 – Institute of Physical Chemistry, University of Innsbruck, Innsbruck, Austria

2 – Fachgebiet Keramische Werkstoffe/Chair of Advanced Ceramic Materials, Institut für Werkstoffwissenschaften und -technologien, Technische Universität Berlin, Berlin, Germany

3 – Ernst Ruska Center for Spectroscopy and Microscopy with Electrons, Jülich, Germany

4 – Advanced Light Source, Lawrence Berkeley National Laboratory Berkeley, California, USA

5 – University Service Center for Transmission Electron Microscopy, TU Wien, Vienna, Austria

simon.penner@uibk.ac.at

*In situ* X-ray diffraction in combination with catalytic tests in dry reforming of methane (DRM) have been performed to unveil the strong structural dynamics of LaNiO<sub>3</sub> catalysts in the pre-catalytically active phase and during the DRM reaction. Structure-activity correlations reveal polymorphic changes of the LaNiO<sub>3</sub> structure (before DRM activity is observed), oxygen-deficient LaNiO<sub>2</sub>, as well as a Ruddlesden Popper La<sub>2</sub>NiO<sub>4</sub> phase with moderate DRM activity and finally, Ni<sup>0</sup>/La<sub>2</sub>O<sub>3</sub> as the most catalytically active phase. In parallel with the decomposition of La<sub>2</sub>NiO<sub>4</sub>, a monoclinic La<sub>2</sub>O<sub>2</sub>CO<sub>3</sub> species is formed, which – in addition to act as the CO<sub>2</sub>-activated species - stabilizes the Ni<sup>0</sup> particles, as it occurs simultaneously with the formation of Ni<sup>0</sup> during the decomposition of La<sub>2</sub>NiO<sub>4</sub> (Figure 1 and 2). We show that La<sub>2</sub>NiO<sub>4</sub> is one of the crucial intermediate structures in the formation of the active Ni<sup>0</sup>/La<sub>2</sub>O<sub>3</sub> phase and we provide direct proof that for the *in situ* decomposition of LaNiO<sub>3</sub> in a DRM mixture to form the active phase, it seems obvious to start directly from the Ruddlesden-Popper phase La<sub>2</sub>NiO<sub>4</sub>. Heating LaNiO<sub>3</sub> in hydrogen – as it is usually carried out to prepare the active phase - yields the same Ni<sup>0</sup>/La<sub>2</sub>O<sub>3</sub> phase, although the sequence of structural transformations to the active phase is strikingly different. The intermediate La<sub>2</sub>NiO<sub>4</sub> structure is not observed and the reduction of the pre-cursor Ni<sup>2+</sup> species (i.e. monoclinic LaNiO<sub>2.5</sub>) takes place within seconds. On the contrary, the decomposition of intermediate La<sub>2</sub>NiO<sub>4</sub> in the DRM mixture towards the active phase occurs on a larger time scale (minutes), and hence, under more controlled conditions. Exemplified for the DRM reaction and the LaNiO<sub>3</sub> structure, only the knowledge about the sheer complexity of the structural dynamics allows the unequivocal assignment of participating structures and phases to their respective catalytic performance and, therefore, allows definite conclusions about the formation and the properties of the final active phase.

## IOP-III-1

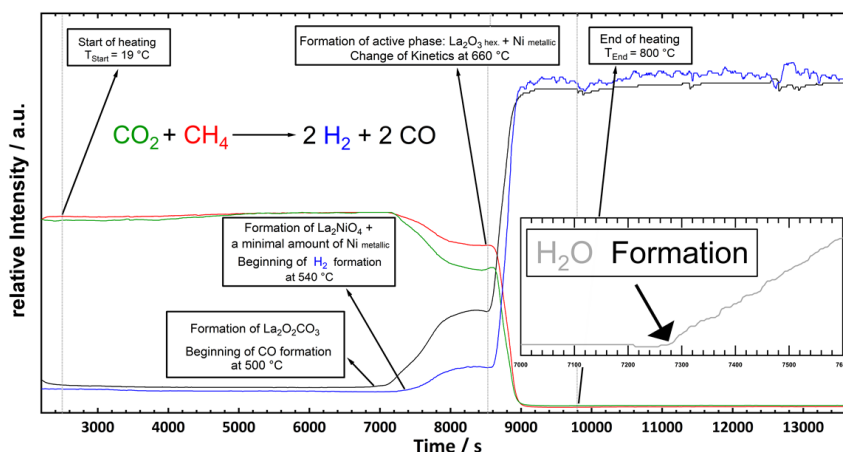


**Figure 1:** Dry reforming measurement using  $\text{LaNiO}_3$  as catalyst. Heating was carried out in a DRM mixture ( $\text{CO}_2:\text{CH}_4:\text{He} = 1:1:3$ ) in a total gas flow of  $100 \text{ mL min}^{-1}$  and a heating ramp of  $400 \text{ }^\circ\text{C h}^{-1}$  from room temperature to  $800 \text{ }^\circ\text{C}$ . The respective signals of the gases are shown in the diagram are  $\text{CO}_2$  (green),  $\text{CH}_4$  (red),  $\text{H}_2$  (blue),  $\text{CO}$  (black). The *in situ* detected structural changes are assigned to the respective temperatures to obtain a proper structure-activity correlation. The formation of reaction water starting at approximately  $520 \text{ }^\circ\text{C}$  is shown as inset.

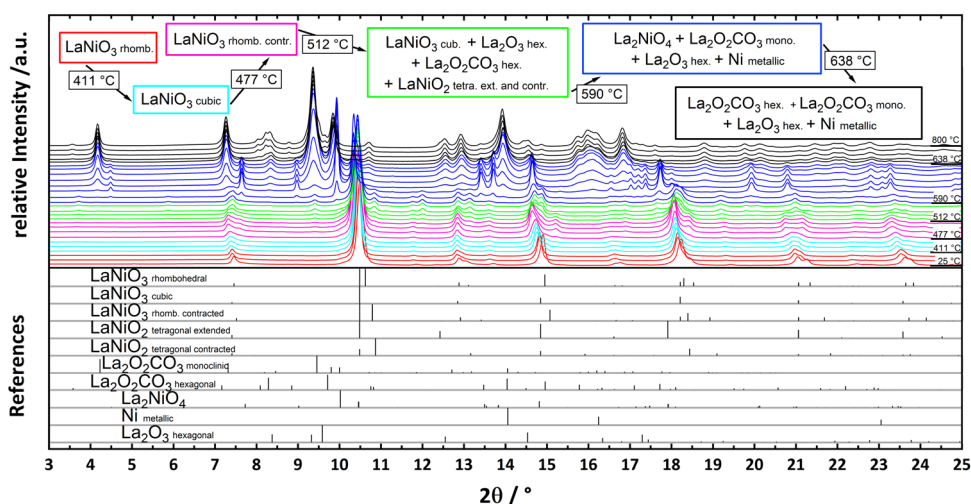


**Figure 2:** *In-situ* collected XRD patterns on  $\text{LaNiO}_3$  during DRM. Conditions as in Figure 1.

**Acknowledgement.** S. Penner acknowledges funding from the Austrian Science Fund (FWF) within the SFB project F4503-N16 “Functional Oxide Surfaces and Interfaces” and the DACH project I2877-N34. The authors further thank the Advanced Light Source (which is supported by the Director, Office of Science, Office of Basic Energy Sciences, of the U.S. Department of Energy under Contract No. DE-AC02-05CH11231), where *in situ* XRD measurements were conducted at beamline 12.2.2 in the framework of the AP program ALS-08865.

## OP-III-2

### Detailed Mechanism of Ethanol Transformation into Syngas on Nanocomposite Catalysts

Sadykov V.A.<sup>1,2</sup>, Ereemeev N.F.<sup>1</sup>, Rogov V.A.<sup>1,2</sup>, Sadovskaya E.M.<sup>1,2</sup>, Bobin A.S.<sup>1,2</sup>, Avdeev V.I.<sup>1</sup>, Chesalov Yu.A.<sup>1</sup>, Smal E.A.<sup>1</sup>, Lukashevich A.I.<sup>1</sup>, Krasnov A.V.<sup>1</sup>, Simonov M.N.<sup>1,2</sup>, Roger A.-C.<sup>3</sup>

1 – Boreskov Institute of Catalysis, Novosibirsk, Russia

2 – Novosibirsk State University, Novosibirsk, Russia

3 – University of Strasbourg, Strasbourg, France

sadykov@catalysis.ru

Catalysts based on Mg-doped alumina supports (including ordered mesoporous MgAl<sub>2</sub>O<sub>4</sub> spinel prepared by the one-pot evaporation induced self-assembly method using Pluronic P123 as a template [1]) loaded with fluorite PrCeZrO, perovskite PrNi<sub>0.95</sub>Ru<sub>0.05</sub>O<sub>3</sub> and spinel MnCr<sub>2</sub>O<sub>4</sub> oxides possessing a high lattice oxygen mobility and reactivity and promoted by Ru, Ru+Ni possess a high activity and coking stability in transformation of natural gas and biofuels (ethanol, glycerol, etc) into syngas at short contact times [1-3], which makes them promising for the practical application. Their optimization requires knowledge of detailed reaction mechanism elucidated by modern experimental and theoretical techniques. This work presents results of studies of mechanism of ethanol transformation into syngas (partial oxidation, steam/dry reforming) reactions by combination of transient kinetic methods (<sup>18</sup>O SSITKA, pulse microcalorimetry, FTIRS) using earlier described approaches [4-6]. Enthalpies and activation energies of elementary steps were estimated by DFT calculations using the ESPRESSO program package and ultrasoft pseudopotentials with exchange-correlation Perdew-Wang functional [7-10]. The reaction pathways were studied by the Climbing Image Nudged Elastic Band method (CI-NEB) [11].

For Ru(Ni)-promoted catalysts with optimized compositions their performance in reactions of ethanol transformation into syngas in the intermediate temperature range was high with efficient first-order specific rate constants up to ~ 1/m<sup>2</sup>s at 450 °C being close to those for Ru-promoted bulk complex oxides [4] and correlating with the number of accessible metal sites estimated by FTIRS of adsorbed CO. Main by-products are methane and acetaldehyde, minor – acetone, diethylether, C<sub>2</sub>H<sub>4</sub>, etc, their yield decreasing with the reaction temperature.

By *in situ* FTIRS in flow cells the surface species (ethoxy, adsorbed ethanol, acetaldehyde, acetate, etc) were identified and their thermal stability and reactivity were estimated. Acetate species were shown to be spectators for all types of catalysts. Transformation of ethoxy species by dehydrogenation was found to be a fast step, while the rate-determining stage is C-C bond rupture in thus formed acetaldehyde. Reactivity of intermediates was found to be the highest for catalysts containing PrCeZrO mixed oxide.

Ethanol transformation in pulses fed to the catalysts in the steady-state proceeds with the rate and products selectivities close to those in mixed pulses of ethanol with oxidant. The step of the oxides surface reoxidation by oxidants (CO<sub>2</sub>, H<sub>2</sub>O, O<sub>2</sub>) is fast producing, along with

## OP-III-2

CO or H<sub>2</sub>, reactive oxygen species rapidly migrating along the surface/domain boundaries to metal sites. Their interaction with adsorbed intermediates produces also acetaldehyde, H<sub>2</sub> and CO<sub>x</sub> under pulses of oxidants. Hence, for these types of catalysts in the steady-state the mechanism of EtOH reforming reactions can be described by a step-wise bifunctional redox scheme. The strength of oxygen bonding with the steady-state surface of complex oxides corresponds to bridging M<sub>2</sub>O forms (heat of O<sub>2</sub> adsorption ~ 500-600 kJ/mol for fluorite and perovskite-like supports, and ~400 kJ/mol for spinel).

Analysis of kinetics of the <sup>18</sup>O transfer into reaction products (CO, CO<sub>2</sub>, CH<sub>3</sub>CHO) allowed to estimate the rates of steps and present a scheme of the reaction mechanism including 1) fast CH<sub>3</sub>CHO formation on mixed metal oxide sites; 2) rate-limiting stage of surface oxygen species incorporation into CH<sub>3</sub>CHO with C-C bond rupture yielding CO (from -COH fragment) and CO<sub>2</sub> (from CH<sub>3</sub>- fragment) along with H<sub>2</sub> and H<sub>2</sub>O; 3) water gas shift reaction by redox mechanism affecting CO/CO<sub>2</sub> ratio and their oxygen isotope fraction. The highest surface oxygen mobility in these catalysts was shown for PrCeZrO surface layers.

According to results of DFT calculations, C<sub>2</sub>H<sub>5</sub>OH adsorption as ethoxy species on Me<sup>n+</sup> cations of support with proton of OH group transfer to the surface oxygen atom is characterized by the energy barrier up to 50 kJ/mole. Transformation of ethoxy complex into adsorbed acetaldehyde by C-H bond splitting and H transfer to the surface oxygen has the energy barrier up to 150 kJ/mole. Since this stage is endothermic ( $\Delta H$  up to 100 kJ/mole), the surface coverage by acetaldehyde is to be low agreeing with FTIRS data. Incorporation of surface oxygen species bound with transition or rare-earth cations into C-C bond of adsorbed acetaldehyde with its rupture is characterized by the energy barrier up to 260 kJ/mole, while for Ru=O oxygen species the energy barrier is much lower (~150 kJ/mole). Hence, promotion by Ru facilitates this rate-limiting stage providing a high syngas yield not accessible even for Pt-promoted complex oxides [4].

**Acknowledgement.** This work was supported by the Russian Science Foundation (grant 16-13-00112) and by the Russian Fund of Basic Research (grant RFBR-CNRS 18-58-16007\_a).

### References:

- [1] S. Pavlova, Y. Fedorova, V. Sadykov, et al, *Catal. Sustain. Energy* 5 (2018) 59.
- [2] V. Sadykov, N. Mezentsseva, M. Simonov, J. Ross, et al, *Int. J. Hydr. Energy* 40 (2015) 7511.
- [3] V. Sadykov, S. Pavlova, E. Smal, et al, *Catal. Today* 293–294 (2017) 176.
- [4] L. Pinaeva, E. Sadovskaya, V. Sadykov, et al, *Chem. Eng. J.* 333 (2018) 101.
- [5] V. Sadykov, O. Chub, Yu. Chesalov, et al., *Top. Catal.* 59 (2016) 1332.
- [6] M.N. Simonov, V.A. Sadykov, V.A. Rogov, et al., *Catal. Today* 277 (2016) 157.
- [7] P. Giannozzi, S. Baroni, N. Bonini, et al, *J. Phys. –Condens. Matt.* 21 (2009) 395502.
- [8] D.Vanderbilt, *Phys. Rev.B.* 41 (1990) 7892.
- [9] J. Perdew, J. Chevary, S. Vosko, et al, *Phys. Rev.B.* 46 (1992) 6671.
- [10] J. Perdew, Y. Wang, *Phys. Rev.B.* 45 (1992) 13244.
- [11] G. Henkelman, B. Uberuaga, H. Jonsson, *J. Chem. Phys.* 113 (2000) 9901.

**Kinetic Studies and Optimization of Heterogeneous Catalytic Oxidation Processes for the Green Biorefinery of Wood**

Kuznetsov B.N.<sup>1</sup>, Sudakova I.G.<sup>1</sup>, Garyntseva N.V.<sup>1</sup>, Tarabanko V.E.<sup>1</sup>, Djakovitch L.<sup>2</sup>, Rataboul F.<sup>2</sup>

*1 – Institute of Chemistry and Chemical Technology SB RAS, FRC KSC SB RAS,  
Krasnoyarsk, Russia*

*2 – IRCELYON, Lyon, France*

*bnk@icct.ru; inm@icct.ru*

The huge resources of lignocellulosic biomass are presented by wood which can be used as an important renewable feedstock for production of valuable chemicals and biofuels. The promising approaches to the development of high-tech processes of lignocellulosic biomass conversion into valuable chemicals and biofuels are based on the fractionation of its main components – polysaccharides and lignin. Oxidative catalytic fractionation of biomass can be considered as a key stage of wood biorefinery.

This presentation describes the oxidation processes of catalytic fractionation of hardwood and softwood by H<sub>2</sub>O<sub>2</sub> and O<sub>2</sub> on the cellulose, aromatic aldehydes and organic acids.

Air dry sawdust (fraction 2–5 mm) of aspen-wood, birch-wood, abies-wood, pine-wood were used as initial raw materials. Catalytic processes of wood conversions were studied with the use of stirring fixed-bed reactors. FTIR, XRD, SEM, solid state <sup>13</sup>C CP/MAS and chemical methods were used for study the solid products. Low molecular mass products were identified by GC, HPLC and GC-MC methods.

Two different ways of biomass wood catalytic fractionation were researched, namely, peroxide oxidation in the medium of acetic acid – water and oxidation by oxygen in alkaline medium. Solid catalysts and optimal conditions of oxidation processes were selected for conversion of wood biomass to cellulose, aromatic aldehydes and organic acids.

Suspended TiO<sub>2</sub> catalyst was used for wood peroxide fractionation on microcrystalline cellulose and organic acids at mild conditions (100 °C, atmospheric pressure) in the acetic acid – water medium. For all type of wood the processes are described by the first order equations and have the activation energies 76–94 kJ/mol. (Table). The optimized conditions of hardwood and softwood fractionation processes were established by experimental and mathematical methods.

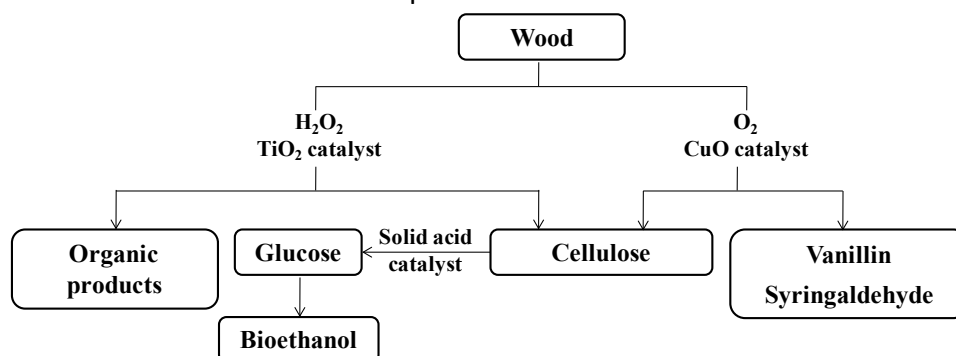
Oxidation of wood by oxygen to aromatic aldehydes and cellulose was accomplished in water-alkaline medium in the presence of suspended catalyst Cu(OH)<sub>2</sub>. The copper catalyst intensifies the oxidation of wood lignin by O<sub>2</sub> to aromatic aldehydes at 150–160 °C. At optimum conditions the total yield of vanillin and syringaldehyde reaches to 43 % mas. relative to hardwood lignin. Oxidation of softwood lignin by oxygen gives mainly vanillin with the yield to 18 % mas.

### OP-III-3

**Table.** Rate constants and activation energies of wood peroxide delignification with 1 % TiO<sub>2</sub> catalyst (H<sub>2</sub>O<sub>2</sub> – 5 % mas., CH<sub>3</sub>COOH – 25 % mas., LWR – 15, 4 h)

Temperature, °C	$k \cdot 10^{-4}, c^{-1}$	Activation energy, kJ/mol
<b>Aspen wood</b>		
70	0.18	76
80	0.56	
90	1.19	
100	1.56	
<b>Birch wood</b>		
70	0.14	82
80	0.32	
90	0.98	
100	1.49	
<b>Abies wood</b>		
70	0.08	86
80	0.19	
90	0.49	
100	1.23	
<b>Pine wood</b>		
70	0.07	94
80	9.20	
90	0.62	
100	2.17	

Based on the heterogeneous catalytic processes of wood oxidation and cellulose hydrolysis the green biorefinery of wood to microcrystalline cellulose, vanillin, syringaldehyde, organic acids and bioethanol was developed.



Scheme of green biorefinery of wood

**Acknowledgement.** The reported study was supported by the Russian Science Foundation (Grant N 16-13-10326). This work is part of GDRI “Catalytic biomass transformation” between France and Russia.

#### References:

- [1] B.N. Kuznetsov, I.G. Sudakova, N.V. Garyntseva, A.A. Kondrasenko, A.V. Pestuniv, L. Djakovitch, F. Rataboul, *React Kinet Mech Cat* (2018) DOI 10.1007/s11144-018-1518-6.
- [2] V.E. Tarabanko, K.L. Kaygorodov, E.A. Skiba, N.V. Tarabanko, Yu.V. Chelbina, O.V. Baybakova, B.N.Kuznetsov, L. Djakovitch, *J Wood Chem Technol*, 37 (2017) 43

## Impact of Metal Ratio in the Bimetallic Three-Way Catalyst on Mechanism of the Catalysed Reactions

Vedyagin A.A.<sup>1</sup>, Kenzhin R.M.<sup>1</sup>, Tashlanov M.Y.<sup>1,2</sup>, Stoyanovskii V.O.<sup>1</sup>, Plyusnin P.E.<sup>2,3</sup>,  
Shubin Y.V.<sup>2,3</sup>, Slavinskaya E.M.<sup>1</sup>, Mishakov I.V.<sup>1,2</sup>

1 – Boreskov Institute of Catalysis, Novosibirsk, Russia

2 – Novosibirsk State University, Novosibirsk, Russia

3 – Nikolaev Institute of Inorganic Chemistry SB RAS, Novosibirsk, Russia

vedyagin@catalysis.ru

As well known, three-way catalysts (TWC) are widely used for purification of exhaust gases from gasoline engines [1, 2]. These gases contain nitrogen oxides, unburnt hydrocarbons and carbon monoxide. Simultaneous oxidation of CO and hydrocarbons along with reduction of NO<sub>x</sub> can be realized over precious metals (Pt, Pd, Rh) supported on various oxides solely or in combination [3, 4]. In our recent research [5-7], supported Pd-Rh alloy anchored to specific sites on the surface of alumina was found to exhibit good enough stability (diminished palladium surface migration and rhodium bulk diffusion). The preparation conditions, including environment of treatment procedures and presence of hydroxyl groups on the support's surface, could play a defining role.

The precise study on Pd-Rh alloy system has shown that, in accordance with phase diagram, these metals are partly miscible [8]. The most area of the diagram is represented by non-miscibility. Thereby, bimetallic Pd-Rh species with a ratio within this area can be considered as metastable. Here, the important role of metal-metal interaction and its effect on activity and stability of the bimetallic catalysts should be emphasized [7]. Another significant point defining the catalytic performance of TWC is metal-support interaction [9].

The present research was aimed to study in more detail the effect of Pd:Rh ratio on the catalytic performance of Pd-Rh/ $\gamma$ -Al<sub>2</sub>O<sub>3</sub> three-way catalysts. It was found that the Pd:Rh ratio affects significantly the conversion of different component of a reaction gas mixture.

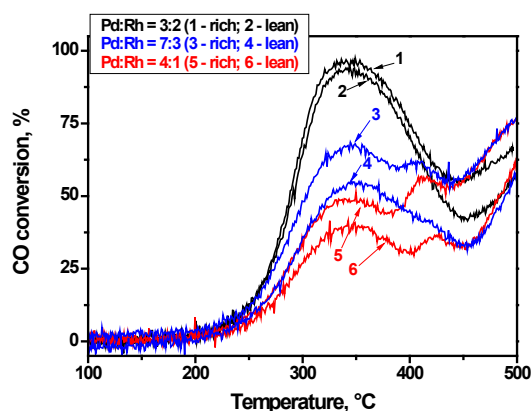


Figure 1. TWC light-off curves for CO conversion over Pd-Rh/ $\gamma$ -Al<sub>2</sub>O<sub>3</sub> samples with varied Pd:Rh ratio under rich and lean conditions.

### OP-III-4

The shape of light-off curves for CO conversion presented in Fig. 1 indicates that the processes taking place over the catalysts are quite complicated. Carbon monoxide undergoes oxidation at temperatures near 200 °C regardless to the Pd:Rh ratio. Then, with the temperature increase the curves have slightly different slope indicating the difference in the reaction rates. The curves go through a maximum at 340-350 °C, and then CO conversion decreases. Samples Pd:Rh(7:3) and Pd:Rh(4:1) show second maximum at 410-420 °C. For these samples, curves corresponded to lean conditions lie noticeably below that for rich conditions. It should be noted that conversion of oxygen takes place at temperatures of 240 °C and above. Hereby, while no oxygen or NO conversion was observed within a range of 200-240 °C, CO conversion can be assigned to a water-gas shift reaction. At higher temperatures, CO oxidation reaction also starts to take place. Nitrogen oxide undergoes conversion starting from 250-260 °C. Contrary, the Pd:Rh ratio has no significant effect on propylene conversion, while temperature region of NO conversion is evidently shifted toward higher temperatures. Thus, it can be concluded here that Pd:Rh ratio affects the catalytic behavior of bimetallic Pd-Rh/ $\gamma$ -Al<sub>2</sub>O<sub>3</sub> three-way catalysts changing the mechanism of the reactions. The highest activity of Pd:Rh(3:2) sample is believed to be facilitated by higher involvement of NO in the catalytic processes. Oppositely, the Pd:Rh(7:3) and Pd:Rh(4:1) samples were shown to catalyse the reactions via different routes.

**Acknowledgement.** The study was financially supported by the Ministry of Education and Science of the Russian Federation within the framework of subsidizing agreement of October 23, 2017 (No. 14.581.21.0028, unique agreement identifier RFMEFI58117X0028) of the Federal Target Program “Research and development in priority directions of the progress of the scientific and technological complex of Russia for the years 2014–2020.

#### References:

- [1] R.M. Heck, R.J. Farrauto, *Appl. Catal. A-Gen.* 221 (2001) 443–457.
- [2] M.V. Twigg, *Appl. Catal. B-Environ.* 70 (2006) 2–15.
- [3] M. Shelef, G.W. Graham, *Catal. Rev. Sci. Eng.* 36 (1994) 433-457.
- [4] H.S. Gandhi, G.W. Graham, R.W. McCabe, *J. Catal.* 216 (2003) 433–442.
- [5] A.A. Vedyagin, M.S. Gavrilov, A.M. Volodin, V.O. Stoyanovskii, E.M. Slavinskaya, I.V. Mishakov, Y.V. Shubin, *Top. Catal.* 56 (2013) 1008-1014.
- [6] A.A. Vedyagin, A.M. Volodin, V.O. Stoyanovskii, R.M. Kenzhin, E.M. Slavinskaya, I.V. Mishakov, P.E. Plyusnin, Y.V. Shubin, *Catal. Today* 238 (2014) 80-86.
- [7] A.A. Vedyagin, A.M. Volodin, R.M. Kenzhin, V.O. Stoyanovskii, Y.V. Shubin, P.E. Plyusnin, I.V. Mishakov, *Catal. Today* 293–294 (2017) 73-81.
- [8] Y.V. Shubin, P.E. Plyusnin, S.V. Korenev, *J. Alloy. Compd.* 622 (2015) 1055-1060.
- [9] T. Zheng, J. He, Y. Zhao, W. Xia, J. He, *J. Rare Earth.* 32 (2014) 97-107.

## The Benefit of Catalytic Materials Cooperation in the Hydrodeoxygenation of Aliphatic Oxygenates

Vlasova E.N.<sup>1,2</sup>, Shamanaev I.V.<sup>1</sup>, Aleksandrov P.V.<sup>1,2</sup>, Nuzhdin A.L.<sup>2</sup>, Bukhtiyarova G.A.<sup>1,2</sup>

1 – Borekov Institute of Catalysis, Novosibirsk, Russia

2 – Novosibirsk State University, Novosibirsk, Russia

*gab@catalysis.ru*

The triglyceride-based feedstocks (non-edible vegetable oils, animal fats, waste cooking oils) are the attractive renewables for the production of valuable motor fuel component – mixture of C<sub>12</sub>-C<sub>18</sub> alkane, that are fully compatible with the petroleum-derived gas oil and improves its properties. Hydrodeoxygenation (HDO) of triglycerides can be performed in the stand-alone units or via the co-processing with the petroleum oil in the existing refinery, in both cases sulfide Co(Ni)Mo/Al<sub>2</sub>O<sub>3</sub> catalysts are employed. The drawback of the sulfide catalyst is the deactivation due to sulfur loss and necessity of sulfiding agent feeding to the reactor. One of the approaches to solve this problem is the development of sulfur-free catalyst containing base metals, their carbides, nitrides or phosphides. As well, co-processing of triglycerides (TG) with petroleum feeds is the cost-effective solution improving the fuel properties and avoiding the addition of sulfur-containing component, like dimethyldisulfide (DMDS) to preserve the sulfide state of Co(Ni)Mo/Al<sub>2</sub>O<sub>3</sub> catalysts. HDO of TG can proceed via H<sub>2</sub>O removal (direct HDO pathway – dHDO) or through the oxygen removal in the form of CO/CO<sub>2</sub> (HDeCo<sub>x</sub> route), which can lead to the additional hydrogen consumption in the methanation reaction and demands separation of carbon oxides.

In the current work we illustrate the enhancing of catalytic activity or selectivity through the cooperation of catalytic systems with different functionality in the HDO of aliphatic compounds. Firstly the peculiarities of stack-bed technology are discussed which use avoid CO<sub>x</sub> formation during the ULSD production from the mixture of straight run gas oil (SRGO) and rapeseed oil (RSO). Then the enhancement of catalytic activity of Ni<sub>2</sub>P/SiO<sub>2</sub> catalyst in methyl palmitate (MP) hydrodeoxygenation is shown, which is result of catalyst dilution with  $\gamma$ -alumina.

The Ni<sub>2</sub>P/SiO<sub>2</sub> and sulfided MoS<sub>2</sub>/Al<sub>2</sub>O<sub>3</sub> and Co(Ni)Mo/Al<sub>2</sub>O<sub>3</sub> catalysts were prepared by the impregnation of supports with the solution of precursors with the subsequent drying and activation immediately before experiment in the catalytic reactors [1,2]. The catalysts were studied using chemical analysis (ICP-AES), N<sub>2</sub> physisorption, H<sub>2</sub>-TPR, XRD, XPS and TEM. The hydrotreatment of straight run gas oil and RSO mixtures was performed using granulated MoS<sub>2</sub>/Al<sub>2</sub>O<sub>3</sub> and CoMo/Al<sub>2</sub>O<sub>3</sub> catalysts. Sulfur, nitrogen, oxygen, mono- and polycyclic aromatic hydrocarbons and other properties of products were determined as described in [3]. The HDO of MP was carried out in the trickle-bed down-flow reactor over Ni<sub>2</sub>P/SiO<sub>2</sub> catalyst

### OP-III-5

mixed with SiC or alumina (volume ratio 1:8); accompanied by GC analysis of liquid and gas phases, as well oxygen analysis using Vario EL Cube analyzer.

To prevent CO<sub>x</sub> formation in the SRGO-RSO hydrotreatment we proposed using the selective MoS<sub>2</sub>/Al<sub>2</sub>O<sub>3</sub> catalyst in the front bed of the reactor and sulfide CoMo/Al<sub>2</sub>O<sub>3</sub> or NiMo/Al<sub>2</sub>O<sub>3</sub> catalysts in the second layer. The comparison of the behavior of CoMo/Al<sub>2</sub>O<sub>3</sub>, NiMo/Al<sub>2</sub>O<sub>3</sub> catalysts and the stacked-bed catalytic systems (MoS<sub>2</sub>/Al<sub>2</sub>O<sub>3</sub>–Co(Ni)Mo/Al<sub>2</sub>O<sub>3</sub>) in the SRGO-RSO hydrotreatment (340°C, 4.0 MPa, H<sub>2</sub>/feed - 600 Nm<sup>3</sup>/m<sup>3</sup>, LHSV- 1.5 h<sup>-1</sup>; RSO content – 10,15 and 30 wt.%) showed, that the quality of the products depends more on the amount of RSO than on the nature of the catalysts. In the case of stacked-bed system we did not detect CO<sub>x</sub> among the reaction products that pointed out to the selective transformation of RSO via HDO routes in the front layer, containing MoS<sub>2</sub>/Al<sub>2</sub>O<sub>3</sub> catalyst. Thus, the cooperation of MoS<sub>2</sub>/Al<sub>2</sub>O<sub>3</sub> catalyst (providing selective HDO of RSO) and traditional hydrotreating catalysts (providing the deep hydrotreating of SRGO) allows ULSD production from SRGO-RSO mixture without CO<sub>x</sub> formation, that increase the yield of diesel fuel and avoid a technological problems associated with the purification of recycle hydrogen.

The study of Ni<sub>2</sub>P/SiO<sub>2</sub> catalyst mixed with the inert (SiC) or acidic (γ-Al<sub>2</sub>O<sub>3</sub>) material in methyl palmitate HDO (250–330°C, 3.0 MPa, H<sub>2</sub>/feed - 600 Nm<sup>3</sup>/m<sup>3</sup>, WHSV 5 h<sup>-1</sup>) let us see, that MP conversion increases significantly when γ-Al<sub>2</sub>O<sub>3</sub> is used instead of SiC. HDO of aliphatic esters into hydrocarbons proceeds through a complicated reaction network, including hydrogenation-dehydrogenation, hydrogenolysis of C–O and C–C bonds, hydrolysis, dehydration reactions. MP conversion to the oxygenated intermediates is shown to be the rate-determining step over the Ni<sub>2</sub>P/SiO<sub>2</sub>–SiC system, and could be increased due to the acceleration of ester hydrolysis over acid sites of alumina of Ni<sub>2</sub>P/SiO<sub>2</sub>–γ-Al<sub>2</sub>O<sub>3</sub> system. Thus, synergism of Ni<sub>2</sub>P/SiO<sub>2</sub> and γ-Al<sub>2</sub>O<sub>3</sub> physical mixture in MP HDO could be explained by the cooperation of the metal sites of Ni<sub>2</sub>P/SiO<sub>2</sub> and acid sites of γ-Al<sub>2</sub>O<sub>3</sub> in the providing of metal- and acid-catalyzed reactions. This observation would play an important role in the development of the effective catalyst for the HDO of fatty acid esters over supported phosphide catalysts.

**Acknowledgement.** The authors are grateful to Dr. I. V. Deliy, Dr. V.P. Pacharukova and Dr. E.Yu. Gerasimov for assistance in this study. The work was supported by the Ministry of Education and Science of the Russian Federation, project № 14.575.21.0128, unique identification number RFMEFI57517X0128.

#### References:

- [1] I.V.Deliy, I.V.Shamanaev, P.V.Aleksandrov et al., *Catalysts* 8 (2018) 515:1-23.
- [2] E.N. Vlasova, G.A. Bukhtiyarova, et al., *Catalysis Today* (2019). DOI: [10.1016/j.cattod.2019.06.011](https://doi.org/10.1016/j.cattod.2019.06.011).
- [3] E.N. Vlasova, I. V. Deliy, A. L. Nuzhdin, et al, *Kinet. Catal.* 55 (2014) 481.

## Some Regularity and Peculiarity of SCR NO-NH<sub>3</sub> Behaviour of Cu-ZSM-5 with Different Copper Electronic State

Yashnik S.A., Ismagilov Z.R.

*Boreskov Institute of Catalysis, Novosibirsk, Russia*

*yashnik@catalysis.ru*

Due to the Euro-6 emission standards for light- and heavy-duty diesel vehicles, ammonia-based selective catalytic reduction of NO<sub>x</sub> (SCR NO-NH<sub>3</sub>) over Cu-zeolite proposed by Komatsu et. al. in 1994 [1] has become again the sought-after technology for NO<sub>x</sub> emissions control [2]. The results reported in this communication focus on UV-Vis DR, DRIFT, and ESR experiments with three Cu-ZSM-5 catalysts during NH<sub>3</sub> adsorption-desorption and SCR NO-NH<sub>3</sub>. The catalysts were previously shown [3] to possess various SCR NO-NH<sub>3</sub> behaviours due to different copper species: the isolated Cu<sup>2+</sup> ions, the structures of Cu<sup>2+</sup> ions with extra-framework oxygen (EFO), and CuO nanoparticles [4]. Cu-ZSM-5 with high concentration of isolated Cu<sup>2+</sup> ions and Cu-structures with EFO exhibited high activity in SCR NO-NH<sub>3</sub> at 180-350 °C, whereas 2%Cu(0)-Cu-ZSM-5 and 3.5%Cu(3)-Cu-ZSM-5 with isolated Cu<sup>2+</sup> ions and CuO-like nanoparticles, respectively, were more active at 350-500 °C [3].

According to TPD-NH<sub>3</sub> and DRIFT, the Cu-ZSM-5 catalysts differ by their capacity to ammonia adsorption. At 25 °C, the sample 2.0%Cu(0)-ZSM-5, having the isolated Cu<sup>2+</sup> ions, adsorbs NH<sub>3</sub> as: 1) weak-bonded on silanol groups (desorbed at 220-240 °C, Fig.1a a.b. 3745 cm<sup>-1</sup>), 2) coordinated in [Cu(NH<sub>3</sub>)<sub>n</sub>]<sup>2+</sup> (300-375 °C), and 3) strong-bonded on SiOHAl (430-450 °C, Fig.1a a.b. 3608 cm<sup>-1</sup>). Their adsorption heats were 75±5, 95±5, 110±10 kJ/mol, respectively. The molar ratio of the NH<sub>3</sub> desorbed in TPD-NH<sub>3</sub> at 300-375 °C to the Cu-content in the sample, ν(NH<sub>3</sub>)/νCu, was close to 1.7-2.0. However, parameters of ESR (g<sub>||</sub> = 2.24, g<sub>⊥</sub> = 2.06, A<sub>||</sub> = 180 G) and UV-Vis DR (d-d transition at 15800 cm<sup>-1</sup>, Fig.1b) spectra illustrated a formation of [Cu(NH<sub>3</sub>)<sub>4</sub>]<sup>2+</sup> complex from [Cu(O)<sub>4</sub>]<sup>2+</sup> during ammonia adsorption. The amount of the adsorbed NH<sub>3</sub>/NH<sub>4</sub><sup>+</sup> (Fig. 1a) as well as ν(NH<sub>3</sub>)/νCu ratio (shift of a.b. to 13500/14100 cm<sup>-1</sup>, n=1-2, Fig.1b) rapidly decreased with an increasing adsorption temperature from 25 to 200-400 °C and under O<sub>2</sub>/(NO+O<sub>2</sub>)-containing mixtures. A twofold decrease of the intensity of the band at 13500 cm<sup>-1</sup> in combination with the appearance of Cu<sup>2+</sup>-Cu<sup>+</sup> IVT at 21800 cm<sup>-1</sup> indicate the reduction of some Cu<sup>2+</sup> ions to Cu<sup>+</sup> under ammonia at 400 °C. These changes were reversible, at least when the ammonia adsorption – desorption cycles (200 – 400 °C) were repeated 5 times.

In comparison with the catalyst 2.0%Cu(0)-ZSM-5, the catalyst 2.9%Cu(6)-ZSM-5 adsorbs a slightly lower amount of ammonia (540 instead of 615 μmol/g<sub>cat</sub>). This was due to low concentration of SiOHAl-groups, while its ratio of ν(NH<sub>3</sub>)/νCu was near 2.5 – 3, and energy of d-d transition was equal to 15200 cm<sup>-1</sup>. Besides, the catalyst 2.9%Cu(6)-ZSM-5 was characterized by lower value of NH<sub>3</sub> adsorption heat (50-95 kJ/mol). At 300 and 400 °C,

## OP-III-6

ammonia was adsorbed in TPD-NH<sub>3</sub> only over the strong sites of the catalyst [3], apparently as NH<sub>4</sub><sup>+</sup>, while there was [Cu(NH<sub>3</sub>)<sub>n</sub>]<sup>2+</sup> (1266-1272 cm<sup>-1</sup> in DFIRT and 13800 cm<sup>-1</sup> in UV-Vis DR) as well as SiO(NH<sub>4</sub><sup>+</sup>)Al (3608 cm<sup>-1</sup>) in SCR NO-NH<sub>3</sub> condition.

The catalyst 3.5%Cu(3)-ZSM-5 with CuO-like nanoparticles showed in TPD-NH<sub>3</sub> experiment an additional ammonia desorption peak - at 175-205 °C attributed to the weakly bound NH<sub>3</sub> adsorbed on the CuO-like species. Its adsorption heat was 55±5 kJ/mol, while the heat of NH<sub>3</sub> adsorption on other 3 types of site decreased to 30-35 kJ/mol, indicating on weakening interaction between ammonia and the catalyst surface.

Under SCR NO-NH<sub>3</sub> conditions (600 ppm NH<sub>3</sub>, 400 ppm NO and 5 vol% O<sub>2</sub>), ammonia adsorption on the catalyst 2.9%Cu(6)-ZSM-5 lasted 1.5-2 hours at 200 °C, then the ammonia appeared in the gas mixture after the catalyst bed, but NO/NO<sub>2</sub> was not detected. Here NH<sub>3</sub> and NO conversion were equal to 42% and 100%, respectively. In (NO+O<sub>2</sub>+Ar) mixture, the strong-bound ammonia was intensively removed at a temperature about 350-400 °C (Fig.1a). After NH<sub>3</sub> removal, NO<sub>2</sub> was registered in the gas mixture (45-50 ppm) as well as on the catalyst surface (1627 cm<sup>-1</sup> in DRIFT), whereas NO concentration was near 200 ppm, and mono/bidentate nitrate groups was observed in DRIFT (1572, 1598 cm<sup>-1</sup>). These facts allow us to conclude that the "fast route" (NO+NO<sub>2</sub>+ 2NH<sub>3</sub> → 2N<sub>2</sub> + 3 H<sub>2</sub>O [1]) of SCR NO-NH<sub>3</sub> took place on 2.9%Cu(6)-ZSM-5.

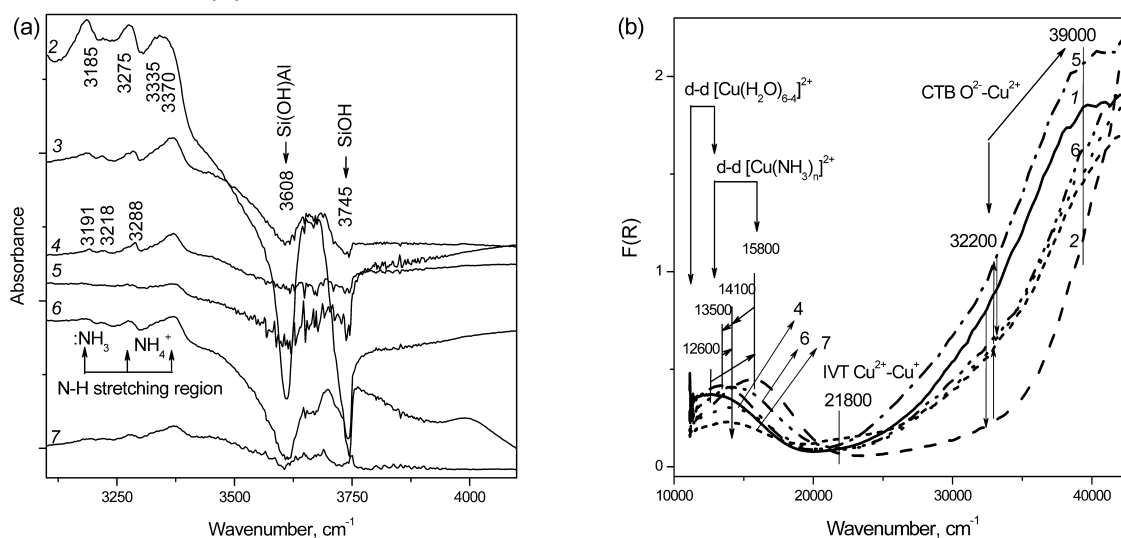


Fig. 1. DRIFT (a, subtracted (1)) and UV-Vis DR (b) spectra of 2.0%Cu(0)-ZSM-5 treated in O<sub>2</sub>/400°C (1) and then (2) NH<sub>3</sub>/25°C, (3) NH<sub>3</sub>/200°C, (4) NH<sub>3</sub>/200°C-(NO+O<sub>2</sub>)/200°C, (5) NH<sub>3</sub>/200°C-(NO+O<sub>2</sub>)/400°C, (6) NH<sub>3</sub>/200°C-(NO+O<sub>2</sub>)/200°C-NH<sub>3</sub>/200°C, (7) NH<sub>3</sub>/200°C-(NO+O<sub>2</sub>)/200°C-NH<sub>3</sub>/400 °C.

**Acknowledgement.** This work was supported by the Ministry of Science and Higher Education (project # AAAA-A17-117041710086-6).

### References:

- [1] T. Komatsu, M. Nunokawa, S. Moon, T. Takahara, S. Namba, T. Yashima, *J. Catal.* 148 (1994) 427.
- [2] J. Li, H. Chang, L. Ma, J. Hao, R. T. Yang, *Catal. Today* 175 (2011) 147.
- [3] S.A. Yashnik, Z.R. Ismagilov, *Top. Catal.* 62 (2019) 179.
- [4] S.A. Yashnik, Z.R. Ismagilov, *Appl. Catal. B.* 170-171 (2015) 241.

## OP-III-7

### **Mechanism of Activation of Molecular Oxygen by Homogeneous Vanadium Substituted Polyoxometalates**

Khenkin A.M.

*Weizmann Institute of Science, Rehovot, Israel*

*alex.khenkin@weizmann.ac.il*

The reactivity of various vanadium-substituted polyoxometalates with different structures and oxidation potentials was compared for the electron transfer-oxygen transfer oxidation of organic substrates. Electron transfer initiates the C-H bond activation. Analysis of reactivity via an outer sphere electron transfer model demonstrates that in addition to the oxidation potential, the polyoxometalate structure and charge are important parameters in the electron transfer reaction. A further comparative study for electron transfer and oxygen transfer reactivity showed that the eventual formation of the oxygenated product, although initiated by electron transfer was dependent on other factors. The reduced vanadium substituted polyoxomolybdates are reoxidized by molecular oxygen whereas vanadium substituted polyoxotungstates are stable to reoxidation under ambient conditions. The reasons for these differences will be discussed.

## Mechanistic Study on the Oxidation of Organic Sulfides and Sulfoxides with H<sub>2</sub>O<sub>2</sub> over Zr-Based Metal-Organic Frameworks

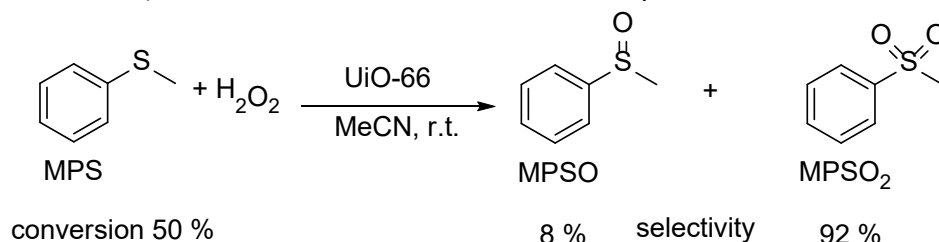
Zalomaeva O.V.<sup>1</sup>, Evtushok V.Yu.<sup>1,2</sup>, Glazneva T.S.<sup>1,2</sup>, Kholdeeva O.A.<sup>1,2</sup>

1 – Boreskov Institute of Catalysis, Novosibirsk, Russia

2 – Novosibirsk State University, Novosibirsk, Russia

zalomaeva@catalysis.ru

Metal-organic frameworks (MOFs) have attracted great attention as potential heterogeneous catalysts due to a unique combination of properties, such as hybrid nature, open crystalline structures, ultrahigh surface areas, tunable pore size and surface properties. Zr-based MOFs are of particular interest due to their outstanding stability [1]. The zirconium terephthalate UiO-66 was found to be active in a range of catalytic reactions, including the oxidative desulfurization of fuels with aqueous H<sub>2</sub>O<sub>2</sub> [2]. The mechanism of H<sub>2</sub>O<sub>2</sub> activation over UiO-66 remains a matter of discussion. The UiO-66-catalyzed oxidation of methyl phenyl sulfide (MPS) with H<sub>2</sub>O<sub>2</sub> in methanol was suggested to involve the formation of electrophilic Zr(IV) hydroperoxo species formed at defect sites of the MOF [3]. However, we found that selectivity of MPS oxidation over UiO-66 and some other Zr-MOFs strongly depends on the solvent nature. When the reaction is carried out in MeCN, the corresponding sulfone becomes the predominated product even at rather low substrate conversions (e.g., 92% selectivity at 50% MPS conversion), which is not characteristic of electrophilic oxidation.



The product analysis of the oxidation of the test substrate thianthrene 5-oxide, Hammett plot and competitive sulfide-sulfoxide oxidation strongly support nucleophilic character of the oxidizing species formed upon interaction of H<sub>2</sub>O<sub>2</sub> and UiO-66 in MeCN. FTIR spectroscopic study using CDCl<sub>3</sub> as a probe molecule confirmed the presence of basic sites in the Zr-MOF that can be responsible for the nucleophilic activation of hydrogen peroxide, leading to the highly selective formation of sulfones.

**Acknowledgement.** This work was supported by the Russian Science Foundation (grant 18-29-04022) and by the Ministry of Science and Higher Education of the Russian Federation (project AAAA-A17-117041710080-4).

### References:

- [1] Y. Bai, Y. Dou, L.-H. Xie, W. Rutledge, J.-R. Li, H.-C. Zhou, *Chem. Soc. Rev.* 45 (2016) 2327.
- [2] C. M. Granadeiro, S. O. Ribeiro, M. Karmaoui, R. Valenca, J. C. Ribeiro, B. de Castro, L. Cunha-Silva, S. S. Balula, *Chem. Commun.* 51 (2015) 13818.
- [3] R. Limvorapitux, H. Chen, M.L. Mendoca, M. Liu, R.Q. Snurr, S.T. Nguyen, *Catal. Sci. Technol.* 9 (2019) 327.

## Methane Activation on Cu/H-ZSM-5 Zeolites: A Spectroscopic Investigation of Methane Interaction with Different Cu-Sites

Gabrienko A.A.<sup>1,2</sup>, Yashnik S.A.<sup>1</sup>, Stepanov A.G.<sup>1,2</sup>

1 – Boreskov Institute of Catalysis, Novosibirsk, Russia

2 – Novosibirsk State University, Novosibirsk, Russia

*gabrienko@catalysis.ru*

### Scope

Nowadays, zeolites loaded with copper attract much attention as potential catalysts for methane processing to valuable chemicals via selective oxidation to methanol [1, 2]. Performed fundamental and applied studies admit a crucial role of  $\text{Cu}^{2+}$  and/or  $\text{Cu}^+$  cationic species present in the zeolites for methane activation [3-6]. Though, the mechanism of methane activation, for instance, the pathway of methane C–H bond dissociation (homolytic or heterolytic), is still unknown. Therefore, it is an interesting problem to investigate the interaction of methane with different Cu-sites that might be present in zeolites in order to inquire into the mechanism of methane-to-methanol transformation.

This paper presents a summary of our work devoted to the study of the properties of Cu-containing zeolites with respect to methane chemical activation. Particularly, the ability of different Cu-species, isolated  $\text{Cu}^{2+}$  cations and CuO-like clusters, introduced into the HZSM-5 zeolite to provide methane C–H bond dissociation have been investigated. A set of the spectroscopic methods, namely, DRIFTS, UV–vis DRS, and solid-state MAS NMR has been applied aiming to obtain valuable information on the peculiarities of methane interaction with the surface sites of Cu/H-ZSM-5 zeolite.

### Results

For such study, it is crucial to characterize the state of Cu-sites in the zeolite reliably.

Therefore, the state and composition of  $\text{Cu}^{2+}$  species loaded into the H-ZSM-5 zeolite via

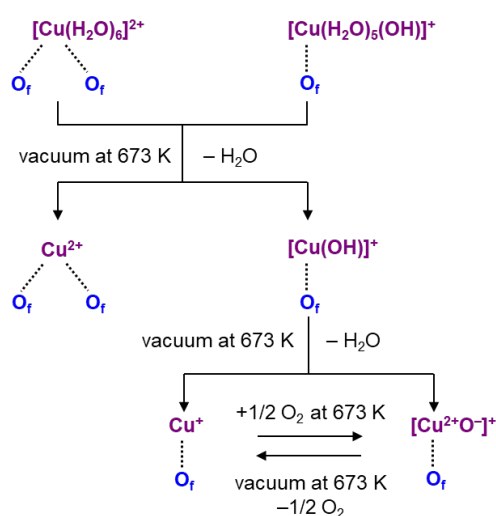


**Figure 1.** Formation of different Cu-sites in a Cu/H-ZSM-5 zeolite.

different approaches have been analyzed with UV–vis DRS method. The formation of isolated  $\text{Cu}^{2+}$  cations of different composition attached to the surface Si–O–Al sites of the zeolite as well as CuO small clusters inside the zeolite channels has been observed and rationalized taking into account previously reported data (Figure 1).

The specific interaction of methane adsorbed at the Cu/H-ZSM-5 zeolite with different Cu-sites has been also studied with in situ spectroscopic techniques. DRIFTS has revealed the formation of the molecular complex between methane and isolated  $\text{Cu}^{2+}$  sites which is characterized by

### OP-III-9

polarized C–H bond. The polarization of the C–H bond in such molecular complex leads to the weakening of the bond and, therefore, its efficient dissociation on  $\text{Cu}^{2+}$  and CuO sites. This proposition has been confirmed by the monitoring of the promoting effect of Cu species on the H/D exchange between methane and Brønsted acid sites of the Cu/H-ZSM-5 zeolites with  $^1\text{H}$  MAS NMR approach in situ.

The surface intermediates formed after methane C–H bond dissociation on  $\text{Cu}^{2+}$  sites have been detected with  $^{13}\text{C}$  CP/MAS NMR spectroscopy. It has been obtained that methane chemical activation assisted by both  $\text{Cu}^{2+}$  sites and Brønsted acid sites has led to surface methoxy species which is considered to be an intermediate towards methanol formation.

The mechanism of methane activation has been offered (Figure 2).

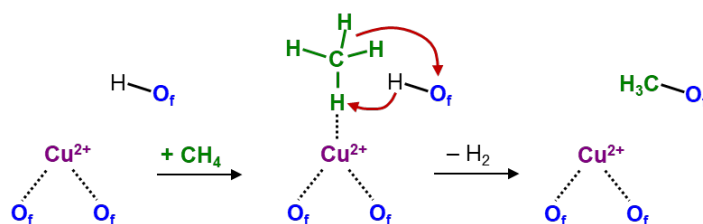


**Figure 2.** Methane activation on  $\text{Cu}^{2+}$  sites of a Cu/H-ZSM-5 zeolite.

Further, the properties of surface methoxy species to interact with various substrates (water, CO, benzene, etc.) have been monitored with  $^{13}\text{C}$  CP/MAS NMR. Possible pathways, alternative to methane-to-methanol reaction, of methane chemical transformation have been established.

**Acknowledgement.** This work was supported by Russian Science Foundation (grant no. 18-7300016).

#### References:

- [1] E.M.C. Alayon, M. Nachtegaal, M. Ranocchiari, J.A. van Bokhoven, CHIMIA 66 (2012) 668.
- [2] P. Vanelderen, R.G. Hadt, P.J. Smeets, E.I. Solomon, R.A. Schoonheydt, B.F. Sels, J. Catal. 284 (2011) 157.
- [3] G. Li, P. Vassilev, M. Sanchez-Sanchez, J.A. Lercher, E.J.M. Hensen, E.A. Pidko, J. Catal. 338 (2016) 305.
- [4] S. Grundner, M.A.C. Markovits, G. Li, M. Tromp, E.A. Pidko, E.J.M. Hensen, A. Jentys, M. Sanchez-Sanchez, J.A. Lercher, Nat. Commun. 6 (2015) 7546.
- [5] P. Tomkins, A. Mansouri, S.E. Bozbag, F. Krumeich, M.B. Park, E.M.C. Alayon, M. Ranocchiari, J.A. van Bokhoven, Angew. Chem. 128 (2016) 5557.
- [6] S.E. Bozbag, E.M.C. Alayon, J. Pecháček, M. Nachtegaal, M. Ranocchiari, J.A. van Bokhoven, Catal. Sci. Technol. 6 (2016) 5011.

## Differential Selectivity Patterns of Mizoroki-Heck Reaction: Novel Data on the Reaction Mechanism and Active Species Nature

Kurokhtina A.A., Larina E.V., Yarosh E.V., Lagoda N.A., Schmidt A.F.  
*Chemical Department of Irkutsk State University, Irkutsk, Russia*  
*kurokhtina@chem.isu.ru*

Mizoroki-Heck reaction has been intensively studied for two last decades. Some fundamental aspects of the mechanism of catalytic systems operation established to the moment are commonly accepted and don't raise any questions. However, some principal issues of the reaction mechanism are still debated. Namely, the data on the type of active Pd complexes (cationic, anionic, or neutral) reported in literature are controversial. Also there are the papers considering 'ligand-free' nature of active species despite the presence of organic ligands in the catalytic system, whereas other ones propose presence of organic ligands in the coordination sphere of active complexes. In our opinion, reliable data on the nature of active catalyst can be obtained by the studies of differential selectivity of the catalytic systems. Differential selectivity is independent on the active species concentration (that may vary significantly under varying experimental conditions) and is determined by the nature of such species only, so any changes of its value is indicative of the changes of active species. Such changes can be easily tracked by using phase trajectories of the reaction. We carried out comparative study of differential selectivity of Mizoroki-Heck reaction with aryl bromides using 'ligand-free' and phosphine-containing catalytic systems under competition of two alkenes. The insensitivity of the differential selectivity to the nature of halide anions presenting in the reaction system along with its sensitivity to the additives of tertiary phosphine ligand indicated entrance of the latter in the coordination sphere of active Pd species participating in the elementary step determining the reaction selectivity of competing alkenes. At the same time, the regioselectivity of  $\alpha$ - and  $\beta$ -arylated alkenes strongly depended on both the concentration and nature of phosphine ligands and halide anions presenting in the system pointing to the entrance of both halide anions and phosphine ligand in the coordination sphere of the active complexes responsible for the formation of the regioisomers. Moreover, based on the analysis of kinetic models corresponding to different hypotheses of the catalytic cycle mechanism, the insensitivity of differential selectivity of competing alkenes to the presence of different halide salts along with the dependence of differential regioselectivity of  $\alpha$ - and  $\beta$ -regioisomers on the nature of such salts unambiguously points to presence of an irreversible elementary step between two steps of the catalytic cycle determining the values of these two selectivities.

**Acknowledgement.** This work was supported by the Russian Science Foundation, grant 19-73-10004.

## New Macromolecular Cross-Metathesis Reaction in the Mixtures of Polynorbornene with Polydienes Mediated by Grubbs' Catalysts: A Kinetic Study

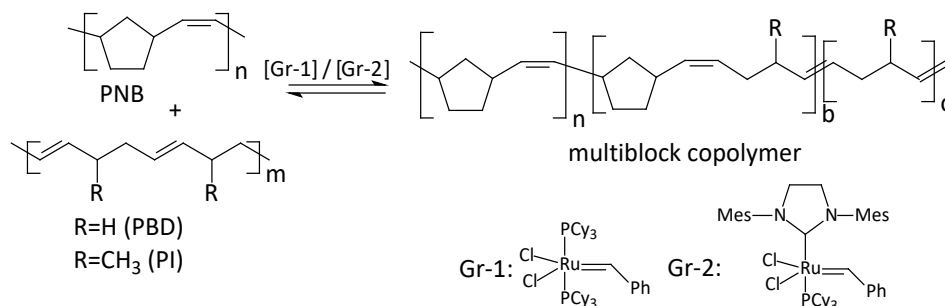
Morontsev A.A.<sup>1</sup>, Denisova Yu.I.<sup>1</sup>, Gringolts M.L.<sup>1</sup>, Peregudov A.S.<sup>2</sup>, Kudryavtsev Y.V.<sup>1</sup>,  
Finkelshtein E.Sh.<sup>1</sup>

<sup>1</sup> – A.V. Topchiev Institute of Petrochemical Synthesis RAS, Moscow, Russia

<sup>2</sup> – A.N. Nesmeyanov Institute of Organoelement Compounds, RAS, Moscow, Russia  
gringol@ips.ac.ru

The cross-metathesis reaction between various polymers containing carbon double bonds in the main chain is a new approach to the synthesis of statistical multiblock copolymers (MBC) with interesting mechanical properties and enhanced durability [1]. Through the interaction of commercial polynorbornene (“Norsorex”) and polycyclooctene (“Vestenamer”), we obtained new norbornene (NB) and cyclooctene (CO) MBC, which are difficult to obtain from the corresponding monomers [2]. Based on the study of the polynorbornene (PNB) and polycyclooctene (PCO) reaction kinetics, the sequence of individual stages was determined and a kinetic model of the process was developed [3].

In this work, new MBCs were synthesized from PNB and industrial polydienes, namely, polybutadiene (PBD) and *cis*- and *trans*- polyisoprene (PI) in the presence of Ru-carbene Grubbs' catalysts. The conditions for obtaining copolymers with different average block lengths were determined and thermal and crystalline properties of the copolymers were studied. The kinetics of the process was investigated by *in situ* <sup>1</sup>H NMR monitoring of the transformations of Ru-carbene complexes as the reaction active centers, and by *ex situ* <sup>13</sup>C NMR control of the chain structure and degree of MBC blockiness.



It was found that in the PNB/PBD system, along with the MBC, cyclooligomers are formed as a result of intramolecular metathesis, mainly in the chains of PBD. The cyclooligomers yield can be reduced by increasing the polymers concentration in the reaction mixture.

For the first time the influence of the monomer unit stereo-structure on the cross-metathesis reaction of polymers was studied for *cis*- and *trans*- PI. It was established that the isomerization of *cis*-C=C to *trans*-C=C in *cis*-PI and *trans*-C=C to *cis*-C=C in *trans*-PI proceeded during the cross-metathesis. *Trans*-C=C bonds in PI are more active both in the isomerization reaction and in the cross-metathesis with PNB. Grubbs' catalyst of the 2nd generation allows

### OP-III-11

one to change the average block length in the copolymers over a wide range, up to 4.5 monomer units. PI is the least active polymer in the reaction with PNB in the series of previously studied polycycloctenes and polydienes. This could be explained by low activity of tri-substituted double C=C bonds in the metathesis reaction. The applicability of the previously developed kinetic model for the description of the studied process was shown. The constants of the elementary stages of the process were determined. The fastest of them is the interaction of Ru-PNB carbenes with double bonds in PBD chains. It proceeds two orders of magnitude faster than the interaction of Ru-PBD carbenes with double bonds in PNB chains. The reaction mechanism and possible reasons for different polymer reactivities are discussed.

**Acknowledgement.** This work was supported by the Russian Foundation for Basic Research (Project 17-03-00596)

#### References:

- [1] M. Gringolts, Yu. Denisova, E. Finkelshtein, Y. Kudryavtsev, Beilstein J. Org. Chem. 15 (2019) 218.
- [2] M.L. Gringolts, Yu.I. Denisova, G.A. Shandryuk, L. B. Krentsel, A.D. Litmanovich, E.Sh. Finkelshtein, Y.V. Kudryavtsev, RSC Adv. 5 (2015) 316.
- [3] Yu. Denisova, M. Gringolts, A.S. Peregudov, L.B. Krentsel, E. A. Litmanovich, A. D. Litmanovich, E. Sh. Finkelshtein, Y. V. Kudryavtsev, Beilstein J. Org. Chem. 11 (2015) 1796.

## Different Efficiency of $Zn^{2+}$ Cations and ZnO Species in Activation of Propane on Zn-Modified Zeolite BEA

Arzumanov S.S., Gabrienko A.A., Toktarev A.V., Stepanov A.G.  
 Boreskov Institute of Catalysis, Novosibirsk, Russia  
 stepanov@catalysis.ru

### Introduction

Zinc containing zeolites represent efficient catalysts for aromatization of  $C_{2+}$  alkanes. [1] The role of different zinc species as well as Brønsted acid sites (BAS) should be understood in details to unravel the successive stages of alkane transformation and improve technology for alkane aromatization. In this study, in situ MAS NMR spectroscopy was applied to clarify activation and conversion of propane on zinc-modified zeolite. Two zeolite catalysts, containing either  $Zn^{2+}$  cations or small ZnO clusters ( $Zn^{2+}/HBEA$  and  $ZnO/HBEA$  samples) were specially synthesized. Kinetics of H/D exchange of propane with BAS and propane conversion, was studied to explore peculiarities of propane interaction with zinc species of different nature.

### Results and Discussion

$Zn^{2+}/HBEA$  zeolite containing  $Zn^{2+}$  cations provides regioselective H/D exchange of BAS with methyl groups of propane. The rate is higher by one order of magnitude and activation

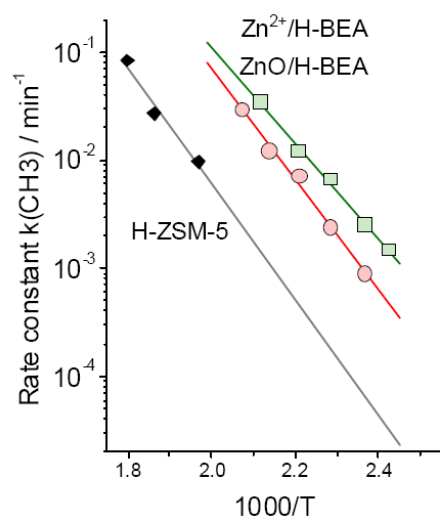


Fig.1. Arrhenius plot for the H/D exchange in methyl groups of propane on H-ZSM-5,  $Zn^{2+}/HBEA$ , and  $ZnO/HBEA$  zeolites.

energy is lower compared to the H/D exchange for propane on pure-acidic zeolite (Fig.1). Much slower rate was observed for H/D exchange in the  $CH_2$  group of propane on  $Zn^{2+}/HBEA$  (Fig.2) with the kinetic parameters similar to pure-acid form zeolite. It was suggested that  $Zn^{2+}$  cations form a transient complex [2] of BAS with C-H bond of methyl group of propane providing a significant promotion of the hydrogen exchange in propane methyl groups. The absence of accelerating effect of Zn on H/D exchange with the  $CH_2$  implied occurrence of the exchange of this group of propane with involvement of pentacoordinated carbonium ion as a transition state. [3]

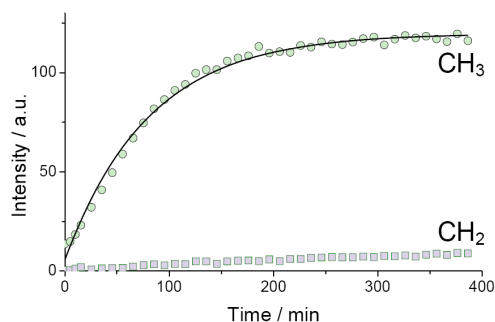


Fig.2. Kinetics of H/D exchange in propane-D<sub>8</sub> on Zn<sup>2+</sup>/H-BEA zeolite at 453K.

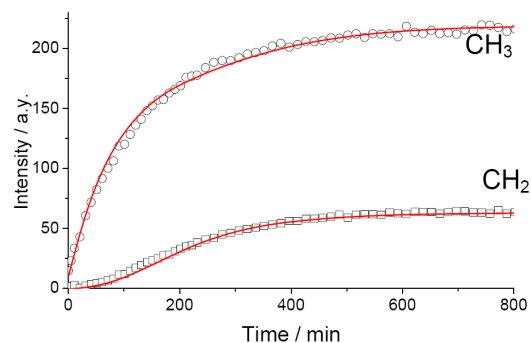


Fig.3. Kinetics of H/D exchange in propane-D<sub>8</sub> on ZnO/H-BEA zeolite at 453K.

Different kinetic behaviour for H/D exchange was observed for ZnO/HBEA zeolite. Both CH<sub>2</sub> and CH<sub>3</sub> groups of propane are involved in the H/D exchange with equal rates, but higher than for pure acid form zeolite. However, the CH<sub>2</sub> kinetics exhibits an induction period for ca. 100 min (Fig.3). Regioselective H/D exchange in the methyl groups during induction period is succeeded presumably by intramolecular process of hydrogen scrambling which can be provided by carbenium-ion species (isopropyl cation). This hypothesis is supported by <sup>13</sup>C MAS NMR data showing formation of small amounts of propylene on ZnO/HBEA zeolite at the end of induction period. Protonation of propane by BAS can provide isopropyl cation formation. Interestingly, Zn<sup>2+</sup>/H-BEA performs propane dehydrogenation easier, compared to ZnO/H-BEA. However, the formed propylene does not violate the regioselectivity of the H/D exchange in the methyl groups. The reason could be a higher stability of propylene complex with Zn<sup>2+</sup> cations, which does not allow protonation of propylene. Thus, different kinetic behaviour of H/D exchange for Zn<sup>2+</sup>/H-BEA and ZnO/H-BEA zeolites reflecting difference in activation of propane by these differently modified with Zn zeolites may be related with different stability of propene complex with Zn<sup>2+</sup> cations and ZnO species.

**Acknowledgement.** The research was supported by Russian Science Foundation, grant 19-43-04101).

#### References:

- [1] Y. Ono, Catal. Rev.-Sci. Eng. 34 (1992) 179.
- [2] S.S. Arzumanov, A.A. Gabrienko, D. Freude, A.G. Stepanov, Catal. Sci. Technol. 6 (2016) 6381.
- [3] S.S. Arzumanov, S.I. Reshetnikov, A.G. Stepanov, V.N. Parmon, D. Freude, J. Phys. Chem. B 109 (2005) 19748.

## Interaction of Ethylene with Methane and its Pyrolysis Products on a Resistive FeCrAl Alloy Catalyst

*Sigaeva S.S., Anoshkina E.V., Temerev V.L., Shlyapin D.A.  
Center of New Chemical Technologies BIC, Omsk, Russia  
s\_in\_cube@mail.ru*

The methane molecule does not contain specific centers and has high bond strength of C-H, so its activation for subsequent conversion into valuable products requires high temperatures and the presence of homogeneous or heterogeneous catalysts [1]. Technologies of involvement of methane in reactions with participation of other hydrocarbons are of special interest. Such processes carry out either in two stages [2] or in two-section reactors [3,4]. The ideas of physical separation or separate fulfillment of various stages of chemical process are the cornerstone of a way. At the same time, each stage proceeds under optimal conditions.

The investigation of the joint methane and ethylene transformation in the two-section reactor with activation of methane on a surface of the FeCrAl alloy spiral was the purpose of this work.

Process takes place in the T-shaped reactor. The FeCrAl alloy spiral heated by electric current is located in the bringing tube on a joint with the main section. The spiral, which is heated to 700-1100 °C, are blown by cold gas mixture consisting 15-75 % methane in nitrogen or pure nitrogen. On the border of the first and second sections there is a contact of the stream containing pyrolysis products (including methyl radicals) with ethylene – nitrogen mixture (30 % C<sub>2</sub>H<sub>4</sub>). The following facts were established: a significant increase in the conversion of ethylene in contact with the flow of methane-nitrogen mixture which was converted on the FeCrAl spiral, a decrease in the yield of acetylene and trans-butene - the products of ethylene conversion and an increase in the yields of propylene, propadiene and isobutene - the products of the interaction of ethylene with methyl radicals. This facts can be interpreted as evidence of the interaction of methyl radicals with ethylene. Increasing the temperature of the FeCrAl alloy spiral leads to an increase in the yield of the main products, except for propylene. The maximum in the yield of propylene is observed at a temperature of 950-1000 °C. The increase of methane concentration in the mixture leads to an increase in ethylene conversion and increases the yield of isobutene, as well as the yield of trans-butene and acetylene decreases. The maximum propylene yield is achieved at the following conditions: 1) 30% methane concentration in the gas mixture; 2) flow rate of 200 ml/min; 3) temperature of FeCrAl alloy spiral - 900 °C. The mechanism of the main products formation providing the stage of interaction of ethylene and methyl radicals is offered (Fig. 1).



## Kinetics of Levulinic Acid Hydrogenation to Gamma-Valerolactone Using Ru-Containing Polymeric Catalysis

Matveeva V.G., Protsenko I.I., Nikoshvili L.Zh., Sulman E.M.  
*Tver Technical University, Tver, Russia*  
*sulman@online.tver.ru*

The advanced biofuels of the second generation are mainly produced from lignocellulosic biomass, one of the most inexpensive and abundant raw materials. Levulinic acid (LA) is a substance, which can be obtained from cellulosic biomass via acid hydrolysis [1]. Hydrogenation of LA to gamma-valerolactone (GVL) is one of the most promising reactions in the field of biomass valorization to fine chemicals and liquid transportation fuels [2]. Investigations are mainly focused on hydrogenation of LA and its esters by molecular hydrogen in the presence of metal catalysts. Application of supported metal catalysts is especially advantageous, owing to simplicity of product recovery and catalyst recycling [3]. Currently, the conventional catalyst of the LA hydrogenation is 5%-Ru/C [4], the use of which allows achieving high yields of GVL. In order to achieve high degrees of the LA conversion, the use of ruthenium nanoparticles (NPs) with high surface areas is important. However, for successful use of Ru NPs in the LA hydrogenation the former should be stabilized. A successful solution to this problem is possible via the use of stabilizing agents, the most promising among which are porous polymers.

This work is devoted to the use of ruthenium containing catalysts based on hyper-cross-linked polystyrene (HPS) in hydrogenation of LA to GVL. Ru-containing NPs immobilized in HPS were synthesized at variation of Ru loading and type of HPS (functionalized or without functional groups). Hydrogenation of LA was carried out in Parr Series 5000 Multiple Reactor System in aqueous medium. Samples of reaction mixture were analyzed via HPLC method.

Influence of substrate-to-catalyst ratio, reaction temperature and hydrogen partial pressure was investigated. Kinetic modelling was carried out by formal kinetic approach and all constants were calculated using well established Levenberg-Marquardt algorithm. It was found that the behaviour of HPS-based catalysts containing RuO<sub>2</sub> as an active phase is in good agreement with Langmuir-Hinshelwood mechanism considering uncompetitive adsorption of the reagents.

**Acknowledgement.** This work was supported by the Russian Foundation for Basic Research (project 18-58-80008).

### References:

- [1] D. Sivasubramaniam, N.A.S. Amin, Chem. Eng. Transactions, 45 (2015) 907.
- [2] R.O.M.A. De Souza, L.S.M. Miranda, L. Rafael L., Green Chem., 16 (2014) 2386.
- [3] M.G. Al-Shaal, M. Calin, I. Delidovich, R. Palkovits, Catal. Commun., 75 (2016) 65.
- [4] M. Selva, M. Gottardo, A. Perosa, ACS Sustain. Chem. Eng., 1 (2013) 180.

**Stereospecific Propylene Polymerization over Supported Titanium-Magnesium Catalysts: Study of the Effect of Catalyst Composition on the Distribution of Active Sites According to Stereospecificity**

Zakharov V.A., Nikolaeva M.I., Matsko M.A., Barabanov A.A., Sukulova V.V.  
*Boreskov Institute of Catalysis, Novosibirsk, Russia*  
*zva@catalysis.ru*

Supported titanium-magnesium catalysts (TMC) are multisite catalytic systems; they contain different types of active sites (AS) which produce polypropylene (PP) with different stereoregularity. In this case polymer produced is the composite, which contains the individual fractions of PP with different stereoregularity. The modern method of the fractionation of polymers (temperature rising elution fractionation – TREF) allows to separate the PP on individual fractions, with different isotacticity which are formed on different types of active sites. So experimental data on the formation and distribution of these PP fractions correspond to the formation and distribution of active sites with different stereospecificity in the catalytic system.

We have used for study the method of preparative fractionation (p-TREF) for analysis of PP samples produced over TMC with composition  $\text{TiCl}_4/\text{MgCl}_2$  nID +  $\text{AlEt}_3/\text{ED}$  (ID – electronodonor compound in the composition of supported catalysts, ED – electronodonor compound introduced into polymerization together with  $\text{AlEt}_3$  cocatalyst).

Data are obtained on the effect of the composition of this catalytic system on the amount and distribution of individual PP fractions with different isotacticity which are formed on four types of active sites: nonstereospecific sites (NS), sites with low isospecificity (IS1), isospecific sites (IS2) and highly isospecific sites (IS3).

The scheme of the formation of active sites with different isospecificity is discussed and possible mechanisms of the effect of ID and ED on the formation and distribution of these sites.

Data on values of propagation rate constant ( $K_p$ ) at polymerization on the active sites with different isospecificity are obtained by method of inhibition of polymerization with  $^{14}\text{CO}$ . It is found  $K_p$  values increase in the row active sites:  $\text{NS} < \text{IS1} < \text{IS2} < \text{IS3}$ . These data correlate with data on the increase of molecular mass of PP produced on these sites.

**Acknowledgement.** This work was carried out under the budget project no. 0303-2016-0009 for Boreskov Institute of Catalysis.

## Olefins and Dienes Polymerization over Ziegler-Natta Catalysts Modified with Various Chlorohydrocarbons

Salakhov I.I.

*R&D Centre PJSC Nizhnekamskneftekhim, Nizhnekamsk, Russia*

*i.i.salahov@gmail.com*

Processes of polymerization of dienes and olefins in the presence of various Ziegler-Natta-based catalyst systems causes natural interest due a high stereospecificity of the catalysts. Studies of this kind are connected mainly with attempts to improve stereospecificity of the rubbers, in terms of PP – to achieve better isotacticity and crystallinity, concerning PE – to achieve control over its molecular characteristics, copolymer density within a wide range and comonomer distribution. Meanwhile, the activity of the polymerization system of monomer is also important being responsible for catalyst performance.

As known, classical Ziegler-Natta catalysts used in ionic-coordinate polymerization of olefins and dienes represent a combination (or a complex) of transition metal (Me) and aluminum alkyl (AA).

Due interaction between Me and AA occur a formation of active sites, enabling to synthesis of the stereospecific polymers [1,2]. However, for such types catalysts metal reduction reactions by aluminum alkyl are typical and as a result, decreasing of activity of the catalyst system. [1,3]. Therefore, for maintaining of the activity of Ziegler-Natta catalysts additionally alkyl aluminum chlorides are used. At the same time, the use of alkylaluminum chlorides (AACl) in the synthesis of a catalytic complex has several significant drawbacks: these substances are pyrophoric, have a high cost, and are unstable to moisture and oxygen.

One of the ways to active of Ziegler-Natta catalysts is an introduction of chlorine-containing hydrocarbon compounds (CCHC) in the catalytic complex or direct to the polymerization process, allowing to reactive of catalyst.

This report presents the results of studies of the effect of chlorine-containing hydrocarbons on various types of Ziegler-Natta catalysts on titanium-magnesium (Ti-Mg) and vanadium (V) in (co)polymerization of olefins, and as well as on neodymium (Nd) in butadiene polymerization. Chlorohydrocarbons, which are aliphatic, alicyclic, cyclodiene, and aromatic compounds with a different content of chlorine atoms, are considered. Kinetic of polymerization of olefins and dienes in presence of chlorohydrocarbons was considered, comparative data was presented on the effectiveness of their influence on the process, and a mechanism for the activation of catalytic systems was proposed.

It has been shown that the alicyclic compound in the process of polymerization of both propylene and ethylene shows a significant increase in the activity of the Ti-Mg catalyst, as well as an improvement in the morphology of polypropylene and polyethylene particles.

## OP-III-16

In the process of polymerization of butadiene on the Nd catalyst instead of alkyl aluminum chloride, was proposed to use of hexachloro-p-xylene (HCPX), which is a cheap, low-toxic and non-flammable product. It has been established, that Nd catalyst with hexachloro-p-xylene has a high polymerization rate of butadiene, comparable to the catalysts obtained in the presence of alkyl aluminum chlorides [4]. It is noted that in polybutadiene, synthesized on a catalyst with hexachloro-p-xylene, the molecular weight distribution(MWD) is narrower than that of a polymer obtained in the presence of a catalyst with alkyl aluminum chloride.

At synthesis of ethylene-propylene rubber was investigated an effect of hexachloro-p-xylene in comparison with aliphatic, alicyclic and cyclodiene compounds on the copolymerization of olefins. It was revealed that when hexachloro-p-xylene is added to the V-catalyst, the activity of the catalytic system increases several times as compared with the control synthesis without the addition of CCHC and with other chlorohydrocarbons, which leads to a change in the copolymerization constants. Besides, its introduction has a positive effect on the compositional uniformity of the polymer.

The received results of studying the effect of chlorine-containing hydrocarbon compounds on the polymerization of olefins and dienes in the presence of Ziegler-Natta catalysts have shown, that this direction is one of the effective ways to improve the technology for the synthesis of polyolefins and rubbers, because allows to increase of production units and to solve the problems of improving the quality of polymers by reducing ashes, increasing production safety by using more inert components.

### References:

- [1] W. Saltman, *The Stereo Rubbers* (1977) 897.
- [2] T. Taniike, M. Terano, *Adv. Polym. Sci.* 257 (2013) 81.
- [3] H. Trischler, T. Höchfurtner, M. Ruff, C. Paulik, *Kinetics and Catalysis* 54(5) (2013) 559.
- [4] I. Salahov, I. Akhmetov, V. Kozlov, *Polym. Sci., Ser. B*, 53(2011) 391.

## Effect of Surface Oxidation Degree on Catalytic Activity of Metallic Ni and Co

Bychkov V.Yu., Tulenin Yu.P., Slinko M.M., Korchak V.N.  
*Semenov Institute of Chemical Physics RAS, Moscow, Russia*  
*bychkov@chph.ras.ru*

It is well known that catalytic activities of Ni and Co depend on their oxidation state. Reduced metallic Ni and Co can catalyse partial oxidation of hydrocarbons, methane dry reforming, hydrogenation. On the contrary, nickel and cobalt oxides are active in total oxidation of hydrocarbons. However, only some data can be found in the literature about catalytic activities of Ni and Co at intermediate surface oxidation states. To eliminate this lack we have studied an effect of step-wise oxidation of Ni and Co surfaces on their catalytic activity in ethylene oxidation.

Samples of Ni or Co foils (5\*5 mm) were loaded into a flow-through reactor, pre-reduced in H<sub>2</sub> before catalytic testing and kept in He flow of 20 ml/min. Then the samples were treated by 0.5 ml alternative pulses of the testing reaction mixture (0.2% C<sub>2</sub>H<sub>4</sub>-0.25% O<sub>2</sub>-1% Ar-He) and the oxidizing mixture (1% O<sub>2</sub>-1% Ar-He). A time interval between the pulses was 1 min. Gas compositions of outlet gas were measured with a mass-spectrometer OmniStar GSD 301. Catalytic activities were tested at 600 and 700°C for the Ni foil and at 500, 600, 700, and 800°C for the Co foil. TPR testing in a thermobalance SETSYS EVOLUTION has allowed to estimate oxygen monolayer coatings of the samples: ~0.013 μmol O<sub>2</sub> and 0.063 μmol O<sub>2</sub> for Ni and Co samples correspondingly.

Fig.1 shows gas concentrations in C<sub>2</sub>H<sub>4</sub>-O<sub>2</sub>-Ar-He pulses after their contact with the Ni foil at 600°C. First C<sub>2</sub>H<sub>4</sub>-O<sub>2</sub> pulse contacted with pre-reduced metallic Ni. Following pulses contacted with partially oxidized Ni. It is seen that reduced Ni is active mainly in partial ethylene oxidation to CO and H<sub>2</sub>, slightly oxidized Ni catalyses total oxidation to CO<sub>2</sub> and H<sub>2</sub>O, and more oxidized Ni is much less active. Similar results were observed at 700°C.

Variations of Co catalytic activity were found to depend greatly on the reactor temperature. Although the rate of H<sub>2</sub> and CO production was maximal in first C<sub>2</sub>H<sub>4</sub>-O<sub>2</sub> pulses at all temperatures, this rate remained high at 500 and 600°C with the sample oxidation up to 4 and 2 μmol O<sub>2</sub> correspondingly (see Fig.2a), but decreased fast with the oxidation at 700 and 800°C (Fig.2b). In contrast to Ni, the rate of CO<sub>2</sub> formation did not increase for slightly oxidized Co. At 500°C CO<sub>2</sub> concentration was rather high for metallic Co, remained stable with the sample oxidation up to ~4 μmol O<sub>2</sub>, then decreased twice and kept stable again during further oxidation of the catalyst. On the contrary, at 700°C in the range of oxidation degree of 1-3.5 μmol O<sub>2</sub> the sample had a very low catalytic activity. Unexpectedly, CO<sub>2</sub> formation grew in the oxidation range of 4-5 μmol O<sub>2</sub> and decreased with further oxidation. This phenomenon was observed also at 600°C, but was absent at 800°C.

### OP-III-17

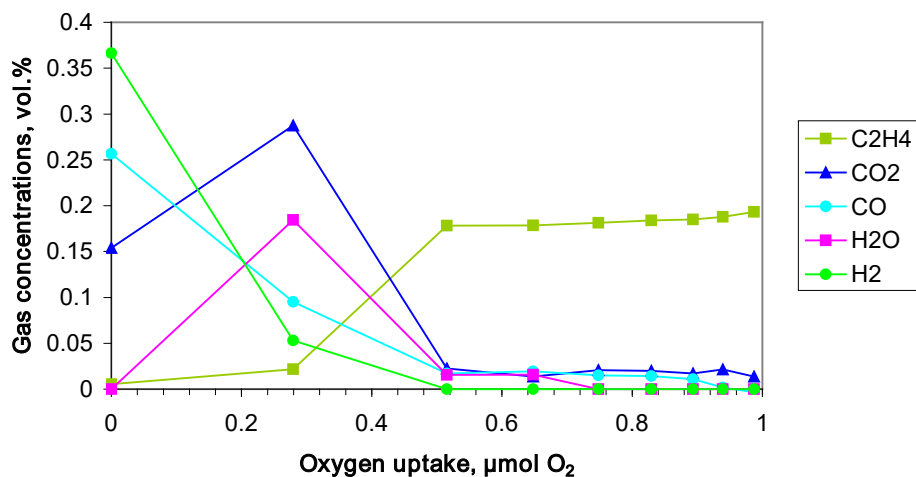


Fig.1 Effect of step-wise oxidation on catalytic activity of Ni foil during ethylene oxidation at 600°C

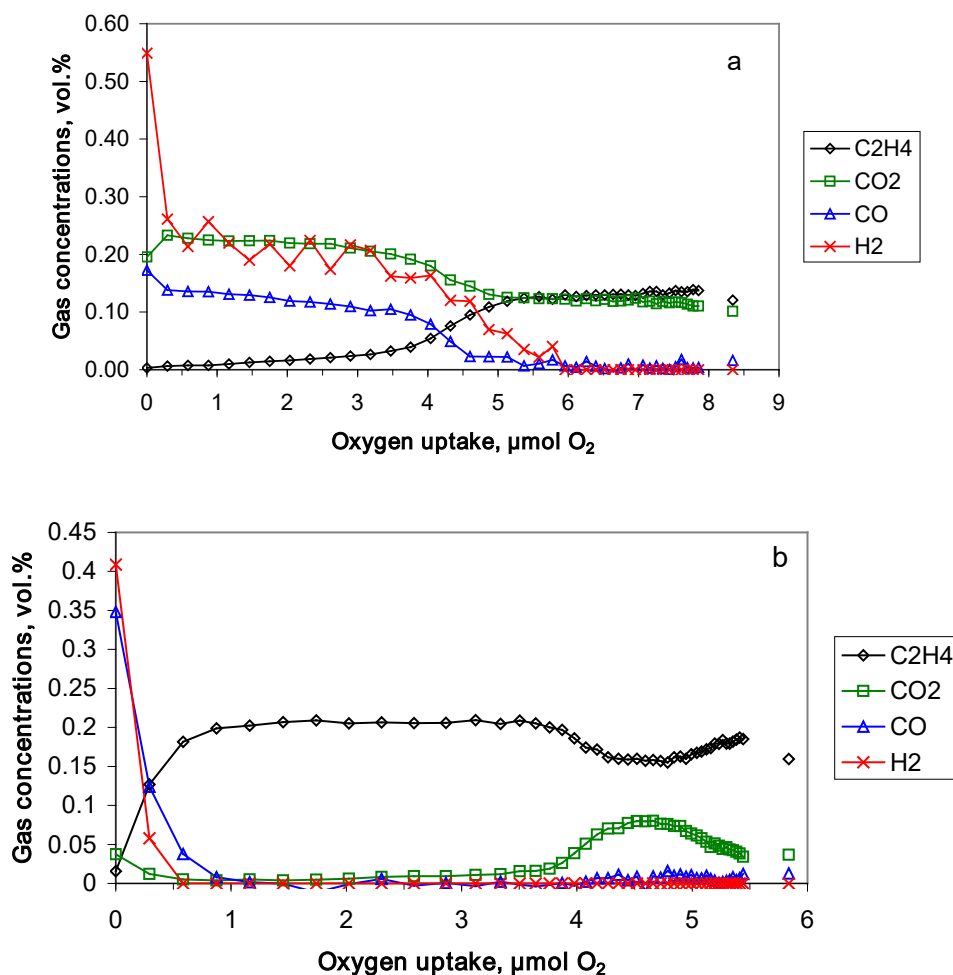


Fig.2 Effects of step-wise oxidation on catalytic activity of Co foil during ethylene oxidation at 500°C (a) and 700°C (b).

**Acknowledgement.** This work was supported by the RFBR, grant 19-03-00096.

**Near Ambient Pressure XPS: New Horizons**

Mammadov S., Socaciu-Siebert L., Meyer M., Dietrich P., Schaff O., Thissen A.  
*SPECS Surface Nano Analysis GmbH, Berlin, Germany*  
*samir.mammadov@specs.com*

Over the last decades, development of XPS systems that can work far beyond the standard ultrahigh vacuum conditions has seen a significant progress. Starting from operando studies of surface reactions in catalysis, the applications soon have been enhanced towards studies of processes at liquid surfaces, mainly using freezing/melting cycles, liquid jets or liquid films on rotation disks or wheels. Thus, Near Ambient Pressure (NAP)-XPS has become a rapidly growing field in research, inspiring many scientists to transfer the method to completely new application fields.

Nowadays, this analysis technique is utilized not only at synchrotrons, but also as standard analysis tool in user friendly laboratory systems. The development of pure laboratory NAP-XPS systems with optimized sample environments, like special sample holders, Peltier coolers and operando liquid cells combined with full automation and process control provides possibilities for the preparation and analysis of a multitude of liquid samples or solid-liquid interfaces on a reliable daily base. Modern NAP-XPS systems can be customized to unique research requirements of each laboratory and give the possibility to perform XPS measurements from UHV to 100 mbar atmosphere environment.

In this work, we present the existing solutions and future development routes to new instruments and material analysis methods being functional under near-ambient working conditions.

A new fully automated NAP-XPS system EnviroESCA, which allows high-throughput analysis of wide range of sample materials and sizes under various environmental conditions will be introduced.

Application examples of existing in situ methods (NAP-XPS or NAP-SPM), such as operando studies of solid-liquid interfaces, solid-gas interfaces for catalyst research applications will be presented.

Finally, opportunities and limits will be discussed from the perspective of a supplier of scientific instruments.

## Coupling Multilayers Regulated by pH with Photocatalytically Active Surface for Bionic Devices and Infochemistry

Ryzhkov N.V.<sup>1</sup>, Nesterov P.<sup>1</sup>, Nikolaev K.<sup>1</sup>, Yurchenko S.O.<sup>2</sup>, Skorb E.V.<sup>1</sup>

1 – ITMO University, Saint Petersburg, Russia

2 – Bauman Moscow State Technical University, Moscow, Russia

skorb@scamt-itmo.ru

We follow how the research moved from light regulated feedback sustainable systems and control biodevices to the current focus on infochemistry in aqueous solution [1]. A major part of the work focuses on the photogeneration and use of localized ion concentration gradient. In situ scanning vibration electrode (SVET) and scanning ion-selective electrode techniques (SIET) are efficient for spatiotemporal evolution of ions on the surface of titania (Figure). pH-sensitive polyelectrolytes (PEs)—here, polyethylenimine (PEI) and poly(sodium styrene sulfonate) (PSS)—multilayers with different PEs architecture are composed with a feedback loop for bionic devices [2].

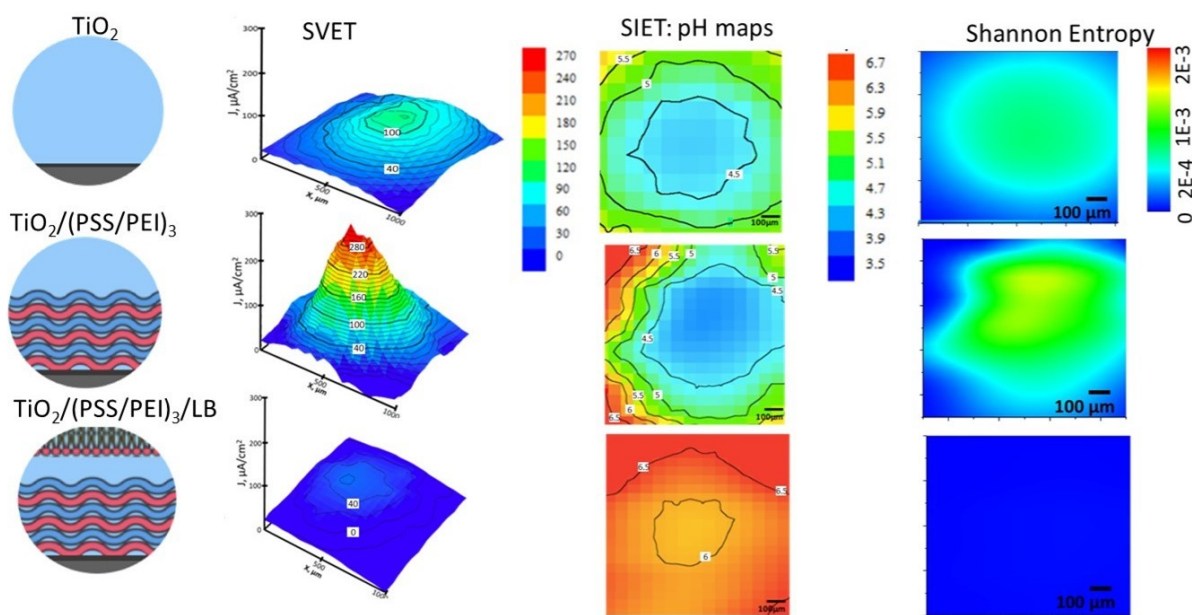


Figure. Representation of photoelectrode–solution interface, anodic activity (SVET current density maps), pH SIET maps, and correlated maps of Shannon entropy of adjusted to electrode media respectively under at 365 nm of  $5 \text{ mW}/\text{cm}^2$  LED irradiation in 50 mM NaCl for bare nanostructured  $\text{TiO}_2$ ,  $\text{TiO}_2/\text{PEs}$ , and  $\text{TiO}_2/\text{PEs}/\text{LB}$ .

We show here that pH-regulated PEs multilayers can change their properties—film thickness and stiffness [3], permeability [4], hydrophilicity, and / or fluorescence [5]—in response to light instead of the classical acid/base titration. The lipid bilayer (LB) was deposited on top of positive polymer cushion from dispersion of negative vesicles and may

## IOP-IV-1

provide efficient termination of proton pumping from the surface localizing them in confined nanovolume which is promising for cosmetic test systems [6].

One more idea is to correlate self-organization vs. Shannon's entropy. Processes of self-organization are discussed [2] to be closely related to change in entropy of the system. Typically, this occurs with spatial change in thermodynamic (as temperature, density, and pressure) as well as chemical parameters and, in particular, ion composition of the system. In our case, the changes of temperature, density, and pressure are negligible, while the local electrochemical influence affects directly the ion-distribution in the solution. Note that the spatial pH-redistribution occurs self-consistently, being accompanied by local electric potential redistribution during the free-energy minimisation of the system. In result, the self-organization and the redistribution of pH-fields are directly associated with each other and, thus, the change of entropy can be illustrated using the fields of pH.

The pH SIET maps were calculated vs total entropy for given discrete spatial distribution of pH (distribution of the system states) can be calculated with summation over the S-values in all spatial points of the system (Figure). This situation with discrete distribution of pH field is typical for experiments we performed, since the size of a 'cell' (small open volume of the solution) wherein pH is measured is determined by the electrode size.

**Acknowledgement.** This work was supported by the Russian Science Foundation, grant 17-79-20186. ITMO Fellowship and Professorship Program is thanked for Infrastructural Support.

### References:

- [1] N. V. Ryzhkov et al. *Langmuir* (2019) DOI: 10.1021/acs.langmuir.9b00633.
- [2] N. V. Ryzhkov et al. *Frontiers in Chem.* (2019) DOI: 10.3389/fchem.2019.00419.
- [3] S. A. Ulasevich et al. *Angew. Chem. Int. Ed.* 55 (2016) 13001.
- [4] S. A. Ulasevich et al. *Macromol. Biosci.* 16 (2016) 1422.
- [5] A. A. Nikitina et al. *Bioconjugate Chem.* 29 (2018) 3793.
- [6] N. V. Ryzhkov et al. *J. Royal Society Interface* 16 (2019) 20180626.

**Organic Molecules Oxidation on Hybrid Titania – Cadmium Sulfide  
Photocatalyst Active under Visible Light**

Rempel A.A.<sup>1,2,3</sup>, Valeeva A.A.<sup>2,3</sup>, Weinstein I.A.<sup>2</sup>, Kozlova E.A.<sup>4</sup>, Dorosheva I.B.<sup>1,2,3</sup>,  
Kuznetsova Yu.V.<sup>3</sup>, Selishchev D.S.<sup>4</sup>

*1 – Institute of Metallurgy UB RAS, Ekaterinburg, Russia*

*2 – NANOTECH Centre, Ural Federal University, Ekaterinburg, Russia*

*3 – Institute of Solid State Chemistry UB RAS, Yekaterinburg, Russia*

*4 – Borekov Institute of Catalysis, Novosibirsk, Russia*

*rempe.limet@mail.ru*

Nanostructural titania attract vast attention of researchers working on creation of photocatalysts for selective oxidation occurring on metal oxide semiconductors under the action of solar light. Photocatalytic processes under the action of solar light attract particular attention because of their potential in environmental restoration [1].

In the present work, material design to create photocatalysts with specified structure and properties were proposed. A new method for the synthesis of complex hybrid titania nanotubes with cadmium sulfide nanoparticles inside nanotubes has been suggested. The method includes a combination of different technique: anodization of Ti foil for titania nanotubes growing [2], chemical condensation of CdS [3], and sol-gel synthesis of TiO<sub>2</sub> [4]. Decoration of titania nanotubes by CdS nanoparticles was performed by centrifuging after the preliminary pumping out of air. Then titania nanotubes with CdS particles inside were covered by TiO<sub>2</sub> produced by sol-gel method. The X-ray diffraction techniques including diffraction under a grazing incident beam, X-ray photoelectron microscopy, high-resolution electron microscopy, and optical methods, have been used to comprehensively evaluate the synthesized samples and determine their chemical and phase composition, as well as the size of the nanoparticles and their morphology. A high activity of the hybrid photocatalysts in oxidation reaction of acetone to carbon under visible light with 450 nm is probably due to heterojunctions between CdS and TiO<sub>2</sub> nanoparticles that provide a more efficient and longer charge separation than pure CdS or TiO<sub>2</sub> does.

**Acknowledgement.** The study was supported by the RFBR (Project No. 17-03-00702).

**References:**

- [1] E.A. Kozlova, V.N. Parmon, Russian Chemical Reviews 86 (2017) 870.
- [2] A.A. Valeeva, E.A. Kozlova, A.S. Vokhmintsev, R.V. Kamalov, I.B. Dorosheva, A.A. Saraev, I.A. Weinstein, A.A. Rempel, Scientific Reports 8 (2018) 9607.
- [3] A.A. Rempel, E.A. Kozlova, T.I. Gorbunova, S.V. Cherepanova, E.Yu. Gerasimov, N.S. Kozhevnikova, A.A. Valeeva, E.Yu. Korovin, V.V. Kaichev, Yu.A. Shchipunov, Catal. Comm. 68 (2015) 61.
- [4] I.B. Dorosheva, A.A. Valeeva, A.A. Rempel, AIP Conference Proceedings, 1886 (2019) 020006.

### OP-IV-3

## Isobutanol Dehydration over Ag-ZP Catalysts Obtained by Sol-Gel Method

Pylinina A.I., Mikhalenko I.I.

Peoples Friendship University of Russia (RUDN-University), Moscow, Russia

imikhalenko@mail.ru

Framework of complex zirconium orthophosphates derived from  $\text{NaZr}_2(\text{PO}_4)_3$  named NZP is of NASICON-type (Na-Super Ionic Conductors) solid electrolytes. This family of ceramic materials promises to be good catalysts for both acid-base and oxidation–reduction reactions due to easy varying its content by replacement of  $\text{Na}^+$  ions or  $\text{Zr}^{+4}$  by cations ( $\text{M}^+$ ,  $\text{M}^{2+}$ ) without structure change. Earlier we reported results about  $\text{M}^{2+}$  in  $\text{Na}_{1-2x}\text{M}^x\text{Zr}_2(\text{PO}_4)_3$  and  $\text{Na}_3\text{ZrM}^+(\text{PO}_4)_3$  with  $\text{Cu}^{+2}$ ,  $\text{Ni}^{+2}$ ,  $\text{Co}^{+2}$ ,  $\text{Zn}^{+2}$  for isopropanol, butanol-1, butanol-2 conversions [1]. Catalysts  $\text{AgZr}_2(\text{PO}_4)_3$ , prepared by sol-gel (SG) and co precipitation methods, were tested in oxidation reactions *ethylene glycol*  $\rightarrow$  *glyoxal* and *ethanol*  $\rightarrow$  *acetaldehyde* [2].

No	Samples, mode of preparation		Py <sub>ads</sub>	$\Sigma W^{\uparrow}_{653}$ %	$S^{\uparrow}_{653}$ %	Ea <sup>↑</sup> kJ/mole
1	$\text{NaZr}_2(\text{PO}_4)_3$	SG, 900°C	7	15 / 18	95 / 100	<b>92 / 96</b>
2	$\text{AgZr}_2(\text{PO}_4)_3$	SG, 900°C	51	54 / 44	100 / 100	<b>44 / 81</b>
3	$\text{AgZr}_2(\text{PO}_4)_3$	SG, 300°C	68	93 / 77	85 / 74	<b>53 / 60</b>
4	$\text{AgZr}_2(\text{PO}_4)_3$	IE, 900°C	48	73 / 26	79 / 70	<b>80 / 129</b>
5	1% $\text{Ag}^+$ / $\text{NaZr}_2(\text{PO}_4)_3$	SG-P, 900°C	28	44 / 25	89 / 69	<b>60 / 108</b>

The present work was aimed at studying of isobutanol dehydrating reaction for desirable product of Isobutene conversion over Ag-ZP (SG). The precursors for SG samples were NaCl and  $\text{ZrOCl}_2 \times 8\text{H}_2\text{O}$  (1),  $\text{AgNO}_3$  and  $\text{ZrN}_2\text{O}_7 \times 8\text{H}_2\text{O}$  (2,3) and  $\text{H}_3\text{PO}_4$ . To compare with NZP and AZP one catalyst was synthesized by ions exchange method of  $\text{Na}^+$  in NZP to  $\text{Ag}^+$  (4) and another by  $\text{AgNO}_3$  impregnation of NZP (5). Specific area of all samples was  $\sim 5\text{-}8 \text{ m}^2/\text{g}$ .

XRD analysis confirmed the similar rhombohedra structure NZP, AZP. For sample 2 the phases  $\text{Zr}_{2,25}(\text{PO}_4)_3$  and  $\text{ZrP}_2\text{O}_7$  were found too. Silver presence increased the surface acidity (pyridine adsorption in mM/g) in 4-10 times. The  $i\text{-C}_4\text{H}_9\text{OH}$  conversion was studied in a flow regime at temperatures 273-673 K (mixture of alcohol vapour and He passed with  $\omega=1.1 \text{ L}\cdot\text{h}^{-1}$  through catalyst's layer  $\sim 2 \text{ mm}$  of thickness, GCh). All catalysts were treated in He flow at 673 K, 1 h and then in Alc+He at 673 K, 1 h (standard procedure). Data of catalytic activity in rising temperature mode ( $\uparrow$ ) are shown in a table for the first (numerator) and repeated tests (denominator): total alcohol conversion  $\Sigma W$  and selectivity of isobutene  $S^{\text{C}=\text{C}}$  at 653 K, apparent activation energy  $Ea^{\text{C}=\text{C}}$ , calculated from the Arrhenius plots of olefin yield.

For 1 and 2 catalysts  $S^{\text{C}=\text{C}}=100\%$ , but in case of 3,4,5 samples dehydrogenation reaction occurred too. The thermal hysteresis was found and discussed for these systems.

#### References:

- [1] E. I. Povarova, A. I. Pylinina, I. I. Mikhalenko, *Prot. Met. and Phys. Chem. Surf.* 50 (2014) 331.  
 [2] N. V. Dorofeeva, V.O.Vodyankina et al. *Studies in Surf. Sci. Catal.* 175 (2010) 759.

## Photocatalytic CO<sub>2</sub> Reduction over Cd<sub>1-x</sub>Zn<sub>x</sub>S-Based Photocatalysts: Effect of the Phase Composition on the Reaction Rate and Product Distribution

Kozlova E.A.<sup>1,2</sup>, Lyulyukin M.N.<sup>1,2</sup>, Markovskaya D.V.<sup>1,2</sup>, Kozlov D.V.<sup>1,2</sup>

1 – Boreskov Institute of Catalysis, Novosibirsk, Russia

2 – Novosibirsk State University, Novosibirsk, Russia

kozlova@catalysis.ru

The chemical binding of CO<sub>2</sub> is an urgent problem not only from the standpoint of its use as a carbon source but also as a method to reduce its concentration in the atmosphere. Carbon dioxide is regarded as a source for production of useful organic compounds [1]. However, CO<sub>2</sub> is the thermodynamically and kinetically stable molecule. Thus, conversion of CO<sub>2</sub> into useful organic compounds can be achieved only under intensive physical exposure. One of the promising techniques is photocatalytic reduction of CO<sub>2</sub>. Among the various photocatalysts used for photocatalytic reduction of CO<sub>2</sub>, metal sulfides (e.g., CdS and Cd<sub>1-x</sub>Zn<sub>x</sub>S) have attracted considerable attention as the photocatalysts for CO<sub>2</sub> reduction under visible light due to their appropriate band gaps and catalytic functions [2].

This study was aimed at the synthesis of Cd<sub>1-x</sub>Zn<sub>x</sub>S solid solutions for the photocatalytic reduction of carbon dioxide under visible light. Photocatalysts, based on solid solutions of cadmium and zinc sulfides, which are sensitive to visible light, were synthesized [3]. The photocatalysts were characterized by X-ray diffraction, UV-VIS diffuse reflectance spectroscopy, and low-temperature N<sub>2</sub> adsorption techniques and were tested in the gas-phase photocatalytic reduction of CO<sub>2</sub> under visible light ( $\lambda = 450$  nm). All the synthesized Cd<sub>1-x</sub>Zn<sub>x</sub>S solid solutions were capable to provide the chemical transformations of CO<sub>2</sub> under the conditions considered. Carbon monoxide and methane were identified as the main carbon dioxide reduction products. It has been shown that Cd to Zn ratio strongly affects the reaction rate and products distribution. The highest activity under the action of visible light was possessed by the photocatalyst Cd<sub>0.91</sub>Zn<sub>0.09</sub>S. It should be noted that the rate of CO<sub>2</sub> reduction in the presence of synthesized sulfide samples is higher than the values for photocatalysts based on cadmium and zinc sulfides recently published in the literature [4]. It was shown that the addition of hydrogen to the system leads to a change in the rate of formation and distribution of CO<sub>2</sub> reduction products under the action of visible light in the presence of sulfide photocatalysts.

**Acknowledgements.** This work was supported by RFBR grant 18-03-00775.

### References:

- [1] T. Sakakura, J.C. Choi, H. Yasuda, *Chem. Rev.* 107 (2007) 2365-2387.
- [2] E.A. Kozlova, V.N. Parmon, *Russ. Chem. Rev.* 86 (2017), 870-906.
- [3] E.A. Kozlova, M.N. Lyulyukin, D.V. Markovskaya, D.S. Selishchev, S.V. Cherepanova, D.V. Kozlov, *Photochem. Photobiol. Sci.* (2019) Advance Article, doi: 10.1039/C8PP00332G.
- [4] X. Meng, G. Zuo, P. Zong, H. Pang, J. Ren, X. Zeng, S. Liu, Y. Shen, W. Zhou, J. Ye, *Appl. Catal. B-Environ.* 237 (2018) 68-73.

**Hydrogenation of Monoterpenoids Catalyzed by Gold and Platinum Catalysts**

Demidova Yu.S.<sup>1,2</sup>, Suslov E.V.<sup>3</sup>, Mozhajcev E.S.<sup>3</sup>, Simakova O.A.<sup>4</sup>, Volcho K.P.<sup>2,3</sup>,  
Salakhutdinov N.F.<sup>2,3</sup>, Simakova I.L.<sup>1,2</sup>, Murzin D.Yu.<sup>5</sup>

1 – Borekov Institute of Catalysis, Novosibirsk, Russia

2 – Novosibirsk State University, Novosibirsk, Russia

3 – Novosibirsk Institute of Organic Chemistry, Novosibirsk, Russia

4 – Georgia Institute of Technology, Atlanta, USA

5 – Åbo Akademi University, Turku/Åbo, Finland

demidova@catalysis.ru

Bio-derived natural extractives such as monoterpenes due to their molecular structure represent very attractive starting materials for the synthesis of fine chemicals, pharmaceuticals and intermediates. Stereo-, regio- and chemoselective hydrogenation of compounds with multiple unsaturations is commonly considered to be of interest for synthesis of the desired products with a high efficiency. The main goal of this work was to expand fundamental knowledge on competitive hydrogenation of different functional groups aiming at the development and improvement of approaches and methodologies for stereo- and chemoselective hydrogenation of monoterpenoids oximes and nitro-derivatives to valuable compounds.

Liquid-phase hydrogenation of the oximes of monoterpenoids and their nitro-derivatives was carried out in a batch reactor at 373-393 K under H<sub>2</sub> atmosphere. The reaction mixture was analyzed by GC, GC-MS and NMR. Gold and platinum catalysts comprising Au and Pt on metal oxides, such as TiO<sub>2</sub>, ZrO<sub>2</sub>, Al<sub>2</sub>O<sub>3</sub>, were prepared by the deposition-precipitation and impregnation methods. The catalysts were characterized by a set of physicochemical methods, including TEM, XPS, to determine the parameters influencing the catalytic activity.

Stereo- and chemoselective carvone hydrogenation to dihydrocarvone catalyzed by Au/TiO<sub>2</sub> catalyst with predominant formation of the *trans*-isomer was reported for the first time [1]. This novel approach is of great interest giving a possibility to obtain industrially valuable dihydrocarvone via direct carvone hydrogenation. The highest total selectivity to dihydrocarvone (62%) was achieved at a nearly complete carvone conversion (90%) after 13 h, with the *trans*-to-*cis*-dihydrocarvone ratio being ca. 1.8.

As a subsequent step, a one-pot process consisting of sequential transformations of carvone oxime, which is a key intermediate in carvone synthesis from limonene to dihydrocarvone, was studied. Dihydrocarvone synthesis was shown to occur via carvone formation with the subsequent hydrogenation of its conjugated C=C double bond (Fig. 1) [2].

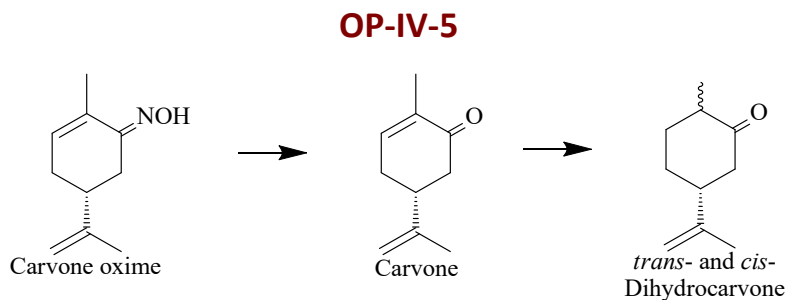


Fig.1. Carvone oxime transformation to *trans*-/*cis*-dihydrocarvone over gold catalysts.

Application of Au/TiO<sub>2</sub> catalyst for both deoxygenation and selective hydrogenation of olefinic C=C functional group is reported for the first time. A combination of these steps provides a possibility to optimize synthesis of dihydrocarvone from carvone oxime. Despite a carvone oxime reaction rate lower than that of carvone, a significant increase in the stereoselectivity towards *trans*-dihydrocarvone was observed when carvone oxime was hydrogenated. The ratio between *trans*- and *cis*- dihydrocarvone was close to 4.0 compared to 1.8 achieved for carvone hydrogenation. Application of the gold catalysts to control selectivity seems to be promising in the particular case of dihydrocarvone synthesis from carvone oxime as well as in consecutive chemoselective hydrogenation of different functional groups in general. The effect of the catalyst support, active metal and the reaction conditions, including solvent, temperature and hydrogen pressure was studied. The reaction regularities for oxime and nitro-derivatives of fenchone, menthone, camphor were also explored and discussed in detail.

**Acknowledgement.** This work was supported by the Russian Science Foundation, grant 18-33-20175.

**References:**

- [1] Yu.S. Demidova, E.V. Suslov, O.A. Simakova, I.L. Simakova, K.P. Volcho, N.F. Salakhutdinov, D.Yu. Murzin, *Catal. Tod.* 241 (2015) 189-194.
- [2] Yu.S. Demidova, E.V. Suslov, O.A. Simakova, I.L. Simakova, K.P. Volcho, N.F. Salakhutdinov, D.Yu. Murzin, *J. Mol. Catal.* 420 (2016) 142-148.

## The Effect of Template Nature and the Composition of Double and Triple Oxide Catalysts Based on CeO<sub>2</sub> in CO Oxidation

Lokteva E.S., Kaplin I.Yu., Golubina E.V., Maslakov K.I., Zhilyaev K.,  
Shishova V.V., Tikhonov A.V.

*Lomonosov Moscow State University, Moscow, Russia*  
*e.lokteva@rambler.ru*

Mixed oxide catalysts on the base of ceria demonstrate promising properties in various catalytic reactions, including CO oxidation [1,2]. Additional improvement of low-temperature activity can be achieved by modification with the oxides of the metals with changeable oxidation state, such as CuO<sub>x</sub> [3] or MnO<sub>x</sub> [4]. The structure and texture of the catalyst have strong influence on catalytic action and can be influenced using different templates during synthesis. The aim of this work was to track the influence of the template nature on the catalytic action of CeZrO<sub>x</sub> (CZ, Ce:Zr=4) and CeSnO<sub>x</sub>, pristine and modified with MnO<sub>x</sub> or CuO<sub>x</sub>. Three types of templates were used: surfactant etyltrimethylammonium chloride (CTAB), polymer Pluronic 123 and biotemplate wood sawdust (SD). CZ [5], Ce<sub>0.9</sub>Sn<sub>0.1</sub>O<sub>2</sub> and Cu/Ce<sub>0.9</sub>Sn<sub>0.1</sub>O<sub>2</sub> [2] prepared without template were used for comparison. Modifiers (MnO<sub>x</sub> or CuO<sub>x</sub>) were co-precipitated Ce, Zr or Sn oxides; only Mn-CZ-IM catalyst was prepared by subsequent wet impregnation of CZ with Mn acetate solution. Calcination temperature of 500°C was used as providing more defect structure and better catalysts than higher values (e.g. 600°C). CO oxidation was performed in continuous-flow system with fixed-bed of catalyst and pulse feeding of stoichiometric mixture of reagents (2%CO, 1%O<sub>2</sub>, balance He). Temperature was raised to 400°C with 50°C increments. The catalysts were investigated by XRD which confirmed fluorite structure of mixed CZ or cerium-tin oxides; temperature-programmed reduction (TPR) and XPS which revealed the presence and the ratios of Ce<sup>3+</sup>/Ce<sup>4+</sup>, Mn<sup>2+</sup>/Mn<sup>3+</sup> and Cu<sup>+</sup>/Cu<sup>2+</sup> in the corresponding systems and the conditions of their reduction. The texture was investigated using N<sub>2</sub> low-temperature adsorption-desorption and SEM (the relevant SEM images are shown in Fig.1, S<sub>BET</sub> values in Table 1). Energy-dispersive spectroscopy (EDS) during SEM was used to confirm the uniform distribution of the elements on the surface of catalysts. The nominations of the catalysts, the S<sub>BET</sub> values, Ce<sup>3+</sup>/Ce<sup>4+</sup> and M<sup>(n-1)+</sup>/M<sup>n+</sup> ratios on the surface (where M=Mn, with n=3, or Cu, with n= 2), found by XPS, the content of M, CO conversion at 200 °C (X<sub>CO</sub>), and the temperatures of 50% CO conversion (T<sub>50</sub>) are presented in Table 1.

The comparison with co-precipitated analogs demonstrates that the use of all templates leads to significant increase of S<sub>BET</sub>. However the addition of MnO<sub>x</sub> decreases S<sub>BET</sub> due to deterioration of complexation. Modification of CZ with Mn or Cu reduces Ce<sup>3+</sup>/Ce<sup>4+</sup> ratio. The highest Mn<sup>2+</sup>/Mn<sup>3+</sup> ratio was achieved in Mn-CZ-IM catalyst, in which manganese oxides were introduced by post-impregnation.

## OP-IV-6

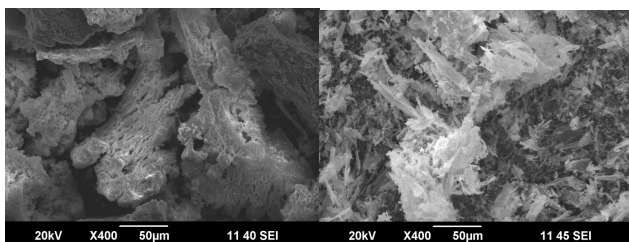


Fig. 1. SEM images of CZ(CTAB) (left) and CZ(SD)

The use of SD template provides better CZ catalyst than CTAB, as  $T_{50}$  is reduced twice; both templated samples start working at much lower temperature than co-precipitated analog. For  $Ce_{0.9}Sn_{0.1}O_2$  the addition of any template (P123 or CTAB) provide also significant reduce of light-off temperature for CO oxidation.

Table 1. Physicochemical characteristics and catalytic properties in CO oxidation

Sample	M, wt.%	$S_{BET}$ , $m^2/g$	$Ce^{3+}/Ce^{4+}$	$M^{(n-1)+}/M^{n+}$	$X_{CO}$ % (200°C)	$T_{50}$ , °C
CZ [5]	-	112	0.18	-	0	400
CZ (CTAB) [6]	-	165	0.19	-	8	305
CZ (SD) [6]	-	45	0.14	-	52	150
Cu/CZ (CTAB) [6]	11	89	0.00	0.23	96	50
Cu/CZ (SD) [6]	9	93	0.02	0.25	97	90
Mn-CZ (CTAB)	6.3	40	0.03	0.14	87	160
Mn-CZ-IM (CTAB)	7.5	48	0.11	0.46	91	150
Mn-CZ(P123)	8	116	No data	No data	5	340
$Ce_{0.9}Sn_{0.1}O_2$ [2]	-	31	0.16	-	3	370
$Ce_{0.9}Sn_{0.1}O_2$ (CTAB)	-	93	0.14	-	20	225
$Ce_{0.9}Sn_{0.1}O_2$ (P123)	-	83	No data	No data	30	237
Cu/ $Ce_{0.9}Sn_{0.1}O_2$ [2]	7	No data	No data	No data	98	175
Cu/ $Ce_{0.9}Sn_{0.1}O_2$ (CTAB)	8	84	0.06	No data	100	<100

Even more significant improvement can be achieved by modification of CZ with  $MnO_x$  and especially with  $CuO_x$ , or  $Ce_{0.9}Sn_{0.1}O_2$  with  $CuO_x$ . The  $T_{50}$  values for  $CuO_x$ -modified CZ and  $Ce_{0.9}Sn_{0.1}O_2$  are below 100 °C and comparable with that for the catalysts based on noble metals.

The reasons of the difference in catalytic properties is discussed in terms of texture features, the bulk vs surface distribution of modifiers, their electronic state, influencing the amount of active oxygen on the surface and in the bulk of the catalysts.

**Acknowledgement.** The authors acknowledge the Program of Development of Lomonosov Moscow State University for the access to XPS equipment.

### References:

- [1] W. Liu, M. Flytzanistephanopoulos, *J. Catal.* 153 (1995) 304.
- [2] J.L. Ayastuy A. Iglesias-González, M. A. Gutiérrez-Ortiz, *Chem. Eng. J.* 244 (2014).
- [3] J.L.Cao, Y.Wang, T.Y.Zhang, S.H. Wu, Z.Y. Yuan // *Appl.Catal. B.* 78 (2008) 120.
- [4] P. Venkataswamy, K.N. Rao, D. Jampaiah, B.M. Reddy, *Appl. Catal. B Environ.* 162 (2015) 122.
- [5] И.Ю.Каплин, Е.С.Локтева, Е.В.Голубина и др. *Кинетика и катализ*, 2017 (58), № 5, 598.
- [6] I.Yu.Kaplin, E.S.Lokteva, E.V.Golubina et al. *RSC advances*, 2017 ( 81) 51359.

## OP-IV-7

### Photocatalytic Reduction of CO<sub>2</sub> over Me (Pt, Ru, Pd, Au)/TiO<sub>2</sub> catalysts

Maniecki T.P.<sup>1</sup>, Shtyka O.<sup>1</sup>, Ciesielski R.<sup>1</sup>, Kędziora A.<sup>1</sup>, Maniukiewicz W.<sup>1</sup>,  
Zakrzewski M.<sup>1</sup>, Dubkov S.<sup>2</sup>, Gromov D.<sup>2</sup>

1 – *Technical University of Lodz Faculty of Chemistry, Institute of General and Ecological Chemistry, Lodz, Poland*

2 – *Moscow Institute of Electronic Technology (MIET), Moscow, Russia*  
*tmanieck@p.lodz.pl*

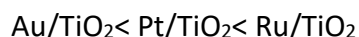
Photocatalytic reduction of CO<sub>2</sub> is still in the focus of the interest of many research groups. Depending on the reaction conditions, CO can be converted into methane, methanol or other oxygenates.

The current research work deals with UV-assisted methanation of CO (i.e. Sabatier reaction).



This reaction is usually carried out over Pt, Pd, Ni, Co) catalysts supported on different oxides (Al<sub>2</sub>O<sub>3</sub>, SiO<sub>2</sub>, CeO<sub>2</sub>, ZrO<sub>2</sub>, etc.) in the temperature range from 250 to 500°C depending on the type of catalyst used in the reaction. The application of UV irradiation can potentially shift the course of the process towards lower temperatures. Therefore, it was attempted to investigate the effect of metal type and loading as well as the influence of UV irradiation on the methanation of CO. The Pt, Ru, and Au catalysts were prepared by traditional wet impregnation technique using corresponding metal salts. The metals were deposited on a commercial titanium oxide (Degussa, P-25). The physicochemical properties of obtained catalysts were investigated using TPR, TPD, and SEM-EDS techniques. The catalytic activity tests were performed in a flow photocatalytic microreactor in the temperature range from 25 to 350°C. The UV light was generated using a Hg quartz lamp of total power near 800W.

It was confirmed that application of UV radiation allows lowering the methanation temperature of about 70° C without significant decrease in methane yield. The activity of prepared catalysts can be represented as follows:



## OP-IV-8

### Carbon Dioxide Methanation over Ni Catalysts Supported on TiO<sub>2</sub> Nanotubes

Mondragón-Galicia G.<sup>1</sup>, Gutierrez-Wing C.<sup>1</sup>, Carrera Nuñez O.<sup>1,2</sup>, Vega Hernandez M.<sup>2</sup>,  
Gutierrez Martinez A.<sup>1</sup>, Perez Hernandez R.<sup>1</sup>

*1 – Instituto Nacional de Investigaciones Nucleares, Mexico, Mexico*

*2 – Benemerita Universidad Autonoma de Puebla, Facultad de Ingeniería Química, Puebla,  
Mexico*

*raul.perez@inin.gob.mx*

In the present work, PdNi/TiO<sub>2</sub>-NT catalysts were synthesized and evaluated in CO<sub>2</sub> methanation. The catalysts were calcined at 400 °C/1h and activated in H<sub>2</sub> flow at 450 °C/1h. The nanocatalysts were characterized by nitrogen adsorption-desorption (BET), scanning electron microscopy (SEM), Transmission electron microscopy (TEM), X-ray diffraction (XRD), programmed temperature reduction (TPR). The catalytic activity results showed that the Pd<sub>20</sub>Ni/TiO<sub>2</sub>-NT and 20Ni/TiO<sub>2</sub>-NT samples had similar behavior than that of the rest of the catalysts after 250 °C, with a maximum conversion of 50% at 325 °C. However, the 10Ni/TiO<sub>2</sub>-NT catalyst at 375 °C showed a CO<sub>2</sub> conversion ca. 60% and decreased to 55% at the maximum reaction temperature. Although, 20Ni/TiO<sub>2</sub>-NT and Pd<sub>20</sub>Ni/TiO<sub>2</sub>-NT samples show a high selectivity towards methane than the other catalysts. This behavior can be associated to a better dispersion of Ni on TiO<sub>2</sub>-NT as shown by SEM and TEM results.

The catalytic activity in the CO<sub>2</sub> methanation reaction was carried out using a fixed flow quartz reactor, 0.1 g of the catalyst was used in a temperature range of 200 to 400 °C with steps of 50 °C and a stabilization time of 7 h each temperature at atmospheric pressure in an automatic multitask unit RIG-100 ISR Inc. A K-type thermocouple was inserted into the catalyst bed to measure and control the bed temperature. The catalyst was activated prior to the test using a H<sub>2</sub> flow (60 ml/min) from room temperature to 400 °C using a heating ramp of 10 °C/min and holding at this temperature for 1h. The sample was brought up to the reaction temperature in He and the reaction mixture was introduced. For the reaction, 30 mL of the CO<sub>2</sub> (5%)/He mixture and 30 mL of the CH<sub>4</sub> (5%)/He mixture. The effluent gases from the reactor were analyzed using gas chromatography, using a Gow-Mac 580 equipped with a two-column system (5 Å molecular sieve at 45 °C and Porapack Q columns at 110°C), the double injector is controlled using Clarity software V.7.2.0.73 and TDC.

X-ray diffraction (XRD) patterns of synthesized TiO<sub>2</sub> nanotube and Ni/TiO<sub>2</sub>-NT catalysts, showed the monoclinic phase of the oxi-hydroxi-TiO<sub>2</sub> (PDF 36-0654). For Ni loaded TiO<sub>2</sub>-NT, showed peaks assigned to Ni cubic (PDF: 65-2868) and nickel titanate (PDF 04-006-1789).

Fig. 1 shows the field emission scanning electron microscopy (FESEM) micrographs of TiO<sub>2</sub> nanotube and 20Ni/TiO<sub>2</sub>-NT. Fibrous-like structures with diameters of approximately 10 nm

## OP-IV-8

and several hundred nanometers in length was obtained for TiO<sub>2</sub> nanotube (Fig.1a) in the 20Ni/TiO<sub>2</sub>-NT spots bright were observed and they were consistent with Ni (Fig. 1b)

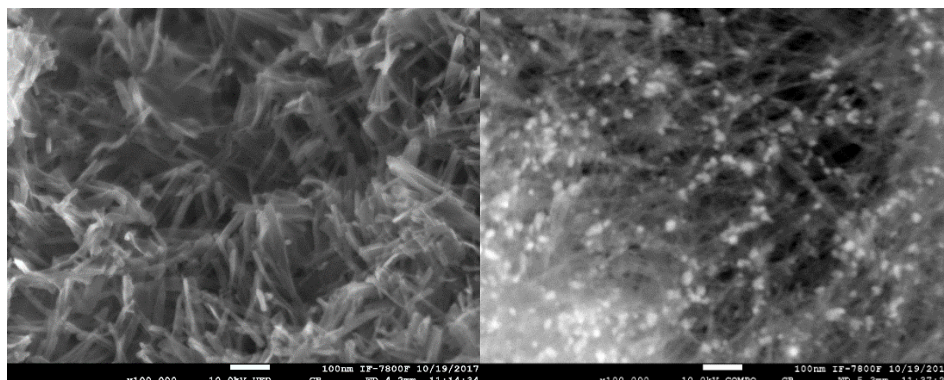


Fig. 2. SEM image of the (a) TiO<sub>2</sub>-NT, (c) 20Ni/TiO<sub>2</sub>-NT.

The effect of Ni on CO<sub>2</sub> methanation reaction was examined in the Ni/TiO<sub>2</sub>-TN as a function of reaction temperature. The CO<sub>2</sub> conversion in the region of low temperature was high in the 20Ni/TiO<sub>2</sub>-NT and bimetallic Pd20Ni/TiO<sub>2</sub>-NT nanocatalysts than other samples evaluated in this contribution. Selectivity toward methane was observed in all regions of the reaction temperatures in all samples.

### Conclusions

CO<sub>2</sub> methanation was investigated over Ni/TiO<sub>2</sub>-NT catalysts with different Ni contents (5, 10 and 20wt%) and modified with Pd. The positive effect of Ni on CO<sub>2</sub> methanation was observed over 20Ni/TiO<sub>2</sub>-NT and Pd<sub>20</sub>Ni/TiO<sub>2</sub>-NT catalysts respectively.

**Acknowledgement.** This research was supported by the SENER-CONACYT 226151, ININ CA-607.

## The Features of the Decalin Dehydrogenation over Platinum Catalysts Supported over Various Silica-Alumina Carriers

Pimerzin Al.A.<sup>1</sup>, Martynenko E.A.<sup>1</sup>, Savinov A.A.<sup>1</sup>, Verevkin S.P.<sup>1,2</sup>, Pimerzin A.A.<sup>1</sup>

1 – Samara State Technical University, Samara, Russia

2 – Institute of Chemistry, University of Rostock, Germany

al.pimerzin@gmail.com

One of the promising technology for lossless long-term energy accumulation and further transportation comes from hydrogen energetics. Hydrogen storage by chemical binding in a suitable organic compound, called liquid organic hydrogen carrier (LOHC) – is a perspective not expensive and safe technology [1].

The naphthalene - decalin pair looks like an efficient hydrogen carrier. It is not expensive and meets most of the LOHC requirements. There are a numerous studies of the naphthalene hydrogenation to decalin in the scientific literature, while the dehydrogenation reaction is still actively studied. One of the issues is the development of the effective and stable catalyst for dehydrogenation of saturated cyclic compounds.

The presented study devoted to the decalin dehydrogenation over platinum containing catalysts (2 %wt. Pt) supported on various silica-alumina carriers: Al<sub>2</sub>O<sub>3</sub>, SiO<sub>2</sub>, SBA-15, MCM-48, and MCM-41. Catalytic activity examinations were carried out using flow type catalytic unit with fixed-bed catalyst under the following conditions: temperature range 300-335°C, hydrogen pressure of 0.5 MPa, liquid hour speed velocity (LHSV) 12-120 h<sup>-1</sup> and hydrogen to feed ratio of 500 nm<sup>3</sup>/m<sup>3</sup>. The decalin (1 %wt.) in toluene was used as a feedstock.

It was shown that support nature has a sufficient effect on the active phase properties of the supported Pt-catalysts. The catalysts supported on mesostructured silicates such as MCM-48, SBA-15 exhibited the highest activity in the decalin dehydrogenation. Such results correlate with active particles dispersion on the surface of the prepared catalysts. The influence of temperature, hydrogen pressure, and LHSV on the reaction rate constants was studied.

Obtained results allow to conclude, that Pt-catalysts supported on mesostructured silicates and exhibited high dehydrogenation activity could be used for the development of new technologies for energy accumulation and transportation on the basis of LOHC.

**Acknowledgement.** This research was supported by the Government of Russian Federation (decree №220 of 9 April 2010) agreement №14.Z50.31.0038.

### References:

[1] Preuster P., Papp C., Wasserscheid P. Acc. Chem. Res., 2017, V.50, №.1,74–85.

## Catalytic Chemistry of Dimethoxymethane: Carbonylation, Steam Reforming and Partial Oxidation

Badmaev S.D., Pechenkin A.A., Paukshtis E.A., Belyaev V.D., Sobyenin V.A.  
*Boreskov Institute of Catalysis, Novosibirsk, Russia*  
*sukhe@catalysis.ru*

In recent years, dimethoxymethane (DMM) has attracted a growing interest as an ecologically benign raw material with a wide scope of applications. DMM, as well as methanol and dimethyl ether is an easy to synthesize oxygenated compound of C1 chemistry. It is worth emphasizing that DMM is a noncorrosive, nontoxic compound. The report discusses the features of catalytic processes for the conversion of DMM into hydrogen/syngas and C2-oxygenates.

The results indicate:

- the possibility of a vapour-phase carbonylation of DMM on a different kind of solid acids. We found that the rate of the reaction increases with the strength of Bronsted acid sites according to the Bronsted-Evans-Polanyi-Semenov correlation [1].

- the promise of a steam reforming of DMM to hydrogen-rich gas for fuel cell feeding. Bifunctional CuO–ZnO/Al<sub>2</sub>O<sub>3</sub> catalyst containing on its surface both acidic and copper-based sites is active and selective for DMM steam reforming to hydrogen-rich gas with low (<1 vol.%) CO content. The hydrogen-rich gas can be used for direct feeding of high temperature polymer electrolyte membrane fuel cell (HT PEMFC) without any further CO removal [2].

- the feasibility of syngas production by partial oxidation of DMM using supported noble metal catalysts at low temperature. In particular, Pt/CeO<sub>2</sub>-ZrO<sub>2</sub> catalyst provided complete conversion of DMM with high syngas production rate at GHSV = 10000 h<sup>-1</sup> and T = 400 °C showing high promises for solid oxide fuel cells (SOFC) [3].

Of course, the use of DMM as a raw material for the production of other products is at an early stage. Further research is needed in this field.

**Acknowledgement.** This work was supported by Ministry of Science and Higher Education of the Russian Federation (project № AAAA-A17-117041710088-0).

### References:

- [1] S.D. Badmaev, A.V. Smorygina, E.A. Paukshtis, V.A. Sobyenin, V.N. Parmon, *Kinet. Catal.* 59 (2018) 99.
- [2] S.D. Badmaev, A.A. Pechenkin, V.D. Belyaev, V.A. Sobyenin, *Int. J. Hydrogen Energy* 40 (2015) 14052.
- [3] S.D. Badmaev, N.O. Akhmetov, T.B. Shoynkhorova, P.A. Simonov, V.D. Belyaev, V.A. Sobyenin, Russian Patent Application № 2018142709, 2018.12.03.

## Why Ni/Silicalite-1 Catalyst Shows High Stability and Reactivity in Dry Reforming of Methane?

Vovk E.I.<sup>1</sup>, Zhou X.<sup>1</sup>, Liu Z.<sup>1</sup>, Guan C.<sup>1</sup>, Yang Y.<sup>1</sup>, Kong W.<sup>2</sup>, Si R.<sup>3</sup>

*1 – ShanghaiTech University, Shanghai, China*

*2 – Shanghai Advanced Research Institute, Shanghai, China*

*3 – Shanghai Synchrotron Radiation Facility, Shanghai, China*

*evovk@shanghaitech.edu.cn*

Dry reforming of methane (DRM) is a reaction between two greenhouse gases (CH<sub>4</sub> and CO<sub>2</sub>) being converted into syn-gas (H<sub>2</sub>+CO) [1]. DRM is a highly endothermic reaction which requires high operating temperatures (>850°C). At high temperatures sintering is a common issue of catalyst deactivation. Deactivation of Ni catalyst in DRM process is also accompanied by carbon deposition (coking) induced by methane decomposition and CO disproportionation (Boudouard reaction). Noble metal catalysts show high resistance toward coke formation in DRM. Despite the better performance of noble metal catalysts, Ni-based catalyst is preferred for the DRM process due to economic concern.

In the current work we investigated catalyst obtained by encapsulating Ni clusters (2.5 nm) into microporous silicalite-1 (aluminum free zeolite with MFI structure). Ni/silicalite-1 catalyst was compared with Ni/SiO<sub>2</sub> catalyst which was prepared by impregnation method. It was also compared with conventional Rh/SiO<sub>2</sub> catalyst. For the Ni/silicalite-1 sample, no deactivation and coking under a wide range of conditions was observed, where carbon formation is thermodynamically favored. XPS study has been performed in ThermoFischer ESCALAB 250Xi photoelectron spectrometer equipped with high pressure gas cell (HPGC 300, Fermi Instruments).

XPS analysis of Ni/silicalite-1 demonstrates the presence of a peak with binding energy (BE) 856.2 eV in Ni 2p<sub>3/2</sub> region, which has a similar spectrum shape to previously reported nickel silicate [2]. This peak in Ni/silicalite-1 sample suggests the presence of Ni-O-Si species which indicates a strong metal-support interaction. After oxidation of this sample at 400°C there are no changes of the Ni-O-Si species (Figure 1). Upon oxidation, Ni<sup>0</sup> transforms into NiO. Reduction of Ni/silicalite-1 catalyst in hydrogen at 600°C leads to partial reduction of nickel into Ni<sup>0</sup> while a significant portion of Ni-O-Si still remains. The behavior of Ni-O-Si feature in both oxidizing and reducing conditions clearly indicates its very high stability.

HRTEM of Ni/silicalite-1 has shown that after reduction in hydrogen (1 bar) at 700°C the number of Ni particles (with size of around 2.5 nm) increases. While, EDS shows the concentration of Ni is not changed. This supports that before reduction, Ni-O-Si is the highly dispersed single atom feature which is not visible in HRTEM; only after reduction and sintering into Ni clusters, it becomes detectable by HRTEM. EXAFS data confirm the presence of Ni-O-Si species and support this conclusion.

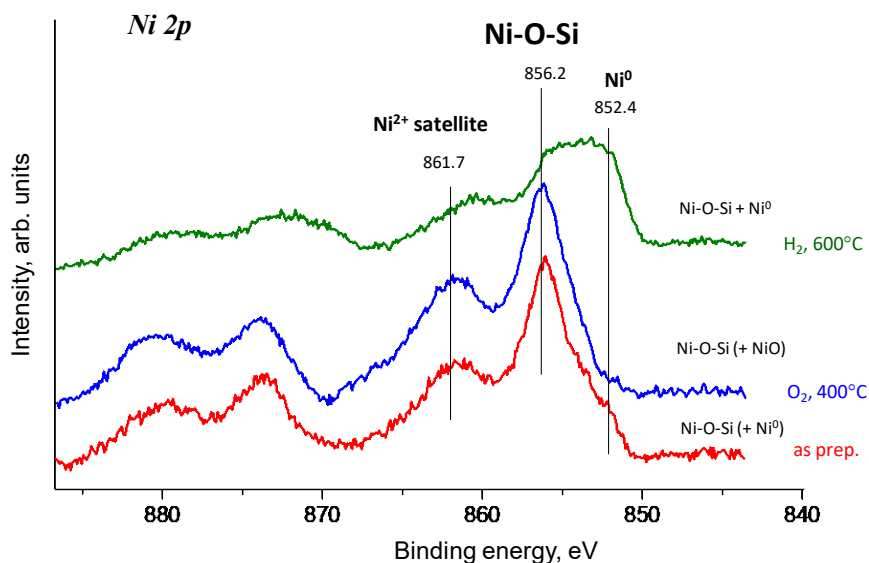


**Figure 1.** Ni 2p core level photoelectron spectra of Ni/silicalite-1 catalyst (as prepared, after oxidation in spectrometer and subsequent reduction).

Ni/silicalite-1 is a novel oxygen-philic interfacial catalyst system, consisting mainly of Ni-O-Si species intercalated into silicalite framework. We also attribute Ni-O-Si feature to be formed at the interface between Ni nanoparticles and the silicalite support. The small metallic Ni clusters are surrounded by these species which stabilizes Ni nanoparticles, preventing its sintering and carbon deposition (coking). Heterojunction Ni-O-Si species may play an important role in the reaction mechanism, providing oxygen atoms for methane oxidation and oxygen vacancy sites for CO<sub>2</sub> activation. The role of this species in the reaction mechanism is discussed.

Detection of Ni-O-Si provides fundamental understanding of high stability and reactivity of Ni/silicalite-1 catalyst which makes it also interesting for commercial application.

#### References:

- [1] M.C.J. Bradford, M.A. Vannice, *Catalysis Reviews*, 41 (1999) 1-42.
- [2] R.B. Shalvoy, B.H. Davis, P.J. Reucroft, *Surface and Interface Analysis*, 2 (1980) 11-16.

**Formic Acid Production via Methane Peroxide Oxidation over Oxalic Acid Activated Fe-MFI Catalysts. Mechanistic Insights**

Taran O.P.<sup>1,2</sup>, Yashnik S.A.<sup>1</sup>, Boltenkov V.V.<sup>1</sup>, Parkhomchuk E.V.<sup>1</sup>, Sashkina K.A.<sup>1</sup>,  
Babushkin D.E.<sup>1</sup>, Parmon V.N.<sup>1</sup>

*1 – Institute of Chemistry and Chemical Technology SB RAS, FRC KSC SB RAS, Krasnoyarsk*

*2 – Boreskov Institute of Catalysis, Novosibirsk, Russia*

*oxanap@icct.krasn.ru*

Formic acid is a widely used, readily biodegradable and low corrosive commodity chemical considered now as one of promising hydrogen storage materials due to its easily controlled dehydrogenation to H<sub>2</sub> and CO<sub>2</sub> [1]. Formic acid can be produced from methane [1-3] which is one of most abundant and renewable carbon resource on our planet [4]. Fe- and Cu-containing hydroxides and zeolites were shown earlier to catalyze the peroxide oxidation of light paraffins [5], and, recently, of methane to methanol and/or formic acid at a high enough selectivity under mild conditions (323 K) [12, 45, 46]. However, we failed to find any literature data concerning influence of structural and textural characteristics of the zeolite catalysts on the process selectivity.

The present study we studied in detail the influence of Fe-ZSM-5 zeolites properties such as the zeolite morphology (the crystallite size and texture properties) and structure of Fe-containing species inside the zeolite channels on the catalysts selectivity to partial peroxide oxidation of methane to formic acid. The catalysts of different morphology (nanosize, microsize, and bulky (Fig. 1)) were prepared, activated with an oxalic acid solution and characterized by UV-vis DR, ESR, NH<sub>3</sub>-TPD, <sup>27</sup>Al NMR. The activation caused transformation of isolated iron cations from tetrahedral framework oxygen surrounding to octahedral extraframework oxygen surrounding with simultaneous formation of oligomeric Fe oxo-clusters that led to an increase in the selectivity to formic acid and to a decrease in the selectivity to CO<sub>2</sub> and methanol.

We also revised the effect of addition of the reaction intermediates (methanol and formic acid) on the conversion and selectivity of the peroxide oxidation of methane. Peroxide oxidation of methanol and formic acid also were studied over initial and activated bulky catalysts.

The obtained data and regularities of the peroxide oxidation of methane, methanol and formic acid support the formulated hypothesis on different mechanisms of oxidation of methane over Fe-MFI catalysts. Evidently, the heterogeneous route is characteristic of the transformations of methane to formic acid, when the active sites are formed via interaction of oligomeric oxo-clusters of Fe-ions with H<sub>2</sub>O<sub>2</sub>. The radical mechanism seems more probable for oxidation of methane to methanol and methanol to CO<sub>2</sub>. These mechanisms will be discussed in the presentation.

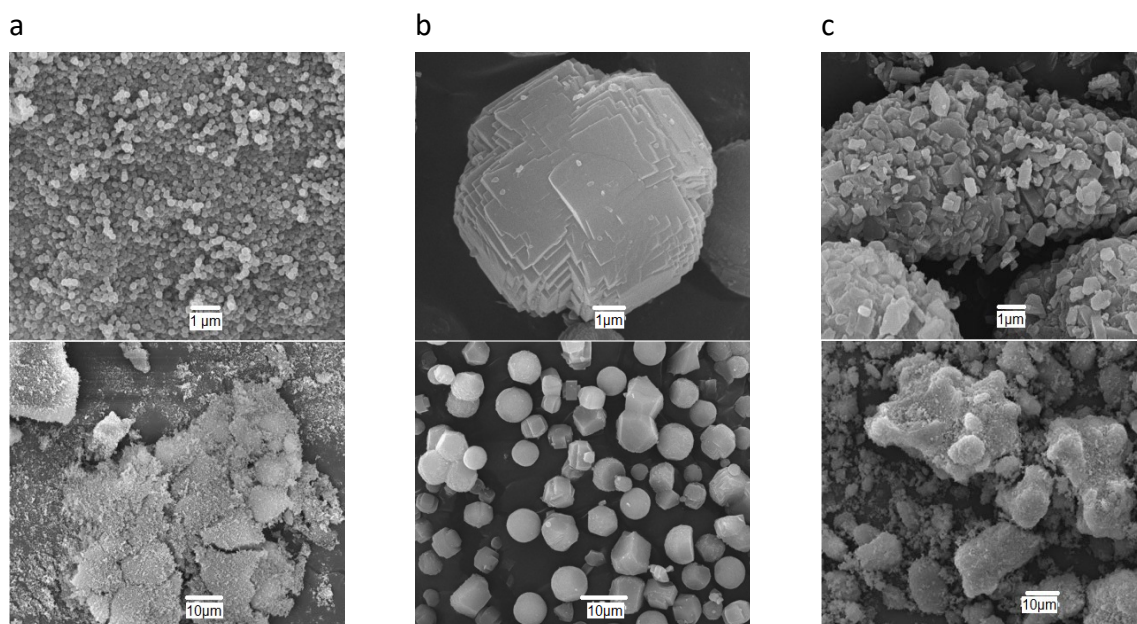


**Figure 1.** SEM images of Fe-silicalite Nanocrystals (a), Fe-silicalite Microcrystals (b) and Commercial Fe-ZSM-5 (c) at different magnifications.

**Acknowledgement.** Acknowledgement. This work was supported by the Russian Science Foundation, grant 17-73-30032.

#### References:

- [1] Bulushev, D.A., Ross, J.R.H. *ChemSusChem* 11 (2018) 821.
- [2] Rahman, A.K.M.L., Kumashiro, M., Ishihara, T. *Catal Commun* 12 (2011) 1198.
- [3] Taran, O.P., Yashnik, S.A., Boltenev, V.V., Parkhomchuk, E.V., Sashkina, K.A., Ayusheev, A.B., Babushkin, D.E., Parmon, V.N. *Topics in Catalysis* 2019.10.1007/s11244-019-01151-8.
- [4] Thauer, R.K. *Angew Chem Int Ed.* 49 (2010) 6712.
- [5] Kuzmin, A.O., Elizarova, G.L., Matvienko, L.G., Savinova, E.R., Parmon, V.N. *Mend Commun* 8 (1998) 210.
- [6] Hammond, C., Dimitratos, N., Lopez-Sanchez, J.A., Jenkins, R.L., Whiting, G., Kondrat, S.A., Ab Rahim, M.H., Forde, M.M., Thetford, A., Hagen, H., Stangland, E.E., Kang, J.H., Moulijn, J.M., Willock, D.J., Hutchings, G.J. *ACS Catal* 3 (2013) 1835.
- [7] Hammond, C., Dimitratos, N., Jenkins, R.L., Lopez-Sanchez, J.A., Kondrat, S.A., Ab Rahim, M.H., Forde, M.M., Thetford, A., Taylor, S.H., Hagen, H., Stangland, E.E., Moulijn, J.M., Taylor, S.H., Willock, D.J., Hutchings, G.J. *ACS Catal* 3 (2013) 689.
- [8] Hammond, C., Forde, M.M., Ab Rahim, M.H., Thetford, A., He, Q., Jenkins, R.L., Dimitratos, N., Lopez-Sanchez, J.A., Dummer, N.F., Murphy, D.M., Carley, A.F., Taylor, S.H., Willock, D.J., Stangland, E.E., Kang, J., Hagen, H., Kiely, C.J., Hutchings, G.J. *Angew Chem Int Ed* 51 (2012) 5129.

## Mechanistic Studies of Methanol Synthesis Reaction over Cu and Pd-Cu Catalysts

Ciesielski R., Zakrzewski M., Kubicki J., Maniukiewicz W., Kedziora A., Maniecki T.P.  
*Lodz University of Technology, Lodz, Poland*  
*radoslaw.ciesielski@p.lodz.pl*

The main purpose of this work was determination the influence of the active phase composition on the physicochemical and catalytic properties of Cu and Pd-Cu catalysts supported on CeO<sub>2</sub>:Al<sub>2</sub>O<sub>3</sub> binary oxides in the methanol synthesis reaction. Within the work, the effect of catalysts composition on the mechanism of methanol synthesis reaction from H<sub>2</sub> and CO<sub>2</sub> mixture was also studied.

In order to achieve the purpose of the work, monometallic Cu/support and bimetallic Pd-Cu/support catalysts were prepared using the conventional wet impregnation method. As a support for the catalytic systems, CeO<sub>2</sub>:Al<sub>2</sub>O<sub>3</sub> binary oxide system, was used. The physicochemical properties of prepared catalytic systems were studied using BET, TPR-H<sub>2</sub>, TPD-NH<sub>3</sub>, XRD, SEM-EDS and FT-IR techniques. The catalytic activity tests in methanol synthesis were carried out using a gradientless reactor at 220 °C under pressure of 3.5 MPa.

The BET results showed that specific surface area of the investigated catalysts decrease with the addition of copper and palladium oxides. The reducibility measurements suggested an interaction between copper species and palladium evidenced by the shifts of the reduction effects visible on the TPR profile recorded for Pd-Cu catalysts. The simultaneous presence in the same place of palladium and copper oxide was confirmed by SEM-EDS measurements. The obtained EDS spectra of bimetallic catalysts after reduction at 300°C clearly showed a wide variation in elemental composition. Therefore, it can be concluded that the surface of the catalyst is not homogeneous. The XRD results recorded for investigated catalysts reduced at 300 °C displays reflections characteristic for crystalline Cu, CeO<sub>2</sub>, and CeAlO<sub>3</sub> phases, respectively. Additionally, in the case of bimetallic catalysts, PdCu phase was also observed. The presence of PdCu alloy phase confirmed the interaction of Pd and CuO during the reduction process and can explain the shift of TPR result observed on the reduction curves recorded for palladium catalysts. The acidity measurements showed that increase of copper concentration into the support decreases the total acidity in the opposite to bimetallic systems. The promotion effect of palladium on the catalytic activity of copper supported catalyst in methanol synthesis reaction was proven. The improvement of the activity of bimetallic Pd-Cu catalyst in methanol synthesis reaction is explained by the alloy formation. Based on the results of FTIR measurements and available literature data, it was observed that hydrogen molecules adsorb dissociatively on the metallic copper surface to form hydrogen atoms, increasing the hydrogen spillover effect to the metal-carrier interface. In contrast, CO<sub>2</sub> is adsorbed on the oxygen vacancies of the support to form carbonates which can further undergo hydrogenation to methanol.

## The Role of Structural, Redox and Acid-Base Properties of Monolayer $\text{MgVO}_x/\text{Al}_2\text{O}_3$ Catalysts in Oxidative Dehydrogenation of Propane

Kharlamova T., Timofeev K., Vodyankina O.  
Tomsk State University, Tomsk, Russia  
kharlamova83@gmail.com

Due to the favourable redox and adsorption properties of the surface two-dimensional  $\text{VO}_x$  species, the supported vanadium catalysts are among the most promising systems for ODH of propane [1, 2]. However, the low selectivity of the process caused by rapid consecutive propylene overoxidation remains a challenge. Both metal oxide support and additives can alter the electronic properties of the  $\text{VO}_x$  active site that affect the observed selectivity towards propylene and reactivity of the catalyst [2]. The catalyst acidity can also play a crucial role in the adsorption and overoxidation of the propylene formed [2].

The modification of the alumina-supported vanadia catalyst by  $\text{MgO}$  to form the surface magnesium vanadate species was shown to result in the improvement of the propane selectivity [3, 4]. Here we present the study of the tailor-made  $\text{MgVO}_x/\text{Al}_2\text{O}_3$  materials with the emphasis on the relationships between the structure of the vanadia species, acid-base and redox properties of the catalyst surface and the response to the catalyst performance.

A series of the  $\text{MgVO}_x/\text{Al}_2\text{O}_3$  samples was prepared with vanadia monolayer coverage characterized by the formation of the surface  $\text{MgVO}_x$  species with different structures. The structure of the  $\text{MgVO}_x$  species is shown to depend on the Mg content. The metavanadate  $[(\text{V}_2\text{O}_6)^2-]_n$  structures are formed in the samples with the Mg/V molar ratio  $\leq 0.8$ . Further increase in the magnesium content to up to the Mg/V molar ratio = 1.7 leads to the formation of the dimeric  $[\text{V}_2\text{O}_7]^{4-}$  moieties in the surface  $\text{MgVO}_x$  species.

The  $\text{MgVO}_x/\text{Al}_2\text{O}_3$  samples show a reduced catalytic activity, but an increased selectivity towards propene in comparison with the unmodified  $\text{VO}_x/\text{Al}_2\text{O}_3$  sample. The increase of the Mg/V ratio leads to the increase of the V–O bond strength in the  $\text{MgVO}_x/\text{Al}_2\text{O}_3$  samples, which well correlates with the decrease in their catalytic activity. However, there is no correlation between the V–O bond strength and the selectivity. The analysis of the acid-base properties of the surface and the propylene adsorption show that the high acidity leads to the reduction of the selectivity towards propylene due to its strong adsorption yielding the surface carboxylate structures.

**Acknowledgement.** This work was supported by “The Tomsk State University Academic D.I. Mendeleev Fund Program” grant.

### References:

- [1] J.T. Grant, C.A. Carrero, F. Goeltl, et al, *Science*, 2016, 354 (6319), 1570–1573.
- [2] J.T. Grant, J.M. Venegas, W.P. McDermott, I. Hermans, *Chem. Rev.*, 2018, 118 (5), 2769–2815.
- [3] T. Kharlamova, E. Sushchenko, T. Izaak, O. Vodyankina, *Catal. Today*, 2016, 278, 174–184.
- [4] E.D. Sushchenko, T.S. Kharlamova, T.I. Izaak, O.V. Vodyankina, *Kinet. Catal.*, 2017, 58 (5), 630–641.

## **Titania-Zirconia Coatings of a Capillary Microreactor for the Selective Hydrogenation of 2-Methyl-3-Butyn-2-ol Using a PdZn/Ti<sub>x</sub>Zr<sub>1-x</sub>O<sub>2</sub> Catalyst: Stability, Effect of the Catalyst's Activation Conditions and a Kinetic Study**

Okhlopkova L.B.<sup>1</sup>, Kerzhentsev M.A.<sup>1</sup>, Ismagilov Z.R.<sup>1,2</sup>

*1 – Boreskov Institute of Catalysis, Novosibirsk, Russia*

*2 – Institute of Coal Chemistry and Material Science FRC CCC SB RAS, Kemerovo, Russia  
mila65@catalysis.ru*

The introduction of microcapillary reactors with catalytic coatings into fine organic synthesis and pharmaceutical industry allows to comply with strict environmental requirements and control of selectivity in successive reactions [1]. Multicrystalline titania-zirconia oxide coatings have increased thermal stability as compared to titanium dioxide coatings [2]. The aim of the present work is to study stability of titania-zirconia with embedded PdZn nanoparticles in selective hydrogenation of 2-methyl-3-butyn-2-ol, the effect of activation conditions on their catalytic properties and to perform the kinetic interpretation of the data obtained.

### **Experimental**

The catalytic coatings of 1 wt.% PdZn/Ti<sub>x</sub>Zr<sub>1-x</sub>O<sub>2</sub> (x = 1, 0.8, 0.5) were synthesized via self-assembly on the inner surface of a 0.53-mm-long capillary reactor with a length of 10 m. Coatings were tested in the selective hydrogenation of MBY at 333 K and 1 atm. H<sub>2</sub>. The obtained coatings were subjected to activation under different conditions. The kinetic parameters of Langmuir–Hinshelwood model were calculated using Matlab software.

### **Results and discussion**

The productivity of the microcapillary reactor after 32 hours of continuous stream increases in the series PdZn/TiO<sub>2</sub> < PdZn/Ti<sub>0.8</sub>Zr<sub>0.2</sub>O<sub>2</sub> < PdZn/Ti<sub>0.5</sub>Zr<sub>0.5</sub>O<sub>2</sub> at constant selectivity (more than 96%) and productivity of the catalysts (1.2, 1.5 and 1.3 gMBE/s/gPd) due to thickening of the coating. The high selectivity for PdZn nanoparticles embedded to titania-zirconia matrix is due to the decrease in the constant of direct hydrogenation and the ratio of the alkene and alkyne adsorption constants derived by kinetic modelling. The reactor productivity increased and the selectivity decreased on the PdZn/Ti<sub>0.8</sub>Zr<sub>0.2</sub>O<sub>2</sub> coating in time-on-stream experiments, while productivity and selectivity have increased on the PdZn/TiO<sub>2</sub> coating during long-term test up to 88 h (Fig. 1). The observed changes in the activity and selectivity on mixed titania-zirconia coatings can be explained by an increase in the ratio of the alkene and alkyne adsorption constants and rise of the constants of 2-methyl-3-butyn-2-ol, 2-methyl-3-buten-2-ol and direct hydrogenation reactions.

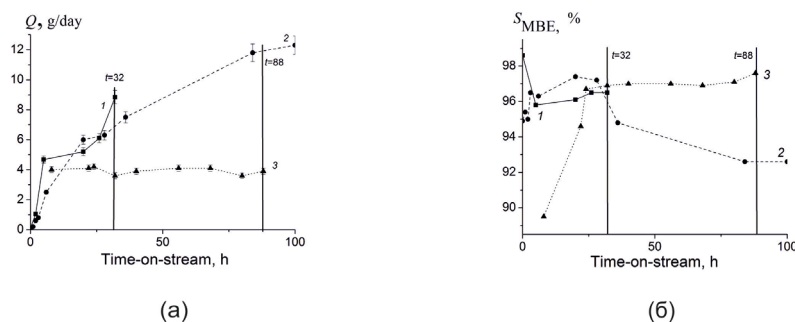


Fig. 1. Effect of time-on-stream on reactor productivity (a) and selectivity (b) in the hydrogenation reaction of MBY on PdZn/Ti<sub>0.5</sub>Zr<sub>0.5</sub>O<sub>2</sub> (1), PdZn/Ti<sub>0.8</sub>Zr<sub>0.2</sub>O<sub>2</sub> (2) and PdZn/TiO<sub>2</sub> (3) films. Reaction conditions:  $C_{MBY,0} = 1.0-2.0$  mol/l, gas flow rate 6.0 ml/min,  $p_{H_2} = 1$  atm, 313 K

Reduction at 573 K decreased the activity of the PdZn/Ti<sub>0.8</sub>Zr<sub>0.2</sub>O<sub>2</sub> coating by 2.6 times, and the selectivity of 2-methyl-3-buten-2-ol formation does not change. Similar regularities were obtained for PdZn/Ti<sub>0.5</sub>Zr<sub>0.5</sub>O<sub>2</sub>. The selectivity on the PdZn/Ti<sub>0.8</sub>Zr<sub>0.2</sub>O<sub>2</sub> coating increased to 94.7% after oxidation-reduction treatment in air at 573 K for 2 h and in H<sub>2</sub> at 573 K for 2 h. The high selectivity level of the oxidized-reduced coatings is due to the decrease in the constant of 2-methyl-3-buten-2-ol hydrogenation and the ratio of the alkene and alkyne adsorption constants.

### Conclusions

The coatings of 1 wt.% PdZn/TiO<sub>2</sub> and PdZn/Ti<sub>x</sub>Zr<sub>1-x</sub>O<sub>2</sub> ( $x = 1, 0.8, 0.5$ ) on the inner surface of a capillary reactor 0.53 mm in diameter, 10 m in length were synthesized. Coatings were tested in the selective hydrogenation of 2-methyl-3-buten-2-ol at 333 K and 1 atm. H<sub>2</sub>. The higher selectivity of reaction on the titania-zirconia films can be explained by a decrease in the constant of direct hydrogenation and the ratio of the alkene and alkyne adsorption constants derived by kinetic modelling. The effect of the composition of the support on the productivity and selectivity of the catalytic films depends on the duration of the tests. The activity increases and the selectivity decreases with increasing reaction time for mixed titania-zirconia coatings as a result of the oxidation of the active component, the destruction of the PdZn alloy, and the formation of carbon deposits on its surface.

**Acknowledgement.** This work was supported by budget project No. AAAA-A17-117041710090-3 for Boreskov Institute of Catalysis.

### References:

- [1] A. Renken, L. Kiwi-Minsker, *Adv. Catal.*, 2010, vol. 53, p. 47. doi 10.1016/S0360-0564(10)53002-5.
- [2] L. B. Okhlopko, M. A. Kerzhentsev, Z. R. Ismagilov, *Kinetics and catalysis*, 2019.





**Content**



**School-Conference  
for young scientists  
"CATALYSIS FOR ENERGY,  
FUELS, RENEWABLES"**

**OPS-1 ÷ OPS-15**



**NiMoP Catalyst in the Hydroprocessing of Mixture of Straight-Run Diesel Fuel and Secondary Light Fractions Obtained by Catalytic Steam Cracking of Vacuum Residue**

Stolyarova E.A.<sup>1</sup>, Saiko A.V.<sup>1</sup>, Zaikina O.O.<sup>1,2</sup>, Sosnin G.A.<sup>1,2</sup>, Yeletsky P.M.<sup>1</sup>,  
Klimov O.V.<sup>1</sup>, Yakovlev V.A.<sup>1</sup>, Noskov A.S.<sup>1</sup>

1 – Boreskov Institute of Catalysis, Novosibirsk, Russia

2 – Novosibirsk State University, Novosibirsk, Russia  
*sea@catalysis.ru*

One of promising ways of heavy oil feedstocks upgrading, which can be alternative to conventional approaches based on carbon rejection (visbreaking, coking, catalytic cracking) and hydrogen addition (hydrotreatment, hydrocracking) is a catalytic steam cracking (CSC) [1]. The light fractions obtained in the CSC are distillates of secondary thermocatalytic processes by their characteristics. Their using as components of commercial diesel fuel is impossible without pre-hydrotreatment. Combined hydrotreating of secondary distillates with straight-run diesel fraction is an effective process for improving their consumer and operational characteristics.

NiMoP catalysts supported by  $\gamma$ -Al<sub>2</sub>O<sub>3</sub> are traditionally used in the hydrotreating process [2]. They show high activity in hydrodesulfurization (HDS) and hydrodenitrogenation (HDN), as well as the hydrogenation (HYD) of unsaturated and aromatic hydrocarbons, which are contained in heavy fractions in significant quantities.

This work describes the effect of NiMoP hydrotreating catalyst in hydroprocessing of a mixture of straight-run diesel fuel blended with secondary light fractions obtained from vacuum residue (VR) via CSC.

NiMoP catalyst supported by  $\gamma$ -Al<sub>2</sub>O<sub>3</sub> was prepared to obtain 12 wt.% of Mo; 4 wt.% of Ni; 1.5 wt.% of P in the final catalyst. It has surface area 150 m<sup>2</sup>/g (by BET), average pore diameter 104 Å, average pore volume 0.41 cm<sup>3</sup>/g. The sample was tested in the hydrotreating of two different mixtures, which contained straight-run diesel fraction (DF) as well as diesel fraction (DVR) and gasoline fraction (GVR) obtained as a result of CSC of VR. The experimental conditions were the following: P<sub>H<sub>2</sub></sub> = 7 MPa, T = 340 °C, LHSV = 1.0 h<sup>-1</sup>, H<sub>2</sub>/feed ratio = 500.

Properties of mixture feed (MF), liquid hydrotreated product (HDP) and products of rectification of the HDP: diesel fraction (DFP) and gasoline fraction (GFP) were measured. The selected results are shown in the table:

## OPS-1

Parameter	70% DF + 30% DVR				70% DF + 25% DFP + 5% GVR			
	MF	HDP	GFP	DFP	MF	HDP	GFP	DFP
S content, ppm	7000	9.16	0.98	8.28	6000	8.81	0.94	7.89
N content, ppm	1000	1.29	0.12	1.17	250	1.45	0.15	1.22
Content of aromatic hydrocarbons, wt. %								
Monoaromatic	19.1	14.2	-	15.0	18.9	14.6	-	15.6
Diaromatic	8.5	0.68	-	0.76	8.2	0.76	-	0.81
Polyaromatic	2.2	0.07	-	0.07	2.0	0.07	-	0.06
Summary content of aromatic hydrocarbons	29.8	14.95	-	15.83	29.1	15.43	-	16.47
Temperature of IBP <sup>1</sup>								
50%	117	89	12	182	79	72	10	188
90%	275	262	147	262	272	259	142	267
FBP <sup>2</sup>	343	337	194	343	342	336	179	339
	378	380	220	377	377	379	204	376

<sup>1</sup> – Initial boiling point; <sup>2</sup> – Final boiling point

Hydrotreating process lets to obtain liquid hydrotreated product and the rectification diesel and gasoline fractions which have better physical-chemical characteristics than initial mixture feed, for example, cetane number, octane number, freezing temperature, content of sulfur, nitrogen, aromatic hydrocarbons and others.

Variation of initial mixture composition by addition of different secondary light fractions obtained as a result of CSC of VR showed a strong influence on the properties of resulted liquid hydrotreated product as well as diesel and gasoline fractions obtained after rectification of the hydrotreated product.

Using of NiMoP hydrotreating catalyst lets to obtain diesel and gasoline fraction having sufficient physical-chemical properties to use in compounding of motor fuel. In this way, using of NiMoP catalysts in the hydrotreating of mixture feed containing secondary light fractions obtained through catalytic steam cracking of vacuum residue allows to engage these components to the further oil refining.

**Acknowledgement.** This work was supported by Ministry of Science and Higher Education of the Russian Federation (project AAAA-A17-117041710077-4)

### References:

- [1] P.M. Eletsii et al. / Journal of Siberian Federal University. Chemistry. 10 (2017) 545.  
 [2] Yu.V. Vatutina et al. / Applied Catalysis B: Environmental 199 (2016) 23–32.

## OPS-2

### Determination of the Type and Reactivity of Carbon Deposits in the Mixed Reforming of Methane

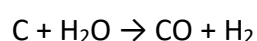
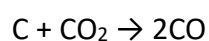
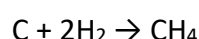
Zakrzewski M., Shtyka O., Ciesielski R., Kedziora A., Maniecki T.

*Lodz University of Technology, Institute of General and Ecological Chemistry, Lodz, Poland  
801012@edu.p.lodz.pl*

The methane reforming process leading to synthesis gas has been known for many years. It was found that Ni, Pd, Pt, Ru, Rh, Ir proved to be effective components of the catalytic systems in this reaction. However, one of the main problems of methane reforming is the deactivation of catalysts due to the carbon deposition [1]. It was found that systems based on noble metals are less sensitive to the formation of a carbon deposit [2, 3]. However, due to their availability and cost, Ni-based catalysts are often preferred, which are characterized by high activity and low resistance to carbon deposition. Therefore, it is desirable to develop an active promotion of nickel catalysts that will provide high activity and resistance to carbon deposit formation.

CeO<sub>2</sub> is an effective promoter and/or support for nickel catalysts. The addition of cerium oxide improves the activity of alumina based catalysts used in vehicles for controlling exhaust emissions. CeO<sub>2</sub> has the ability to store and/or release oxygen during the process, when there is a change in the concentration of the gas phase. This phenomenon is referred to as oxygen storage capacity [4]. The presence of cerium oxide in the catalyst also has influence on the increase of the dispersion of the active phase as well as increase the phase transition temperature  $\gamma$ -Al<sub>2</sub>O<sub>3</sub> (used as a support) into the  $\alpha$ -Al<sub>2</sub>O<sub>3</sub> characterized by a low specific surface area [5, 6].

Deactivation of heterogeneous catalysts is associated with many factors. One of these factors are carbon deposits generated in many catalytic reactions involving hydrocarbons or carbon monoxide. They cause a decrease in activity, changes in catalyst selectivity and blocking the flow of reagents through the bed. The deposit formed on catalysts can be removed by various factors, for example carbon dioxide, hydrogen or water vapor:



Due to the attractiveness of biogas as a renewable raw material, it is readily used as a substrate for the production of synthesis gas. Therefore, the gas supplied to the reactor contains biogas, biohydrogen and carbon dioxide derived from side reactions occurring during sugar production. Water vapor (as an additional oxidizing agent) was selected for additional substrates, while argon is used to dilute the input mixture. The ratio of the mixture entering the reactor is CH<sub>4</sub> : CO<sub>2</sub> : H<sub>2</sub> : H<sub>2</sub>O : Ar = 2 : 2 : 1 : 0.9 : 1.25. The most important reactions occurring during mixed reforming of methane are:



## OPS-2

The aim of this work was to determine the type and the reactivity of the carbon deposit formed during the process of the mixed reforming of methane. In order to achieve the intended purpose of this work the monometallic nickel ( $20\%Ni/Al_2O_3$ ,  $x\%CeO_2-20\%Ni/Al_2O_3$  –  $x$ : 0.1, 0.5, 1, 5) and bimetallic ( $x\%Ru-20\%Ni/Al_2O_3$  –  $x$ : 0.1, 0.5, 1, 5) catalysts were prepared. The monometallic catalysts were prepared by wet impregnation method from aqueous solutions of nickel nitrate and cerium nitrate. While, bimetallic Ru – Ni catalysts were prepared by the subsequent impregnation method from aqueous solutions of ruthenium chloride. The physicochemical properties of mono and bimetallic catalysts after calcination and reaction processes were examined using various techniques such as: XRD, SEM, TG, TOC and TPSR methods. The activity tests in mixed reforming of methane reaction were carried out in the temperature range 700 - 750°C in a flow quartz microreactor under atmospheric pressure. The catalyst load in each experiment was 0.4 g and the stream composition was:  $H_2/CH_4/CO_2/Ar/H_2O = 1/2/2/1.25/0.9$  (volumetric ratio), respectively.

The analysis of the total carbon content in the case of the investigated catalysts being after reaction showed that the amount of the carbon detected on the catalyst surface depends strongly on the composition of the catalyst. The total carbon content for all studied catalysts being after 3h on stream was in the range 2-10% wt. of carbon. The formation of the carbon deposit was also confirmed by TG (Fig. 1. A) and SEM (Fig. 1. B) measurements. Within the pictures is contained carbon deposits form on  $1\%Ru-20\%Ni/Al_2O_3$  catalyst surface. The pictures show the so-called „carbon whiskers”. The spectrum EDS confirms the presence of carbon in the catalytic system and other catalyst components such Al, Ru, Ni and O. The TPSR (temperature programmed surface reaction) and TG-DTA (Fig. 1 A.) measurements were performed for investigated catalysts and the obtained results showed the occurrence of the three types of the carbon deposit which is formed during the reaction. These three types of carbon deposit are  $C\alpha$ , polymeric (low temperature effect -  $C\beta$ ) and graphitic (high temperature effect -  $C\gamma$ ) type of carbon, respectively.

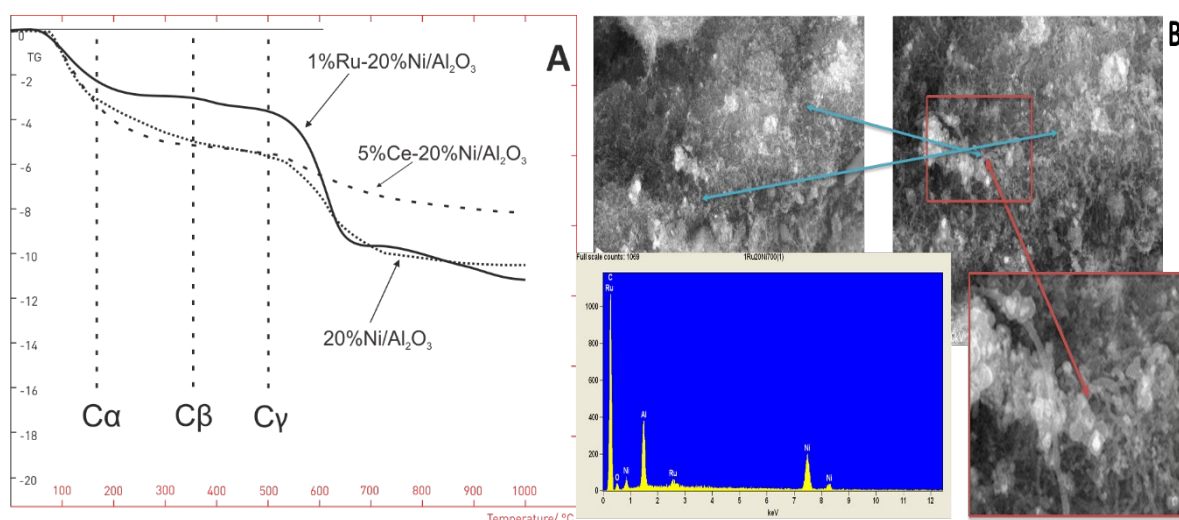


Fig. 1. A) TG curves for  $20\%Ni/Al_2O_3$ ,  $1\%Ru-20\%Ni/Al_2O_3$  and  $5\%Ce-20\%Ni/Al_2O_3$ ; B) SEM-EDS spectra for  $1\%Ru-20\%Ni/Al_2O_3$  catalyst after mixed reforming of methane at 700°C.

## OPS-2

**Acknowledgement.** This work was partially funded from NCBIr – Grant no. BIOSTRATEG2/297310/13/NCBIr/2016.

### References:

- [1] S. Wang, G.Q. Lu, G.J. Millar, *Energy and Fuels* 10 (1996) 896.
- [2] A.T. Ashcroft, A.K. Cheethan, M.L.H. Green, P.D.F. Vernom, *Science* 352 (1991) 225.
- [3] J.R. Rostrup-Nielsen, J.H.B. Hansen, *J. Catal.* 144 (1993) 38.
- [4] H.C. Yao, Y.F.Y. Yao, *J. Catal.* 86 (1984) 254.
- [5] J. Soria, J.M. Coronado, J.C. Conesa, *J. Chem. Soc. Faraday Trans.* 92 (1996) 1619.
- [6] C. Morterra, V. Bolis, G. Magnacca, *J. Chem. Soc. Faraday Trans.* 92 (1996) 1991.

## OPS-3

### ***In situ* XPS and MS Study of Methane Oxidation over Bimetallic Pt-Pd/Al<sub>2</sub>O<sub>3</sub> Catalysts**

Chetyrin I.A., Bukhtiyarov A.V., Prosvirin I.P., Bukhtiyarov V.I.

*Boreskov Institute of Catalysis, Novosibirsk, Russia*

*chia@catalysis.ru*

Lean burn gas engines currently become more attractive due its ability to use various gases as natural gas, biogas and synthetic methane [1]. However, well known problem is release of a small amount of unburned methane into the exhaust. For the combustion of the residual methane from the exhaust of gas engines the Pd/Al<sub>2</sub>O<sub>3</sub> catalysts usually used due to their high catalytic activity at relatively low temperatures (< 500°C) [2-4]. The activity of palladium catalysts in total methane oxidation depends on several factors as the particles size, the phase composition, and the charge state of the active component [5-7]. Specifically, using the *in situ* techniques the formation of an active but unstable mixed Pd<sup>0</sup>-PdO phase has been detected [8-9]. Nevertheless one of the main problems for these catalysts is a low stability in a reaction conditions. Most of researches suggest that the reason is a deactivation of active sites/component by the water steam, which is a reaction product as well as exhaust component [2-4]. Probably the formation of surface hydroxyls on the Pd surface or on the support hinders oxygen exchange between support and active sites and therefore leads for loss of activity. Adding Pt prevents the deactivation of catalysts under wet conditions and improves catalytic activity [1, 10-11]. However the reasons of synergetic effects exhibiting in Pt-Pd bimetallic catalysts still under discussion. Some researchers suppose that Pt is acts as promoter stabilizing the mixed Pd<sup>0</sup>-PdO phase, which is an active component of monometallic palladium catalysts [12-13]. Other researchers consider that Pt acts as component of the active site and participates in the hydrocarbons oxidation process. The systematic investigation of the total methane oxidation over bimetallic Pt-Pd/Al<sub>2</sub>O<sub>3</sub> catalysts using the NAP XPS technique could help to get more reliable data concerning surface structure and chemical composition of active metals depending on different reaction conditions.

The aim of this work the application of *in situ* XPS and MS techniques combination for investigation of electronic and catalytic properties of bimetallic Pt-Pd nanoparticles supported on  $\gamma$ -Al<sub>2</sub>O<sub>3</sub> with a different Pd:Pt ratio in comparison with monometallic Pd/Al<sub>2</sub>O<sub>3</sub> under methane oxidation reaction.

It has been shown that the bimetallic catalysts demonstrate the higher catalytic activity compared to monometallic catalysts (Pt/Al<sub>2</sub>O<sub>3</sub> and Pd/Al<sub>2</sub>O<sub>3</sub>). Moreover the bimetallic catalysts with a lower Pt amount have been more active in a reaction compared to the samples with a higher Pt concentration.

The chemical states of the palladium and platinum depending on the reaction conditions as well as on Pt:Pd ratio has been investigated using NAP XPS. It has been shown that both the

### OPS-3

metallic and oxidized Pd and Pt species coexist at the catalyst surface during the methane oxidation reaction. The active sites formation occurs already at room temperature under reaction mixture. Thus using of *in situ* techniques are necessary for the investigation of the active sites in Pd-Pt bimetallic catalysts.

Linear correlation between TOF values and Pd<sup>2+</sup>/Pd<sup>0</sup> ratios has been revealed under lean feed conditions. This allows us to suggest that that Pd<sup>2+</sup> favors the total methane oxidation reaction and the concentration of Pd oxidized species depends on Pt content.

**Acknowledgement.** This work was conducted within the framework of budget project for Boreskov Institute of Catalysis.

#### References:

- [1] A.T. Gremminger, H.W. P. de Carvalho, R. Popescu, J.-D. Grunwaldt, O. Deutschmann., *Cat. Tod.* 258 (2015) 470.
- [2] P. Briot, M. Primet, *Appl. Catal.* 68 (1991) 301.
- [3] T.R. Baldwin, R. Burch, *Appl. Catal.* 66 (1990) 337.
- [4] K. Persson, K. Jansson, S. Järas, *J. Catal.* 245 (2007) 401.
- [5] Y. Ozawa, Y. Tochihara, M. Nagai, S. Omi, *Chem. Eng. Sci.*, 58 (2003), 671.
- [6] P. Castellazzi, G. Groppi, P. Forzatti, A. Baylet, P. Marecot, D. Duprez, *Catal. Today*, 105 (2010), 18.
- [7] P. Castellazzi, G. Groppi, P. Forzatti, E. Finnochio, G. Busca, *J. Catal.*, 275 (2010), 218.
- [8] W. R. Schwartz, L. D. Pfefferle, *J. Phys. Chem. C*, 116 (2012), 8571.
- [9] M. A. Mashkovtsev, A. K. Khudorozhkov, I. E. Beck, A. V. Porsin, I. P. Prosvirin, V. N. Rychkov, V. I. Bukhtiyarov, *Catal. Ind.*, 3 (2011), 350.
- [10] T.R. Johns, R. S. Goeke, V. Ashbacher, P. C. Thüne, J.W. Niemantsverdriet, B. Kiefer, C. H. Kim, M. P. Balogh, A. K. Datye, *J. Catal.* 328 (2015) 151.
- [11] G. Lapisardi, P. Gelin, A. Kaddouri, E. Garbowski, S. Da Costa, *Top. Catal.* 42–43 (2007) 461.
- [12] N.M. Kinnunen, J.T. Hirvi, M. Suvanto, T.A. Pakkanen, *J. Mol. Catal. A: Chem.* 356 (2012) 20.
- [13] E.D. Goodman, Sh. Dai, A-Ch. Yang, C.J. Wrasman, A. Gallo., S.R. Bare , A.S. Hoffman, T.F. Jaramillo, G.W. Graham, X. Pan, M. Cargnello. *ACS Catal.* 7 (2017), 4372.

## OPS-4

### ***In situ* NAP-XPS Study of Cu-Fe-Al-Based Nanocomposite Catalysts of CO Oxidation**

Tsapina A.M.<sup>1</sup>, Selivanova A.V.<sup>1</sup>, Saraev A.A.<sup>1</sup>, Fedorov A.V.<sup>1</sup>, Vorokhta M.<sup>2</sup>,  
Šmíd B.<sup>2</sup>, Kaichev V.V.<sup>1</sup>

1 – Boreskov Institute of Catalysis, Novosibirsk, Russia

2 – Charles University, Prague, Czech Republic

*amtsapina@catalysis.ru*

Fe-based catalysts have been the subject of intense research in the past due to a wide application in various fields, such as water-gas shift reactions, the Fisher-Tropsch synthesis, partial oxidation of H<sub>2</sub>S, and ammonia synthesis. Recently, it has been showed that the Fe<sub>2</sub>O<sub>3</sub>-Al<sub>2</sub>O<sub>3</sub> catalysts demonstrate moderate activity in the oxidation of CO [1]. Moreover, their activity can be increased by promotion with copper. The CuO-, Fe<sub>2</sub>O<sub>3</sub>-, and Al<sub>2</sub>O<sub>3</sub>-based nanocomposite catalyst with 5% copper oxide and Fe<sub>2</sub>O<sub>3</sub>:Al<sub>2</sub>O<sub>3</sub> = 82:18 showed the maximum of catalytically activity among the other CuO-, Fe<sub>2</sub>O<sub>3</sub>-, and Al<sub>2</sub>O<sub>3</sub>-based catalysts [1, 2]. Since these catalysts feature high activity in addition their low cost and environmentally friendly they could be used in the catalytic combustion of non-traditional fuels such as peat, lignite, wood or food waste, sewage sludge, and the other industrial wastes. This technology is based on the gasification of solid fuels with following catalytic combustion of resultant gases. In this contribution, we focus on the study of Cu-Fe-Al catalysts in the CO oxidation because the resultant gases consist of CO, H<sub>2</sub>, and H<sub>2</sub>O mainly. The chemical interactions occurring at the gas-substrate interface are crucial during the reduction process of these catalysts. The Near Ambient Pressure X-ray photoelectron spectroscopy (NAP-XPS) method is an indispensable method for obtaining information about the chemical states and the relative concentration of atoms on the surface of the catalysts directly under the reaction conditions.

The catalyst (5% of CuO, 78% of Fe<sub>2</sub>O<sub>3</sub>, and 17% of Al<sub>2</sub>O<sub>3</sub>) was synthesized from the iron, aluminium and copper nitrate salts mixed in the required ratios, and then the preliminary dried powder was calcined at 700°C for 1 h in air. The NAP-XPS study of the chemical composition of the Cu-Fe-Al catalyst surface under the reaction conditions was performed at Charles University in Prague, Czech Republic. The experiments were performed on a photoelectron spectrometer (SPECS Surface Nano Analysis, GmbH Germany) which is equipped with a PHOIBOS-150 Hemispherical Energy Analyser coupled with a differentially pumped electrostatic pre-lens system. DeviSim reaction cell installed in the analysis chamber allows obtaining *in situ* XPS spectra directly in the gas mixture flow at pressures up to 20 mbar in a wide range of temperatures. Spectra were obtained using Al K $\alpha$  X-ray radiation ( $h\nu = 1486.6$  eV). The powder of the catalyst was deposited on a stainless steel mesh attached to a special sample holder. The catalyst of optimal composition and reference CuO and CuFe<sub>2</sub>O<sub>4</sub>

## OPS-4

samples were investigated in a flow of CO and a mixture of CO and O<sub>2</sub> (2:1) in the temperatures ranging from room temperature up to 600°C. The total pressure was 1 mbar.

According to the XPS data, it was established that copper is mainly in the Cu<sup>2+</sup> state in the fresh Cu-Fe-Al catalyst, iron is in the Fe<sup>3+</sup> state. Heating the catalyst under the CO flow is accompanied by gradual reduction of copper and iron cations, so that already at 300°C copper is in the Cu<sup>1+</sup> state and then it reduces to metallic Cu<sup>0</sup>. The Fe2*p* spectrum demonstrated presence of Fe<sup>2+</sup> even at 400° C. The peaks of metallic iron appear additionally in the Fe2*p* spectrum at 500° C. Catalyst reduction hardly occurs under the flow of a CO and O<sub>2</sub> mixture, the state of the catalyst remains practically unchanged up to 500° C. Thus, an increase in the partial pressure of O<sub>2</sub> leads to increasing the reduction temperature. Copper and iron cations in the bulk spinel CuFe<sub>2</sub>O<sub>4</sub> structure are in the Cu<sup>2+</sup> and Fe<sup>3+</sup> state. Heating CuFe<sub>2</sub>O<sub>4</sub> in a CO flow leads to copper is partly reduced to Cu<sup>0</sup> at 200°C and then it is fully reduced to a metallic state at 400°C without passing through any intermediate states. In the Fe2*p* XPS spectra, peaks of metallic iron and Fe<sup>2+</sup> begin to appear additionally even at 300°C. The reduction temperature of copper and iron in CuFe<sub>2</sub>O<sub>4</sub> is lower than it of the catalyst. Furthermore the reduction temperature of copper in the Cu-Fe-Al catalyst is higher than copper(II) oxide. Copper in CuO begin to reduce during the heating process in CO already at 150°C with the formation of an intermediate component Cu<sub>2</sub>O at 175°C. Finally copper is fully reduced at 200°C. This means that the addition of alumina and the preparation of the catalyst in the form of nanoscale composite results in an increase in the copper and iron cations reduction temperature.

It can be concluded that the chemical state of the copper and iron cations on the surface of the Cu-Fe-Al catalyst and the reference samples of CuFe<sub>2</sub>O<sub>4</sub> and CuO in CO oxidation was determined by NAP-XPS technique. This approach allows us to determine the reduction temperature of copper and iron as well as phase transitions of the Cu-Fe-Al-nanocomposite catalyst in the temperature range up to 600°C under the reaction conditions. There was found that the reduction of the copper cations in the catalyst to metallic state proceeds with formation of Cu<sup>1+</sup> intermediate state. The presence of alumina in the catalyst makes copper and iron more difficult for reducing. Moreover, increasing the reduction temperature occurs when oxygen is added to a reaction mixture.

**Acknowledgement.** This work was supported by the Russian Science Foundation, grant 17-73-20157.

### References:

- [1] A.V. Fedorov, A.M. Tsapina, O.A. Bulavchenko, A.A. Saraev, G.V. Odegova, D.Yu. Ermakov, Y.V. Zubavichus, V.A. Yakovlev, V.V. Kaichev, *Catal. Lett.* 148 (2018) 3715.
- [2] O.A. Bulavchenko, Z.S. Vinokurov, A.A. Saraev, A.M. Tsapina, A.L. Trigub, E.Yu. Gerasimov, A.Yu. Gladky, A.V. Fedorov, V.A. Yakovlev, V.V. Kaichev, *Inorg. Chem.* (2019) in press.

## OPS-5

### ***In situ* Study of Methanol Adsorption on Pt(111) and Pd(111) at Low Temperatures by Polarization Modulation Infrared Reflection Absorption Spectroscopy**

Selivanova A.V.<sup>1</sup>, Tsapina A.M.<sup>1</sup>, Medvedeva Yu.I.<sup>2</sup>, Saraev A.A.<sup>1</sup>, Kaichev V.V.<sup>1</sup>, Bukhtiyarov V.I.<sup>1</sup>

1 – Boreskov Institute of Catalysis, Novosibirsk, Russia

2 – Novosibirsk State Technical University, Novosibirsk, Russia

avselivanova@catalysis.ru

The adsorption of various molecules on the different metal surfaces has been the subject of several studies in the past. The small molecules such as CO, O<sub>2</sub> and H<sub>2</sub>O were studied basically. The investigations of more complex molecules such as methanol, ethanol, etc. have been less. Many researchers observed that the molecules adsorb intact to form isolated species or ordered structures over solid surfaces at low temperatures according to Brunauer-Emmett-Teller theory. Methanol was reported to adsorb through a classical layer-by-layer growth mechanism. It should be stressed that this model was based on the hypothesis that molecules of methanol exist in the gas phase as monomers only. However, water, methanol, formaldehyde, etc. exist as clusters not only in the liquid phase, but also in the gas phase due to strong H-bonds. It is very likely that these clusters can adsorb intact at least at low temperatures, thereby breaking the layer-by-layer growth of the adsorption layer.

To elucidate the adsorption mechanism we performed an *in situ* study of the adsorption of methanol on Pd(111) and Pt(111) at temperatures between 80 and 120 K using TPD and polarization modulation infrared reflection-absorption spectroscopy (PM IRRAS) [1]. PM IRRAS is quite suitable for the analysis of species residing at gas-solid and gas-liquid interfaces because at a high (grazing) angle of incidence, the absorption of *p*-polarized IR radiation by thin films on metal surfaces is enhanced so that even adsorbed species with a concentration of several hundreds of monolayer can be observed in the *p*-polarized infrared reflection spectrum [2]. Because the contribution of the absorbance of the adsorbed species to the *s*-polarized infrared reflection spectrum is negligible, the difference between *s*- and *p*-reflectivities yields surface species information. The ratio between the difference and sum reflectivity can be used to compensate the gas phase absorbance, hence yielding a vibrational surface spectrum. This technique becomes especially popular in the field of *in situ* studies of the adsorption of various molecules on atomic-smooth metal surfaces in a wide pressure range from ultrahigh vacuum (UHV) to near ambient pressures (NAP).

The experiments were carried out in a custom-designed UHV/NAP instrument that consists of two stainless steel chambers. The first chamber denoted as the UHV chamber was used for preparation and characterization of the samples under study. The UHV chamber was equipped by a PHOIBOS-150-MCD-9 hemispherical energy analyzer, an XR-50 X-ray source with a dual Al/Mg anode, and an IQP-10/63 ion source (SPECS Surface Nano Analysis GmbH).

## OPS-5

The UHV chamber was also equipped by a  $xyz\phi$  manipulator with a sample holder that provided transfer of the sample under study from the UHV chamber to the second chamber denoted as the catalytic cell. The catalytic cell was attached to a VERTEX 80v FTIR spectrometer (Bruker Optic GmbH) via two differentially pumped BaF<sub>2</sub> windows for input and output IR radiation. The spectrometer was equipped by a mercury-cadmium telluride detector and a photoelastic modulator PEM-100 (Hinds instruments, Inc.) which provided a modulation of the polarization of IR radiation with frequency of 42 kHz. Sum ( $p + s$ ) and difference ( $p - s$ ) signals collected by the detector were processed in real time.

We studied the formation and subsequent transformation of the adsorption layer on the Pd(111) and Pt(111) single crystal surfaces during methanol exposure at 80, 90, and 100 K and following heating to 120 K. We found that methanol adsorbs molecularly to form clusters containing several hydrogen-bonded CH<sub>3</sub>OH molecules at temperatures below 100 K. However, these clusters have low thermal stability and decompose even at 100 K to form isolated chemisorbed methanol molecules. As a result, at a temperature between 100 and 120 K methanol adsorbs intact to produce adsorbed isolated molecules. These adsorbed species fast desorb at a temperature above 120 K. The adsorption of methanol on the palladium and platinum surface at 80-90 K does not proceed via the layer-by-layer mechanism.

### References:

- [1] V.V. Kaichev, A.V. Selivanova, A.M. Tsapina, A.A. Saraev, V.I. Bukhtiyarov, J. Phys. Chem. C (2019) in press.
- [2] G. Rupprechter, Adv. Catal. 51 (2007) 133-263.

## OPS-6

### Study of the Zinc Addition Influence on the Pd/Sibunit Catalyst of Selective Acetylene Hydrogenation

Glyzdova D.V.<sup>1</sup>, Afonassenko T.N.<sup>1</sup>, Domanina T.P.<sup>1</sup>, Leont'eva N.N.<sup>1</sup>, Prosvirin I.P.<sup>2</sup>,  
Bukhtiyarov A.V.<sup>2</sup>, Shlyapin D.A.<sup>1</sup>

1 – Center of New Chemical Technologies BIC, Omsk, Russia

2 – Boreskov Institute of Catalysis, Novosibirsk, Russia

omsk-glyzdova@mail.ru

Bimetallic Pd-Zn catalysts are widely used in hydrocarbon conversion processes (steam reforming of methanol and methanol synthesis, selective hydrogenation, oxidation processes, etc.) and are characterized by high yield of target products and stability under the reaction conditions due to the formation of joint Pd-Zn phases. The modifier atoms in the bimetal structure “dilute” neighboring palladium atoms and effectively isolate them from each other, so such Pd–Zn–Pd-ensembles of active sites are formed on the catalyst surface [1]. In the case of selective acetylene hydrogenation for Pd-Zn-Pd the possibility of C<sub>2</sub>H<sub>2</sub> adsorption on two neighboring Pd atoms in the di-σ-bound form, which is mostly converted into alkane, is almost excluded. In these conditions more possible form of the alkyne adsorption is a weaker π-complex, which facilitates the desorption of ethylene and, accordingly, leads to an increase in its yield. It should be noted that the amount of the introduced modifier has a significant effect on the catalyst properties [2]. In addition to that, the optimum of the Pd:Zn ratio is determined not only by the joint phase composition, but also by the textural and structural properties of the support, which affect the degree of the Pd and Zn interaction. In this regard, the aim of this work was to study the effect of the zinc amount on the composition, structure, electronic state of the active component and the catalytic properties of Pd-Zn/Sibunit systems in the selective hydrogenation of acetylene to ethylene.

The carbon material Sibunit (Sib) was used as a support [3]. Samples were obtained by an incipient wetness impregnation with joint aqueous solution of Pd(NO<sub>3</sub>)<sub>2</sub> and Zn(NO<sub>3</sub>)<sub>2</sub> with following stages of air drying (120 °C, 2 h) and reduction in a hydrogen stream (500 °C, 5 hours). The modifier content was varied from Pd:Zn = 1:0.1 to 1:4. Catalytic tests were carried out in flow reactor, in a stream of gas mixture containing 4 vol.% C<sub>2</sub>H<sub>2</sub> + 96 vol.% H<sub>2</sub> at 35-95 °C.

It was found by XRD and EXAFS that in the Pd-Zn(1:0.25)/Sib sample palladium and zinc interact with the formation of a solid substitution solution based on palladium FCC. The crystal lattice parameter of palladium decreases (from 3.886 to 3.844 Å), due to the incorporation of a smaller zinc atom in the lattice [4], and the distance between the neighboring Pd-Pd atoms increases from 2.75 to 2.85 Å. For the catalyst with the equimolar Pd-Zn(1:1)/Sib composition, the bimetallic compound fraction increases, and the crystal lattice transforms into the tetragonal characteristic of the intermetallic PdZn phase. In the Pd:Zn = 1:4 catalyst, the excess of Zn exists as an oxide phase, and bimetallic scattering paths (according to EXAFS) are strongly

## OPS-6

disordered (Debye–Waller factor — 0.0184 Å) and are determined only by the K-edge of palladium. It also should be noted that increasing of zinc part in the samples also leads to a shift of the Pd3d signal in the XPS spectra towards higher binding energies values compared to the monometallic sample (from 335.5 eV to 335.8 ± 0.05 eV). According to XPS data for the Pd:Zn = 1:0.25 ratio, only a small part of palladium is situated as a PdZn alloy nanoparticles, but with an increase in the amount of introduced zinc, almost all surface of palladium goes into nanoalloy and just a small part exists as individual Pd<sup>0</sup> nanoparticles.

The introduction of zinc into the Pd/Sibunit composition has a noticeable effect on its catalytic properties. Thus, an increase in the zinc content to Pd:Zn > 1:0.5 is accompanied by a shift of the acetylene conversion curve (X (C<sub>2</sub>H<sub>2</sub>) = 50%) to higher temperatures (from 45 to 77°C), which indicates a depression in catalytic activity. It is assumed that the observed effect is caused by blocking a part of the active sites by the formed zinc oxide, found by the EXAFS and X-ray powder diffraction methods. The dependence of ethylene selectivity on the zinc amount in the sample has an extreme character with a maximum at 74% achieved on catalysts with Pd:Zn = 1:0.5 - 1:1. It is ~ 8 % rel. higher than the selectivity obtained on monometallic Pd/Sibunit reference sample (68%). It is assumed that the optimum for the selectivity of ethylene formation is achieved on catalysts containing the highest number of bimetallic particles, and depends on the degree of their structure order.

**Acknowledgement.** This work was supported by the Ministry of science and high education of the Russian federation in relating with Program of fundamental scientific investigation of State Academies of Sciences on 2013-2020 years in the direction V.46, project №V.46.2.5 (project No. AAAA-A17-117021450096-8) and under the support of the Haldor Topsoe. The most experiments were carried out using the equipment of Scientific Research Center "Kurchatov Institute" (Moscow), Boreskov Institute of Catalysis (Novosibirsk) and Omsk Research Collaboration Centre SB RAS (Omsk).

### References:

- [1] H. Zhou, X. Yang, L. Li, X. Liu, Y. Huang, X. Pan, A. Wang, J. Li, T. Zhang, *ACS Catalysis*. 6 (2016) 1054-1061.
- [2] Z. Wang, L. Yang, R. Zhang, L. Li, Z. Cheng, Z. Zhou, *Catal. Today*. 264 (2015) 37-43.
- [3] D.V. Glyzdova, A.A. Vedyagin, A.M. Tsapina, V.V. Kaichev, A.L. Trigub, M.V. Trenikhin, D.A. Shlyapin, P.G. Tsyruльников, A.V. Lavrenov, *Appl. Catal.*, A. 563 (2018) 18-27.
- [4] A.V. Chistyakov, M.A. Gubanov, V. Yu. Murzin, P. A. Zharova, M. V. Tsodikov, V. V. Kriventsov, A. E. Gekhman, I. I. Moiseev, *Russian Chemical Bulletin, International Edition*. 63 (2014) 88-93.

## The Formation of Precatalysts for Selective Ethylene Dimerization in System $\text{NiBr}_2[\text{bis}(3,5\text{-Dimethylpyrazol-1-yl)Methane}]/\text{PPh}_3$

Zubkevich S.V.<sup>1</sup>, Tuskaev V.A.<sup>1,2</sup>, Gagieva S.Ch.<sup>1</sup>, Pavlov A.A.<sup>2</sup>, Bulychev B.M.<sup>1</sup>

1 – Moscow State University, Chemical Department, Moscow, Russia

2 – Nesmeyanov Institute of Organoelement Compounds, RAS, Moscow, Russia

zubkevich.sergey@gmail.com

The catalytic systems for C-C coupling of olefins based on nickel complexes are valued for their versatility. These catalytic systems can catalyse processes such as selective oligomerization of ethylene [1], polymerization of olefins [2] and copolymerization of polar and non-polar olefins [3]. Since the discovery of  $\text{PPh}_3$  promoting effect on the activity of nickel based catalytic systems [4] a series of attempts to establish the mechanism of this effect have been taken [5-8].

In present work we had chosen nickel (II) bromide complex with bis(3,5-dimethylpyrazol-1-yl)methane (**1**) as a model system to study its interaction with  $\text{PPh}_3$  in different solvents, such as acetonitrile, dichloromethane and toluene. There is always an equilibrium in solution between molecular and ionic forms of complexes and free  $\text{PPh}_3$  (Fig. 1), according to the UV-Vis and  $^1\text{H}$  NMR data. This effect was observed even in non-polar solvents, such as dichloromethane or toluene.

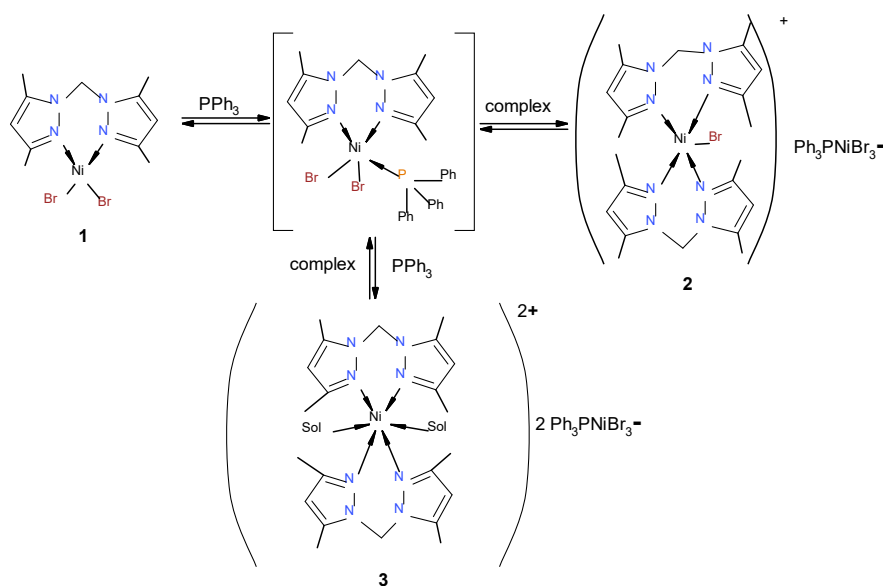


**Figure 1.** Proposed equilibrium for system  $\text{NiBr}_2[\text{bis}(3,5\text{-dimethylpyrazol-1-yl)Methane}]/\text{PPh}_3$  in solution

The complex **1** readily regroups upon the addition of  $\text{PPh}_3$  to its solution in dichloromethane and gives a set of signals in  $^1\text{H}$  NMR spectra, some of them uniquely refer to complex anion  $[\text{NiBr}_3\text{PPh}_3]^-$ . The structures of complex cations were proposed based on X-ray data of individual ionic compounds of nickel with coordinated bis(3,5-dimethylpyrazol-1-yl)methane and  $\text{PPh}_3$ , obtained from THF (**2**) and  $\text{CH}_3\text{CN}$  (**3**) (Fig. 2). Individual complexes **2**

## OPS-7

and **3** when dissolved in dichloromethane also undergo rearrangements and finally reach the equilibrium, but **3** possess higher stability and its complete transformation takes more than 6 hours at r.t.

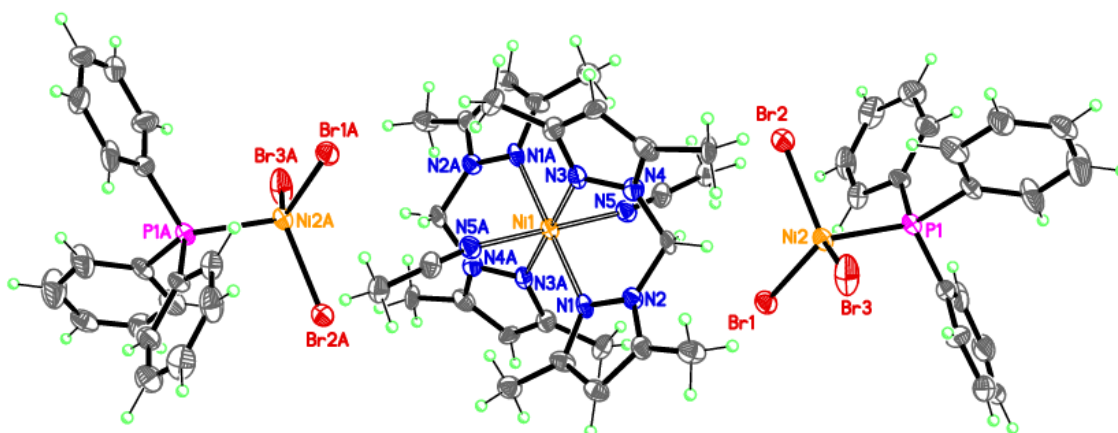


**Figure 2.** General view of complex **3** in crystal in thermal ellipsoid representation ( $p=50\%$ ).

Both the studied system **1**/ $\text{PPh}_3$  (with variations of ratios between the complex and  $\text{PPh}_3$ ) and individual compounds **2** and **3** form catalytic systems upon activation with  $\text{Et}_2\text{AlCl}$ . These systems selectively produce butenes from ethylene (selectivity up to 100%), but the share of butene-1 does not exceed 15%.

The activation of **1**/ $\text{PPh}_3$  with  $\text{Et}_2\text{AlCl}$  was studied by  $^{31}\text{P}$  NMR. The data shows that the addition of activator results in complete coordination of  $\text{PPh}_3$  to Ni and the formation of a compound (or compounds) closest to active species. However, more studies, including EPR measurements and DFT calculations, need to be performed in course of future work to determine the composition of the resulting solution.

**Acknowledgement.** This work was supported by the Russian Foundation of Basic Research, grants 18-03-01112 (synthesis and studies of rearrangements with  $\text{PPh}_3$ ) and 18-33-20091 (ethylene oligomerization).

### References:

- [1] Bryliakov, K. P.; Antonov, A. A. *J. Organomet. Chem.*, 2018, 867, 55–61.
- [2] Wang, J.; Wang, L.; Yu, H.; Ullah, R. S.; Haroon, M.; Zain-ul-Abdin; Xia, X.; Khan, R. U. *Eur. J. Inorg. Chem.*, 2018, 2018 (13), 1450–1468.
- [3] Carrow, B. P.; Nozaki, K. *Macromolecules*, 2014, 47 (8), 2541–2555.
- [4] Schmidt, F. K.; Tkach, V. S.; Kalabina, A. *Pet. Chem. U.S.S.R.*, 1972, 12 (1), 18–25.
- [5] Peuckertt, M.; Keim, W. *Organometallics*, 1983, 2 (5), 594–597.
- [6] Pietsch, J.; Braunstein, P.; Chauvin, Y. *New J. Chem.*, 1998, 22 (5), 467–472.
- [7] Sun, W. H.; Zhang, W.; Gao, T.; Tang, X.; Chen, L.; Li, Y.; Jin, X. *J. Organomet. Chem.*, 2004, 689 (5), 917–929.
- [8] Schmidt, F. K.; Titova, Y. Y.; Belykh, L. B. *Kinet. Catal.*, 2016, 57 (1), 61–71.

## Mechanistic Insights into the Selective Catalytic Reduction of NO Revealed by Modulated-Excitation Raman Spectroscopy

Nuguid R.J.G.<sup>1,2</sup>, Nachtegaal M.<sup>2</sup>, Ferri D.<sup>2</sup>, Kröcher O.<sup>1,2</sup>

1 – Ecole Polytechnique Fédérale de Lausanne (EPFL), Lausanne, Switzerland

2 – Paul Scherrer Institut, Villigen, Switzerland

rob.nuguid@epfl.ch

Raman spectroscopy is the preferred characterization technique for metal oxide-based catalysts [1]. Here we combined Raman spectroscopy with modulated excitation to study V<sub>2</sub>O<sub>5</sub>/TiO<sub>2</sub>, the most widely used selective catalytic reduction (SCR) catalyst. Our novel approach revealed in-depth mechanistic insights that go beyond what is achievable with conventional Raman experiments under steady-state conditions.

ME was performed by pulsing NH<sub>3</sub> in a gas feed of NO/H<sub>2</sub>O/O<sub>2</sub>/Ar at 250 °C while simultaneously recording Raman spectra and monitoring SCR activity. The *in situ* Raman spectra of the V<sub>2</sub>O<sub>5</sub>/TiO<sub>2</sub> catalyst sample exhibit features that are in agreement with previous studies. The peak at 1031 cm<sup>-1</sup> originates from V=O stretch while those at 395, 512, and 636 cm<sup>-1</sup> are characteristic of TiO<sub>2</sub> in the anatase phase [2].

In the time-resolved spectra of V<sub>2</sub>O<sub>5</sub>/TiO<sub>2</sub>, no obvious spectral changes were apparent (Figure 1A). However, after applying phase-sensitive detection (PSD) [3], changes around the VO<sub>x</sub> and TiO<sub>2</sub> peaks were amplified (Figure 1B, green). While the VO<sub>x</sub> peak broadened significantly in the presence of NH<sub>3</sub> and H<sub>2</sub>O in the time-resolved spectra, a narrow peak appeared at 1031 cm<sup>-1</sup> in the phase-resolved spectra. Hence, only a well-defined fraction of the VO<sub>x</sub> species act as catalytic active centers while the majority remain largely unresponsive. Based on the energy position of the VO<sub>x</sub> peak in the phase-resolved spectra, these SCR-active species correspond to the coordinatively unsaturated VO<sub>x</sub> sites.

When TiO<sub>2</sub> alone was subjected to the same pulsing procedure, no phase-resolved signal was observed (Figure 1B, blue), confirming that NH<sub>3</sub> remains strongly adsorbed on TiO<sub>2</sub> at 250 °C. This observation, together with the observation that TiO<sub>2</sub> peaks appeared in the phase-resolved spectra of V<sub>2</sub>O<sub>5</sub>/TiO<sub>2</sub>, implies that TiO<sub>2</sub> acts as a reservoir of NH<sub>3</sub> molecules, which can be delivered to VO<sub>x</sub> to react if NO is present.

These mechanistic insights could be extracted from the Raman spectra only due to the increased sensitivity offered by ME and PSD. Therefore, our approach opens up new possibilities in deciphering structure-reactivity relationships of metal oxide catalyst systems.

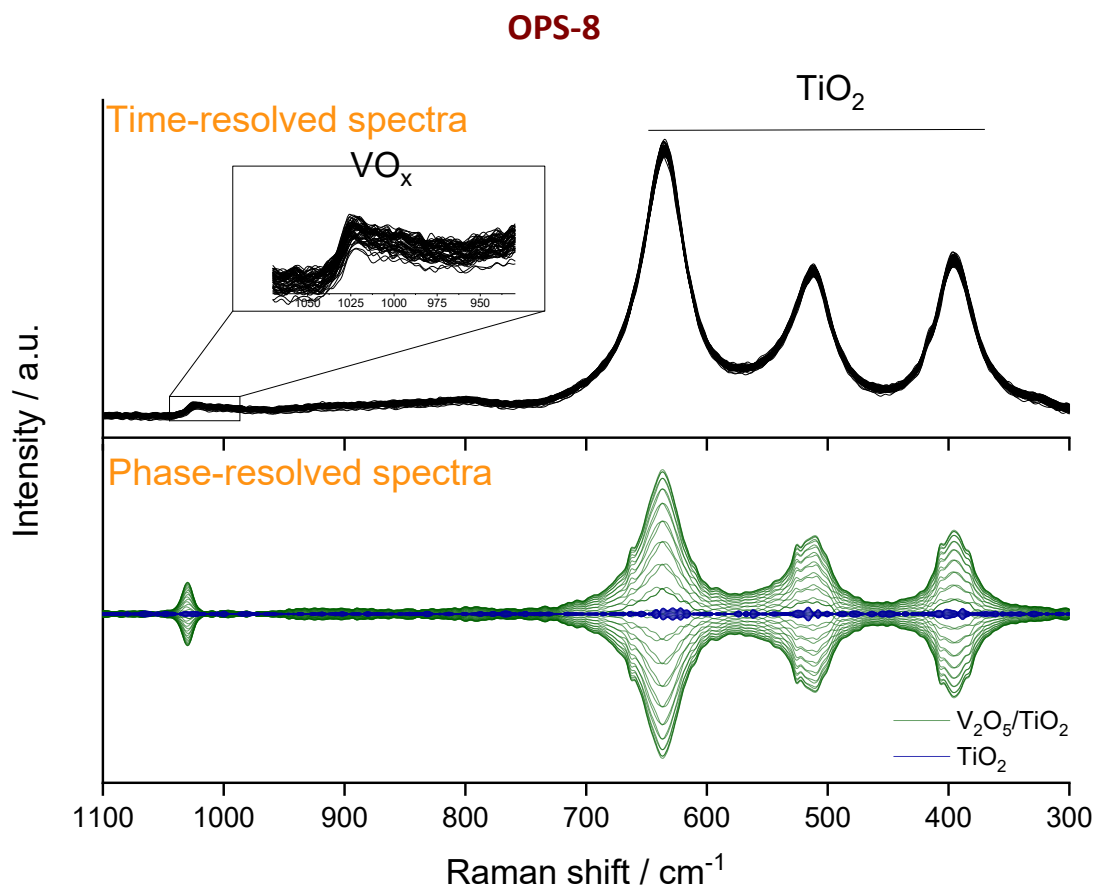


Figure 1. (A) Time-resolved Raman spectra and (B) the corresponding phase-resolved spectra of V<sub>2</sub>O<sub>5</sub>/TiO<sub>2</sub> during 30-s pulses of 500 ppm NH<sub>3</sub> in a gas feed of 500 ppm NO, 2 vol% H<sub>2</sub>O, and 5 vol% O<sub>2</sub> balanced in Ar at 250 °C. The phase-resolved spectra of TiO<sub>2</sub> are also shown for comparison.

**Acknowledgement.** This work was supported by the Swiss National Science Foundation, grant #200021\_172669/1.

**References:**

- [1] I.E. Wachs, *Catal. Today* 27 (1996) 437.
- [2] I. Giakoumelou, C. Fountzoula, C. Kordulis, S. Boghosian, *J. Catal.* 239 (2006) 1.
- [3] D. Baurecht, U.P. Fringeli, *Rev. Sci. Instrum.* 72 (2001)3782.

## DFT Simulation of the Molecular Structure of VO<sub>x</sub>/TiO<sub>2</sub> Catalysts

Nikitina N.A., Pichugina D.A., Kuz'menko N.E.  
 Lomonosov Moscow State University, Moscow, Russia  
 nnikitina1719@gmail.com

V<sub>2</sub>O<sub>5</sub>–TiO<sub>2</sub> is used as a catalyst in various processes: cyclohexane oxidation [1], sulfur dioxide oxidation [2], reduction of nitrogen oxides by ammonia [3]. Different types of V<sub>2</sub>O<sub>5</sub>/TiO<sub>2</sub> system are known: VO<sub>x</sub> monomeric particles, (VO<sub>x</sub>)<sub>2</sub> dimeric particles, (VO<sub>x</sub>)<sub>n</sub> polymeric structures supported on TiO<sub>2</sub>. The vanadium state in V<sub>2</sub>O<sub>5</sub>/TiO<sub>2</sub> as well as the mechanism of active sites formation has been unclear yet.

In this work, we simulated the interaction between TiO<sub>2</sub> (anatase) support and V<sub>2</sub>O<sub>5</sub> including separate VO<sub>x</sub> fragments, dimeric (VO<sub>x</sub>)<sub>2</sub>, and monolayer V<sub>2</sub>O<sub>5</sub>. The catalytic model was constructed as (001) - (2 × 4) TiO<sub>2</sub> (anatase) surface. The catalyst is a periodic surface with four Ti-O layers and a VO<sub>x</sub> layer. VO<sub>x</sub> particles are created by substitution of surface Ti atoms. Plane-wave DFT calculations were performed using the VASP code on the supercomputer at Moscow State University [4]. A projector augmented wave pseudopotential scheme was employed with a 400 eV cutoff energy. Exchange-correlation energies were calculated with the Perdew–Burke–Ernzerhof functional of the generalized gradient approximation (GGA).

According to the calculation of adsorption energy, the monomeric form of V<sub>2</sub>O<sub>5</sub> is the most stable. To estimate reactivity, the d-band structures of V<sub>2</sub>O<sub>5</sub>/TiO<sub>2</sub> were analyzed. The V<sub>2</sub>O<sub>5</sub> deposition on TiO<sub>2</sub> shifts the density of d-states of titanium atoms to the Fermi level. The narrow distribution of electron density in the V<sub>2</sub>O<sub>5</sub>/TiO<sub>2</sub> system indicates a high chemical activity. The contribution of vanadium atoms to the density of d-states increases for system's in the order: separate VO<sub>x</sub> fragments < dimeric (VO<sub>x</sub>)<sub>2</sub> < monolayer V<sub>2</sub>O<sub>5</sub>. This is due to the massive increase in vanadium oxide in the systems. Theoretical studies have shown that the V<sub>2</sub>O<sub>5</sub>/TiO<sub>2</sub> system is complex and dynamic.

**Acknowledgement.** This work was supported by RFBR Grant 18-33-00431.

The research is carried out using the equipment of the shared research facilities of HPC computing resources at Lomonosov Moscow State University.

### References:

- [1] A. Bellifa, D. Lahcene, Y.N. Tchenar, A. Choukchou-Braham, R. Bachir, S. Bedrane, C. Kappenstein Appl. Catal. A Gen. 305 (2006) 1.
- [2] P. Ji, X. Gao, X. Du, C. Zheng, Z. Luoa, K. Cen Catal. Sci. Technol. 6 (2016) 1187.
- [3] I. Giakoumelou, C. Fountzoula, C. Kordulis, S. Boghosian J. Catal. 239 (2006) 1.
- [4] V. Sadovnichy, A. Tikhonravov, Vl. Voevodin, V. Opanasenko "Lomonosov": Supercomputing at Moscow State University. In Contemporary High Performance Computing: From Petascale toward Exascale (Chapman & Hall/CRC Computational Science), Boca Raton, USA, CRC Press (2013) 283.

## A Theoretical Study of the Effects of Promoters of Silver Catalysts for Ethylene Epoxidation

Salaev M.A., Salaeva A.A., Vodyankina O.V.  
Tomsk State University, Tomsk, Russia  
mik.salaev@gmail.com

For many years, ethylene epoxidation brings about the interest of both industry and academic community due to a large number of applications of the ethylene oxide [1]. The silver-based catalysts supported on  $\alpha$ -alumina are traditionally used in the process. Various promoters, including chlorine, rhenium, alkali metals, etc., were shown to enhance the catalyst performance, with Cl and Cs being the most extensively studied both experimentally and theoretically [2-3]. Recently, the theoretical approaches were also used to study the effects of two promoters simultaneously presenting in the model [4,5]. Due to the low amounts of the promoters used, there are the limitations in the experimental study of their roles, while theoretical methods allow shading the light on the nature of the promoting effects. Thus, the roles played by promoters (in particular, Cl, Re and alkali metals) in the process under consideration are still debating.

In the present work we computationally study the promoting effects of chlorine, rhenium and alkali metals in silver catalysts for ethylene epoxidation using the density functional approach. We developed the models containing neutral relaxed Ag clusters and/or substrate and/or atomic oxygen species and/or promoter(s) and calculated them using the Gaussian'09 program package (Revision C.01) installed at SKIF "Cyberia" supercomputer of Tomsk State University. Molecular and atomic oxygen, ethylene, oxametallacycle, and ethylene oxide were taken as substrates. Atomic chlorine, alkali metals (AM=Li, Na, K, Rb, and Cs), rhenium oxyanion ( $\text{ReO}_4$ ) were taken as the promoter moieties. The B3LYP/Lanl2DZ level of theory was used for initial optimization of the models developed, then the resulted geometries were reoptimized using the Lanl2DZ and 6-31G\* basis sets for Ag, Re, Na, K, Rb, and Cs, and C, H, O, and Li atoms, respectively. The nature of the stationary point was checked. The IRC calculations were used to determine the transition states. The binding energies were calculated as the difference between the total energies of the model, substrate(s) and cluster.

The new insights on the nature of co-promotion of Ag catalysts with the promoters under consideration, including synergistic effects, are provided. The effects of promoters on the geometries and the binding energies of the substrates as well as on the transition states and the process mechanism are shown. The roles played by the promoters are discussed.

**Acknowledgement.** The work was supported by the Russian Science Foundation (grant No. 18-73-00296).

### References:

- [1] S. Rebsdat, D. Mayer, 2012, Ethylene Oxide. Ullmann's Encyclopedia of Industrial Chemistry.
- [2] T.C.R. Rocha, M. Hävecker, A. Knop-Gericke, R. Schlögl, J. Catal. 312 (2014) 12-16.
- [3] S. Linic, M.A. Barteau, J. Am. Chem. Soc., 126 (2004) 8086-8087.
- [4] M.O. Özbek, I. Önal, R.A. van Santen, ChemCatChem, 5 (2013) 443-451.
- [5] Z. Li, L. Zhu, J.-F. Chen, D. Cheng, Ind. Eng. Chem. Res., 57 (12) (2018) 4180-4185.

## Theoretical Investigation of Active Metal Sites in Pt- and Pd-Functionalized Metal-Organic Frameworks

Skorynina A.A.<sup>1</sup>, Olsbye U.<sup>2</sup>, Lillerud K.P.<sup>2</sup>, Lamberti C.<sup>1,3</sup>, Soldatov A.V.<sup>1</sup>, Bugaev A.L.<sup>1</sup>

1 – Southern Federal University, Rostov-on-Don, Russia

2 – University of Oslo, Oslo, Norway

3 – University of Turin, Turin, Italy

*alinaskorynina@rambler.ru*

The object of our research is metal-organic frameworks (MOFs) with UiO-67 topology, first synthesized at the University of Oslo 10 years ago [1]. This class of materials has a three-dimensional porous structure with high surface area. Due to the diversity of species, MOFs are used in such areas as luminescent sensors, catalysts, filters, storage and transportation of light gases, and many others [2]. Using noble metals to functionalize metal-organic frameworks is a promising way for constructing new materials for catalytic application [3, 4]. Although numerous successful synthesis of MOFs functionalized by metal ions and metal nanoparticles were reported, the exact mechanisms of structural evolution of the metal sites in many cases is still unknown. Determination of these mechanisms as well as investigation of the intermediate active sites formed during the synthesis is important for tailoring the specific catalytic properties of materials. In this work, we investigate structural changes in UiO-67 functionalized by Pd and Pt depending on the activation conditions by a combination of theoretical and experimental techniques.

Functionalization of UiO-67 by Pd and Pt was achieved via substitution of 10% standard biphenyl dicarboxylate linkers by  $MCl_2$ -2,2-bipyridine-5,5-dicarboxylic acid ( $MCl_2$ bpydc, M = Pd, Pt) [5, 6]. The obtained materials were further activated by heating to 300 °C in inert (He) and reducing ( $H_2/He$ ) atmospheres. Evolution of the atomic and electronic structure was monitored by *in situ* extended X-ray absorption fine structure (EXAFS), X-ray absorption near edge structure (XANES) spectroscopies and X-ray powder diffraction (XRPD). All spectroscopic data for Pd *K*- and Pt *L*<sub>3</sub>-edges were analysed simultaneously by MCR-ALS approach [7] to determine the number of pure species formed during the activation and their spectra.

To interpret the experimental data, we have performed DFT-calculations and XANES simulation by FDMNES code for different potential intermediates. The atomic models included the initial  $MCl_2$ bpydc linker and a number of possible reaction pathways in presence of  $H_2$ : substitution of both chlorine atoms by hydrogen atoms with formation of  $Cl_2$  molecule, substitution of one chlorine by hydrogen atom with formation of HCl molecule; detachment of one or two chlorines with formation of HCl molecules, detachment of  $MCl_2$  fragment from the linker with its substitution by two hydrogens bonded to nitrogen atoms of the linker; and simulating inert conditions: simple detachment of  $MCl_2$  fragment, detachment of chlorines

## OPS-11

with formation of Cl<sub>2</sub> molecule. All reaction pathways were ranked according to the calculated reaction enthalpies and XANES spectra were calculated for the most probable ones.

The reaction pathways with the lowest reaction enthalpies were verified by good agreement between calculated and experimentally observed XANES spectra. For UiO-67-Pd, detachment of PdCl<sub>2</sub> is the most probable pathway in both inert and H<sub>2</sub> atmospheres which correlate with experimental results. For UiO-67-Pt, four different structures have been identified. In the presence of hydrogen, detachment of one chlorine atom should occur first. The second possible transition in the same environment is the detachment of PtCl<sub>2</sub> from the linker with the addition of two hydrogen atoms to nitrogen atoms with the further formation of Pt nanoparticles at temperatures above 200 °C. While formation of bare Pt-sites occurs from 200 to 300 °C in the inert flow [8]. Thus, the XANES spectroscopy supported by theoretical calculations allowed verifying and describing transitional experimental spectra.

**Acknowledgement.** This work was supported by the Russian Science Foundation, grant 18-73-00189.

### References:

- [1] Cavka J. H., et al., *J. Am. Chem. Soc.* 130 (42) (2008) 13850-13851.
- [2] Evans J. D., et al., *Coordination Chemistry Reviews*. 380 (2019) 378–418.
- [3] Tanabe K. K., Cohen S. M., *Chem Soc Rev.* 40 (2) (2011) 498-519.
- [4] Wang Z., Cohen S. M., *Chem Soc Rev.* 38 (5) (2009) 1315-29.
- [5] Braglia L., et al., *Phys Chem Chem Phys.* 19 (40) (2017) 27489-27507.
- [6] Bugaev A. L., et al., *The Journal of Physical Chemistry C.* 122 (22) (2018) 12029–12037.
- [7] Jaumot J., et al., *Chemometrics and Intelligent Laboratory Systems.* 140 (2015) 1-12.
- [8] Bugaev A. L., et al., *Catalysis Today.* (2019) *in press*, doi: 10.1016/j.cattod.2019.03.054.

## Structural, Microstructural and Optical Characterization of Bi<sub>2</sub>O<sub>3</sub>-Cu<sub>2</sub>O Heterojunctions for Photocatalytic Applications

Ayala-Ayala M.T.<sup>1</sup>, Bahnemann D.<sup>2</sup>, Muñoz-Saldaña J.<sup>1</sup>

1 – Centro de Investigación y de Estudios Avanzados del Instituto Politécnico Nacional,  
Querétaro, Mexico

2 – Leibniz Universität Hannover, Hannover, Germany  
maria.ayala@cinvestav.mx

In this work, spherical nanoparticles of tetragonal  $\beta$ -Bi<sub>2</sub>O<sub>3</sub> synthesized by flame spray were used as a p-type semiconductor to obtain Bi<sub>2</sub>O<sub>3</sub>-Cu<sub>2</sub>O heterojunctions to enhance their photocatalytic properties. Cu<sub>2</sub>O is a p-type semiconductor that exhibits high photocurrent density and remarkable photoactivity for hydrogen generation by water splitting. Analytical grade Cu<sub>2</sub>O powder was used without further purification. Bi<sub>2</sub>O<sub>3</sub>-Cu<sub>2</sub>O heterojunctions were synthesized by high energy ball milling as a function of time to study the physical coupling of both semiconductors as well as structural defects and thus their correspondent optical properties. The structural parameters were measured as a function of milling time by X-ray diffraction and Rietveld refinement to evaluate their effect on photoabsorption, photoluminescence and thus photocatalytic properties. Scanning electron microscopy (SEM) and BET surface area evidenced that as prepared Bi<sub>2</sub>O<sub>3</sub> powder has a nanometric size distribution while commercial Cu<sub>2</sub>O powder shows a micrometric particle size with irregular morphology. From reflectance spectra and Tauc plot using Kubelka Munk theory the band gap energy of Bi<sub>2</sub>O<sub>3</sub> and Cu<sub>2</sub>O were 2.5 eV and 2.0 eV, respectively showing that both catalysts can be activated under visible light irradiation. UV-vis-NIR spectrophotometry evidenced an enhancement on the photoabsorption in the Bi<sub>2</sub>O<sub>3</sub>-Cu<sub>2</sub>O heterojunction presenting two shoulders in the reflectance spectra respective to the present phases. This effect seems to be attributed to efficient coupling of both catalysts that promotes charge carrier transport. Photoluminescence spectra of Bi<sub>2</sub>O<sub>3</sub> shows that photorecombination can be diminished by coupling with Cu<sub>2</sub>O. These results evidenced that Bi<sub>2</sub>O<sub>3</sub> with a narrow band gap semiconductor heterojunction stimulates the photoinduced charge transport and separation which increases the photoactivity of the composite. Moreover, the photorecombination of the electron-hole pair as seen in the PL spectra decreased with increasing of milling time on the synthesis of Bi<sub>2</sub>O<sub>3</sub>-Cu<sub>2</sub>O generating thus an efficient coupling of both semiconductors. If the number of emitted electrons resulting from the recombination between excited electrons and holes is increased, the PL intensity increases and consequently, the photoactivity decreases.

## Photocatalytic Hydrogen Evolution from Glucose Aqueous Solutions under Visible Light Irradiation

Kurenkova A.Yu.<sup>1</sup>, Markovskaya D.V.<sup>1,2</sup>, Kozlova E.A.<sup>1,2</sup>

*1 – Boreskov Institute of Catalysis, Novosibirsk, Russia*

*2 – Novosibirsk State University, Novosibirsk, Russia*

*kurenkova@catalysis.ru*

Today, there is a great demand for alternative energy sources because of the increasing emission of green-house gases, world ocean contamination, and fossil fuel depletion. Photocatalytic water splitting is a promising way to convert sunlight energy to the chemical one. H<sub>2</sub> could be produced from water solution under light irradiation in the presence of photocatalyst. To achieve the higher efficiency for photocatalytic water splitting, many researchers have involved electron donors as “sacrificial agents” which can react irreversibly with the photoinduced hole. Great amount of compounds can be used as sacrificial agents, but biomass components are of a particular interest. Using biomass-derived compounds, one can produce H<sub>2</sub> with the usage of renewable energy sources only, namely: solar light, water, and biomass. Cd<sub>1-x</sub>Zn<sub>x</sub>S solid solution with a controllable bandgap width and band-edge position is an efficient photocatalyst for H<sub>2</sub> production from water solutions under visible light. To improve the photocatalytic activity of Cd<sub>1-x</sub>Zn<sub>x</sub>S solid solution, many modification approaches have been developed. Our previous work [1] has shown that the hydrothermal treatment of Cd<sub>0.3</sub>Zn<sub>0.7</sub>S photocatalyst changes the crystal structure from cubic lattice to hexagonal one which is beneficial for photocatalytic reaction [2]. Moreover, deposition of the Pt particles onto the photocatalyst surface is known to increase the hydrogen evolution rate [3].

This work was aimed at the study of photocatalytic hydrogen reaction from glucose solution under visible light irradiation. A series of Cd<sub>0.3</sub>Zn<sub>0.7</sub>S photocatalysts was prepared by the coprecipitation method with subsequent hydrothermal treatment at different temperatures in a range of 80–140 °C in air atmosphere. Afterwards, the Pt particles were deposited on the surface of prepared samples. Photocatalytic hydrogen evolution was carried out by the following method. The aqueous suspension with the catalyst (50 mg), NaOH, and glucose was placed in a sealed reactor, purged with Ar and illuminated by a 450-nm LED (48 mV/cm<sup>2</sup>) under continuous stirring. Hydrogen was analyzed by gas chromatography.

Among the prepared photocatalysts, the sample treated at 120 °C showed the highest activity equaled to 0,5 mmol H<sub>2</sub> · g<sup>-1</sup> · h<sup>-1</sup>. This 1% Pt/Cd<sub>0.4</sub>Zn<sub>0.6</sub>S/ZnS photocatalyst was chosen for the further experiments devoted to the study of the influence of initial concentration of NaOH and glucose. The experimental data are presented in Fig.1.

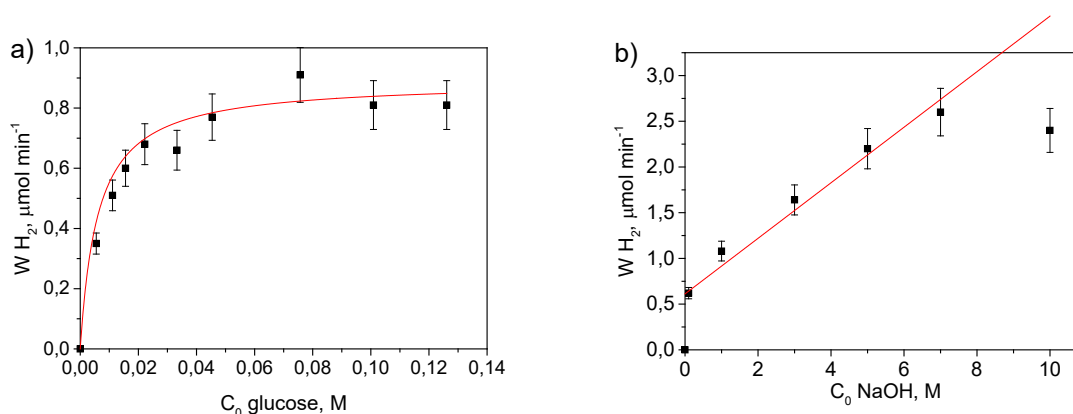


Fig. 1. The H<sub>2</sub> evolution rate over the 1% Pt/Cd<sub>0.4</sub>Zn<sub>0.6</sub>S/ZnS photocatalyst in dependence on a) the initial concentration of glucose (C<sub>0</sub>(NaOH) = 0.1 M); b) the initial concentration of NaOH (C<sub>0</sub>(glucose) = 0.016 M). Conditions: C(cat) = 0,5 g·L<sup>-1</sup>, V = 100 mL, λ = 450 nm.

The data obtained allowed us to propose a kinetic model for the description of dependence the reaction rate on the initial concentration of substrates:

$$W = \frac{A \cdot C(\text{glu}) + B \cdot C(\text{glu}) \cdot C(\text{NaOH})}{1 + D \cdot C(\text{glu})},$$

where A and B are the apparent rate constant, D is the adsorption constant of glucose, C(glu) and C(NaOH) are the initial concentration of glucose and sodium hydroxide, respectively.  $A = k_1 \cdot K_a(\text{glu}) = 139 \pm 35 \text{ mL} \cdot \text{min}^{-1}$ ,  $B = k_2 \cdot K_a(\text{glu}) = 69 \pm 14 \text{ mL}^2 \cdot \text{mol}^{-1} \cdot \text{min}^{-1}$ ,  $D = K_a(\text{glu}) = 164 \pm 48 \text{ M}^{-1}$ . The activity value at 10 M sodium hydroxide was not taken into account as only little amount of glucose had been dissolved in the reaction solution. It should be noted that the semi-empirical equation includes such features of the hydrogen production as the monomolecular reactions occurring on the surface of the photocatalyst with the participation of adsorbed glucose and the linear dependence of the reaction rate on the sodium hydroxide content. Moreover, one can predict photocatalytic activity under different conditions such as glucose or NaOH concentration by the usage of given kinetic model.

**Acknowledgement.** The reported study was funded by RFBR and Novosibirsk region according to the research project № 19-43-543009.

**References:**

- [1] A.Y. Kurenkova, P.A. Kolinko, S.V. Cherepanova, E.A. Kozlova, Mater. Today Proc. 11 (2017) 11371.
- [2] J. Zhanga, S. Wagehc, A. A. Al-Ghamdi, J. Yua, Appl. Catal. B: Environ. 192 (2016) 101.
- [3] E.A. Kozlova, A.Yu. Kurenkova, P.A. Kolinko, A.A. Saraev, E.Yu. Gerasimov, D.V. Kozlov, Kinet. Catal. 58 (2017) 431

## Kinetic Features of Mediator Bioelectrocatalytic Oxidation of Glucose by «Crude» Bacterial Extracts

Dmitrieva M.V., Zolotukhina E.V., Gerasimova E.V., Dobrovolskiy Yu.A.  
*Institute of Problems of Chemical Physics Chernogolovka, Russia*  
*angel.maria@mail.ru*

Bioelectrocatalytic processes are one of the most interesting objects in modern electrochemistry. High selectivity and sensitivity of biocatalysts to the large number of substrates as well as evident perspectives of their use in sensors and fuel cell applications are the main reason of such interest. Bioelectrocatalytic systems can be divided into two types: enzymatic fuel cell working on pure enzymes and microbial fuel cell. However, the main problem of obtaining pure enzymes is a very complicated and long procedure of their synthesis and purification and short lifetime period, which considerably restricts of their application in real systems due to an economic inexpediency. The production of microbial catalysts is quite simple in comparison, but the lifecycle and stability of the microbial fuel cell are restricted and moreover, the waste products in the electrolyte can affect on the electrochemical cell operation. So, the combination of advantages of pure enzymes and microbial fuel cells looks very attractive for practice. Such combination can be realized by the use of protein extracts obtained from microbial cells.

In our previous work [1] the idea of the use of "crude" protein extract in biocatalytic reaction has been already checked.

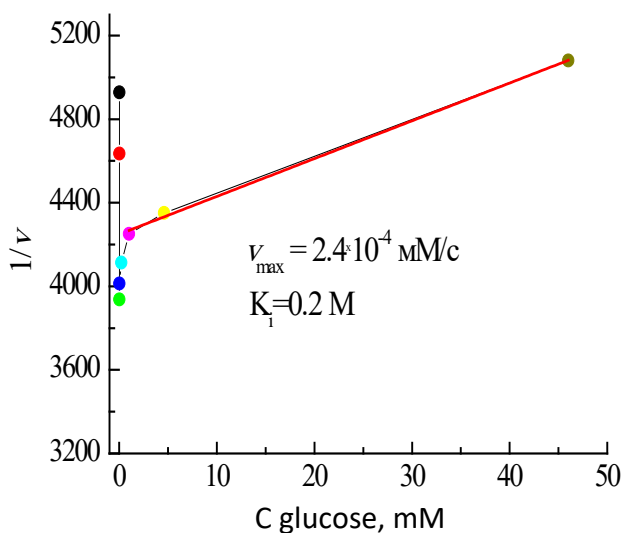


Figure 1. The influence of concentration of substrate (glucose) on bioelectrocatalytic reaction with the participation of the "crude" bacterial extracts.

"Crude" protein extract of microbial cells was studied as a bioelectrocatalyst in glucose oxidation reaction. Such extract obtained from *Escherichia coli* BB culture was considered in this work as a model system containing all enzymes of bacteria lifecycle. This system

demonstrated the mediating mechanism of interaction with an inert glassy carbon electrode in buffer solution with glucose as a substrate.

This work is dealing with study of influence of some experimental conditions (temperature, co-enzyme content, mediator content, substrate content and enzyme content)

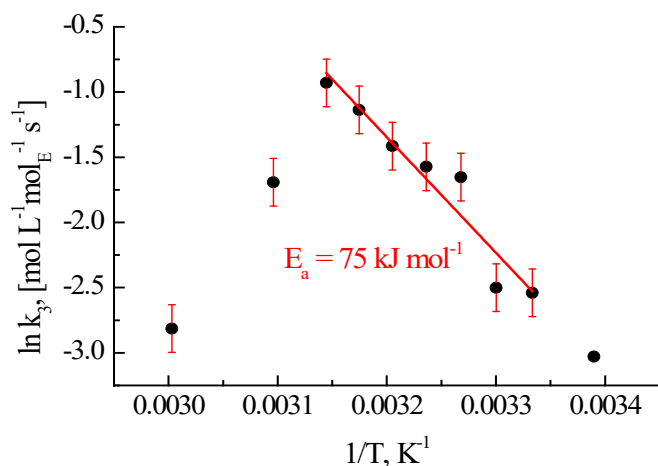


Figure 2. Dependence of the rate constant of glucose oxidation reaction on temperature.

on bioelectrochemical activity of crude extracts obtained from culture of *E.coli BB* in glucose oxidation reaction. The obtained experimental data allowed to establish the kinetic features of the mediator oxidation of glucose by «crude» extracts. Reaction rate constant,  $k$ , calculated from the slope of the initial part of the kinetic curve (Fig. 1) was  $0.06 \text{ mol}^{-1} \text{ s}^{-1}$ . When studying the effect of substrate concentration (glucose) on the initial

reaction rate, it was found that the resulting dependence of the reaction rate on the glucose concentration is typical for the case of substrate inhibition. The estimated value of the substrate inhibition constant was 0.2 M. The study of kinetic curves in the temperature range from 27 to 60 °C allowed us to obtain the activation energy value for the optimal pH value and buffer composition. Fig. 2 demonstrates the dependence of the rate constant  $k$  on temperature. Obtained extracts were also tested in asymmetric fuel biocells with various design. It was shown that specific power density of these cells depends strongly not only type of extract and used fuel, but also on the materials of the structural part of the cell as well as its design. Obtained results indicate the perspective of further research and practical application of a new type of bioelectrocatalyst.

**Acknowledgement.** This work was supported by the Grant of the President of the Russian Federation № SP-2619.2018. This study was carried out with the use of resources of Competence Center of National Technology Initiative in IPCP RAS.

#### References:

[1] M. Dmitrieva, E. Zolotukhina, E. Gerasimova, A. Terent'ev, Yu. Dobrovol'skii, Dehydrogenase and electrochemical activity of *Escherichia coli* extracts, *Applied Biochemistry and Microbiology*. 53 (2017) 458-463.

## Synergetic Effect of Polychromatic Irradiation in the Reactions of Photocatalytic Oxidation on the Surface of N-Doped Titanium Dioxide

Kovalevskiy N.S.<sup>1,2</sup>, Selishchev D.S.<sup>1,2</sup>, Svintsitskiy D.A.<sup>1,2</sup>, Selishcheva S.A.<sup>1,2</sup>, Kozlov D.V.<sup>1,2</sup>

1 – Boreskov Institute of Catalysis, Novosibirsk, Russia

2 – Novosibirsk State University, Novosibirsk, Russia

*nikita@catalysis.ru*

One of the important fields of scientific and technical research is photocatalysis as an efficient method for transformation of light energy to carry out useful chemical processes, e.g., photocatalytic oxidation for the efficient purification of water and air from hazardous chemical and biological agents. Titanium dioxide is the most active and stable photocatalyst for the oxidation processes both in liquid and gas phases. At the same time, a substantial hindrance for active expand of TiO<sub>2</sub> photocatalysts is a wide band gap of titanium dioxide that corresponds to the fundamental ability for the absorption of UV light only. This fact hinders its application under solar light due to the solar radiation spectrum has less than 5% of radiation in that region compared to all the radiation with wavelengths less than 780 nm. Therefore, an enhancement of TiO<sub>2</sub> action spectrum is an important task.

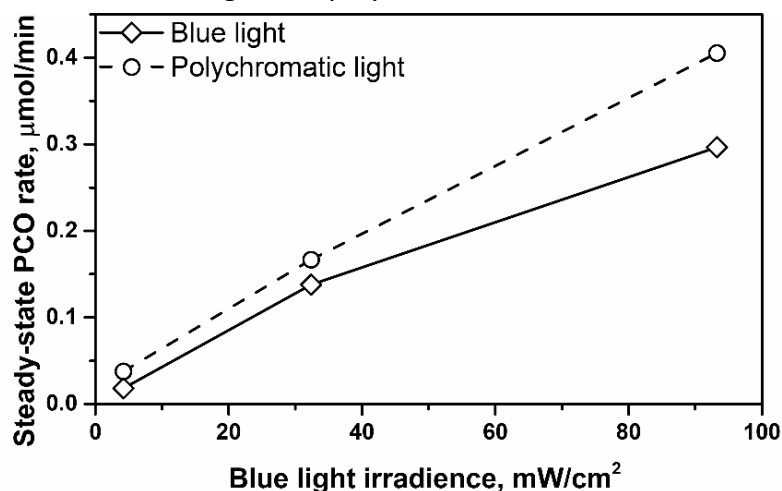
A shift of the TiO<sub>2</sub> absorption band edge towards the visible region can be achieved using several ways, namely, sensitization with dyes, doping with metals, plasmon resonance, modification with other semiconductors, and doping with non-metal atoms. The TiO<sub>2</sub> doped with nitrogen exhibited a very high activity under visible light [1]. The nitrogen impurities were shown to induce the formation of localized energy levels in the band gap of TiO<sub>2</sub> that results in reducing the energy for electron excitation and a redshift of the absorption band edge up to 550 nm. However, DFT calculations and EPR spectroscopy studies showed that the impurity level of nitrogen is partly unoccupied [2]. As a result, an electron under blue light (450 nm) can be excited from the impurity level to the conduction band, as well as from the valence band to the impurity level. The first process leads to the photocatalytic process, because a long-lived electron-hole pair is formed. The second process leads to the undesirable recombination and decreases the photon efficiency. Additional irradiation with wavelength longer than 550 nm can increase the photon efficiency due to the excitation of an electron from the valence band to the impurity level and an increase in its occupation. Therefore, this study was aimed to experimentally confirmed this assumption by investigation the effect of polychromatic irradiation on the photocatalytic activity of N-doped TiO<sub>2</sub>.

For this purpose, the N-doped TiO<sub>2</sub> photocatalysts were prepared via the precipitation from titanil sulfate solution with ammonium hydroxide. After aging, the precipitate was separated by centrifugation and washed. Finally, the precipitate was calcined at 350 °C followed by the grind. The effect of additional irradiation with wavelength longer than 550 nm on the steady-state photocatalytic activity was investigated using a test reaction of the acetone oxidation in a

## OPS-15

continuous-flow set-up. The experiments were performed under blue light (450 nm) and under combination of blue (450 nm) and red (630 nm) light. The irradiance of blue light was 4, 32, or 93 mW/cm<sup>2</sup>. The irradiance of blue component in polychromatic irradiation was the same, while the irradiance of red component was 10, 65, 177 mW/cm<sup>2</sup>, respectively.

The oxidation under red light only was checked under the first step. No activity was observed for red light even at the maximum irradiance, because the energy of light is not enough for the excitation of electrons to the conduction band. Further, the photocatalytic activity was compared under blue light and polychromatic irradiation.



Up to 2-fold increase in the rate of photocatalytic oxidation was observed under polychromatic irradiation compared to the rate under blue light. The red light increases the occupation of the impurity level that increases the probability of electron excitation from this impurity level to the conduction band of TiO<sub>2</sub> under blue light. As a result, the efficiency of blue light utilization is increased. The experiments with several amounts of irradiance shown that the photocatalytic oxidation rate non-linearly increases under blue light as the irradiance increases. This is due to an increasing recombination of charge carriers. On the contrary, the photocatalytic activity under polychromatic light has a linear dependence, and the steady-state photocatalytic oxidation rate is higher under the same irradiance of blue light.

This study shows a synergetic effect of polychromatic irradiation, when an additional red light increases the efficiency of blue light utilization by N-doped TiO<sub>2</sub>. Therefore, the N-doped TiO<sub>2</sub> photocatalysts have a promise for efficient photocatalytic oxidation under solar light, which is a polychromatic irradiation with a wide range of wavelengths.

**Acknowledgement.** This work was supported by the Russian Foundation for Basic Research [grant number 18-29-17055], the Russian Foundation for Basic Research and the government of Novosibirsk region of the Russian Federation [grant number 19-43-543038], and the Russian President Grant [grant number 075-15-2019-1086 (MK-3483.2019.3)]

### References:

- [1] S. Kumar, L. Devi, J. Phys. Chem. A. 115 (2011) 13211.
- [2] C. Di Valentine, G. Pacchioni, J. Phys. Chem. B. 109 (2005) 11414.



# **POSTER PRESENTATIONS**

**Section I. Basic concepts, theory and modeling in catalysis**  
**PP-I-1 ÷ PP-I-16**

**Section II. Physical methods, including in situ and operando techniques, in catalysis**  
**PP-II-1 ÷ PP-II-14**

**Section III. Kinetics and mechanisms of catalyzed processes**  
**PP-III-1 ÷ OP-III-54**

**Section IV. Advanced catalyst systems addressing current challenges: energy, materials, sustainability**  
**PP-IV-1 ÷ OP-IV-69**



## Computer Simulation System for the Catalytic Dewaxing Process

Belozertseva N.E., Belinskaya N.S.  
Tomsk Polytechnic University, Tomsk, Russia  
*belozertsevanatasha@mail.ru*

In recent years, Russia has witnessed an increase in the production of diesel fuel. One of the most modern processes for the production of diesel fuel is the catalytic dewaxing process.

However, despite the growth of knowledge regarding this process, its optimization with regard to the composition of the feed, mechanisms of the occurring reactions, the activity of the catalyst and possible deviations (abnormal situations) in the operation of the installation has not been implemented at the moment.

The urgency of the catalytic dewaxing process modeling is due to the fact that the main goal will be achieved, which is to obtain diesel fuel that meets international standards, with minimal economic and production costs.

In this paper, a computer simulation system was created for the catalytic dewaxing process. This computer simulation system can be used as a simulator for personnel working at the industrial unit and as a tool for monitoring the process parameters and offer the options for optimizing operating parameters when the final characteristics of the product do not match the required grade of diesel fuel.

To create this computer simulation system, the catalytic dewaxing process was studied in detail, namely:

- main reactions occurring in this process and their thermodynamic and kinetic parameters;
- composition and properties of feed and hydrogen-containing gas;
- technological parameters of the process [1].

All the data obtained were aimed at creating a computer simulation system for the catalytic dewaxing process. The algorithm for the application of the system is presented in Figure 1.

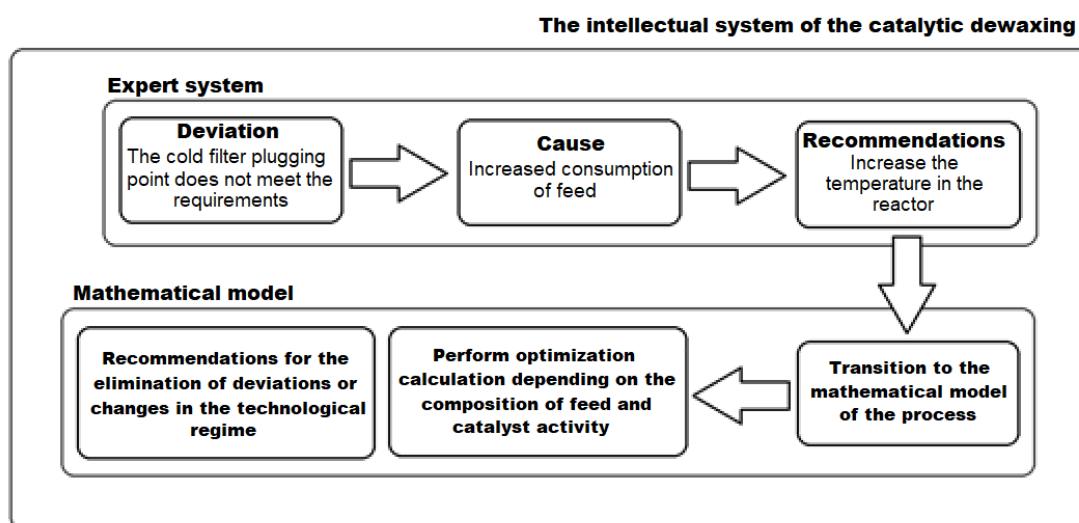


Figure 1 - Algorithm of application of the intellectual system of the catalytic dewaxing process

## PP-I-1

The developed modelling system can be applied at the industrial enterprise in a real mode of operation of a catalytic dewaxing unit to recommend actions in the event of the abnormal situation, taking into account the composition of the processed feed and the activity of the catalyst.

**Acknowledgement.** This work was supported by the Russian Foundation for Basic Research, project No. 18-38-00585 “Studying physico-chemical patterns and the development of non-stationary mathematical model of the petroleum middle distillates catalytic dewaxing process”.

### References:

[1] Belinskaya N.S., Frantsina E.V., Ivanchina E.D., Popova N.V., Belozertseva N.E. Determination of optimal temperature of catalytic dewaxing process for diesel fuel production // Petroleum and Coal. – 2016. – Vol. 58(7). – P. 695-699.

## The Interface Effect of Gold Nanoparticles and Pyrolytic Graphite on Hydrogen Adsorption

Dohlikova N.V., Gatin A.K., Sarvadii S.Y., Haritonov V.A., Rudenko E.I., Grishin M.V., Shub B.R.  
 Semenov Institute of Chemical Physics RAS, Moscow, Russia  
 dohlikovanv@gmail.com

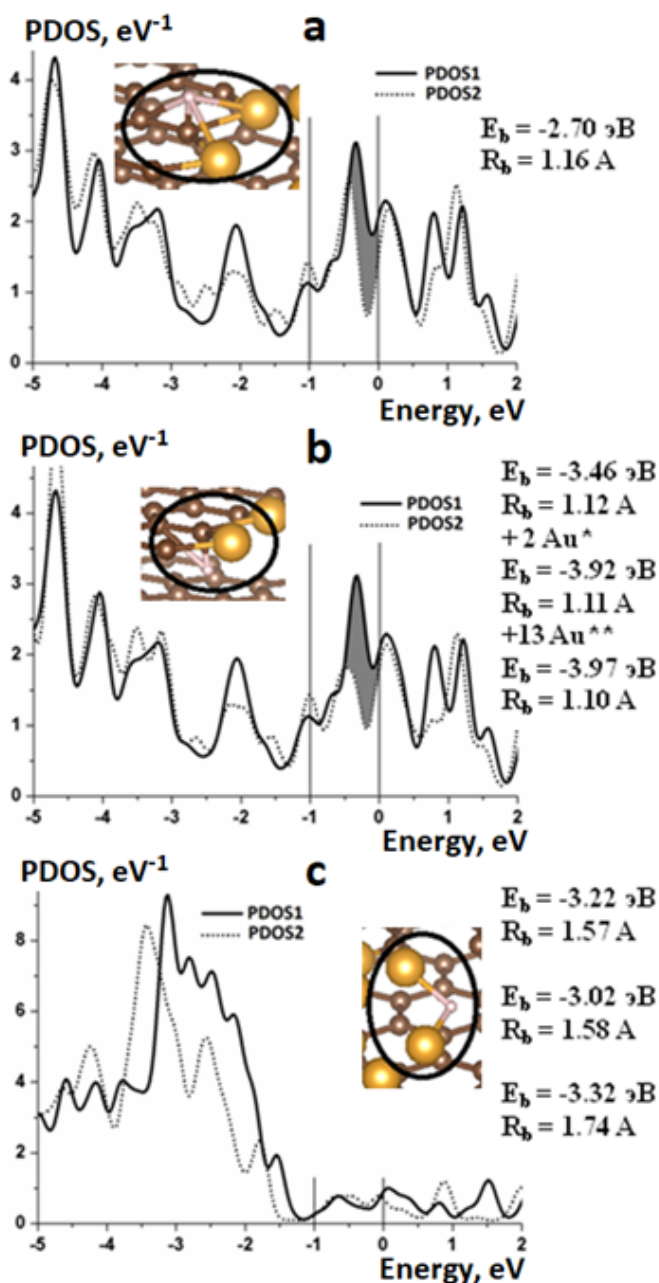


Fig. 1. The sum of projected densities of states (PDOS) of atoms near the adsorbed hydrogen (outlined in an inset near the graph); PDOS1 - before adsorption, PDOS2 - after adsorption; a - above the interface, b - under the interface, c - on the gold cluster. For part b,  $+2\text{Au}^*$  - bond energy for two relaxed gold atoms closest to adsorbed hydrogen,  $+13\text{Au}^{**}$  - bond energy for all relaxed gold atoms.

The interface of deposited metal nanoparticle and a substrate can play a large role in the adsorption processes. It is due to the inhomogeneous electronic structure arising from the nanoparticle atomic structure transformation and the contact difference of nanoparticle and substrate chemical potentials. The hydrogen adsorption on gold nanoparticles ( $\approx 5$  nm) deposited on a highly oriented pyrolytic graphite (HOPG) was investigated using scanning tunnelling microscopy/spectroscopy (STM/STS) [1]. Since STM/STS allows one to measure the sample surface local properties, it was found that the most preferred area of a hydrogen adsorption is the interface of gold nanoparticles and a HOPG substrate. While hydrogen is stably chemisorbed on the gold nanoparticles surface, this leads to the metal-semiconductor transition of the latter. The hydrogen adsorption DFT-simulation on the interface of a gold cluster and a graphite plane edge (supercluster  $\text{Au}_{13}\text{C}_{138}$ ) was carried out. It showed that the largest change of density of states (DOS) in the Fermi level vicinity undergoes in the case of interface adsorption, which is consistent with the results of the STS experiments. The difference in the

## PP-I-2

interface-cluster adsorption energy is small. It means that hydrogen adatoms migration is associated with transitions through a significant activation barrier. The greatest influence on the binding energy of hydrogen atoms with a gold cluster has the nearest gold atoms mobility, which indicates that the hydrogen interaction with the supercluster Au<sub>13</sub>C<sub>138</sub> is locally. As one can be seen, the computer simulation results are in qualitative agreement with the experimental data. The calculation results are shown in Fig.1.

**Acknowledgement.** This work was supported by the Russian Foundation for Basic Researches, grant 17-03-00275. Calculations were performed on the computational resources of the Joint Supercomputer Center RAS

### References:

[1] Grishin M.V. et. al, Kinet. Catal. 56 (2015) 539.

## Computer Simulation of the Kinetics of a Multistage Process as a Method of Studying the Mechanism of Catalytic Naphtha Reforming

Dyusembaeva A.A., Vershinin V.I.  
Dostoevsky Omsk State University, Omsk, Russia  
aykend@mail.ru

To describe the catalytic reforming, kinetic models reflecting a set of successive partial reactions of the first and pseudo-first order are used. The reactions describe reversible and irreversible conversions of individual hydrocarbons (e.g., *n*-heptane) and/or narrow groups of structurally similar hydrocarbons (e.g, xylenes). Kinetic models are systems of differential equations in which the coefficients are the rate constants ( $k_j$ ) measured in laboratory conditions for partial reactions. The values of the constants are refined by solving the inverse problem of chemical kinetics as applied to the features of the simulated reactors and the real conditions of reforming. Kinetic models take into account not only the change in the concentration and temperature of the reaction mixture, but also the gradual coking of the active sites of the catalyst [1]. An adequate description of reforming is achieved by the proper choice of partial reactions considered in the model. Thus, a relatively simple model [2] takes into account 27 partial reactions occurring with the participation of 16 components of the reaction mixture in the range of 490-525°C on different active sites of the Pt-Sn catalyst. Using the model [2], it is possible to predict the content of components in the final product (platformate) knowing the composition of the raw material and the reforming conditions. Calculations are carried out using specially developed software, a single calculation takes less than 1 min. The prediction errors do not exceed 2 rel. % for the target reforming products, i.e., individual C<sub>6</sub>-C<sub>8</sub> arenes.

The use of an adequate model developed at Omsk State University [2] allows us to predict the effect of technological factors on the composition of platformate, as well as to optimize the reforming conditions [3]. However, we believe that the model [2] can also be applied to study the mechanism of catalytic reforming, in particular, to identify those partial reactions that most affect the yield of the target products. In the course of the computer experiment, we alternately varied the values of all  $k_j$  (by  $\pm 5$ ,  $\pm 10$ ,  $\pm 15\%$  relative to the nominal value) and recorded changes in the expected contents of the target products (benzene, toluene, and the sum of xylenes). The sensitivity coefficient  $S_{ij}$  for the  $i$ th composition index and for the  $j$ th reaction was calculated by the general formula

$$S_{ij}^k = \frac{k_j \partial Y_i}{Y_i \partial k_j} = \frac{\partial \ln Y_i}{\partial \ln k_j} , \quad (1)$$

where  $Y_i$  is the expected content of the  $i$ th product in platformate. The justification of the formula (1), as well as the methodology and the results of a computer experiment are

### PP-I-3

described elsewhere [4]. All calculations were performed for 505°C, which corresponds to the middle of the temperature range allowed by the technological regulations (490–525°C). The values of  $S_{ij}$  found for 27 partial reactions were compared in absolute value. The reactions for which the  $S_{ij}$  values are maximal have the greatest effect on the yield of the  $i$ th product.

According to our data, the yield of benzene is most affected by reaction 2, i.e., the dehydrocyclization of *n*-hexane. Reactions 5 and 9, which represent different stages of the dehydrocyclization of *n*-heptane and isoheptanes, have the greatest effect on the yield of toluene and xylenes. Apparently, the reactions 2, 5 and 9 are the limiting stages of the multistage reforming process. The critical level of variation of the rate constants for these reactions is close to 10 rel. %. Larger variations of the constants lead to statistically significant changes in the composition of platformate. On the contrary, the variation of the rate constants for the paraffin dehydrogenation and isomerization reactions as well as for the side reactions of hydrocracking almost does not affect the expected composition of platformate. It should be considered that the rate constants  $k_2$ ,  $k_5$  and  $k_9$  at a temperature of 505°C are much lower than the rate constants for the competing dehydrogenation and isomerization reactions. This is consistent with our assumptions about the limiting stages of a multistage process. Probably, it is useful to determine the sensitivity of the model to variations in the kinetic parameters not only when studying the reforming mechanism, but also when studying other multistage catalytic processes. The only problem is that not all of these processes have detailed kinetic models that are adequate in a wide range of variable parameters and that allow appropriate computer experiments to be carried out.

**Acknowledgement.** This work was supported by the Russian Foundation for Basic Research (grant 16-43-550479).

#### References:

- [1] N. Ostrovsky, A. Belyi // *Khim. Prom-st.* 76 (1999) 522.
- [2] A. Dyusembaeva, V. Vershinin // *Catalysis in Industry.* 9 (2017) 10.
- [3] A. Dyusembaeva, V. Vershinin // *Kataliz v promyshlennosti (Catalysis in Industry).* 10 (2018) no 5, 70.
- [4] A. Dyusembaeva, V. Vershinin // *Kinetic and Catalysis.* 60 (2019) 106.

## Catalysis of Hydrogen Atom Transfer in Water Complexes with Organic Compounds

Grinvald I.I., Kalagaev I.Yu., Spirin I.A., Kapustin R.V., Petukhov A.N.  
Nizhny Novgorod State Technical University, Nizhny Novgorod, Russia  
grinwald@mts-nn.ru

The hydrogen atom transfer is one of phenomena, which attracts the attention of many researchers, because it plays an important role in chemical and biological processes. A similar transfer can be a crucial step in different catalytic reactions. In most cases it relates to the formation of hydronium ion in water systems. However there is a quite restricted set of experimental data concerning this transformation.

In the present work the hydrogen atom transfer and interaction of hydronium ion with organic molecules in solid films and KBr matrix by FTIR spectroscopy was studied. There were used two ways of preparation of the solid phase. In the first one the KBr powder was saturated by water vapour and then mixed with the organic species and was pressed in a pallet for FTIR spectra recording. In the other one the solid film on the optical window was prepared from acetone solution, to which water was added. There were considered three water-organic compounds systems, having different mechanisms of hydrogen atom transfer.

*Triazole-water system in solid film.* Triazole has an agostic hydrogen atom, which can transfer to the oxygen atom of a water molecule. It leads to the formation of hydronium ion complex with triazole molecule. This transformation manifests in IR spectra as an appearance of a set of new bands in 1900-1800  $\text{cm}^{-1}$  region, having no isotopic shift in a heavy water system. At heating of the films the bands disappear.

*Diaminoboran, morpholinboran-water systems in solid films.* These organic species can form dihydrogen bond with hydrogen atom of water molecule in water complexes. The new bands, assigned to this type of binding in 3400-3300  $\text{cm}^{-1}$  range were observed. The mentioned bands have an isotopic shift predicted from theoretical considerations. Such an interaction leads to the following transformation with hydronium ion occurrence. The new bands at 1720-1710  $\text{cm}^{-1}$  indicate the hydrogen atom transfer in water complexes. The suggested interpretation is confirmed by IR spectra of heavy water samples.

*1-Butyl-3-methylimidazolium chloride and tetrafluoroborate-water systems in KBr matrix.* These organic species are, so called, room temperature ionic liquids. In these systems the new bands in 3520-3490  $\text{cm}^{-1}$  region were observed. The range of location and isotopic shift in heavy water systems prove the assignment of these bands to water complexes of ionic liquids. At the same time the new band at 2108  $\text{cm}^{-1}$  demonstrates the formation of hydronium ion in system at the transformation of complexes.

*DFT study.* The calculations have shown that in the presented systems water complexes with hydrogen atom transfer can form. In this transformation the agostic hydrogen atom (the first system), dihydrogen binding (the second system) and interaction of anion atoms in initial organic molecule or KBr matrix with water (the third system) can participate.

## Breaking the Rules in Zirconocene-Catalyzed $\alpha$ -Olefin Oligomerization: DFT Visualization of Zr-Al and Zr-Al<sub>2</sub> Mechanistic Concepts

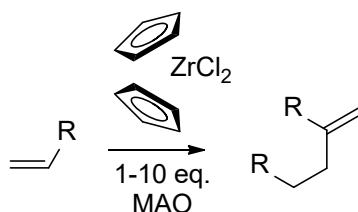
Ivchenko P.V.<sup>1,2</sup>, Nifant'ev I.E.<sup>1,2</sup>, Vinogradov A.A.<sup>1</sup>

1 – A.V. Topchiev Institute of Petrochemical Synthesis, RAS, Moscow, Russia

2 – M.V. Lomonosov Moscow University, Department of Chemistry, Moscow, Russia  
phpasha1@yandex.ru

Conventional concept of zirconocene-catalyzed polymerization of  $\alpha$ -olefins implies the involvement of cationic alkylzirconium catalytic species [1]. This model seems to be reasonable for conventional<sup>1</sup> activation of zirconocene pre-catalysts by  $10^3$ – $10^4$  of methylalumoxanes (MAO) or by perfluoroaryl borates. Strictly speaking, the cationic model requires significant refinement from the standpoint of the formation of close or separated ion pairs [2–7]. If the reaction is preceded by the initiation with minimal excess of MAO,<sup>2</sup> or proceeds in the presence of organoaluminium scavenger (perfluoroaryl borate activation), the direct participation of Zr-Al heterobimetallic species [8–10] is very possible.

Low MAO loading is used in selective dimerization of  $\alpha$ -olefins [11] (Scheme 1). The cationic concept (Fig. 1A) fails to interpret the experimental observations for this process. Recently we proposed the probable cause of high selectivity in the formation of methylenealkanes [12, 13]. We assumed that the driving force of  $\beta$ -hydride elimination after the insertion of the second molecule of  $\alpha$ -olefin is a formation of Zr-( $\mu$ -H)-Al fragment in heterobimetallic complex; and the chemical nature of the second bridging ligand (H, Cl, F, Alkyl) determines the activation barrier of  $\beta$ -hydride elimination (Fig. 1B).



**Scheme 1.** Dimerization of  $\alpha$ -olefins

In our presentation we will discuss the results of DFT modeling (M06X/DGTZVP) of the reaction profiles of  $\alpha$ -olefin oligomerization for  $(\eta^5\text{-C}_5\text{H}_5)_2\text{Zr}(\mu\text{-H})(\mu\text{-X})\text{-AlMe}_2$  species. These results allowed us to interpret the difference in catalytic behavior of  $(\text{C}_5\text{H}_5)_2\text{ZrX}_2$  (X = Cl, F, Me) in the presence of single MAO molecules. However, this simple bimetallic model does not accurately reflect the empirical regularities, and we have developed a more complex trinuclear mechanistic concept (Fig. 1C) that correlates with the molecular structures of neutral and cationic zirconium-aluminium complexes [8–10].

<sup>1</sup> *in academia* ☺

<sup>2</sup> reaction conditions that are actual for chemical industry

## PP-I-5

The free energies of transition states of  $\beta$ -hydride elimination, that were found for trinuclear mechanism, are in good agreement with the experimental results. The possibility of the using of binuclear and trinuclear models to analyze the reactivity of zirconocenes of different structural types in the presence of organoaluminium compounds is also considered in our presentation.

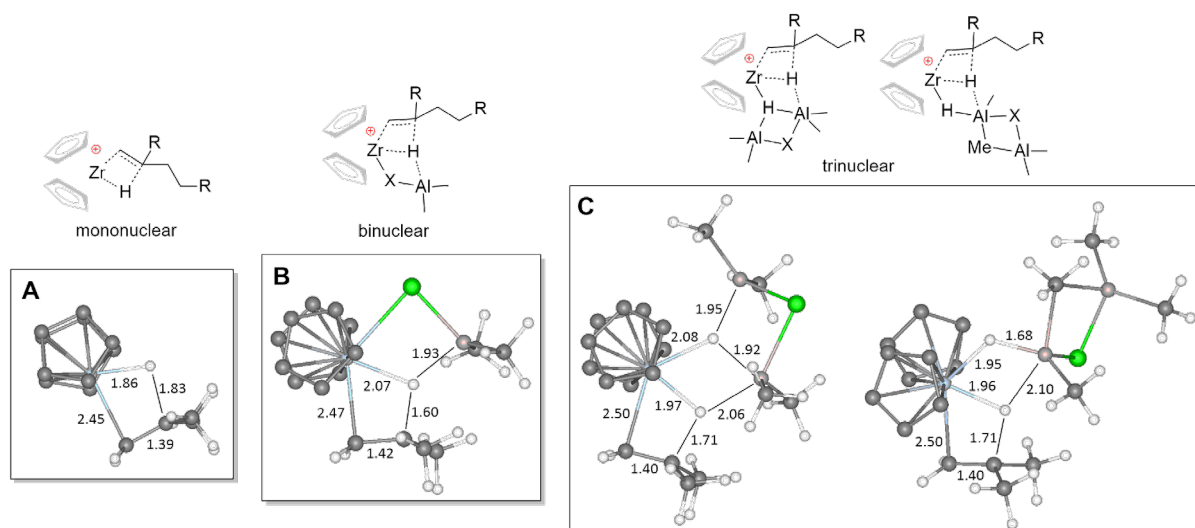


**Figure 1.** Transition states of  $\beta$ -hydride elimination stage for traditional cationic (mononuclear, A), binuclear (B) and trinuclear (C) mechanisms. Hydrogen atoms in Cp rings are omitted for clarity

We sincerely hope for a fruitful discussion of the novel mechanistic concepts in the course of our report.

**Acknowledgement.** This work was supported by the Russian Science Foundation, grants 18-13-00351 and 18-73-10128.

### References:

- [1] W. Kaminsky, A. Laban, *Appl. Catal. A: General* 222 (2001) 47.
- [2] S. Beck, S. Lieber, F. Schaper, A. Geyer, H.H. Brintzinger, *J. Am. Chem. Soc.* 123 (2001) 1483.
- [3] C.L. Beswick, T.J. Marks, *Organometallics* 18 (1999) 2410.
- [4] M.S.W. Chan, K. Vanka, C.C. Pye, T. Ziegler, *Organometallics* 18 (1999) 4624.
- [5] I.E. Nifant'ev, L.Yu. Ustynyuk, D.N. Laikov, *Organometallics* 20 (2001) 5375.
- [6] G. Theurkauff, A. Bondon, V. Dorcet, J.-F. Carpentier, E. Kirillov, *Angew. Chem. Int. Ed.* 54 (2015) 6343.
- [7] G. Theurkauff, M. Bader, N. Marquet, A. Bondon, T. Roisnel, J.-P. Guegan, A. Amar, A. Boucekine, J.-F. Carpentier, E. Kirillov, *Organometallics* 35 (2016) 258.
- [8] S.M. Baldwin, J.E. Bercaw, H.H. Brintzinger, *J. Am. Chem. Soc.* 130 (2008) 17423.
- [9] S.M. Baldwin, J.E. Bercaw, H.H. Brintzinger, *J. Am. Chem. Soc.* 132 (2010) 13969.
- [10] S.M. Baldwin, J.E. Bercaw, L.M. Henling, M.W. Day, H.H. Brintzinger, *J. Am. Chem. Soc.* 133 (2011) 1805.
- [11] J. Christoffers, R.G. Bergman, *J. Am. Chem. Soc.* 118 (1996) 4715.
- [12] I.E. Nifant'ev, A.A. Vinogradov, A.A. Vinogradov, P.V. Ivchenko, *Catal. Commun.* 79 (2016) 6.
- [13] I. Nifant'ev, P. Ivchenko, A. Tavtorkin, A. Vinogradov, A. Vinogradov, *Pure Appl. Chem.* 89 (2017) 1017.

**Generalized Quantum-Chemical Principle and the Theory of Catalysis by Polyedres as a Basis Formulating the Mechanisms of Chemical and Catalytic Processes**

Kolesnikov I.M.

*Gubkin Russian State University of Oil and Gas, Moscow, Russia*

To date, many different modifications of mechanisms have been developed: radical theory, carbonium ion theory, radical cation mechanism, basic and acid catalysis, homogeneous and heterogeneous catalysis, and other approaches to the formulation of mechanisms for the transformation of inorganic and organic substances.

In all these theories, the mechanism of preliminary excitation of reagent molecules is not shown, while molecules in the ground state cannot react. For the first time, Taylor for heterogeneous catalysis conditions stated that chemisorbed (excited) molecules can be subjected to catalytic transformation. However, they did not formulate in detail the elementary stages of the catalytic process.

The elementary stages of the catalytic process (as well as any chemical non-catalytic process) were determined on the basis of the Generalized Quantum-Chemical Principle formulated by the author in the twentieth century.

Moreover, for catalytic processes, the mechanism is formulated on the basis of the theory of catalysis by polyhedra for homogeneous and heterogeneous systems. The generalized quantum chemical principle was developed in the following formulation: **the chemical (catalytic) reaction can take place at all elementary stages while simultaneously fulfilling the requirements imposed on the reacting system by the Hund rule, Pauli principles, energy correspondence, phase sign matching, and preservation of orbital symmetry. Violation of any of these requirements imposes a ban on the implementation of the elementary stage or increases the likelihood of its breaking.**

This principle is simple in formulation and rigorous in content. Based on it, it is easy to choose the only possible path for a chemical (catalytic) reaction. To illustrate the principle, elementary stages of the process of dimerization of ethylene molecules in the presence of an aluminosilicate catalyst are considered.

## Nuclear Spin Catalysis: From Chemical Physics to Living Cells

Koltover V.K.

*Institute of Problems of Chemical Physics, RAS, Chernogolovka, Moscow Region, Russia*

*koltover@icp.ac.ru*

Cells are composed from atoms of chemical elements, many of which have magnetic and nonmagnetic stable isotopes. In physics and chemistry, magnetic isotope effects (MIEs) have long been known for a number of magnetic isotopes, among them  $^{13}\text{C}$ ,  $^{17}\text{O}$ ,  $^{29}\text{Si}$ ,  $^{33}\text{S}$ ,  $^{73}\text{Ge}$ , and  $^{235}\text{U}$  [1]. Not long ago, MIEs have been discovered in experiments with living cells. In studies of effects of different isotopes of magnesium, magnetic  $^{25}\text{Mg}$  and nonmagnetic  $^{24}\text{Mg}$ , on the post-radiation recovery of the yeast *Saccharomyces* irradiated by short-wave UV light or X-rays, it has been revealed that the recovery process of the cells, enriched with the magnetic  $^{25}\text{Mg}$ , proceeds two times faster than the post-radiation recovery of the cells, enriched with the nonmagnetic  $^{24}\text{Mg}$  [2, 3]. In the experiments with another cell model, bacteria *E. coli*, it has been found that bacterial cells adapt essentially faster to the growth media enriched with magnetic  $^{25}\text{Mg}$  compared to the media enriched with the nonmagnetic isotopes of magnesium. Besides, the cells enriched with  $^{25}\text{Mg}$  demonstrate the reduced activity of the important antioxidant enzyme, superoxide dismutase, by comparison to the cells enriched with the nonmagnetic  $^{24}\text{Mg}$  [4, 5]. Thus, it has been discovered that living cell perceive the nuclear magnetism. Furthermore, MIEs have been revealed in studies of the most important molecular motor of cell bioenergetics, myosin isolated from smooth muscle. The rate of the ATP hydrolysis, driven by myosin, is 2.0-2.5 times higher with  $^{25}\text{Mg}$  than that with the nonmagnetic  $^{24}\text{Mg}$  or  $^{26}\text{Mg}$  [6]. The similar MIE has been revealed with zinc. While  $\text{Zn}^{2+}$  performs the cofactor function less efficiently than  $\text{Mg}^{2+}$ , the rate of the ATP hydrolysis driven by myosin is 40-50 percent higher with the magnetic  $^{67}\text{Zn}$  as compared to the nonmagnetic  $^{64}\text{Zn}$  or  $^{68}\text{Zn}$  [7]. Moreover, the beneficial MIE of  $^{25}\text{Mg}$  has been discovered in the reaction of ATP hydrolysis catalyzed by mitochondrial  $\text{H}^+$ -ATPase, isolated from yeast cells and reconstituted into the proteoliposome membrane [8]. On its own, factual evidence of MIE unambiguously indicates that there is a spin-selective rate-limiting step, the “bottle-neck” in the chemo-mechanical cycle of the enzyme that is accelerated by the nuclear spins of  $^{25}\text{Mg}$  or  $^{67}\text{Zn}$ . The nuclear spin catalysis in the molecular motors may be explained as follows. The energy released during ATP hydrolysis is not large enough to trigger the electron-conformational excitation of the macromolecule into the singlet excited state. It is sufficient to trigger a low-level triplet state. However, the transition from the ground state ( $S = 0$ ) into the triplet state ( $S = 1$ ) is forbidden by the spin conservation law. The magnetic isotope’s nuclear spin eliminates the spin ban providing the required spin conversion into the triplet state, thereby providing the acceleration of the chemo-mechanical cycle of the enzyme. The

## PP-I-7

alternative explanation of the nuclear spin catalytic effects suggests a virtual radical-ion pair in the enzyme's active center, which interferes with the ATP hydrolysis. Creating the spin ban, the magnetic isotope prevents the undesired reverse reaction of ATP synthesis thereby promoting the direct ATP hydrolysis reaction [9]. The hypothesis about the key-role of such a virtual radical-ion pair in ATP synthesis at oxidative phosphorylation was stated about 50 years ago [10]. Although detailed mechanisms of ability of the biocatalysts to perceive the nuclear magnetism require further investigations, there are the grounds to believe that this new field, nuclear spin catalysis, highlights promising venues for future research with possible applications of the stable magnetic isotopes in medicine for creating novel anti-stress drugs including the low-toxic anti-radiation protectors.

**Acknowledgement.** This work was supported by Russian Foundation for Basic Research, grant no. 14-04-00593 and was realized in accordance with the State task (state registration No. 01201361868).

### References:

- [1] K.M. Salikhov, Y.N. Molin, R.Z. Sagdeev, A.L. Buchachenko. Spin Polarization and Magnetic Field Effects in Radical Reactions (Elsevier, Amsterdam, 1984).
- [2] V. Koltover, Y. Kutlakhmedov, D. Grodzinsky. *Mol. Biol. Cell* 22 (2011) 441.
- [3] L.V. Avdeeva, T.A. Evstyukhina, V.K. Koltover, V.G. Korolev, Y. A. Kutlakhmedov. *Nuclear Physics and Atomic Energy* 20 (2019), in press.
- [4] V.K. Koltover, V.K. Koltover, U.G. Shevchenko, L.V. Avdeeva, E.A. Royba, V.L. Berdinsky, E.A. Kudryashova. *Doklady Biochem. Biophys.* 442 (2012) 12.
- [5] L.V. Avdeeva, V.K. Koltover. *Moscow Univ. Chem. Bull.* 71 (2016) 160.
- [6] V.K. Koltover. R.D. Labyntseva, V.K. Karandashev, S.A. Kosterin. *Biophysics* 61 (2016) 200.
- [7] V.K. Koltover, R.D. Labyntseva, S.A. Kosterin. *Myosin: Biosynthesis, Classes and Function* (Nova Science Publ., New York, USA, 2018), pp. 135-158.
- [8] V.K. Koltover, P. Graber, V.K. Karandashev, I. Starke, P. Turina. Abstracts of 11th International Conference "Biocatalysis: Fundamentals and Applications" (Innovations and High Technologies, MSU Ltd., Moscow, 2017), pp. 50-51. ISBN 978-5-9500292-3-3.
- [9] V.K. Koltover. *J. Mol. Liquids* 235 (2017) 44.
- [10] V.K. Koltover, L.A. Blumenfeld. *Mol. Biol.* 6 (1972) 130.

## DFT Study of Adsorption of Au-Au, Au-Re and Au-Mn Dimers at Ceria Nanoparticle

Laletina S.S., Shor A.M., Nasluzov V.A., Ivanova-Shor E.A.  
*Institute of Chemistry and Chemical Technology SB RAS, Federal Research Center  
"Krasnoyarsk Scientific Center SB RAS", Krasnoyarsk, Russia  
laletina.ss@icct.krasn.ru*

In the recent years, a number of explorations exhibited that the bimetallic clusters has the distinctive catalytic, structural, electronic, magnetic and optical properties. Especially, transition metal-doped gold clusters have been becoming a growing interest because transition metal elements possess intricate d-orbital bonding, strong electron correlation, and spin-orbit coupling, which strongly influence the chemical and physical properties of host gold clusters [1]. They are promising to be used in medicine, catalyst and optics.

The intermetallic antiferromagnetic MnAu compound has been attracting considerable interest for antiferromagnetic spintronics due to its high Neel temperature and strong spin-orbit coupling and their potential applications in GMR and TPR devices [2]. ReAu alloys showed activity for catalytic cyclization of hydrocarbons [3]. ReAu/ceria are highly selective and active for water-gas shift reaction, especially for high H<sub>2</sub>O/CO ratios [4]. ReAu alloys are biocompatible and their binuclear clusters can be potentially used as bioprobe [5] or metal based drugs [6].

Problem is that these binuclear systems are poorly studied. The aim of the work was to establish the relationship between the composition, structure, and properties of homo- and heteronuclear gold dimers (Au<sub>2</sub>, MnAu and ReAu) adsorbed at ceria cluster using the density functional method. We have determined the adsorption modes of atoms and dimers at Ce<sub>21</sub>O<sub>42</sub> cluster and the strength of metal-oxide interactions. Spin state of metal species at ceria nanoparticle has been clarified.

**Acknowledgement.** The reported study was also funded by Russian Foundation for Basic Research, Government of Krasnoyarsk Territory, Krasnoyarsk Regional Fund of Science in frameworks of research project «New compounds based on gold and noble metals: synthesis, physicochemical properties, catalytic activity» (grant № 18-4443-240010). The authors thank Siberian Supercomputer Center (www.sccc.ru) and the Supercomputing Center of Lomonosov Moscow State University [7] for provided computational resources.

### References:

- [1] A. Villa, D. Wang, D.S. Su, L. Prati, *Catal. Sci. Technol.* 5 (2015) 55.
- [2] X. Wei et al., *J. App. Phys.* 523 (2011) 1.
- [3] T. Plunkett, *J. Catal.* 35 (2004) 330.
- [4] B. S. Çağlayan, A. E. Aksoylu, *Catal. Communications.* 12 (2011) 1206.
- [5] A. Liang, J. Li, C. Jiang, Z. Jiang, *Bioprocess and Biosyst. Eng.* 33 (2010) 1087.
- [6] S. P. Fricker, *Dalton Transactions*, 43 (2007) 4903.
- [7] V. Sadovnichy, A. Tikhonravov, V. Voevodin, V. Opanasenko, "Lomonosov": Supercomputing at Moscow State University. In *Contemporary High Performance Computing: From Petascale toward Exascale* (Chapman & Hall/CRC Computational Science), pp.283-307, Boca Raton, USA, CRC Press, 2013.

## Tuning the Structure of Active Sites and Catalytic Performance of Pd-Ag/Al<sub>2</sub>O<sub>3</sub> Selective Hydrogenation Catalyst by CO and O<sub>2</sub> Adsorption-Induced Segregation

Mashkovsky I.S., Rassolov A.V., Smirnova N.S., Baeva G.N., Bragina G.O., Stakheev A.Yu.  
N.D. Zelinsky Institute of Organic Chemistry RAS, Moscow, Russia  
*im@ioc.ac.ru*

In this study, we used the adsorption-induced segregation to control the performance of Pd–Ag<sub>2</sub>/Al<sub>2</sub>O<sub>3</sub> catalyst. The choice of PdAg composition was related to the fact that it widely used in the selective hydrogenation of hydrocarbons with multiple bonds [1-4]. Furthermore, as it was previously reported, these systems are highly selective in liquid-phase hydrogenation of terminal and internal alkynes [5-6].

The main idea of this research was to study the possibility to tune the structure of active sites and, consequently, the catalytic characteristics of Pd-Ag catalysts by using CO and O<sub>2</sub> adsorption-induced surface segregation. The catalytic effect of this treatment was investigated in liquid-phase diphenylacetylene (DPA) hydrogenation.

The Pd–Ag<sub>2</sub>/Al<sub>2</sub>O<sub>3</sub> catalyst was obtained by the incipient wetness co-impregnation of Al<sub>2</sub>O<sub>3</sub> (Sasol, S<sub>BET</sub> = 56 m<sup>2</sup>/g) with an aqueous solutions of palladium and silver nitrates. The catalyst was dried at room temperature and reduced in a 5% H<sub>2</sub>/Ar flow (550°C, 2 h). The structure of Pd–Ag nanoparticles was characterised by TEM, H<sub>2</sub>-TPD, H<sub>2</sub>-TPR and CO-DRIFTS techniques. The catalytic tests were performed in *n*-hexane at room temperature and P(H<sub>2</sub>) = 5 bar.

It is remarkable that CO-DRIFT spectrum of the freshly reduced Pd–Ag<sub>2</sub>/Al<sub>2</sub>O<sub>3</sub> catalyst exhibits only one intensive absorption band with a maximum at 2049 cm<sup>-1</sup> characteristic of the linearly adsorbed CO. This observation indicates the formation of Pd<sub>1</sub> sites isolated by neighboring Ag atoms.

The CO-DRIFTS data allow us to conclude that the CO induced segregation treatment of the Pd–Ag<sub>2</sub>/Al<sub>2</sub>O<sub>3</sub> catalyst at an elevated temperature (200°C) leads to surface enrichment in Pd and the formation of Pd<sub>2</sub> dimer centres which apparently consist of two neighbouring palladium atoms on the surface. The formation of these centres is revealed by the appearance of relatively narrow band at 1979 cm<sup>-1</sup> characteristic of the two-point CO adsorption [7].

The CO-DRIFTS spectrum of Pd–Ag<sub>2</sub>/Al<sub>2</sub>O<sub>3</sub> catalyst treated in O<sub>2</sub> indicates even more pronounced surface modification as compared to the treatment in CO. Thus the adsorption band of linear CO shifts toward 2071 cm<sup>-1</sup> suggesting the change in the electronic state of supported Pd.

The catalytic results obtained in the liquid-phase hydrogenation of DPA made it possible to conclude that the treatment of the Pd–Ag<sub>2</sub>/Al<sub>2</sub>O<sub>3</sub> catalyst in CO increases DPA hydrogenation rate from ~ 3 to ~ 7 mmolH<sub>2</sub> g<sub>cat</sub><sup>-1</sup> min<sup>-1</sup> compared to the freshly reduced Pd-

## PP-I-9

Ag<sub>2</sub>/Al<sub>2</sub>O<sub>3</sub>. Remarkably, the selectivity in the formation of the target diphenylethylene essentially does not change and remains identical to the selectivity of the freshly reduced Pd-Ag<sub>2</sub>/Al<sub>2</sub>O<sub>3</sub> catalyst. Thus at 100% DPA conversion target selectivity is ~ 95-96% for both samples.

The O<sub>2</sub> induced segregation treatment results in further increase in hydrogenation rate from ~ 3 to ~10 mmolH<sub>2</sub> g<sub>cat</sub><sup>-1</sup> min<sup>-1</sup>, however, selectivity is notably reduced. Presumably, this is resulted from transformation of isolated Pd<sub>1</sub> active sites into multiatomic Pd<sub>n</sub> active centres observed by CO-DRIFTS.

The data obtained in this research demonstrate that the adsorption-induced segregation provides a convenient method for modification of the surface structure and, as a consequence, the catalytic performance of bimetallic Pd–Ag catalysts in selective hydrogenation of acetylenic compounds.

**Acknowledgement.** Financial support of the Russian Foundation for Basic Research (grant no. 16-29-10788) is gratefully acknowledged.

### References:

- [1] Y. Liu, J. Zhao, Y. He, J. Feng, T. Wu, D. Li, *J. Catal.* 348 (2017) 135.
- [2] M. Kuhn, M. Lucas, P. Claus, *Ind. Eng. Chem. Res.* 54 (2015) 6683.
- [3] M.T. Ravanchi, S. Sahebdehfar, *Appl. Catal. A: General.* 525 (2016) 197.
- [4] M.T. Ravanchi, S. Sahebdehfar, M.R. Fard, S. Fadaeeraeyeni, P. Bigdeli, *Chem. Eng. Technol.* 39 (2016) 301.
- [5] A.V. Rassolov, P.V. Markov, G.O. Bragina, G.N. Baeva, I.S. Mashkovsky, A.Yu. Stakheev, I.A. Yakushev, M.N. Vargaftik, *Kinet. Catal.* 57 (2016) 853.
- [6] A.V. Rassolov, D.S. Krivoruchenko, M.G. Medvedev, I.S. Mashkovsky, A.Yu. Stakheev, I.V. Svitanko, *Mendeleev Commun.* 27 (2017) 615.
- [7] A.J. McCue, J.A. Anderson, *J. Catal.* 329 (2015) 538.

## Mild Oxidative-Reductive Treatments as an Effective Way to Tune the Surface Structure and Catalytic Properties of PdIn Catalyst in Liquid-Phase Hydrogenation of Substituted Alkynes

Mashkovsky I.S.<sup>1</sup>, Smirnova N.S.<sup>1</sup>, Markov P.V.<sup>1</sup>, Baeva G.N.<sup>1</sup>, Bragina G.O.<sup>1</sup>,

Bukhtiyarov A.V.<sup>2</sup>, Prosvirin I.P.<sup>2</sup>, Bukhtiyarov V.I.<sup>2</sup>, Stakheev A.Yu.<sup>1</sup>

1 – N.D. Zelinsky Institute of Organic Chemistry RAS, Moscow, Russia

2 – Borekov Institute of Catalysis, Novosibirsk, Russia

*im@ioc.ac.ru*

Nowadays increasing attention is paid to intermetallic compounds (IMCs) as highly stable heterogeneous catalysts. The unique combination of ionic and covalent bonding results in the homogeneity of both crystal and electronic structures of IMCs providing exclusive catalytic characteristics. Recently, PdIn system was reported as one of the promising IMCs for hydrogenation of substituted alkynes in gas- and/or liquid-phase [1-3].

One of specific properties of PdIn IMCs is high oxophilicity of indium which can lead to the instability of IMCs. On the other hand selective oxidation of In component may provide a new technique of tuning catalytic characteristics by controlled oxidative treatment. Therefore the main objective of this research was to explore the effect of mild oxidation on the surface structure and catalytic performance of PdIn/Al<sub>2</sub>O<sub>3</sub> in selective hydrogenation of diphenylacetylene (DPA).

The catalyst was obtained by impregnation of Al<sub>2</sub>O<sub>3</sub> («Sasol»  $S_{\text{BET}} = 56 \text{ m}^2/\text{g}$ ) with a solution of the Pd(OAc)<sub>4</sub>In(OAc) heterometallic acetate-bridged complex [4] in dilute acetic acid (pH 2.8). The sample was dried in air at room temperature and reduced in 5%H<sub>2</sub>/Ar flow at 500 °C for 3 h. For studying an effect of oxidative treatment, the freshly reduced PdIn/Al<sub>2</sub>O<sub>3</sub> catalyst was exposed to commercial synthetic air (20 vol% O<sub>2</sub>/N<sub>2</sub>) at 25 and 150°C, and its surface structure was investigated by DRIFT-CO and XPS techniques. The catalytic properties were studied in the liquid-phase hydrogenation of diphenylacetylene (DPA). After oxidation experiments, the catalyst was re-reduced at 250°C in order to explore the reversibility of changes in the surface structure and catalytic performance caused by oxidation.

Analysis of the XPS and DRIFT-CO data allow us to conclude that oxidation significantly affects the surface structure of PdIn nanoparticles. Since its high oxophilicity, the In component is presumably transformed into the InOx surface species after the oxidation treatment. This results in the deterioration of isolated Pd<sub>1</sub> sites and the formation of Pdn multiatomic centers (presumably dimeric), as indicated by the appearance of a bridge-bonded CO band in DRIFT-CO spectra. It is important to note, that the Pd site-isolated structure can be easily recovered by reduction even at 250°C. This treatment is accompanied by a decrease in the surface In/Pd ratio to a value characteristic of

## PP-I-10

the intermetallic PdIn surface ( $\sim 1.01$ ). The disappearance of the bridge-bonded CO band and the shift of the linear adsorbed CO band to  $2066\text{ cm}^{-1}$  in DRIFT-CO spectra evidenced the complete restoration of isolated Pd<sub>1</sub> sites.

The effect of oxidation/reduction treatments on the performance of PdIn/Al<sub>2</sub>O<sub>3</sub> in DPA hydrogenation was evaluated by comparing H<sub>2</sub> uptake profiles and TOF values for the freshly reduced catalyst and the catalyst treated in 20%O<sub>2</sub>/N<sub>2</sub> at 25 and 150°C. The data obtained allow us to conclude that oxidation significantly increases the rate of hydrogenation. Thus, turnover frequency in alkyne hydrogenation (TOF<sub>1</sub>) increases twofold after oxidation at room temperature (from 0.018 to 0.044 s<sup>-1</sup>) and almost by an order of magnitude (to 0.17 s<sup>-1</sup>) after oxidation at 150°C. The activity enhancement presumably stems from the transformation of isolated Pd<sub>1</sub> to multiatomic Pdn surface sites as evidenced by DRIFT-CO and XPS.

Remarkably that despite this transformation PdIn/Al<sub>2</sub>O<sub>3</sub> retains high selectivity in diphenylethylene formation even after oxidation at 150°C. Presumably this observation suggests that the high selectivity of PdIn/Al<sub>2</sub>O<sub>3</sub> can be result of the hindering of subsurface hydride formation (since PdIn is not capable to adsorb hydrogen) rather than site isolation of Pd<sub>1</sub> centers. It is important that the subsequent reduction at 250°C completely restores the catalytic characteristics of PdIn/Al<sub>2</sub>O<sub>3</sub>, which is in good agreement with DRIFT-CO and XPS data.

Our experimental results allow us to conclude that the mild partial oxidation is a promising and effective tool for tuning surface structure and catalytic performance of PdIn hydrogenation catalysts.

**Acknowledgement.** Catalyst characterization by CO-DRIFTS and XPS was granted by the Russian Science Foundation (Grant RSF # 19-13-00285). The methodology of catalyst preparation and catalytic test procedure were developed by the Russian Science Foundation (Grant RSF # 16-13-10530). Authors are grateful to Prof. M. N. Vargaftik and Dr. I. A. Yakushev (N. S. Kurnakov Institute of General and Inorganic Chemistry, Russian Academy of Sciences) for supplying us with the Pd(OOCMe)<sub>4</sub>In(OOCMe) complex, which was used as a precursor for the catalyst preparation.

### References:

- [1] M. Neumann et al., *J. Catal.* 340 (2016) 49.
- [2] Y. Cao et al., *ACS Catal.* 7 (2017) 7835.
- [3] Q. Feng et al., *J. Am. Chem. Soc.* 139 (2017) 7294.
- [4] I.P. Stolarov et al., *Inorg. Chem.* 57 (2018) 11482.

## Catalysis in Adsorbed Domens and Layers

Mel'gunov M.S.

*Boriskov Institute of Catalysis, Novosibirsk, Russia*

*max@catalysis.ru*

Permanent expansion of the variety of precursors, products and conditions requires the extension of our ideas about mechanisms of catalytic transformations. By now, adsorbed phase in heterogeneous catalysis is usually not considered in any kind other than within the Langmuir model. However, substances under sub-critical conditions can form adsorbed layers of various thickness on the surface, or liquid-like domens in narrow pores. By this contribution we consider possible benefits and disadvantages that such states can introduce into catalytic transformations.

The thickness of adsorbed layers depends on temperature and partial pressure of substance vapor and can be found in a range of 1 nm (thin films) - 10 nm and more (thick films). Potential electrostatic and dispersion interaction energy between catalyst surface and substance molecules, surface curvature play role, as well. Adsorbed phase cannot be considered as the bulk liquid or gas, because its main properties are enlarged density exceeding the density of a bulk liquid, enhanced mass transfer (compared to transport rate through gaseous phase through channels of the same aperture). Possible benefits of steady-state adsorbed layers or domains to catalysis are:

- 1) Improved opportunity of interphase "gas,vapor – liquid(adsorbed phase)" reactions, involving gases, such as hydrogen, oxygen or CO, which poorly dissolve in liquids;
- 2) Possibility to provide catalytic liquid(adsorbed) phase reactions in truly isolated, or interconnected nanometer reactors that are feed with reagents through gaseous or vapor phase.

Several practical examples that can be considered as candidates for advanced catalysis in adsorbed domens and layers are discussed in a talk.

**Acknowledgement.** This work is supported by Ministry of Science and Higher Education of the Russian Federation (project AAAA-A17-117041710079-8).

## Dual-Zone Zeolite Catalyst for Complex Abatement of Power Plant and Automotive Emissions

Mytareva A.I., Bokarev D.A., Baeva G.N., Belyankin A.Yu., Stakheev A.Yu.  
*N.D. Zelinsky Institute of Organic Chemistry RAS, Moscow, Russia*  
*aim@ioc.ac.ru*

One of the main requirements for power plant and vehicle emission control technologies is a high efficiency in NO<sub>x</sub>, CO, hydrocarbons, and residual ammonia abatement in a wide temperature range (150–500 °C) [1]. In order to convert pollutants to harmless CO<sub>2</sub>, N<sub>2</sub> and H<sub>2</sub>O complex systems consisting several separate catalytic blocks such as selective catalytic reduction catalyst (SCR), oxidation catalyst (OC), and ammonia-slip oxidation catalyst (ASC) are widely used. In addition to the complexity, the systems are also very expensive, since they contain Pt and Pd. In this study we demonstrate the potential opportunity to simplify and to reduce cost of emission control system by integration oxidation (OC, PF, and ASC) and reduction (SCR) catalytic functions in a single FeBeta | Mn-Ce/FeBeta dual-zone catalyst.

The dual-zone catalyst comprises two catalytic beds: 1) commercial FeBeta (“Zeolyst”; Si/Al=12.5; 0.9 wt% Fe), and 2) 16%Mn-16%Ce/FeBeta prepared by incipient wetness co-impregnation of parent Fe-zeolite by aqueous solution of manganese (II) nitrate and cerium (III) nitrate. Catalytic activities of FeBeta, 16%Mn-16%Ce/FeBeta and FeBeta | Mn-Ce/FeBeta dual-zone catalyst in NH<sub>3</sub>-SCR were measured using gas composition containing 500 ppm NO, 100–800 ppm NH<sub>3</sub>, 10 vol% O<sub>2</sub>, 6 vol% H<sub>2</sub>O balanced with N<sub>2</sub> (300 ml/min). In order to investigate efficiency of the dual-bed catalyst in simultaneous removal of NO<sub>x</sub>, CO, and hydrocarbon, 200 ppm CO and/or 500 ppm *n*-C<sub>4</sub>H<sub>10</sub> were added to the feed gas.

It was found that FeBeta is a highly efficient catalyst in the NH<sub>3</sub>-SCR at temperatures above 300 °C: 90–95 % of NO<sub>x</sub> are selectively converted to N<sub>2</sub> and H<sub>2</sub>O. Mn-Ce/FeBeta demonstrates superior performance at 180–350 °C. As the reaction temperature increases above 350 °C, NO<sub>x</sub> conversion over Mn-Ce/FeBeta decreases because of NH<sub>3</sub> overoxidation on Mn-Ce active centres.

The dual-zone catalyst provides high activity (NO<sub>x</sub> conversion > 80 %) and N<sub>2</sub>-selectivity in the NH<sub>3</sub>-SCR within 180–500 °C. By comparing catalytic results obtained for the individual catalytic beds and dual-bed system it can be concluded that excellent performance of the dual-bed catalyst stems from superimposition of FeBeta and Mn-Ce/FeBeta performances. Thus, at 180–350 °C nitrogen oxides are reduced over Mn-Ce/FeBeta (downstream bed). As the temperature increases above 350 °C the NH<sub>3</sub>-SCR proceeds mainly over FeBeta (upstream bed), providing high NO<sub>x</sub> to N<sub>2</sub> conversion.

Catalytic performance of FeBeta | Mn-Ce/FeBeta was studied in the NH<sub>3</sub>-SCR at different NH<sub>3</sub>/NO ratio (0.2–1.6). At NH<sub>3</sub>/NO < 1 nitrogen oxides are not completely reduced due to insufficient ammonia concentration. When NH<sub>3</sub>/NO ratio is increased above 1, NO<sub>x</sub> conversion

## PP-I-12

exceeds 80–90 % within 180–500 °C. It is remarkable, that even at  $\text{NH}_3/\text{NO} = 1.6$  residual ammonia ( $\text{NH}_3\text{-slip}$ ) is not observed at temperatures above 300 °C. Detailed analysis of the reaction products indicates that  $\text{NH}_3$  excess is selectively converted to  $\text{N}_2$  *via* intrinsic  $\text{NH}_3\text{-SCR}$  process.

In addition to high efficiency in the  $\text{NH}_3\text{-SCR}$  FeBeta||Mn-Ce/FeBeta dual-bed system demonstrates promising activity in simultaneous carbon monoxide and hydrocarbons removal. Almost complete CO removal and high *n*-C<sub>4</sub>H<sub>10</sub> conversion is achieved at 200–500 °C. It should be noted, that oxidation reactions proceed over FeBeta||Mn-Ce/FeBeta independently of  $\text{NH}_3\text{-SCR}$  and do not affect on  $\text{NO}_x$  removal efficiency.

The data obtained demonstrate that the FeBeta||Mn-Ce/FeBeta dual-zone catalyst would be highly suitable for complex power plant and diesel vehicle emission abatement as it gives high  $\text{NO}_x$  reduction, and CO, hydrocarbons, residual  $\text{NH}_3$  oxidation efficiencies over a wide temperature range.

### References:

[1] I.Nova, E.Tronconi. Urea-SCR technology for DeNO<sub>x</sub> after treatment of diesel exhausts. Springer, New York (2014) P. 716.

## Synthesis of Titanium Oxide Coatings with a Given Band Gap Value

Sarvadiy S.Yu., Kharitonov V.A., Dokhlikova N.V.  
 Semenov Institute of Chemical Physics RAS, Moscow, Russia  
 sarvadiy15@mail.ru

The relatively small work function for pure titanium (3.95 eV) [1] and the small band gap ( $E_g < 0.1$  eV) for a range of its oxides [1–3] make titanium a promising material from the perspective of creating of model catalytic systems. In this research by means of atomic force microscopy and scanning tunneling microscopy and spectroscopy methods we established the peculiarities of the spatial distribution of the oxide layer formed on the surface of the titanium coating after its interaction with oxygen at different temperatures. It was found that non-stoichiometric oxide  $TiO_x$  is formed on the surface of titanium, where  $1.75 < x < 2$ , as a result of its interaction with oxygen. Measuring the band gap at various points over the sample surface allowed us to map the spatial distribution of the oxide phase over the titanium surface and to create the histogram of the frequency distribution of different band gap values. With an increase in the duration of the annealing of the sample in oxygen, a gradual increase in the oxide band gap is observed. It is shown that changing the temperature and duration of annealing in oxygen allows to create titanium oxide coatings with a given band gap value.

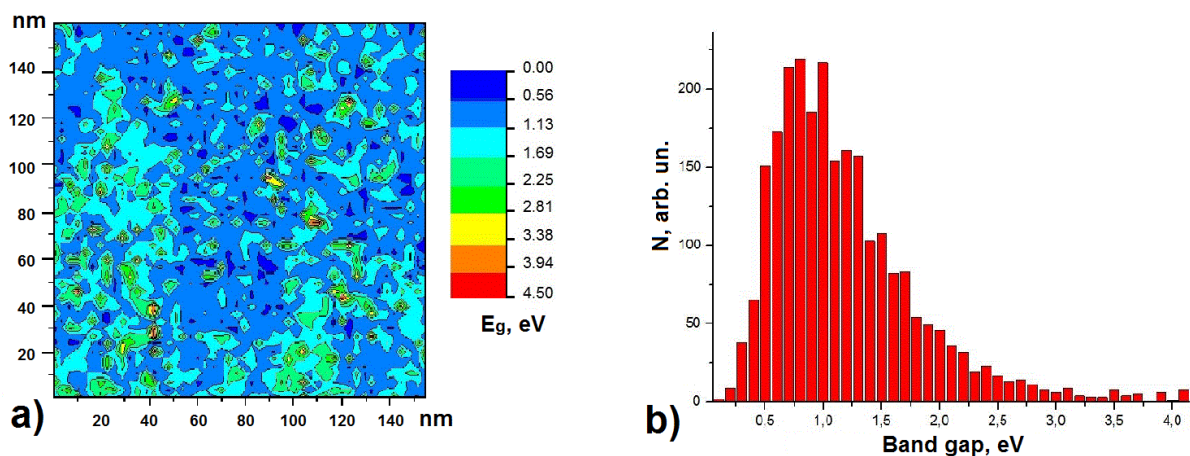


**Fig. 1.** For the sample oxidized in  $O_2$  at  $T = 300$  K: a - the oxide phase distribution over the selected surface area (140 nm  $\times$  140 nm), b - the histogram of the frequency distribution of various band gap values over the same surface area.

**Acknowledgement.** This work was supported by the RFBR grant 18-33-00020.

### References:

- [1] V. Ern, A.C. Switendick, Phys. Rev. 137 (1965) 1927.
- [2] V.E. Henrich, P.A. Cox, The Surface Science of Metal Oxides. Cambridge University Press, 1996.
- [3] D. Reyers-Coronado, G.R. Gattorno, M.E.E. Pesqueira et al., Nanotechnology, 19 (2008) 145605.

## Influence of Size Effect on the Hydrogen Adsorption on the Surface of Supported Gold Nanoparticles

Gatin A.K., Grishin M.V., Sarvadiy S.Yu., Shub B.R.  
*Semenov Institute of Chemical Physics RAS, Moscow, Russia*  
*sarvadiy15@mail.ru*

Gold is a perfect example of a material that is inert in its massive form and highly active in the nanoscale form. The reasons for the increase in activity with the reduction in particle size to nanometers may be various, including size quantization, nanoparticles being charged due to interaction with the substrate, an increase in the specific fraction of low-coordinated gold atoms, etc.

Experimentally, chemisorption of hydrogen on the surface of gold nanoparticles was discovered relatively recently [1–5]. In our previous works [4,5], using scanning tunneling microscopy and spectroscopy (STM/STS), we observed dissociative adsorption of hydrogen on gold nanoparticles deposited on graphite. This study shows the influence of size effect on the ability of gold nanoparticles supported on highly oriented pyrolytic graphite (HOPG) to adsorb dissociatively hydrogen on their surface.

The experiments were carried out at a facility consisting of a scanning tunneling microscope, Auger spectrometer, quadrupole mass spectrometer, and auxiliary equipment at 300 K and a residual gas pressure of  $2 \times 10^{-10}$  Torr. As STM probes, we used tips made of platinum–iridium and tungsten wires using the standard methods.

Nanoparticles were deposited on the surface of HOPG using the impregnation method. To achieve this, an aqueous solution of  $\text{HAuCl}_4$  with a metal concentration of  $5 \times 10^{-6}$  g/mL was applied over the surface of the substrate. Then, the sample was dried, placed in a vacuum chamber, and annealed in ultra-high vacuum at 500–750 K for several hours. The required duration of annealing was established using the results of an STM study of the surface morphology of the sample.

The purpose of this study was to establish a correlation between the nanoparticle size and their adsorption properties in relation to molecular hydrogen. In our previous report [6], it was shown, that molecular hydrogen isotope (deuterium) chemisorbed dissociatively on the surface of gold nanoparticles with a size of 5–6 nm. In the case of such nanoparticles, hydrogen adsorption leads to a drastic change in the electronic structure of the surface of nanoparticles and significantly decreases the conductivity of the STM tunneling contact formed by STM tip and gold nanoparticles.

In presented work we investigate the changes in the conductivity of gold nanoparticles with different size after exposure to 2000 Langmuir of hydrogen. It was shown that exposure to hydrogen leads to decreasing of conductivity of nanoparticles with size of 5-9 nm. In the case of nanoparticles with a size of more than 10 nm, the exposure of the sample to hydrogen

## PP-I-14

did not lead to any noticeable changes in the electronic structure of nanoparticles. Thus, we can conclude that hydrogen was dissociatively chemisorbed on the surface of gold nanoparticles with a size of 5–9 nm, while hydrogen chemisorption was not observed for gold nanoparticles with a size of  $\geq 10$  nm.

**Acknowledgement.** This research was funded by the Russian Science Foundation, project 18-73-00195.

### References:

- [1] M. Manzoli; A. Chiorino, F. Vindigni.; F. Boccuzzi, *Catal. Today* 181 (2012) 62.
- [2] I.P. Silverwood, S.M. Rogers, S.K. Callear, S.F. Parker, C.R.A. Catlow, *Chem. Commun.* 52 (2016) 533.
- [3] W.L. Watkins, Y. Borensztein, *Phys. Chem. Chem. Phys.* 19 (2017) 27397.
- [4] A.K. Gatin, M.V. Grishin, A.A. Kirsankin, V.A. Kharitonov, B.R. Shub, *Nanotechnol. Russia*, 8 (2013) 36.
- [5] M.V. Grishin, A.K. Gatin, N.V. Dokhlikova, A.A. Kirsankin, A.I. Kulak, S.A. Nikolaev, B.R. Shub, *Kinet. Catal.* 56 (2015) 532.
- [6] A.K. Gatin, M.V. Grishin, N.V. Dokhlikova, N.N. Kolchenko, Sarvadii S.Yu., B.R. Shub, *Kinet. Catal.* 59 (2018) 820.

## Pt, Pd, Ru on Sibunit: Synergistic Effect in Hydrogenation Reactions

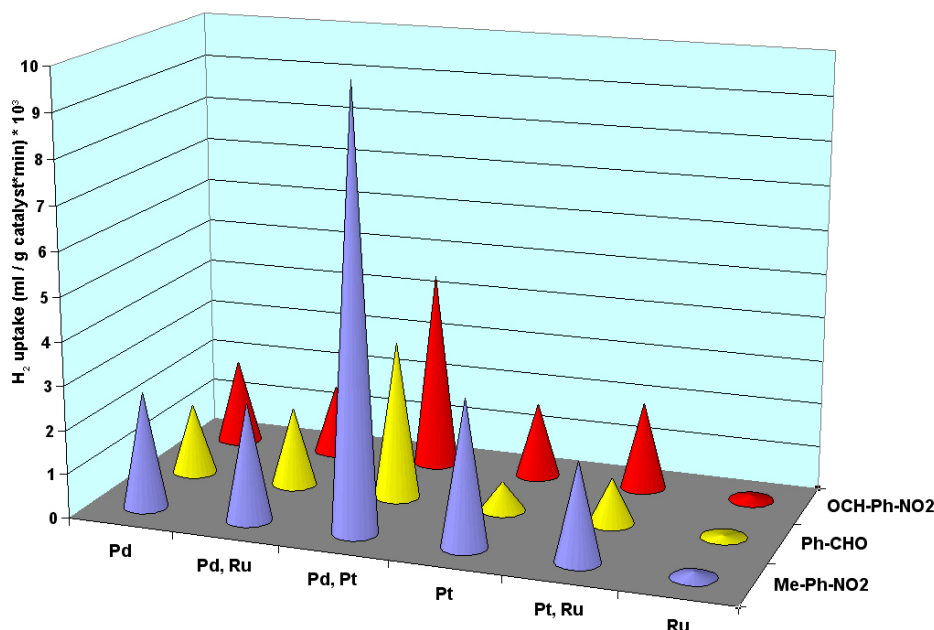
Troitskii S.Yu., Prosvirin I.P.

Boriskov Institute of Catalysis, Novosibirsk, Russia

tsy@catalysis.ru

For the synthesis of bimetallic deposited catalysts, a procedure of sequential or simultaneous impregnation of the support with compounds of active components is often used. After that, the samples are calcined and the initial compounds are reduced to the metal state. Polymetallic contacts in this method of synthesis are formed as a result of migration of active components on the surface of the support during calcination and reduction.

In the current work, bimetallic precursors of active centers were obtained as a product of simultaneous hydrolysis of  $[\text{PtCl}_4]^{2-}$ ,  $[\text{PdCl}_4]^{2-}$  and  $[\text{RuCl}_5\text{H}_2\text{O}]^{2-}$  complexes. Conditions of hydrolysis were chosen on the basis of a preliminary study of the processes of hydrolysis of individual compounds. The resulting samples were deposited on the surface of the carbon material Sibunit and reduced with sodium borohydride at room temperature, and then in a  $\text{H}_2$  flow at  $100^\circ\text{C}$  and  $200^\circ\text{C}$ . The data of catalytic activity of samples (1% of each metal on Sibunit) in hydrogenation reactions of 2-nitrotoluene, benzaldehyde and 4-nitrobenzaldehyde are presented:



The reduction of samples by hydrogen leads to a certain leveling of the synergistic effect and a decrease in the activity of all catalysts. Perhaps this is due to the metal particles sintering. According to electron microscopy, the average diameter of the particles in the catalyst Pd,Pt / C, reduced  $\text{NaBH}_4$  about 2 nm, after hydrogen reduction at  $200^\circ\text{C}$  - 5-8 nm.

## PP-I-15

It was found that the optimal molar ratio Pd:Pt in bimetallic catalysts Pd,Pt/C in the nitro group reduction reactions is – 1:3.

Data on the oxidation state of the active component of catalysts obtained by XPS. It was found that the reduction of catalysts using NaBH<sub>4</sub> leads to the reduction of Pt<sup>2+</sup> (72.2 eV) to Pt<sup>0</sup> (71.4 eV), but almost all Ru<sup>3+</sup> remains in the oxidized state (281.6 eV). In Pd/C samples, a significant proportion (1/3) is Pd<sup>2+</sup> (337 eV). Reduction the catalysts with H<sub>2</sub> flow at 100° C convert all active components to the metal state (Ru – 280,4 eV, Pd – 335,5 eV). Just f small fraction of Pd and Ru remain oxidized. The hydrogenation reaction of benzaldehyde leads to almost complete reduction of all metals independent on pretreatment. It is interesting to note that in catalysts containing Pt, the second metal is completely reduced by hydrogen and, like platinum itself, does not contain oxidized forms. This can indicate the formation of bimetallic contacts, using the proposed method of the catalysts preparation.

**Acknowledgement.** This work was supported by Ministry of Science and Higher Education of the Russian Federation (project AAAA-A17-1170410090-3).

## Mathematical Modeling of Reaction Benzylbutyl Ethersynthesis

Vovdenko A.G.<sup>1</sup>, Vovdenko M.K.<sup>1</sup>, Koledina K.F.<sup>1,2</sup>, Gubaydullin I.M.<sup>1,2</sup>

1 – Institute of Petrochemistry and Catalysis RAS, Ufa, Russia

2 – Ufa State Petroleum Technological University, Ufa, Russia

vovdenkoann@gmail.com

Benzyl butyl ether having fruity and floral aromas is a valuable aromatic substance and is widely used for flavoring products of the perfumery, cosmetic and food industries. Benzyl butyl ether is permitted in many countries for use as a food flavoring.[1]Benzyl butyl ether is synthesized through benzyl alcohol and butanol etherification with copper bromide as catalyst.Reactionscheme [2] is represented in Table 1 below.

Table 1. Reaction scheme of Benzyl alcohol and butanol.

No	Elementary stage
1	$\text{PhCH}_2\text{OH}(\mathbf{X}_1) + \text{CuBr}_2(\mathbf{X}_2) \rightarrow [\text{PhCH}_2]^+[\text{CuBr}_2(\text{OH})]^- (\mathbf{X}_3)$
2	$[\text{PhCH}_2]^+[\text{CuBr}_2(\text{OH})]^- (\mathbf{X}_3) + \text{BuOH}(\mathbf{X}_4) \rightarrow [\text{PhCH}_2\text{OBu}]\text{H}^+ [\text{CuBr}_2(\text{OH})]^- (\mathbf{X}_5)$
3	$[\text{PhCH}_2\text{OBu}]\text{H}^+ [\text{CuBr}_2(\text{OH})]^- (\mathbf{X}_5) \rightarrow \text{PhCH}_2\text{OBu}(\mathbf{X}_6) + \text{H}_2\text{O}(\mathbf{X}_7) + \text{CuBr}_2(\mathbf{X}_2)$
4	$[\text{PhCH}_2]^+[\text{CuBr}_2(\text{OH})]^- (\mathbf{X}_3) + \text{PhCH}_2\text{OH}(\mathbf{X}_1) \rightarrow [\text{PhCH}_2\text{OHCH}_2\text{Ph}]^+ [\text{CuBr}_2(\text{OH})]^- (\mathbf{X}_8)$
5	$[\text{PhCH}_2\text{OHCH}_2\text{Ph}]^+ [\text{CuBr}_2(\text{OH})]^- (\mathbf{X}_8) \rightarrow \text{PhCH}_2\text{OCH}_2\text{Ph} (\mathbf{X}_9) + \text{H}_2\text{O}(\mathbf{X}_7) + \text{CuBr}_2(\mathbf{X}_2)$
6	$\text{BuOH}(\mathbf{X}_4) + \text{CuBr}_2(\mathbf{X}_2) \rightarrow [\text{Bu}]^+[\text{CuBr}_2(\text{OH})]^- (\mathbf{X}_{10})$
7	$[\text{Bu}]^+[\text{CuBr}_2(\text{OH})]^- (\mathbf{X}_{10}) + \text{BuOH}(\mathbf{X}_4) \rightarrow [\text{BuOHBu}]^+[\text{CuBr}_2(\text{OH})]^- (\mathbf{X}_{11})$
8	$[\text{BuOHBu}]^+[\text{CuBr}_2(\text{OH})]^- (\mathbf{X}_{11}) \rightarrow \text{BuOBu}(\mathbf{X}_{12}) + \text{H}_2\text{O}(\mathbf{X}_7) + \text{CuBr}_2(\mathbf{X}_2)$
9	$[\text{Bu}]^+[\text{CuBr}_2(\text{OH})]^- (\mathbf{X}_{10}) + \text{PhCH}_2\text{OH}(\mathbf{X}_1) \rightarrow [\text{PhCH}_2\text{OBu}]\text{H}^+ [\text{CuBr}_2(\text{OH})]^- (\mathbf{X}_5)$

Mathematical model was established on the basisof mass of action law and experiments results [3].Mathematic model was solved in MATLAB software. Elementary stages rate constants values for 140 °C represented below as example.

Table 2. Elementary stages rate constants for 140 °C.

No of stage	Elementary stage rate constant	Dimensions	No of stage	Elementary stage rate constant	Dimensions
1	1.70136	lit/(mole·s)	6	0.00062957	lit/(mole·s)
2	2.056031	lit/(mole·s)	7	0.116993	s <sup>-1</sup>
3	0.052503	lit/(mole·s)	8	1.9554e-004 s <sup>-1</sup>	s <sup>-1</sup>
4	1.9224	lit/(mole·s)	9	0.15	lit/(mole·s)
5	0.113	lit/(mole·s)	-	-	

Concentrations profiles of reagent ( $\mathbf{X}_1$ ) and products ( $\mathbf{X}_6, \mathbf{X}_9$ ) (calculated and experimental) are shown below on Fig.1-Fig.3.

## PP-I-16

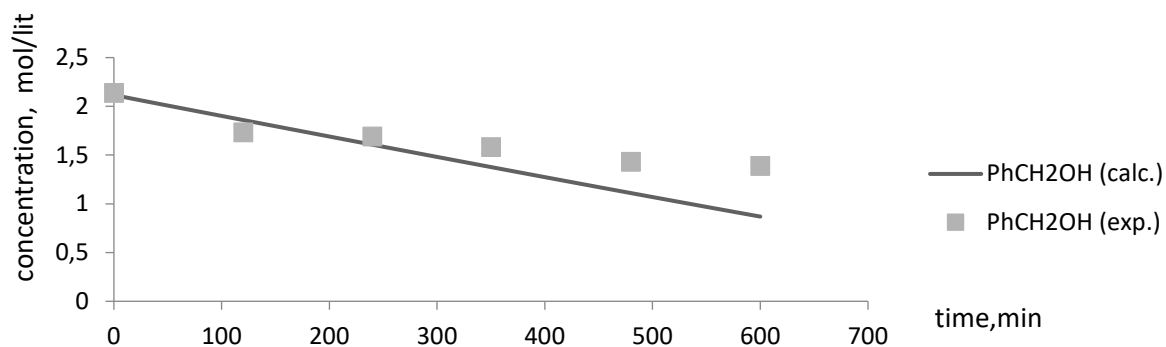


Fig.1 Benzyl alcohol concentration change profile

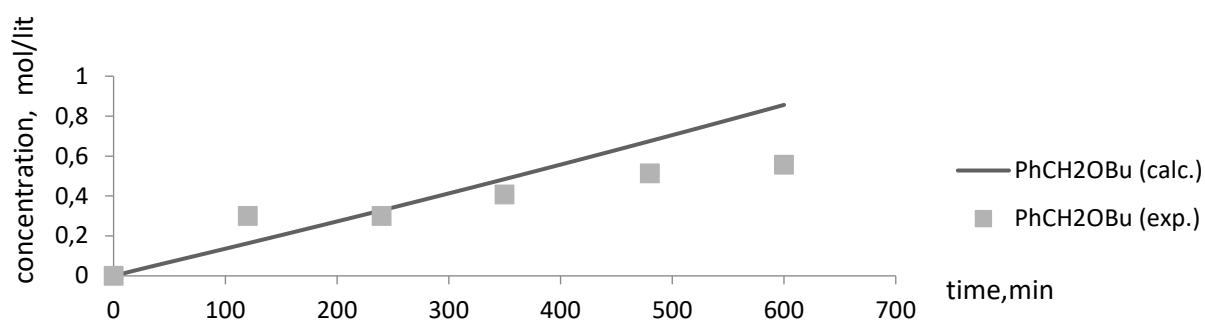


Fig.2 Benzyl alcohol concentration change profile

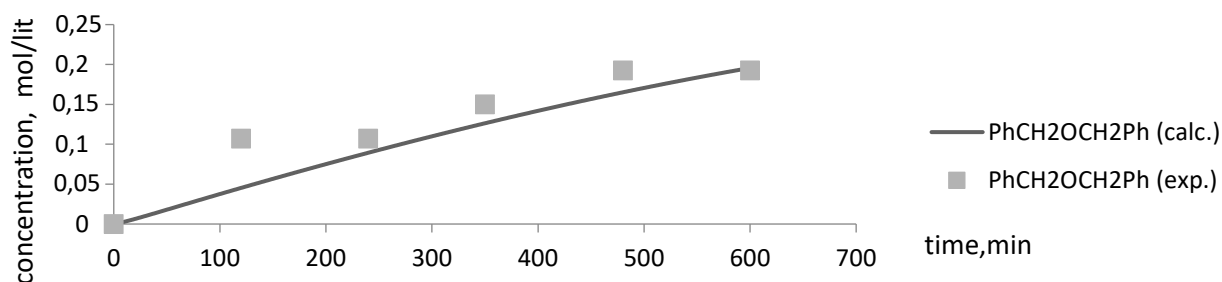


Fig.3 Benzyl alcohol concentration change profile

Experimental data obtained in Ufa Federal Research Center RAS, Institute of Petrochemistry and Catalysis was used [2] in order to analyze and validate calculations results.

### References:

- [1] Encyclopedia of food and color additives (ed. George A. Burdock) CRC Press, 1997, 264.
- [2] Bayguzina A. R., Gimaletdinova L. I., Khusnutdinov R. I. *Russ J Org Chem* 2018, Vol. 54, No. 8, pp. 1148–1155; doi: 10.1134/S1070428018080055.
- [3] Koledina K, Koledin S and Gubaydullin I. 2017 *CEUR Workshop Proceedings* 19665-9.

## Influence of CO Oxidation Conditions on the MnO<sub>x</sub>-ZrO<sub>x</sub> Catalyst Structure: In Situ XRD and MS Study

Vinokurov Z.S.<sup>1,2</sup>, Bulavchenko O.A.<sup>1,2</sup>, Afonasenko T.N.<sup>3</sup>, Tsybulya S.V.<sup>1,2</sup>

1 – Boreskov Institute of Catalysis, Novosibirsk, Russia

2 – Novosibirsk State University, Novosibirsk, Russia

3 – Center of New Chemical Technologies BIC, Omsk, Russia

isizy@catalysis.ru

Manganese based oxides are active catalysts in several oxidation and reduction reactions, such as oxidation of CO, VOCs, oxidative coupling of methane, selective reduction of nitrobenzene, CO hydrogenation. Their catalytic properties arise from the ability of manganese to form oxides with wide range of oxidation states and from their oxygen storage capacity in the crystalline lattice. The catalytic activity of Mn based oxides correlates with the operating conditions. For example, the phase composition and the chemical state of the Mn-based catalysts may be changed significantly depending on the fuel (CO, H<sub>2</sub>, hydrocarbons) rich or lean conditions. The fuel rich condition corresponds to a more reducing environment which favors the reduction of oxygen lean MnO<sub>x</sub> species, whereas the fuel lean condition corresponds to an oxidative environment promoting the formation of oxygen rich MnO<sub>x</sub> species. For Mn-containing oxides, oxidation reactions are known to proceed through the Mars-van Krevelen mechanism oxidizes by the lattice oxygen from the structure of oxide to produce CO<sub>2</sub> and the resulting reduced structure replenishes oxygen from the gas phase. Depending on the conditions (CO/O<sub>2</sub> ratio), competition between the reaction of CO with molecular or lattice oxygen of the oxide can occur.

Series of Mn<sub>x</sub>Zr<sub>1-x</sub>O<sub>4</sub> catalyst with different x were synthesized by coprecipitation of nitrates with further calcination at 650 °C for 4 h. The catalysts with a composition of Mn<sub>0.4</sub>Zr<sub>0.6</sub>O<sub>2</sub>–Mn<sub>0.6</sub>Zr<sub>0.4</sub>O<sub>2</sub> exhibited a maximum catalytic activity in CO oxidation reaction. Mn-Zr catalyst consists of Mn<sub>3</sub>O<sub>4</sub>, Mn<sub>2</sub>O<sub>3</sub> and Mn<sub>x</sub>Zr<sub>1-x</sub>O<sub>4</sub> solid solution. In this study, we have used XRD and MS for investigation the Mn-Zr oxide catalyst under reaction conditions with different CO/O<sub>2</sub> ratio. In pure CO environment, the reduction of Mn ions occurs in the volume of solid solution Mn<sub>x</sub>Zr<sub>1-x</sub>O<sub>2</sub> and the transformation of manganese oxides proceeds as follows Mn<sub>2</sub>O<sub>3</sub> → Mn<sub>3</sub>O<sub>4</sub> → MnO proceeds. The structure of the catalyst does not change during CO oxidation at a stoichiometric ratio of CO/O<sub>2</sub>=2:1 and in excess of oxygen. When the ratio of CO/O<sub>2</sub> is increased to 4, the environment changes to a reducing one. Up to 400°C, there is an interaction of CO with only molecular oxygen; at 400-450°C, manganese cations are reduced. In situ XRD reveals that catalyst structure is stable during conditions of catalytic

## PP-II-1

reaction but excess of reducing agent such as CO can change the active component. This process is reversible and, reoxidation leads to the formation of the catalyst similar to the initial state.

**Acknowledgement.** The reported study was funded by RFBR according to the research project № 19-43-543012 and the framework of the budget project for Boreskov Institute of Catalysis.

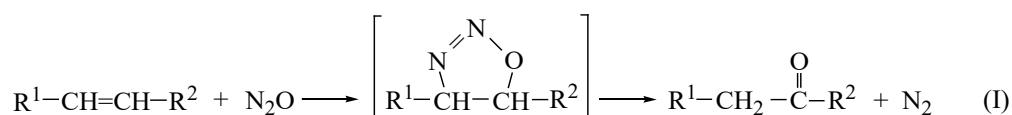
## PP-II-2

### Gas-Phase Selective Oxidation of Propane-Propylene Mixture with Nitrous Oxide

Parfenov M.V., Ivanov D.P., Dubkov K.A., Kharitonov A.S.  
*Boriskov Institute of Catalysis, Novosibirsk, Russia*  
*dubkov@catalysis.ru*

The light hydrocarbon fractions of oil refining, in particular the olefin-containing gases of catalytic cracking, are valuable raw materials for the chemical industry. Their wider use for the production of useful chemical products remains an urgent problem. One of the promising approach is the selective conversion of olefin-containing gases into oxygenates.

The discovery of the nitrous oxide (N<sub>2</sub>O) ability to convert olefins into carbonyl compounds with a selectivity above 90% [1, 2] and industrial implementation of this method for cyclopentanone and cyclododecanone production by BASF [3] open new prospects in this field. Such oxidation proceeds via a non-radical mechanism through the 1,3-dipolar cycloaddition of N<sub>2</sub>O to the C = C bond. Decomposition of [1,2,3]-oxadiazoline intermediate with release of N<sub>2</sub> leads to ketone or aldehyde:



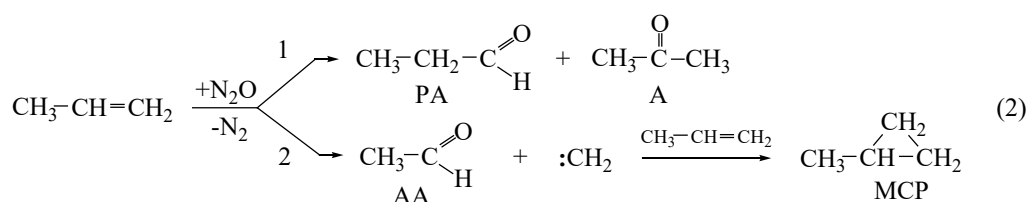
The present work presents a new method for producing carbonyl compounds by the gas-phase N<sub>2</sub>O-oxidation of propylene in the propane-propylene mixture (PPM) without its separation. The PPM contained 15% propane, 85% propylene and was similar in composition to the propane-propylene fraction of the typical catalytic cracking process. The reaction was carried out in a flow reactor (25 cm<sup>3</sup>) at 350-550°C and a pressure of 1-7 atm. A flow rate of the reaction mixture (10% N<sub>2</sub>O and 90% PPM) was 25 cm<sup>3</sup>/min.

It is seen from the table that the conversion of N<sub>2</sub>O (X<sub>N<sub>2</sub>O</sub>) and propylene (X<sub>R</sub>) increases with increasing temperature and pressure. At a pressure of 7 atm and 450°C, the N<sub>2</sub>O conversion reaches 74.6%, the conversion of propylene is 12.5%, and the total selectivity to carbonyl products S(O)<sub>Σ</sub> exceeds 74%. The total productivity for these products is 10.3 g/L·h.

№	P atm	T °C	X <sub>N<sub>2</sub>O</sub> %	X <sub>R</sub> %	Selectivity (S), %					S(O) <sub>Σ</sub> %
					A	AA	PA	MCP	Other	
1	1	450	3.9	0.6	38.3	26.7	24.7	2.0	8.4	89.7
2		500	13.9	2.2	36.4	24.0	22.6	4.7	12.5	83.0
3		550	42.1	5.9	32.5	24.1	14.0	2.0	27.4	70.6
4	4	400	14.8	2.3	35.2	28.9	18.6	5.3	12.0	82.7
5		450	46.4	7.9	33.1	21.9	18.3	5.0	21.7	73.3
6	7	350	8.8	1.3	32.5	35.2	15.3	4.8	12.1	83.0
7		400	28.4	4.7	33.9	27.2	17.4	6.0	15.5	78.5
8		450	74.5	12.5	36.8	21.3	16.5	6.1	19.2	74.6

## PP-II-2

The reaction leads to the formation of propanal (PA, selectivity is 14-25%), acetone (A, 32-38%), acetaldehyde (AA, 21-35%) and methylcyclopropane (MCP, 2-6%). Based on these data, the main routes for the oxidation of propylene in PPS are established (Scheme 2):



According to this scheme, the N<sub>2</sub>O oxygen adds to propylene with the formation of carbonyl products, and the molecular nitrogen (N<sub>2</sub>) is released. Depending on the carbon atom in the C=C bond to which the oxygen atom is attached, the oxidation leads to propanal (PA) or acetone (A) (route 1). The oxidation with the cleavage of the initial C=C bond (route 2) gives acetaldehyde (AA) and methylene: CH<sub>2</sub>. Highly active methylene then readily reacts with propylene, yielding methylcyclopropane (MCP). N<sub>2</sub>O does not react with alkanes and is consumed only for the formation of carbonyl products from propylene.

The presented results show that the gas-phase oxidation of propylene in the propane-propylene mixture with nitrous oxide at 350-550°C and a pressure up to 7 atm allows obtaining carbonyl products (acetone, propanal and acetaldehyde) with a total selectivity near 75%. In addition, the reaction yields a valuable cyclopropane derivative (methylcyclopropane), which is formed with selectivity up to 6%. The total selectivity of propylene conversion to useful products is at least 80%. The productivity to carbonyl products can be increased by increasing the operating pressure or the N<sub>2</sub>O concentration in the reaction mixture.

**Acknowledgement.** This work was conducted within the framework of the budget project #AAAA-A17-117041710083-5 for Boreskov Institute of Catalysis.

### References:

- [1] E. Starokon, K. Dubkov, D. Babushkin, V. Parmon, G. Panov, *Adv. Synth. Catal.* 346 (2004) 268-274.
- [2] K. Dubkov, G. Panov., V. Parmon, *Russ. Chem. Rev.* 86 (2017) 510.
- [3] <http://www.chemicalonline.com/article.mvc/BASF-Starts-Up-A-New-Production-Facility-For-0001>.

## Zeolite Brønsted Acidity: Direct Quantitative Characterization by Joint FTIR Spectroscopy and Solid-State $^1\text{H}$ MAS NMR Approach

Gabrienko A.A.<sup>1,2</sup>, Danilova I.G.<sup>2</sup>, Stepanov A.G.<sup>1,2</sup>  
1 – Novosibirsk State University, Novosibirsk, Russia  
2 – Borekov Institute of Catalysis, Novosibirsk, Russia  
*a.gabrienko@g.nsu.ru*

Zeolites are applied for numerous commercial applications. These crystalline materials, having unique microporous nature and strong Brønsted acidity, find broad usage in heterogeneous catalysis [1, 2]. Zeolite Brønsted acidity, caused by the presence of bridging Si–O(H)–Al or silanol Si–OH groups [3], attracts much attention since it determines the activity and selectivity of zeolite-based catalysts for acid-governed reactions. For adequate prediction of zeolite catalytic properties, it is crucial to have a reliable and feasible approach to measure the quantity of different hydroxyl O–H groups or Brønsted acid sites (BAS).

Fourier transform infrared (FTIR) spectroscopy is broadly applied nowadays for probing the concentration and strength of acid sites in zeolite catalysts [4, 5]. FTIR spectroscopy is able to measure zeolite Brønsted acidity directly by the observation of the absorption bands corresponding to different O–H groups or BAS. However, the accuracy of direct assessment of the quantity of different O–H groups by FTIR method suffers from the uncertainty of the integrated molar absorption coefficients,  $\epsilon$ . The  $\epsilon$  values reported by different authors might differ by an order of magnitude [6].

This report, based on the paper published recently [7], aims to demonstrate an elegant approach for reliable determination of the integrated molar absorption coefficients. The approach is based on joint work of  $^1\text{H}$  MAS NMR and FTIR spectroscopy techniques. The feasibility and accuracy of the proposed methodology have been verified on a series of zeolite samples.

The concentration of different O–H groups for H-ZSM-5 and H-ZSM-23 zeolite samples with different Si/Al ratio has been reliably established with  $^1\text{H}$  MAS NMR, using methane and benzene as internal standards. Further, same zeolite samples have been analyzed with FTIR spectroscopy to obtain the integrated absorbance of the IR bands related to the O–H groups. As the result, the values of the integrated molar absorption coefficients have been derived by comparing  $^1\text{H}$  MAS NMR and FTIR data. The  $\epsilon$  coefficients have been reliably determined to be  $3.06 \pm 0.04$  and  $1.50 \pm 0.06 \text{ cm} \times \mu\text{mol}^{-1}$  for the IR bands at 3605–3615 and 3740–3747  $\text{cm}^{-1}$ , respectively. Interestingly, the  $\epsilon$  values are similar for both H-ZSM-5 and H-ZSM-23 zeolites. It is also obtained that the  $\epsilon$  values are constant with respect to the concentration of O–H groups for H-ZSM-5 and H-ZSM-23 zeolites.

The determined  $\epsilon$  coefficients can be further used for reliable quantitative assessment of zeolite Brønsted acidity with the aid of the widely available and relatively simple methodology of FTIR spectroscopy.

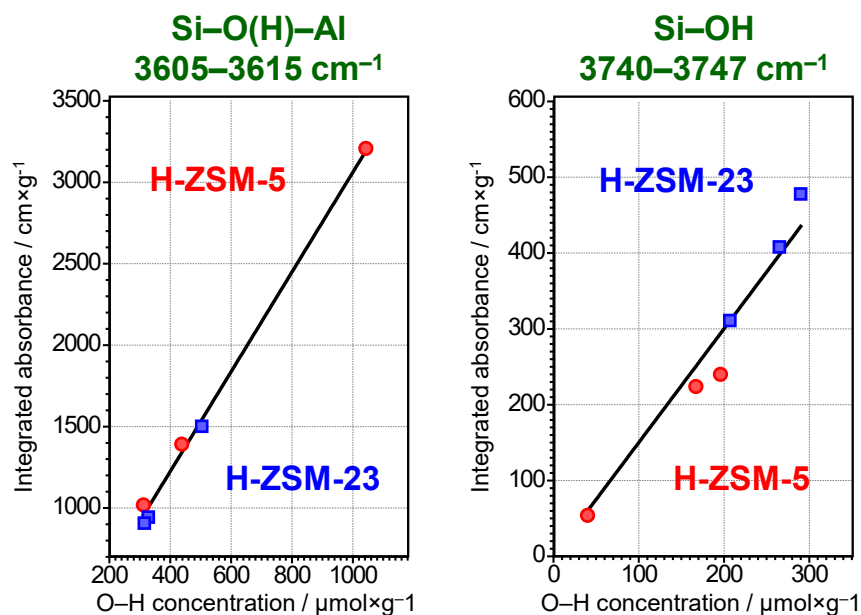


**Figure 1.** Integrated intensity of the IR band versus the concentration of the O–H groups for H-ZSM-5 and H-ZSM-23 zeolites.

**Acknowledgement.** This work was supported by Russian Foundation for Basic Research (grant no. 18-03-00189).

#### References:

- [1] E.T.C. Vogt, B.M. Weckhuysen, *Chem. Soc. Rev.* 44 (2015) 7342.
- [2] P. Schwach, X.L. Pan, X.H. Bao, *Chem. Rev.* 117 (2017) 8497.
- [3] A.A. Gabrienko, I.G. Danilova, S.S. Arzumanov, A.V. Toktarev, D. Freude, A.G. Stepanov, *Microporous Mesoporous Mat.* 131 (2010) 210.
- [4] A. Corma, *Chem. Rev.* 95 (1995) 559.
- [5] W.E. Farneth, R.J. Gorte, *Chem. Rev.* 95 (1995) 615.
- [6] K. Hadjiivanov, *Adv. Catal.* 57 (2014) 99.
- [7] A.A. Gabrienko, I.G. Danilova, S.S. Arzumanov, L.V. Pirutko, D. Freude, A.G. Stepanov, *J. Phys. Chem. C* 122 (2018) 25386.

## X-ray Absorption Spectroscopy Study of Metal-Organic Frameworks Functionalized by Pd for Catalytic Hydrogenation of CO<sub>2</sub>

Kamyshova E., Skorynina A., Bugaev A., Soldatov A.  
Southern Federal University, Rostov-on-Don, Russia  
kamyshova.liza@gmail.com

Metal-organic frameworks (MOFs) are new promising porous materials, constructed from organic linkers and metal-oxide units [1]. Additional useful properties can be achieved by the functionalization of MOFs, which allows obtaining new structures with specific properties. UiO-66/67/68 family shows an incredible thermal and chemical stability, which makes them promising for catalysis. Also, in the case of UiO-66/67/68, functionalization has played an important role in enhancing the material potentialities, by insertion of other metals in the inorganic cornerstones and by functionalization of linkers by additional metals.

This research is aimed to investigate the structure and catalytic properties of series of new UiO-67 metal-organic frameworks functionalized with palladium by in situ and operando X-ray absorption spectroscopy (XAS). The main goals were to prove the successful incorporation of Pd atoms in the structure of UiO-67, and monitor the formation of either metal nanoparticles (NPs) or single-atom Pd active sites upon activation in H<sub>2</sub> and He, and also determine the structure-reactivity relationships and the stability of the synthesized materials during catalytic hydrogenation of carbon dioxide.

The synthesized materials were studied at the European Synchrotron Radiation Facility (ESRF) by simultaneous Pd K-edge XAS and X-ray diffraction (XRD). XAS was used as the main experimental technique, because of its sensitivity to the local atomic environment around palladium atoms. At the same time, XRD confirmed the stability of UiO-67 crystal structure during the formation of catalytically active species [2]. We used 4 samples with 5% and 10% of linkers functionalized with palladium via pre-made linker synthesis (PMLS) and post-synthesis functionalization (PSF). Each sample was activated by heating to 300°C (2°C/min) in a flow of 10% H<sub>2</sub>/He and pure He. After reaching 300°C, the catalysts was left at that temperature to allow the formation of particles. The evolution of local environment around Pd atoms was monitored by Pd K-edge (24350 eV) EXAFS and XANES spectroscopies. The activated material was cooled down to 50°C, and high-quality EXAFS data was collected. Then, the materials were exposed to a mixture of H<sub>2</sub>/CO<sub>2</sub>/He (6:1:3) at 100, 200 and 300 °C and *operando* XAS spectra were collected, while the output of the as mixture was analysed by online mass spectrometer.

We performed a Fourier-analysis of the whole series of EXAFS data collected during the activation and determined the key steps in formation of active Pd-species: removal of Cl-ligands, detachment of Pd from the linkers, formation and growth of Pd NPs. By simultaneous analysis of the whole series of EXAFS spectra we obtained the temperature dependence of

## PP-II-4

the Pd-N and Pd-Cl coordination numbers, as well as evolution of structural parameters of the formed Pd nanoparticles [3]. The XANES spectra collected during the catalytic hydrogenation of CO<sub>2</sub> were normalized and will be further processed by principle component analysis and multivariate techniques.

Therefore, we have proved successful incorporation of Pd atoms into the structure of the linker in UiO-67 MOF. The initial structure has Pd in square planar coordination with two chlorine and two nitrogen atoms, acting as a precursor for catalytically active Pd NPs confined inside the pores of UiO-67. We collected and analysis in situ EXAFS data and provided detailed structural information about the evolution of the local surrounding of Pd atoms. Analysis of operando XANES data which is expected to provide structure-reactivity relationships for CO<sub>2</sub> hydrogenation is now in progress.

**Acknowledgement.** This research was supported by the Russian Science Foundation, project № 18-73-00189.

### References:

- [1] Butova V. V., Soldatov M. A., Guda A. A. et al. Metal-organic frameworks: structure, properties, methods of synthesis and characterization // Russian Chemical Reviews. -- 2016. -- T. 85, № 3. -- C. 280-307.
- [2] Bugaev A. L., Guda A. A., Lomachenko K. A. et al. Operando study of palladium nanoparticles inside UiO-67 MOF for catalytic hydrogenation of hydrocarbons // Faraday Discussions. -- 2018. -- T. 208. -- C. 287-306.
- [3] Kamysheva E. G. et al. Formation and growth of Pd nanoparticles in UiO-67 MOF by in situ EXAFS // Radiation Physics and Chemistry. -- 2019, doi: 10.1016/j.radphyschem.2019.02.003.

## The Nature of Active Sites in PdCo/C Catalysts Prepared by Pyrolysis of Wood Sawdust Impregnated with Pd(NO<sub>3</sub>)<sub>2</sub> and Co(NO<sub>3</sub>)<sub>2</sub> in Hydrodechlorination of Chlorobenzene

Klokov S.V.<sup>1</sup>, Lokteva E.S.<sup>1</sup>, Golubina E.V.<sup>1</sup>, Maslakov K.I.<sup>1</sup>, Isaikina O.Y.<sup>1</sup>, Trenikhin M.V.<sup>2,3</sup>

1 – Lomonosov Moscow State University, Moscow, Russia

2 – Omsk State Technical University, Omsk, Russia

3 – Omsk Scientific Centre of SB of RAS, Omsk, Russia

*servadklokov@gmail.com*

Hydrodechlorination (HDC) is a promising disposal method for organochlorine wastes due to the absence of dioxins in products and possibility of HDC products reuse. Catalysts containing transition metal nanoparticles (Pd, Ni, Fe etc.) demonstrate good performance in HDC [1]. However, they are easily deactivated under the influence of reaction by-product, HCl. There is the need in development of new types of stable catalysts.

We showed that Pd/C [2] and Co/C [3] obtained by shortened method including the pyrolysis of sawdust impregnated with metal nitrate solution are effective in HDC of chlorobenzene (CB), but the active component differs in nature: it comprises predominantly Pd<sup>0</sup> in Pd/C and mainly CoO in Co/C. Therefore it is important to study the mechanism of catalytic action of bimetallic PdCo/C. In this work PdCo/C catalysts were prepared by the same method, tested in chlorobenzene HDC and compared with monometallic Pd/C and Co/C catalysts. Characteristics of catalysts are presented in Table 1.

*Table 1. Characteristics of PdCo/C catalysts*

Catalyst	S <sub>BET</sub> , m <sup>2</sup> /g	Pd loading, mass.% (AAS data)	Co loading, mass.% (AAS data)	d <sub>n</sub> , nm (TEM data)
Pd/C	148 ± 15	0.56	-	3.7
PdCo(1.1)/C	210 ± 21	0.85	0.77	6.5
PdCo(0.7)/C	164 ± 16	1.07	1.48	4.1
Co/C	261 ± 26	-	1.30	3.9

According to low-temperature nitrogen adsorption, XPS and Raman spectroscopy, carbon material obtained by pyrolysis of wood sawdust impregnated with metal nitrate solution contains amorphous carbon and is similar in structure to carbon of low activation degree. Cobalt promotes better activation of carbon material in comparison to palladium.

According to TPR H<sub>2</sub> and XPS, palladium in the catalysts is present in the reduced state (Pd<sup>0</sup>) in contrast to cobalt which is present in oxidized state (mainly CoO). According to TEM, metals-containing nanoparticles are located on the surface and in the bulk of carbon material. Nanoparticles located on the surface are coated with thin carbon shell. The interplanar spacings for major part of Pd-containing particles in Pd/C are 2.26-2.37 Å, but the other particles have increased interplanar spacing (2.34-2.37 Å) probably due to PdC<sub>x</sub> formation on

## PP-II-5

the surface of Pd particles. In PdCo(0.7)/C a few of nanoparticles with interplanar spacing of 2.36-2.41 Å, characteristic to PdCoO<sub>2</sub>, were observed, that indicates closer contact between two metals in PdCo(0.7)/C in comparison with PdCo(1.1)/C.

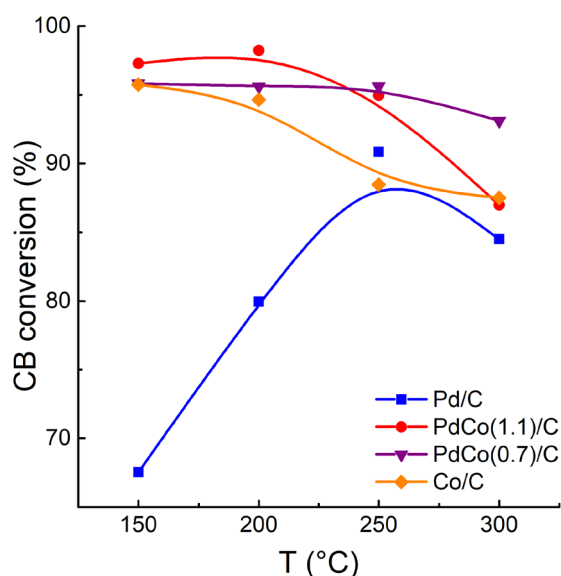


Figure 1. Chlorobenzene conversion vs temperature

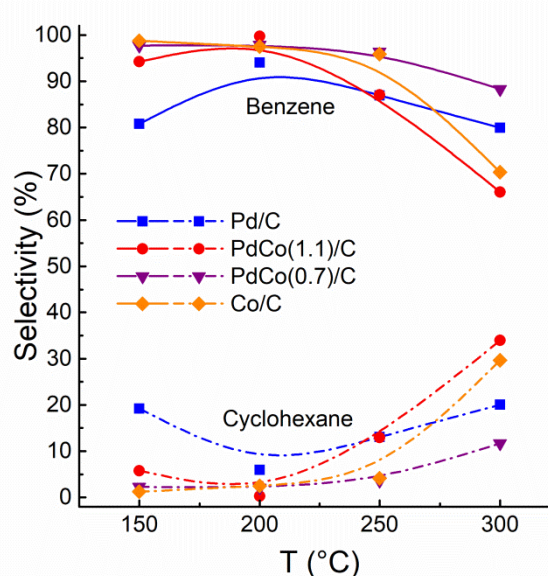


Figure 2. Selectivity to benzene and cyclohexane vs temperature

Catalysts were tested in HDC of CB in a fixed bed continuous flow reactor at 250-300°C for 18-20 h. All catalysts were active in CB transformation to benzene. Conversion of CB at low temperatures (150-200°C) is higher on Co-containing catalysts than on Pd/C. In contrast to Pd/C where active sites comprise Pd<sup>0</sup>, whereas in Co/C mainly CoO constitutes the active component, as it was suggested in [3]. An improved efficiency of PdCo/C in comparison with Pd/C and Co/C may be explained by joint action of Pd<sup>0</sup> and CoO, especially on the border between two phases, with additional effect of PdCoO<sub>2</sub>.

According to XPS investigation of catalysts after catalytic tests, the chlorination of metals and the destruction of the carbon shell under the influence of HCl by-product in reaction medium were observed. The second process provides an increase of the metal surface available for adsorption of reagents adsorption and activation. Analysis of the elemental composition and electronic state of the elements after catalysis showed that in the bimetallic catalysts cobalt containing particles are chlorinated more easily than palladium ones.

**Acknowledgement.** This work was supported by RFBR according to the research project №18-33-00785.

### References:

- [1] M.A. Keane ChemCatChem 3 (2011) 800.
- [2] S.V. Klovov, E.S. Lokteva, E.V. Golubina et al. Catal. Commun. 77 (2016) 37.
- [3] S.V. Klovov, E.S. Lokteva, E.V. Golubina et al. Appl. Surf. Sci. 463 (2019) 395.

## Advances in Characterization of Aluminum Oxides Porous Structure

Mel'gunova E.A., Krapivina E.A., Mel'gunov M.S.  
*Boreskov Institute of Catalysis, Novosibirsk, Russia*  
*melena@catalysis.ru*

Aluminum oxides are probably the most common materials for catalysis and adsorption applications. Most often, their porous structure is characterized by means of adsorption methods, usually by nitrogen adsorption at ca. 77.4K. The values of textural parameters namely the specific surface area, pore volume and their size distributions calculated by means of widespread BET and BJH methods are more-or-less reproducible, but their relevance to real values is questionable due to known oversimplifications [1]. Application of alternative techniques is less common, and introduces considerable uncertainty, which usually is not discussed. Unfortunately, the method of isotherm comparison (IC), which was elaborated to overcome the drawbacks of the BET method suffers from ambiguity of choice of a reference material, and a linear region; methods based on molecular statistics (NLDFT, Monet Carlo, etc.) sometimes unreasonably poorly fit the experiment [2]; by unknown reasons the thermodynamically correct Deryagin-Broekhoff-de Boer (DBdB) method [3] did not find proper place in the study of alumina-based catalysts.

Due to absence of proper reference materials, which could be independently characterized by means of alternative (not adsorption) techniques, all known methods were used for years without reliable verification. Tuning of known methods for measurement of textural parameters has become possible after elaboration of template hexagonally ordered mesoporous [4] and anodic alumina [5]. In this presentation we discuss the advances of the DBdB method, applied with the reliable high-precision  $t$ -curve [2] that surprisingly well correspond to data obtained by means of alternative non-adsorption methods. We show that this method gives the most reliable values for the surface area and pore size in aluminas, and discuss how these parameters, calculated by means of BET, IC, BJH, and NLDFT measured in catalytic literature can be recalculated to DBdD values.

**Acknowledgement.** This work is supported by Ministry of Science and Higher Education of the Russian Federation (project AAAA-A17-117041710079-8).

### References:

- [1] Thommes M. et al. Physisorption of gases, with special reference to the evaluation of surface area and pore size distribution (IUPAC Technical Report) // Pure and Applied Chemistry. 2015. Vol. 87, № 9–10. P. 1051–1069.
- [2] Mel'gunov M.S. et al. Nitrogen adsorption at ca. 77.4 K on partially hydrated and anhydrous  $\alpha$ - $\text{Al}_2\text{O}_3$  // Adsorption. 2019.
- [3] Ustinov E.A., Do D.D., Jaroniec M. Equilibrium Adsorption in Cylindrical Mesopores: A Modified Broekhoff and de Boer Theory versus Density Functional Theory // J. Phys. Chem. B. 2005. Vol. 109, № 5. P. 1947–1958.

## PP-II-6

[4] Bruschi L. et al. Capillary Condensation and Evaporation in Alumina Nanopores with Controlled Modulations // *Langmuir*. 2010. Vol. 26, № 14. P. 11894–11898.

[5] Petukhov D.I. et al. Experimental and Theoretical Study of Enhanced Vapor Transport through Nanochannels of Anodic Alumina Membranes in a Capillary Condensation Regime // *The Journal of Physical Chemistry C*. 2016. Vol. 120, № 20. P. 10982–10990.

## Zirconium-Assisted Activation of Palladium to Boost Syngas Production by Methane Dry Reforming

Köpfle N.<sup>1</sup>, Götsch T., Grünbacher M.<sup>1</sup>, Carbonio E.A.<sup>2</sup>, Hävecker M.<sup>2</sup>, Knop-Gericke A.<sup>2</sup>, Schlicker L.<sup>3</sup>, Doran A.<sup>4</sup>, Kober D.<sup>3</sup>, Gurlo A.<sup>3</sup>, Penner S.<sup>1</sup>, Klötzer B.<sup>1</sup>

*1 – Institute of Physical Chemistry, University of Innsbruck, Innsbruck, Austria*

*2 – Department of Inorganic Chemistry Fritz-Haber-Institute of the Max-Planck-Society, Berlin, Germany*

*3 – Fachgebiet Keramische Werkstoffe/Chair of Advanced Ceramic Materials, Institut für Werkstoffwissenschaften und -technologien, Technische Universität Berlin, Berlin, Germany*

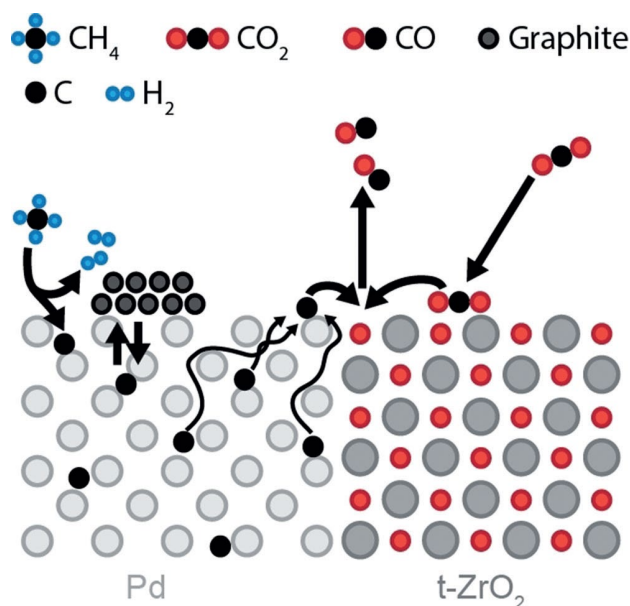
*4 – Advanced Light Source, Lawrence Berkeley National Laboratory Berkeley, California, USA  
simon.penner@uibk.ac.at*

C-saturated Pd<sup>0</sup> nanoparticles with an extended phase boundary to ZrO<sub>2</sub> evolve from a Pd<sup>0</sup>Zr<sup>0</sup> precatalyst under CH<sub>4</sub> dry reforming conditions. This highly active catalyst state fosters bifunctional action: CO<sub>2</sub> is efficiently activated at oxidic phase boundary sites and Pd<sub>x</sub>C provides fast supply of C-atoms toward the latter.

In conclusion, the surface-near regions of a bulk PdZr pre-catalyst are oxidatively decomposed under realistic DRM conditions and the resulting Pd<sup>0</sup> nanoparticles provide an appropriate near-surface carbon loading at the resulting Pd<sup>0</sup>/t-ZrO<sub>2</sub> interface at about 700°C, as depicted in Scheme 1. This, in turn, creates optimized conditions for bifunctional catalyst operation: Pd<sup>0</sup> regions favor fast supply of reactive C-atoms toward the phase boundary, whereas Zr(ox) sites [1,2] assist in CO<sub>2</sub> activation and the transfer of CO<sub>2</sub>-derived oxygen to the latter, thus providing optimum conditions for high CO activity. Empirical attempts to control coking of, for example, Ni by specifically active supports such as CeZrO<sub>x</sub>[3-5] seem to make use of this principle. Faster C-depletion of the metallic component via an accelerated phase boundary reaction can directly lower the C concentration of the metal particles and thus initially disfavor nucleation and growth of graphite-type C-species, but also enhance the relative amount of redissolution of the latter in the metal as C<sub>bulk</sub> under stationary reaction conditions. This scenario provides a solid basis for directional promotion of microkinetic steps leading both to enhanced activity and improved control of carbon chemistry during DRM. Important implications for knowledge-based DRM catalyst synthesis, at least if C-dissolving metals such as Ni and Pd are involved, are: 1) optimization of phase boundary dimensions and CO<sub>2</sub> activation properties of the support; 2) adjustment of (bi)metal particle size to achieve C<sub>bulk</sub> depletion even in metallic regions with the largest distance to the phase boundary; 3) use of (bi)metallic catalysts with suppressed nucleation- and growth kinetics of graphite-type C-species, at least within the DRM temperature range; and 4) high abundance and reactivity of interfacial C<sub>ads</sub> species, achievable via optimized CH<sub>4</sub> adsorption/sticking at the metallic surface and fast bulk/surface diffusion to not too strongly C-binding sites at

## PP-II-7

or close to the phase boundary. As shown in this work, the use of intermetallic precursors such as  $\text{Pd}_x\text{Zr}_y$  is one way to match these criteria.



**Scheme 1.** Proposed DRM mechanism leading to enhanced CO formation at the Pd/t-ZrO<sub>2</sub> interface.

**Acknowledgement.** This work was financially supported by the Austrian Science Fund through grant F4503-N16. N.K. acknowledges a PhD position via doctoral programme “reactivity and catalysis” of the University of Innsbruck. The authors thank the HZB/ BESSY II staff for their support of the in situ XPS measurements at beamline ISSS-PGM. Financial support by the project CALIPSOplus under the Grant Agreement 730872 from the EU Framework Programme for Research and Innovation HORIZON 2020 is acknowledged. This research used resources of the Advanced Light Source, which is a DOE Office of Science User Facility under contract no. DE-AC02-05CH11231. L.S. acknowledges the funding of his work by an ALS doctoral fellowship.

### References:

- [1] J. H. Bitter, K. Seshan, J. A. Lercher, *J. Catal.* 1998, 176, 93.
- [2] J. H. Bitter, K. Seshan, J. A. Lercher, *J. Catal.* 1997, 171, 279.
- [3] A. Wolfbeisser, O. Sophiphun, J. Bernardi, J. Wittayakun, K. Föttinger, G. Rupprechter, *Catal. Today* 2016, 277, 234.
- [4] S. Damyanova, B. Pawelec, K. Arishtirova, M. M. Huerta, J. L. G. Fierro, *Appl. Catal. B* 2009, 89, 149.
- [5] M. M. Makri, M. A. Vasiliades, K. C. Petalidou, A. M. Efstathiou, *Catal. Today* 2016, 259, 150.

## Photocatalytic Hydrogen Production over Titania-Based Photocatalysts

Selivanova A.V.<sup>1</sup>, Kurenkova A.Y.<sup>1</sup>, Tsapina A.M.<sup>1</sup>, Saraev A.A.<sup>1,2</sup>,  
Kozlova E.A.<sup>1,2</sup>, Kaichev V.V.<sup>1,2</sup>

1 – Boreskov Institute of Catalysis, Novosibirsk, Russia

2 – Novosibirsk State University, Novosibirsk, Russia

vvk@catalysis.ru

The rapid depletion of hydrocarbon resources makes it necessary to harness a wide range of new chemical energy carriers and alternative or unconventional sources of energy. Particular attention is paid to the use of hydrogen as fuel. Photocatalytic hydrogen production is, as well as photocatalytic carbon dioxide reduction, are one of the most promising methods of solar energy conversion. The production of hydrogen via the photocatalytic water splitting is possible when the conduction band edge of a semiconductor is more negative than the electrochemical hydrogen production potential and when the valence band edge is more positive than the oxygen production potential. TiO<sub>2</sub> (E<sub>g</sub> = 3.2 eV) is a widely used photocatalyst for hydrogen production from water solution of glycerol under UV light irradiation. However, the solar spectrum contains only about 3-5% of the UV range irradiation. Thus, sensibilization of titanium dioxide to visible light is an important task. One of the promising methods for shifting the absorption edge of titanium dioxide is the deposition of transition metals [1].

This work was aimed at the synthesis of titania-based photocatalysts with deposited metals (Au, Pt, Pd, Cu, Ni, and Ag). Commercial titania samples Hombifine N (100% anatase) and Degussa P25 (70% anatase, 30% rutile) were used for the photocatalysts preparation. The photocatalysts were characterized by X-ray photoelectron spectroscopy, X-ray absorption spectroscopy, UV-VIS diffuse reflectance spectroscopy, X-ray diffraction, low-temperature N<sub>2</sub> adsorption technique and tested in the photocatalytic hydrogen production from aqueous solutions of glycerol under visible light (λ = 450 nm). Recently glycerol (C<sub>3</sub>H<sub>8</sub>O<sub>3</sub>) is considered as a prospective electron donor for the photocatalytic hydrogen production because it is a by-product of the vegetable oil transesterification into biodiesel [2]. It has been shown that the photocatalysts based on Degussa P25 possesses higher activity in comparison to the photocatalysts based on Hombifine N due to heterojunctions between anatase and rutile phases of titania. It turned out that an increase in activity during the deposition of copper and nickel is comparable to an increase in activity during the deposition of platinum, which is a very promising result.

**Acknowledgement.** This work was supported by the Russian Science Foundation, grant 19-73-20020.

### References:

- [1] E.A. Kozlova, V.N. Parmon, Russ. Chem. Rev. 86 (2017) 870-906.
- [2] D.I. Kondarides, V.M. Daskalaki, A. Patsoura, X.E. Verykios. Catal. Lett. 122 (2008) 26-32.

**Atomic Structure and Catalytic Properties of Bimetallic Nanoparticles PtM (M = Ni, Co, Cu) in Metall-Carbon PtM/C Electrocatalysts for Low-Temperature Fuel Cells**

Shemet D.B., Pryadchenko V.V., Menshikov V.S., Nevelskaya A.K., Guterman V.E., Bugaev L.A.  
*Southern Federal University, Rostov-on-Don, Russia*  
*shemetdabo@mail.ru*

Composite materials based on multicomponent platinum-containing nanoparticles are widely studied because they are promising catalysts for the electroreduction reaction of oxygen in low-temperature fuel cells. Platinum-containing nanoparticles are very promising due to high thermodynamic stability of platinum and due to specific chemical activity of this metal. However, the cost of pure platinum particle is one of the main factors restricting the wide application of low-temperature fuel cells. Such expenses can be decreased by using multimetal nanoparticles or non-platinum nanoparticles.

The studied catalysts were obtained by two different methods of synthesis: simultaneous and sequential reduction of the precursors to the carbon substrate. As a result, nanoparticles that have a structural form were obtained. In the case of sequential reduction, the proposed nanoparticles with the core-shell structure were obtained.

Samples were heat treated in an inert zone. The electrochemically activated surface area and the specific catalytic activity of the obtained catalysts were determined by the method of cyclic voltammetry. The study of changes in the size of the electrochemically active surface area of catalysts and specific activity during long-term cyclic voltammetry made it possible to establish synthesis conditions and post-processing results based on the catalysts obtained.

The size characteristics of the nanoparticles (average nanoparticle size, size dispersion) were found using powder X-ray diffraction. Using a specialized synchrotron radiation source BASSY II, X-ray absorption spectra (XAS) were obtained in the near threshold (XANES) and extended (EXAFS) energy zones.

Using the technique based on the Fourier transform of the EXAFS spectra, the values of the parameters of the near environment of metal atoms in nanoparticles in different structural states were obtained.

**Acknowledgement.** This work was supported by grants from the Russian Foundation for Basic Research № 18-32-00632 мол\_a.

## Adsorption and Oxidation of Carbon Monoxide on Co - ZSM-5 Zeolites

Shilina M.I.<sup>1</sup>, Gloriozov I.P.<sup>1</sup>, Zhidomirov G.M.<sup>1,2</sup>

1 – Lomonosov Moscow State University, Moscow, Russia

2 – Boreskov Institute of Catalysis, Novosibirsk, Russia

*mish@kinet.chem.msu.ru*

Zeolites are useful microporous matrices for creating well-defined isolated active sites in a controlled environment. These materials are extensively applied as selective catalysts for a wide variety of chemical processes. Cobalt modified zeolites ZSM-5 prepared by impregnation were the most active in the catalytic oxidation of CO at relatively low temperatures, slightly above 100 °C [1]. It was proposed that oxocations  $[\text{Co}_x\text{O}_y]^{n+}$  ( $n = 1, 2$ ) with Co(III) prevailing in their structure play a crucial role in CO adsorption and catalytic oxidation.

In this work using quantum-chemical DFT calculations we analysed the geometry of the extra-framework cations and cobalt-oxocomplexes in the direct channel of the cobalt-containing ZSM-5 zeolite depending on the distribution of aluminium. A fragment of a crystal cell consisting of 222 atoms was chosen as a model cluster. The geometries, adsorption energies, and IR spectra of adsorbed CO on exchangeable  $\text{Co}^{2+}$  cations and polynuclear Co-oxocations of different composition were calculated.

The interaction of CO with Co-ZSM-5 was investigated by a combination of IR spectroscopy and DFT calculations employing the  $\omega/r$  correlation for calculations of CO stretching frequencies in order to gain more insight on  $\text{Co}^{2+}$  cation coordination in the ZSM-5 zeolite and site-specificity of CO stretching frequency in IR spectra of CO/Co-ZSM-5 system. Experimental data were interpreted on the basis of a good agreement between experimental and theoretical results. Detailed analysis of both theoretical and experimental results reveals that no individual band can be assigned to specific type of CO–Co complex or to a one type of  $\text{Co}^{2+}$  sites. On the contrary, several different type of carbonyl complexes contribute to each vibrational band discerned in the experimental IR spectra. The new absorption band at  $2215 \text{ cm}^{-1}$  was assigned to the carbonyl complexes on Co(III) located in oxocations  $[\text{Co}_2\text{O}_2]^{2+}$ . The data of quantum chemical DFT calculations showed that the most likely active centres in the oxidation of CO by oxygen on Co-ZSM-5 are the polynuclear oxocations  $[\text{Co(III)}-(\mu\text{-O})_2\text{-Co(III)}]^{2+}$ . The possible ways for the oxidation of carbon monoxide under these species were analysed.

**Acknowledgement.** All calculations were performed using the MBC100k cluster at the Joint Supercomputer Center (JSCC) (Moscow, Russia).

### References:

[1] M.I. Shilina, T.N. Rostovshchikova, S.A. Nikolaev, O.V. Udalova, *Mater.Chem.Phys.*, 223 (2019) 287.

## In Situ High Energy XRD Study of Reduction Process of Transition Metal Oxides in Supercritical Isopropanol

Shmakov A.N., Nesterov N.S., Yakushkin S.S., Martyanov O.N.  
Boreskov Institute of Catalysis, Novosibirsk, Russia  
shurka@catalysis.ru

Because of the development of chemical technology, the emergence of new materials and the improvement of engineering solutions, supercritical (SC) fluid technologies become more and more economically attractive for carrying out various chemical processes (extraction, separation, chemical reactions). The use of SC environment allows the creation of unique functional materials that are difficult and sometimes impossible to produce using traditional approaches. It is known that isopropanol in the SC state ( $T_{crit}=235^{\circ}\text{C}$ ,  $P_{crit}=53$  bar) provides the reduction of transition metal oxides, particularly cobalt oxide ( $\text{Co}_3\text{O}_4$ ), at temperatures lower than that of reduction in pure hydrogen [1]. Thus, it was shown by the ferromagnetic resonance method that this feature of the SC isopropanol avoids the high-temperature sintering of metal particles upon reduction and makes SC isopropanol a promising reducing agent for the preparation of dispersed metallic catalysts [2].

To reveal phase transitions of  $\text{Co}_3\text{O}_4$  under SC conditions the High Energy X-ray diffraction experiment was carried out at Beamline No.8 of VEPP-4M storage ring operating as synchrotron radiation source with electron energy 4.5 GeV. The mixture of cobalt oxide powder and isopropanol was placed in glass capillary with outer diameter of 1 mm and inner diameter of 0.5 mm, sealed and mounted in front of area X-ray detector at distance 650 mm. Sample was heated to temperature up to  $420^{\circ}\text{C}$  with air blower, the temperature was controlled with thermocouple positioned to capillary as close as possible. The high energy of radiation, 112.3 keV ( $\lambda=0.01104$  nm), was chosen for diffraction experiment to minimize radiation absorption in capillary walls. Area detector Toshiba FDX4343R was used to detect Debye rings and pattern treatment was done with Fit2D software.

Under isopropanol SC conditions the reduction of  $\text{Co}_3\text{O}_4$  begins at  $210^{\circ}\text{C}$  and transforms the initial oxide to CoO at temperature range  $210\div 340^{\circ}\text{C}$ . At higher temperature metallic Co with cubic structure appears.

**Acknowledgement.** This work was supported by Ministry of Science and Higher Education of the Russian Federation (project AAAA-A19-119020890025-3).

### References:

- [1] Gubin, S.P., Buslaeva, E.Y. Supercritical isopropanol as a reducing agent for inorganic oxides. *Russ. J. Phys. Chem. B.* **3**, 1172–1186 (2009). doi:10.1134/S1990793109080077.
- [2] Nesterov, N.S., Simentsova, I.I., Yudanov, V.F., Martyanov, O.N. A comparative FMR study of the reduction of Co-containing catalysts for the Fischer–Tropsch process in hydrogen and supercritical isopropanol. *J. Struct. Chem.* **57**, 90–96 (2016). doi:10.1134/S0022476616010108.

## IR Study of Hydrogen Atom Transfer in Hydrates of Alkali Metal Halides

Spirin I.A., Grinvald I.I., Kalagaev I.Yu., Kapustin R.V.

*Nizhny Novgorod Technical State University n.a. R.E. Alekseev, Nizhny Novgorod, Russia  
ivan.sn.92@mail.ru*

Proton solvates are involved in most processes occurring in solutions. They play a special role in homogeneous acid catalysis. Sustainable solvates of the proton acting as reagents or ionizing agents and can form various intermediate complexes. The structure of the proton solvates determined the mechanism of transformation in solutions.

The present work discusses the IR spectroscopy investigation of the proton transport phenomenon and hydrate formation in alkali metal halides. The IR study was carried out for the films deposited on an optical window. Briefly, the method of films preparation can be described as follows. A certain volume of alkali salts solution was diluted in acetone. Then the solid films were crystallized from these solutions for spectra recording.

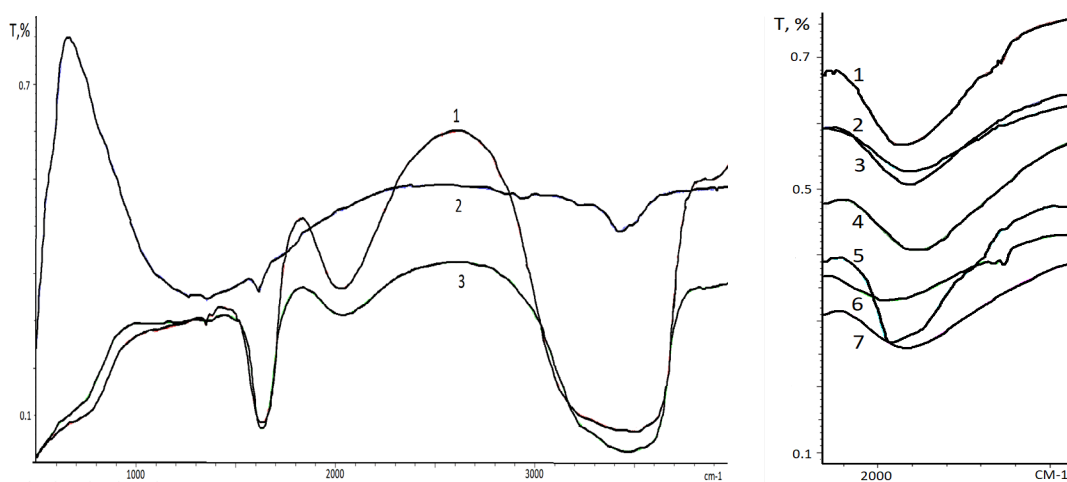


**Figure 1.** IR spectra of inorganic salts films obtained by crystallization from acetone.

On the left side, the KI films spectra with a different ratio of aqueous salt solution in acetone are shown: the concentration of salt in water solution grows at going from spectrum 1 to 3. On the right side IR spectra of salts films in the  $2300\text{--}2000\text{ cm}^{-1}$  region are presented: 1 - LiBr, 2 - NaCl, 3 - LiF, 4 - KCl, 5 - NaBr, 6 - KI, 7 - KBr.

The appearance of new bands and shift of the initial bands in the region of stretching vibration in hydronium ion ( $2300\text{--}2000\text{ cm}^{-1}$ ) to the formation of adduct with salt anion  $(\text{H}_2\text{O})\text{H}^+\cdots\text{X}^-$  ( $\text{X}^- = \text{F}^-, \text{Cl}^-, \text{Br}^-, \text{I}^-$ ) is assigned. In contrast to the common opinion that the rise of anion electronegativity from iodine to fluoride ion leads to an increase of the water stretching vibration red shift, in our study an opposite picture was found: the shift of OH-stretching vibration in hydronium ion grows at going from fluoride to iodide. In this work an attempt to interpret this phenomenon is given.

## Dynamics of the Atomic and Electronic Structure of Nanoparticles of Noble Metals during Catalytic Reactions

Usoltsev O.A.<sup>1</sup>, Bugaev A.L.<sup>1</sup>, Skorynina A.A.<sup>1</sup>, Tereshchenko A.A.<sup>1</sup>, Lomachenko K.A.<sup>2</sup>,  
Guda A.A.<sup>1</sup>, Groppo E.<sup>3</sup>, Pellegrini R.<sup>4</sup>, Lamberti C.<sup>1,3</sup>, Soldatov A.V.<sup>1</sup>

1 – Southern Federal University, Rostov-on-Don, Russia

2 – European Synchrotron Radiation Facility, Grenoble, France

3 – University of Turin, Turin, Italy

4 – Chimet SpA - Catalyst Division, Arezzo, Italy

oleg-usol@yandex.ru

Noble metal nanoparticles are widely used in catalysis and electrochemistry due to remarkable advantages over most analogues, the main of which is the large surface area of nanoparticles. The atomic and electronic structure of the near-surface regions determine the catalytic properties. A few percent change in catalytic activity and selectivity can significantly affect the lifetime of the catalyst and, ultimately, increase or decrease the cost of the final products. We focus on the formation of the carbide phase in palladium nanoparticles (Pd NPs) on a carbon substrate exposed to acetylene and ethylene at 100 °C. The formation of the carbide phase was observed *in situ* (Fig. 1.) using X-ray absorption near edge structure (XANES), extended X-ray absorption fine structure (EXAFS) and X-ray powder diffraction (XRPD).

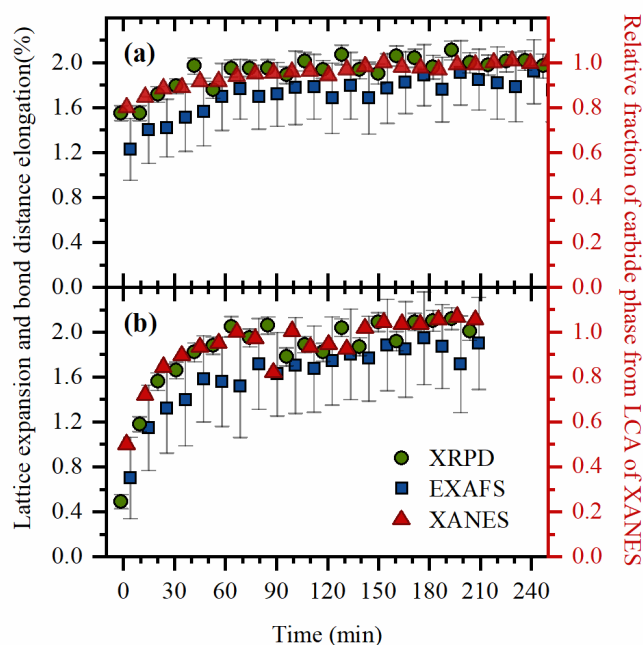


Fig. 1. Evolution of the cell parameter calculated from XRPD refinement (green circles, left ordinate axis), first shell Pd–Pd interatomic distances from EXAFS (blue squares, left ordinate axis) and relative fraction of carbide component from LCA of XANES during exposure of Pd NPs to acetylene (a) and ethylene (b) at 100 °C.

## PP-II-13

We obtained the time evolution of the unit cell parameter applying using Rietveld refinement to XRPD and first-shell Fourier-analysis to EXAFS data simultaneously with relative carbon concentration in the sample using linear combination analysis of XANES spectra. The results represent *in situ* determined carbide formation rates in Pd NPs under the influence of acetylene and ethylene at 100 °C. This allows us to divide the carbide phase formation in two stages: rapid emergence immediately after the supply of hydrocarbons that probably corresponds to surface carbide formation, and more slow and gradual expansion of the cell parameter, which is observed for several hours that may correspond to the penetration of carbon atoms into the bulk of Pd NPs. Summing up, we would like to point out that the rate of formation of carbide phase in acetylene is higher than in ethylene. However, the final structures obtained after continuous exposure are identical.

**Acknowledgement.** This work was supported by Russian Foundation for Basic Research (RFBR) according to the research project number 18-32-00856.

### References:

[1] Skorynina A., Tereshchenko A., Usoltsev O. et al, Radiation Physics and Chemistry (2018).

## **Operando XRD Study of the Self-Sustained Reaction Rate Oscillations in the Oxidation of Methane over Palladium**

Vinokurov Z.S.<sup>1,2</sup>, Saraev A.A.<sup>1,2</sup>, Zaguzova V.V.<sup>3</sup>, Lashina E.A.<sup>1,2</sup>, Kaichev V.V.<sup>1,2</sup>

1 – Boreskov Institute of Catalysis, Novosibirsk, Russia

2 – Novosibirsk State University, Novosibirsk, Russia

3 – Novosibirsk State Technical University, Novosibirsk, Russia

vinokurovzs@catalysis.ru

The self-sustained kinetic oscillations in the catalytic oxidation of methane over Pd foil have been studied at atmospheric pressure using X-ray diffraction and mass spectrometry. The *operando* study was performed at the High Precision Diffractometry station at the synchrotron radiation facilities of the VEPP-3 storage ring (Siberian Synchrotron and Terahertz Radiation Center, Novosibirsk, Russia). The experiments were carried out on a high-precision X-ray diffractometer equipped with a collimation system, a position sensitive parallax-free linear OD-3M detector [1], a high temperature flow reaction chamber, flow mass controllers and a quadruple-type gas analyser UGA-100 [2]. The reaction chamber was made from stainless steel and had a construction similar to a XRK-900 (Anton Paar GmbH). To prevent a contribution to the catalytic reaction from reactor walls, the inside of the reaction chamber was coated by  $\alpha$ -Al<sub>2</sub>O<sub>3</sub> using a detonation spraying technique. The X-ray wavelength of 1.0102 Å was set by a single reflection of the “white beam” of synchrotron radiation from a Si(220) single-crystal monochromator. The catalyst temperature was measured by a K-type thermocouple spot-welded directly to the sample.

It was found that the regular reaction-rate oscillations appear under oxygen-deficient conditions and the period of oscillations varies between approximately 30 and 1000 s. CO, CO<sub>2</sub>, H<sub>2</sub>, and H<sub>2</sub>O were detected as products. The oscillations of the products and reactants are accompanied by the regular variation of the catalyst temperature with peak-to-peak amplitude of more than 15 degrees Celsius. The *operando* measurements have revealed the periodic change of the sample surface (~10µm depth) phase composition (Fig. 1). XRD reflections intensities corresponding to Pd and PdO were altering simultaneously with the partial pressures of products and reactants, as well as with the catalyst temperature. The satellite reflexes of Pd appear when the system is in a higher activity state. We refer these to the palladium-carbon solid solution. The carbon dissolution in the Pd lattice causes its expansion and shifts the metal reflections to lower angles [3] as it was observed in the experiment. The experiment has shown a higher activity of metallic Pd in the reaction than PdO oxide. Hence, the driving force of the oscillations is periodical oxidation and reduction of palladium. The obtained data will help to establish the mechanism of methane oxidation over palladium.

## PP-II-14

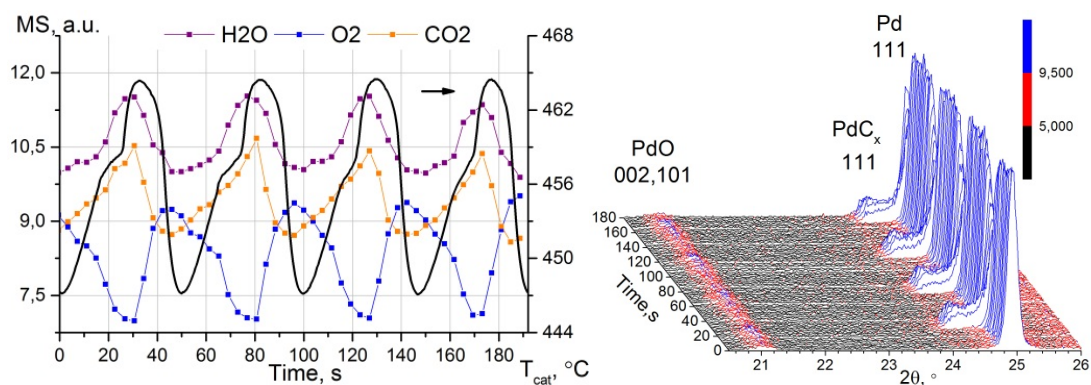


Fig. 1. MS/Temperature oscillations (left) and corresponding X-ray diffraction patterns (right) obtained for reactants molar ratios CH<sub>4</sub>:O<sub>2</sub>:He = 5:1:25. Total flow is 60 sccm.

**Acknowledgement.** This work was supported by RFBR, project No. 19-03-00419.

### References:

- [1] V.M. Aulchenko, O.V. Evdokov, V.D. Kutovenko, B.Ya. Pirogov, M.R. Sharafutdinov, V.M. Titov, B.P. Tolochko, A.V. Vasiljev, I.A. Zhogin, V.V. Zhulanov, Nucl. Instrum. Methods Phys. Res. A 76 (2009) 603.
- [2] A.A. Saraev, Z.S. Vinokurov, V.V. Kaichev, A.N. Shmakov, V.I. Bukhtiyarov, Catal. Sci. Technol. 7 (2017) 1646.
- [3] G.L. Selman, P.J. Ellison, A.S. Darling, Plat. Met. Rev. 14 (1970) 14.

## Specifics of Propane Dehydrogenation over Silica Supported Gallium Catalysts

Agafonov Yu.A.<sup>1</sup>, Gaidai N.A.<sup>1</sup>, Botavina M.A.<sup>2</sup>, Lapidus A.L.<sup>1</sup>

<sup>1</sup> – N.D.Zelinsky Institute of Organic Chemistry RAS, Moscow, Russia

<sup>2</sup> – University of Torino, Department of IPM Chemistry and NIS Centre, Torino, Italy  
 plassey@mail.ru

Gallium oxides catalysts exhibit high activity in dehydrogenation of light paraffins. Side processes, such as cracking and coke formation decrease of yield of olefins. Using of porous silicates as catalytic supports which are characterized by high specific surface and good resistance to coke formation can be effectively for paraffins dehydrogenation processes. This work devoted to the investigation of an influence of nature of silica support, carbon oxides (CO and CO<sub>2</sub>) and conditions of pre-treatment on efficiency of silica supported gallium catalysts. Early, it was shown for chromium oxide catalysts that CO<sub>2</sub> which can interact with hydrogen, forming at propane dehydrogenation, results in the shift of reaction equilibrium, and partly oxidizes coke and catalyst surface, what increases the catalyst stability at long-duration work [1-3]. An important role in paraffins dehydrogenation over gallium catalysts can play the oxidation state of the active surface, which depends on the pre-treatment conditions and the composition of the reaction mixture.

Catalysts were prepared by wet impregnation of silicagels KSKG (330-360m<sup>2</sup>/g) and Silica for chromatography (Acros -480-550m<sup>2</sup>/g) from water solutions of gallium nitrates and direct one-pot synthesis embedding Ga species in the siliceous mesoporous framework of MCM-41. Catalysts under investigation are contained 5-40 % wt. of Ga on silicagels and 1-3 %wt. Ga in MCM-41. Catalyst structure and adsorption properties were controlled by X-ray diffraction, N<sub>2</sub> adsorption, TPR-H<sub>2</sub> and TPD-NH<sub>3</sub>. The catalytic tests were carried out in a flow reactor at 600°C, volume space velocity 200 h<sup>-1</sup>, atmospheric pressure. The reaction products were analyzed by GC methods. Unstationary phenomena were investigated using the transient response method in the flow reactor of small volume connected with mass-spectrometer. Results of investigations on propane dehydrogenation in CO<sub>2</sub> (30% vol.) presence showed (Fig.1) that catalysts prepared by one-pot method demonstrated more high specific activity and stability in propene formation than the catalysts made by wet impregnation.

According to TPR-H<sub>2</sub> data, catalysts Ga-MCM were characterized by high dispersity. It was shown in [4] that high

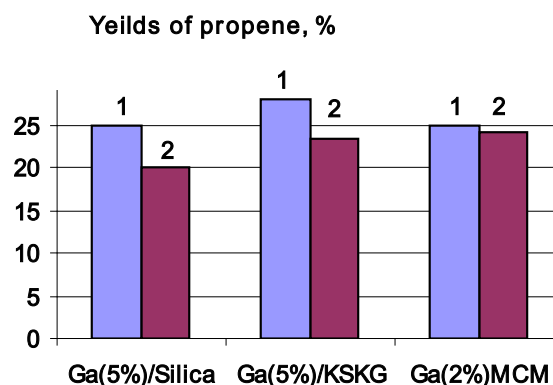


Figure 1. Results of propane dehydrogenation over gallium-catalysts in CO<sub>2</sub> (30% vol.) presence: **1** - after 30 min and **2** - 300 min of work.

metal dispersity (Ni) in silica framework is accompanied by an intense decrease of coke formation. We observed the analogical effect for Ga-MCM. One of reasons of it can be a decrease of possibility for interaction between adsorbed olefins and further growth of chain because of an increase of distance between centers of their adsorption. Dehydrogenation of

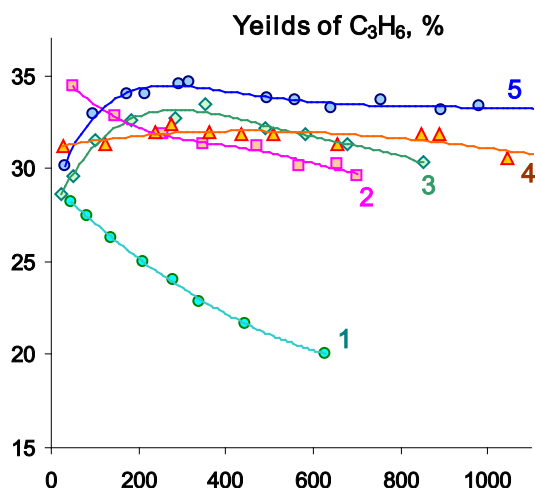


Figure 2. Results of propane dehydrogenation over Ga(10%)/KSKG at different conditions:

- 1 -pre-treat. in  $O_2$  (600°C), react.mix.- $C_3H_8$ : $CO_2$ (30%): $N_2$
- 2 -pre-treat. in  $O_2$  (600°C), react.mix.- $C_3H_8$ :  $N_2$
- 3 -pre-treat. in  $H_2$  (630°C), react.mix.- $C_3H_8$ :  $N_2$
- 4 -pre-treat. in  $O_2$  (600°C), react.mix.- $C_3H_8$ : $CO$ (20%):  $N_2$
- 5 -pre-treat. in  $H_2$  (700°C), react.mix.- $C_3H_8$ :  $N_2$

propane over gallium catalysts proceeds through heterolytic dissociation reaction pathway with the formation of Ga-hydrides [5]. In this case  $CO_2$  would have the negative influence on this process due to its oxidized properties and can inhibit the hydride formation. Really, this effect is detected in stationary (fig.2) and unstationary experiments. Propene yield and stability was minimal over oxidized catalyst in the  $CO_2$  presence (line 1). Other effect is observed in the case of CO introduction (line 4 at Fig.2), it is seen that stability of oxidized gallium catalysts rises. May be it is connected to a reducing of Ga-particles or/and with decrease of coke deposition. Really, the pre-treatment of Ga-catalysts by  $H_2$  at 630°C (line 3) and 700°C (line 5) considerably increase the stability and activity in propene formation.

The results of TPR- $H_2$  for Ga-MCM and Ga/KSKG demonstrated what the process of Ga reduction is started from 520°C, that is, Ga-oxide phase is partly reduced in the reaction conditions (600°C). In addition, the reducing of Ga-particles may be accompanied an increase in their dispersion has positive influence on the catalytic activity at paraffins dehydrogenation.

The comparison of responses  $(He+C_3H_6)/(He+CO_2)$  and  $(He+CO_2)/(He+C_3H_6)$  at 200°C per the time of replacing one component by another showed that  $CO_2$  is tied more firmly than  $C_3H_6$ . Also it was shown that the delay of  $C_3H_6$  appearance in gas phase (at 600°C) is increased in the following row of responses:  $[He/(C_3H_8+He)] < [He/(C_3H_8+CO_2)] < [(He+CO_2)/(C_3H_8+CO_2)]$ . Thus,  $CO_2$  precludes the interaction of propane with an active surface.

#### References:

- [1] K.Takehira, Y.Ohishi, T.Shishido,T.Kawabata,K.Takaki, Q.Zhang, Y.Wang. J. Catalysis. 224 (2004) 404.
- [2] Yu.A.Agafonov, N.A.Gaidai, A.L.Lapidus. Russian Chemical Bulletin. 63 (2014) 381.
- [3] Yu.A.Agafonov, N.A.Gaidai, A.L.Lapidus. Kinetics and catalysis. 59 (2018) 744.
- [4] Z.Liu, J.Zhou, K.Cao, W.Yang, H.Gao, Y.Wang, H.Li. Applied Catalysis B: Environmental. 125 (2012) 324.
- [5] S.E.Collins, M.A. Baltanás, J.L.Garcia Fierro, A.L.Bonivardi. J. Catalysis. 211 (2002) 252.

## PP-III-2

### HZSM-5 Supported Pt- and Pd-Catalysts Doped by Ni for Hydro-Isomerisation of n-Hexane

Luu Cam Loc<sup>1</sup>, Dao Thi Kim Thoa<sup>2</sup>, Nguyen Tri<sup>1</sup>, Ha Cam Anh<sup>2</sup>, Gaidai N.A.<sup>3</sup>, Agafonov Yu.A.<sup>3</sup>, Lapidus A.L.<sup>3</sup>

1 – Institute of Chemical Technology, Vietnam Acad. Sci. Techn., Ho Chi Minh City, Vietnam

2 – Ho Chi Minh City University of Technology, Ho Chi Minh City, Vietnam,

3 - N.D. Zelinsky Institute of Organic Chemistry, Russian Acad. Sci., Moscow, Russia  
plassej@mail.ru

The catalyst for isomerisation has been developed continuously: the very first generation was liquid Lewis acid followed by solid super acids (amorphous and crystalline silica-alumina), and then was bi-functional catalysts containing noble metals supported on various acidized carriers. Current industrial catalyst for hydro-isomerisation is bi-functional catalysts on the basis of Pt supported on halogenated alumina. Although being very active and can be operated at moderate temperature, this type of catalyst requires complicated operation, causes corrosion, and being very sensitive to feeding impurities like sulfur compounds and water [2].

Table. Results of activities and stability of Pt- and Pd-catalysts in n-hexane isomerisation.

Catal.	$\tau$ (h)		Temperature, °C			
			225	250	275	300
Pd HZSM	1	X, %		56,9	84,5	91,4
		S <sub>i-C6</sub> , %		<b>86,5</b>	62,7	24,4
		Y <sub>i-C6</sub> , %		49,3	<b>53,0</b>	22,3
Pt HZSM	3	X <sub>n-C6</sub> , %	35,9	59,2	70,4	84,6
		S <sub>i-C6</sub> , %	<b>95,4</b>	85,2	59,6	34,1
		Y <sub>i-C6</sub> , %	34,3	<b>50,5</b>	42,0	28,9
Pd-Ni HZSM	>30	X, %	43,0	60,3	75,4	77,2
		S <sub>i-C6</sub> , %	<b>96,7</b>	90,6	<b>76,6</b>	38,5
		Y <sub>i-C6</sub> , %	41,6	54,3	<b>57,7</b>	29,5
Pt-Ni HZSM	12	X, %	50,8	72,2	78,7	88,5
		S <sub>i-C6</sub> , %	<b>95,8</b>	89,5	67,3	38,4
		Y <sub>i-C6</sub> , %	48,7	<b>64,6</b>	53,0	34,0

The use of zeolites as an acidic support could eliminate such problems. In our previous studies [3], catalysts on the basis of Pt and Pd supported on HZSM-5

have been comparable activity but less stable. Yoshioka [4] also confirmed that, the addition of a second metal onto the noble metal catalysts to form bimetallic catalysts was proved to cause a significant increase in catalytic activity and selectivity toward branched isomers. For instance, the introduction of 0.4wt.% Ni

onto 0.2 wt.% Pt/SAPO-5 or Pt/SAPO-11 catalysts led to increase in the n-hexane conversion, isomerisation selectivity and stability of the catalyst in n-hexane isomerisation[2].

Mono and bimetallic catalysts were synthesized by impregnations: 0.8 wt% Pd/HZSM5, 0.8wt%Pd+1.0wt%Ni/HZSM5, 0.35wt% Pt/HZSM5, 0.35wt%Pd+1.0wt%Ni/HZSM5. After the

## PP-III-2

metal loading, samples were dried, air calcinated at 400°C for 2h and reduced at 400°C for 2h in the hydrogen flow. The catalysts were investigated by BET, XRD, TEM, NH<sub>3</sub>-TPD, TPR-H<sub>2</sub>. Catalytic activity in n-hexane isomerisation was tested in a micro-flow reactor under atmospheric pressure at 200-325°C. The response method was used to compare adsorption characteristics of catalysts at n-hexane isomerisation at partial pressure of n-hexane-0.066 atm., molar ratio of H<sub>2</sub>: n-hexane-14.2, the temperature-250°C (weight 1.0 g).

Ni exhibited the geometric and electronic effects toward Pd/HZSM-5 and Pt/HZSM-5. On these bimetallic systems, noble metal was stabilized in highly dispersed state and facilitated their reduction. Effect of promoter resulted in the improvement activity and stability for both systems (table). Hydrogen spill over phenomenon played an important role in the mechanism of coke removal.

Important results are obtained by the non-stationary method:

The comparison on the following responses: H<sub>2</sub>/(H<sub>2</sub>+n-C<sub>6</sub>H<sub>14</sub>), He/(H<sub>2</sub>+n-C<sub>6</sub>H<sub>14</sub>), H<sub>2</sub>/(He+n-C<sub>6</sub>H<sub>14</sub>), He/(He+n-C<sub>6</sub>H<sub>14</sub>) showed that adsorption capacities on n- and iso-C<sub>6</sub>H<sub>14</sub> for promoted-catalysts were higher than these for mono-metallic catalysts.

In the responses He/H<sub>2</sub>, it was found that the adsorption strength and amount of hydrogen in the case of the Ni-promoted catalysts is also significantly higher than for mono-metallic catalysts.

The increase in the amount of formed isohexanes in the response (He+n-C<sub>6</sub>H<sub>14</sub>)/(H<sub>2</sub>+n-C<sub>6</sub>H<sub>14</sub>) can mean that hydrogen takes participation in the isomerization reaction.

**Acknowledgement.** This work was supported by the Russian Science Foundation Investigations №15-53- 54026 Viet\_a and VAST.HTQT. Nga. 02/15-16.

### References:

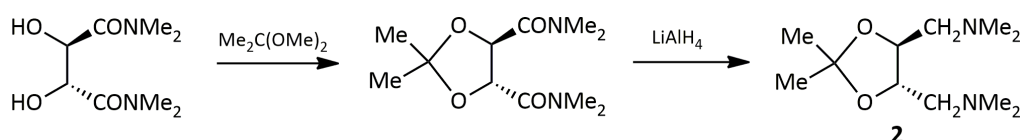
- [1] Kaufmann, T.G., et al., Catalysis science and technology for cleaner transportation fuels. Catalysis Today, 2000. 62(1): p. 77-90
- [2] Eswaramoorthi, I. and N. Lingappan, Hydroisomerisation of n-hexane over bimetallic bifunctional silicoaluminophosphate based molecular sieves. Applied Catalysis A: General, 2003. 245(1): p. 119-135.
- [3] Cam Loc Luu, T.K.T.D., Tri Nguyen, Thanh Huong Bui, Thi Ngoc Yen Dang, Minh Nam Hoang, Si Thoang Ho, Effect of carriers on physico-chemical properties and activity of Pd nano-catalyst in n-hexane isomerization. Advances in Natural Science, 2013. 4: p. 1-9.
- [4] Yoshioka, C.M.N., T. Garetto, and D. Cardoso, n-Hexane isomerization on Ni-Pt catalysts/supported on HUSY zeolite: The influence from a metal content. Catalysis Today, 2005. 107–108(0): p. 693-698.

## Hydrogenation of Dimethyl Itaconate over Rhodium Nanoparticles, Modified by Optically Active Quarternary Ammonium Salts

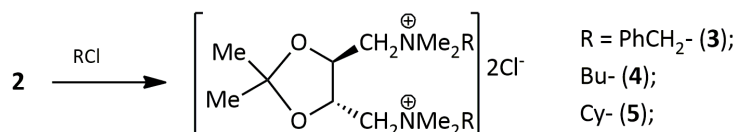
Badyrova N.M., Nindakova L.O.

Irkutsk National Research Technical University (IRNITU), Irkutsk, Russia  
n.m.badyrova@istu.edu

Colloidal solutions of Rh nanoparticles (Rh NPs), modified by three optically active quaternary ammonium salts, were tested in the hydrogenation of dimethyl ester of itaconic acid (DME IA). The cationic complex of rhodium bis-cyclooctadiene-rhodium(I) trifluoromethanesulfonate  $[\text{Rh}(\text{cod})_2]^+\text{TfO}^-$ , **1**, was used as the metal precursor. The diamine **2** is synthesized by cyclization of the diamide (R,R)(+)-tartaric acid and 2,2-dimethoxypropane followed by reduction dicarboxamide with  $\text{LiAlH}_4$  in a known manner [1]:



Synthesis of optically active quaternary ammonium salts was performed by interaction of the diamine **2** with two equivalents of the organic halides according to the scheme:



The table shows the results of the DME IA hydrogenation over the complexes  $\text{Rh}(\text{S,S-2})_2]^+\text{TfO}^-$  and **1** in the presence of quaternary ammonium salts **3**, **4** and **5**. The hydrogenation of 1,5-cyclooctadiene molecules and the reduction of Rh(I) to elemental rhodium proceed during induction time.

Table - Hydrogenation of DME IA over Rh nanoparticles ( $C_{\text{Rh}} = 1.5 \text{ mmol/L}$ ,  $\text{Sub/Rh} = 170$ ; solvent – methanol:toluene = 2:1,  $P_{\text{H}_2} = 1 \text{ atm}$ ).

NN	System	$w_{\text{max}}$ mmol/(L*h)	$(A)_{\text{max}}$ mol/(g-at Rh*h)	ee, % (config.)
1 <sup>a</sup>	$[\text{Rh}(\text{S,S-2})_2]^+\text{TfO}^-$	1050	684	2.1 (S)
2	$[\text{Rh}(\text{S,S-2})_2]^+\text{TfO}^-$	238	154	11.3 (S)
3	$[\text{Rh}(\text{S,S-2})_2]^+\text{TfO}^- + \mathbf{3}$	213	142	11.0 (S)
4	$[\text{Rh}(\text{cod})_2]^+\text{TfO}^- + \mathbf{3}$	300	200	15.2 (S)
5	$[\text{Rh}(\text{cod})_2]^+\text{TfO}^- + \mathbf{4}$	278	185	25.1 (S)
6	$[\text{Rh}(\text{cod})_2]^+\text{TfO}^- + \mathbf{5}$	320	215	30.2 (S)

Microheterogeneous nature of the catalyst is confirmed by the hydrogenation of toluene into methylcyclohexane after full reduction of the DME IA ( $\text{TOF} = 15\text{-}20 \text{ mol H}_2/(\text{g-at Rh}\cdot\text{h})$ ) and HR TEM images of Rh NP.

### References:

[1] D. Seebach, H.O.Kalinowski, B.Bastini, G.Crass, H.Daum, H.Doerr. Helv. Chim. Acta. 60 (1977) 301.

## The Mechanism of Ortho-Para Conversion of Protium on the Nanoparticles of Silver and Gold in the Field of Low Temperatures

Boeva O.A., Vorakso I.A., Kudinova E.S., Paniukova N.S., Nesterova N.I., Zhavoronkova K.N.

*D. Mendeleev University of Chemical Technology of Russia, Moscow, Russia*  
*olga\_boeva@mail.ru*

On the one hand, the ortho-para reaction conversion has fundamental interest, because it involves a transition with a revolution of nuclear spin and rotation. On the other hand, it is an important technological process in the liquefaction of hydrogen. Hydrogen is an efficient energy source which is used in fuel cells and rocket fuel. The storage of hydrogen in liquid form is a high-density storage method. When normal hydrogen is liquefied with a ratio of ortho-para modifications equal to 3 then about 40% of the initially liquefied hydrogen evaporates during 100 hours. It happens through to release of rotational energy at o-p conversion occurring in liquid hydrogen. There no transformation of gaseous state of ortho-para without catalyst. Therefore, the development of a highly efficient and stable catalyst for this process is an opportune and urgent objective.

This work discusses the magnetic mechanism of ortho-para conversion of protium occurring on metal nanoparticles of the IB group-silver and gold. It shows that in contrast to massive metals, silver and gold become highly active catalytic systems which can capable of adsorbing hydrogen and converting at liquid nitrogen temperatures (77 K) during the transition to the nanostructured state. The conversion rate does not depend on the particle size [1] and increases during the reaction in magnetic field. Moreover, the comparison of specific catalytic activities of nanoparticles in ortho-para reactions of protium conversion and deuterio-hydrogen exchange [2], which are differing by several tens of times, confirms the assumption of the magnetic mechanism of the conversion reaction. In that way, we can state not only high catalytic properties of silver and gold nanoparticles, but also their acquisition of new magnetic properties than other diamagnetic metals.

### References:

- [1] Boeva O.A., Odintsov A.A., Solovov R.D., Abkhalimov E.V., Zhavoronkova K.N., Ershov B.G. Low-temperature ortho-para hydrogen conversion catalyzed by gold nanoparticles: Particle size does not affect the rate // International Journal of Hydrogen Energy. - 2017. - Vol. 42. - P. 22897 – 22902.
- [2] Boeva O. A., Ershov B. G., Zhavoronkova K. N., Odintsov A. A., Solovov R. D., Abkhalimov E. V., Evdokimenko N. D. Catalytic properties of gold nanoparticles in H<sub>2</sub>-D<sub>2</sub> exchange and ortho-para hydrogen conversion // Doklady Physical Chemistry. – 2015. – V. 463. – Part 2. – P. 165-167.

## Investigation the Transformations Regularities of Stable Gas Condensate Hydrocarbons during Their Processing on Zeolite Catalysts

Bogdanov I.A., Altynov A.A., Kirgina M.V.  
Tomsk Polytechnic University, Tomsk, Russia  
*bogdanov\_ilya@mail.ru*

Nowadays such a valuable hydrocarbon feedstock, as stable gas condensate (which mainly consists of hydrocarbons which have more than 5 carbon atoms), that is a by-product of oil and natural gas production, is used not rationally at most fields. Stable gas condensate is pumped into the reservoir for maintain pressure, returned to oil for improve flow properties, or flared. At the same time, in the oil refining field is increased number of process which uses zeolite catalysts. This fact is due to the high activity and selectivity of these type of catalysts, their low cost and high resistance of zeolites to deactivation and to effects of catalytic poisons [1-4]. Therefore the aim of this work is investigation the transformations regularities of gas condensates hydrocarbons during their processing on zeolite catalysts. Using a zeolite catalyst and a stable gas condensate as a feedstock, a series of experiments were carried out on a laboratory catalytic unit. During the study, the technological conditions of the process such as temperature, pressure and feedstock space velocity were changing (table 1).

Table 1. Technological conditions of the process

Test number	Temperatures, °C	Pressure, MPa	Feedstock space velocity, ml/min
1	375	2.5	0.33
2	400	2.5	0.33
3	425	2.5	0.33
4	400	3.5	0.33
5	400	4.5	0.33
6	400	2.5	0.5
7	400	2.5	0.67

To determine the group hydrocarbon composition of feedstock gas condensate and derived products, chromatographic analysis was carried out [5]. The results of determining the group hydrocarbon composition of feedstock gas condensate and derived products are presented in table 2.

As it can be seen from the results presented in table 2, the common for most derived products is the maximum content of iso-paraffin hydrocarbons and the minimum content of olefin hydrocarbons. With increasing temperature of process the content of aromatic hydrocarbons increases. This is due to increase in the rate of target aromatization reaction.

### PP-III-5

Table 2. Group hydrocarbon composition of feedstock gas condensate and derived products

Test number	Hydrocarbon group content, % vol.				
	n-paraffins	iso-paraffins	naphthenes	olefins	aromatic hydrocarbons
1	33.25	43.94	7.74	4.81	10.26
2	24.36	37.86	9.37	4.31	24.07
3	25.86	38.98	6.29	3.62	25.25
4	38.58	29.05	5.49	6.73	20.14
5	32.3	41.38	3.32	3.04	19.98
6	31.27	46.35	1.72	4.44	16.28
7	30.59	45.27	5.17	6.33	12.7
Feedstock	40.64	38.25	19.35	1.14	0.62

As the process pressure is changed the predominant group of hydrocarbons in the derived products changes. So for the product obtained during the test at a pressure of 3.5 MPa paraffin hydrocarbons predominate, while for products obtained during the tests at pressures of 2.5 MPa and 4.5 MPa, the iso-paraffin hydrocarbons predominate. Also as the pressure increases, aromatic hydrocarbons content decreases. This is fact due to decrease in the selectivity of paraffins conversion to aromatic hydrocarbons as far as high pressure is advantageous for cracking reactions.

At the same time, products obtained at feedstock space velocity of 0.33 ml/min and 0.67 ml/min are characterized by a minimum content of olefinic hydrocarbons, and a product obtained at a feedstock space velocity of 0.5 ml/min by a minimum content of naphthenic hydrocarbons. As the feedstock space velocity increases, the content of aromatic hydrocarbons decreases. This is due to decrease in the residence time and as a result, decrease in the depth of aromatization.

#### References:

- [1] Primo A, Garcia H. Zeolites as catalysts in oil refining // *Chemical Society Reviews* – 2014. – Vol. 43 (22). – P. 7548-7561.
- [2] Srivastava R. Synthesis and applications of ordered and disordered mesoporous zeolites: Present and future prospective // *Catalysis Today* – 2018. – Vol. 309. – P. 172-188.
- [3] Feliczak-Guzik A. Hierarchical zeolites: Synthesis and catalytic properties // *Microporous Mesoporous Mater* – 2018. – Vol. 259. – P. 33–45.
- [4] Maria V. Kirgina, Ilya A. Bogdanov, Andrey A. Altynov, Nikolay S. Krinitsyn Feasibility studies of jet fuels using as a low-temperature additive to straight-run diesel fuels // *Petroleum and Coal*. – 2019 – Vol. 61(1). – P. 120-127.
- [5] EN ISO 22854:2008 "Liquid petroleum products – Determination of hydrocarbon types and oxygenates in automotive-motor gasoline – Multidimensional gas chromatography method" [Electronic source]. – URL: <https://www.iso.org>, free access. – Accessed date: 05.02.2019.

## Butadiene-1,3 Hydrogenation on Palladium Nanoparticles Supported on Modified Alumina

Boretskaya A.V., Il'yasov I.R., Lamberov A.A.  
Kazan Federal University, Kazan, Russia  
*ger-avg91@mail.ru*

Alumina supported palladium catalysts were synthesized and investigated. The pseudoboehmite ("Pural SB", Sasol) was modified with the acidic (acetic acid and ammonium fluoride) and basic (sodium hydroxide and cesium nitrate) additives and was calcined at 550 °C for obtained of  $\gamma$ -Al<sub>2</sub>O<sub>3</sub> support. According to the results of the thermoprogrammed desorption of ammonia (TPD NH<sub>3</sub>), modification with acidic additives leads to a decrease in the share of weak acid sites and an increase in the share of very strong centers compared with the unmodified sample (table 1). The samples of aluminum oxides containing sodium and cesium have a low acidity as a result the suppression of strong acid sites.

Table 1 – The number of acid sites (N) of the aluminum oxides

Sample	$\Sigma N, \mu\text{mol/g}$	Weak $T_d < 250$	Medium $250 \leq T_d < 350$	Strong $350 \leq T_d < 450$	Very strong $T_d \geq 450$
Al <sub>2</sub> O <sub>3</sub>	819	369	246	147	57
Al <sub>2</sub> O <sub>3</sub> (Ac)	1044	438	313	198	95
Al <sub>2</sub> O <sub>3</sub> (F)	853	350	256	188	59
Al <sub>2</sub> O <sub>3</sub> (Na)	552	254	193	105	-
Al <sub>2</sub> O <sub>3</sub> (Cs)	356	153	132	71	-

$T_d$  – the temperature of ammonia desorption, °C

The deposition of the active component was carried out from palladium acetylacetonate in benzene. Before analysis and catalytic tests the palladium systems were subjected to preliminary treatment: oxidation at 400 °C (2 hours), holding for 10 minutes in He and subsequent reduction for 2 hours at the same temperature.

Table 2 –Size ( $d_{Pd}$ ), fraction of the reduction (Pd<sup>0</sup>) and oxidized (PdO) palladium particles

Sample	$d_{Pd}, \text{nm}$	$v(\text{Pd}^0), \%$	$v(\text{PdO}), \%$
Pd/Al <sub>2</sub> O <sub>3</sub>	5-20	72	28
Pd/Al <sub>2</sub> O <sub>3</sub> (Ac)	~ 1	75	25
Pd/Al <sub>2</sub> O <sub>3</sub> (F)	~ 1	70	30
Pd/Al <sub>2</sub> O <sub>3</sub> (Na)	5-30	91	9
Pd/Al <sub>2</sub> O <sub>3</sub> (Cs)	3-20	100	0

The structural and electronic characteristics of the supported palladium particles were studied by transmission electron microscopy (TEM) and X-ray photoelectron spectroscopy

### PP-III-6

(XPS), respectively. Although palladium particles on the supports modified with acidic additives are characterized by the smallest size, its electronic states differ slightly in comparison with the catalyst on an unmodified support (table 2). Introduce of the alkaline additives leads to an increase in the concentration of reduced palladium. For catalyst based on cesium containing support, palladium particles in oxidized state are not observed.

Tests of the palladium catalysts were carried out in the hydrogenation of butadiene-1,3 (BD) in a flow-through reactor at atmosphere pressure. The Pd/Al<sub>2</sub>O<sub>3</sub>(Na) and Pd/Al<sub>2</sub>O<sub>3</sub>(Cs) are demonstrated higher values of BD conversion already at low temperatures. The values of selectivity to butene-1 (BE) for these samples are similar with unmodified catalyst Pd/Al<sub>2</sub>O<sub>3</sub>. The Pd/Al<sub>2</sub>O<sub>3</sub>(Ac) and Pd/Al<sub>2</sub>O<sub>3</sub>(F) catalysts are demonstrated lower conversion of BD than other samples at reaction temperatures from 15 °C to 60 °C (fig. 1). However, Pd/Al<sub>2</sub>O<sub>3</sub>(Ac) is reached the total conversion of BD early than Pd/Al<sub>2</sub>O<sub>3</sub>, Pd/Al<sub>2</sub>O<sub>3</sub>(F) and Pd/Al<sub>2</sub>O<sub>3</sub>(Na). The Pd/Al<sub>2</sub>O<sub>3</sub>(Ac) and Pd/Al<sub>2</sub>O<sub>3</sub>(F) samples are provided higher values of selectivity to BE throughout the catalytic test range.

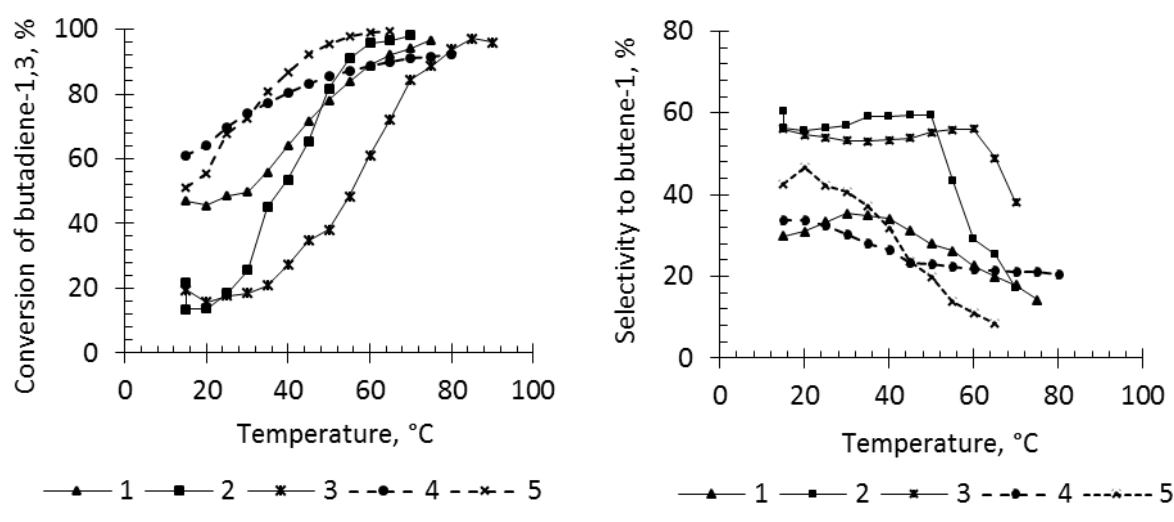


Figure 1 – Kinetics curves of catalytic tests of the palladium systems: 1- Pd/Al<sub>2</sub>O<sub>3</sub>; 2 - Pd/Al<sub>2</sub>O<sub>3</sub>(Ac); 3 - Pd/Al<sub>2</sub>O<sub>3</sub>(F); 4 - Pd/Al<sub>2</sub>O<sub>3</sub>(Na); 5 - Pd/Al<sub>2</sub>O<sub>3</sub>(Cs)

The modification of alumina supports with basic additives contributes to increase of concentration reduced palladium and high values of BD conversion. The acidic modifiers leads to stabilization of the small palladium particles (~ 1 nm) with electronic states are similar with ones of unmodified catalyst. Possibly, it promotes to a single-center adsorption of BD and higher selectivity to BE.

**Acknowledgement.** The work performed at the expense of subsidies allocated within the state support of the Kazan (Volga Region) Federal University in order to increase its competitiveness among the world's leading scientific and educational centers.

## Benzylic C-H Hydroxylations in the Presence of Bioinspired Mn Complexes: the Origin of Acetate Products

Ottenbacher R.V.<sup>1,2</sup>, Sun W.<sup>3</sup>, Sun, Q.<sup>3</sup>, Bryliakov K. P.<sup>1,2</sup>

1 – Borekov Institute of Catalysis, Novosibirsk, Russia

2 – Novosibirsk State University, Novosibirsk, Russia

3 -State Key Laboratory for Oxo Synthesis and Selective Oxidation, Lanzhou Institute of Chemical Physics, Chinese Academy of Sciences, Lanzhou, China

bryliako@catalysis.ru

The oxidation of benzylic C-H groups by “green” oxidant hydrogen peroxide, mediated by *bis*-amine-*bis*-pyridine manganese complexes, occurring in the presence of carboxylic acid additives (typically acetic acid), has been reported to afford acetate as byproduct (Figure 1) [1, 2].

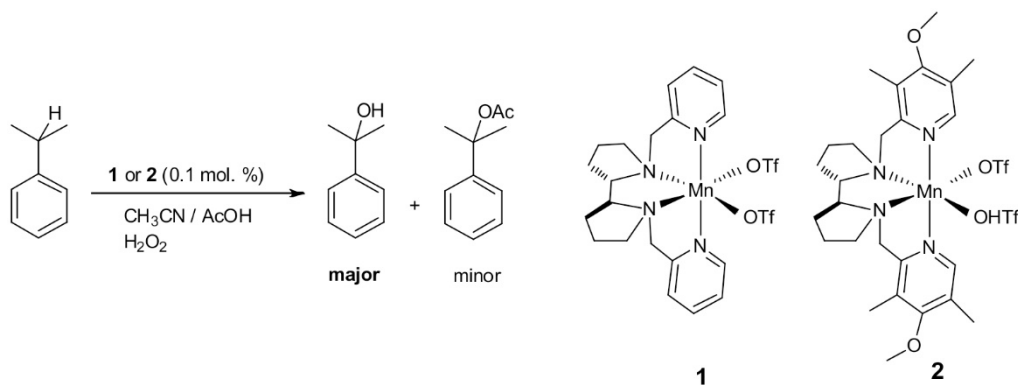


**Figure 1.** The oxidation of cumene in the presence of bioinspired manganese complexes.

Herewith, the details of molecular mechanism of manganese catalyzed benzylic C-H oxidation are examined, using the formation of acetate as a mechanistic probe. The correlation between the alcohol/acetate ratio (alcohol selectivity) and the presence of electron-donating groups at the aminopyridine ligand core has been revealed. Isotopic labeling studies witness that the oxygen atom in the cumyl alcohol originates from the  $\text{H}_2\text{O}_2$  molecule, while the oxygen of the acetate comes from the acetic acid. These data rule out acid-catalyzed Fischer esterification of the initially formed cumyl alcohol, and provide evidence for a different mechanism of cumyl acetate formation. Possible mechanistic alternatives are discussed.

**Acknowledgement.** KPB and RVO thank RFBR (# 16-29-10666).

### References:

- [1] Shen, D., Miao, C., Wang, S., Xia, C., Sun, W. *Org. Lett.* 16 (2014) 1108-1111.  
 [2] Ottenbacher, R. V.; Talsi, E. P.; Bryliakov, K. P. *ACS Catalysis* 5 (2015) 39-44.

## On the Role of Nanoscale Particles Formed on the Basis of Nickel (II) Complexes and Aluminum Alkyl Halides in Catalysis of Propene Oligomerization

Bykov M.V., Suslov D.S., Pakhomova M.V., Tkach V.S., Schmidt A.F.  
Irkutsk State University, Irkutsk, Russia  
bykov@chem.isu.ru

Unsaturated short chained hydrocarbons are low priced educts for polymerization, oligomerization and metathesis application, produced by thermal cracking processes. Especially the dimerization of propylene plays an important role for the formation of gasoline with a high octane number. As a result branched hexenes can be obtained and used as gasoline blending compounds [1–4]. Catalyst systems on the base of Ni(acac)<sub>2</sub> with mono-/bidentate phosphines (PR<sub>3</sub> or P<sup>^</sup>P = PPh<sub>3</sub>, P(i-Pr)<sub>3</sub>, PCy<sub>3</sub>, P(o-An)<sub>3</sub>, dppm, dppe, dppp, dpph, dppbac) or phosphine-free activated with aluminum alkyl halides, modified with proton donor compounds in octane and/or dichloroethane generate active catalysts *in situ* that dimerize propylene, giving product mixtures of *n*-hexenes and methylpentenes. These catalysts are highly active and stable, with propene turnover number as high as (2–5)·10<sup>4</sup> mol of C<sub>3</sub>H<sub>6</sub>/((mol of Ni)h) observed. TON and TOF are dependent on the reaction temperature, nature of the phosphine ligand, proton donor compound, and aluminum cocatalyst. Reaction conditions and phosphine nature can be adjusted that lead to selectivity to 2,3-Dimethylbutene-2 comprising more than 40% of the total product distribution.

Differential selectivity of the propene dimerization under noncompeting conditions with a varying set of reaction parameters was determined using Schmidt's [5] phase trajectories approach. The results allow for conclusions to be drawn regarding the character of active species to be nanosized nickel particles using the ligand-free catalytic system. Formation of nano-Ni particles were also confirmed by TEM results of reactions mixtures.

**Acknowledgement.** This work was supported by the joint grant of Russian Foundation for Basic Research (RFBR) and the Government of Irkutsk region according to project number 17-43-380010.

### References:

- [1] J.R.V. Lang, C.E. Denner, H.G. Alt, J. Mol. Catal. A Chem. 322 (2010) 45.
- [2] P.-A.R. Breuil, L. Magna, H. Olivier-Bourbigou, Catal. Letters. 145 (2015) 173.
- [3] F.K. Schmidt, Y.Y. Titova, L.B. Belykh, M. Gomboogiin, J.J. Titova, L.B. Belykh, M. Gomboogiin, Pet. Chem. 50 (2010) 205.
- [4] Y.Y. Titova, L.B. Belykh, A. V. Rokhin, O.G. Soroka, F.K. Schmidt, Kinet. Catal. 55 (2014) 35.
- [5] A.F. Schmidt, A.A. Kurokhtina, E. V. Larina, Catal. Sci. Technol. 4 (2014) 3439.

## Study of the Properties of Bimetallic Polymer Catalysts

Bykova L.N., Vitkovskaya R.F., Rumynskaya I.G., Novoselov N.P.  
*St. Petersburg State University of Industrial Technology and Design, Russia*  
*bykova.liubov@gmail.com*

Due to the use of large amount of water in technological processes of many enterprises, in particular, textile and light industry, a significant amount of industrial waste-water is generated, with which over 95 % of various impurities and solid wastes are transported (synthetic dyes, surfactants, organic and mineral acids, chlorides, sulphates, heavy metal ions, etc.). In this regard, there is a need for effective treatment of waste-water generated after the dyeing process. The most advanced technology for the purification, neutralization and utilization of waste-water is the catalytic method. Along with catalysts used in industry, it is necessary to develop new types, in particular, polymer nano-composites with catalytic properties, as well as the improvement of their "active" properties by introducing promoters.

In this paper were studied metal - containing fibre catalysts developed on the basis of modified PAN fibres [1]. As a catalytic active centres, immobilized complexes  $\text{Co}^{3+}$  and pairs  $\text{Co}^{3+} + \text{Fe}^{3+}$  ions, fixed on a polymer base, were studied. For this, the modified PAN fibres were treated with aqueous solutions of  $[\text{Co}(\text{NH}_3)_6]\text{Cl}_3$  и  $\text{FeCl}_3 \cdot 6\text{H}_2\text{O}$  salts for 1, 10, 30 and 60 minutes. The catalytic activity of the samples was determined by the method of quasi-static oxidation of the anthraquinone dye acid blue 45 [2]. The destruction of the dye was carried out in the presence of oxygen, as well as a combination of oxygen with hydrogen peroxide. The registration of the decomposition of the dye was carried out optically on a Specord M-40 spectrophotometer. The coordination mechanisms and the distribution of metals on a polymeric carrier were studied using IR spectroscopy on FMS 1201 and on a JEOL JSM-6390 scanning electron microscope.

From the histograms presented in fig. 1, it can be seen that the sample, treated for 10 minutes with  $\text{Co}^{3+}$  salt and working under oxidation conditions only with oxygen, has the highest oxidising ability. The oxidizing ability of the catalyst is significantly reduced when hydrogen peroxide is used as an additive to oxygen, which, according to IR spectroscopy, is due to the destruction of part of the  $\text{Co}^{3+}$  complexes on the surface of the fibrous support by peroxide. It should be noted that the catalytic activity of the material containing both  $\text{Co}^{3+}$  and  $\text{Fe}^{3+}$  ions also markedly decreases. As was shown in [2], the activity of metal - containing polymer catalysts is due to the addition of metals to heterocyclic N - oxides.

### PP-III-9

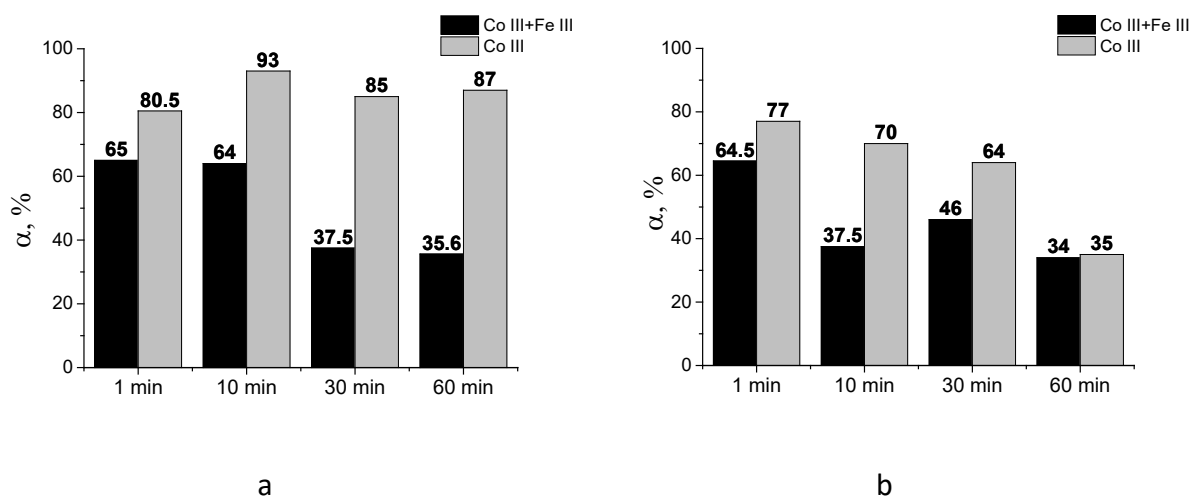


**Figure 1.** The dependence of the degree of oxidation of the anthraquinone dye on the fibrous material with aqueous solutions of salts of the metals  $\text{Co}^{3+}$  and  $\text{Fe}^{3+}$  from 1 to 60 minutes; a - air oxygen; b - air oxygen and hydrogen peroxide.

Previous studies have shown that a catalyst containing  $\text{Co}^{3+}$  is much more efficient than iron-containing. In this case, the accumulation of active centres with  $\text{Co}^{3+}$  occurs more slowly than with  $\text{Fe}^{3+}$ . The presence in solution of two dissimilar ions leads to the competition of metals for the place near the oxygen of N-oxides. The decisive role on the process of diffusion of trivalent ions to the functional groups of the ligands is played by their size, therefore the number of iron-containing complexes on the fibre is much larger. This explains the decrease in the oxidizing ability of the catalyst containing metals. Thus, in this case, the introduction of the second metal as a promoter into the active part did not lead to an increase in the oxidative capacity of the catalyst.

#### References:

- [1] Vitkovskaya R.F., Rumynskaya I.G., Smirnov A. Yu. Chem. Fibers. 2008. №3. - 26-28 pp.
- [2] Smirnov A. Yu., Vitkovskaya R.F. // Bulletin SPSUTD, October, 2010. №3, 12 - 14 pp.

## Pyrrole Ring Formation Mechanisms in Carbohydrate – Aryl Amine Condensations

Cherepanov I.S.  
Udmurt State University, Izhevsk, Russia  
cherchem@mail.ru

Non-enzymatic browning (Maillard reaction) products in carbohydrate – amine systems play important practical role as synthetic antioxidants and pharmaceutical medicines, which activity is defined by the nature of melanoidin's structural fragments [1,2]. Such structures are the substituted pyrroles [2], showing essential antioxidant activity [1], at the same time formation mechanisms the pyrrole heterocycles in melanoidin formation in literature are considered only for limited number of systems, generally for reactions of monosaccharide with amino acid [2]. In present paper on the base of experimental data obtained (elemental analysis, UV-Vis, IR-Fourier transform and mass spectroscopy), mechanisms of pyrroles formation in the carbohydrate – *p*-toluidine systems, which melanoidins are characterized by reducing properties [3], are detailed.

Synthesis of melanoidins was carried out according to techniques [3] described earlier, IR-Fourier transform spectra of final non-dialyzable products were registered with various spectral resolution in several areas, that allowed to carry out in details the signals assignment to structural elements. Mass spectra of melanoidins are characterized by a large number of various intensity signals, depending on temperature condition of pyrolysis, from which the peaks assigning to fragmentation of N-arylpyrroles are allocated. The analysis of experimental data shows the high extent of heterocyclic ring substitution, assuming pyrrole formation by the condensation reactions. Two main pathways of the substituted heterocycles formation are considered; the first of them is the classical mechanism of Knorr acid catalysed condensation: corresponding aminoketone forms from the Amadori compound and 3-deoxyosone. Alternative scheme including aldol type condensation of the same substrate to form intermediate, which cyclized to  $\beta,\beta'$ -disubstituted N-aryl-4,5-dihydropyrrol-2-carbaldehyde. The last mechanism may be considered as modified Knorr reaction [4], but the electron donating groups in substituted anilines accelerate the heterocyclisation, and this pathway is supposed more correct. Further reactions undergo as acid catalysed intermolecular electrophilic substitution in  $\alpha'$ -position of pyrrole ring, forming together with other aliphatic [2] and aromatic [3] fragments the high molecular melanoidin structure.

### References:

- [1] F. Hidalgo, F. Nogales, R. Zamora. *J. Agric. Food Chem.* 51 (2003) 5703.
- [2] J. Gerrard. *Aust. J. Chem.* 55 (2002) 299.
- [3] I. Cherepanov, G. Abdullina, V. Kornev. *Butlerov Communication.* 46 (2016) 51.
- [4] Y. Zhang, Y. Jiang, X. Liang. *Chin. J. Chem.* 15 (1997) 371.

## The Dehydration Mechanism of Methyl Lactate over Phosphates

Chernyshev D.O., Dubrovsky V.S., Varlamova E.V., Suchkov Y.P., Kozlovskiy R.A.  
*D. Mendeleev University of Chemical Technology of Russia, Moscow, Russia*  
 varlamova@yandex.ru

### Introduction

Acrylic acid (AA) is an important monomer for the production of polymers, the request on polymers based on AA increases annually. In connection with unstable prices for fossil hydrocarbons, the biggest companies form requests for alternative AA technologies in order to be able to diversify production facilities. One of such technologies is the production of lactic acid and its esters by fermentation of plant materials and its subsequent catalytic dehydration in AA or its esters.

The key role in questions for create effective catalytic system based on understanding of reaction mechanism. Despite the fact that dehydration reaction is well studied, the “classic” catalysts [1], for example  $Al_2O_3$ , do not show high efficiency in ML dehydration reaction to AA. In fact, more optimistic results was achieve with catalytic systems based on sulfate, phosphate and zeolites. For catalytic systems based on zeolite salts there is a nuance, after introduction into structure alkali, alkaline earth or lanthanide metal cations [2] they an activity increase. So preliminary we can proposal that effective catalytic system must contain some balance between acid/base properties.

### Experimental part

Investigation of the catalyst systems were carried out in a vertical cylindrical reactor with a fixed catalyst bed  $10\text{ cm}^3$  in a nitrogen stream, at temperatures ranging  $360\text{--}410^\circ\text{C}$  and a contact time of 1.0 second, ML water solution was feed to the reactor in a weight ratio 20/80. The products composition was determined using GC. Activity of catalysts were evaluated for ML conversion ( $X_{ML}$ , wt. %) and the selectivity to AA ( $S_{AA}$ , wt. %).

### Results

In our previous article [3] was highlight a good activity of phosphate salts in combination with stability in dehydration reaction of ML. For first raw estimation of different phosphate structure influence on activity and selectivity was chose the following salts type: metha-, pyro-, ortho- and hydroxyapatite. These type of phosphates has a different structure and Ca/O mole ratio and it is provide different acid/base properties. The table #1 are contained information about catalytic activity of different types phosphate salts.

**Table #1, catalyst activity and Ca/O mile ratio**

Sample	CaMP	CaPP	CaOP	CaHAP
Ca/O	0.42	0.62	0.94	0.96
$X_{ML}$	31.6	38.0	53.6	77.6
$S_{AA}$	4.5	15.0	18.5	34.4

## PP-III-11

Based on information from the table #1, we can observe a good correlation of ML conversion and AA selectivity in comparison with Ca/O mole ratio. The ratio of deactivation/time on stream also decrease in with increase ratio Ca/O. These results allow to assume that the ML dehydration reaction proceed over phosphate salts according to concerted mechanism. Below on the simple scheme (fig. #1), present the theoretically possible mechanism of the ML dehydration.

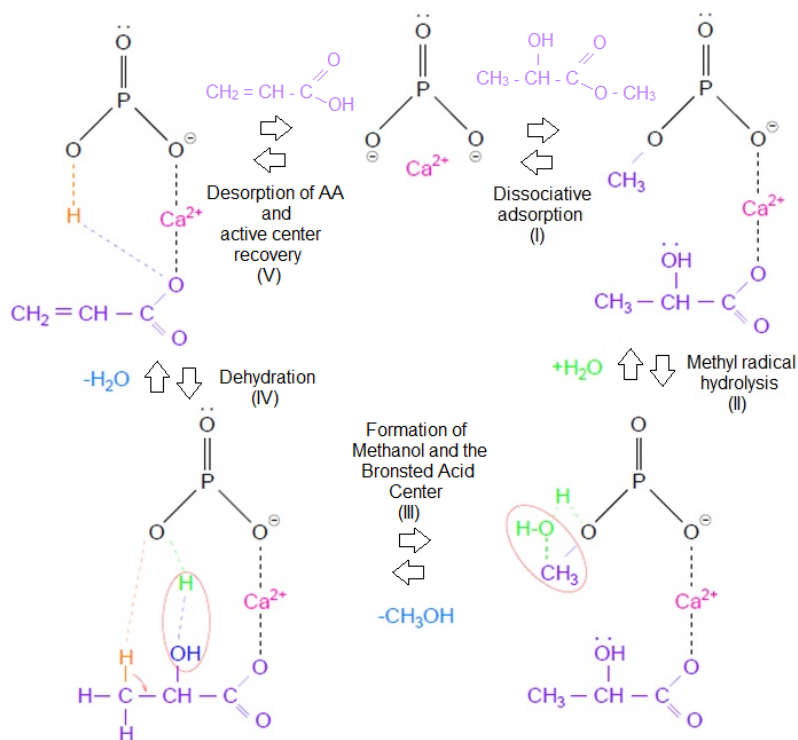


**Figure 1, ML dehydration mechanism**

## Results

The first raw comparison of activity different type phosphates with Ca/O mole ratio are implied that ML dehydration proceed according to concerted mechanism. More detail research is needed in future with phosphates salts as catalyts.

## References:

- [1] Changyuan W., Guiying L., Changhai D., Influence of Adding  $\text{KH}_2\text{PO}_4$  on  $\text{WO}_3\text{-}\gamma\text{Al}_2\text{O}_3$  solid acid catalyst for the synthesis of AA from LA, Adv. Mat. Res. Vols 912-914 (2014) pp 178-181.
- [2] E.A.Gorbatenko, E.I.Provalova, E.V. Varlamova, R.A. Kozlovski, V.F. Shvets, Production of MA based on LA from renewable materials, Success in chemistry and chemical technology, 2008, vol. XXII, p. 24-29.
- [3] Chernyshev D.O., Suslov A.V., Varlamova E.V, Suchkov Y.P., Staroverov D.V., Study of the structure of silicon-phosphate-calcium catalyst in dehydration of ML to AA, Success in chemistry and chemical technology, 2014, vol. XXVII, p. 29.

## Catalytic Coking of High Molecular Hydrocarbons

Chichkan A.S., Chesnokov V.V.

*Boreskov Institute of Catalysis, Novosibirsk, Russia*

*AlexCsh@yandex.ru*

Delayed coking is the most common coking process. Delayed coking units produce sponge and needle coke. Needle coke is produced from highly aromatic feedstocks [1]. In the production of electrodes, it is preferred to use needle coke, since its specific electrical resistance and thermal expansion coefficient are less than those of sponge coke.

The first aim of this study was to investigate the effect of the active component (iron, cobalt, nickel) deposited on the Sibunite support on the morphology of the carbon nanomaterials formed during the pyrolysis of hexane, undecane, and hexadecane. And then we investigated the mechanism of coking of anthracene, a fused-ring aromatic hydrocarbon, and the effect of carbon nanotubes (CNTs) on the morphology and crystal structure of the resulting coke.

The samples of CoO/Sibunite, and Fe<sub>2</sub>O<sub>3</sub>/Sibunite catalysts were prepared by impregnation. Carbon formation on the prepared samples in the pyrolysis of high-molecular paraffin hydrocarbons—hexane, undecane, and hexadecane—at 500, 600, and 700°C was studied. It was found that:

1. Carbon is deposited on the 10%CoO/Sibunite catalyst in the form of three morphological forms: (1) multiwalled carbon nanotubes (MCNTs), (2) MCNTs with numerous linkers in the channel, and (3) carbon nanofibers with stacked graphite layers in the fibers.

2. Carbon is deposited on the 10%Fe<sub>2</sub>O<sub>3</sub>/Sibunite catalyst in the form of carbon nanotubes or carbon nanofibers, whose diameter exceeds that of nanotubes.

The anthracene coking process was investigated in the temperature range of 400–600°C [2]. It was shown that at a temperature of 450°C, intermolecular interaction of two anthracene molecules begins involving the elimination of hydrogen and the formation of a C–C bond between the middle rings. Increasing the coking temperature to 500–600°C leads to the formation of poorly crystallized graphite. In the case of pure anthracene, spherical carbon particles of about a micron in size are produced. The addition of carbon nanotubes leads to the formation of the carbon “coat” covering the surface of CNTs. Carbon nanotubes act as nuclei of the new phase.

**Acknowledgement.** This work was supported by the Russian Science Foundation, grant 17-73-30032.

### References:

- [1] J. H. Gary, G. E. Handwerk, and M. J. Kaiser, *Petroleum Refining: Technology and Economics* (CRC, Boca Raton, 2007), 5th Ed.
- [2] V. V. Chesnokov, A. S. Chichkan, and E. A. Paukshtis, *Petroleum Chemistry*, 59 (2019) 186.

## Palladium-Catalyzed Allylation and Hydroallylation of Norbornadiene: Key Intermediates and Mechanism

Durakov S.A., Flid V.R., Shamsiev R.S.

MIREA - Russian Technological University, Institute of Fine Chemical Technologies named after M.V. Lomonosov, Moscow, Russia  
s.a.durakov@mail.ru

The catalytic allylation reaction of norbornadiene (NBD) is not similar to the well-known allylic substitution reactions [1]. The peculiarity of this reaction is the controlled variation in the nature of the addition of an allyl fragment to the NBD, which can undergo significant changes, up to the breaking of the C-C bond. This reaction opens up exceptional opportunities for single-stage synthesis of a wide range of strained polycyclic hydrocarbons containing methylene, vinyl and methylenecyclobutane fragments.

The allylation of NBD with allyl formate (AF) in the presence of Pd - catalysts differs from reactions with other allyl ethers in the nature of the hydrogen transfer, allowing also to synthesize structures containing allyl fragments [2].

The principal difference between the two described directions is that in the first case the allyl group, joining to the NBD, loses the hydrogen atom (oxidative allylation), and in the second case it attaches the hydrogen atom from the formyl moiety (reductive allylation). Such a diversity of interaction directions is not observed in the case of nickel catalytic systems.

On the basis of a complex of physicochemical, kinetic, electrochemical, and isotopic methods, the schemes of the mechanisms of allylation reactions and hydroallylation of NBD in the presence of palladium complexes are substantially supplemented and specified. The directions and the variability of the stages of  $\beta$ -hydride transfer in the interaction of NBD and AF are experimentally established [3,4]. Isotopic and kinetic methods have confirmed the key role of these stages in the catalytic cycle, and methods for regulating their directions have been proposed [5]. It is shown that the direction of the hydride transfer during the formation of all products is of a general nature and is associated with the breaking of the C – H bond located in the  $\beta$ -position relative to the metal atom, and this stage can occur with the participation of an allylic, norbornenyl or formyl hydrogen atom.

The possibility of regulating the directions of palladium-catalyzed allylation for a wide range of NBN and NBD derivatives using AF as an allylation agent has been demonstrated.

**Acknowledgement.** This work was supported by the Russian Science Foundation (RSF), grant № 18-13-00415.

### References:

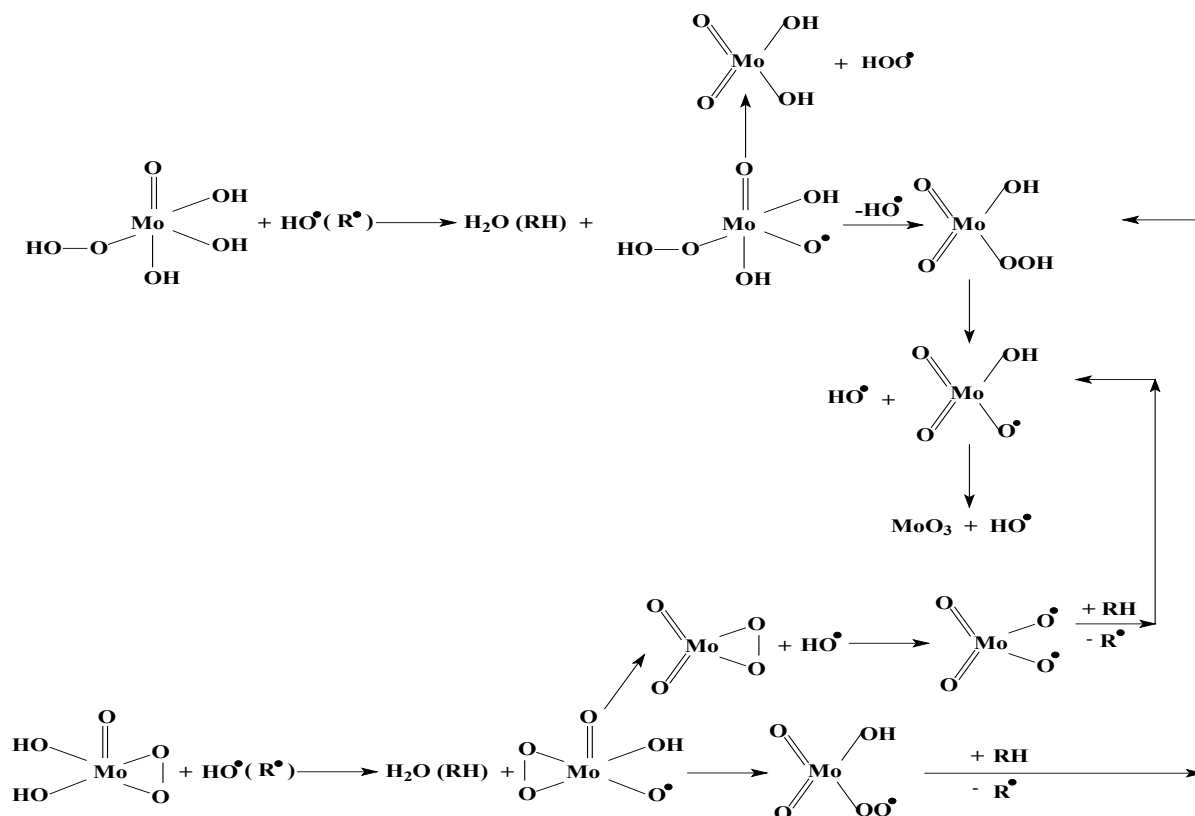
- [1] N.A. Butt, W.Zhang, Chem. Soc., Rev. 44, (2015), 7929.
- [2] I. P. Stolyarov, A. E. Gekhman, I. I. Moiseev, A. Yu. Kolesnikov, E. M. Evstigneeva, V. R. Flid, Russ. Chem. Bull., 56, (2007), 309.
- [3] S. A. Durakov, R. S. Shamsiev, V. R. Flid, A. E. Gekhman, Kinet. Katal., 60, (2019), 1.
- [4] V. R. Flid, S. A. Durakov, T. A. Morozova, Russ. Chem. Bull., 65, (2016), 2639.
- [5] S. A. Durakov, R. S. Shamsiev, V. R. Flid, A. E. Gekhman, Russ. Chem. Bull., 67, (2018), 2234.

## The Mechanism of Decomposition and Stabilization of Molybdenum Epoxidation Catalysts for Olefinic Hydrocarbons

Elimanova G.G., Batyrshin N.N., Kharlampidi Kh.E.  
Kazan National Research Technological University, Kazan, Russia  
yelimanova@mail.ru

At the stage of epoxidation of propylene with ethylbenzene hydroperoxide in the process of the joint production of propylene oxide and styrene, a molybdenum compound soluble in alkyl aromatic hydrocarbons is used as a catalyst, which is obtained by the reaction of metallic (Mo) and ethyl benzene hydroperoxide (HPB) in ethyl alcohol (CMC) [1]. The catalyst has a low thermal and temporal stability. The possibility of stabilization of CMC by nitrogen-containing compounds is presented in [2]. A significant decrease in the rate of deactivation of the catalyst in the presence of Mannich base (PMB), a typical inhibitor of radical chain processes, suggested that the destruction of the catalyst is a homolytic process.

In further studies, the destruction of homogeneous molybdenum catalytic complexes derived from metallic molybdenum, hydrogen peroxide (PMC) and isopropyl benzene hydroperoxide (MC) was considered. By accelerating the radical-chain reaction of liquid-phase oxidation of styrene with oxygen in the presence of molybdenum catalysts ( $-2 - 4$  orders of magnitude), it has been experimentally proved that deactivation of the molybdenum catalyst begins with homolytic decomposition.



### PP-III-14

The process of deactivation of molybdenum complexes is accompanied by the formation of insoluble forms of molybdenum-containing compounds (precipitation). The analysis of a deposit by a gravimetric method allowed to assume that the deposit which is formed at deactivation consists of mix of trioxide of molybdenum and molybdenic acid. Based on all the above facts, a scheme for the deactivation of molybdenum catalysts for the epoxidation of olefinic hydrocarbons has been proposed.

#### References:

- [1] L. P. Karpenko, B. R. Serebryakov, R. E. Galanterik, et al., *Zh. Prikl. Khim.* 1975, 8, pp. 1706 -1709.
- [2] G.G. Elimanova, N.N. Batyrshin, Kh.E. Kharlampidi, *Kinetics and Catalysis*, 2017, Vol. 58, No. 1, pp. 46–50.

## Sterically Crowded Dimeric Diisobutylaluminum Aryloxides: Synthesis, Characteristics, and Application as Activators in Homo- and Copolymerization of Olefins

Faingol'd E.E., Zharkov I.V., Bravaya N.M., Panin A.N., Saratovskikh S.L.,  
Babkina O.N., Shilov G.V.

*Institute of Problems of Chemical Physics RAS, Chernogolovka, Moscow Region, Russia*  
*fevgeny@mail.ru*

Sterically crowded isobutylaluminum aryloxides with tert-butyl group in the 2 and 6 positions of aryloxy group are individual monomeric compounds and effective activators of dimethyl bisindenyl metallocene catalysts of olefin polymerization [1,2]. The interesting task was to synthesize new isobutylaluminum aryloxides with different substituents in ortho-positions of aryloxy group, to study their structural peculiarities and to test new compounds as metallocene catalyst activators. In the work a row of diisobutylaluminum aryloxides bearing different sterically crowded substituents in ortho-positions of aryl ligand (ArO)Al<sup>i</sup>Bu<sub>2</sub> (ArO=2-<sup>t</sup>Bu-C<sub>6</sub>H<sub>4</sub>O (**Al<sub>TBP</sub>**), 2-Me,6-<sup>t</sup>Bu-C<sub>6</sub>H<sub>3</sub>O (**Al<sub>MTBP</sub>**), 2,6-<sup>i</sup>Pr<sub>2</sub>-C<sub>6</sub>H<sub>3</sub>O (**Al<sub>DIPP</sub>**), 2-Ph-C<sub>6</sub>H<sub>4</sub>O (**Al<sub>PP</sub>**), 2,6-Ph<sub>2</sub>-C<sub>6</sub>H<sub>3</sub>O (**Al<sub>DPP</sub>**), 1-C<sub>10</sub>H<sub>7</sub>O (**Al<sub>N-1</sub>**) was synthesized by the reaction of triisobutylaluminum with appropriate phenol. Molecular structures of **Al<sub>MTBP</sub>**, **Al<sub>DIPP</sub>**, **Al<sub>PP</sub>**, **Al<sub>DPP</sub>**, and **Al<sub>N-1</sub>** were determined by X-ray crystallography. X-ray and NMR analysis were shown a dimeric [(ArO)Al<sup>i</sup>Bu<sub>2</sub>]<sub>2</sub> structure of the synthesized compounds. All dimeric diisobutylaluminum aryloxides were tested as activators of *rac*-Et(2-MeInd)<sub>2</sub>ZrMe<sub>2</sub> in homopolymerization of ethylene, propylene, copolymerization of ethylene with propylene and terpolymerization of ethylene/propylene/5-ethylidene-2-norbornene. It was shown that only **Al<sub>MTBP</sub>** and **Al<sub>DPP</sub>** work as effective activators in all polymerization processes, with activity of **Al<sub>MTBP</sub>** system being significantly higher than that of **Al<sub>DPP</sub>**. The evaluation of dimerization energies of synthesized aryloxides by means of DFT calculations showed **Al<sub>MTBP</sub>** and **Al<sub>DPP</sub>** to form the least stable dimers. The activation of *rac*-Et(2-MeInd)<sub>2</sub>ZrMe<sub>2</sub> was modeled as bonding of diisobutylaluminum aryloxide with zirconocene followed by the first insertion of ethylene into Zr<sup>+</sup>-Me bond. DFT calculations demonstrated the process to be the most favorable for **Al<sub>MTBP</sub>** and **Al<sub>DPP</sub>** which well corresponds to experimental observations.

**Acknowledgement.** This work was supported by the Russian Foundation for Basic Research, grant 15-03-02307-a.

### References:

- [1] Faingol'd E.E., Bravaya N.M., Panin A.N., Saratovskikh S.L., Babkina O.N. Patent RU 2588496 C2, 27.06.2016.  
[2] Faingol'd E.E., Bravaya N.M., Panin A.N., Babkina O.N., Saratovskikh S.L., Privalov V.I. J.Appl.Polym.Sci. 2016, V. 133, P. 43276.

## Molybdenite-Based Hydrodesulfurization Catalysts Prepared under the Conditions of Cryo-Mechanical Activation

Fedushchak T.A.<sup>1</sup>, Uyimin M.A.<sup>2</sup>, Maykov V.V.<sup>2</sup>, Mikubaeva E.V.<sup>1</sup>, Zhuravkov S.P.<sup>3</sup>, Vosmerikov A.V.<sup>1</sup>, Stasieva L.A.<sup>1</sup>, Prosvirin I.P.<sup>4</sup>, Zaykovsky V.I.<sup>4</sup>, Kogan V.M.<sup>5</sup>

1 – Institute of Petroleum Chemistry SB RAS, Tomsk, Russia

2 – Institute of Metal Physics UB RAS, Ekaterinburg, Russia

3 – National Research Tomsk Polytechnic University, Tomsk, Russia

4 – Boreskov Institute of Catalysis, Novosibirsk, Russia

5 – N.D. Zelinsky Institute of Organic Chemistry RAS, Moscow, Russia

taina@ipc.tsc.ru

Solid-phase methods for the preparation of bulk sulfide catalysts for hydrotreating petroleum fractions meet the requirements of 'green chemistry'. The catalysts are usually prepared in planetary mills by mechanical grinding of commercial molybdenite ( $\text{MoS}_2$ ), as a size precursor of the active component, in the presence of organic solvents [1] or their trace amounts [2]. The disadvantages of these methods are the unstable level of hydrodesulfurization ability, the tendency to carbonization [1], and the initial presence of S–O structures, which are easily hydrolyzed to sulfuric acid ( $\text{pH} = 2.1$ ) on the catalyst surface [2]. In addition, the above mentioned catalysts need to be preactivated with S-toxic reagents.

Earlier, the efficiency of grinding of solid substrates for the purpose to obtain nanopowder reagents using a combination of mechanochemical grinding and low temperatures ( $T < 77\text{K}$ ) has been shown [3]. A similar approach was applied in this study.

The aim of this study is to prepare hydrotreating catalysts by mechanochemical grinding of molybdenite under cryogenic conditions and determine the specificity of their structures and catalytic activity in the model reaction of hydrogenolysis of dibenzothiophene and diesel fraction components.

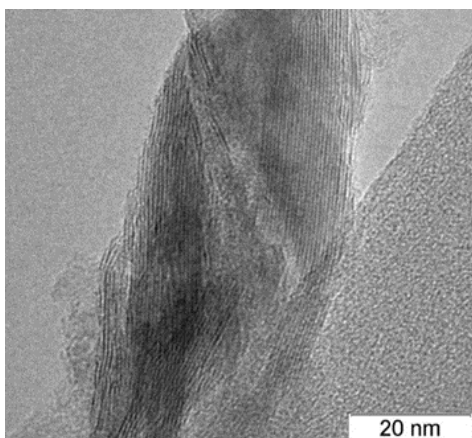


Fig. 1. Electron micrograph of the cryo-catalyst.

Physico-chemical analysis of the powders was performed using X-ray diffraction phase analysis (XRD; D8-Discover X-ray diffractometer, Bruker, Germany), X-ray photoelectron spectroscopy (XPS; SPECS photoelectron spectrometer using  $\text{AlK}\alpha$  radiation), and sedimentation analysis (DC24000 disc centrifuge; CPS Instruments, USA).

The pH values of aqueous phases of powder suspensions were measured using a HANNA HI 2215 pH-meter. The X-ray fluorescence analysis of

### PP-III-16

hydrogenates for the content of residual sulfur ( $S_{res}$  as an estimated criterion of catalyst activity) was performed using a SW-D3 Spectroscan.

It was found out that the hydrodesulfurization ability of cryo-MoS<sub>2</sub> in the model reaction of hydrogenolysis of dibenzothiophene ( $S_{init} = 500$  ppm;  $S_{res} < 5$  ppm) and components of the diesel fraction ( $S_{init} = 500$  ppm;  $S_{res} = 10$  ppm) is quite high. It was also revealed that cryo-MoS<sub>2</sub> does not require any step of activation with hydrogen sulfide/dimethyl disulfide as compared to the catalysts described in [1, 2]. It is more resistant to chemical degradation during storage and retains the ability to be used cyclically in model reactions.

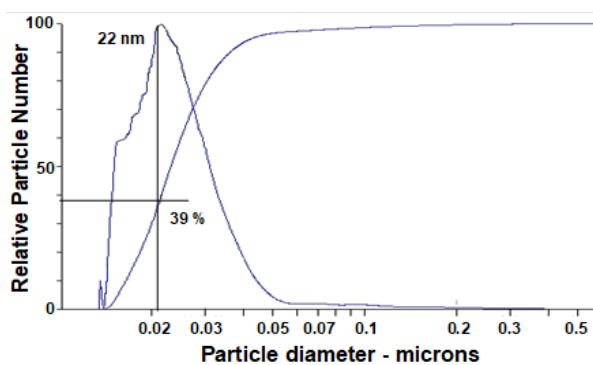


Fig.2. Relative size of nano-particles of cryo-catalyst.

The dispersity of the resulted catalyst cryoparticles (Fig. 1; Fig. 2) lies in the nanoscale ranges 12-22 nm (39 wt. %) and 23-55 nm (61 wt. %).

According to XRD data, the multiplicity of shortening of the basal edges during cryo-grinding does not exceed 2. The interplanar spacing in close-packed nanocrystallites of cryo-MoS<sub>2</sub>, the

level of internal elastic stresses ( $\Delta d/d \cdot 10^3 = 1.4$ ) in them, and the magnitude of microstrains in unit cells ( $c/a = 3.901$ ) differ little from the initial values for molybdenite ( $c/a = 3.888$ ).

These data suggest the formation of a product with a virtually defect-free structure. Meanwhile, a pronounced tendency to obtain highly defective catalytic systems via mechanical activation is observed in the literature [1]. It follows from the XPS results that ratios of sulfate/sulfide anions ( $SO_4^{2-}/S^{2-}$ ) as well as  $Mo^{6+}/Mo^{4+}$  are present on the surface of cryo-MoS<sub>2</sub> nanoparticles in 3,6 times lower amount than it is reported in [2].

On the basis of a detailed analysis of the composition of formed hydrodesulphurisates, the possible structure of catalytically active sites and hydrogenating/cracking mechanisms of cryo-powder catalysts were discussed.

**Acknowledgement.** The work was performed in the framework of the project No. V.46.2.1. of the Program of basic research of State Academies of Sciences and within the scope of works for a topic 'Magnet', No. AAAA-A18-118020290129-5.

#### References:

- [1] K. Masato, U. Kunio, K. Yasunori, I. Fumikazu, Applied Catalysis A: General. 276 (2004) 241.
- [2] T. Feduschak, A. Akimov, M. Morozov et al., Comptes Rendus Chimie.19. (2016) 1315.
- [3] E. Stepanov, G. Kotelnikov, Izv. VUZov. Chemistry and Chem. Technol. 46 (2003) 26.

## Kinetic Experiment of Dry Reforming of Methane on Mo<sub>2</sub>C/CeZrO<sub>2</sub> Catalysts

Gavrilova N.N., Osipenko N.N., Nazarov V.V., Sapunov V.N., Skudin V.V.  
*D. Mendeleev University of Chemical Technology, Moscow, Russia*  
*ngavrilova@muctr.ru*

Molybdenum carbide is one of the most interesting compounds among transition metal carbides due to its promising physical and chemical properties: high temperature stability and mechanical strength, resistant to poisoning and catalytic activity in various reaction.

Dry reforming of methane is the reaction that has received much attention as an effective way to syngas production by converse both abundant gases: carbon dioxide and methane.

Molybdenum carbide exhibits high catalytic activity in dry reforming of methane and resistant to carbon deposition [1]. However, Mo<sub>2</sub>C oxidation to form inactive MoO<sub>2</sub> occurs during reaction condition. Oxidative stability can be improved by the introduction of promoters or the use of support [2, 3]. Ceria-zirconia solid solutions can be used as support for Mo<sub>2</sub>C catalyst.

Synthesis of Mo<sub>2</sub>C/Ce<sub>x</sub>Zr<sub>1-x</sub>O<sub>2</sub> catalytic systems was carried out by the sol-gel method. Solid solutions Ce<sub>x</sub>Zr<sub>1-x</sub>O<sub>2</sub> with different composition ( $x = 0.9, 0.8, 0.5$  and  $0.2$ ) were used as catalyst supports. The synthesized catalysts were characterized in terms of morphology, phase composition and porous structure. Catalytic activity and stability were investigated in the reaction of carbon dioxide conversion of methane (DRM). The reaction was carried out in a reactor with a fixed bed of catalyst in the temperature range of 800-900°C.

Kinetic studies were carried out on Mo<sub>2</sub>C and Mo<sub>2</sub>C/Ce<sub>x</sub>Zr<sub>1-x</sub>O<sub>2</sub> catalysts. The calculation of the specific rate constants showed that the Mo<sub>2</sub>C/Ce<sub>0.5</sub>Zr<sub>0.5</sub>O<sub>2</sub> catalyst has the highest catalytic activity. The reaction mechanism, which explains the high stability of this catalyst, was proposed.

It was shown that supported Mo<sub>2</sub>C/Ce<sub>x</sub>Zr<sub>1-x</sub>O<sub>2</sub> catalysts were more oxidative stable than unsupported Mo<sub>2</sub>C, whose loss of activity was observed after a 60 min of experiment. Oxidation of supported Mo<sub>2</sub>C/Ce<sub>x</sub>Zr<sub>1-x</sub>O<sub>2</sub> was not observed for 600 min under the reaction conditions.

**Acknowledgement.** The work was supported by Mendeleev University of Chemical Technology of Russia. Project Number 028-2018.

### References:

- [1] J.B. Claridge, A.P.E. York, C. Márquez-Alvarez, A.J. Brungs, J. Sloan, S.C. Tsang, M.L.H. Green. *J. Catal.* 180 (1998) 85.
- [2] A.J. Brungs, A.P.E. York, J.B. Claridge, C. Marquez-Alvarez, M.L.H. Green. *Catal. Lett.* 70 (2000) 117.
- [3] A. R.S. Darujati, W. J. Thomson. *Chem. Eng. Sci.* 61 (2006) 4309.

## Hydrogen Production from Formic Acid Decomposition over Pd/C Catalysts: Effect of Deposition of N-Containing Precursors on Carbon Support

Golub F.S.<sup>1</sup>, Beloshapkin S.A.<sup>2</sup>, Bolotov V.A.<sup>1</sup>, Parmon V.N.<sup>1</sup>, Bulushev D.A.<sup>1</sup>

1 – Boreskov Institute of Catalysis, Novosibirsk, Russia

2 – University of Limerick, Limerick, Ireland

Fedorglb@gmail.com

Most of the currently used energy resources are fossil fuels. At the same time, there is an active search for renewable energy sources. One of the interesting renewable fuels is hydrogen, but there are difficulties with its storage and transportation. An approach to solving these problems is to store and generate hydrogen using molecules with high hydrogen content like formic acid (4.4 %) that can be obtained from biomass at mild conditions.

Earlier, we showed that doping of the carbon support by nitrogen leads to an increase of the activity of supported Pd catalysts in hydrogen production from formic acid. The obtained pyridinic nitrogen sites can strongly interact with metal atoms and such interaction allows reaching a high dispersion of the active component, up to atomic [1]. The objective of the present research was further development of the N-doped carbon supports for Pd-catalysts for efficient hydrogen generation from formic acid. Thus, we used a Sibunit carbon as a mesoporous support (348 m<sup>2</sup>/g). N-doping of the Sibunit was performed by post-deposition of different substances which contain pyridinic nitrogen atoms like melamine, 1,10-phenanthroline and 2,2'-bipyridine followed by calcination at 400°C. As a result, we synthesized a series of N-doped carbon supports with a wide range of surface areas: from 8 to 301 m<sup>2</sup>/g.

Preparation of 1 % wt Pd catalysts was performed by impregnation of synthesized supports with a Pd acetylacetonate acetone solution followed by their reduction in a 2.5% HCOOH/Ar flow at 300°C. Reaction rates were determined in a fixed bed reactor at low conversions at different temperatures. Catalysts based on C<sub>x</sub>N<sub>y</sub>/C supports, which were prepared from a mixture of melamine and Sibunit (1:2) in a muffle furnace (2 hours) or under microwave heating conditions (140 s), showed the highest catalytic activity as seen in Fig. 1. These samples are about 3.5 times more active than the Pd/C catalyst without nitrogen and catalysts prepared from bipyridine and phenanthroline. The most active samples showed the lowest apparent activation energy (32 kJ/mol). The selectivity of hydrogen formation for the majority of catalysts was in the range 91-96 %, while that for the most active Pd/C<sub>x</sub>N<sub>y</sub>/C (muf) sample was 98 %. A stability test of the Pd/C<sub>x</sub>N<sub>y</sub>/C (muf) sample demonstrated no significant changes in the catalyst activity for 5 h at 300°C.

Using HRTEM we established that the mean Pd particle size in the catalysts does not depend strongly on the nature of the support and corresponds to the range of 2.0-2.6 nm. Using XPS study we found a difference in the ratios of nitrogen forms: pyridinic (398.8 eV) and tertiary N

(400.2 eV) due to different nature of the N precursors. Fig. 2 shows Pd 3d spectra for the studied samples which demonstrate two doublet signals. The high binding energy (BE) component we attribute to an oxidized Pd state (Pd<sup>2+</sup>) which can exist in the state of highly dispersed surface oxide formed by oxidation Pd-particles by atmospheric oxygen or by single atom Pd<sup>2+</sup> species strongly interacting with N, O or C defect sites of the carbon support. The low BE component we attribute to a metallic Pd state. A strong shift of the Pd 3d<sub>5/2</sub> lines for the Pd/C<sub>x</sub>N<sub>y</sub>/C catalysts up to 336.4 eV as compared to metallic highly dispersed Pd particles (335.8 eV) for the Pd/C catalyst, indicates that this is an electron-deficient state of Pd which strongly interacts with the surface of the N-doped carbon support. Bipyridine and phenanthroline based samples showed intermediate BE shifts (up to 336.0 eV) and much lower surface N concentrations.

Thus, the best precursor for N-doping of the Sibunit carbon is melamine. The high activity, H<sub>2</sub> selectivity and stability of the Pd catalysts based on melamine-doped Sibunit is explained by strong interaction between the nitrogen species of the support and highly dispersed Pd particles (2 nm), which are present in the electron-deficient state (Fig. 3).

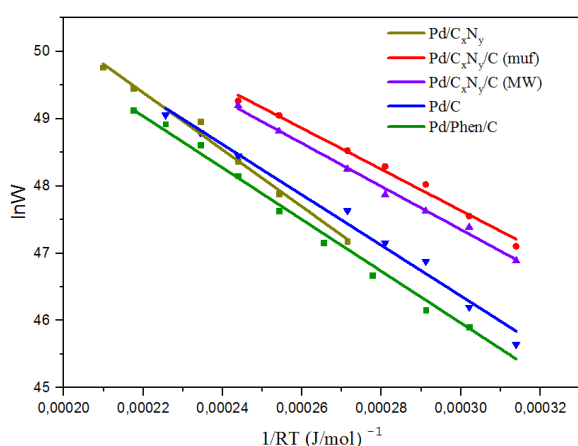


Fig. 1. Arrhenius plots for formic acid decomposition

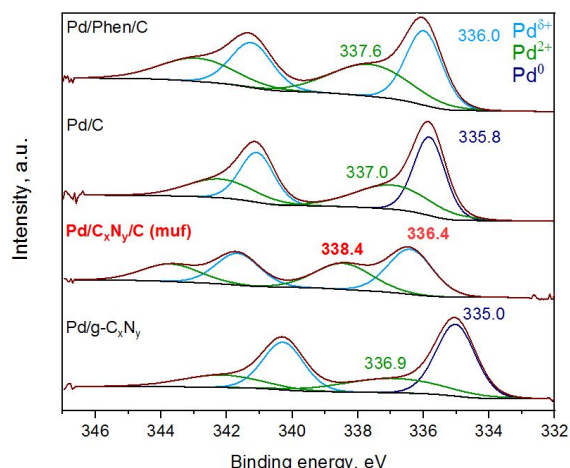


Fig. 2. Pd 3d XPS-spectra

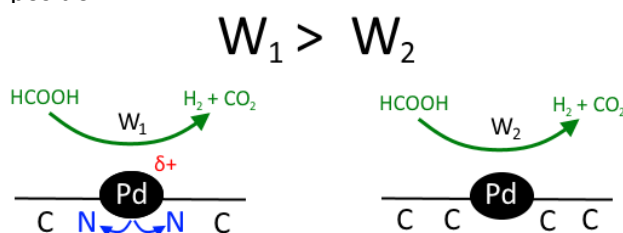


Fig. 3 Possible conclusion about nitrogen influence on the catalytic activity

**Acknowledgement.** This research was supported by the Russian Science Foundation, grant 17-73-30032.

**References:**

[1] O. Y. Podyacheva, D. A. Bulushev, A. N. Suboch, D. A. Svintsitskiy, A. S. Lisitsyn, E. Modin, A. Chuvilin, E. Y. Gerasimov, V. I. Sobolev, V. N. Parmon, ChemSusChem 11 (2018) 3724-3727.

## Catalytic Transformations of 1-Heptene and n-Heptane over Selected Zeolites at 170–260 °C

Gorokhova E.O.<sup>1</sup>, Kulchakovskaya E.V.<sup>1</sup>, Asalieva E.Yu.<sup>1</sup>, Sineva L.V.<sup>1,2</sup>, Mordkovich V.Z.<sup>1,2</sup>

*1 – Technological Institute for Superhard and Novel Carbon Materials,*

*Troitsk, Moscow, Russia*

*2 – INFRA Technology LLC, Moscow, Russia*

*gorokhovaeo@tisnum.ru*

Zeolites manifest advantages over most other heterogeneous catalysts, including crystalline ones, where active sites are located at the outer faces or defective lattice sites. To determine the structural features of catalytically active sites, one can use the data obtained by X-ray diffraction analysis (XRD) or by spectroscopy. In petrochemical and refining industries the zeolites are widely used as catalysts for the various hydrocarbon conversions such as isomerization, cracking, oligomerization, alkylation, etc. [1]. Zeolites are used as components of the supports for Fischer–Tropsch synthesis catalysts.

Fischer–Tropsch synthesis (FTS) is a heterogeneous catalytic process of formation of liquid hydrocarbons and waxes mixture from CO and H<sub>2</sub>. FTS catalysts consist of active metal (Co, Fe) and support (Al<sub>2</sub>O<sub>3</sub>, SiO<sub>2</sub>, TiO<sub>2</sub>, zeolites). The use of zeolite as a support in such catalyst generates additional catalytic activity in secondary transformations of hydrocarbons formed on cobalt active sites. Such transformations, which take place on the zeolite acid sites, can be cracking, isomerization, alkylation or redistribution of hydrogen [2]. Cracking and isomerization of hydrocarbons are the most important industrial processes, but the mechanisms of those reactions are not disclosed enough in the temperature range important for FTS. Therefore, for a better understanding of these catalytic reactions, it is interesting to study the transformations of zeolites on individual hydrocarbons.

In this work, we investigate the catalytic transformations of 1-heptene and n-heptane over zeolites HBeta–25, HZSM–5, HY5, HY30 and HY60 at 170–260°C.

During the investigation, 1 ml of 1–heptene or n–heptane was added to each selected zeolite with rate 0.2 ml every 10 minutes. The synthesis was carried out in a flow reactor in a stream of inert gas (He) at atmospheric pressure in the temperature range 170–260°C.

All studied zeolites were not active in n-heptane transformations and were active in 1–heptene ones. Main products of 1–heptene transformations were C<sub>3</sub>–C<sub>10</sub> (olefins, paraffins, iso-olefins, iso-paraffins). It is interesting to note that the reaction product gas contained significant amounts of CO and CO<sub>2</sub>, the presence of which allowed suggesting that this effect is the result of a change in the crystal lattice and subsequent extraction of oxygen from a zeolite to gas phase.

### PP-III-19

To identify the structural features of HBeta–25 and HZSM–5 zeolites before and after the contact with 1–heptene, XRD was performed to confirm the assumption of the effect of 1-heptene on the crystal lattice.

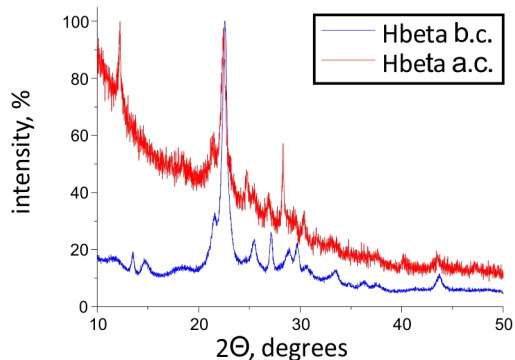


Fig 1. Comparison of X–ray pattern of zeolite HBeta–25 before and after the contact with 1-heptene

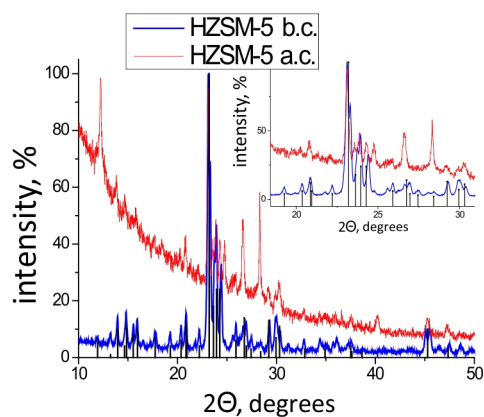


Fig 2. Comparison of X–ray pattern of zeolite HZSM–5 before and after contact with 1-heptene and  $\text{Al}_2\text{O}_3$  54  $\text{SiO}_2$  data. Inset — an enlarged fragment

The figures show X–ray diffraction patterns of HBeta–25 zeolites (Fig. 1) and HZSM–5 (Fig. 2) before and after the addition of 1–heptene.

Significant conversion of heptane to gaseous products, as well as major variation in the composition of the liquid products of the interaction of n–heptane with zeolites were not detected.

The following conclusions can be drawn:

- 1) CO and CO<sub>2</sub> were detected in the products of the interaction of 1-heptene with zeolites, which is explained by the extraction of oxygen from the zeolite lattice. This assumption is confirmed by XRD.
- 2) In both cases, after the 1-hour long catalytic process, the d–spacing changed unevenly in different directions. Such a change indicates, as shown by the analysis of the elementary cell, a decrease in the concentration of lattice oxygen.

**Acknowledgement.** This work was supported by The Ministry of Science and Higher Education of Russian Federation in terms of the state assignment to TISNCM.

#### References:

- [1] M.L. Putzma, Catalysis. Chemistry and mechanism. World–ACS. (1980) 409.
- [2] J. Cejka, A. Corma, S. Zones. Zeolites and Catalysis. Wiley–VCH. (2010) 881.

## Interaction of Hydrogen, Carbon Monoxide and Oxygen with Films Consisting of Gold and Copper Nanoparticles

Grishin M.V.<sup>1</sup>, Gatin A.K.<sup>1</sup>, Dohlikova N.V.<sup>1</sup>, Kulak A.I.<sup>2</sup>, Sarvadii S.Yu.<sup>1</sup>, Shub B.R.<sup>1</sup>

*1 – Semenov Institute of Chemical Physics RAS, Moscow, Russia*

*2 – The Institute of General and Inorganic Chemistry NAS Belarus, Minsk, Belarus*

*mvgrishin68@yandex.ru*

The progress of modern industrial chemistry is largely due to the use of new catalysts based on nanoparticles. This approach had become the main direction in the creation of new catalysts. The purpose of our work was to determine the features of the interaction of H<sub>2</sub>, CO and O<sub>2</sub> with single gold and copper nanoparticles that are part of films on the surface of highly organized pyrolytic graphite (HOPG).

To create the film, the aqueous solutions H<sub>2</sub>AuCl<sub>4</sub> and/or Cu(NO<sub>3</sub>)<sub>2</sub> were applied on the substrate and calcined in a vacuum. All the measurements were carried out using scanning tunneling microscopy and spectroscopy at a pressure of residual gases  $p \leq 2 \cdot 10^{-10}$  Torr.

The studying of films consisted of gold and copper nanoparticles, as well as the gold-copper film itself was fulfilled. It was found that Au and Cu nanoparticles had a spherical shape with a diameter of about 3-6 nm. Previously, we established the features of interaction of gold nanoparticles with H<sub>2</sub>, O<sub>2</sub> and CO. The dissociative adsorption of H<sub>2</sub> on Au nanoparticles took place at 300 K. The oxygen activation required of the pre-adsorbed hydrogen atoms on the surface of Au nanoparticles. The sequential exposure of Au nanoparticles first in H<sub>2</sub>, then in O<sub>2</sub>, and again in H<sub>2</sub> led to the H<sub>2</sub>O molecules formation. The interaction of adsorbed H atoms with CO led to the formation of HCO, and exposure in oxygen resulted in H<sub>2</sub>O and CO<sub>2</sub> formation. The copper film consisted of nanoparticles covered with Cu<sub>2</sub>O and CuO. The exposure of this film in CO led to a partial reduction of the surface oxides, while hydrogen adsorption on the oxide-free copper nanoparticles caused a transformation of their electronic structure from the metal type to the semiconductor one. The exposure in O<sub>2</sub> resulted in both the oxidation of impurity-free Cu nanoparticles and the removal of adsorbed hydrogen atoms. It was found that the bimetallic coating formed by gold and copper nanoparticles with virtually no nanoparticles of mixed composition. The interaction of Cu and Au nanoparticles helped to prevent complete oxidation of copper. With respect to CO adsorption the bimetallic film showed properties of copper film. The H<sub>2</sub> adsorption on a bimetallic film led to the same effects as on the gold film.

Quantum chemical modelling generally confirmed the experimental results.

**Acknowledgement.** This work was supported by the Russian Foundation for Basic Researches, grants 17-03-00275 and 18-03-00013. Computation was carried out in Joint SuperComputer Center of the Russian Academy of Sciences.

## Kinetic Model of Sonochemiluminescence Process of Aqueous Solution of Ruthenium Tris-Bipyridyl Chloride (II)

Mannanova G.I.<sup>1</sup>, Koledina K.F.<sup>1,2</sup>, Gubaydullin I.M.<sup>1,2</sup>

1 – Institute of Petrochemistry and Catalysis of RAS UFIC, Ufa, Russia

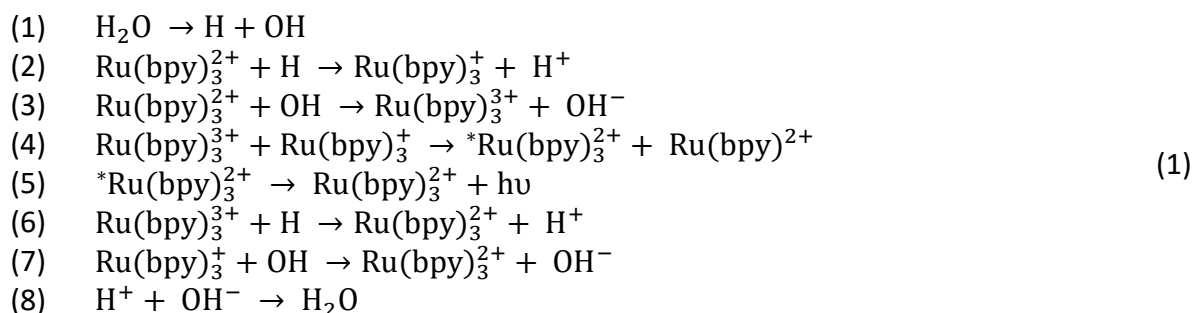
2 – Ufa State Oil Technical University, Ufa, Russia

gulshat.islamova.2017@mail.ru

The luminescence produced by ultrasound in solutions is called sonoluminescence [1]. Sonochemiluminescence—one of the varieties of this process, in which light is emitted during chemical reactions of sonolysis products, falling from cavitation bubbles in the volume of the solution.

Currently, there is an active study of the process of sonochemiluminescence of aqueous solutions of Tris-bipyridyl ruthenium chloride [2]. This process is a promising way to develop analytical determination of various substances. This work is devoted to the development of a kinetic model of this process for the purpose of theoretical justification of its mechanism.

On the basis of experimental data in [2], a preliminary scheme of chemical transformations occurring during sonolysis of a neutral aqueous solution  $\text{Ru}(\text{bpy})_3^{2+}$  with the formation of an electronically excited product  $^*\text{Ru}(\text{bpy})_3^{2+}$  emitting light was proposed.



To check the correctness of the presented mechanism, atomic-molecular and stoichiometric matrices were composed,  $X_i$ -substances participating in the reaction:

$$\begin{array}{c}
 \left[ \begin{array}{c} X_i \\ X_1 \\ X_2 \\ X_3 \\ X_4 \\ X_5 \\ X_6 \\ X_7 \\ X_8 \\ X_9 \end{array} \right] \begin{array}{c} \text{H}_2\text{O} \\ \text{H} \\ \text{OH} \\ \text{Ru}^{2+} \\ \text{Ru}^{3+} \\ \text{OH}^- \\ \text{Ru}^+ \\ ^*\text{Ru}^{2+} \\ \text{H}^+ \end{array} \\
 \text{AM}[9;3]=
 \end{array}
 \begin{array}{c}
 \left[ \begin{array}{ccc} \text{H} & \text{O} & \text{Ru} \end{array} \right] \\
 \begin{array}{ccc} 2 & 1 & 0 \\ 1 & 0 & 0 \\ 1 & 1 & 0 \\ 0 & 0 & 1 \\ 0 & 0 & 1 \\ 1 & 1 & 0 \\ 0 & 0 & 1 \\ 0 & 0 & 1 \\ 1 & 0 & 0 \end{array}
 \end{array}
 \text{SM}[8;9]=
 \begin{array}{c}
 \left[ \begin{array}{cccccccccc} X_1 & X_2 & X_3 & X_4 & X_5 & X_6 & X_7 & X_8 & X_9 \end{array} \right] \\
 \begin{array}{cccccccccc} -1 & +1 & +1 & 0 & 0 & 0 & 0 & 0 & 0 \\ 0 & -1 & 0 & -1 & 0 & 0 & +1 & 0 & +1 \\ 0 & 0 & -1 & -1 & +1 & +1 & 0 & 0 & 0 \\ 0 & 0 & 0 & +1 & -1 & 0 & -1 & +1 & 0 \\ 0 & 0 & 0 & +1 & 0 & 0 & 0 & -1 & 0 \\ 0 & -1 & 0 & +1 & -1 & 0 & 0 & 0 & +1 \\ 0 & 0 & -1 & +1 & 0 & +1 & -1 & 0 & 0 \\ +1 & 0 & 0 & 0 & 0 & -1 & 0 & 0 & -1 \end{array}
 \end{array}$$

### PP-III-21

The product of stoichiometric and atomic-molecular matrices was obtained zero matrix (SMxAM = 0), which confirms the correctness of the mechanism. [3]

According to the schemes of chemical transformations (1) on the basis of the law of mass action, the reaction rates in stages are as follows:

$$\begin{aligned} W_1 &= -k_1 \cdot [X_1], \text{ где } [k_1] = [1/s]; \\ W_2 &= -k_2 \cdot [X_4] \cdot [X_2], \text{ где } [k_2] = [l/(mol \cdot s)]; \\ W_3 &= k_3 \cdot [X_4] \cdot [X_3], \text{ где } [k_3] = [l/(mol \cdot s)]; \\ W_4 &= k_4 \cdot [X_5] \cdot [X_7], \text{ где } [k_4] = [l/(mol \cdot s)]; \\ W_5 &= k_5 \cdot [X_8], \text{ где } [k_5] = [1/s]; \\ W_6 &= k_6 \cdot [X_5] \cdot [X_2], \text{ где } [k_6] = [l/(mol \cdot s)]; \\ W_7 &= -k_7 \cdot [X_7] \cdot [X_3], \text{ где } [k_7] = [l/(mol \cdot s)]; \\ W_8 &= -k_8 \cdot [X_8] \cdot [X_6], \text{ где } [k_8] = [l/(mol \cdot s)]. \end{aligned}$$

Experimental studies are carried out under ideal mixing conditions, in a closed system, i.e. the volume of the reaction mass is constant. Correctly describe the study in such conditions is the condition of ideal mixing. [4]

On the basis of the presented mechanism the kinetic model of the process is made:

$$\left\{ \begin{aligned} \frac{d[X_1]}{dt} &= -k_1[X_1] + k_8[X_6][X_9] \\ \frac{d[X_2]}{dt} &= k_1[X_1] - k_2[X_2][X_4] - k_6[X_2][X_5] \\ \frac{d[X_3]}{dt} &= k_1[X_1] - k_3[X_3][X_4] - k_7[X_3][X_7] \\ \frac{d[X_4]}{dt} &= -k_2[X_2][X_4] - k_3[X_3][X_4] + k_4[X_5][X_7] + k_5[X_8] + k_6[X_2][X_5] + k_7[X_3][X_7] \\ \frac{d[X_5]}{dt} &= k_3[X_3][X_4] - k_4[X_5][X_7] - k_6[X_2][X_5] \\ \frac{d[X_6]}{dt} &= k_3[X_3][X_4] + k_7[X_3][X_7] - k_8[X_6][X_9] \\ \frac{d[X_7]}{dt} &= k_2[X_2][X_4] - k_4[X_5][X_7] + k_7[X_3][X_7] \\ \frac{d[X_8]}{dt} &= k_4[X_5][X_7] - k_5[X_8] \\ \frac{d[X_9]}{dt} &= k_2[X_2][X_4] + k_6[X_2][X_5] - k_8[X_6][X_9] \end{aligned} \right.$$

where  $X_1 - H_2O$ ,  $X_2 - H$ ,  $X_3 - OH$ ,  $X_4 - Ru^{2+}$ ,  $X_5 - Ru^{3+}$ ,  $X_6 - OH^-$ ,  $X_7 - Ru^+$ ,  $X_8 - *Ru^{2+}$ ,  $X_9 - H^+$

Thus, the kinetic model of the process is obtained. On the basis of this model, the inverse kinetic problem of selecting adequate values of the reaction rate constants will be further solved.

#### References:

- [1] V.A. Borisenok Acoustic journal 3 (2015) 333.
- [2] G.L. Sharipov, A.M. Abdrakhmanov, B.M. Gareev, L.R. Ekshembееva, R.Koroliov Proceedings of the Ufa scientific centre of RAS 3 (2017) 15.
- [3] I. M. Gubaydullin, L. V. Saifullin, M. R. Enikeev / / Publishing house of BSU, Ufa, 2011.

## Models of the Reaction Unit of Catalytic Cracking

Mannanova G.I.<sup>1</sup>, Gubaydullin I.M.<sup>1,2</sup>

1 – Institute of Petrochemistry and Catalysis of RAS UFIC, Ufa, Russia

2 – Ufa State Oil Technical University, Ufa, Russia

gulshat.islamova.2017@mail.ru

The main component in the production of commercial motor gasoline is currently gasoline catalytic cracking. In addition, catalytic cracking refers to a group of processes that increase the depth of oil refining. The chemistry and mechanism of this process is complex and there are many different views on this. This report presents a number of models developed by domestic and foreign scientists.

In 1995, Picault offered his four lump model (Fig.1). In this model, a small number of components [1], were chosen to describe a complex gaseous mixture of CC products, which provides ease of calculation. The influence of rate constants and activation energy on the raw material is a known limitation of the four lump model, this must be taken into account when processing the results.

A large number of reactions with the formation of low-molecular components from high-molecular hydrocarbons takes place in the CC Elevator reactor. The article [2] describes a six-component kinetic model of the process (Fig. 2), which describes reactions involving vacuum gas oil, gasoline, and light gaseous products of CC, including  $C_3H_6$  and  $C_2H_4$  and the two species toxicogenic structures (coking structures 1 and coking structures 2).

Another six-component model was developed for the light fractions of hydrocarbon, CC on the Fe/HZSM-5 catalyst. The formalized scheme of transformations presented in Fig. 3 describes the transformation of light fractions of UV [3].

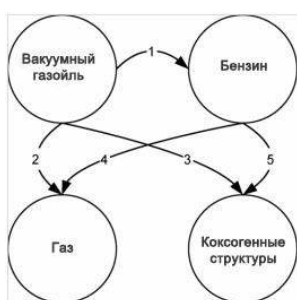


Figure 1 – Schematic representation of the four lump model of pitault and et al.(1995)

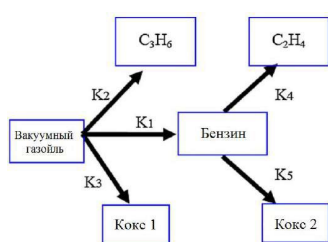


Figure 2 – diagram of the six-component transformations

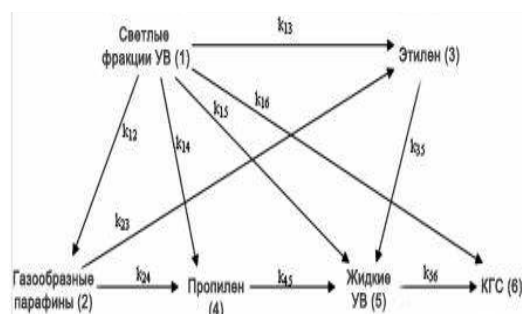


Figure 3 – Scheme of transformations of the six-component model

The paper [4] presents a complex scheme of transformations with nine lump, taking into account the aromatization reactions of gasoline CC. In this scheme of transformations, aromatization reactions are first composed into h-paraffins, iso-olefins, olefins, aromatic

## PP-III-22

hydrocarbons, coking structures, light hydrocarbons and hydrogen. Three main types of reactions between these components were considered in the scheme of aromatization reactions transformations, for example, dehydrogenation and cyclization of paraffins, isomerization of paraffins and cracking of low molecular weight hydrocarbons. In order to simplify, less important reactions were excluded from the transformation scheme. The nine-component model of gasoline CC is shown in Fig. 4 [4].

The eleven lump model is shown in Fig. 5. In this complex model, in addition to chemical constants, such physical parameters of homologous hydrocarbons as density, heat capacity, viscosity, thermal conductivity, heat of formation of active forms and molecular masses are taken into account. Since the model with eleven components contains a single group describing both coke and light hydrocarbon gases, their characteristics have been determined as a weighted average of these varieties. Coke content of 30% and 70% of light hydrocarbon gas was confirmed [5].

The 14-lump kinetic model [6] used to describe catalytic cracking reactions is shown in Fig. 6. The more components a model includes, the more kinetic parameters need to be determined and, accordingly, more experimental data will be required. Light fraction is composed of nonaromatic hydrocarbons (paraffinic hydrocarbons, naphthenic) and aromatic hydrocarbons. In the process of CC, non-aromatic hydrocarbons can easily turn into paraffinic hydrocarbons. Aromatic hydrocarbons can't recirculated with the formation of gaseous products, decyclization reactions of aromatic hydrocarbons do not occur in the operating conditions of heavy raw materials [7]. Liquid hydrocarbons are products of polymerization, aromatization, and condensation. Since the reaction temperature of the CC is very high, some gaseous products with high molecular weight may be subjected to secondary cracking reactions. In addition, olefins can be converted into liquid hydrocarbons by polymerization and aromatization reactions.

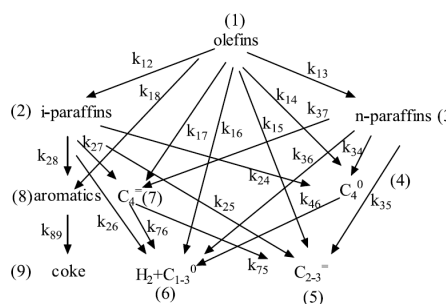


Figure 4 – nine lump model CC gasoline

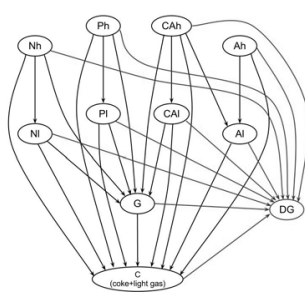


Figure 5 – Eleven lump kinetic model

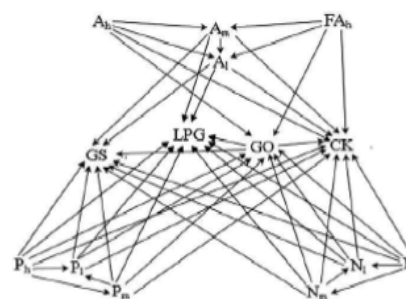


Figure 6 – 14-lump scheme of CC transformations

Thus, currently there are many different approaches to modeling the process of catalytic cracking. Different models are caused by different composition of raw materials, technological conditions of the process, different types of catalysts and designs of reaction devices. The

## PP-III-22

problem of creating an adequate model for calculating the parameters of the catalytic cracking process is currently relevant.

### References:

- [1] Pitault I., Forissier M., Bernard J.R. J. Chem. Eng. 73 (1995) 498.
- [2] Behjata Y. Chemical engineering research and design. 89 (2011) 978.
- [3] Li T., Pougatch K., Salcudean M., Grecov D. Chem. Eng. Res. Des. 87 (2009) 1451.
- [4] Kang X. Guo X. Energy Sources. – Part A. 35 (2013) 343.
- [5] Barbosa A.C. Lopes G.C. Chemical engineering transactions. 32 (2013) 637.
- [6] Zhang. China University of Petroleum. (2005) 129.
- [7] Sedighi M. E. Keyvanloo K, Towfighi J. Korean J Chem Eng. (2010) 203.

## Polyoxotungstate Supported on Carbon Nanotubes (CNT) as Effective Heterogeneous Catalyst for Epoxidation of Olefins

Ivanchikova I.D.<sup>1</sup>, Evtushok V.Yu.<sup>1,2</sup>, Suboch A.N.<sup>1,2</sup>, Podyacheva O.Yu.<sup>1,2</sup>, Kholdeeva O.A.<sup>1,2</sup>

1 – Boreskov Institute of Catalysis, Novosibirsk, Russia

2 – Novosibirsk State University, Novosibirsk, Russia

*idi@catalysis.ru*

Epoxides are valuable intermediates for the manufacture of a wide range of commercial chemical products. The selective epoxidation of olefins with environmentally benign oxidant is the most ecological and economical route to the production of epoxides. The construction of highly efficient and truly heterogeneous and recyclable epoxidation catalysts is a challenging goal of the modern oxidation catalysis.

In this work, we present a new environmentally benign method for the synthesis of epoxides based on polyoxotungstate  $[PW_4O_{24}]^{3-}$  ( $PW_4$ ) supported on nitrogen free and nitrogen doped carbon nanotubes (CNTs and N-CNTs) as a heterogeneous catalyst and aqueous hydrogen peroxide as green oxidant. Two series of catalysts  $PW_4/CNTs$  and  $PW_4/N-CNTs$  containing 10-15 wt % of  $PW_4$  have been prepared and characterized by elemental analysis,  $N_2$  adsorption, SEM, TEM, and Raman spectroscopy. Their catalytic performance was assessed in the selective oxidation of cyclooctene (CyO) as a model substrate under mild reaction conditions (50 °C). In contrast to the oxidation of alkylphenols over a CNTs-supported polyoxometalate [1], N-free carbon supports revealed better selectivity for the alkene epoxidation. The best results (CyO conversion 93% and epoxide selectivity 97%) were observed with  $PW_4/CNTs$  in dimethyl carbonate as solvent. Remarkably, the epoxidation over CNTs-supported  $PW_4$  proceeds ca. 3.5 times faster than with homogeneous  $PW_4$ . After optimization, the  $PW_4/CNTs$  catalysts demonstrated fairly good catalytic performances for the epoxidation of various alkenes (cyclohexene, caryophyllene, etc.). The catalysts are stable to metal leaching and reveal truly heterogeneous nature of the catalysis. They can be easily recovered by simple filtration, regenerated by evacuation and reused several times with the maintenance of the catalytic performance.

**Acknowledgement.** This work was supported by the Russian Science Foundation (grant 19-03-00172) and by the Ministry of Science and Higher Education of the Russian Federation (project AAAA-A17-117041710080-4).

### References:

[1] V. Yu. Evtushok, A. N. Suboch, O. Yu. Podyacheva, O. A. Stonkus, V. I. Zaikovskii, Yu. A. Chesalov, L. S. Kibis, O. A. Kholdeeva, *ACS Catal.* 8 (2018) 1297–1307.

## Size Effect in the Oxidation of CO and Methane on Pd/TiO<sub>2</sub> Catalysts

Kaichev V.V., Maksimov G.M., Fedorov A.V., Gerasimov E.Yu., Tsapina A.M., Selivanova A.V.,  
Saraev A.A.

*Boreskov Institute of Catalysis, Novosibirsk, Russia*  
*vvk@catalysis.ru*

Two 1%Pd/TiO<sub>2</sub> catalysts with different dispersion were tested in the oxidation of CO and methane in a flow-circulation reactor [1]. Catalyst 1 was synthesized by sorption of aqua sol of Pd(II) polyhydroxy complex stabilized with niobium polyoxometalate and following reduction in hydrogen at 300°C. According to TEM, the supported nanoparticles are characterized by the narrow size distribution in a range between 0.5 and 1.5 nm with the mean particle size of 0.8 nm. However, the CO adsorption technique indicates that the mean particle size is equal to 2.1 nm. Catalyst 2 was synthesized by sorption of aqua sol of metallic palladium stabilized with tungsten polyoxometalate. According to TEM, the supported nanoparticles are characterized by the narrow size distribution in a range between 1 and 7 nm with the mean particle size of 3.3 nm. This value agrees well with the CO adsorption data indicating that the mean particle size is equal to 3.0 nm.

In spite of a small difference in the mean particle size these catalysts demonstrate different activity in the reactions under study. Catalyst 1 is high active in the CO oxidation. According to kinetic measurements its turnover frequency (TOF) is approximately 0.12 s<sup>-1</sup> whereas catalyst 2 demonstrates the TOF value near 0.021 s<sup>-1</sup> only. In contrast, catalyst 2 is more active in the oxidation of methane. We have found that its turnover frequency is 0.62 s<sup>-1</sup> whereas the catalytic activity of catalyst 1 is extremely low and corresponds TOF = 0.0054 s<sup>-1</sup>. To elucidate the reasons of size effects in these reactions we performed the NAP XPS study. We found that supported palladium can change the chemical state under reaction conditions and redox properties of palladium depend on the particle size. Metallic palladium and PdO have different catalytic performance that can lead to the size effect in the oxidation of CO and methane. NAP XPS measurements indicated that both metallic palladium and oxidized palladium (Pd<sup>2+</sup>) existed in the catalysts in the CO oxidation at 673 K under the oxygen excess (the total pressure was 1 mbar, the molar ratio CH<sub>4</sub>:O<sub>2</sub> = 1:20).

**Acknowledgement.** This work was supported by RFBR, project No. 18-43-540010.

### References:

[1] A. V. Fedorov, A. M. Tsapina, O. A. Bulavchenko, A. A. Saraev, G. V. Odegova, D. Yu. Ermakov, Y. V. Zubavichus, V. A. Yakovlev, V. V. Kaichev, *Catal. Lett.* 148 (2018) 3715.

## Kinetic Model of the Reaction of Dimethylcarbonate with Alcohols in the Presence Metal Complex Catalysts

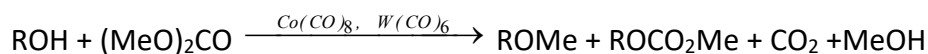
Koledina K.F.<sup>1,2</sup>, Koledin S.N.<sup>2</sup>, Gubaydullin I.M.<sup>1,2</sup>

1 – Institute of Petrochemistry and Catalysis, Russian Academy of Sciences, Ufa, Russia

2 – Ufa State Petroleum Technological University, Ufa, Russia

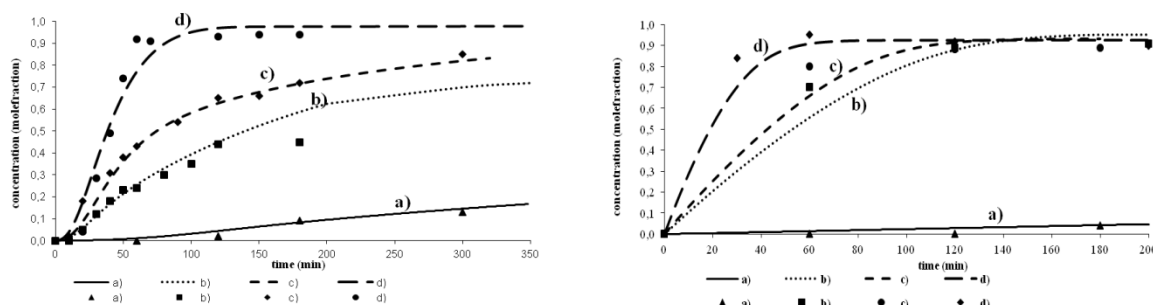
koledinakamila@mail.ru

Catalytic reaction between dimethyl carbonate (DMC) and alcohols in the presence of  $W(CO)_6$  и  $Co_2(CO)_8$  is considered in this article. DMC is one from the “green chemistry” reagents. In [2,5] authors synthesized alkyldimethyl ether and alkyldimethylcarbonates by diol and dimethylcarbonate reaction in the presence of  $W(CO)_6$ ,  $Co_2(CO)_8$ . These catalysts show high catalytic activity during the reaction between DMC and alcohols. After changing catalyst from  $W(CO)_6$  to  $Co_2(CO)_8$  alkylmethylcarbonates are formed [2].



ROH, ROME,  $ROCO_2Me$  ( $R=C_6H_{13}$ ) are detectable result substances.

The graphs in Fig. 1 show the corresponding parameters of calculated values and the experimental data.



a) Changing  $ROCO_2Me$  concentration for the reaction of DMC with alcohols in the presence of  $Co_2(CO)_8$ , with:

a)  $T = 150^\circ C$ , 0.002 mol of the catalyst;

b)  $T = 200^\circ C$ , 0.001 mol of the catalyst;

c)  $T = 180^\circ C$ , 0.002 mol of the catalyst;

d)  $T = 180^\circ C$ , 0.003 mol of the catalyst.

b) Changing ROME concentration for the reaction of DMC with alcohols in the presence of  $W(CO)_6$ , with:

a)  $T = 160^\circ C$ , 0.001 mol of the catalyst;

b)  $T = 180^\circ C$ , 0.002 mol of the catalyst;

c)  $T = 160^\circ C$ , 0.003 mol of the catalyst;

d)  $T = 200^\circ C$ , 0.003 mol of the catalyst

**Fig. 1.** Comparison between experimental (marks) and simulated values (lines)

The general scheme of the reactions in the presence of  $Co_2(CO)_8$  and  $W(CO)_6$  with the calculated activation energies shown in Fig. 9.

The catalysts  $Co_2(CO)_8$  and  $W(CO)_6$  (18) are involved in the catalytic cycle not themselves, but as active particles (12 and 22). This stages have the largest activation barrier. In the original form  $Co_2(CO)_8$  and  $W(CO)_6$  are not transformed during the reaction. They can not be isolated unchanged after the reaction. Differences begin at the stage of formation a catalytically active

form. In the case of  $\text{Co}_2(\text{CO})_8$  (3) formation of catalytically active particles (12) occurs from reaction with the initial alcohol ROH (1). In the the case of the  $\text{W}(\text{CO})_6$  catalytically active particle (22) is formed by separating CO (16) and activation energy of this stage  $E_{1,\text{II}}=132,6$  kJ/mol. Next, the complexes (12 and 22) react with dimethyl carbonate (2) to form (14, 20) and the methoxy anion (11).

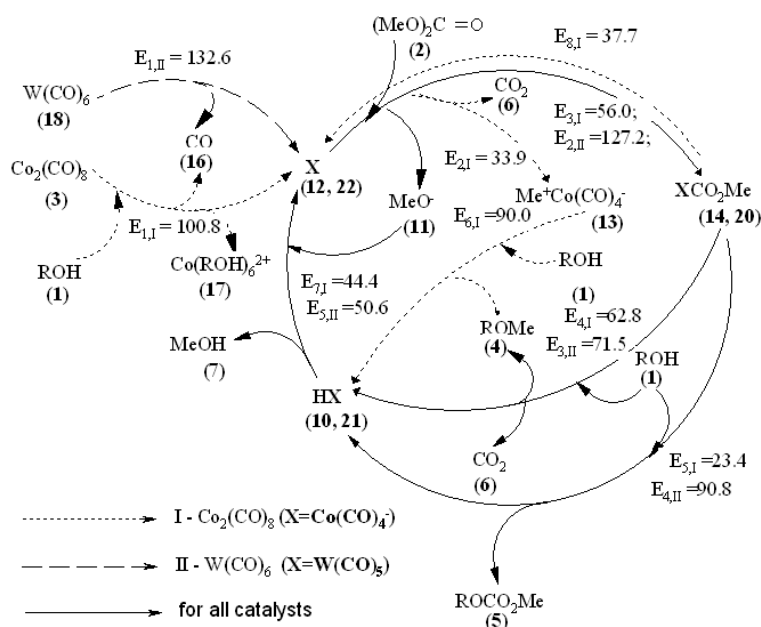


**Fig. 2.** Kinetic model of the reaction of dimethylcarbonate with alcohols in the presence metal complex catalysts

Next, complexes (14 and 20) react with the initial alcohol (1) to form target products (4) and (5). In the first case, the activation energy of formation (4) is more than (5) ( $E_{4,\text{I}}=62,8$  kJ/mol vs  $E_{5,\text{I}}=23,4$  kJ/mol). In the second case, on the contrary, the activation energy (4) is less than (5) ( $E_{3,\text{II}}=71,5$  kJ/mol vs  $E_{4,\text{II}}=90,8$  kJ/mol). As a result, in the first case large quantities  $\text{ROCO}_2\text{Me}$  are formed, and in the second  $\text{ROMe}$ . Simultaneously, in both cases a complex HX (10 and 21) is formed. In a next step HX reacts with previously formed  $\text{MeO}^-$  (11) resulting in by-product (7) and complexes (12 and 22). Then the catalytic cycle closes. For these steps similar activation energies are obtained ( $E_{7,\text{I}}=44,4$  kJ/mol and  $E_{5,\text{II}}=50,6$  kJ/mol).

**Acknowledgement.** The reported study was funded by the President of the Russian Federation SP-669.2018.5 stipends and RFBR according to the research projects No. 18-07-00341, 18-37-00015.

#### References:

- [1] R.I. Khusnutdinov, N.A. Shchadneva, Y.Y. Mayakova, *Rus J Org Chem* 50(6) (2014) 790–795.
- [2] K.F. Koledina, S.N. Koledin, N.A. Shchadneva, I.M. Gubaidullin, *Rus J Phys Chem A*. 91(3) (2017) 444–449.
- [3] K.F. Koledina, S.N. Koledin, N.A. Shchadneva, Y.Yu. Mayakova, I.M. Gubaidullin, *Rus J Phys Chem React Kinet Mech Cat*. 121(2) (2017) 425-438.

## Differential Selectivity Measurements of Phosphine-Containing and Phosphine-Free Catalytic Systems of Mizoroki-Heck Reaction with Aromatic Carboxylic Anhydrides

Larina E.V., Lagoda N.A., Yarosh E.V., Kurokhtina A.A, Schmidt A.F.  
*Irkutsk State University, Chemical Department, Irkutsk, Russia*  
*tendu90@mail.ru*

The results of the kinetic study of attractive for fine organic synthesis modification of well-known Mizoroki-Heck reaction with aromatic carboxylic anhydrides [1] are presented. To establish the nature of the active complexes of phosphine-containing and ligand-free catalytic systems of this reaction, the comparative study of the differential selectivity of competitive reactions was conducted. It is known that in the Mizoroki-Heck reaction with aromatic carboxylic anhydrides the addition of an inorganic halide salt increases the catalytic activity significantly [1]. Therefore, the study of the differential selectivity of ligand-free and phosphine-containing catalytic systems was carried out in the presence of inorganic halide salt. The study of differential selectivity patterns, in contrast to traditional studies of catalytic activity (reaction rate), unambiguously reveals possible changes in the nature of active complexes formed by varying conditions [2]. Two types of competing experiments were carried out: reactions where two aromatic carboxylic anhydrides or two alkenes competed were used to investigate the nature of the active complexes involved in the activation of these substrates. Comparative study of phosphine-containing and phosphine-free catalytic systems demonstrated that the differential selectivity of the reaction under competition of two aromatic anhydrides or two alkenes did not depend on the presence of a tertiary phosphine additive. Such pattern was found for systems containing 2 equiv of phosphine and 6 equiv of various inorganic salts (LiCl, NaCl, NaBr, LiBr, NBu<sub>4</sub>Br) to Pd. This result indicates that palladium complexes do not containing phosphine ligands in their coordination sphere are active in the catalytic cycle steps where activation of aromatic carboxylic anhydride or activation of alkene proceed. However, for catalytic systems containing less than 6 equiv LiCl it was found that limiting Pd/Cl ratios exist, when the tertiary phosphine ceases to be part of the active complexes.

**Acknowledgement.** This work was supported by the Russian Foundation for Basic Research, grant № 18-33-00362 mol\_a.

### References:

- [1] M. S Stephan, A. J. J. M. Teunissen, G. K. M. Verzijl, J. G. de Vries, *Angew. Chem. Int. Ed.* 37 (1998) 662.
- [2] A.F. Schmidt, A.A. Kurokhtina, E.V. Larina, *Catal. Sci. Technol.* 2014. V. 4 (10). P. 3439.

## The Effect of Pd/Al<sub>2</sub>O<sub>3</sub> Modification with Si,W-Heteropolyacid on the Mechanism of 1,3,5-Trichlorobenzene Multi-Phase Hydrodechlorination

Lokteva E.S.<sup>1</sup>, Golubina E.V.<sup>1</sup>, Gurbanova U.D.<sup>2</sup>, Kharlanov A.N.<sup>1</sup>

1 – Lomonosov Moscow State University, Moscow, Russia

2 – Baku Branch of Lomonosov Moscow State University, Baku, Azerbaijan

e.lokteva@rambler.ru

Hydrodechlorination (HDC) provides the convenient way to transform chlorinated organics which are well-known ecotoxicants into hydrocarbons. The most active are Pd catalysts, so the development of improved Pd-containing systems is of practical and theoretical importance. In this work 2 wt.% of Pd was supported by wet impregnation on two types of alumina (E, produced by Engelhard, and C, produced by calcination of boemite at 600°C), both pristine and modified with 20 wt.% of H<sub>8</sub>[Si(W<sub>2</sub>O<sub>7</sub>)<sub>6</sub>]×6H<sub>2</sub>O (HPS), and tested in multi-phase HDC [1] of 1,3,5-trichlorobenzene (TCB, 3.5×10<sup>-4</sup> M, isooctane, 0.1 g of catalyst, Aliquat-336 as interphase transfer agent, 20% KOH water solution, 5 ml/min of H<sub>2</sub>, 50°C). TEM HR demonstrated uniform distribution of HPS and Pd on the surface of alumina, Pd particle size is less than 20 nm and increases in the raw Pd/HPS/Al<sub>2</sub>O<sub>3</sub> (C) < Pd/HPS/Al<sub>2</sub>O<sub>3</sub> (E) < Pd/Al<sub>2</sub>O<sub>3</sub> (C) < Pd/ Al<sub>2</sub>O<sub>3</sub> (E). According to TPR data, significant part of Pd easily reduces even at RT and form PdHx in H<sub>2</sub>, but the other part is more difficult to reduce, and it is lower in HPS-modified catalysts. This fraction grows after catalytic tests.

Table 1. Catalytic properties

Catalyst	TOF, h <sup>-1</sup>	t <sub>50</sub> , min
Pd/Al <sub>2</sub> O <sub>3</sub> (E)	11	180
Pd/Al <sub>2</sub> O <sub>3</sub> (C)	30	250
Pd/ΓΠC-Al <sub>2</sub> O <sub>3</sub> (E)	18.2	62
Pd/ΓΠC-Al <sub>2</sub> O <sub>3</sub> (C)	34.6	105

Using IR DO spectroscopy after CO adsorption, it was found that relatively large Pd<sup>0</sup> particles are the major form of palladium in non-modified catalysts. In modified catalysts the fraction of Pd<sup>0</sup> is much lower, and single Pd<sup>+</sup> and Pd<sup>2+</sup> ions are also found. The features of Lewis

acidity of the catalysts surface and the presence of HPS and/or the products of its thermal decomposition define the possibility of TCB adsorption and activation not only on Pd, but also on a support. Then adsorbed moieties can be reduced with hydrogen spilling over the surface from Pd and W centers. Also the new types of active centers can be formed on the border between Pd and HPS particles. All listed phenomena provide an improvement of catalysts activity (Table 1, t<sub>50</sub> is time of 50% TCB conversion) and stability in aggressive reaction medium after modification of a support with HPS. The catalysts on Al<sub>2</sub>O<sub>3</sub> (E) have better performance due to the feature of structure, as it was found by TEM and XRD.

**Acknowledgement.** The authors acknowledge the Program of Development of Lomonosov Moscow State University for the access to XPS equipment.

### References:

[1] Tundo P., Perosa A., Zinovyev S. J. Mol. Catal. A: Chemical. 2003 (204-205) 747.

## Influence of the Affinity of Metal Precursor to Polymeric Support on Activity of Ligandless Catalysts of Suzuki Cross-Coupling

Nikoshvili L.Zh.<sup>1</sup>, Matveeva V.G.<sup>1</sup>, Sulman E.M.<sup>1</sup>, Kiwi-Minsker L.<sup>2</sup>

1 – Tver Technical University, Tver, Russia

2 – Tver State University, Tver, Russia

*nlinda@science.tver.ru*

At present, ligandless catalysts of cross-coupling reactions are the subject of intensive study. Regarding to such catalysts, the term “cocktail” type catalysts is proposed, because ligandless catalytic systems contains simultaneously different forms of palladium (bulk nanoparticles (NPs), soluble Pd(II) species, soluble Pd(0) species) [1]. It is assumed that these forms of the catalyst are mutually transformed into each other during the reaction, and aryl-halide plays an important role in these transformations [2, 3]. In this context, the rates of palladium dissolution and precipitation, as well as reaction location (in the solution or inside the pores of catalytic support) are of crucial importance. In this work different combinations of polymeric supports (hyper-crosslinked polystyrene (HPS)) and palladium precursors (chlorine-containing precursors and palladium acetate) were studied in the Suzuki reaction.

For as-synthesized unreduced Pd/HPS catalysts containing mostly Pd (II) as an active phase, it was shown that Pd activation occurs under the action of arylboronic acid, which in turn leads to the formation of noticeable amounts of the homocoupling product and to the deposition of Pd(0) NPs. In this case, the ratio of arylboronic acid and aryl-halide as well as the presence of the excess of base play crucial role in ensuring a high yield of cross-coupling product. Moreover, it was found that, in some cases, fast Pd precipitation, which is in turn due to high migration ability of palladium salt inside the polymer, is responsible for fast catalyst deactivation during the reaction. In contrast, in the case of optimal combinations of Pd precursor for the samples with highest activity, the process of NPs formation occurs relatively slow and results to rather small NPs (about 2-4 nm). In the case of catalysts preliminarily reduced in hydrogen flow, Pd(0) NPs are “reservoirs” of active soluble catalytic species formed under the influence of aryl-halide.

As a result of this study, Pd-containing HPS-based catalytic systems with high activity (complete conversion of aryl-halide for the reaction time about 1 h) working at mild reaction conditions (60°C, ethanol-water mixture as a solvent) and at the absence of phase-transfer agents were developed.

**Acknowledgement.** This work was supported by the Russian Science Foundation, grant 15-19-20023.

### References:

- [1] D.B. Eremin, V.P. Ananikov, *Coord. Chem. Rev.*, 346 (2017) 2.
- [2] A.F. Schmidt, A.A. Kurokhtina, E.V. Larina, *Kinetics and Catalysis*, 53 (2012) 84.
- [3] A.A. Kurokhtina, A.F. Schmidt, *ARKIVOC*, 11 (2009) 185.

## Influence of a Hydrothermal Treatment of the Amorphous Aluminum Compounds on the Properties of the Obtained Aluminum Hydroxides

Mukhamediarova A.N., Boretsky K.S., Egorova S.R., Ermolaev R.V., Lamberov A.A.  
*Butlerov Institute of Chemistry KFU, Kazan, Russia*  
*anm030693@gmail.com*

$\gamma$ -Al<sub>2</sub>O<sub>3</sub> is widely used in the petrochemical industry physicochemical properties of which determine its using as a catalyst, catalyst carrier, and adsorbent [1]. On an industrial scale,  $\gamma$ -Al<sub>2</sub>O<sub>3</sub> is produced by heat treatment of its precursors pseudoboehmite (PB) or boehmite. The most common methods for obtaining PB are the precipitation of aluminum hydroxide from Al-containing acidic solutions with a base [2] and the hydrolysis of aluminum alkoxides [3]. These methods allow to control the phase composition and properties of the obtained aluminum hydroxides. However, in both cases, in addition to the target product, the formation of X-ray amorphous compounds is possible. In the first case, incompletely hydrolyzed aluminum salts, in the second, residues of organic fragments are formed [2, 3]. On the one hand, the amorphous component is undesirable in the production of the catalyst due to it reduces the filterability of the precipitate and makes it difficult to wash the pseudoboehmite from impurity ions (Na, Fe, etc.), which are catalytic poisons. In addition, the amorphous component has a low specific surface area [4]. Therefore, the amount of the amorphous component in the pseudoboehmite composition is tried to be minimized. However, on the other hand, the amorphous component is able to provide a positive effect on the catalyst. Amorphous base salts can provide the plastic properties of the catalyst precursor during molding and, after the calcination step, decompose with the formation of a new binding alumina phase [5]. Also, in the recent publications [6], we noted that by transforming the amorphous component of pseudoboehmite using hydrothermal treatment, it is possible to control the properties of the resulting catalyst of the skeletal isomerization of n-butylenes to isobutylene.

There is no systematic study of non-crystalline aluminum compounds in the scientific literature, but these compounds affect the properties of the products obtained from them, which is catalysts particularly. The amorphous aluminum compounds resulting from various methods of obtaining differ in phase composition and properties. The high-purity amorphous aluminum hydroxide is obtained by hydrolysis of organoaluminum compounds. It contains organic residues. The anionic residues of precursor salts are present in the structure of amorphous compounds, obtained by precipitation and thermal decomposition of aluminum nitrate methods. Thus, the purpose of this study was a comparative analysis of various methods for producing amorphous aluminum compounds, such as the precipitation method, thermal decomposition of aluminum salts and alcoholates, and investigation of the properties

### PP-III-29

of hydrothermal treatment (HT) products obtained from them at 110-150 °C for 3 h at the initial pH of the aqueous suspension and the pressure of saturated water vapor.

Amorphous aluminum compounds were obtained by precipitation method using ammoniac-nitrate technology (pH = 6.0; 25 °C), heat treatment of aluminum nitrate (350 °C / 1 h) and the hydrolysis product of organoaluminum compound (550 °C / 2 h), which are the following mixtures:

- amorphous aluminum hydroxide (20.2 wt%) + basic salt (66.0 wt%) + pseudoboehmite (13.8 wt%);
- amorphous aluminum hydroxide (16.3 wt%) + basic salt (83.7 wt%);
- amorphous alumina (100 wt%), respectively.

The amorphous aluminum compound obtained by the precipitation method and the products of its hydrothermal treatment are non-porous ( $S < 5 \text{ m}^2/\text{g}$ ,  $V < 0.02 \text{ cm}^3/\text{g}$ ), the aluminas obtained from it have an acidity of the surface up to  $200 \mu\text{mol NH}_3/\text{g}$ . The amorphous aluminum compound obtained by heat treatment of aluminum nitrate has a porous system with  $S=29 \text{ m}^2/\text{g}$ ,  $V=0.04 \text{ cm}^3/\text{g}$ , and the acidity of the alumina obtained from it is  $116 \mu\text{mol NH}_3/\text{g}$ . After HT we observed phase transformation of amorphous compound into boehmite with increasing of  $S$  to  $161 \text{ m}^2/\text{g}$ ,  $V$  to  $0.17 \text{ cm}^3/\text{g}$  and the acidity of  $\gamma\text{-Al}_2\text{O}_3$  obtained from it up to  $291 \mu\text{mol NH}_3/\text{g}$ . Amorphous alumina has a big system of pores ( $S=334 \text{ m}^2/\text{g}$ ,  $V=0.9 \text{ cm}^3/\text{g}$ ) and high surface acidity ( $652 \mu\text{mol NH}_3/\text{g}$ ). After HT a complete phase transformation into boehmite is observed, which is accompanied by a decreasing of  $S$  to  $127 \text{ m}^2/\text{g}$ ,  $V$  to  $0.55 \text{ cm}^3/\text{g}$ . The acidity of  $\gamma\text{-Al}_2\text{O}_3$  obtained from boehmite is  $203 \mu\text{mol NH}_3/\text{g}$ .

**Acknowledgement.** This work was funded by the Russian Foundation for Basic research according to the research project № 18-33-00559.

#### References:

- [1] A. Ivanova, G. Litvak, G. Kryukova, S. Tsybulya, E. Paukshtis, *Kinet. Catal.* 41 (2000) 122.
- [2] C. Oh, Y. Yi, S. Kim, T. Tran, M. Kim, *Powder Technol.* 235 (2013) 556.
- [3] B. Yoldas. *J. Appl. Chem. Biotechnol.* 23 (1973) 803.
- [4] B. Lippens, J. de Boer. *J. Catal.* 4 (1965) 319.
- [5] C. Ma, X. Zhou, X. Xu, T. Zhu, *Mater. Chem. Phys.* 72 (2001) 374.
- [6] I. Mukhambetov, S. Egorova, A. Mukhamed'yarova, A. Lamberov, *Appl. Catal. A* 554 (2018) 64.

## Polymerization of Propylene on Metal-Complex Catalysts in the Presence of Carbon Nanoparticles

Palaznik O.M., Nedorezova P.M., Polshikov S.V., Klyamkina A.N.

*N.N. Semenov Institute of Chemical Physics, Russian Academy of Science, Moscow, Russia  
polned@mail.ru*

Investigated the polymerization of propylene in bulk monomer with the use of catalyst systems based on *rac*-Me<sub>2</sub>Si(2-Me-4PhInd)<sub>2</sub>ZrCl<sub>2</sub>/MAO and TiCl<sub>4</sub>-(C<sub>2</sub>H<sub>5</sub>)<sub>2</sub>AlCl in the presence of nanoplates of graphene obtained by the chemical (GNP), or thermal reduction of graphite oxide (TROG), highly dispersed graphite (NG) and single-walled carbon nanotubes (SWCNT). According the data of X-ray diffraction analysis, the used graphene nanoplates contain 3-5 layers of graphene. The specific surface area of the GNP-510 m<sup>2</sup>/g, TROG-620 m<sup>2</sup>/g, NG – 480m<sup>2</sup>/g, SWNT – 390 m<sup>2</sup>/g.

The introduction of carbon nanoparticles into the reaction medium during polymerization on the metallocene catalytic system leads to a decrease in its activity (by 1.5 – 2 times), but practically does not affect on the stereoregularity of the synthesized PP. Analysis of kinetic dependences indicates a more stable form of dependence of the polymerization rate on time in the presence of nanocarbon fillers.

The content of the atactic fraction in PP synthesized on a metallocene catalyst is 1 wt.% by weight. When polymerizing propylene on TiCl<sub>4</sub> - (C<sub>2</sub>H<sub>5</sub>)<sub>2</sub>AlCl, the content of the atactic fraction is 50% by weight. At the same time, in the presence of graphene nanoplates, as well as in the presence of graphite or hexagonal boron nitride, there is a significant increase in the activity of the catalytic system TiCl<sub>4</sub> - (C<sub>2</sub>H<sub>5</sub>)<sub>2</sub>AlCl (3 to 5 times) and stereoregularity of the synthesized PP. The strong modifying effect of graphite-like fillers is due to the fact that they act as macroligands in the formation of active centers on their surface [1]. It was shown that in the nanocomposites produced on TiCl<sub>4</sub> - (C<sub>2</sub>H<sub>5</sub>)<sub>2</sub>AlCl the content of PP atactic fraction in composites of PP/TROG is 4-5 wt.% , in composites PP/GNP is 7-10 wt.%, in composites PP/NG is 2 wt.%, while in composites of PP/SWNT is 30-40 wt.%. Low content of irregular fractions in PP obtained in the presence of graphene nanoparticles or highly dispersed graphite is due to the structure used particles. The presence of a greater number of defects and functional groups on the surface of GNP and TRGO compared to NG provides a higher content of atactic fraction. The presence of 3-4 layers of graphene in crystallites is sufficient for the formation of isospecific centers of propylene polymerization using the system TiCl<sub>4</sub>-(C<sub>2</sub>H<sub>5</sub>)<sub>2</sub>AlCl.

On both catalytic systems PP crystallizes in the form of alpha-modification. When using a metallocene catalyst, the degree of crystallinity of the PP is 65-67%, and when polymerizing on TiCl<sub>4</sub> -(C<sub>2</sub>H<sub>5</sub>)<sub>2</sub>AlCl the degree of crystallinity of the PP is 54-56 %.

### PP-III-30

SEM of nascent samples of composite materials indicates a different character of polymer growth on the surface of carbon nanoparticles depending on the type of catalytic system (Fig.1, 2).

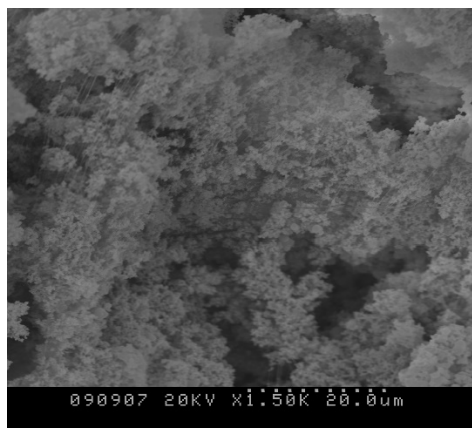


Figure 1. SEM microphotographs of the composite powders of mcPP/GNP (5 wt. %)

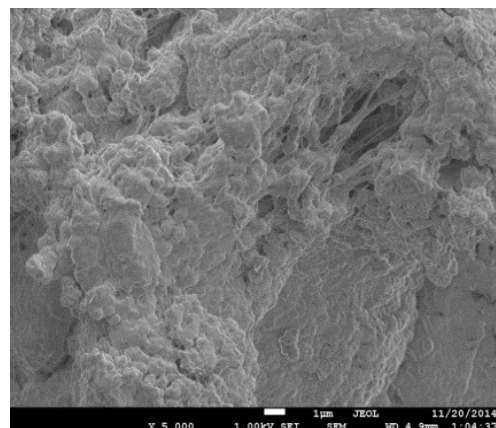


Figure 2. SEM microphotographs of the composite powders Ti PP /TROG (2.5 wt.%)

In case of metallocene catalytic system, polymer grows normally to the surface of filler (Fig. 1). In case of titanium catalyst, polymer replicates the shape of GNP or TRGO particles, arranging in the plane of filler particles surface (Fig.2). The difference in the character of polymer growth on the surface of particles is explained by the extremely high activity of uniformly distributed active centers of the metallocene catalytic system.

The effect of metallocene and titanium catalytic systems on the properties of nanocomposites is investigated in detail.

**Acknowledgement.** This work was supported by the Russian Science Foundation, grant № 18-33-00573 мол\_a.

#### References:

[1] P.M. Nedorezova, N.M. Galashina, V.I. Tsvetkova, T.A. Sukhova., S.L. Saratovskikh, O.N. Babkina, F.S. Dyachkovskii // Eur. Polym. J. 1996. V. 32. N 9. P. 1161.

## Catalysis of Hydroperoxide Decomposition Reactions in the Presence of Group I Metal Compounds

Nurullina N.M., Batyrshin N.N., Kharlampidi Kh.E.  
Kazan National Research Technological University, Kazan, Russia  
nyryllina@mail.ru

The compounds of non-transition metals ( $ML_n$ ) are highly effective catalysts for the “soft” initiation of the process of oxidation of hydrocarbons into relevant hydroperoxides [1].

We have researched the catalytic activity of Na, K, Rb 2-ethylhexanoates (MEH) in the decomposition of isopropylbenzene hydroperoxide (IPBHP), the primary oxidation product of isopropylbenzene. The dependence of the rate of the gross decomposition of the hydroperoxide on its concentration has the form of a “saturation” curve, which indicates the complexation between the components of the catalytic system.

The studied salts are ordered by catalytic activity as follows: Rb > K > Na.

It has been kinetically proven that the decomposition of the hydroperoxide is preceded by the formation of the hydroperoxide-catalyst complex. The stoichiometry of the complexes (1:1) was established, the estimated 6-membered structure of the complex was considered. The kinetic, activation and thermodynamic parameters of the decomposition were determined.

For the first group metals, the values of the enthalpy of complexation and the reaction rate of the decomposition correlate with the ionization potentials (ref. to the following table). With the increasing radius of the metal ion, the ionization potential decreases in the subgroup from top to bottom. The lower the ionization potential, the weaker the bond between the metal and the oxygen atom of the hydroperoxide in the complex, so the decomposition proceeds easier.

Table. Comparison of the kinetic parameters of the IPBHP decay ( $[Cat] = 5 \cdot 10^{-3}$  mol/L)

Catalyst	K (110°C), L/mol	-ΔH, kJ/mol	-ΔS, J/mol·K	$k_3 \cdot 10^2$ (110°C), s <sup>-1</sup>	A <sub>0</sub> , s <sup>-1</sup>	E <sub>a</sub> , kJ/mol	Conditional radius of ion E <sup>+</sup> , nm	Standard electrode potential $E_{E^+/E^0}^0$	Ionization potential, eV	
									IP <sub>1</sub> E <sup>0</sup> → E <sup>+</sup>	IP <sub>2</sub> E <sup>+</sup> → E <sup>2+</sup>
NaEH	1.4	83.9	215.9	5.9	$2.11 \cdot 10^9$	77.3	0.098	-3.05	5.14	47.3
KEH	1.6	72.9	187.6	9.7	$3.06 \cdot 10^{13}$	105.6	0.133	-2.92	4.34	31.8
RbEH	1.3	66.6	171.4	13.7	$4.07 \cdot 10^{12}$	102.4	0.149	-2.93	4.18	27.5

For a more detailed study of the reaction mechanism, quantum-chemical calculations were performed in the Priroda software package. The structures of the molecules of IPBHP, all the studied metal compounds and the reaction products of the primary decomposition of

### PP-III-31

the hydroperoxide, RO<sup>•</sup> and OH<sup>•</sup> radicals, were optimized. Then the structures of the intermediates were modeled and optimized.

Quantum-chemical modeling fully confirmed our assumptions about complexation, and specifically about the 6-member structure of intermediate complexes.

Obviously, the decomposition proceeds in steps, since the process requires high energy costs:



In this scheme, the first stage is the formation of a complex. The second stage is the O–O-bond breaking with the RO<sup>•</sup> radical detachment and the OH<sup>•</sup> radical temporary retention in the coordination sphere of the metal. The third stage is the catalyst regeneration with the release of the hydroxyl radical into the reactional volume. It was established that the limiting stage is the second reaction (2), the subsequent stage of the decomposition requires less energy.

Based on the parameters of the decomposition of IPBHP in the presence of metal-containing catalysts, it was established and quantum-chemically confirmed that in the intermediate activated ROOH–MEH complexes, in addition to hydrogen bonds, the bond between the metal and the oxygen atom of the hydroperoxide is also getting formed.

**Acknowledgement.** The work was done with the financial support of the Ministry of Education and Science of the Russian Federation as a part of the state mission No. 10.956.2017 (PNIL 25.17).

#### References:

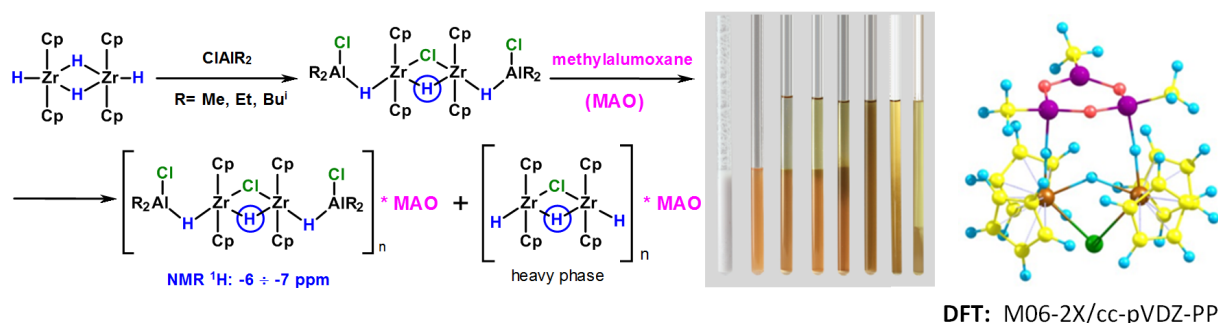
[1] N.M. Nurullina, N.N. Batyrshin, Kh.E. Kharlampidi, *Kinetics and Catalysis*. Vol. 48. No. 5, 649 (2007).

## Bimetallic Zr,Al- Hydrides as Active Intermediates in Alkene Di- and Oligomerization

Parfenova L.V., Kovyazin P.V., Bikmeeva A.Kh., Islamov D.N., Tyumkina T.V.  
*Institute of Petrochemistry and Catalysis of RAS, Ufa, Russia*  
 luda\_parfenova@ipc-ras.ru

Alkene dimers and oligomers represent a large class of compounds, required in various industries. Among the catalytic methods for the alkene di- and oligomerization, approaches that use Ziegler-Natta type systems consisting of metallocenes or postmetallocenes in combination with organoaluminum or organoboron co-catalysts have great potential for the development. It has been repeatedly suggested that metal hydride cations could be the catalyst active forms in the alkene di-, oligo- and polymerization [1]. However, the literature contains scarce experimental information on the structure of the possible adducts and intermediates. All of them, as a rule, refer to the zirconocene and hafnocene hydride derivatives [2-4].

In order to establish the role of metal hydride intermediates in the terminal alkene di- and oligomerization, which run in the presence of catalytic systems metallocene-  $XAlBu_2$  - activator (alkyl(aryl)alumoxanes or pentafluorophenyl borates), we studied the structure and reactivity of bimetallic Zr,Al-hydride complexes formed in the reaction of zirconocene dihydride with chlorodialkylalanes and polymerization activators. Thus, in the systems  $[Cp_2ZrH_2]_2-ClAlR_2$  ( $R = Me, Et, iBu$ ) we observed the formation of new bimetallic Zr, Al - hydride complexes  $Cl(R_2)Al(\mu-H)Cp_2Zr(\mu-H)(\mu-Cl)Cp_2Zr(\mu-H)Al(R_2)Cl$ , characterized by the upfield signals of the bridge Zr-H-Zr hydride in the  $^1H$  NMR spectra in the range  $-7 \div -6$  ppm [5]. It was shown that the new complexes have high affinity to MAO and boron activator  $(Ph_3C)[B(PhF_5)_4]$  and give both toluene-soluble derivatives and poorly soluble heavy adducts. The hydrodynamic radii and volumes of the adducts were found using the DOSY method.



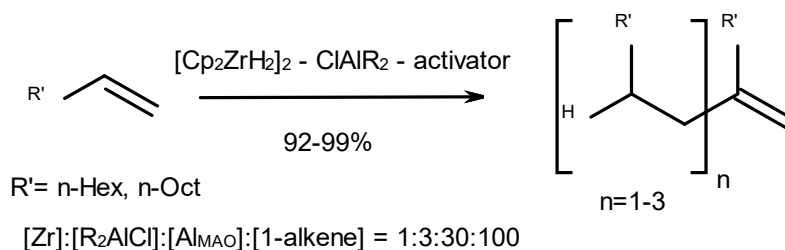
A quantum-chemical study of the possible binding sites of new Zr, Al- hydride complexes to MAO in the case of complete replacement of organoaluminum linkers demonstrated the possible participation of terminal Zr-H bond hydrides and a chlorine atom of the the Zr-Cl-Zr bridge. The consideration of various models of MAO - one-, two- and three-dimensional

### PP-III-32

structures as matrices for binding with the complexes showed the preferable participation of simple chains with  $(\text{MeAlO})_n$  or/and hexagons with  $(\text{MeAlO})_3$  unit.

The applicability of the MALDI TOF/TOF method for mass-spectral study of the complexes of zirconocene hydrides with MAO was shown for the first time. As a result, the fragments  $(\text{AlMeO})_7 \cdot (\text{AlMe}_3) \cdot [\text{Cp}_2\text{ZrH}_2]_2$  and  $(\text{AlMeO})_9 \cdot (\text{AlMe}_3) \cdot [\text{Cp}_2\text{ZrH}_2]_2$  with  $m/z$  948.94 and 1064.44, correspondingly, were found.

The reactivity of adducts of zirconocene hydrides with MAO and  $(\text{Ph}_3\text{C})[\text{B}(\text{PhF}_5)_4]$  towards the alkenes was studied on the example of hexene-1 and octene-1. The reaction takes place in 4-16 hours at room temperature with alkene conversion of 92-99% and the formation of dimers and trimers of alkenes with a starting  $n$ -alkyl group and a terminal methylene double bond, which indicates the participation of hydride intermediates in the first stage of the reaction and chain termination as a result of  $\beta$ -CH activation. Increasing of the reaction temperature to  $60^\circ\text{C}$  shortens the time of the process to 0.5 h. The use of various types of substituents in  $\text{R}_2\text{AlCl}$  significantly affects the ratio of dimers and oligomers. Thus, in a system containing  $\text{Me}_2\text{AlCl}$ , dimers are formed with high selectivity, whereas in the presence of  $\text{Bu}^i_2\text{AlCl}$  only trimers are found.



Thus, it was shown that the new hydride clusters, due to their ability to chemically bind with three-coordinated Al or B atoms, can be used as probes for study the activator structure, and also could serve as model for the detailed research of catalyst activation and alkene transformation stages.

**Acknowledgement.** The work was supported by the Russian Foundation of Basic Research, grant 18-03-01159a.

#### References:

- [1] E. Y. H. Chen, T. Marks, Chem. Rev. 100 (2000) 1391.
- [2] C. Götz, A. Rau, G. Luft, J. Mol. Catal. A: Chem. 184 (2002) 95.
- [3] K. P. Bryliakov, E. P. Talsi, A. Z. Voskoboinikov, S. J. Lancaster, M. Bochmann, Organometallics 27 (2008) 6333.
- [4] M. B. Steven, E. B. John, H.-H. Brintzinger, J. Am. Chem. Soc. 132 (2010) 13969.
- [5] L.V. Parfenova, P.V. Kovyazin, T.V. Tyumkina, D.N. Islamov, A.R. Lyapina, S.G. Karchevsky, P.V. Ivchenko, J. Organomet. Chem., 851 (2017) 30.

## Investigation of the Mechanism of Triethoxysilane Dismutation over Ion-Exchange Resin in a Free Base Form via Operando FTIR Technique

Makarov D.A., Vorotyntsev A.V., Petukhov A.N., Markov A.N.  
Nizhny Novgorod State Technical University n.a. R.E. Alekseev, Nizhny Novgorod, Russia  
*dm.makarov.lmcp@gmail.com*

At this moment, most of the polycrystalline silicon is produced via the Siemens process and its modifications. There are several certain disadvantages concerning Siemens process i.e. high cost of the product, high energy consumption (about 100kWh/kg) due to high temperatures (850 – 1000 °C) used, formation of toxic and corrosive compounds as by-products (SiCl<sub>4</sub>, HCl, Cl<sub>2</sub>), slowness of the process (about 1kg/h) [1,2]. The main alternative to the Siemens process is the Union Carbide process. The main point of the later is to obtain polysilicon via thermal decomposition of monosilane obtained by dismutation of trichlorosilane catalyzed by ion-exchange resins containing quaternary ammonium groups [3]. Silane can be obtained not only by disproportionation of trichlorosilane but also by catalytic dismutation of triethoxysilane (TES), which is more advantageous way due to the ease of separation of the products (silane is the only gaseous product of the reaction), the safety (TES and tetraethoxysilane are much less volatile and toxic than their chloro analogues), the simplicity of the reaction apparatus construction.

In order to investigate the nature of the interaction between TES and anion-exchange resin in a free base form, *in situ* Operando FTIR studies of TES – Amberlyst A21 free base and TES – Amberlyst A21 – ethylmethylketone systems were conducted. In addition, the temperature stability of the catalytic complex being formed during the reaction course was investigated.

According to the obtained data, pentacoordinated silicon containing complex is being formed after TES was introduced to Amberlyst A21 resin. The reaction between TES and ion-exchange resin proceeds fairly rapidly and the catalytic complex showed stability up to at least 100 °C (neat ion-exchange resin starts to decompose at 40 °C). The TES – Amberlyst A21 free base system reacts with a carbonyl compound to give silicon derivative of the corresponding alcohol. The observations mentioned above allowed to conclude that disproportionation of TES over ion-exchange resin in a free base form is likely to proceed as an exchange reaction between pentacoordinated silicon complex and another ethoxysilane molecule which yields in tetraethoxysilane and less substituted silane molecule.

**Acknowledgement.** The reported study was financially supported by Russian Foundation of Basic Research (projects No. 18-33-00914).

### PP-III-33

#### References:

- [1] A.F.B. Braga, S.P. Moreira, P.R. Zampieri, J.M.G. Bacchin, P.R. Mei, *Sol. Energy Mat. Sol. Cells* 92 (2008) 418–24.
- [2] B.S. Xakalashé, M. Tangstad, *South. Afr. Pyromet. 2011 Int. Conf.* (Johannesburg: Southern African Institute of Mining and Metallurgy, 2011) p 83.
- [3] A. Ciftja, T.A. Engh, M. Tangstad *Refining and Recycling of Silicon: A Review* (Trondheim: Norwegian University of Science and Technology, 2008).

## Alternation in Kinetics of C<sub>1</sub>-C<sub>2</sub> Hydrocarbon Oxidation in the Presence of Model OCM Catalysts

Lomonosov V.I., Gordienko Yu.A., Ponomareva E.A., Sinev M.Yu.  
*Semenov Institute of Chemical Physics RAS, Moscow, Russia*  
*katerinaii@inbox.ru*

Oxidative coupling of methane (OCM) is a promising one-step process for ethylene production. It proceeds via the heterogeneous generation of primary methyl radicals and their further transformation into other species in a series of multiple homogeneous and heterogeneous steps. Ethane is the second (after methane) most abundant component of natural and petroleum gases and it also forms as an intermediate molecular product in the OCM reaction. Thus, it seems practical to investigate joint catalytic oxidation of C<sub>1</sub>-C<sub>2</sub> hydrocarbons and determine the effects of their reciprocal influence that is due to a close similarity in their oxidation mechanisms. Being much less reactive than ethane, methane is known to inhibit homogeneous oxidation of ethane [1]. As to OCM catalysts, they inhibit homogeneous oxidation of C<sub>2</sub>-hydrocarbons [2] due to their dual function: they activate alkane molecules, and also contribute to the termination of chain propagation by trapping free radicals. The resulting kinetic effects can be very complex.

In the present work we investigated the C<sub>1</sub>-C<sub>2</sub> hydrocarbon oxidation in the identical conditions in the presence of two efficient model OCM catalysts – NaWMn/SiO<sub>2</sub> and Ca-La/Al<sub>2</sub>O<sub>3</sub>. Experiments were performed in the temperature range of 720-860°C at 25-125 ml/min flow rates using the reactant mixtures of various composition. The experimental data were supplemented with the simulations in the framework of the heterogeneous-homogeneous kinetic model suggested earlier [3].

It was found that in separate oxidation, methane reactivity is higher over the Ca-La/Al<sub>2</sub>O<sub>3</sub> catalyst, whereas in the presence of NaWMn/SiO<sub>2</sub>, ethane reacts faster and the 'conversion vs. contact time' kinetic curves preserve an S-shape character typical for homogeneous chain development (Fig.1). If both alkanes are present in the initial mixture, non-additivity in their activation and product formation is manifested, which becomes more evident at higher temperatures and ethane concentrations (Fig.2).

According to the results of simulations, methane decreases the rate of ethane and ethylene oxidation as an efficient radical scavenger; while ethane accelerates the methane conversion owing to an increase the rate of chain branching. Due to a dual character of the catalyst action mentioned above, the particular manifestation of the reciprocal influence of free radicals and catalytic active sites depends on the concentration and specific activity of the latter. As a result, over Ca-La/Al<sub>2</sub>O<sub>3</sub> which is more active in the alkane molecule activation, ethane reacts slower due to the termination of chain process.

### PP-III-34

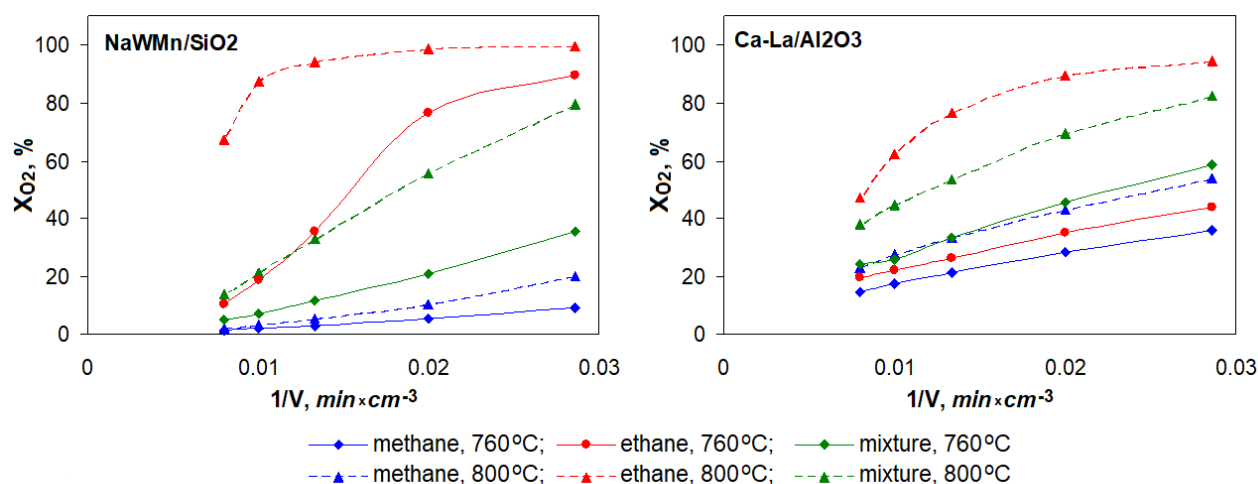


Fig. 1. Oxygen conversion as a function of the inverse flow rate for oxidation of methane, ethane and their mixture over NaWMn/SiO<sub>2</sub> (left) and Ca-La/Al<sub>2</sub>O<sub>3</sub> (right).

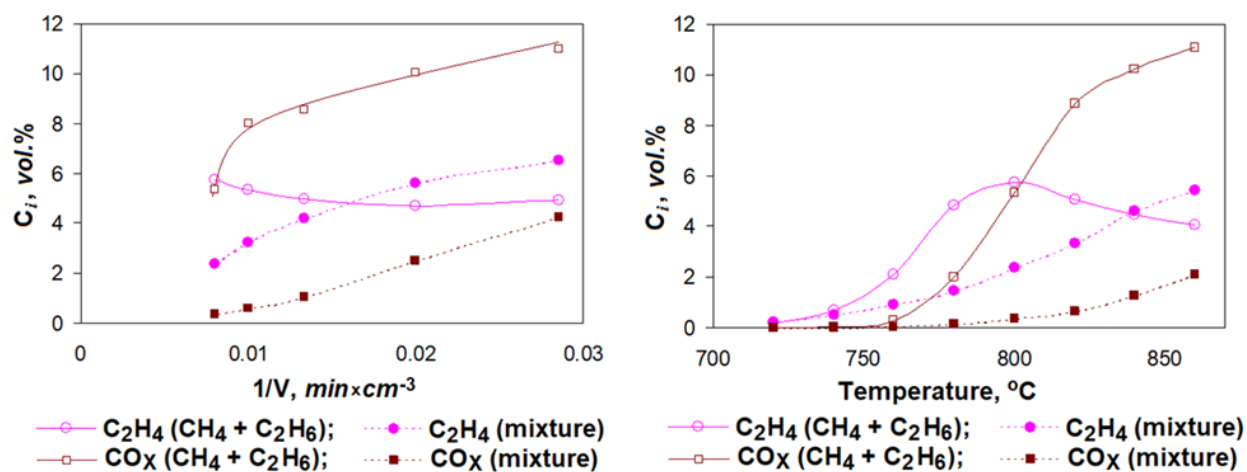


Fig. 2. Concentrations of ethylene and CO<sub>x</sub> as functions of inverse flow rate at 800°C (left) or as functions of temperature at a flow rate of 125 ml/min (right) for oxidation of ethane (solid line) and methane-ethane mixture (dashed line) over NaWMn/SiO<sub>2</sub> catalyst.

**Acknowledgement.** This work was supported by the Russian for Basic Research (RFBR), grant number 18-33-00798; and as a part of the Governmental task for ICP RAS 0082-2014-0007, state registration number AAAA-A18-118020890105-3.

#### References:

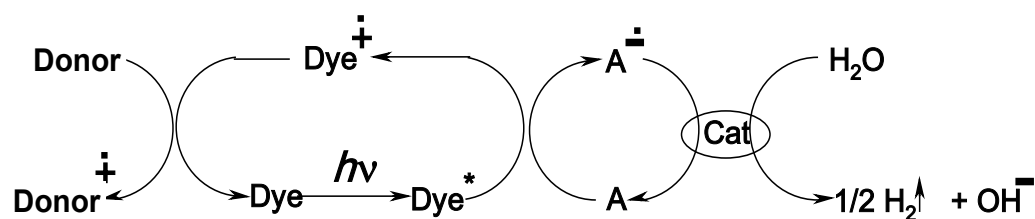
- [1] J.C. Mackie, J.G. Smith, P.F. Nelson, R.J. Tyler, Energy Fuels. 4 (1990) 277.
- [2] V.I. Lomonosov, T.R. Usmanov, M.Y. Sinev, V.Y. Bychkov, Kinet Catal. 55 (2014) 474.
- [3] M.Y. Sinev, Russian Journal of Physical Chemistry B. 1 (2007) 412.

## Photocatalysis of Hydrogen Evolution from Water by Systems Based on Boron Chelates with Diheterylamine

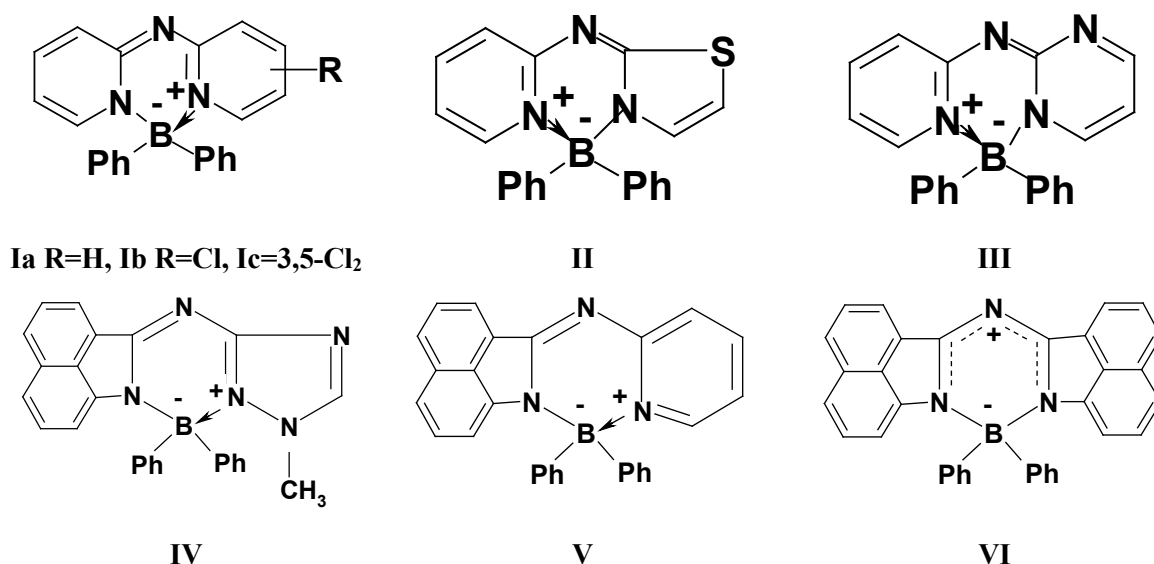
Ponyaev A.I., Glukhova Y.S., Frolov A.N.

*Saint-Petersburg State Institute of Technology (Technical University), Saint-Petersburg, Russia  
ponyaev@technolog.edu.ru*

In solar energy accumulation systems, photochromic transformations of dyes-photosensitizer are an intermediate in the way hydrogen is generated during the photosplitting of water into hydrogen.



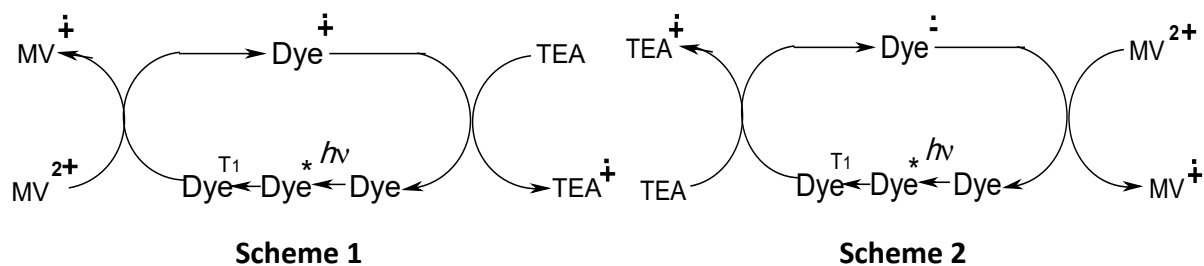
Photophysical and photochemical properties of monoazacyanines (I-VI) containing a boron chelating fragment were studied and the kinetics of the photocatalytic process of hydrogen evolution was studied by chromatographic method. To search for the most effective photocatalysts, the relationship «the structure of an organic dye - the efficiency of water photocleavage» was studied.



Irradiation of azacyanines (I-VI) in the presence of N,N'-dimethyl-4,4'-dipyridylum diperchlorate (methylviologen **MV<sup>2+</sup>**) and triethanolamine (**TEA**) with light with  $\lambda \geq 400 \text{ nm}$  causes photo-reduction of methylviologen. The formation of the radical-cation of methylviologen **MV<sup>+•</sup>** can be estimate by the appearance of a blue color of the solution and the increase in absorption at 605 nm.

### PP-III-35

Azacyanine dyes based on boron chelates with diheterylamine are of interest from the point of view of photocatalysis, since they simulate a structural fragment of phthalocyanines and are stable upon irradiation. Chelates (**I-VI**) have a developed  $\pi$ -system and an unshared electron pair on the nitrogen mesoatom, therefore methylviologene can be reduced by oxidizing (scheme 1) and reducing (scheme 2) redox cycles involving cation- and anion-radicals of photosensitizers (**I-VI**).



Analysis of the spectral-luminescent and electrochemical parameters of azacyanines made it possible to estimate the contribution of the oxidative and reductive mechanisms to the photo-reduction of methylviologen. Calculated by the Rem-Weller equation, the changes in the free electron transfer energy  $\Delta G$  in schemes (1, 2) indicate that chelates (**I-V**) act as a strong electron donor and photoreduction proceeds by the oxidative mechanism (scheme 1). With an increase in the conjugation chain, the contribution of the oxidative mechanism decreases and, in conformity with the  $\Delta G$  values, the photo-reduction of methylviologen already by azacyanine (**VI**) occurs mainly by the reduction cycle (scheme 2).

Flash photolysis was used to study oxygen-free solutions of chelate (**Ib**) in ethanol. In this case, a short-lived photoinduced form is formed with the absorption spectrum maxima at 570 and 670 nm, the kinetics of back reaction of which is described by the pseudo-first-order kinetics. By analogy with the literature data of the photoinduced form, the structure of the chelate radical-cation (**Ib**) is attributed. The rate constant of back reaction of the photoinduced form increases with increasing chelate concentration. Such concentration behavior is characteristic of radical-cations whose disappearance follows the dimerization mechanism. When methylviologen is added, the spectrum of the photoinduced form with  $\lambda_{\max}$  570 and 670 nm is replaced with the spectrum with  $\lambda_{\max}$  605 nm, which is characteristic of the methylviologen radical cation **MV<sup>•+</sup>**.

When irradiated with light with wavelengths  $\lambda > 400$  nm, for 4 hours of a degassed aqueous-alcoholic solution (20 ml) containing one of chelates (**I-VI**), methylviologen, ethylenediaminetetraacetic acid as a sacrificial donor and a colloidal platinum stabilized by polyvinylpyrrolidone, is released molecular hydrogen (3.8 to 4.4 ml).

**Acknowledgement.** This work was supported by the Ministry of Science and Higher Education of the Russian Federation (4.4697.2017 / 6.7) and the Russian Foundation for Basic Research, grant 19-08-01232.

## Catalytic Cracking of Deuterated Hydrocarbons as Method for Investigation of Hydrogen Transfer on Zeolite-Containing Catalyst

Potapenko O.V., Plekhova K.S., Altinkovitch E.O., Krol O.V., Sorokina T.P., Doronin V.P.  
*Center of New Chemical Technologies BIC, Omsk, Russia*  
*potap@ihcp.ru*

Hydrogen transfer reactions occurring during the conversion of hydrocarbons on zeolite-containing catalysts are very important. According to catalytic cracking process, these reactions determine the olefinicity of the C<sub>3</sub> and C<sub>4</sub> fractions, octane characteristics of the gasoline product, and the amount of sulfur in liquid products. When considering petrochemical orientation catalytic cracking process the hydrogen transfer reaction should be minimized. At the same time, the selectivity of the thiophenic compounds conversion to hydrogen sulfide is mainly determined by the hydrogen transfer from paraffinic and naphthenic compounds.

Analysis of the cracking products of model deuterated hydrocarbons and their mixtures with protium form of hydrocarbons and thiophenic compounds makes it possible to evaluate the catalysts activity in the intermolecular hydrogen transfer reactions [1]. In the work, co-conversion of 1-hexene, cyclohexane-d<sub>12</sub> and 2-methylthiophene on mono- and bi-zeolite cracking catalysts were investigated. As the initial zeolites, we used zeolite Y in the HRE- form, zeolites ZSM-5 in the H-form, and also samples treated with alkali (OH/HZSM-5) or phosphorus compounds (P/HZSM-5). The catalyst matrix included alumina and bentonite clay with a ratio by weight – 1: 1.

**Table 1.** Distribution of deuterium in gaseous cracking products during the conversion of feedstock containing cyclohexane-d<sub>12</sub> on catalysts with different ratios of the HREY and P/HZSM-5 zeolites (fixed-bed, 590°C, WHSV = 2.5 h<sup>-1</sup>) [2]

Component	HREY : P/HZSM-5 ratio in catalyst		
	30/10	20/20	10/30
Methane	1.7	1.2	0.8
Ethane	1.1	1.4	1.3
Ethylene	4.8	8.3	13.9
Propane	14.0	14.3	14.8
Propylene	14.9	21.0	28.5
Isobutane	7.2	6.1	4.0
n-Butane	2.6	2.6	2.5
Butylenes	3.2	8.0	13.5
Total	49.4	62.9	79.3

An increase in the ratio of P/ZSM-5 and HREY zeolites (Table 1) in the cracking catalyst composition contributes to the conversion of cyclohexane with the formation of

### PP-III-36

predominantly unsaturated compounds. It is confirmed by the increase in the deuterium amount redistributed to ethylene, propylene and butylene. An increase in the amount of a wide-porous Y-type zeolite leads to a redistribution of deuterium into isobutane, which can be considered as the main product of the intermolecular hydrogen transfer reaction, formed from the tertiary  $C_4H_9^+$  carbocation. The content of deuterium in normal saturated cracking products does not depend on the composition of the catalytic system.

Modification of ZSM-5 zeolite with an alkali allows an increase in the catalytic system activity in the intermolecular hydrogen transfer reactions. In the case of the conversion of sulfur-containing feed, high catalyst activity in the hydrogen transfer reactions contributes to a decrease in the content of sulfur compounds in the liquid cracking products and an increase in the yield of hydrogen sulfide.

Modification of zeolite ZSM-5 with phosphorus compounds leads to reduce the activity of the catalytic system in hydrogen transfer reactions. The conversion of model mixture 1-hexen-cyclohexane- $d_{12}$  observed an increase of deuterium redistributed in  $C_2$ - $C_4$  olefins.

**Acknowledgement.** The work was carried out according to the state task of the IHP SB RAS (project registration number AAAA-A17-117021450095-1).

#### References:

- [1] O.V. Potapenko, V.P. Doronin, T.P. Sorokina, O.V. Krol', V.A. Likholobov. A study of intermolecular hydrogen transfer from naphthenes to 1-hexene over zeolite catalysts. // *Applied Catalysis A: General*, 516 (2016), 153-159.
- [2] O.V. Potapenko, K.S. Plekhova, D.B. Gilyazutdinov, O.V. Krol', T.P. Sorokina, V.P. Doronin. Cotransformations of n-hexadecane, hexene-1, and cyclohexane over dual-zeolite cracking catalysts // *Petroleum Chemistry*, 59 (2019), N. 4, 447-454.

## Catalytic Generation of Radicals in Mixed Micelles {Acetylcholine – Hydroperoxide}

Potapova N.V., Kasaikina O.T.

*Semenov Institute of Chemical Physics RAS, Moscow, Russia*

*Pot.natalia2010@yandex.ru*

Acetylcholine (ACh) refers to neurotransmitters in the peripheral and central nervous system. ACh is excreted by the endings of the vegetative and motor nerve fibers, the excess is removed by cholinesterase. The accumulation of ACh excess leads to an acceleration of the transmission of nerve impulses (excitation), and then the impulse blocking and paralysis. Choline is a part of phosphatidylcholines (PC), natural zwitterionic surfactants that perform metabolic and structural functions in cell membranes. It was found [1,2] that in organic media, ACh catalyzes the radical decomposition of hydroperoxides (ROOH) similar to cationic surfactants ( $S^+$ ).

It was shown [3] that the interaction of phosphatidylcholine with  $CaCl_2$  leads to the initial PC reverse micelles distraction and release of the choline fragment. The resulting system is able to catalyze the radical decomposition of hydroperoxides and initiate radical chain processes. Earlier [2,4], we established that a moderate magnetic field (0.15–0.6 T) reduces the rate of radical generation in reversed mixed micelles  $\{S^+ - ROOH\}$  and  $\{ACh - ROOH\}$ . We have studied the influence of the combinations of PC (Egg lecithin) with salts of Ca and Mg on the decomposition of hydroperoxides using the kinetic model of chain oxidation of  $\beta$ -carotene. It was found that taken separately PC,  $CaCl_2$  and  $MgSO_4$  do not affect ROOH decomposition. Equimolecular mixtures of (PC –  $CaCl_2$ ) and (PC- $MgSO_4$ ) catalyze radical decomposition of hydroperoxide (tert-butyl hydroperoxide) and initiate the  $\beta$ - carotene oxidation. The rate of  $\beta$ - carotene oxidation and chain initiation caused by micellar systems (PC –  $CaCl_2$ ) and (PC- $MgSO_4$ ) was found to decrease in moderate magnetic field (0,15 T). Contrary to that, in the case of homogeneous initiation of  $\beta$ - carotene oxidation by azoinitiator AIBN or homogeneous mixture  $ROOH + Fe(acac)_3$  the same magnetic does not affect the rate of the process.

It is possible that the nucleation and development of atherosclerosis is to some extent related to the oxidative polymerization of unsaturated lipids and lipoproteins on the adsorption layers of PC and ACh, initiated in the presence of  $Ca^{2+}$  and  $Mg^{2+}$  ions and lipoperoxides.

**Acknowledgement.** This work was supported by the Russian Science Foundation, grants 17-03-00364 и 18–33–00742.

### References:

- [1] D.A.Krugovov, E.A.Mengele, O.T.Kasaikina. *Rus.Chem.Bull.*, 8. (2014) 1837.
- [2] O.T.Kasaikina, N.V.Potapova, et al. *Kin. Cat.*, 58 (5), (2017) 567.
- [3] E.A.Mengele, O.T.Kasaikina et al. *Coll.J.*, 20 (6), (2008) 805.
- [4] O.T.Kasaikina, L.M.Pisarenko *Rus.Chem.Bull.*, 10. (2015) 2319

## New Cocatalyst for Alkene Polymerization Reactions with Transition Metal Catalysts

Rishina L.A.<sup>1</sup>, Kissin Y.V.<sup>2</sup>, Gagieva S.Ch.<sup>3</sup>, Lalayan S.S.<sup>1</sup>

1 – Semenov Institute of Chemical Physics, Rus. Acad. Sci., Moscow, Russia

2 – Rutgers, The State University of New Jersey, Department of Chemistry and Chemical Biology, USA

3 – Moscow State University, Department of Chemistry, Moscow, Russia  
rishina@polymer.chph.ras.ru

We investigated cocatalyst effects in alkene homopolymerization and copolymerization reactions with transition metal catalysts of different types. Polymerization results are discussed for ethylene, propylene and higher 1-alkenes (1-hexene, 1-octene, 1-decene, vinyl cyclohexane, 3-methyl-1-butene), as well as copolymerization of ethylene with linear 1-alkenes. Several transition metal compounds were used in combination with a binary cocatalyst  $\text{Al}(\text{C}_2\text{H}_5)_2\text{Cl}/\text{Mg}(\text{C}_4\text{H}_9)_2$  at the  $[\text{Al}]:[\text{Mg}]$  molar ratio  $>2.5$ . The list of catalysts includes traditional catalysts of the  $\text{TiX}_n$  type ( $\text{TiCl}_4$ ,  $\text{Ti}(\text{O}i\text{-C}_3\text{H}_7)_4$ ,  $\text{TiCl}_3$ ) and post-metallocene titanium complexes  $\text{LTiX}_2$  with various organic ligands  $L$ .

The binary  $\text{Al}(\text{C}_2\text{H}_5)_2\text{Cl}/\text{Mg}(\text{C}_4\text{H}_9)_2$  cocatalyst greatly increases activity of traditional catalysts in comparison with  $\text{Al}(\text{C}_2\text{H}_5)_2\text{Cl}$  and activity of post-metallocene complexes in comparison with MAO. The reaction products are high molecular linear polyethylene, amorphous atactic polypropylene, polymers of higher 1-alkenes and ethylene/1-alkene copolymers containing from 1 to 20 mol % of 1-alkenes. Active centers in all the catalyst systems are nonuniform with respect to their kinetic parameters (based on GPC data of polymers), copolymerization ability (DSC data) and stereospecificity (fractionation, DSC and  $^{13}\text{C}$  NMR data). Most active centers produce essentially atactic polypropylene but the catalysts also contain active centers producing a small fraction (5-10%) of moderately isotactic polypropylene. The isospecific centers operate according to the enantiomorphic stereocontrol mechanism the same as the active centers in common Ziegler-Natta catalysts.

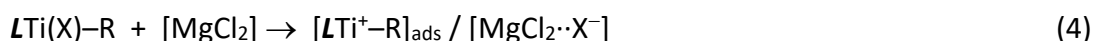
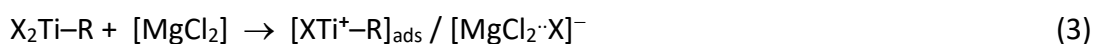
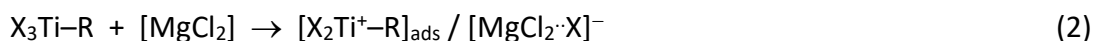
Two reasons for the high activity of ternary  $\text{TiX}_4 - \text{Al}(\text{C}_2\text{H}_5)_2\text{Cl}/\text{Mg}(\text{C}_4\text{H}_9)_2$  and  $\text{LTiX}_2 - \text{Al}(\text{C}_2\text{H}_5)_2\text{Cl}/\text{Mg}(\text{C}_4\text{H}_9)_2$  systems and for multi-center nature of these catalysts can be proposed. First, interaction between  $\text{Al}(\text{C}_2\text{H}_5)_2\text{Cl}$  and  $\text{Mg}(\text{C}_4\text{H}_9)_2$  leads to *in situ* formation of highly dispersed  $\text{MgCl}_2$  with Lewis-acidic surface:



The combination of  $\text{Al}(\text{C}_2\text{H}_5)_2\text{Cl}$  and  $\text{Mg}(\text{C}_4\text{H}_9)_2$  was used in this research at  $[\text{Al}]:[\text{Mg}] >2.5$ . Any Ti compound  $\text{TiX}_4$  or complex  $\text{LTiX}_2$ , which is added to the  $\text{Al}(\text{C}_2\text{H}_5)_2\text{Cl}/\text{Mg}(\text{C}_4\text{H}_9)_2$  cocatalyst at the last step of the catalyst preparation, reacts both with the unreacted excess of  $\text{Al}(\text{C}_2\text{H}_5)_2\text{Cl}$  and with  $\text{Al}(\text{C}_2\text{H}_5)_2(\text{C}_4\text{H}_9)$  formed in Reaction 1.

### PP-III-38

Reactions between titanium compounds  $TiX_4$  or  $LTiX_2$  and organoaluminum compounds  $AlR_3$  and  $AlR_2Cl$  produce various alkylated  $Ti^{IV}$  and  $Ti^{III}$  complexes of the  $X_iTi-R$  type ( $i = 3$  or  $2$ ) and  $LTi(X)-R$  type. These complexes can be adsorbed on the Lewis-acidic  $MgCl_2$  surface and form cationic species containing the  $Ti^+-C$  bond:



Such cationic species are commonly regarded as catalytically active centers in alkene polymerization reactions with Ziegler-Natta catalysts.

Another reason for the high activity of the  $TiX_4 - Al(C_2H_5)_2Cl/Mg(C_4H_9)_2$  and  $LTiX_2 - Al(C_2H_5)_2Cl/Mg(C_4H_9)_2$  systems could be an interaction between  $Al(C_2H_5)_2Cl$  and  $Mg(C_4H_9)_2$  [or  $Mg(C_4H_9)Cl$ , the intermediate product in Reaction 1], which leads to the formation of ion pairs  $[Mg-C_4H_9]^+ [A]^-$  and  $[Mg-Cl]^+ [A]^-$ , where  $[A]^- = [Al(C_2H_5)_2(C_4H_9)_2]^-$  or  $[Al(C_2H_5)_2(C_4H_9)Cl \cdots Al(C_2H_5)_2(C_4H_9)_2]^-$ . Such ion pairs can convert  $X_3Ti^{IV}-R$ ,  $X_2Ti^{III}-R$  and  $LTi(Cl)-R$  complexes into other types of cationic active centers containing the  $Ti^+-R$  bond, for example:



As a result, all the  $TiX_4$  ( $LTiX_2$ ) -  $Al(C_2H_5)_2Cl/Mg(C_4H_9)_2$  catalysts contain several types of active centers, which differ in solubility, kinetic stability, stereospecificity and the average molecular weight of polymer material they produce.

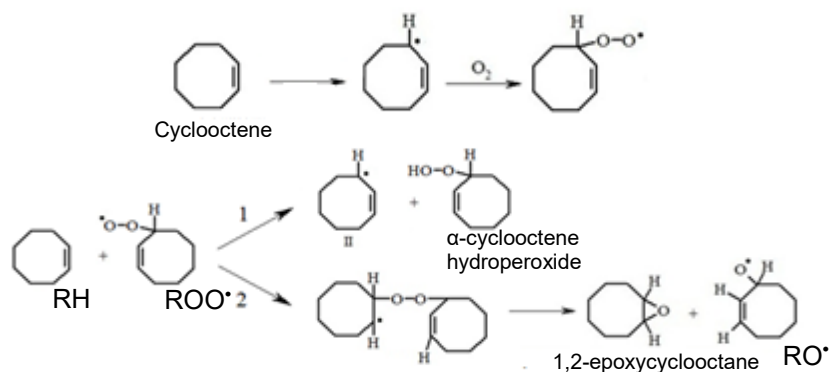
The data obtained in this research show that combinations of a  $TiX_4$  ( $LTiX_2$ ) and the binary  $Al(C_2H_5)_2Cl/Mg(C_4H_9)_2$  cocatalyst can be viewed as special types of supported catalysts.

**Acknowledgement.** This work was supported by the Russian Science Foundation, grant № 18-13-00375.

## The Mechanism of Cyclooctene Epoxide Formation in the Process of Catalytic Liquid-Phase Oxidation of Cyclooctene by Molecular Oxygen

Shangareev D.R., Antonova T.N., Sivova T.S., Abramov I.G.  
 Yaroslavl State Technical University, Yaroslavl, Russia  
 antonovatn@ystu.ru

It is known [1] that in the process of initiated liquid-phase oxidation of cyclooctene — cycloolefin with average cycle size and with a rehybridized double bond by molecular oxygen — unlike other olefins, cyclooctene epoxide (1,2-epoxycyclooctane) is formed with a yield of up to 70%. The process proceeds by a radical-chain mechanism, where peroxy radicals ( $\text{ROO}\cdot$ ) become principal radicals leading the chain. However, this radical can participate both in the formation of cyclooctene hydroperoxide (1) and in the reaction of cycloaddition to cyclooctene — the main way to form 1,2-epoxycyclooctane (2).



To increase the yield of obtaining the target epoxide, in this process it is proposed to use a catalytic system with a pronounced regulating function, which makes it possible to correct the mechanism of epoxide formation in such a way that it becomes possible to eliminate direction 1 in the above scheme and the reaction of the cycloaddition while keeping the radical-chain way of transformation of the original cyclooctene by using a catalytic system comprising an organic compound of d-metal and substituted phthalimide [2]. In this case, the process of obtaining epoxide proceeds through the formation of an intermediate catalytic complex, d-metal atoms, radicals  $\text{ROO}\cdot$ , cyclooctene molecules due to their donor-acceptor interaction taking part in the formation of this complex. Inside this complex, polarized of the bond  $-\text{O}-\text{O}-$  in the radical  $\text{ROO}\cdot$ , so both oxygen atoms take part in the formation of epoxide. As a result of the use of the catalytic system, the yield of the desired epoxide increases to 84–88%.

### References:

- [1] M.M. Mogilevich, E.M. Pliss. Oxidation and oxidative polymerization of unsaturated compounds, M.: Khimiya, 1990.  
 [2] Catalytic system for the oxidation of cyclooctene to epoxide by molecular oxygen Chemical / Sivova T.S. // 5th International School-Conference on Catalysis «Catalyst Design: From Molecular to Industrial Level»: Abstracts. –Novosibirsk, 2018. – P.278.

## Polyoxide Catalysts Based on Pillared Clays for the Oxidative Dehydrogenation of Ethane to Ethylene

Shorayeva K.A.<sup>1</sup>, Massalimova B.K.<sup>1</sup>, Sadykov V.A.<sup>2</sup>, Nauryzkulova S.M.<sup>1</sup>, Altynbekova D.T.<sup>1</sup>,  
Jetpisbayeva G.D.<sup>1</sup>

*1 – Taraz State University, Taraz, Kazakhstan*

*2 – Boreskov Institute of Catalysis, Novosibirsk, Russia*

*k.a.shorayeva@mail.ru*

One of the most important and key monomers of the organic synthesis is ethylene, which in recent years has seen a high consumption growth in the world. The particular interest is the production of ethylene by the method of oxidative dehydrogenation at relatively low temperatures using effective catalytic systems for the selective oxidative dehydrogenation of ethane to ethylene [1].

We have synthesized polyoxide Mo-, La-, Nb-containing catalysts based on Zr-, Al-, Zr/Al-pillared clays. It has been used montmorillonite and kaolinite natural clays of Kazakhstan deposits for the preparation of pillared clays [2]. The use of pillared clays as a carrier and carrying out the process of catalytic oxidative dehydrogenation of ethane to ethylene at a low temperature allows saving energy costs, and thus leads to cheaper process and cost of the synthesized catalysts.

The process of catalytic oxidative dehydrogenation was carried out on the “OXI-1” installation at temperatures of 400–460 °C and contact time of 0,1–15 s. The initial reaction mixture (% vol.) was C<sub>2</sub>H<sub>6</sub> : O<sub>2</sub> : N<sub>2</sub> = 10:10:80. The studies were carried out on a flow-type installation at atmospheric pressure in a tubular quartz reactor with a fixed catalyst bedding of a fraction of 0,25-0,50 mm. The analysis of the initial materials and the reaction products was carried out using the chromatographic method on a “Chromos GK-1000” device. The amount of the obtained target product was from 45,1 to 91,2 % as a result of varying of the reaction temperature, the composition of the initial reaction mixture, the space velocity, the content and composition of the active phase of the catalyst.

New catalysts have a high potential for use in the development of perspective catalytic systems and can be considered as universal tools for use in the process of oxidative dehydrogenation of ethane to ethylene.

### References:

[1] Che-Galicia G., Ruiz-Martinez R.S., Chemical Engineering Journal. 280 (2015) 682-694.

[2] Kalmakhanova M.S., Massalimova B.K., Herald of L.N. Gumilyov Eurasian National University. №6 (121). 2017. 16-19.

## Copper Containing Catalysts Based on CeO<sub>2</sub>- ZrO<sub>2</sub> Supports for Ethanol Conversion

Sil'chenkova O.N., Bychkov V.Yu., Matyshak V.A.  
*Semenov Institute of Chemical Physics RAS, Moscow, Russia*  
*son1108@yandex.ru*

Introduction. Ethanol is widely applied in chemical industry for production of various chemicals. For the last years an ethanol conversion reactions are considered as a very efficient way of hydrogen production for fuel cells. Apparently several reactions of ethanol conversion such as a water-gas reforming, partial oxidation and oxidative water-gas reforming have been investigated in the presence of supported oxide catalysts. Among them copper containing catalysts based on CeO<sub>2</sub>- ZrO<sub>2</sub> supports were found to be very promising ones for ethanol conversion. In the present work an attempt has been made to elucidate mechanism of ethanol conversion via investigating nature and transformation routes of surface compounds formed by interaction of ethanol at the surface of copper containing catalysts based on CeO<sub>2</sub>- ZrO<sub>2</sub> supports by spectrokinetic method.

Experimental. Set of supports of composition CeO<sub>2</sub>, 0.8CeO<sub>2</sub>-0.2ZrO<sub>2</sub>, 0.5CeO<sub>2</sub>-0.5ZrO<sub>2</sub>, 0.2CeO<sub>2</sub>-0.8ZrO<sub>2</sub>, ZrO<sub>2</sub> was prepared by Pechini method. The supported 5% CuO catalyst samples were synthesized by impregnation procedure. The both catalysts and supports were characterized by set of tools such as XRD, ESR, ESDR, TPR H<sub>2</sub> as well as by measurements of specific surface area, FTIR spectroscopy of CO adsorption and thermal desorption of CO and CO<sub>2</sub>. FTIR spectroscopy was applies for investigation of surface intermediates in the course of ethanol conversion.

Mass-spectroscopic analysis of ethanol conversion products was performed by OmniStar GSD 301 (Pfeiffer) followed by simultaneous measurements of sample weight with TGA SETSYS Evolution System (Setaram).

Results and discussion. Application of these experimental methods allowed to identify the activity of the catalyst surface as a function of ZrO<sub>2</sub> concentration in catalyst support:

- according to XRD data copper containing mixed oxides catalysts are the solid solutions of cubic structure with a lattice parameter which is linearly decreases with increasing ZrO<sub>2</sub> concentration what causes increase of crystallites concentration with high crystal-face indexes as well as increase of the terminal oxygen atoms concentration on the catalyst surface.
- decreasing average clusters size correlates with increase of the catalyst specific surface area.
- increasing bond-strength of surface oxygen atoms with increase of ZrO<sub>2</sub> concentration.
- coordination of Cu<sup>2+</sup> ions is changing from plane quadrate in case of CeO<sub>2</sub> to octahedral one with some tetrahedral distortion in case of ZrO<sub>2</sub>.

### PP-III-41

Thus, varying ratio between CeO<sub>2</sub> and ZrO<sub>2</sub> in the catalyst support it is possible to change properties of the supported active phase.

Ethoxy-, acetate-, formate groups and condensation products were detected as the main surface intermediates of ethanol conversion. Rate of their conversion into reaction products decreases with increasing bond-strength of oxygen atoms in CuO clusters.

Acetic and crotonic aldehydes, acetone, butene are formed from by conversion of condensation products. Hydrogen, CO and CO<sub>2</sub> are formed by the following reaction route:



No formation of surface formate complexes was observed over catalysts with a high bond-strength of oxygen atoms. It was also observed that in the absence of the surface formate complexes decrease of hydrogen formation and no CO formation had taken place. It means that in the selected catalyst candidates on the base of CeO<sub>2</sub> - ZrO<sub>2</sub> supports one may regulate their efficiency toward hydrogen formation over Cu/CeO<sub>2</sub> or toward CO formation over Cu/ZrO<sub>2</sub> catalysts.

**Acknowledgement.** This work was supported by the Russian Foundation for Basic Research, grant 18-03-00627 A.

## Improvement of Selectivity to $\gamma$ -Valerolactone in Hydrodeoxygenation of Lignocellulose Derived Levulinic Acid by Ir Catalyst Modification

Simakova I.L.<sup>1,2</sup>, Demidova Yu.S.<sup>1,2</sup>, Devi N.<sup>3</sup>, Dhepe P.<sup>3</sup>, Bokade V.<sup>3</sup>

1 – Boreskov Institute of Catalysis, Novosibirsk, Russia

2 – Novosibirsk State University, Novosibirsk, Russia

3 – CSIR-National Chemical Laboratory, Pune, India

simakova@catalysis.ru

Nano-phased transition bimetallic catalytic systems attract significant attention due to their tunable physical and chemical properties [1]. Compared to monometallic counterparts, the bimetallic systems are usually more advantageous and often exhibit enhanced efficiency because of the synergism between two metal centers. The cooperative effect of noble and non-noble metals for designing the bimetallic catalysts benefits for sustainable catalyst development [2, 3]. In this work this approach is extended to bimetallic systems comprising noble Ir and a non-noble Re or Sn metals to develop effective catalysts for complex processing of lignocellulose derived levulinic acid (LA) into valuable chemicals and biofuels, e.g.  $\gamma$ -valerolactone (GVL) (Fig. 1).

LA (CA) (98%, Acros Organics, Belgium) in polar aprotic 1,4-dioxane was hydrogenated in a batch reactor at 140-180°C, 20-30 bar of H<sub>2</sub>. Ir, ReOx or IrReOx catalysts were prepared by impregnation with IrCl<sub>3</sub> and HReOx precursors, respectively, followed by hydrogenation at TPR conditions and characterized by TEM, XRD, XPS, TPR [4]. Reaction components were analyzed by GLC using BP20 capillary column (60 m/0.25 mm/0.25  $\mu$ m) (Chromos GC-1000).

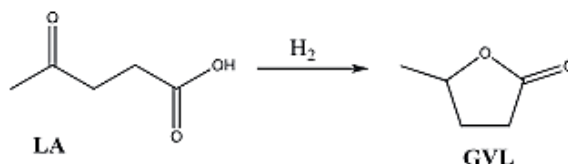


Fig. 1. LA transformation to GVL

The composition of IrReOx centers was tailored by sequence of metal introduction, variation of Ir/Re ratio, reduction temperature and estimated by the ability of bimetal IrRe center to transform LA into GVL predominantly. Samples of catalysts were characterized by TEM, XRD, XRF and N<sub>2</sub> physisorption. The regularities obtained for LA hydrogenation were applied for development of selective GVL synthesis (Fig. 2). The role of Re was found to strengthen terminal C=O group adsorption on ReOx sites compared to monometallic Ir providing high catalytic activity and selectivity in C=O hydrogenation [5].

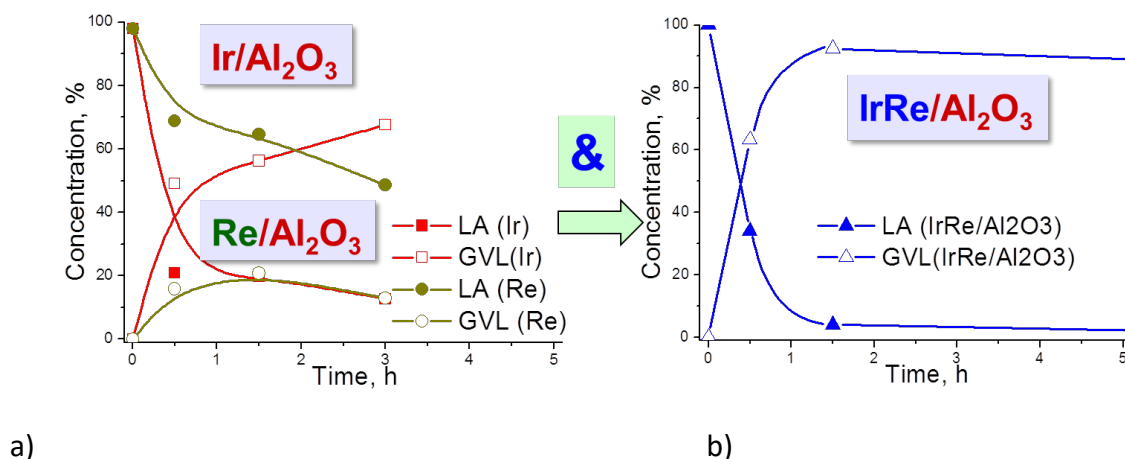


Fig. 2. LA transformation to GVL over a) Ir/Al<sub>2</sub>O<sub>3</sub> and ReOx/Al<sub>2</sub>O<sub>3</sub>, b) IrReOx/Al<sub>2</sub>O<sub>3</sub>. Reaction conditions 4%Ir4%Re/C, 165°C, 20 bar, 1,4-dioxane, catalyst mass 240 mg.

Application of the bimetallic IrReOx catalysts to control selectivity seems to be promising in the case of GVL synthesis from LA. The general and kinetic regularities for LA hydrogenation over mono- and bimetallic IrReOx catalysts were discussed in detail.

**Acknowledgement.** This work was supported by RFBR Grant 18-53-45013 IND\_a.

#### References:

- [1] J. Bozell, G. Petersen, *Green Chem.* 12 (2010) 539–554.
- [2] M. Tamura, K. Tokonami, Y. Nakagawa, K. Tomishige, *ACS Sustainable Chem. Eng.* 5 (2017) 3685–3697.
- [3] Q. Yu, X. Zhang, B. Li, J. Lu, G. Hu, A. Jia, C. Luo, Q. Hong, Y. Song, M. Luo, *J. Mol. Catal. A: Chem.* 392 (2014) 89–96.
- [4] I.L. Simakova, Yu.S. Demidova, S.A. Prikhodko, M.N. Simonov, A.Yu. Shabalin, *J. Siberian Federal University Chemistry* 3 (2015 8) 439-449.
- [5] I.L. Simakova, Yu.S. Demidova, S.A. Prikhodko, M.N. Simonov, A.Yu. Shabalin, *J. Siberian Federal University Chemistry* 9 (4) (2016) 443-453.

## Reactor with Membrane Catalyst: Experimental Evaluation and Intensification Hypothesis

Gavrilova N.N., Sapunov V.N., Skudin V.V.  
*D. Mendeleev University of Chemical Technology, Moscow, Russia*  
*skudin@muctr.ru*

The main purpose of the development and creation of any membrane reactors is the intensification of the processes occurring in them. Membrane catalyst is a device in which the catalytically active substance is placed on the membrane surface. The reaction and transport of the substance are mated in the pore space in such a device. In addition, an extremely important feature of such catalysts is the possibility of conjugation of exergonic and endergonic processes. This circumstance leads to the intensification of the whole process, allowing the reactions prohibited by Gibbs.

Although the membrane catalyst (RMC) reactors have been known for a long time, but only in the aftermath of 10–20 years did a new direction appear in their design. The review [1] presents the various applications and advantages of such reactors. As advantages of such reactors, the authors of the works call a significant decrease in the process temperature, complete removal of impurities with low concentrations from mixtures, an increase in the conversion rate of the initial reagents, a decrease in contact time, a decrease in the amount of active substance required to achieve the same results as in traditional reactor.

An objective comparison of the effectiveness of reactors with membrane and traditional catalysts is an important scientific and practical task. The main difficulty of this comparison is that these catalysts have a different principle for influencing reagents. The kinetic experiment allows us to solve this fundamental problem. A recently published paper [2] showed that under dry reforming of methane (DRM) conditions, the specific constant found for the initial rate of the limiting stage of this process — methane dissociation into carbon and hydrogen — for traditional and membrane catalysts can differ by two orders of magnitude. That is, the initial rate of dissociation of methane (endergonic process) on a membrane catalyst is hundreds of times higher than on a traditional catalyst! Since the composition of the reaction mixture and the process temperature when comparing the catalysts were the same, the main differences were in the smaller mass of the active substance in the membrane catalyst and its device. Therefore, the reason for the intensification of the DRM process should be sought in the conjugation of exergonic and endergonic processes. It was found that the phenomenon of thermal creep (or also thermal transpiration) occurs on the membrane catalyst, causing gas circulation through the pore structure of this catalyst and increasing the real contact time.

### References:

- [1] T. Westermann, T. Melin. *Chemical Engineering and Processing* 48 (2009) 17.
- [2] A. V. Alexandrov, N. N. Gavrilova, V. R. Kislov, V. V. Skudin. *Petr. Chem.* 57 (2017) 804.

## On the Nature of Active Sites of Ethylene Polymerization in the Presence of Nickel(II)- $\alpha$ -Diimine Complexes

Soshnikov I.E.<sup>1,2</sup>, Semikolenova N.V.<sup>1</sup>, Antonov A.A.<sup>1,2</sup>, Bryliakov K.P.<sup>1,2</sup>, Talsi E.P.<sup>1,2</sup>

1 – Boreskov Institute of Catalysis, Novosibirsk, Russia

2 – Novosibirsk State University, Novosibirsk, Russia

talsi@catalysis.ru

One of the most important features of nickel(II) N,N- $\alpha$ -diimine polymerization catalysts (LNi<sup>II</sup>Br<sub>2</sub>, where L = neutral bidentate N,N- $\alpha$ -diimine ligands) is their ability to produce branched polyethylenes by ethylene homopolymerization via “chain-walking” mechanism. Unfortunately, these catalysts suffer from the rapid deactivation at high temperatures, preventing their industrial application [1]. In this context, a detailed understanding of the mechanism of their catalytic action could put the design of thermally stable and highly active nickel catalysts on a rational basis. However, the nature and properties of Ni(II) species formed in the systems LNi<sup>II</sup>Br<sub>2</sub>/MAO and LNi<sup>II</sup>Br<sub>2</sub>/MMAO (MAO = methylalumoxane, MMAO = modified methylalumoxane) was poorly understood until recently.

Using <sup>1</sup>H, <sup>13</sup>C and <sup>1</sup>H-<sup>13</sup>C correlation NMR spectroscopy we have established the nature of the Ni(II) complexes formed upon the activation of the pre-catalyst L<sup>1</sup>NiBr<sub>2</sub> (complex **1**, Figure 1) with MAO and MMAO (L<sup>1</sup> = 1,4-bis-2,4,6-dimethylphenyl-2,3-dimethyl-1,4-diazabuta-1,3-diene). The heterobinuclear ion pair [L<sup>1</sup>Ni<sup>II</sup>( $\mu$ -Me)<sub>2</sub>AlMe<sub>2</sub>]<sup>+</sup>[MeMAO]<sup>-</sup> (complex **2**, Figure 1) was observed at the initial stage of the reaction of L<sup>1</sup>NiBr<sub>2</sub> with MAO at -40 °C, whereas the ion pair [L<sup>1</sup>Ni<sup>II</sup>-<sup>t</sup>Bu]<sup>+</sup>[MeMMAO]<sup>-</sup> (complex **3**, Figure 1) predominates at the initial stage of the reaction of L<sup>1</sup>NiBr<sub>2</sub> with MMAO under the same conditions. Further warming the samples **1**/MAO and **1**/MMAO up to 25 °C leads to a rapid reduction of the Ni(II) centre to the EPR-active monovalent state (Ni(I), S = 1/2). The cationic Ni(I) complex **4** (Figure 1) with proposed structure [L<sup>1</sup>Ni<sup>I</sup>]<sup>+</sup>[MeMMAO]<sup>-</sup> (more than 70  $\pm$  20% of total Ni content) and aluminum complex with anion-radical of N,N- $\alpha$ -diimine ligand L<sup>( $\cdot^-$ )</sup>AlMe<sub>2</sub> (complex **5**, Figure 1) were found in the catalyst system **1**/MMAO at 25 °C.

The catalytic studies have shown that system **1**/MMAO displays activity toward ethylene polymerization at 50 °C, producing branched polyethylene (43 br/1000 C) with high molecular weight (M<sub>w</sub> = 76 000 g/mol) and narrow MWD (M<sub>w</sub>/M<sub>n</sub> = 1.9). It was surprising that complex **1** pre-activation with MMAO during 1 hour at 25 °C does not lead to the catalyst activity lost: only 2-fold activity decrease was found. The PE obtained has similar M<sub>w</sub> (90 000 g/mol), MWD (2.4), and branching (39 br/1000 C) values.

According to EPR data, the addition of ethylene (600 eq.) to the sample **1**/MMAO containing complex **4** at -70 °C leads to a visible decrease of the intensity of resonances of **4** (g<sub>||</sub> = 2.21, g<sub>⊥</sub> = 2.06, A<sub>⊥(2N)}</sub> = 1.06 mT) and appearance of those of a new complex **6** (g<sub>||</sub> = 1.99, A<sub>|| (1N)}</sub> = 1.51 mT, g<sub>⊥</sub> = 2.34). In contrast to complex **4**, complex **6** exhibits hfs from one nitrogen

atom. The concentration of **6** in the reaction mixture is strongly dependent on the amount of ethylene added ( $[4]/[6] = 15$  at  $n(\text{C}_2\text{H}_4)/n(\text{Ni}) = 200$ , and  $[4]/[6] = 4$  at  $n(\text{C}_2\text{H}_4)/n(\text{Ni}) = 600$ ). After complete ethylene consumption, **6** disappears, and initial concentration of **4** is restored. The EPR spectra of **4** and **6** are significantly different. The EPR spectrum of **4** is typical for Ni(I) species with  $g_{\parallel} > g_{\perp}$  and displays hfs from two nitrogen atoms  $A^{\perp} = 1.06$  mT. Complex **6** displays EPR spectrum with  $g_{\parallel} < g_{\perp}$  and hfs from one nitrogen atom  $A_{\parallel} = 1.51$  mT. Probably, **6** is adduct of **4** with ethylene  $[\text{L}^1\text{Ni}(\text{C}_2\text{H}_4)]^+[\text{MeMMAO}]^-$ . This assumption is supported by the ease of the reversible conversion between **4** and **6** upon the addition or consumption of ethylene. The dramatic difference between the EPR spectra of **4** and **6** can be caused by significant distortion of geometry of nickel(I) complex **4** upon ethylene coordination.

It is generally accepted that cationic alkyl complexes of Ni(II) are the active species of ethylene polymerization, catalyzed by  $\alpha$ -diimine complexes of nickel [2]. The data obtained here show that predominantly paramagnetic Ni(I) species are present in the catalyst system **1**/MMAO/ $\text{C}_2\text{H}_4$  at room temperature (complexes **4** and **6**), whereas cationic alkyl complexes of Ni(II) (complex **3**) are not observed. Nevertheless, this system appears active in ethylene polymerization. Hence, the exact role of Ni(I) species in ethylene polymerization, catalyzed by  $\alpha$ -diimine complexes of Ni(II) is still unclear and requires further studies.

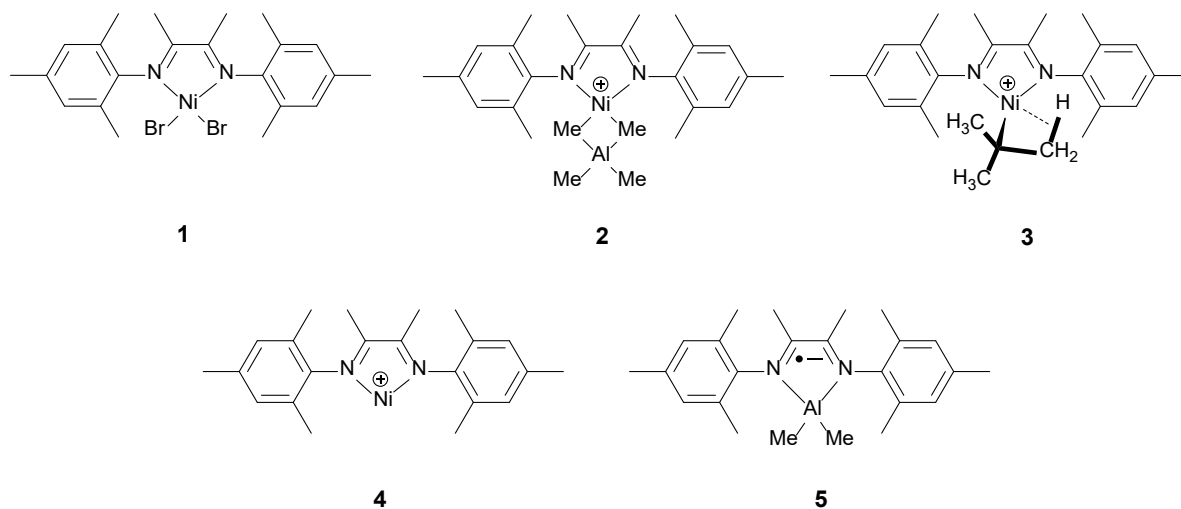


**Figure 1.** Structures of the complexes **1-5** considered in present work.

**Acknowledgement.** This work was supported by the Russian Foundation for Basic Research (grant 18-53-80031) and the National Natural Science Foundation of China (grant 5171102116).

#### References:

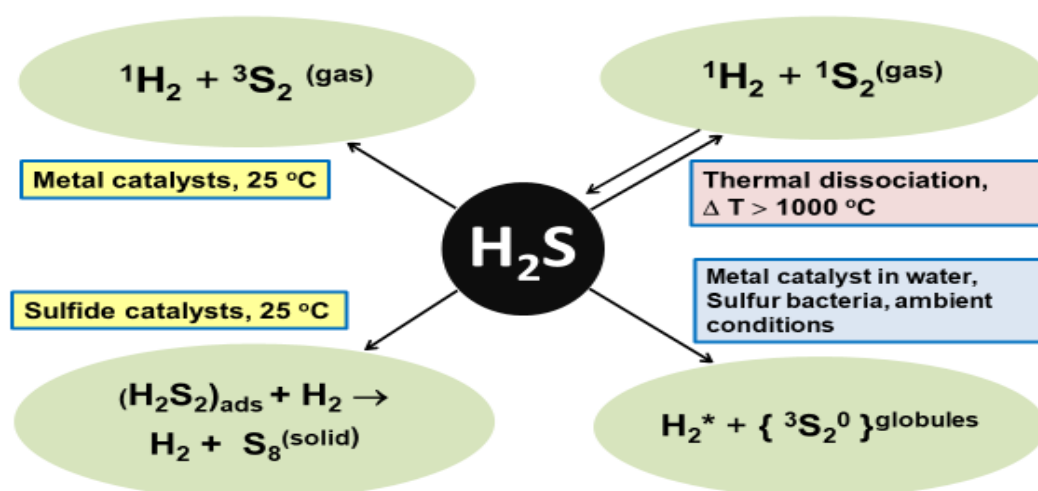
- [1] W.H. Sun, Soc. open sci. 5 (2018) 180367.  
 [2] M.D. Leatherman, S.A. Svejda, L.K. Johnson, M. Brookhart, J. Am. Chem. Soc. 125 (2003) 3068.

## The Key Role of Catalysts in the Low Temperature Process of H<sub>2</sub>S Decomposition: Non-Equilibrium Thermodynamics of Open Systems

Startsev A.N.  
JSC "Katalizator", Novosibirsk, Russia  
startsev@catalyst.su

Four possible pathways of H<sub>2</sub>S decomposition into hydrogen and elemental sulfur are considered (Fig) [1,2]. In the thermal process, H<sub>2</sub>S dissociation results in the formation of diatomic both hydrogen and sulfur molecules in the singlet state according to the rules of the "classical" reversible thermodynamics.

The reaction mechanisms of low-temperature H<sub>2</sub>S decomposition on sulfide and metal catalysts are considered in the framework of thermodynamics of non-equilibrium irreversible processes for open systems [3], since these processes occur at room temperature without supplying thermal energy from the outside due to the internal chemical energy of substrate molecules – hydrogen sulfide.



2

On sulfide catalysts, the irreversible process of H<sub>2</sub>S decomposition proceeds through the stage of formation of disulfane, H<sub>2</sub>S<sub>2</sub>, as a key intermediate, and the reaction products are hydrogen and solid sulfur. The reaction occurs through a number of successive exothermic stages of H<sub>2</sub>S molecule dissociation, in which entropy of the system decreases due to its dissipation into the environment in the form of bound energy TΔS. The remaining part of free energy ΔG is accumulated on the catalyst surface and is used for implementation of the energy-consuming stage of decomposition of adsorbed intermediates and removal of hydrogen in the gas phase.

### PP-III-45

Metal catalyst ensures capture and accumulation of energy from the exothermic processes of adsorption and dissociation of the initial H<sub>2</sub>S molecules into the atomic adsorbed species of hydrogen and sulfur. The stored energy is used for the chemical conversion of adsorbed atomic intermediates into the final reaction products – molecular hydrogen and gaseous diatomic triplet sulfur, followed by its desorption into the gas phase. Hydrogen production from H<sub>2</sub>S is realized at room temperature with the efficiency of 99.6% on metal catalysts immersed into the liquid which is capable well-dissolving H<sub>2</sub>S and diatomic sulfur [4]. These results offer very attractive perspectives for the creation of a new innovative energy-saving technology for the toxic H<sub>2</sub>S disposal instead of the long-outdated energy-consuming technology by the Claus method, while the target product is hydrogen instead of water.

In the process of H<sub>2</sub>S decomposition on metal catalysts at room temperature, the previously unknown diatomic gaseous sulfur in the ground triplet state was obtained, the existence of which was predicted by quantum chemistry. Some properties of the triplet diatomic sulfur and the white globular hexagonal sulfur (an unknown allotrope of solid sulfur) obtained from the saturated aqueous solutions of the triplet sulfur are considered [5]. Similarity of the morphology of hydrophilic white sulfur globules and bacterial colorless sulfur S<sup>0</sup> obtained by sulfur bacteria in the processes of chemosynthesis of organic matter from CO<sub>2</sub> and H<sub>2</sub>S, allowed to develop an alternative hypothesis about the nature of bacterial sulfur S<sup>0</sup> and possible mechanism of chemosynthesis of carbohydrates with participation of sulfur bacteria.

#### References:

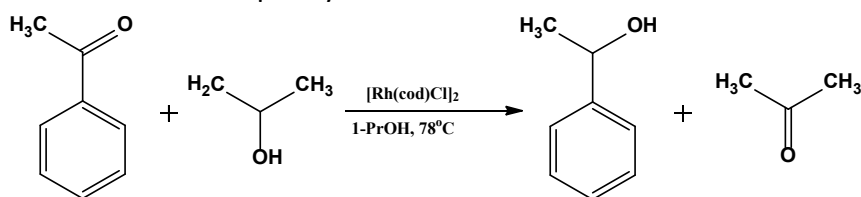
- [1] A. N. Startsev. *Kinet. Catal.*, 57 (2016) 511–522.
- [2] A.N. Startsev, *J Thermodyn Catal.*, 8 (2017) 2.
- [3] I. Prigogine, *Introduction to thermodynamics of irreversible processes*, Sprinfield, Illinois, U.S.A., 1955.
- [4] A.N. Startsev, O.V. Kruglyakova, et al. *J Sulfur Chem.* 37 (2016) 229-240.
- [5] A.N. Startsev, O.V. Kruglyakova, et al. *Russ J Phys. Chem. A.* 89 (2015) 19-23.

## Catalytic Transfer Hydrogenation of Acetophenone over Rhodium Nanoparticles

Goryunova V.D., Strakhov V.O., Nindakova L.O.  
 Irkutsk National Research Technical University, Irkutsk, Russia  
 nindakova@istu.edu

It is known that metal colloids modified with optically active stabilizers, exhibit catalytic activity in asymmetric hydrogenation of ketones [1]. The catalytic properties of metal nanoparticles depend on many parameters, including their size [2], which can be controlled by selecting the conditions of formation of the system [3] and the insertion of additional stabilizers [4].

In the reaction of asymmetric transfer hydrogenation of acetophenone (Aph) in i-PrOH the rhodium nanoparticles were studied, which is formed by reduction of the complex  $[\text{Rh}(\text{COD})\text{Cl}]_2$  using  $\text{N}_1, \text{N}_2$ -bis(thiophene-2-yl-methyl)cyclohexane-1,2-diamine as a modifier. In General, the reaction proceeds according to the scheme presented in the figure with the formation of the enantiomers of 1-phenylethanol.



For additional stabilization of rhodium nanoparticles in the experiments we used polyvinylpyrrolidone (PVP) and cross linked polyvinylpyrrolidone (CL PVP).

So, in the presence of PVP it were achieved rate values (0,35 mol/l\*h) and conversion (29,0 %). When using CL PVP the conversion (17,7 %) decreases, which may indicate that part of the rhodium nanoparticles are inaccessible for the substrate, being located deep in the mesh crosslinked polymer.

The greatest excess of (S)-(-)-enantiomer of the product (46,7 %) were obtained when the reaction is carried out in the absence of polymers. Polymeric stabilizers produce results 41.8 % and 40.8 % for PVP and CL PVP , respectively.

### References:

- [1] H. Bonnemann, G.A. Braun, Chem. Eur. J. 3 (1997) 1200. DOI: 10.1002/chem.19970030805.
- [2] R. Narayanan, M. A. El-Sayed, J. Phys. Chem. B 109 (2005) 12663.
- [3] E. Zhan, C. Chen, Y. Li, W. Shen, Catal. Sci. Technol. 5 (2015) 650-659. DOI: 10.1039/C4CY00900B.
- [4] A. Gniewek, A.M. Trzeciak, Top.Catal. 56 (2013) 1239-1245. DOI: 10.1007/s11244-013-0090-6.

## Trimetallic Naphtha Reforming Catalysts. Properties of the Metal and Acid Functions of Pt–Re–Zr/ $\gamma$ -Al<sub>2</sub>O<sub>3</sub>–Cl

Tregubenko V.Yu.<sup>1</sup>, Vinichenko N.V.<sup>1</sup>, Belopukhov E.A.<sup>1</sup>, Paukhtis E.A.<sup>2</sup>, Belyi A.S.<sup>1</sup>

*1 – Center of New Chemical Technologies BIC, Omsk, Russia*

*2 – Boreskov Institute of Catalysis, Novosibirsk, Russia*

*kalininga\_ihcp1@mail.ru*

The naphtha reforming process is very important in the petroleum refining and petrochemical industries because it is one of the main suppliers of high octane gasoline and aromatic hydrocarbons. A great improvement in the process occurred when a bifunctional metal–acid catalyst was introduced.

Platinum is the best element for the metallic function of the naphtha reforming catalyst. Bimetallic Pt-Re systems have a great stability. Many patents involve catalysts with three elements in the metal function. Zr-modified systems have a great attention in recent publications [1, 2]. The effect of Zr addition is the decrease of acidity and increase of stability of the catalysts.

Our purpose in this work is to deduce the influence of the zirconium and its method of addition on the catalytic properties of the metallic function on the catalytic and acid-related properties of these materials in reforming reactions.

Pt-Re/Al<sub>2</sub>O<sub>3</sub>-ZrO<sub>2</sub> systems were prepared. The supports were prepared by mixing aluminum hydroxide with an zirconium oxide precursor (Zr(ONO<sub>3</sub>)<sub>2</sub>·5H<sub>2</sub>O and Zr(OCl)<sub>2</sub>·8H<sub>2</sub>O). The calculated zirconium oxide content was from 0.1 to 2.0 wt.%. Pt and Re content was in the range of commercial catalysts (0.25 and 0.3 wt.%, respectively). The synthesized catalysts were calcined in a flow of dry air at 500°C for 1 h and reduced in a hydrogen flow at 500°C for 1 h with sulfurization (0.07 wt.% S). The catalysts were tested in a model reaction of n-heptane reforming.

To study Zr effect on the state of platinum centers the infrared diffuse reflection spectroscopy (IR) of adsorbed CO was used.

Table 1 IR CO data

LAS type	LAS -1	LAS-2	LAS-3	LAS-4	ΣLAS-2 и 3	ΣLAS
$\nu_{CO}, \text{cm}^{-1}$	2178-2183	2190-2195	2196-2198	2235		
Sample	Concentration, $\mu\text{mol/g}$					
Pt-Re/Al	51	264	26	0.3	290	341.3
Pt-Re/0.1ZrCl	94	290	35	0.2	325	420.2

### PP-III-47

The acidic properties of the catalysts were studied by IR CO. Four types of Lewis acid sites (LAS) were identified on the samples surface, which correspond to the maxima of the absorption bands at 2179-2180  $\text{cm}^{-1}$  (LAS-1), 2190-2191  $\text{cm}^{-1}$  (LAS-2), 2198-2203  $\text{cm}^{-1}$  (LAS-3) and 2230-2235  $\text{cm}^{-1}$  (LAS-4) (table 1).

According to the classical bifunctional mechanism, the reactions of skeletal isomerisation and cyclisation of n-alkanes start on the metal function with a step of dehydrogenation to n-alkenes. The n-alkene produced is then adsorbed on the acid function where it is transformed to an i-alkene (isomerisation) or a cyclic alkane (cyclisation). The cycloalkanes are dehydrogenated on the metal function and the resulting C<sub>5</sub>-C<sub>6</sub> cyclic alkenes are further inter-isomerised (cyclopentenes to cyclohexenes) on the acid sites. The final step occurs on the metal function, where i-alkanes are produced by hydrogenation of i-alkenes and aromatic hydrocarbons are produced by dehydrogenation of the corresponding cyclohexenes.

Table 2 Kinetic parameters of the aromatization reaction for PtRe/ZrCl samples

Characteristics	PtRe/Al	PtRe/0.1ZrCl	PtRe/0.4ZrCl	PtRe/0.7ZrCl
$k_a \cdot 10^{-2}, \text{s}^{-1} (T = 773 \text{ K})$	3.6	5.0	4.9	4.9
$E_a, \text{kJ/mol}$	152.8	141	142	152.8

Therefore, it can be assumed that for the PtRe/0.1ZrCl reforming catalyst, the increase in activity and selectivity of aromatization is associated with an increase in the concentration of acid sites of medium strength. Moreover, the optimal composition of LAS of medium strength for zirconium-modified n-alkane dehydrocyclization catalysts is represented mainly by LAS type 2, increasing their concentration contributes to an increase in the activity and selectivity. The concentration of more stronger LAS-3 during the course of the modification can be increased, most likely, to a certain limit, while the performance characteristics of the n-heptane aromatization catalyst will increase. A further increase in the concentration of LAS-3 sites will facilitate the course of hydrocracking reactions.

According to the values of the aromatization rate constant and the activation energy (table 2), the optimal amount for modifying Pt-Re/Al<sub>2</sub>O<sub>3</sub> is 0.1-0.4 %wt. ZrO<sub>2</sub>.

**Acknowledgement.** This work was supported by the Ministry of Science and Higher Education of the Russian Federation in relating with the Program of Fundamental Scientific Investigations of State Academies of Sciences on 2013-2020 years, direction V.46, project №V.46.2.4 (No. AAAA-A17-117021450095-1).

#### References:

- [1] M.-Y. Kim, S. Park, G. Seo, K.-S. Song // Catalysts. 3 (2013) 88.
- [2] Long L.-L., Xia K., Lang W.-Z., Shen L.-L., Yang Q., Yan X., Guo Y.-J. // Journal of Industrial and Engineering Chemistry. 51 (2017) 271.

## Low-Temperature Sintering of the Active Components of Pd/C Catalysts

Troitskii S.Yu., Zavarukhin S.G.

*Boriskov Institute of Catalysis, Novosibirsk, Russia*

*tsy@catalysis.ru*

One of the reasons for the deactivation of catalysts containing metals deposited on the surface of carriers is the sintering or migration of particles of active components of these catalysts. There is abundant evidence in the literature on such a decontamination mechanism. However, the described observations and studies of catalytic processes are carried out for processes occurring at a relatively high temperature. Under mild conditions, the possibility of sintering was not considered.

It was assumed that even under conditions of heterogeneous catalysis in the liquid phase, the deactivation of catalysts as a result of sintering is possible even in ambient conditions.

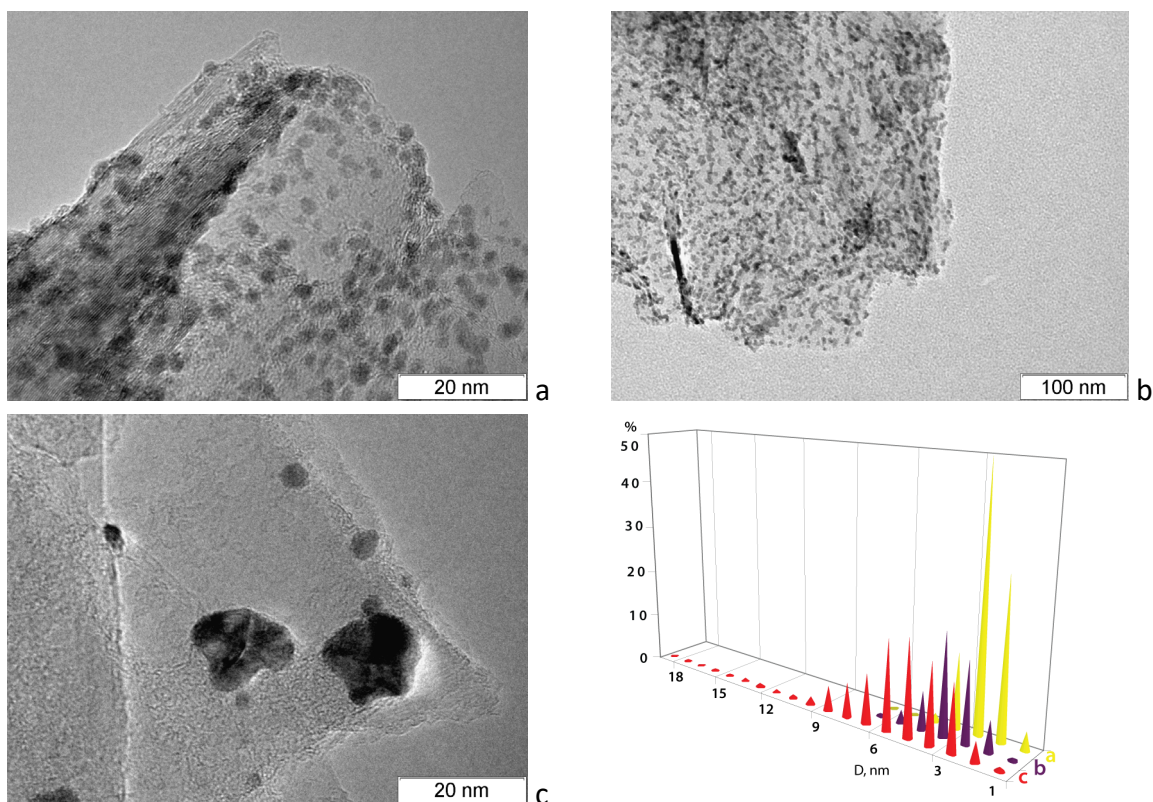


Fig.1. TEM images and corresponding histograms of Pd/C samples: a – Pd PHC/C, b – Pd/C after H<sub>2</sub> reduction, c – Pd/C after cyclohexene hydrogenation.

The main issue was the heat transfer of the energy released in the exothermic reaction from the particles of the active component to the reaction medium and the carrier particle. For experimental confirmation of the possibility of low-temperature sintering were prepared catalysts containing adsorbed on the surface of graphite particles [1] of palladium (II) polynuclear hydroxocomplexes (PHC), 2% Pd/C. The hydrogenation of cyclohexene was

carried out at atmospheric pressure and 20 C, in a reactor equipped with a magnetic stirrer. Firstly the catalysts were tested without reagents by stirring in methanol and 1atm H<sub>2</sub> for 1 hour. The same test was providing in 10% cyclohexene solution in methanol. The results of the TEM study of the catalysts before and after testing are shown in Fig.1.

It is shown that the reduction of palladium hydroxide to metal occurs in the hydrogen medium (established by the EDX method) and a slight increase in particle sizes is observed, possibly due to an increase in the contrast of Pd metal image compared to the PHC. No large metal particles were found. The hydrogenation reaction under the same conditions leads to a significant increase in the average diameter of Pd particles and the formation of very big particles, up to 100 nm.

The use of porous media, such as carbon, makes it difficult to accurately measure changes in the dispersion of the active component of catalysts by TEM due to the high contrast of the carriers themselves. Catalysts Pd/C (4% Pd) before and after the reaction of hydrogenation of nitrobenzene were studied by measuring the CO chemisorption. The average diameter of Pd particles in the initial catalyst is 3.1 nm, and after the reaction (turnover number 200) – 6.4 nm.

The change in the apparent diameter of the particles of the active component can be associated both with the segregation of palladium particles on the surface of the carbon, and with the loss of the active surface as a result of its coating with a carbon film. However, both processes exist only at very high temperatures of the active centers.

Calculations based on the equations of heat and mass transfer allowed to estimate the thermal states of dispersed palladium particles and Pd/C catalysts under the ambient conditions of liquid-phase cyclohexene hydrogenation. It is shown that:

1. Under the cooling of catalyst (2% Pd/C) by methanol, in the stationary process conditions, the temperature of the catalyst grain will be higher than the medium temperature by 0.1 K.
2. In the hypothetical absence of heat transfer between Pd particles and the reaction medium, the temperature of the particles can lifting up to thousands degrees.
3. The hydrogenation process can lead to boiling of methanol in the pores of the carrier for 10 minutes after the start of the reaction.

The calculations confirm the possibility of segregation of the active component particles observed in the experiments. In addition, the possibility of boiling the solvent in the pores of the catalysts can lead to a periodic mechanism of the process accomplished by local overheating and cooling of the reaction zone.

**Acknowledgement.** This work was supported by Ministry of Science and Higher Education of the Russian Federation (project AAAA-A17-1170410090-3).

**References:**

- [1] S. Yu. Troitskii, A. L. Chuvilin, D. L Kochubei, B. N. Novgorodov, E. N. Kolomiichuk, and V. A. Likholobov, Russ. Chem. Bull.,- 1995, - Vol. 44, - N10, - P. 1822.

## Features of the Oxidation of Light Saturated Hydrocarbons under Heterogeneous Catalysis

Vasileva E.A., Mukhamedzyanov R.R., Sitmuratov T.S., Petukhov A.A., Akhmedyanova R.A.  
*Kazan National Research Technological University, Kazan, Russia*  
*elina.vasiljeva@mail.ru*

Saturated hydrocarbons are major sources of raw materials for the chemical industry. Thus, content of linear saturated C<sub>5+</sub> hydrocarbons depends on oil type and ranges from 10 to 70 %. Associated petroleum gas from Siberian fields contain from 134 to 450 g/m<sup>3</sup> of hydrocarbon of C<sub>3</sub>-C<sub>5</sub> structure, depending on the deposit.

It is gaining growing importance rational use of natural gas and the possibility of its processing into liquid products which can be used as motor fuel or additives thereto. The study of gas liquation into liquid hydrocarbons solves problems related to the processing of associated petroleum gas.

Scientific-technical and patent literature review showed that the oxidation of hydrocarbons with oxygen or oxygen-containing gas takes place mainly at the tertiary carbon atom, as breaking of the primary and secondary C-H bond requires much more energy. The oxidation of aliphatic hydrocarbons is an important industrial process for obtaining valuable oxygen-containing organic compounds such as hydroperoxides, alcohols, aldehydes, ketones, carboxylic acids, and many others.

The hydrocarbons oxidation by oxygen proceeds with formation of corresponding hydroperoxide as primary product. On the one hand the metals oxides of variable valence accelerate the oxidation process, on the other hand they decompose the hydroperoxide with formation of associated products [1-8]. Oxides of Co, Mn, Mo, Ni, Fe, Cu, Ag, Cr, and etc are widely used as a heterogeneous catalysts for oxidation of saturated hydrocarbons in gas and liquid phase[1-8].

In this work, isopentane was used as a substrate, and heterogenic catalytic systems based on manganese oxides/alumina oxide and cobalt oxides/alumina oxide were used. The oxidation process was carried out in a titanium reactor at a temperature 120 °C and pressure 3 MPa.

The efficiency of the oxidate, obtained during the oxidation of isopentane, was evaluated as a high-octane additive to automotive gasolines. It is shown that the addition of 3% of the obtained oxidate significantly increases the octane number of the reference fuel.

### References:

- [1] N.N. Semenov. Chain reactions / N. N. Semenov. - L.: Goskhimtekhnizdat, 1934. – 562 pages.
- [2] N.N. Semenov. About some problems of chemical kinetics and reactivity (free radicals and chain reaction.) – 2nd reslave. and additional prod. – M.: Academy of Sciences of the USSR, 1958. - 686 pages.

### PP-III-49

- [3] N.M Emanuel. The chain reaction of hydrocarbons oxidation in the liquid phase/ N. M. Emanuel, E. T. Denisov, Z. K. Mayzus. – M.: Science, 1965. - 375 pages.
- [4] N.M Emanuel. The course of chemical kinetics / N. M. Emanuel, D. G. Knorre. – M.: High school, 1966. – 431 pages.
- [5] N.M Emanuel. Modern state of the theory of chain processes of liquid-phase oxidation of hydrocarbons / N. M. Emanuel // New petrochemical processes and prospects of petrochemistry development. – M.: Chemistry, 1970. – Page 35-56.
- [6] N.M Emanuel. The kinetics of the liquid-phase oxidation of organic substances / N. M. Emanuel // Chemical physics. – 1982. - No. 1. – Page 91-104.
- [7] E. T. Denisov. The boundaries of the chain reaction mechanisms of hydrocarbon oxidation / E. T. Denisov // Chem. physics. – 1982. - No. 1.- p. 105-112.
- [8] N.M Emanuel. The role of the environment in radical-chain oxidation reactions of organic compounds / N. M. Emanuel, T. E. Zaikov, Z.K. Mayzus. – M.: Science, 1973. - 279 pages.

## Isopropylbenzene Oxidation Kinetic Model

Vovdenko M.K.<sup>1</sup>, Vovdenko A.G.<sup>1</sup>, Koledina K.F.<sup>1</sup>, Gubaydullin I.M.<sup>1,2</sup>

1 – Institute of Petrochemistry and Catalysis RAS, Ufa, Russia

2 – Ufa State Petroleum Technological University, Ufa, Russia

Mikhail\_vovdenko@rambler.ru

Isopropylbenzene oxidation process is intermediate stage of phenol and acetone production in so called cumene method. Cumene (isopropylbenzene – IPB) is main raw material for this industrial process. IPB is oxidized by air oxygen in order to obtain hydroperoxide of isopropylbenzene (HP IPB). Then mixture of IPB and HP IPB goes to distillation stage, where concentrated HP IPB is received. After concentration stage HP IPB undergo decomposition during which mixture of phenol and acetone is received [1].

Oxidation of IPB is radical-chain reaction which is initiated by certain radical particles. Also IPB oxidation is autocatalytic process, which means that main product itself serves as source of radical particles, which are necessary for reaction (initiator).

From the analysis of the kinetic models presented in [1] - [4], the reaction scheme represented in Table 1 was developed.

Table 1. Isopropylbenzene oxidation reaction scheme

№	Elementary stage	№	Elementary stage
1	$RH \rightarrow R\bullet + H\bullet$	9	$RO\bullet + ROOH \rightarrow ROO\bullet + ROH$
2	$RH + O_2 \rightarrow R\bullet + HO_2\bullet$	10	$R\bullet + RO_2\bullet \rightarrow ROOR$
3	$ROOH \rightarrow RO\bullet + HO\bullet$	11	$2RO_2\bullet \rightarrow ROOR + O_2$
4	$RH + RO\bullet \rightarrow R\bullet + ROH$	12	$RO\bullet \rightarrow ACP + CH_3\bullet$
5	$RH + HO\bullet \rightarrow R\bullet + H_2O$	13	$CH_3\bullet + O_2 \rightarrow CH_3O_2\bullet$
6	$R\bullet + O_2 \rightarrow ROO\bullet$	14	$CH_3O_2\bullet + RH \rightarrow CH_3COOH + R\bullet$
7	$ROO\bullet + RH \rightarrow ROOH + R\bullet$	15	$RO\bullet + RH \rightarrow \alpha\text{-MS} + H_2O + R\bullet$
8	$2R\bullet \rightarrow RR$	16	$CH_3O_2\bullet + RO_2\bullet \rightarrow ROH + HCOH + O_2$

List of stable components includes RH, ROOH, O<sub>2</sub>, ROH, H<sub>2</sub>O, RR, ROOR, ACP, CH<sub>3</sub>COOH, α-MS, HCOH. The unstable radicals include R•, H•, RO•, HO<sub>2</sub>•, HO•, CH<sub>3</sub>•, CH<sub>3</sub>O<sub>2</sub>•.

In order to determine concentration of radical we made quasi-steady state assumption, which means that equating rates of radicals accumulation during process to zero. For e.g. concentrations of some radicals are represented below:

$$[RO\bullet] = \frac{k_3[ROOH]}{k_4[RH] + k_3[ROOH] + k_{12} + k_{15}[RH]}$$

$$[R\bullet] = \frac{-B_1 + \sqrt{B_1^2 - 4A_1C_1}}{2A_1},$$

### PP-III-50

where

$$A_1 = k_9$$

$$B_1 = k_6[O_2] + k_{10}[RO_2 \bullet]$$

$$C_1 = -(k_1 + k_2[O_2] + k_4[RO_2 \bullet] + k_2[OH \bullet] + k_7[ROO \bullet] + k_7[ROO \bullet] + k_{14}[CH_3O_2 \bullet] + k_{15}[RH])$$

$$[ROO \bullet] = \frac{-B_2 + \sqrt{B_2^2 - 4A_2C_2}}{2A_2},$$

where

$$A_2 = k_7$$

$$B_2 = k_7[RH] + k_{10}[R \bullet]$$

$$C_2 = -(k_6[O_2][R \bullet] + k_9[RO \bullet][ROH])$$

The rate of change of the amount of stable substances in the liquid phase during chemical reactions, is defined as the sum and difference of the reaction rates, where given substance is formed or consumed:

$$R_j = \sum_{i=1}^I W_i,$$

where  $R_j$  – rate of change of the amount of  $j$ -th stable substances in the liquid phase,  $W_i$  – rate of  $i$ -th reaction, where  $j$ -th stable substances is received or consumed,  $I$  – number of reactions, where  $j$ -th stable substances is received or consumed. MATLAB software was used in order to solve this and results were compared with data represented in [1]-[4].

#### References:

- [1] K.Hattori, Y. Tanaka, H.Suzuki, T. Ikawa , H. Kubota, J.of Chem. Eng. of Jap.( 1970) 72-78.
- [2] B. Makalec, G.Kirichenko, E. Strygin, Petrochemistry. 18. (1978) 250-255.
- [3] A. Bhattacharya, Chem. Eng. J. (2008) 308–319.
- [4] A. Mutriskov., O. Maminov, N.Terpilovskyi, Chem. and Chem. Techn. 15 (1972). 411 -413

## Mechanism of Chemical Evaporation of a Platinum Catalyst in an Ammonia Oxidation Reaction

Vyatkin Yu.L.<sup>1</sup>, Balaev A.V.<sup>2</sup>, Savenkov A.C.<sup>3</sup>, Vanchurin V.I.<sup>1</sup>

1 – Russian University of Chemical Technology, D. I. Mendeleev, Moscow, Russia

2 – Ufa State Technical University, Ufa, Russia

3 – Politehnicheskij Kharkov Institute, Kharkov, Ukraine

yuris-vtk2016@yandex.ru

The catalytic process of oxidation of ammonia on platinum Pt takes place in the area of external diffusion, characterized by a high rate of conversion of ammonia, contact time  $(1-3) \cdot 10^{-4}$  seconds. In this case, the thickness of the catalyst layer of 20-25 mm (pack of meshes of the PGE) gas temperature changes from 900 °C to 220°C. Under the influence of the reaction medium, the catalyst grids are loosened and for the period of 3-5 months of operation in the industry, the initial mass of 23-25 kg of platinoids loses 30-50% of its weight [1].

In [2] that flies platinum in the form PtO<sub>2</sub> oxide melting point of oxide 450-480°C [1]. And at an operating temperature of 850 °C, evaporation of platinum can be neglected [3].

The reaction  $Pt_s + O_2^g = PtO_2^g$  is essentially topochemical (gaseous substances react with the catalyst solid). In [4] an attempt is made to study in detail the mechanism of Pt oxidation reaction without ammonia as an example of a model (simpler) system. It was found that the process of oxidation of platinum:

1) Is largely determined by the conditions in the boundary layer and at a pressure of up to 1 ATA describes the equation of the first order of oxygen. 2) the rate of formation and withdrawal of PtO<sub>2</sub> from the surface depends not only on the surface temperature of the catalyst, but also on the temperature of the gas. 3) the oxidation rate of platinum in a simple system does not depend on the linear flow rate up to 220 cm/sec., but in the system with NH<sub>3</sub> such dependence is. It is expressed through the tension of the grids.

The mechanism of platinum oxidation is as follows:

a) Active Pt atoms from the catalyst volume diffuse to the surface, pass through the atomic layer of chemisorbed oxygen on which it is adsorbed the layer of molecular oxygen O<sub>2</sub>.  
b) Active Pt atoms react chemically with O<sub>2</sub> and leave the gas volume. The rate of diffusion of metal atoms in a solid body is small, so the rate of formation of PtO<sub>2</sub> and NO in a system with ammonia differ 10<sup>4</sup>-10<sup>6</sup> times.

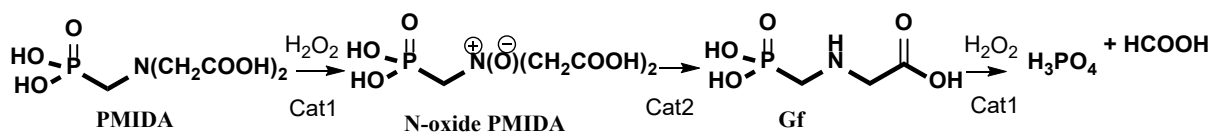
### References:

- [1] Handbook of nitrogen, 2nd edition revised, 1987.
- [2] C. Alcock, G. Hooper, Proc.Roy.Soc., A254, 551 (1960).
- [3] Yu. L. Vyatkin, A. S. Savenkov and others Chem.prom. (1979) №10, p. 620.
- [4] G. Fryburg, H. Petrus, J. Electrochem.Soc. (1961),V. 104,p.104.496.

## Oxidation of N-(Phosphonomethyl)Iminodiacetic Acid with Hydrogen Peroxide in Phase-Transfer Conditions

Yushchenko D.Yu., Pai Z.P., Khlebnikova T.B.  
Boreskov Institute of Catalysis, Novosibirsk, Russia  
dyy@catalysis.ru

N-(phosphonomethyl)-glycine (glyphosate, Gf) is an efficient herbicide [1]. Environment friendly methods of its large-scale synthesis are based on the catalytic oxidation of N-(phosphonomethyl)iminodiacetic acid (PMIDA) with oxygen or hydrogen peroxide in an aqueous solution. Oxidation of PMIDA with aqueous hydrogen peroxide is preferable because it allows carrying out the synthesis at atmospheric pressure; however, it has several disadvantages. The first is the necessity of using two catalysts: Cat1 at the stage of oxidation of PMIDA to N-oxide PMIDA at 70 °C; Cat2 for the rearrangement of N-oxide PMIDA into glyphosate at 40 °C. In addition, it is almost impossible to organize the recycling of catalysts, and the use of an excess amount of H<sub>2</sub>O<sub>2</sub> in the process leads to the over oxidation of the resulting glyphosate [2]. In our previous studies, the problem of catalyst recycling was solved by using bifunctional catalysts based on tetranuclear tungsten polyoxoperoxo complexes [3], but the task of choosing the optimal amount of H<sub>2</sub>O<sub>2</sub> for oxidizing PMIDA to glyphosate remained unsolved.



In this work, the kinetic regularities of catalytic oxidation reactions of PMIDA with 30% aqueous hydrogen peroxide and the formation of Gf, H<sub>3</sub>PO<sub>4</sub> and HCOOH were studied.

Based on the results obtained, a mathematical model that described the processes was chosen. The choice of the model was verified by comparing the calculated and experimental kinetic curves. The required amount of hydrogen peroxide which allowed obtaining the target product glyphosate in 87% yield has been found [4].

**Acknowledgement.** This work was supported by the Russian Foundation for Basic Research, grant 16-29-10691.

### References:

- [1] S.O. Duke, *Pest Manag. Sci.* 74 (2018) 1025–1026.
- [2] J. Tian, H. Shi, X. Li, Y. Yin, L. Chen, *Green Chem.* 14 (2012) 1990.
- [3] Z.P. Pai, D.Y. Yushchenko, T.B. Khlebnikova, V.N. Parmon, *Catal. Commun.* 71 (2015) 102–105.
- [4] Z.P. Paj, D.Y. Yushchenko, T.B. Khlebnikova, V.N. Parmon, RU 2618629, 2017.

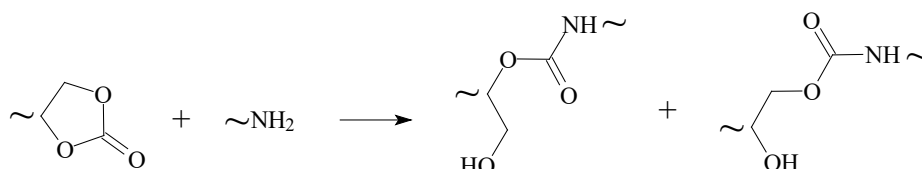
## Kinetics and Quantum Chemical Study of Mechanism of TBD Catalyzed Aminolysis of Cyclocarbonates in DMSO

Zabalov M.V., Levina M.A., Tiger R.P.

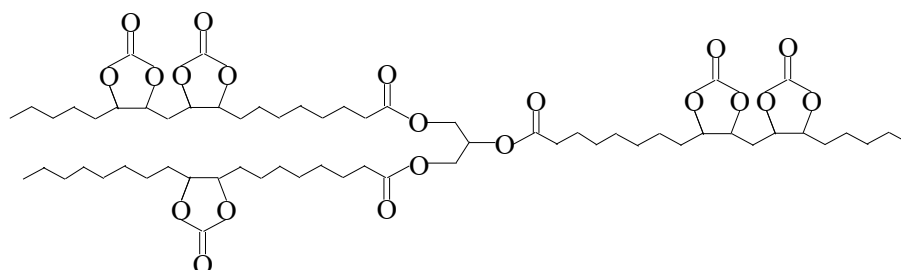
*Institute of Chemical Physics, Russian Academy of Sciences, Moscow, Russia*

*zabalov@chph.ras.ru*

In the base of the classical method of the polyurethane production is the reaction of NCO groups of di- or polyisocyanates with OH groups of di- or polyols. Due to high toxicity of isocyanates and phosgene over recent years a new trend has emerged in this field of researches: the green chemistry of polyurethanes, the aim of which is to replace the urethane formation reactions involving isocyanates with safe reactions, by those based on renewable plant raw materials. The most promising way to synthesize new urethanes is the reaction of primary amines with cyclocarbonates.



TBD (1,5,7-triazabicyclo[4.4.0]dec-5-ene) has the highest catalytic activity in this reaction. The object of the experimental investigation was the reaction of n-butylaminolysis of cyclocarbonate-containing triglyceride based on soybean oil (CSBO) in DMSO with addition or without TBD.



Along with the kinetic study, the quantum chemical calculations by the DFT method of the catalysis mechanism under the action of TBD (using the reaction of methylamine with ethylene carbonate in DMSO as a model one) were carried out.

The patterns of the CSBO catalytic aminolysis testify the first order of reaction by amine and catalyst. The presence of TBD leads to disappearance of the channel with the participation of two amine molecules as it takes place in non-catalytic reaction.

The decrease of the calculated activation energy in DMSO compared to the gas-phase is  $\sim 5$  kcal/mol. The TBD role consists in the proton transfer between the amine and the hydroxyl group formed, and the DMSO role is in the screening of the excess charges formed on the oxygen atoms of the cyclocarbonate group upon the amine addition.

**Acknowledgement.** This work was supported by the RFBR, grant 17-03-00146.

## Aromatic C–H Bond Oxidation by Catalytic Systems Based on an Iron Complex with Ligand TPA Family

Zima A.M.<sup>1,2</sup>, Lyakin O.Y.<sup>1,2</sup>, Bryliakov K.P.<sup>1,2</sup>, Talsi E.P.<sup>1,2</sup>

<sup>1</sup> – Borekov Institute of Catalysis, Novosibirsk, Russia

<sup>2</sup> – Novosibirsk State University, Novosibirsk, Russia

zima@catalysis.ru

Catalytic aromatic hydroxylation is a challenging task due to the very strong C – H bond of the substrate. Only a few examples of synthetic iron-based catalytic systems capable of catalytic selective aromatic hydroxylation are known. It is assumed that in such systems, iron-oxo intermediates are the key species of aromatic hydroxylation.

In this work catalytic systems based on the iron complexes **1** and **2** (Figure 1), H<sub>2</sub>O<sub>2</sub> or CH<sub>3</sub>CO<sub>3</sub>H as an oxidant, and carboxylic acid as an additive were studied.

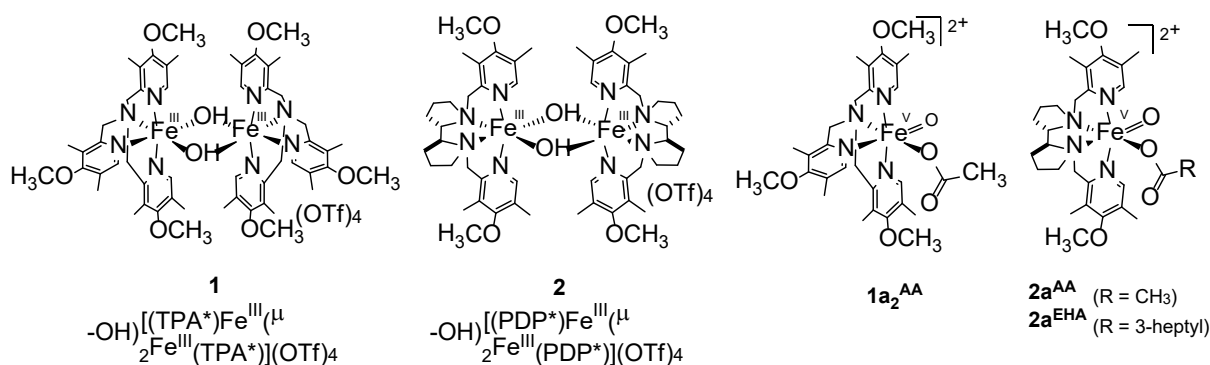


**Figure 1.** Structures of complexes

Catalyst systems **1**/H<sub>2</sub>O<sub>2</sub>(CH<sub>3</sub>CO<sub>3</sub>H)/EHA exhibit EPR spectra of two unstable intermediates, **1a<sub>1</sub><sup>EHA</sup>** and **1a<sub>2</sub><sup>EHA</sup>**, whereas catalyst systems **2**/H<sub>2</sub>O<sub>2</sub>(CH<sub>3</sub>CO<sub>3</sub>H)/AA display EPR spectrum of one unstable intermediate **2a<sup>AA</sup>**. At the beginning of the experiment immediately after mixing the reagents at –70 °C, the concentration of **1a<sub>1</sub><sup>EHA</sup>** is larger than the concentration of **1a<sub>2</sub><sup>EHA</sup>**; subsequently, **1a<sub>1</sub><sup>EHA</sup>** rapidly converts into **1a<sub>2</sub><sup>EHA</sup>**. The presence of an equilibrium between the tautomeric species  $[(\text{TPA}^*)\text{Fe}^{\text{IV}}=\text{O}(\text{OC}(\text{O})\text{CH}_3)]^{2+}$  and  $[(\text{TPA}^*)\text{Fe}^{\text{V}}=\text{O}(\text{OC}(\text{O})\text{CH}_3)]^{2+}$  for **1a<sub>1</sub><sup>EHA</sup>** and **1a<sub>2</sub><sup>EHA</sup>** has been proposed. For linear carboxylic acids used as an additive, the intermediate **1a<sub>2</sub><sup>RCOOH</sup>** strongly predominates in the reaction solution. When branched carboxylic acid was used, the concentration of **1a<sub>1</sub><sup>RCOOH</sup>** can be larger, than the concentration of **1a<sub>2</sub><sup>RCOOH</sup>** at the first moments of the experiment at –70 °C; then, **1a<sub>1</sub><sup>RCOOH</sup>** rapidly converts into **1a<sub>2</sub><sup>RCOOH</sup>**.

It was found that the reactivity of the studied Fe(V)=O species toward substituted benzenes increases in the following order: nitrobenzene < acetophenone < chlorobenzene < benzene < toluene, in accordance with the growth of the electron-rich properties of the substrate, which is consistent with the mechanism of electrophilic substitution in the aromatic ring.

**Acknowledgement.** This work was supported by the RFBR, grant 18-33-00462.

## The Effect of Barium on Behaviour of the OSC-Material in the Composition of Three-Way Catalysts

Alikin E.A.<sup>1</sup>, Denisov S.P.<sup>1</sup>, Baksheev E.O.<sup>1,2</sup>, Kenzhin R.M.<sup>3</sup>, Vedyagin A.A.<sup>3</sup>

1 – Ecoalliance LTD, Novouralsk, Russia

2 - Ural Federal University, Yekaterinburg, Russia

3 – Boreskov Institute of Catalysis, Novosibirsk, Russia

*alikin@eco-nu.ru*

Materials with enhanced oxygen storage capacity (OSC) are an intrinsic part of three-way catalysts (TWC). Typically these materials based on ceria-zirconia solid solution. Ceria damps the fluctuations of oxygen in the exhaust gases, keeping its content on the catalyst's surface equal to the stoichiometric ratio. Such conditions provide an effective oxidation of CO and hydrocarbons to CO<sub>2</sub> and H<sub>2</sub>O simultaneously with reduction of NO<sub>x</sub> to N<sub>2</sub>. Zirconium was found to be the most effective dopant for stabilization of the CeO<sub>2</sub> lattice. On the other hand, it was established that barium has a positive effect on the thermal stability and catalytic activity of the second intrinsic part of TWC - Pd/Al<sub>2</sub>O<sub>3</sub> [1, 2]. As known, Pd can promote OSC effectively, so it has been often deposited on the surface of OSC material. However, the effect of Ba on properties of the OSC materials and Pd/OSC catalytic systems is still poorly reported in the literature. Thereby, the present study was aimed to reveal this effect for the Pd/OSC catalysts.

A solid solution of composition Zr<sub>0.5</sub>Ce<sub>0.4</sub>Y<sub>0.05</sub>La<sub>0.05</sub>O<sub>x</sub> (CZYL) was used as the OSC material. Pd/CZYL catalyst was prepared by an impregnation method as follows. A powder of CZYL support was impregnated with Pd(NO<sub>3</sub>)<sub>2</sub> solution. The resulting powder was milled with distilled water, and the obtained slurry was washcoated onto a cordierite honeycomb (52 cm<sup>3</sup>, Corning). The loading of the active composition in the monolith sample was 60 g/l (typical weight content of OSC component in the monolith). The coated samples were dried at 120 °C for 2 h and calcined at 550 °C for 0.5 h. Pd-Ba/CZYL sample was prepared using the same method with addition of Ba(NO<sub>3</sub>)<sub>2</sub> salt at the milling stage. The loading of Pd and Ba relative to support was 1 and 3 wt.%, respectively.

Measurement of the oxygen storage capacity was performed in a flow reactor system (MEXA-9500 HORIBA) as reported elsewhere [3]. Hydrothermal aging (HTA) of the model samples was performed under the following conditions: T = 1050 °C; t = 4 h; 10% H<sub>2</sub>O + 90% N<sub>2</sub>. The samples after HTA were designated as Pd/CZYL-A and Pd-Ba/CZYL-A. Samples of the washcoat scrubs were investigated by a set of physicochemical methods (BET, XRD, XPS, TEM+EDX etc.).

Table 1 shows BET-BJH results. An addition of barium decreases both the specific surface area (SSA) and the total pore volume (TPV) of the fresh samples. After the HTA the collapse of the structure for the barium-containing sample becomes more dramatic. Figure 1 presents dynamic oxygen storage capacity. As seen, the modification of the Pd/CZYL system with barium leads to a noticeable decrease in OSC for both the fresh and aged samples.

TABLE 1. Pore structure parameters.

Sample	SSA, m <sup>2</sup> /g	TPV, cm <sup>3</sup> /g
Pd/CZYL	71.2	0.52
Pd-Ba/CZYL	60.7	0.37
Pd/CZYL-A	30.5	0.3
Pd-Ba/CZYL-A	20.5	0.06

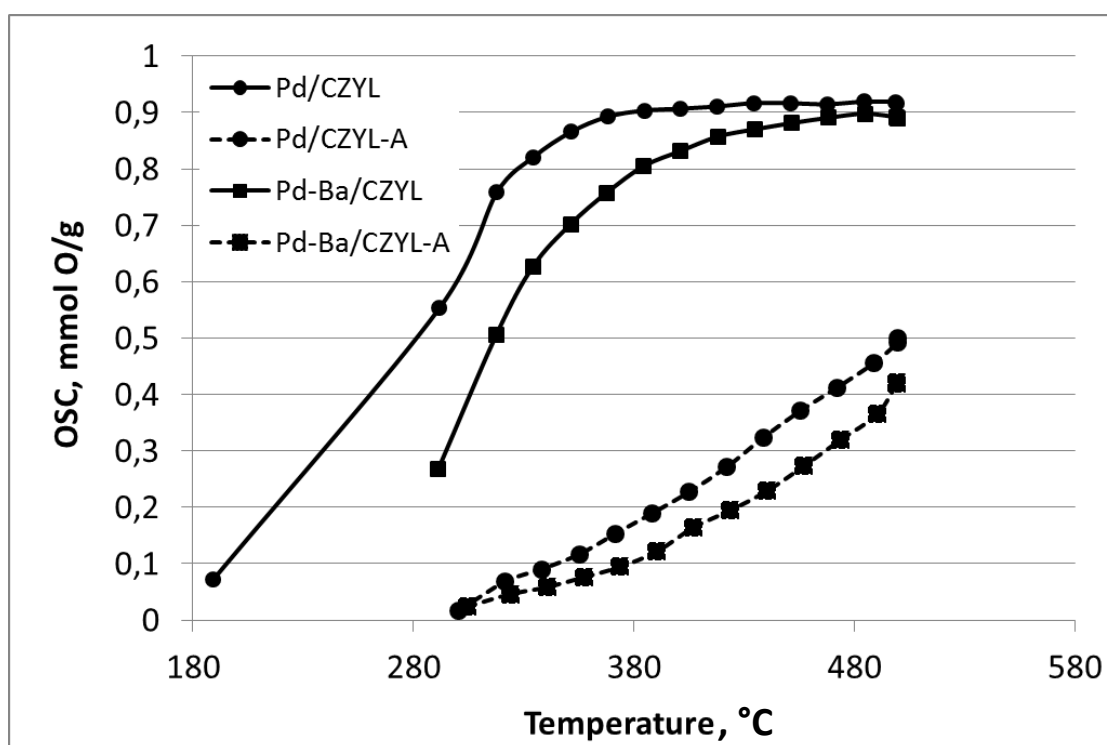


Figure 1 – Dynamic oxygen storage capacity.

The observed negative effect of barium is probably associated with formation of the barium zirconate phase, which was detected by XRD. Thus, it can be concluded that the addition of barium has the negative effect on the properties of the OSC material. This fact should be taken into account when designing the composition of the three-way catalysts.

**Acknowledgement.** The study was financially supported by the Ministry of Education and Science of the Russian Federation within the framework of subsidizing agreement of October 23, 2017 (No. 14.581.21.0028, unique agreement identifier RFMEFI58117X0028) of the Federal Target Program “Research and development in priority directions of the progress of the scientific and technological complex of Russia for the years 2014–2020.”

#### References:

- [1] T. Kobayashi, T. Yamada, K. Kayano, *Appl. Catal. B-Environ.* 30 (2001) 287–292.
- [2] T. Kolli, U. Lassi, K. Rahkamaa-Tolonen, T. Kinnunen, R. Keiski, *Appl. Catal. A-Gen.* 298 (2006) 65-72.
- [3] A.V. Porsin, E.A. Alikin, V.I. Bukhtiyarov, *Catal, Sci, Technol*, 6 (2016) 5891–5898.

## Ethylene Dimerization into 1-Butene and 2-Butene Using Homogeneous and Supported Nickel(II) 2-Iminopyridine Catalysts

Antonov A.A.<sup>1,2</sup>, Semikolenova N.V.<sup>1</sup>, Bryliakov K.P.<sup>1,2</sup>, Talsi E.P.<sup>1,2</sup>

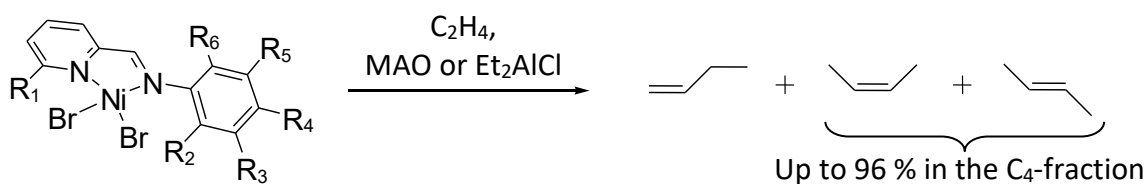
1 – Boreskov Institute of Catalysis, Novosibirsk, Russia

2 – Novosibirsk State University, Novosibirsk, Russia

antonov@catalysis.ru

Butenes (1-butene, *cis*-2-butene, *trans*-2-butene) are widely used in polymer and petrochemical industry. So, 1-butene is produced in the amount of 708000 t per year and one quarter is used in the production of chemicals and polymers, e.g., as a co-monomer for the manufacturing of linear low density polyethylene. As for 2-butene, it is produced mainly in refineries and is converted by approx. three quarters into alkylate gasoline [1]. In parallel, 2-butene can be produced from the ethane-ethylene fraction of hydrocarbon gases via selective ethylene dimerization and then it can be converted to propylene by metathesis with ethylene. The resulting propylene is then hydrated to isopropyl alcohol, which can be used as an octane-raising additive to gasoline [2]. Consequently, catalysts for the selective dimerization of ethylene (especially, into 2-butene), displaying high activity and selectivity towards C<sub>4</sub>-fraction, are greatly demanded at the present time.

In this work, nickel(II) complexes with 2-iminopyridine ligands bearing electron-withdrawing substituents (F, Cl, CF<sub>3</sub>) displayed high activity for ethylene dimerization (up to 9740 kg products·(mol Ni)<sup>-1</sup>·h<sup>-1</sup>·bar<sup>-1</sup>), providing predominantly mixtures of 1-butene and *cis*- and *trans*-2-butene (C<sub>4</sub> selectivity varies from 89 to 100 %). Some effects of the substituents' and the cocatalyst nature on the activity and selectivity of the nickel(II) complexes in ethylene dimerization have been established.



To illustrate, nickel complexes with *o*-trifluoromethyl group in phenyl ring turned out to be more active than catalysts with small *o*-fluoro substituent (the activity for **Ni1** was 7400 and for **Ni4** – 9200 kg products·(mol Ni)<sup>-1</sup>·h<sup>-1</sup>·bar<sup>-1</sup>) upon the activation with methylaluminoxane (MAO) at the same conditions: 2 μmol of Ni, 500 equiv. of cocatalyst, 50 ml of toluene, ethylene pressure 2 bar, time 15 min, *T* = 35 °C.

	R <sub>1</sub>	R <sub>2</sub>	R <sub>3</sub>	R <sub>4</sub>	R <sub>5</sub>	R <sub>6</sub>	X
<b>Ni1</b>	Me	F	H	H	H	H	Cl
<b>Ni2</b>	Me	F	H	H	H	F	Cl
<b>Ni3a</b>	Me	F	H	F	H	F	Cl
<b>Ni3b</b>	Me	F	H	F	H	F	Br
<b>Ni4</b>	Me	CF <sub>3</sub>	H	H	H	H	Cl
<b>Ni5</b>	Me	CF <sub>3</sub>	H	H	H	F	Cl
<b>Ni6</b>	Br	F	H	H	H	F	Br
<b>Ni7</b>	Br	CF <sub>3</sub>	H	H	H	H	Br
<b>Ni8</b>	Me	H	F	H	F	H	Br
<b>Ni9</b>	Me	H	Cl	H	Cl	H	Br

## PP-IV-2

However, increasing the steric bulk in *o*-position of aryl ring with *o*-trifluoromethyl group resulted in the formation of higher oligomers (1-hexene and its isomers). Thus, for **Ni1** at the reaction conditions mentioned above, the C<sub>4</sub>-selectivity was 98 % and selectivity for 2-butenes in C<sub>4</sub>-fraction was 65 %, while for **Ni4**, the C<sub>4</sub>-selectivity and selectivity for 2-butenes in C<sub>4</sub>-fraction decreased to 90 and 52 %, correspondingly. Using MAO as a cocatalyst, the highest selectivity for 2-butenes in C<sub>4</sub>-fraction was determined for the **Ni8** (66 %), containing *m*-fluorine substituents, at ethylene pressure 2 bar, time 30 min, *T* = 35 °C

The replacement of MAO by Et<sub>2</sub>AlCl led to decrease in catalytic activity approx. by a factor of 3. For example, **Ni8** upon the activation with 500 equiv. of cocatalyst at ethylene pressure 2 bar and *T* = 35 °C demonstrated activity 5970 kg products·(mol Ni)<sup>-1</sup>·h<sup>-1</sup>·bar<sup>-1</sup> using MAO and 1790 kg products·(mol Ni)<sup>-1</sup>·h<sup>-1</sup>·bar<sup>-1</sup> using Et<sub>2</sub>AlCl. At the same time, selectivity for 2-butenes in C<sub>4</sub>-fraction increased significantly and reached maximum (96 %) for **Ni8** (6 μmol) activated with 500 equiv. of Et<sub>2</sub>AlCl at ethylene pressure 1 bar, *T* = 35 °C

To evaluate the possibility of immobilization of 2-iminopyridine nickel(II) complexes, the most active and selective catalysts **Ni3b** and **Ni8** were grafted on silica modified with alumina (SiO<sub>2</sub>(Al)), and the resulting heterogeneous catalysts were tested in ethylene dimerization using MAO and Et<sub>2</sub>AlCl.

Grafted complex	n(Ni), [μmol]	Cocatalyst	P(C <sub>2</sub> H <sub>4</sub> ), [bar]	time [min]	<i>T</i> , [°C]	Activity, kg products (mol Ni) <sup>-1</sup> ·h <sup>-1</sup> ·bar <sup>-1</sup>	ΣC <sub>4</sub> /ΣC [%]	2-butenes/ΣC <sub>4</sub> , [%]
<b>Ni8</b>	3.81	MAO	1	15	35	2470	95.3	60.3
<b>Ni8</b>	6.74	Et <sub>2</sub> AlCl	1	15	35	3160	94.9	78.9
<b>Ni3b</b>	1.94	MAO	1	15	35	9740	93.3	57.7
<b>Ni3b</b>	1.15	MAO	1	15	70	2320	98.4	66.3
<b>Ni3b</b>	1.21	MAO	3	15	35	2590	97.0	28.8
<b>Ni3b</b>	1.27	MAO	5	15	35	1650	97.1	21.2

Supported catalysts have demonstrated slightly lower catalytic activities in ethylene dimerization (except **Ni3b**), compared with homogeneous catalysts, while the C<sub>4</sub>-selectivity and selectivity for 2-butenes in the C<sub>4</sub>-fraction have not changed significantly. These catalysts were active even at 70 °C and low ethylene pressure (1 bar). Consistent mechanism of ethylene dimerization to 1- and 2-butenes has been proposed.

**Acknowledgement.** This work was supported by the Ministry of Higher Education and Science of the Russian Federation, unique project identifier RFMEFI60717X0169.

### References:

- [1] M. Bender, ChemBioEng. Rev. 1 (2014) 136.
- [2] A. S. Kharitonov, K. Yu. Koltunov, V. I. Sobolev, V. A. Chumachenko, A. S. Noskov, S. E. Kuznetsov, Catal. Ind. 10 (2018) 115.

## The Influence of Synthesis Parameters on Surface Characteristics of Alumina

Bereskina P.A., Mashkovtsev M.A., Guryanova A.A., Osolihina A.Y.  
*Ural Federal University, Ekaterinburg, Russia*  
*polina.bereskina@urfu.ru*

Alumina ( $\gamma$ - or  $\eta$ -forms) is a widespread material for catalyst, carrier and adsorbent due to high specific surface area values, a wide range of acid and base centres, stability in the temperature interval corresponding to a big number of catalytic reactions. Surface characteristics regulation is an important problem to be solve by controlled variation of the synthesis parameters [1-2]. The purpose of this research is an investigation of the pH influence during synthesis on the surface characteristics of alumina obtained by thermal decomposition of precipitated hydroxides.

The sample synthesis was carried out by hydroxides precipitation while pH values were 6 and 9. Also ammonia was added to the half of suspension with pH=6 to increase this value to 9 after precipitation. Aluminum nitrate solution (1 M) was dropped into a reactor at the constant speed, ammonia solution (10% per mass) was dropped discretely with a relay type switch reacting to pH variation from the set value. The measurement error of pH with the electrode is  $\pm 0,1$  unit. The precipitation was carried out at ambient temperature ( $22 \pm 3^\circ\text{C}$ ). After that, precipitates were filtered, wet cakes were dried at  $130^\circ\text{C}$  for 4 hours and powders were calcinated at  $500^\circ\text{C}$  for 4 hours with a heating rate equaled  $300^\circ\text{C}/\text{h}$ .

Alumina porosity and surface area were investigated with a method of low-temperature nitrogen adsorption with Quantachrome Nova 1200e. The specific surface area was calculated according to the BET theory; the pore size distributions were calculated from a desorption parts of the isotherms by the BJH method. The sample degassation was carried out at  $290^\circ\text{C}$  for 1 hour under vacuum.

Figure 1a shows the adsorption/desorption isotherms and Table 1 shows pore structure parameters.

The specific surface area values of two samples are close:  $245 \text{ m}^2/\text{g}$  for  $\text{Al}_2\text{O}_3$  (pH=9) and  $252 \text{ m}^2/\text{g}$  for  $\text{Al}_2\text{O}_3$  (pH=6), while the pore size and pore shape of the samples being significantly different. The sample precipitated with pH value equalled to 6 and raised to 9 has the lowest specific surface area value), while the pore size and pore shape of this sample being resemble to  $\text{Al}_2\text{O}_3$  (pH=9).

TABLE 1. Pore structure parameters

Sample	Specific surface area (SSA), $\text{m}^2/\text{g}$	Average pores diameter (APD), nm	Total pore volume (TPV), $\text{cm}^3/\text{g}$	Pore type
$\text{Al}_2\text{O}_3$ (pH=6)	252	3,8	0,2	ink-bottle
$\text{Al}_2\text{O}_3$ (pH=6 $\rightarrow$ pH=9)	206	6,2	0,3	ink-bottle
$\text{Al}_2\text{O}_3$ (pH=9)	245	6,3	0,4	ink-bottle

### PP-IV-3

Surface characteristics difference of the samples can be explained with the fact, that pore structure of  $\text{Al}_2\text{O}_3$  (pH=6) was formed during precipitation, however that pore structure of  $\text{Al}_2\text{O}_3$  (pH=9) was shaping primarily during drying. The sample  $\text{Al}_2\text{O}_3$  (pH=6  $\rightarrow$  pH=9) hydrolysed after precipitation, this process changed its pore structure, but pH precipitation value influenced on specific surface area value.

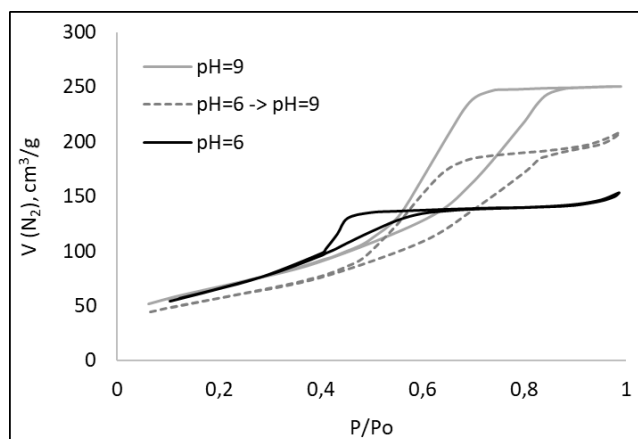


Figure 1 – The adsorption/desorption isotherms:  $\text{Al}_2\text{O}_3$  (pH=6),  $\text{Al}_2\text{O}_3$  (pH=6 $\rightarrow$ 9) and  $\text{Al}_2\text{O}_3$  (pH=9).

Thus, it is found, that pH precipitation significantly influences alumina surface characteristics with the oxides generated from hydroxides by means of the thermal decomposition.

**Acknowledgement.** The study was financially supported by the Ministry of Education and Science of the Russian Federation within the framework of subsidizing agreement of October 23, 2017 (No. 14.581.21.0028, unique agreement identifier RFMEFI58117X0028) of the Federal Target Program “Research and development in priority directions of the progress of the scientific and technological complex of Russia for the years 2014–2020.”

#### References:

- [1] R. Feng, X. Hu, X. Yan, Z. Yan, M. J. Rood, *Microporous Mesoporous Mater.* (2017) 241.
- [2] W. Yu-sheng, M. Jiao, L. Ming-chun, H. Fang, *Chem. Res. Chin. Univ.* (2013) 29.

## Oxidative Desulfurization of Diesel Fuel Catalysed by Brønsted Acidic Ionic Liquids with Heteropolyacids Immobilized on $\gamma$ -Al<sub>2</sub>O<sub>3</sub> and Silica

Bryzhin A.<sup>1</sup>, Gantman M.<sup>2</sup>, Buryak A.<sup>3</sup>, Tarkhanova I.<sup>1</sup>

1 – M.V. Lomonosov Moscow State University, Moscow, Russia

2 – Friedrich-Alexander Universität Erlangen-Nürnberg, Erlangen, Germany

3 – Frumkin Institute of Physical Chemistry and Electrochemistry, Russian Academy of Sciences, Moscow, Russia  
alexandrbr93@gmail.com

The zwitterion (ZI) compound with H<sub>3</sub>PMo<sub>12</sub>O<sub>40</sub> or H<sub>3</sub>PW<sub>12</sub>O<sub>40</sub> immobilized on  $\gamma$ -Al<sub>2</sub>O<sub>3</sub> and Perlkat 97-0 silica gel is a new effective solid catalyst for oxidative desulfurization (ODS) of diesel fuel under mild condition. The catalysts represent supported ionic liquid phases (SILPs). We have previously shown that the use of ZI (4-(3'- ethylimidazolium)-butanesulfonate) promotes an increase in the efficiency of oxide heterogeneous catalysts for the oxidation of sulfur-containing compounds, including the thiophene series [1]. In this work, this IL was used to stabilize heteropolyanions on the surface of mineral carriers in order to obtain catalysts for the oxidative desulfurization of hydrocarbons. To establish the structure of catalysts a wide range of physicochemical methods was used, including surface-assisted laser desorption/ionization (SALDI) mass spectrometry. The prepared compositions were tested in the oxidation of various models (thiophene, dibenzothiophene, thioanisole in isooctane) and diesel fuel with hydrogen peroxide as the oxidant. As a result of the interaction of heteropoly acids with an ionic liquid, the anions of general formula PMe<sub>4</sub> have stabilize on the surface. According to the literature, such HPA fragments are precursors to the active form of catalysts. The most effective catalyst, PMo/SiO<sub>2</sub>, ensure higher stability of heteropolyanions and make the catalyst stable over several successive oxidation cycles despite the fact that the sulfur is converted to sulfuric acid after oxidation of the thiophene. Conversion rate for this catalyst (TOF) was 140 h<sup>-1</sup> for thiophene, 190 h<sup>-1</sup> for dibenzothiophene, and 1230 h<sup>-1</sup> for thioanisole, per mole of HPA.

To increase the efficiency of the process, a method of fractional loading of hydrogen peroxide was used to prevent the side reaction of its decomposition - the conversion value for each of the tested substrates increases by 20-50%. Another important benefit of the reported systems is the desulfurization of diesel fuel with a very high efficiency (residual amount of sulfur < 10 ppm, that meets modern environmental requirements) under mild conditions.

Thus, the combination of the proposed approaches contributes to the deep course of the oxidation process, which makes the proposed oxidizing system promising for practical application.

### Reference:

[1] Ce-, Zr-containing oxide layers formed by plasma electrolytic oxidation on titanium as catalysts for oxidative desulfurization / I. G. Tarkhanova, A. A. Bryzhin, M. G. Gantman, T.P. Yarovaya, I. V. Lukiyanchuk, P.M. Nedozerov, V. S. Rudnev / Surface and Coatings Technology. — 2019. — Vol. 362. — P. 132–140.

## Hydrogenation of Aromatic Hydrocarbons on Mesoporous Silica Doped with Dy and Modified with Ni and Cu

Bulanova A.V., Shafigulin R.V., Filippova E.O., Shmelev A.A., Tokranov A.A.  
 Samara University, Samara, Russia  
 av.bul@yandex.ru

In recent years, the interest of scientists to mesoporous silica gels for use as adsorbents and carriers for catalysts has increased. Mesoporous silica, along with chemical inertness, have an ordered structure and high specific surface.

Hydrogenation of aromatic hydrocarbons is one of the main reactions in the petrochemical industry. The search for new catalysts of hydrogenation reaction with higher catalytic activity and selectivity comparing to industrial catalysts is a demanded direction.

The synthesis of MPS was carried out. The MPS was synthesised by the template method with optimal conditions of the synthesis. Cetyltrimethylammonium bromide (CTAB) was used as a structure-forming substance. To improve the catalytic properties obtained MPS were doped with Dy and modified with nanoparticles of nickel (Dy-Ni/MPS) and copper (Dy-Cu/MPS).

The surface of the synthesized Dy-Ni/MPS was studied using TEM, SEM, BET, XRD, ICP and XRF methods.

The presence of nickel, copper and dysprosium in the sample was detected by XRF and ICP methods. Figure 1 shows the ICP spectrum of Dy-Ni/MPS and Dy-Cu/MPS samples. The specific surface area of Dy-Ni / MPS was 215 m<sup>2</sup>/g.

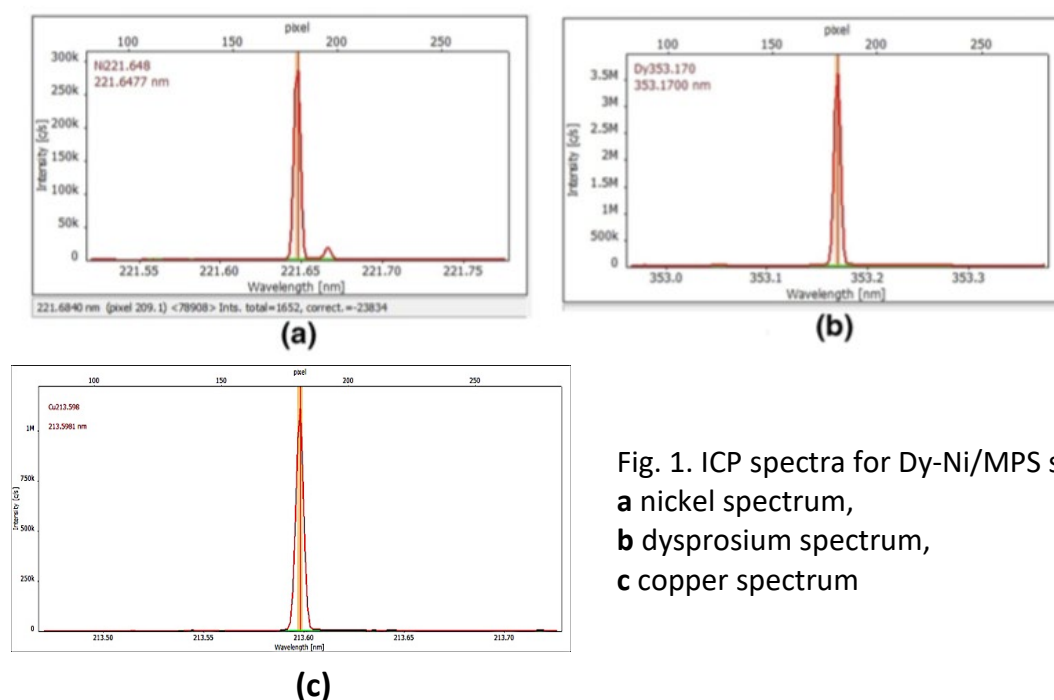


Fig. 1. ICP spectra for Dy-Ni/MPS sample  
**a** nickel spectrum,  
**b** dysprosium spectrum,  
**c** copper spectrum

## PP-IV-5

XRD method was used to analyze the structure of mesoporous silica. Characteristic peaks at low angles indicate that the texture characteristics correspond to the mesoporous silica of MCM-41 type.

TEM analysis pointed out that nickel is predominantly localized in the pores of the silica matrix.

The catalytic activity of the synthesized samples were studied on the example of the hydrogenation reaction of aromatic hydrocarbons in a static mode in the temperature range of 80-170 °C and a hydrogen pressure of 3 atm.

The conversion of ethylbenzene after 10 minutes on the Dy-Ni / MPS catalyst under relatively mild conditions (150°C, pressure 3 atm) reaches 100%, and for o-xylene, m-xylene and p-xylene 100% conversion was achieved after 30 minutes.

Under the same conditions of the hydrogenation reaction on the catalyst Dy-Cu/MPS, the conversion of o-xylene was 30%, of m-xylene 45%, of p-xylene 60% after 45 minutes. Thus, the catalytic activity of Dy-Cu/MPS is lower comparing to Dy-Ni/MPS sample.

The experiment pointed out that the catalytic activity of Dy-Ni/MPS in hydrogenation reactions of aromatic hydrocarbons is higher than that of Dy-Cu/MPS. The sample showed high conversions at relatively low temperatures and pressures.

**Acknowledgement.** This work was supported by the Ministry of Education and Science of the Russian Federation (grant 4.5883. 2017/8.9).

## Production of Composite Materials Based on TiO<sub>2</sub> Modified Particles SiO<sub>2</sub> and Ag

Buzaev A.A.<sup>1</sup>, Rogacheva A.O.<sup>1</sup>, Paukshtis E.A.<sup>2</sup>, Kozik V.V.<sup>1</sup>  
1 – National Research Tomsk State University, Tomsk, Russia  
2 – Boreskov Institute of Catalysis, Novosibirsk, Russia  
*buzae92@icloud.com*

The sol-gel method was used to obtain materials based on spherical TiO<sub>2</sub> composites containing additives SiO<sub>2</sub> and Ag. The texture, surface properties, phase composition of obtained materials were investigated.

It is important task of modern materials science to get new photocatalytic materials based on TiO<sub>2</sub>. Sol-gel synthesis is effective method of obtaining materials with the required performance characteristics. At the same time, modification composite materials based on TiO<sub>2</sub> by metal and oxides particles is promising approach to improving the structural, physicochemical, and functional properties.

The goal of present work is to obtain new composite materials based on spherical TiO<sub>2</sub> composites containing modifying additives SiO<sub>2</sub> and Ag by sol-gel method. Obtained TiO<sub>2</sub>-based composites are spherical of regular geometric shape with a diameter from 202 μm to 706 μm, the surface of which is represented by a spinal relief with smooth plateaus with cracks, according to the SEM results. Parameters of the porous structure and specific surface area of the synthesized materials were estimated by low-temperature nitrogen adsorption using the BET method. It has been established that the specific surface area of the formed materials is 108 m<sup>2</sup>/g. The pore space is represented by through and closed mesopores of spheroidal and cone-shaped geometry with different radii of the inlets. The average pore size is 14.51 nm, and their total volume is 0.13 cm<sup>3</sup>/g. The introduction of Ag additives into the composites led to a decrease in the specific surface area to a value of 82 m<sup>2</sup>/g, a total pore volume of up to 0.8 cm<sup>3</sup>/g, and an their average size of 7.04 nm. When the system was modified with SiO<sub>2</sub> additives, a reverse trend is observed, leading to an increase in the total pore volume to 0.20 cm<sup>3</sup>/g and a specific surface area to 117 m<sup>2</sup>/g. It should be noted that the modified composites based on TiO<sub>2</sub>, containing additives both Ag and SiO<sub>2</sub>, retain the values of specific surface area and total pore volume equal to 105 m<sup>2</sup>/g and 0.14 cm<sup>3</sup>/g, respectively. Control of element consist was carried out using X-ray microanalysis. Due to scanning of modified samples, the content was determined: Ti, O, Ag and Si for composites of the corresponding composition and their uniform distribution over the volume of spherical composites were established. The obtained results show that structural properties of materials can control by varying the amount of additives Ag and SiO<sub>2</sub> and the conditions of the sol-gel synthesis.

**Acknowledgement.** The results were obtained within the framework of the state task of the Ministry of Education and Science of the Russian Federation, project No.10.2281.2017/4.6.

## The Thermal Stability Study of Iron and Cobalts-Containing Catalysts with Layered Perovskite-Like Structure

Chislova I.V.<sup>1</sup>, Yafarova L.V.<sup>1</sup>, Chislov M.V., Zvereva I.A.<sup>1</sup>, Borodina E.M.<sup>2</sup>, Sheshko T.F.<sup>2</sup>

1 – St. Petersburg State University, St. Petersburg, Russia

2 – Peoples' Friendship University of Russia, Moscow, Russia

*i.v.chislova@gmail.com*

The hydrocarbons processing catalysts based on iron and cobalt cations are widely used in production, but the main problem of their industrial use is the coking surfacThee.

The purpose of this study is the characterization of catalysts with a perovskite-like layered structure before and after the carbon dioxide conversion reaction of methane and the Fischer – Tropsch process. The complex ferrites and cobaltites of gadolinium were selected as objects of current study. Samples before and after catalytic processes of carbon dioxide conversion of methane (UKM) and Fischer-Tropsch were under investigation. The sol - gel method for the synthesis of ultrafine GdFeO<sub>3</sub>, GdCoO<sub>3</sub> and their solid solutions was preliminarily developed.

As a result of investigation of the samples before and after catalytic processes, the XRPA method established the phase composition of the catalysts. Using the method of temperature-programmable reduction (TPR) optimal conditions for the catalysts use were selected. The results of the samples surface characteristics obtained by the SEM and BET methods for samples after the catalytic process demonstrate agglomeration and size reduction of nanoparticles. The states of the iron and cobalt atoms in all samples were determined by X-ray photoelectron spectroscopy. To quantify the carbon content in the samples after the catalytic process, a simultaneous thermal analysis was performed with mass spectroscopic determination of the evolved gases.

It was established that complex ferrites and cobaltites of gadolinium are resistant to carbonization in the carbon dioxide methane conversion reaction and the Fisher-Tropsch process, and are stable after high-temperature processes. The results obtained can be used for the implementation of environmentally friendly technological processes, the production of hydrocarbons and syngas conforming to the principles of "green" chemistry.

**Acknowledgement.** This work was supported by the Russian Foundation for Basic Research, grant № 18-33-01209.

Scientific researches were performed at the Center for X-ray Diffraction Methods and Nanotechnology, Center for Studies in Surface Science, Center for Thermogravimetric and Calorimetric Research, Resource center Cultivation of microorganisms of Research park of St. Petersburg State University.

## **Investigation of New Functional Micro-Mesoporous Platinum Containing Catalysts Based on Halloysite Nanotubes and ZSM-5 Type Zeolite for Xylene Isomerization**

Demikhova N.R., Artemova M.I., Nedolivko V.V., Glotov A.P., Vinokurov V.A.  
*Gubkin Russian State University of Oil and Gas, Moscow, Russia*  
*natashademihova@gmail.com*

Due to the growing demand of the chemical industry for aromatic hydrocarbons, there is a strong tendency to develop / optimize heterogeneous catalysts exhibiting high activity in the processing of aromatics. Isomerization of the C-8 aromatic fraction obtained from pyrolysis and catalytic reforming is one of traditional hydro-processing of aromatic hydrocarbons. It is usually carried out at 260-440°C on bi-functional metal-containing catalysts based on zeolites at atmospheric or hydrogen pressure.

Zeolites are widely used as heterogeneous catalysts in the oil industry due to their high activity in the reactions occurring on acid sites. Catalytic activity and selectivity, as a rule, are significantly influenced by size and shape of the zeolite pores, as well as the nature and stability of acid sites. In particular, H-ZSM-5 type zeolite constituting of channel structures formed by 10-membered rings contains many homogeneous microporous structures and has high acidity, which enables application of the material in acid catalysis. However, the microporous structure of H-ZSM-5 prevents large molecules from efficient diffusion during the catalytic process, which leads to blocking of the inlets in the active sites and, as a result, to a decrease in catalytic activity. To solve this problem, catalysts based on micro-mesoporous materials can be used. Such materials formed by micro-mesoporous nanostructures, can allow not only to facilitate the diffusion of large molecules into the pores, but also to increase significantly mechanical and thermal stabilities of the catalysts [1,2]. To reduce the cost of such materials, we suggest using a natural mesoporous clay mineral – halloysite nanotubes.

The structure and chemical composition of halloysite are close to kaolinite, the main difference is that aluminosilicate layers in halloysite are rolled and separated by water molecules. When folding aluminosilicate into the tube there is an aluminum oxide layer inside and the silicon oxide layer is outside. Alumina and silica in the rolled structure of halloysite are located on inner/outer surfaces of the nanotube. Due to their different ionization and dielectric properties, the outer surface is negatively charged in a wide pH range, and the inner surface is positively charged [3,4].

In this work we synthesized new functional micro-mesoporous materials based on halloysite nanotubes (HNT) and zeolite of ZSM-5 type. In preparation of catalyst supports in the form of extrudates, boehmite was used as a binder. The catalyst carrier was prepared by adding boehmite to functional micro-mesoporous materials in 60/40 wt. % ratio. After

## PP-IV-8

platinum addition (0.5 wt. %) we obtained catalysts of the following compositions: Pt/HNT/Al<sub>2</sub>O<sub>3</sub> and Pt/H-ZSM-5 + HNT/Al<sub>2</sub>O<sub>3</sub>.

The composition and structure of the synthesized catalysts were studied by X-ray fluorescent analysis (XRF), low-temperature nitrogen adsorption/desorption, transmission electron microscopy (TEM), and temperature-programmed ammonia desorption (TPD-NH<sub>3</sub>).

H-ZSM-5+HNT micro-mesoporous material has a higher specific surface area compared to the unmodified HNT (188 and 34 m<sup>2</sup> g<sup>-1</sup>, respectively); however, in contrast to the material based on HNT/Al<sub>2</sub>O<sub>3</sub>, the specific surface area and pore volume of the Pt/ H-ZSM-5 + HNT/Al<sub>2</sub>O<sub>3</sub> catalyst appreciably decrease after platinum deposition. It could be explained by blocking of zeolite pores by platinum particles. Nitrogen adsorption-desorption curves for all the samples are of the IV type with a hysteresis loop which indicates the micro-mesoporous structure is saved at all the steps of the synthesis.

The activity and selectivity of the obtained catalysts based on micro-mesoporous supports in isomerization of reforming xylene fraction was investigated in a flow-type laboratory unit with a fixed catalyst bed in the temperature range of 240–460°C under hydrogen pressure of 1 MPa. The highest selectivity to p-xylene (81 %) was obtained over Pt/H-ZSM-5 + HNT/Al<sub>2</sub>O<sub>3</sub> catalyst at 380°C. With increasing temperature, the selectivity with respect to o- and p-xylenes decreased for both catalysts. It may be connected with xylene dealkylation reactions with formation of benzene and toluene. Thus, the total content of dealkylation products for the catalysts studied increased with the temperature growth and was equal for both catalysts. The amount of benzene and toluene also correlated with the concentration of methane and ethane in gaseous reaction products, which reaffirms the occurrence of dealkylation. The hydrogenation products yield on Pt/H-ZSM-5 + HNT/Al<sub>2</sub>O<sub>3</sub> was 3–4 times lower in comparison with Pt/HNT/Al<sub>2</sub>O<sub>3</sub> catalyst. The catalytic system based on H-ZSM-5 + HNT demonstrated the best performance in xylene isomerization. For example, at 400°C in the presence of Pt/H-ZSM-5 + HNT/Al<sub>2</sub>O<sub>3</sub>, the conversions of m-xylene and ethylbenzene were 40 and 81 %, respectively, whereas for the Pt/HNT/Al<sub>2</sub>O<sub>3</sub> catalyst they did not exceed 5 %.

**Acknowledgement.** This work was financially supported by Russian science foundation (project № 19-19-00711).

### References:

- [1] Farshadi, M. and Falamaki, C., *Chin. J. Chem. Eng.*, 2018, vol. 26, no. 1, pp. 116–126.
- [2] Wang, Q., Han, W., Lyu, J., Zhang, Q., Guo, L., and Li, X., *Catal. Sci. Technol.*, 2017, vol. 7, no. 24, pp. 6140–6150.
- [3] Vinokurov, V.A., Stavitskaya, A.V., Chudakov, Ya.A., Glotov, A.P., Ivanov, E.V., Gushchin, P.A., Lvov, Yu.M., Maximov, A.L., Muradov, A.V., and Karakhanov, E.A., *Pure Appl. Chem.*, 2018, vol. 90, no. 5, pp. 825–832.
- [4] A.P. Glotov, E.A. Roldugina, M.I. Artemova, E.M. Smirnova, N.R. Demikhova, V.D. Stytsenko, S.V. Egazar'yants, A.L. Maksimov, V.A. Vinokurov, *Russian Journal of Applied Chemistry*, 2018, Vol. 91, No. 8, pp. 1353–1362.

## 2,4,6-Triphenylpyridine as “Metal-Free” Electrocatalyst of Hydrogen Evolution Reaction (HER)

Dolganov A.V., Tanaseychuk B.S., Chernyaeva O.Yu. , Selivanova Yu.M., Yudina A.Yu.,  
Grigorian K.A., Yurova V.Yu.

*Mordovian Ogarev State University, Saransk, Russia*  
*dolganov\_sasha@mail.ru*

The electrocatalytic activity of new members of the family of “metal-free” electrocatalyst - 2,4,6-triphenylpyridine, was studied in the hydrogen evolution reaction (HER). The electrochemical behavior of electrocatalyst in the presence of acids of various strengths (acetic and perchloric) has been studied in detail. It has been shown that in the presence of strong acids 2,4,6-triphenylpyridine has a high catalytic activity in the hydrogen evolution reaction. In the presence of weak acetic acid, instead of the expected process of formation of molecular hydrogen, the main products of the cathodic electrochemical process were the formation of a compound 2,4,6-triphenyl-1,4-dihydropyridine. It is shown that the nature of the heteroatom has a dramatic effect on the ability of the catalytic system to implement HER. By varying the nature of the heteroatom, as well as its basicity, by varying the substituents at the nitrogen atom, one can “control” the efficiency of the catalytic process. It is important to note, in contrast to the described metal-containing electrocatalytic systems, in which the role of a catalytically active center and a redox center is usually a metal atom, in heterocyclic catalytic systems these centers are separated in the molecule: the redox center is located on 4 carbon atoms , and the main - on the nitrogen atom. Such a structure of the catalyst opens up wide possibilities for creating a catalyst with the necessary (specified) parameters of the catalytic process: (minimum overvoltage value, high speeds of the limiting stages of the catalytic process). For example, varying the value of the redox potential by varying the nature of the substituent at 4 carbon atoms will allow you to adjust the specified value of the redox potential, while varying the substituents at the nitrogen atom will allow you to adjust the basicity of the catalytic center. For metal complexes, the separate variation of the key parameters of the catalyst is impossible; this often results in efficient catalytic systems with a low potential for their further use. The presented results open up a large field for the study of electrocatalytic activity in other heterocyclic compounds, which will make it possible to develop efficient catalytic systems of a new generation.

**Acknowledgement.** This work was supported by the Russian Science Foundation, grant (18-03-00211).

## Formation and Characterization of Photocatalytic Heterostructures Based on TiO<sub>2</sub> NTs/CuO NPs

Dronov A.A., Pinchuk O.V., Zheleznyakova A.V., Savchuk T.P., Kamaleev M.F.,  
Dronova D.A., Gavrilin I.M.

*National Research University of Electronic Technology - MIET, Zelenograd, Russia*  
*Dronov.Alexey@org.miet.ru*

Scientific progress does not stand still, thereby increasing industrial development. In this connection, an energy crisis arises and environmental pollution increases [1–4]. Every year the question of an effective and cheap method of water purification from organic pollutants becomes more acute. One of the potential solutions to this problem may be the photocatalytic decomposition of organic compounds under solar irradiation.

Currently, titanium dioxide has been widely used as a photoelectrode material since the discovery of photochemical water splitting in 1972 [5]. An increase in the efficiency of such systems is usually achieved by increasing the active surface area [6]. In this regard, recently, special attention has been paid to nanoscale dispersions of TiO<sub>2</sub>, characterized by a high specific surface area. In particular, ordered arrays of TiO<sub>2</sub> pores (nanotubes) oriented perpendicularly to the substrate, obtained by anodic oxidation, are one of the promising structures. A distinctive feature of this method of formation is the possibility of controlled variation of the geometric characteristics of anodic titanium oxide nanotubes (TiO<sub>2</sub> NTs), such as length, external and internal diameters, wall thickness, in a wide range specified by the parameters of the anodic process [7]. Also, TiO<sub>2</sub> NTs have good mechanical and chemical stability and fast charge transfer rate along the tube walls [8].

However, the band gap of TiO<sub>2</sub> (3.2 eV) limits the absorption and use of the visible light. An increase in the photoactivity of TiO<sub>2</sub> in the visible range of radiation, as well as an increase in the efficiency of separation and reduction in recombination of charge carriers, can be achieved by using a number of techniques for modifying the surface and structure of the photocatalyst material [9]. To improve the photochemical properties of TiO<sub>2</sub>, it is possible to use various semiconductor nanoparticles for decorating the surface of titanium oxide. Sensitization of semiconductors with TiO<sub>2</sub> NTs can increase the collection of visible light and electron transfer efficiency. One of the most promising materials is copper oxide. Copper oxide is a p-type semiconductor with a narrow band gap (1.2–1.7 eV) and high stability under harsh conditions. Compared to conventional n-type metal oxide sensitizers, CuO nanoparticles deposited on TiO<sub>2</sub> NTs can form a heterojunction, which can have a positive effect on electron transfer and a decrease in carrier recombination. Using the successive ionic layer adsorption and reaction (SILAR) method to obtain nanoparticles of transition metal oxides to create a heterojunction can be a simple and cheap way to increase the photocatalytic activity of TiO<sub>2</sub>.

## PP-IV-10

Arrays of TiO<sub>2</sub> NTs were obtained during anodic oxidation of titanium foil with a voltage of 60 V in fluorine-containing electrolyte based on an ethylene glycol. The obtained structures underwent additional chemical and heat treatment to modify its chemical and phase composition.

Decoration of the TiO<sub>2</sub> NTs surface by CuO nanoparticles (NPs) was done by using the SILAR method. An aqueous solution of CuCl<sub>2</sub> was used as source of copper ions. After completion of the deposition process, the obtained samples were thermally treated in an oven at 300 °C for 2 hours in air to crystallize the deposited CuO NPs.

To study the morphology, chemical and phase composition of the samples, a complex of analytical methods was used, including scanning and transmission electron microscopy and Raman spectroscopy.

The optical properties of the samples under study were carried out using diffuse reflectance spectroscopy.

The photoelectrochemical properties were studied on an Autolab PGSTAT302 potentiostat in a thermostabilized three-electrode cell with a Ag/AgCl reference electrode and a Pt counter-electrode. Investigation of the photocurrent on different wavelength ranges were carried out using a xenon Xe-lamp (150 W, Oriel) and a set of optical filters.

To determine the level of photocatalytic activity of the obtained heterostructures, the methylene blue (MG) oxidation reaction under light irradiation with different wavelength range was performed.

Thus, a comparative analysis of obtained heterostructures with different morphology, chemical and phase composition and their optical, photoelectrochemical and photocatalytic properties was carried out.

Technological parameters for the heterostructures based on TiO<sub>2</sub> NTs/CuO NPs formation were selected for the optimal photocatalytical performance.

**Acknowledgement.** This work was supported by the RFBR, grant 18-29-23038.

### References:

- [1] M. Meng et al., J. of Cleaner Production 177 (2018) 752.
- [2] S.A. Asongu et al., Technol. Forecasting and Social Change 127 (2018) 209.
- [3] Y.Z. Shang et al., Appl. Energy 210 (2018) 660.
- [4] G.B. Bi et al., J. of Cleaner Production 171 (2018) 876.
- [5] A. Fujishima et al., Nature 7 (1972) 37.
- [6] M. Ge et al., J. of Mat. Chem. A 4 (2016) 6772.
- [7] K. Lee et al., Chem. Rev.114 (2014) 9385.
- [8] X. Tian et al., Sep. and Pur. Tech. 209 (2019) 368.
- [9] T. H. Nguyen et al., Adv. Natural Sciences 4 (2013) 025002.

## Oxide Catalysts for Production of Synthesis Gas and its Conversion to Liquid Hydrocarbons

Dossumov K.<sup>1,2</sup>, Ergazieva G.E.<sup>1</sup>, Mironenko A.V.<sup>1</sup>, Ermagambet B.T.<sup>3</sup>, Telbayeva M.M.<sup>1</sup>,  
Myltykbayeva L.K.<sup>1</sup>, Kassenova Zh.M.<sup>3</sup>

*1 – Institute of Combustion Problems, Almaty, Kazakhstan*

*2 – al-Farabi Kazakh National University, Centre of Physical and Chemical Methods of  
Investigation and Analysis, Almaty, Kazakhstan*

*3 – LLP Institute Chemistry of Coal and Technology, Nur-Sultan, Kazakhstan  
ergazieva\_g@mail.ru*

Synthesis gas consisting of a mixture of CO and H<sub>2</sub> in various proportions is an alternative source of raw materials for the petrochemical industry. The main areas of use of synthesis gas [1] oxosynthesis, reduction of iron ore in metallurgy, Fischer-Tropsch synthesis etc. Synthesis gas can be effectively used in the energy sector for the production of heat and electricity in gas turbine and combined-cycle plants, etc. Dry reforming of methane (DRM) is of particular interest because it allows you to simultaneously dispose of two greenhouse gases - methane and carbon dioxide. The main problems of DRM are the low activity of catalysts and their instability to carbonization, as a result of which they lose their effectivity [2]. Therefore, there is still an open question on the development of an active and resistant to carbonization catalyst for the carbon dioxide conversion of methane.

For Fischer – Tropsch synthesis, cobalt systems are considered as promising catalysts, which make it possible to obtain liquid and solid paraffin hydrocarbons from CO and H<sub>2</sub> with selectivity up to 90%. It is known, that the activity and selectivity of cobalt catalysts in the production of liquid hydrocarbons from synthesis gas are influenced by a large number of different factors, for example, the nature of the carrier, promoter, method of preparation, conditions of reduction, etc. [3]. Despite the large number of studies on the choice of carrier, the active phase of cobalt catalysts, the study of influence of the preparation method, conditions for the activation of catalysts. There is no single point of view of the influence of the above factors on the activity of catalysts in the process of producing liquid hydrocarbons by the Fisher-Tropsch method. Therefore, research in this area are relevant.

In this work, the influence of carrier's nature, oxides of transition elements, and the method of preparing catalysts on the direction of DRM to synthesis gas were studied. The transformation of synthesis gas into liquid hydrocarbons on cobalt catalysts was also investigated.

Among carriers ( $\theta$ -Al<sub>2</sub>O<sub>3</sub>,  $\gamma$ -Al<sub>2</sub>O<sub>3</sub> and 4A, 13X, HY, HZSM-5) studied in the production of synthesis gas by DRM,  $\gamma$ -Al<sub>2</sub>O<sub>3</sub> is most effective, the CH<sub>4</sub> conversion is 20 % was determined. It is established that the carrier's efficiency in CH<sub>4</sub> conversion depends on their specific surface. Among the studied oxides (Ni, Cu, Mo, V, Co, Cr, Zr, La, Ce) as the active phase of the catalyst, NiO was the most active in the of DRM. Studying the effect of the preparation method

## PP-IV-11

on the efficiency of 3 wt.% NiO /  $\gamma$ -Al<sub>2</sub>O<sub>3</sub> showed, that the preparation of the nickel catalyst by the “solution combustion” compared to the impregnation method leads to an increase of catalyst’s specific surface from 153 to 161 m<sup>2</sup>/g. Which contributes to an increase in efficiency catalyst, CH<sub>4</sub> conversion increases from 83 to 90% (Tr-850 °C). Effect of modifying additives (MoO<sub>3</sub>, La<sub>2</sub>O<sub>3</sub>, ZrO<sub>2</sub>) on the operating efficiency of 3 wt.% NiO /  $\gamma$ -Al<sub>2</sub>O<sub>3</sub> was studied. It was established that the introduction of MoO<sub>3</sub> into 3 wt.% NiO /  $\gamma$ -Al<sub>2</sub>O<sub>3</sub> leads to an increase in its efficiency in the reaction of the DRM, due to the increase in the textural characteristics of the catalyst. The CH<sub>4</sub> conversion increases from 90 to 96.2% (Tr-850 °C). Modification of 3 wt.% NiO /  $\gamma$ -Al<sub>2</sub>O<sub>3</sub> with MoO<sub>3</sub> leads to an increase in the carbonization stability of the catalyst. Under optimal reaction conditions: CH<sub>4</sub>:CO<sub>2</sub> = 1:1, GHSV = 1500 h<sup>-1</sup>, Tr = 700 °C on a catalyst 4 wt.% NiOMoO<sub>3</sub> / Al<sub>2</sub>O<sub>3</sub>, CH<sub>4</sub> conversion is 86.5%, CO<sub>2</sub> conversion is 79%, concentration of H<sub>2</sub>-50, CO-45 vol.%.

Conversion of synthesis gas to liquid hydrocarbons on the cobalt containing catalyst was studied. Catalyst was prepared by impregnation and “solution combustion” methods. The results of a physicochemical study (TPR-H<sub>2</sub>, SEM and BET) showed that synthesizing cobalt-containing catalysts by “solution combustion” method leads to a decrease in the catalyst recovery temperature, also to an increase in the specific surface of the catalyst from 166 to 171 m<sup>2</sup>/g compared to the impregnation method. Synthesis of a cobalt catalyst by "solution combustion" increases the dispersion of the catalyst, in the composition of the catalyst nanophases with sizes of 10-50 nm are observed. When a H<sub>2</sub>/CO = 2/1 mixture is converted on a cobalt-containing catalyst with REE additives prepared using the “solution combustion” method, at Tr= 300 °C and P= 6 atm, methanol, ethanol and dimethyl ether are formed as liquid products (10-15 vol.%).

The data obtained can be used in the development of new promising catalysts for the direct production of liquid hydrocarbons from methane through synthesis gas.

**Acknowledgement.** This work was supported by the Ministry of Education and Science of the Republic of Kazakhstan, grants № AP05132114 and № BR05236359.

### References:

- [1] Karima Rouibah, Akila Barama, Rafik Benrabaa, Jesus Guerrero-Caballero, Tanushree Kane, Rose-Noelle Vannier, Annick Rubbens, Axel Lofberg, Dry reforming of methane on nickel-chrome, nickel-cobalt and nickel-manganese catalysts, *Int. J. Hydrogen Energy*. 42 (2017) 29725–29734.
- [2] WenmingLiu, Le Li,Xianhua Zhang, Zheng Wang, Xiang Wang, Honggen Peng, Design of Ni-ZrO<sub>2</sub>@SiO<sub>2</sub> catalyst with ultra-high sintering and coking resistance for dry reforming of methane to prepare syngas, *Journal of CO<sub>2</sub> Utilization*. 27 (2018) 297-307.
- [3] E.Y. Asalieve, E.V. Kul’chakovskaya, L.V. Sineva, V.Z. Mordkovich, Effect of rhenium on Fischer-Tropsch synthesis in the presence of cobalt-zeolite catalyst, *Pet. Chem*. 57 (3) (2017) 251–256.

## Homogeneous Catalysts of Oxidation of Thiols by Oxygen in Hydrocarbon Media

Gavrilov Yu.A.<sup>1</sup>, Pletneva I.V.<sup>1</sup>, Nefedov S.E.<sup>2</sup>

*1 – N.N. Semenov Institute of Chemical Physics RAS, Moscow, Russia*

*2 – N. S. Kurnakov Institute of General and Inorganic Chemistry RAS, Moscow, Russia  
yurii.gavrilov@yandex.ru*

It is known that transition metal ions (Cu, Fe) are highly active catalysts for the oxidation of low molecular weight thiols (CH<sub>3</sub>SH, C<sub>2</sub>H<sub>5</sub>SH) with oxygen to disulfides in polar media. At the same time, the oxidation reactions of sulfhydryl derivatives in hydrocarbons catalyzed by metal complexes soluble in non-polar media are of scientific and practical interest. Practical interest in the above-mentioned catalysts is associated with their use in industrial processes of non-extraction (alkali-free) demercaptanization (removal of hydrogen sulfide and light thiols) in natural hydrocarbons and products of their processing [1].

The report presents the results of a study of the synthesis of Cu (+ II) metal complexes soluble in hydrocarbons and the kinetics of the mild oxidation of high molecular weight thiols (C<sub>4</sub> – C<sub>12</sub>) catalyzed by them. Metal complexes were obtained by the interaction of anhydrous CuCl<sub>2</sub> and CuCl with amino alcohols in the medium of aromatic (toluene, ortho-xylene) and aliphatic (heptane) solvents. Amino alcohols compatible with hydrocarbons were used as organic bases. Their general formula is R<sub>3-m</sub>N((CH<sub>2</sub>)<sub>2</sub>OH)<sub>m</sub>, where m = 1, 2 and R is n-butyl or n-octyldecan.

The effect of temperature, concentration, molar ratio of nitrogen-containing ligands and CuCl, oxygen pressure, nature of the solvent and thiol additives (C<sub>12</sub>H<sub>25</sub>SH) at the molar ratio of thiol / CuCl = 2 on the character of pattern of oxidation of Cu (I) to Cu (II) during the formation metal complexes was studied in detail.

The composition of the selected oxidation products of CuCl with oxygen from a solution in toluene in the presence of dibutylaminoethanol responds according to elemental analysis (C, H, N) to the formula Cu<sub>1.1</sub>, N<sub>1.2</sub>, C<sub>10.8</sub> and coincides with the composition of the crystal cell corresponding to the four-core copper complex Cu<sub>4</sub>O<sub>4</sub>C<sub>40</sub>H<sub>80</sub>N<sub>4</sub>Cl<sub>4</sub>, which is confirmed by X-ray diffraction data analysis.

The nature of the observed kinetic patterns of thiol oxidation in the presence of the synthesized complexes practically does not depend on the nature of the hydrocarbon radical. At the same time, a very complex dependence of the oxygen absorption rate (stage of reactivation of the Cu (I) → Cu (II) catalyst) on the catalyst concentration and the thiol / catalyst molar ratio is observed. The form of oxygen absorption kinetic curves changes from hyperbolic (thiol / catalyst molar ratio = 1–1.2) to sigmoid (with RSH / Cu ratio (+ II) ≥ 2.0). When the ratio RSH / Cu (+ II) = 3.0, the duration of the induction period is 5 hours and increases to 27 hours with the ratio RSH / Cu (+ II) = 5.0. The observed patterns are associated,

## PP-IV-12

on the one hand, with a change in the phase state of the catalyst, and, on the other, with the inhibition of the catalyst by the substrate (adsorption of thiols on the surface of the formed CuCl). According to the UV-VIS data of the catalyst solution, after complete thiol conversion, the full identity of the spectra of the initial metal complexes and complexes formed at the reactivation stage of the catalytic thiol oxidation cycle is noted.

$^1\text{H}$ ,  $^{13}\text{C}$  NMR-spectroscopic and FT-IR methods show that the products of thiol oxidation in the presence of synthetic catalysts are only disulfides, while the products of deeper oxidation are absent.

A number of synthesized metal complexes passed pilot tests in the process of non-extraction demercaptanization of gas condensate fuel oil containing  $\text{H}_2\text{S} = 28$  ppm,  $\text{CH}_3\text{SH} = 37$  ppm,  $\text{C}_2\text{H}_5\text{SH} = 124$  ppm. These tests showed that complete removal of these impurities was observed at a contact time of 4 hours, a temperature of 90 °C and a metal consumption (Cu) of 8 ppm.

**Acknowledgement.** This work was supported by the Russian Science Foundation, grant 16-33-00967.

### References:

[1] Gavrilov Yu.A., Isichenko I.V., Pletneva I.V., Silkina E.N. Eurasian Patent №018297 (2013).

## One-Pot Processes of Quinones Syntheses in the Presence of Heteropoly Acid Solutions as Bifunctional Catalysts

Gogin L.L., Zhizhina E.G.

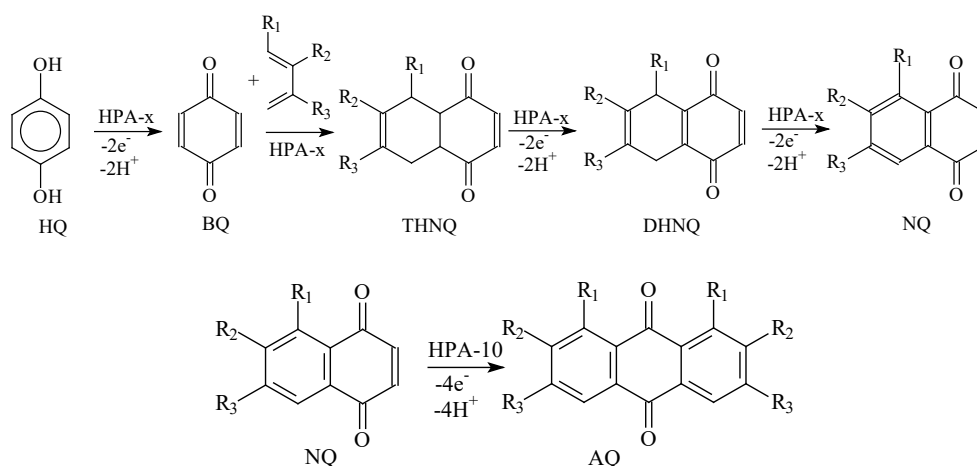
Boreskov Institute of Catalysis, Novosibirsk, Russia

gogin@catalysis.ru

At present, 1,4-naphthoquinones (NQ) and 9,10-anthraquinones (AQ) are important classes of organic compounds with many interesting properties [1-2]. A growing demand for NQ and AQ cannot be provided by existing technologies of their manufacture because ones involve many stages or produce acid effluents. Therefore, at present environmentally safe methods for the synthesis of NQ and AQ are of great demand.

For this purpose diene synthesis from benzoquinone (BQ) or NQ and 1,3-dienes in the presence of oxidizers may be used. As oxidizers heteropoly acids (HPA) can be used. Now processes using aqueous solutions of Mo-V-P heteropoly acids  $H_{3+x}PV_xMo_{12-x}O_{40}$  are widespread [3]. Unlike many other oxidizing agents, the vanadium-containing HPA solutions are able to be regenerated by  $O_2$ . Thus they can catalyze the oxidation of various substrates by  $O_2$ . In the presence of HPA solutions these processes consist of two stages carried out in separate reactors **1** and **2**. In the 1<sup>st</sup> stage a substrate is oxidizing by HPA. In the 2<sup>nd</sup> stage HPA is regenerated by  $O_2$ . It is known that vanadium-containing HPA solutions are strong Brønsted acids and can be used as acid catalysts. Therefore, HPA solutions can be bifunctional (i.e. oxidative and acidic) catalysts.

We have developed new processes of NQ and AQ derivatives production from hydroquinone (HQ) in the presence of HPA solutions [3-4]. At that, we have combined *in a single technological stage* three types of reactions: 1) oxidation of HQ by HPA to benzoquinone (BQ); 2) the acidic-catalyzed Diels-Alder reaction of different 1,3-dienes (1 or 2 mol) with BQ giving substituted 1a,4a-tetrahydro-NQ (THNQ) or 1,4,4a,9a-tetrahydro-AQ (THAQ) respectively; 3) the sequential oxidation of THNQ or THAQ by HPA with the formation substituted NQ or AQ. Thus, our *one-pot* processes are described by scheme 1:



## PP-IV-13

AQ synthesis by this method was studied with the synthesis of 2,3,6,7-tetramethyl-9,10-AQ (TMAQ) as an example [5]. One-pot processes of NQ synthesis was studied too. Results are presented in the Table.

№	Substituents	Yield of product, %	Content main product in precipitate, %
a) Naphthoquinones			
1	$R_1 = H, R_2 = CH_3, R_3 = H$	63	98
2	$R_2 = R_3 = H, R_1 = CH_3$	62	97
3	$R_2 = R_3 = CH_3, R_1 = H$	72	90
4	$R_1 = R_2 = R_3 = H$	41	45*
b) Anthraquinones			
5	$R_1 = H, R_2 = R_3 = CH_3$	76	80**
Conditions: a) $2 \times 10^{-3}$ mol HQ, 10 mL 0.25 M $H_7PMo_8V_4O_{40}$ (HPA-4) water solution, volume ratio HPA-4 : 1,4-dioxane = 1 : 1, reaction time 30 h, temperature 20 °C. HQ conversion $\geq 99\%$ ; b) $1.3 \times 10^{-3}$ mol HQ, 14 mL 0.25 M $H_{17}P_3Mo_{16}V_{10}O_{89}$ (HPA-10) water solution, volume ratio HPA-10 : 1,4-dioxane = 1 : 1; molar ratio diene : HQ = 6.6 : 1, reaction time 24 h, temperature 90 °C. HQ conversion $\geq 99\%$ .			

\*Main product is 1,4,4a,9a-tetrahydro-AQ. \*\*+20% 1,4-dihydro-AQ.

HPA-x solutions are stable at elevated temperatures (160-170°C) and can be fast regenerated by air  $O_2$  [3]. This feature of the HPA-x solutions has ensured high productivity of the processes depicted in the Scheme 1.

**Acknowledgement.** This work was supported by Ministry of Science and Education of Russian Federation (project No. AAAA-A17-117041710081-1).

### References:

- [1] Napthoquinones. Ullmann's Encyclopedia of Industrial Chemistry. 2005. Vol. N.
- [2] Anthraquinones. Ullmann's Encyclopedia of Industrial Chemistry. 2005. Vol. A.
- [3] L.L. Gogin, E.G. Zhizhina, Z.P. Pai, V.N. Parmon, Russ. Chem. Bull. Int. Ed. 64 (2015) 2069.
- [4] E.G. Zhizhina, M.V. Simonova, V.V. Russkih, K.I. Matveev, Catalysis in Industry. 1 (2005) 12.
- [5] L.L. Gogin, E.G. Zhizhina, Z.P. Pai, Kinetics and Catalysis. 59 (2018) 578.

## Influence of Ni Deposition Method on Catalytic Properties of Ni/Al<sub>2</sub>O<sub>3</sub> in Hydrodechlorination of Chlorobenzenes

Golubina E.V., Lokteva E.S., Kavalerskaya N.E., Kharlanov A.N., Maslakov K.I.  
*Lomonosov Moscow State University, Moscow, Russia*  
*golubina@kge.msu.ru*

Hydrodechlorination (HDC) is a remarkable environment friendly and cost saving alternative to the traditional methods for utilization of chlorinated pollutants. HDC of chlorinated organic compounds is sensitive to the electronic state of the supported metal [1, 2]. The active sites of the effective catalyst should contain both reduced and partially oxidized metal. The electronic state of the metal can be tuned by varying the degree of metal-support interaction (MSI). The Ni/Al<sub>2</sub>O<sub>3</sub> catalytic system is not only the efficient catalyst but also the good model because weak MSI results in easily reducible NiO, and stronger MSI provides hardly reducible spinel (as a result of the chemical interaction of Ni with alumina). In this work fundamental regularities on the process of formation of active centers in the Ni/Al<sub>2</sub>O<sub>3</sub> systems prepared by various methods were studied. The influence of Red-Ox treatments on the MSI was established, and the composition of the most active catalytic sites was revealed.

The series of Ni/Al<sub>2</sub>O<sub>3</sub> catalysts were synthesized by different methods in order to vary the degree of MSI. IMP-series: catalysts were prepared by wet impregnation method from Ni(NO<sub>3</sub>)<sub>2</sub> water solution. CP-series: catalysts were prepared by co-precipitation from Ni(NO<sub>3</sub>)<sub>2</sub> and Al(NO<sub>3</sub>)<sub>3</sub> mixture by NaOH at pH 9. DP-series: catalysts were prepared by deposition-precipitation of Ni from Ni(NO<sub>3</sub>)<sub>2</sub> by urea or ammonia. Catalysts precursors were calcined at different temperatures (110–600°C) and reduced with hydrogen at 330 or 450°C. CD-series: Ni was deposited on the alumina from colloid dispersion of 4-5 nm Ni<sup>0</sup> particles.

Catalysts were tested in the hydrodechlorination of chlorobenzene (HDC) at 50–350°C in the gas-phase flow type fixed-bed system. Catalysts after calcination, reduction and catalytic tests were studied by N<sub>2</sub> physisorption, TEM, SEM, IR, and TPR.

The influence of the calcination and reduction parameters on the active sites formation was revealed for the IMP-series. Calcination of the precursor at 400°C and higher temperatures leads to the strong bonding of Ni<sup>2+</sup> species to the alumina surface because of the formation of spinel phase. With increasing the nickel content, the fraction of Ni<sup>2+</sup> species reducible at temperatures 500–600°C increases. Calcination of the catalyst precursor at temperatures below 300°C leads to the formation of weakly bound Ni<sup>2+</sup> species that are reduced to metallic nickel in a hydrogen stream at 300°C. The changes in the surface composition are reflected in the catalytic activity in gas-phase chlorobenzene HDC. Spinel forms of Ni are inactive in this reaction, but they react with hydrogen under the reaction conditions to form Ni<sup>0</sup>, which results in the increase in catalytic activity. The active sites formed by the reduction of weakly bound Ni<sup>2+</sup> species are the most active and stable in chlorobenzene HDC.

## PP-IV-14

The Ni deposition method also affects the composition and properties of the active sites. TPR study of unreduced precursors shows that the deposition-precipitation leads to the formation of different Ni-Al species with the broadest range of reduction temperatures in TPR profile (from 500 to 950°C). Such non-uniform surface composition led to the lowest activity and stability of the Ni/Al<sub>2</sub>O<sub>3</sub>-DP catalysts. The TPR profiles for the catalysts prepared by the co-precipitation method demonstrate only one reduction peak at about 640°C that corresponds to the reduction of the Ni-enriched mixed Ni-Al oxide phase. The presence of only one reduction peak in TPR profile indicates the uniform surface composition of this catalyst. The oxidation of the completely reduced catalyst at low temperature (300°C) makes it possible to obtain a system containing only weakly bound NiO species, completely eliminating the formation of mixed oxide forms. This fact agrees with the results of the IR spectroscopy of adsorbed CO: in reduced Ni/Al<sub>2</sub>O<sub>3</sub>-CP the amount of Ni<sup>0</sup> is 2.7 times higher compared to Ni/Al<sub>2</sub>O<sub>3</sub>-IMP. As a result, the catalysts of CP-series were the most active in chlorobenzene HDC. Moreover, only on Ni/Al<sub>2</sub>O<sub>3</sub>-CP catalysts cracking products were formed at reaction temperatures above 350°C, probably due to their increased Lewis acidity, found by IR spectroscopy of adsorbed benzene.

The study of catalysts synthesized by the deposition of pre-reduced nickel metal particles from colloid dispersion showed that even in this case the interaction of the metal with the support was not avoided. XPS results revealed that only 5% of Ni exists on the surface as metal species, while the rest of it is most likely forms spinel and/or Ni(OH)<sub>2</sub> species. These catalysts exhibited the catalytic activity in chlorobenzene HDC only at high temperatures (250–350°C). In this temperature range relatively weakly bound Ni species can be reduced by hydrogen from the reaction medium. Indeed, the reduction of Ni/Al<sub>2</sub>O<sub>3</sub>-CD by hydrogen immediately before the start of the experiment led to a significant increase in chlorobenzene conversion.

**Acknowledgement.** This work was supported in part by Lomonosov Moscow State University Program of Development.

### References:

- [1] S. Ordóñez, E. Díaz, R.F. Bueres, E. Asedegbega-Nieto, H. Sastre, *J. Catal.* 272 (2010) 158.
- [2] L.M. Gómez-Sainero, X.L. Seoane, J.L.G. Fierro, A. Arcoya, *J. Catal.* 209 (2002) 279.
- [3] S.A. Kachevskii, E.V. Golubina, E.S. Lokteva, V.V. Lunin, *Russ. J. Phys. Chem. A*, 81 (2007) 866.

## The Effect of Sr Substitution in Bulk and Supported $\text{La}_{1-x}\text{Sr}_x\text{FeO}_3$ Perovskites on the Catalytic Activity in $\text{NH}_3$ Oxidation and $\text{N}_2\text{O}$ Decomposition Reactions

Sutormina E.F.<sup>1</sup>, Isupova L.A.<sup>1</sup>, Rogov V.A.<sup>1,2</sup>, Ivanova Y.A.<sup>1</sup>, Vovk E.I.<sup>3</sup>

1 – Boreskov Institute of Catalysis, Novosibirsk, Russia

2 – Novosibirsk State University, Novosibirsk, Russia

3 – ShanghaiTech University, Shanghai, China

*ivanova@catalysis.ru*

Perovskites are attractive materials as catalysts for total oxidation of ammonia as they are less expensive than PGMs, have high thermal stability, show high  $\text{NO}_x$  yield at operating temperatures (850-900°C) of industrial ammonia oxidation process and offer large range of materials through substitution and doping [1]. Moreover, they could reduce  $\text{N}_2\text{O}$  emission due to direct decomposition of nitrous oxide formed as an undesirable by-product on PGM gauzes. The reaction was proposed to follow the Mars–van Krevelen type scheme, which involves the participation of lattice oxygen in  $\text{NH}_3$  oxidation to  $\text{NO}$  and the regeneration of oxygen vacancies by gas-phase  $\text{O}_2$  and/or bulk lattice oxygen. The addition of dopants could promote the catalytic activity of such mix oxides in the reaction due to creation of oxygen vacancies in the perovskite lattice which increase lattice oxygen mobility and facilitate the diffusion of lattice oxygen from the bulk to the surface.

In this work we studied the effect of strontium substitution in bulk and supported  $\text{La}_{1-x}\text{Sr}_x\text{FeO}_3$  perovskites ( $x = 0-0.5$ ) on their catalytic activity in  $\text{NH}_3$  oxidation and  $\text{N}_2\text{O}$  decomposition reactions. The basic features of phase and surface compositions of prepared mix oxides were characterized by BET, XRD, and XPS methods. Redox properties of the catalysts were estimated using  $\text{H}_2$ -TPR at 100-900°C.

It was found that the substitution of lanthanum by strontium generated weakly bound oxygen associated with the formation of  $\text{Fe}^{4+}$  ions.  $\text{La}_{1-x}\text{Sr}_x\text{FeO}_3$  catalysts with  $x=0.2-0.3$  are easily reduced at lower temperature that caused the increase in catalytic activity of these substituted perovskites in the reactions. The further increase in substitution degree resulted in Sr segregation on the catalysts surface accompanied by a decrease in surface area, lower reducibility and catalytic activity as well. For supported samples, the activity in the reactions is weakly dependent on the Sr substitution degree. There is no significant difference between the reduction of 10%  $\text{La}_{1-x}\text{Sr}_x\text{FeO}_3/\text{Al}_2\text{O}_3$  catalysts with  $x=0-0.5$ . This may be due to a significant decrease in the content of active component on the surface of catalysts and the modification of perovskite with aluminum cations.

**Acknowledgement.** This work was conducted within the framework of budget project AAAA-A17-117041710090-3 for Boreskov Institute of Catalysis.

### References:

[1]. S. Royer, D. Duprez, F. Can, X. Courtois, et al, Chem. Rev., 114 (2014) 10292.

## Oxidative Coupling of Methane over Different Sr<sub>2</sub>TiO<sub>4</sub> Catalysts

Ivanova Y.A.<sup>1</sup>, Sutormina E.F.<sup>1</sup>, Nartova A.V.<sup>1,2</sup>, Isupova L.A.<sup>1</sup>

1 – Boreskov Institute of Catalysis, Novosibirsk, Russia

2 – Novosibirsk State University, Novosibirsk, Russia

*ivanova@catalysis.ru*

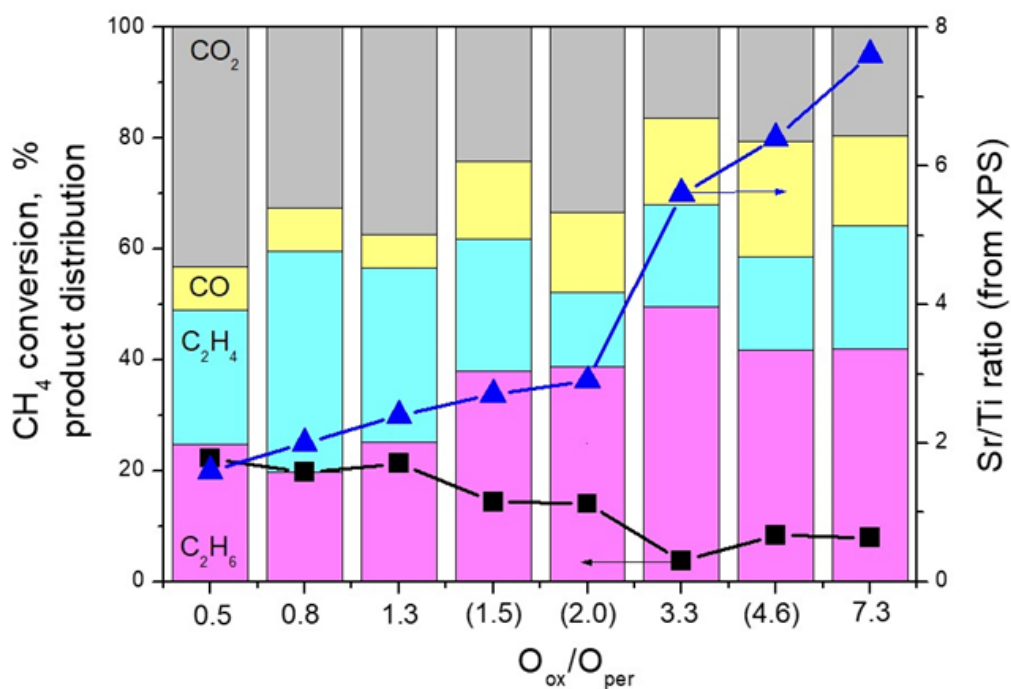
Direct catalytic conversion of methane to C<sub>2</sub> hydrocarbons by oxidative coupling (OCM process) is considered as potential route for the production of useful chemicals and fuels from natural or shale gases [1]. Since the reaction occur via a heterogeneous-homogeneous mechanism, the activity of various catalysts in the reaction is determined by the presence of strongly bound oxygen species, being the active sites for methyl radical generation and high basicity for their fast desorption. Mix oxides with a structure of layered perovskite which are composed of alternating perovskite and oxide layers can be considered as promising catalysts for the OCM reaction. The changes in the cations composition and defect structure of the oxide layers can affect the oxygen bond strength and catalytic activity of these materials.

In this work, the relationship between the surface properties (number or types of oxygen-containing active centers, surface basicity) of the catalysts based on Sr<sub>2</sub>TiO<sub>4</sub> mix oxides with a structure of layered perovskite and their activity in the OCM reaction (methane conversion, C<sub>2</sub>-selectivity) was proposed. For this purpose, a series of Sr<sub>2</sub>TiO<sub>4</sub> catalysts was synthesized using different preparation routes which ensure the predominance of oxide or perovskite layers on the surface [2]. The structural and textural properties of prepared catalysts were studied by adsorption measurements, XRD, SEM, XPS. The changes in surface properties and catalytic activity of the catalysts in time-on-stream experiments (850°C, CH<sub>4</sub>:O<sub>2</sub> = 4, GHSV = 150000 h<sup>-1</sup>, 10 h) were evaluated.

It was found that the phase and surface composition, specific surface area, morphology and catalytic activity in the oxidative coupling of methane of prepared samples strongly depend on the preparation route. According to XPS, there are two main oxygen forms in the samples corresponding to the oxygen in perovskite and oxide/carbonate. The ratio of the oxygen species (O<sub>ox</sub>/O<sub>per</sub>) depends on different degree of surface enrichment with Sr species (Sr/Ti ratio) in the samples.

The segregation of Sr on the surface of catalysts upon the co-precipitation and citrate precursor preparation routes leads to a significant decrease in the specific surface areas that results in lower methane conversion and C<sub>2</sub>-yield on such catalysts despite their higher selectivity to C<sub>2</sub>-hydrocarbons (Fig). The decomposition of the layered perovskites under the reaction conditions followed with the same segregation of Sr compounds on the perovskite surface was found as in the previous work [3]. In general, after the reaction, various catalysts are characterized by similar properties (phase and surface composition, catalytic activity).

## PP-IV-16



Thus, the increase in the Sr centers on the surface of  $Sr_2TiO_4$  catalysts both upon the preparation routes or during the time-on-stream experiments increases the surface basicity and  $C_2$ -selectivity in OCM reaction as well. However, the accompanying decrease in specific surface area and lowering the number of active centers for methane activation reduce the overall  $C_2$ -yield on such catalysts.

**Acknowledgement.** This work was conducted within the framework of budget project AAAA-A17-117041710090-3 for Boreskov Institute of Catalysis.

### References:

- [1] A. Galadima, O. Muraza, J. Indust. Engin. Chem. 37 (2016) 1.
- [2] Y.A.Ivanova, E.F.Sutormina, N.A.Rudina, A.V.Nartova, L.A.Isupova, Catal. Commun. 117 (2018) 43.
- [3] D.V. Ivanov, L.A. Isupova, E. Yu. Gerasimov, L.S. Dovlitova, T.S. Glazneva, I.P. Prosvirin, Appl. Catal. A: General 485 (2014) 10.

## Precipitated K-Promoted Co-Mn-Al Mixed Oxides for Direct NO Decomposition: Preparation and Properties

Jirátová K.<sup>1</sup>, Pacultová K.<sup>2</sup>, Balabánová J.<sup>1</sup>, Karásková K.<sup>2</sup>, Klegová A.<sup>2</sup>, Bílková T.<sup>2</sup>, Jandová V.<sup>1</sup>, Koštejn M.<sup>1</sup>, Obalová L.<sup>2</sup>

1 – Institute of Chemical Process Fundamentals of the CAS, v.v.i., Prague, Czech Republic

2 – VSB-TU of Ostrava, Institute of Environmental Technology, Ostrava, Czech Republic

*jiratova@icpf.cas.cz*

Recent experimental studies showed that K-promoted Co-Mn-Al mixed oxides catalysts could be effective catalysts for the direct decomposition of NO to N<sub>2</sub> and O<sub>2</sub> [1], as it proceeds successfully in the temperature range 600-700 °C. However, stability of the catalyst can be influenced by stability of the promotor (K) at the applied reaction conditions. As was shown in [1], the method of catalyst preparation can affect its activity and stability. Co-precipitation of metals salts by Na salts and following impregnation of wet cake by solution of KNO<sub>3</sub> (Bulk promotion method - BP) led to higher activity and stability of the catalyst than both impregnation of the calcined Co-Mn-Al precursor with a solution of KNO<sub>3</sub> and calcination of corresponding metal nitrates. Disadvantage of the applied method of metal salts co-precipitation by solutions of Na compounds with subsequent impregnation of wet cake is rather complicated preparation procedure. In this contribution, intimate modification of Co-Mn-Al mixed oxides was studied using co-precipitation of a metal nitrates solution with the aqueous solution of K salts.

Co-Mn-Al mixed oxides modified by K were prepared using co-precipitation of a metal nitrates solution with the aqueous solution of K<sub>2</sub>CO<sub>3</sub> and KOH, washing the precipitates to different level of K concentrations and finally calcined at chosen temperature, 500 °C or 700 °C. Numbers 1 to 5 labels the catalysts. The laboratory catalyst prepared by bulk promotion of Co-Mn-Al hydrotalcite-like precursor with K salt was labeled, after drying and calcination, as BP. Commercial Co-Mn-Al catalyst originally designed for direct N<sub>2</sub>O decomposition and laboratory recalcined to 670 °C was included for comparison (labeled as Com). The samples were characterized by AAS, N<sub>2</sub> physisorption (S<sub>BET</sub>), DTG, H<sub>2</sub>-TPR, XRD, XPS, and CO<sub>2</sub>-TPD. The catalysts pre-calcined at 700 °C were tested in direct decomposition of NO (650 °C, 0.5 g, 1000 ppm NO/N<sub>2</sub>, 49 ml min<sup>-1</sup>).

Chemical composition and physico-chemical properties of the prepared catalysts are shown in Table 1. Concentration of K varied from 19 to 0.6 wt. %. DTG measurements of the dried samples showed three areas of maximum weight decrease: 113-136, 206-193 and 448-558°C. The first one can be ascribed to removal of water, second to decomposition of carbonates, and the third one to removal of OH from metal oxyhydroxides.

XRD patterns of the calcined samples confirmed formation of Co<sub>3</sub>O<sub>4</sub> spinel-like phase regardless the K concentration in the catalysts. Surface area of the catalysts with K < 2.4 wt. %

## PP-IV-17

was about  $100 \text{ m}^2 \text{ g}^{-1}$ , and it decreased with increasing K concentration (catalyst with 18.9 wt. % K showed  $S_{\text{BET}} < 1 \text{ m}^2 \text{ g}^{-1}$ ).  $\text{H}_2$ -TPR profiles reflected concentration of K in the catalysts: increasing concentration of K (except the highest concentration 18.9 wt. %) led to gradual decrease in reduction temperature, and simultaneously, to the increase of concentration of strong basic sites. The catalyst with 8 wt. % K exhibited the highest amount of basic sites desorbing during  $\text{CO}_2$ -TPD in the range 25-500 °C and the highest catalytic activity.

Table 1 Composition and surface areas of the catalysts calcined at 500 °C, characteristics of their surface properties ( $\text{CO}_2$ -TPD and  $\text{H}_2$ -TPR) and conversions of NO at 650 °C.

Sample	K wt. %	Co wt. %	Mn wt. %	Al wt. %	$S_{\text{BET}}$ $\text{m}^2 \text{ g}^{-1}$	$\text{CO}_2$ -TPD <sup>a</sup> $\text{mmol g}^{-1}$	$\text{H}_2$ -TPR <sup>a</sup> $\text{mmol g}^{-1}$	$X_{\text{NO}(650)}$ %
1	18.90	28.2	6.0	3.0	< 1	0.01	17.9	23
2	8.20	40.0	8.8	4.0	58	0.14	9.08	61
3	2.39	45.4	10.2	4.7	110	0.13	4.28	46
4	0.92	46.8	10.2	4.7	105	0.05	4.05	0.6
5	0.60	45.6	9.9	4.4	102	0.06	3.77	0
BP	1.90	53.0	12.0	-	94	0.02	3.76	57
Com	2.00	45.3	9.6	5.1	63	0.11	3.34	36

<sup>a</sup>25-500 °C

The investigated method of the K promoted Co-Mn-Al catalyst preparation is easier than the previously studied method of bulk promotion of Co-Mn-Al hydrotalcite-like precursor with a K salt. It leads to more facile reduction of the active components at lower temperature, to higher amount of medium and strong basic sites, and to slightly higher catalytic activity. Higher concentration of potassium in the coprecipitated K-promoted Co-Mn-Al catalysts can be favorable for the durability of the catalytic activity in NO decomposition due to its function as the reservoir of potassium inside the catalyst particles.

**Acknowledgement.** The work was supported from Czech Science Foundation (project No. 18-19519S) and ERDF "Institute of Environmental Technology – Excellent Research" (No. CZ.02.1.01/0.0/0.0/15\_019/0000853). Experimental results were accomplished by using Large Research infrastructure ENREGAT supported by the Ministry of Education, Youth and Sports of the Czech Republic under project No. LM2018098.

### References:

[1] K. Pacultová, V. Drašíková, Ž. Chromčáková, T. Bílková, K. Mamulová Kutlákova, A. Kotarba, L. Obalová, J. Mol. Catal. A: Chemical 428 (2017) 33.

## Synthesis and Properties of Catalyst Based on Titanium Dioxide Modified by Nanomaterials and Catalytic Metals (Pt, Pd) Used in Air Purifiers

Kabachkov E.N.<sup>1,2</sup>, Balikhin I.L.<sup>1,2</sup>, Vershinin N.N.<sup>1</sup>, Efimov O.N.<sup>1</sup>, Kurkin E.N.<sup>1,2</sup>

1 – Institute of Problems of Chemical Physics RAS, Chernogolovka, Moscow region, Russia

2 – Scientific Center of the Russian Academy of Sciences in Chernogolovka, Chernogolovka, Moscow region, Russia

*gurov@icp.ac.ru*

Photocatalytic air purifiers based on titanium dioxide are widely used for air purification from organic toxicants, viruses and bacteria in homes and offices [1]. An essential disadvantage of such purifiers is low efficiency of air purification from carbon monoxide (CO). One of ways of enhancing efficiency of oxidation of CO is introduction of clusters of catalytic metal (Pt, Pd) on nanocarrier surface. We have shown that nanocarriers structurally similar to platinum and palladium clusters show high efficiency in oxidation of CO [2-4]. We synthesized CO oxidation catalysts based on titanium dioxide which includes nanoparticles of cubic structure (nanodiamond (ND), silicon carbide, and titanium nitride) catalytic metal (Pt, Pd) clusters. The catalyst was synthesized by the procedure developed by us earlier [5]. Catalytic oxidation of CO was studied in a low concentration range (<100 mg/m<sup>3</sup>) at room temperature. Such parameters are characteristic of homes and offices. ND (5 nm), SiC (13 nm), TiN (16 nm) and commercial titanium dioxide with average crystallite size of 5-9 nm were used as carriers. The studied catalysts show high catalytic activity in the reaction of oxidation of CO at room temperature. It has been found that CO oxidation rate on the new catalysts is 3 times higher than that for the nanoparticle (ND, SiC, TiN) free catalyst based on titanium dioxide. The new catalysts are promising for the application in catalytic and photocatalytic systems for air purification from toxic gases in homes and offices. At present the catalysts are tested in TIOKRAFT Co. Ltd air purifiers. The tests are aimed at determination of technical parameters of the devices.

### References:

- [1] Mo J. et al. Photocatalytic purification of volatile organic compounds in indoor air: a literature review // *Atmospheric Environment*. – 2009. – T. 43. – №. 14. – C. 2229-2246.
- [2] Vershinin N. N. et al. Synthesis and properties of a platinum catalyst supported on plasma chemical silicon carbide // *High Energy Chemistry*. – 2017. – T. 51. – №. 1. – C. 46-50.
- [3] Vershinin N. N. et al. Synthesis and properties of a CO oxidation catalyst based on plasma-chemical silicon carbide, titanium dioxide, and palladium // *High Energy Chemistry*. – 2018. – T. 52. – №. 1. – C. 90-94.
- [4] Vershinin N. N. et al. The Synthesis and Properties of a Catalyst Based on Titanium Dioxide, Nanodiamond and Pd for CO Oxidation // *Kinetics and Catalysis*. – 2018. – T. 59. – №. 2. – C. 174-178.
- [5] Catalyst and method of its preparation/ N.N.Vershinin, O.N.Efimov, // Russian patent N 2348090 of February 27, 2009.

## Effect of the Nature of Manganese Species in Mn-Ce-Zr Mixed Oxide Systems on Catalytic Properties in CO Oxidation

Kaplin I.Yu., Lokteva E.S., Golubina E.V., Maslakov K.I., Shishova V.V., Fionov A.V.  
*Lomonosov Moscow State University, Moscow, Russia*  
*kaplinigormsu@gmail.com*

Ceria-zirconia mixed systems are promising catalysts for CO oxidation [1]. Additional modification with transition metal oxides allows extending the temperature range of their operation [2]. Manganese oxides can be successfully used as modifiers [3]. The method of Mn introducing can affect the bulk and surface structure of the triple oxide systems. Therefore, this work is aimed to reveal the influence of the preparation method on the structural and catalytic properties of  $\text{MnO}_x\text{-CeZrO}_x$  (Mn-CZ, Ce:Zr = 4) in CO oxidation.

Two types of mixed oxide systems were prepared: (method 1) Mn-CZ ( $S_{\text{BET}} = 40 \text{ m}^2/\text{g}$ ) — by the CTAB-templated (where CTAB is cetyltrimethylammonium bromide) EISA method [2, 4] and (method 2) Mn-CZ IM ( $S_{\text{BET}} = 48 \text{ m}^2/\text{g}$ ) by impregnation of pre-prepared double oxide CZ with manganese acetate. CZ ( $S_{\text{BET}} = 83 \text{ m}^2/\text{g}$ ) and  $\text{MnO}_x$  ( $S_{\text{BET}} = 20 \text{ m}^2/\text{g}$ ) systems were also synthesized by method 1. Then the obtained samples were dried and calcined at  $500^\circ\text{C}$  for 3.5 h (method 1) or at  $400^\circ\text{C}$  for 2 h (method 2). The target Mn content in both systems was 8 wt.%. Catalytic tests were carried out in the fixed-bed microcatalytic setup at pulse feeding of the reaction mixture (2 vol.% CO, 1 vol.%  $\text{O}_2$  in He) in the temperature range from 100 to  $400^\circ\text{C}$ . Analysis of the reaction products was performed by GC.

Bulk and surface composition of prepared systems was investigated by XRD, Raman spectroscopy and XPS. The reflections of  $\text{Mn}_2\text{O}_3$  and the spinel hausmannite phase of  $\text{Mn}_3\text{O}_4$  are observed in the diffraction pattern of  $\text{MnO}_x$ . The XRD patterns of CZ, Mn-CZ and Mn-CZ IM comprise main reflections characterized the cubic fluorite phase. No diffraction peaks of manganese oxides are observed in the patterns of both Mn-modified samples despite the presence of Mn-enriched areas in Mn-CZ IM detected by SEM-EDS. Raman spectroscopy confirmed that both Mn-modified systems contain the CZ mixed oxide phase, but the spectrum of Mn-CZ IM has a separate  $\text{Mn}_3\text{O}_4$  band. This fact, along with the intensity and position of the  $F_{2g}$  line, indicates a weak interaction of manganese with the CZ in Mn-CZ IM. According to XPS results,  $\text{Mn}^{3+}$  prevails on the surface for all Mn-containing samples, while the relative content of  $\text{Mn}^{2+}$  species is at least two times higher of Mn-CZ IM compared to Mn-CZ.

The broad EPR spectra of CZ, Mn-CZ IM, and  $\text{MnO}_x$  with different g-factors (Fig. 1, a) can indicate the presence of paramagnetic particles adsorbed on the surface, and clustered Mn ions. In contrast, the EPR spectrum of Mn-CZ contains hyperfine structure with six intense lines which are related to the presence of isolated  $\text{Mn}^{2+}$  ions located in defect sites with a noncubic symmetry or in the substitutional sites of the CZ lattice. The TPR method also confirms that both modified systems contain  $\text{Mn}^{2+}$  and  $\text{Mn}^{3+}$ .

Catalytic results (Fig. 1, b) show that modification of CZ with manganese oxides contributes to a noticeable increase in CO conversion, especially at the low-temperature range (150 - 350 °C). Mn-CZ IM is somewhat more active in the range from 100 °C to 250 °C. The reducing of the contact times of catalysts with the reaction mixture by decreasing catalyst loadings into the reactors allowed revealing more significant differences between Mn-CZ and Mn-CZ IM. In this case Mn-CZ IM provides higher CO conversion than Mn-CZ, especially at 250–350°C. Moreover, the absence of the hysteresis loop for Mn-CZ IM (Fig. 1, c) indicates the higher stability of this catalyst.

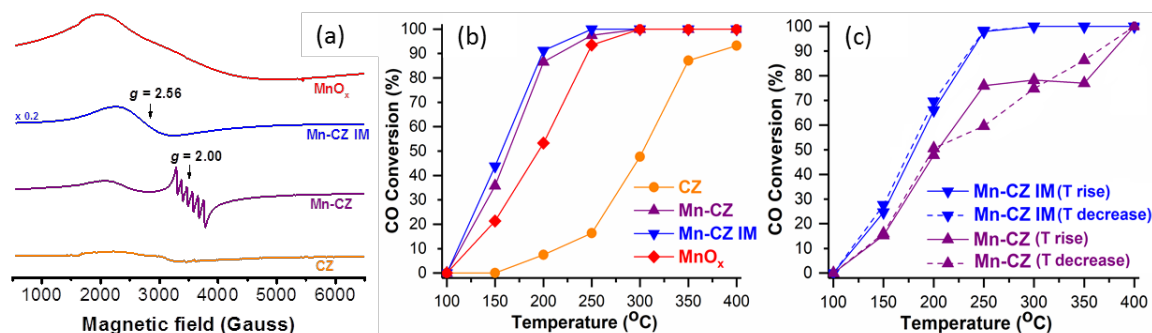


**Figure 1.** EPR spectra (a) and CO conversion plots at 100 mg (b) or 50 mg (c) catalyst loading

Thus, despite decreasing of  $S_{\text{BET}}$  values, modification of CZ by MnO<sub>x</sub> during both synthesis procedures leads to significantly improvement of catalytic properties in CO oxidation. It is probably caused by the presence of separate phases of manganese oxides in various oxidation states, which provide active adsorption centers on the surface. Mn-CZ IM is more active than Mn-CZ in spite of similar properties detected by several physicochemical methods (both contain mixed CZ oxide phase and highly dispersed Mn<sup>2+</sup>, Mn<sup>3+</sup> oxide particles; their specific surface areas are nearly equal). However, the distribution and speciation of manganese in the synthesized catalysts depends on the Mn incorporation technique. In Mn-CZ a minor part of the Mn-modifier is not available for reagents adsorption because of the incorporation of manganese ions into the CZ crystal lattice. In contrast, the presence of surface locations enriched with MnO<sub>x</sub> and other locations comprising mainly CZ and depleted with MnO<sub>x</sub> in Mn-CZ IM can provide the additional adsorption sites and the supply of active oxygen species by spillover mechanism during CO oxidation, respectively.

**Acknowledgement.** This work was maintained by Lomonosov Moscow State University Program of Development.

#### References:

- [1] J. Kašpar, P. Fornasiero, N. Hickey, *Catal. Today*. 77 (2003) 419.
- [2] I.Yu. Kaplin, E.S. Lokteva, E.V. Golubina et al. *RSC advances*, 2017 (81) 51359.
- [3] P. Venkataswamy, K.N. Rao, D. Jampaiah, B.M. Reddy, *Appl. Catal. B Environ.* 162 (2015) 122.
- [4] X.B. Zhao, F. Chen, J. You, X.Z. Li, X.W. Lu, Z.G. Chen, *J. Mater. Sci.* 45 (2010) 3563.

## K/Co-Mg-Mn-Al Mixed Oxide Catalyst System for Direct NO Decomposition

Karášková K.<sup>1</sup>, Pacultová K.<sup>1</sup>, Klegova A.<sup>1</sup>, Fridrichová D.<sup>1,2</sup>, Kiška T.<sup>1</sup>, Jiratová K.<sup>3</sup>, Obalová L.<sup>1</sup>

1 – Institute of Environmental Technology, VSB – Technical University of Ostrava, Ostrava, Czech Republic

2 – Centre Energy Units for Utilization of Non-traditional Energy Source, VSB-Technical University of Ostrava, Ostrava, Czech Republic

3 – Institute of Chemical Process Fundamentals of the CAS, Prague, Czech Republic  
katerina.karaskova@vsb.cz

Direct decomposition of NO is the most attractive as well as the most challenging NO<sub>x</sub> abatement process. This reaction is thermodynamically feasible but due to the high activation energy, the measurable reaction rate can be achieved only at temperatures above 1000 °C. This problem could be solved using the suitable catalysts [1]. In our previous work, the alkali metals (K, Cs) were evaluated as promoters which increased the activity of the Co<sub>4</sub>MnAlO<sub>x</sub> mixed oxide catalyst. However, there are problems with low stability of these alkali metals at reaction temperatures caused by their desorption [2]. The alkali metal stabilization can be achieved by adjusting the catalyst composition and/or preparation procedure. In [3], the enhancement of potassium stability in the composite ferrite catalyst for ethylbenzene dehydrogenation was achieved by phase selective doping with Cr, Mn, Ce, Al, and Mg.

In this study, the effect of Mg partly substituting Co in the Co<sub>4</sub>MnAlO<sub>x</sub> mixed oxide catalyst subsequently modified by different potassium amount, maintaining (Co<sub>x</sub>Mg<sub>y</sub>)/Mn/Al molar ratio constant, was studied. The prepared catalysts were characterized by XRD, BET, TPR-H<sub>2</sub>, TPD-CO<sub>2</sub> and tested for direct NO decomposition in inert gas and in the presence of oxygen.

Spinel structure was detected in all samples. The gradual segregation of two different spinels was observed for the samples with increasing amount of Mg dopant. Simultaneous formation of K-Mn-O phase and the decrease of spinel segregation were found with increasing K content in the catalysts when Mg content was constant. TPR measurements showed that  $T_{max}$  decreased with increasing amount of potassium.

Presence of magnesium and potassium in the Co<sub>4</sub>MnAlO<sub>x</sub> mixed oxide led to the significant increase in catalytic activity for decomposition of NO. Surprisingly, no direct correlation between NO conversion and magnesium content was observed. However, Mg in the catalysts affected stability of K at reaction temperatures positively. DeNO activity depended on the K amount. When the catalyst contained optimum amount of 1 - 2 wt. % K (Fig. 1), maximum NO conversion was achieved.

## PP-IV-20

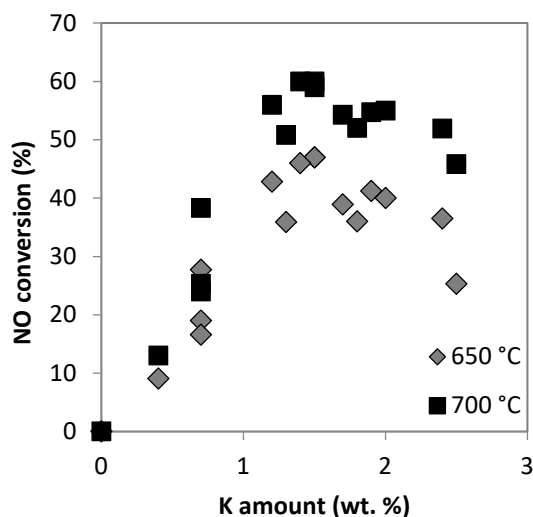


**Fig. 1** Dependence of NO conversion on K amount (AAS) in K-Co-Mg-Mn-Al mixed oxide catalysts. Conditions: 1000 ppm NO in N<sub>2</sub>, GHSV = 6 l g<sup>-1</sup> h<sup>-1</sup>

**Acknowledgement.** This research was funded by ERDF OP RDE project No. CZ.02.1.01/0.0/0.0/15\_019/0000853 and by Czech Science Foundation (No. 18-19519S). Experimental results were accomplished by using Large Research Infrastructures ENREGAT (No. LM2018098) and CATPRO (No. LM2015039) supported by the Ministry of Education, Youth and Sports of the Czech Republic.

### References:

- [1] M. Haneda, H. Hamada, *Comptes Rendus Chimie*, 19 (2016) 1254-1265.
- [2] K. Pacultová, V. Draščíková, Ž. Chromčáková, T. Bílková, K. M. Kutlákova, A. Kotarba, L. Obalová, *Molecular Catalysis*, 428 (2017) 33-40.
- [3] A. Kotarba, W. Bieniasz, P. Kuśtrowski, K. Stadnicka, Z. Sojka, *Applied Catalysis A*, 407 (2011) 100-105.

## Supported Palladium Catalysts of Selective Hydrogenation on the Basis of High-Porous Cellular Materials

Kirgizov A.J., Ilyasov I.R., Laskin A.I. Lamberov A.A.  
*Kazan Federal University, Kazan, Russia*  
*alexey.kirgizov@yandex.ru*

Polyethylene is produced by the polymerization of ethylene, which is produced by cracking naphtha, which includes a small amount of acetylene. Acetylene poisons the catalyst for the polymerization of ethylene and degrades the quality of polyethylene; therefore, it is usually removed by selective hydrogenation [1–3].

A key factor in acetylene hydrogenation is minimization of ethylene loss during acetylene removal, as evidenced by ethylene selectivity in the reaction [2,4].

The catalyst is palladium dispersed on the surface of aluminum oxide [5-7]. The catalyst used should have: high activity, providing a residual content of acetylene and diene compounds in the reaction products to values of ~ 0.0001% by weight.

Granular catalysts with an irregular layer used in industrial hydrogenation processes are characterized by unsatisfactory heat transfer. There are also diffusion limitations when transferring reagents to the active component, due to its location in the depth of the carrier granule.

In this regard, the further development of catalytic systems led to a change in their geometry and shape in the form of regular block honeycomb and mesh structures. A variety of block systems are highly porous cellular materials (HPCMs), which are a spatial framework formed by a system of cells and having a plurality of pores and channels in their structure, which allow to improve radial mixing, increase heat transfer, reduce hydraulic resistance in the catalyst bed.

The initial matrix in the synthesis of HPVM is open-cell polyurethane foam (PUF). In the process of synthesis, the initial matrix of the foam is duplicated and then removed during annealing; as a result, catalyst carriers based on highly porous cellular materials were obtained. Later, selective hydrogenation catalysts based on highly porous cellular carrier were obtained; palladium is an active component in these catalysts. The application of palladium precursor was carried out from the organic phase.

During laboratory tests, the synthesized catalysts showed high values of activity and selectivity in the hydrogenation reaction of acetylene to ethane-ethylene fraction.

### References:

- [1] G.C. Bond, *Catalysis by Metals*, Academic Press, New York, 1962, pp. 281–309.
- [2] A. Molnár, A. Sárkány, M. Varga, *J. Mol. Catal. A* 173 (2001) 185–221.
- [3] H.R. Aduriz, P. Bodnariuk, M. Dennehy, C.E. Gigola, *Appl. Catal.* 58 (1990)227–239.
- [4] D. Mei, M. Neurock, C.M. Smith, *J. Catal.* 268 (2009) 181–195.

## PP-IV-21

[5] Jin Y., Datye A.K., Rightor E., Gulotty R., Waterman W., Smith M., Holbrook M., Maj J., Blackson J. // J. Catal. 2001. Vol. 203. pp. 292-306.

[6] Liying X., Xian G.J., Yee L., Ling K.K., Sheng G.S. Patent 2259877 RF. 2005.

[7] Furlong, B.K. Alumina-supported palladium and palladium/copper catalysts: Characterization and use for selective hydrogenation of 1,3-butadiene. PhD dissertation. Houston: Rice University, 1996. 249 p.

## The Influence of the Nature of the Support on the Inhibitory Effect of Oxygen-Containing Compounds in the Process of co-Hydrotreatment of Model Compounds of Petroleum and Renewable Raw Materials

Kokliukhin A.S.<sup>1</sup>, Ishutenko D.I.<sup>1</sup>, Mozhaev A.V.<sup>1</sup>, Pimerzin A.A.<sup>1</sup>, Nikulshin P.A.<sup>1,2</sup>

1 – Samara State Technical University, Samara, Russia

2 – All-Russia Research Institute of Oil Refining, Moscow, Russia

koklyuhin@yandex.ru

Recently, the development of technologies for the production of biofuels from renewable vegetable raw materials has been more actively pursued. Biofuels play an important role, not only in reducing the associated greenhouse-gases emissions, but also in enabling the gradual independence from fossil sources, rendering low-carbon-highly-sustainable fuels [1]. Much attention is paid to the technology of joint hydroprocessing of plant and oil raw materials in the conditions of existing refineries. That allow minimizing investment costs and implementing the existing capacities of hydrotreating units for a new type of feedstock. But the main problem of inhibiting of target reactions like hydrodesulfurization (HDS) and hydrogenation (HYD) by oxygen-containing compounds, which are contained in renewable plant materials [2].

It was previously found that the use of mesostructured silica as support can significantly increase the activity of a sample in target hydrotreating reactions (HDS and HYD) [3]. Recently we obtained the beneficial effect of trimetallic NiCoMoS active phase compared to bimetallic active phase supported on the alumina in co-hydrotreating of dodecanoic acid, dibenzothiophene (DBT) and naphthalene [4].

The aim of the current research was to investigate the influence of the support on inhibitory effect in co-hydrotreating of dodecanoic acid/guaiacol, DBT and naphthalene in the presence of supported trimetallic NiCoMoS catalysts.

The (Ni)CoMo/Sup (Sup =  $\gamma$ -Al<sub>2</sub>O<sub>3</sub>, SBA-15 or SiO<sub>2</sub>) catalysts with the same surface density of Mo (1.15 at/nm<sup>2</sup>) were prepared by the incipient wetness impregnation technique via the impregnation of the support with an aqueous solution of H<sub>6</sub>[Co<sub>2</sub>Mo<sub>10</sub>O<sub>38</sub>H<sub>4</sub>] (Co<sub>2</sub>Mo<sub>10</sub>-HPA), NiCO<sub>3</sub> and citric acid. Catalysts were airdried at 110°C during 5 h and activated by liquid-phase sulfidation at 340°C during 6 h. Trimetallic samples were analyzed by N<sub>2</sub> adsorption, highly resolution transmission electron microscopy and X-ray photoelectron spectroscopy. Catalytic properties of prepared catalysts were studied in co-hydrotreatment of DBT (2 wt. %), naphthalene (3 wt. %) and oxygen-containing compounds (dodecanoic acid (DA) and guaiacol (Gua)) with different concentrations. These compounds were selected as model components of lignocellulosic- (Gua) and triglycerides-based (DA) feedstocks. Catalytic tests were performed in the fixed-bed microreactor with high pressure of hydrogen.

It was found that the highest turnover frequency (TOF) value in HDS of DBT showed NiCoMo/SBA-15 catalyst, moreover, the highest HYD/DS selectivity was also obtained at SBA-

supported sample. **Fig. 1** shows the graphical dependences of the effect of the partial pressure of inhibitors on the catalytic activity in the reaction of naphthalene HYD on (Ni)CoMo/Sup catalysts.

Moreover, NiCoMo/SBA-15 was less susceptible than other samples to inhibition of target reactions from oxygen-containing compounds, what was also confirmed by the calculated inhibitor adsorption constants.

Similar dependencies were obtained for the reaction of HDS DBT. The sample supported on alumina was significantly inferior to samples synthesized with silica.

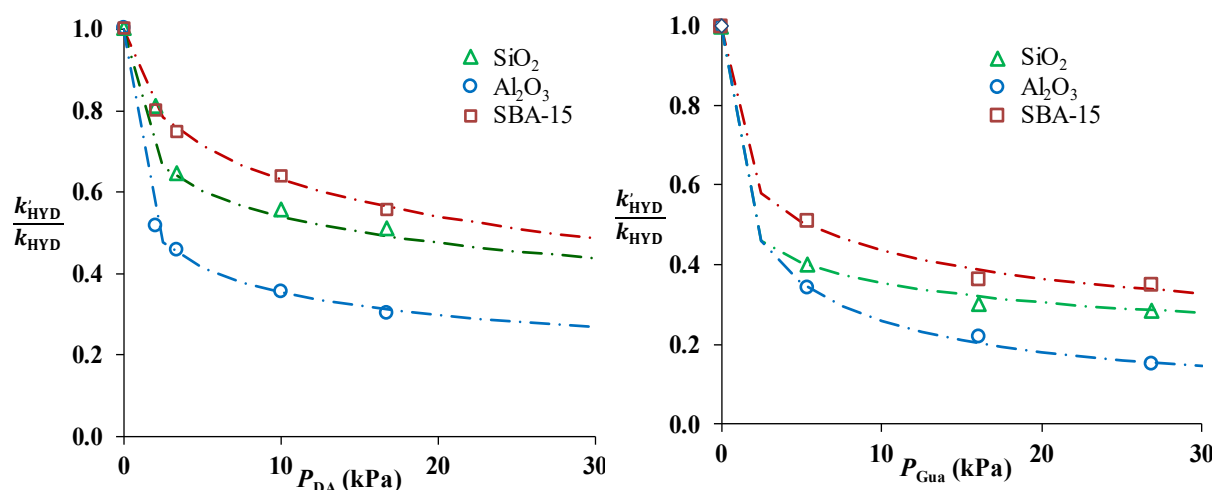


**Fig. 1.** Degree of inhibition of the naphthalene HYD as a function of the Gua and DA partial pressure for the NiCoMo/Sup catalysts. (The points represent experimental data, and the solid lines represent calculated data).

This result can be explained by the fact that these catalysts have optimal morphology and low interaction strength between active phase crystallites and silica-containing carriers.

The study focused on the differences in the state of the inhibitory effect and catalytic properties of NiCoMo catalysts supported on Al<sub>2</sub>O<sub>3</sub>, SiO<sub>2</sub> and SBA-15. It was found that the nature of the carrier has a significant impact not only on the catalytic activity, but on the inhibitory effect of oxygen-containing compounds in the process of co-hydrotreatment. The results show that for further tests on real raw materials it is preferable to use NiCoMo/SBA-15 as catalyst that is highly resistant to oxygen-containing inhibitors and allowing producing a hydrogenated product with ultralow sulfur content.

**Acknowledgement.** The work was financially supported by The Ministry of education and science of Russian Federation, project No 14.574.21.0139 (Unique identifier of applied scientific researches and experimental developments (project number) RFMEFI57417X0139).

#### References:

- [1] S. Bezergianni et al. // Progress in Energy and Combustion Science. 68 (2018) 2964.
- [2] M. Philippe, F. Richard, D. Hudebine, S. Brunet, Appl. Catal. A. 383 (2010) 14.
- [3] A. Kokluhin, M. Nikulshina, A. Sheldaisov-Meshcheryakov, A. Mozhaev, P. Nikulshin, Catalysis Letters. 148 (2018) 2869–2879.
- [4] A. Kokluhin, A. Mozhaev, V. Salnikov, P. Nikulshin, Kinetics and Catalysis. 58 (2017) 463.

## Novel Lanthanide-Grafted Catalytic Systems for Alcohols Acylation and Carboxylic Esters Hydrolysis

Koskin A.P.<sup>1</sup>, Vedyagin A.A.<sup>1,2</sup>

1 – Boreskov Institute of Catalysis, Novosibirsk, Russia

2 – National Research Tomsk Polytechnic University, Tomsk, Russia

koskin@catalysis.ru

The carboxylic acid esterification and carboxylic esters hydrolysis are important synthetic routes in organic chemistry and biodiesel production process. Both reactions are usually performed in the presence of various Lewis acids (e.g.,  $\text{ZnCl}_2$ ,  $\text{CoCl}_2$ ,  $\text{MgBr}_2$ ) [1]. However, Lewis acids have some major drawbacks such as significant deactivation by water. On the other hand, it has been shown that lanthanide (Ln) compounds (e.g.,  $\text{Yb}(\text{SO}_3\text{CF}_3)_3$ ) can act as a mild Lewis acid [2]. An important advantage of such salts in comparison with standard Lewis acids is their stability in proton media and ability to be recycled. The use of the lanthanide compound immobilized catalysts (e.g., Ln-supported on polymer with acidic groups) offers several advantages in preparative procedures. Simplification of the product workup, separation, and isolation as well as reuse of the catalyst including use of the flow-through regime could enhance the economical attractiveness of the approach.

Nafion (DuPont) or other sulphated perfluoropolymers (SFP) as a Ln counter-ions are of particular interest for heterogeneous catalytic systems preparation. The high acidity of  $(\text{CF}_2)\text{SO}_3\text{H}$ -groups provides the high charge density at the  $\text{Ln}^{3+}$ -site, which has a positive effect on the Lewis acidity (fig.1) [3]. However, pure SFP has a low specific surface area and a large part of sulfonic groups are blocked by outer polymer layers which negatively affects to ion-exchange capacity and acid catalysis properties. The use of SFP-containing composites (SFP/support) instead of pure SFP can significantly increase the  $\text{SO}_3\text{H}$ -groups availability [4]. In particular, the use of CNF as a support gave us opportunity to reduce the loading of high-cost sulphated perfluoropolymer without any losses in ion-exchange capacity and catalytic activity [5]. The present research is considered as a step forward from pure Ln-SFP system [3] to the SFP-based systems supported on carbon nanofibers (CNF).

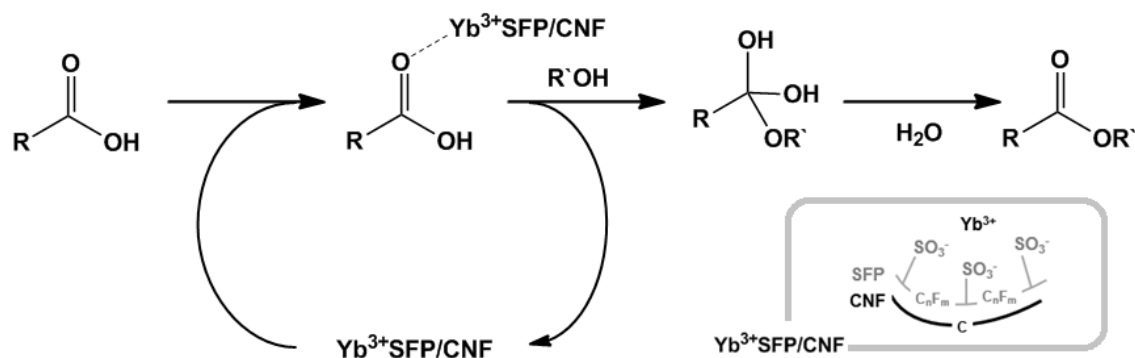


**Figure 1.** Proposed mechanism of carboxylic acid esterification.

## PP-IV-23

In summary, the preparation method of Ln<sup>3+</sup>SFP/CNF composites (where Ln = La, Pr, Eu, Tm, Yb) was proposed. Synthesized catalytic systems are insoluble in the reaction mixture and possess high specific surface area (165 m<sup>2</sup>/g). The catalytic activity of the synthesized composites was studied in acetic, palmitic and oleic acids esterification by ethanol. For the most active of the tested samples (Yb<sup>3+</sup>SFP<sup>580</sup>/CNF), 99% of substrate conversion (X<sub>AcOH</sub>; table 1) was achieved in less than 10 hours of reaction. It was shown that Ln<sup>3+</sup>SFP/CNF compared to Ln(OAc)<sub>3</sub> supported system is characterized by higher esterification initial rates (V<sub>in</sub>; 20.5 and 2.3 mol·h<sup>-1</sup>, consequently), that is connected with higher charge density on active site (Ln cation). Yb-containing systems showed the highest catalytic activity within the studied lanthanides (La, Pr, Eu, Tm, Yb). When comparing of supported and pure SFP systems, it is shown that the efficiency of polymer use (SP = V<sub>in</sub>/m<sub>cat</sub>·W<sub>SFP</sub>, where W<sub>SFP</sub> – weight ratio of SFP in the composite) is raised due to the increased availability of sulfonic groups.

**Table 1.** Esterification of acetic acid by ethanol over the studied lanthanide samples.

Sample	IC <sub>teor</sub> <sup>1</sup> (mmol·g <sup>-1</sup> )	C <sub>Ln</sub> <sup>2</sup> (mmol·g <sup>-1</sup> )	Ethanol acylation by acetic acid <sup>3</sup>		
			X <sub>AcOH</sub> (%)	V <sub>in</sub> (mol·h <sup>-1</sup> )	SP mol·(g·h) <sup>-1</sup>
Yb(OAc) <sub>3</sub> /CNF	–	0.15	16	2.3	–
Yb <sup>3+</sup> SFP <sup>580</sup>	1.72	0.36	99	17.5	17.5
Yb <sup>3+</sup> SFP <sup>1000</sup> /CNF (20 wt. %)	0.2	0.08	99	18.25	91.25
Yb <sup>3+</sup> SFP <sup>850</sup> /CNF (20 wt. %)	0.234	0.11	99	20.1	100.5
Ln <sup>3+</sup> SFP <sup>580</sup> /CNF (20 wt. %) <sup>4</sup>	0.344	0.15	89-99	12.8-20.5	64-102.5

<sup>1</sup>Theoretical ion-exchange capacity of non-grafted precursor

<sup>2</sup>Lanthanide-ion concentration grafted to composite

<sup>3</sup>R.c.: 1 g of Ln-grafted composite, 3M AcOH, 6M EtOH, in 45 ml THF, at 60°C and 10 h.

<sup>4</sup>Ln = La, Pr, Eu, Tm, Yb

**Acknowledgement.** This work was supported by the Russian Science Foundation, grant 18-29-19053.

### References:

- [1] H.T. Nguyen, P.H. Tran, RSC Adv. 6 (2016) 98365.
- [2] S. Kobayashi, M. Sugiura, H. Kitagawa, W.W.L. Lam, Chem. Rev. 102 (2002) 2227.
- [3] L. Yu, D. Chen, J. Li, P.G. Wang, J. Org. Chem. 62 (1997) 3575.
- [4] A. Molnar, Curr. Org. Chem. 15 (2011) 3928.
- [5] A.P. Koskin, R.M. Kenzhin, A.A. Vedyagin, I.V. Mishakov, Cat. Comm. 53 (2014) 83.

**SrO Integration Effect on Structure and Activity of Perovskite-Type Oxides  
GdFeO<sub>3</sub> for DRM and FTS**

Sheshko T.F.<sup>1</sup>, Sharaeva A.A.<sup>1</sup>, Kost V.V.<sup>1</sup>, Kryuchkova T.A.<sup>1</sup>, Chislova I.V.<sup>2</sup>, Zvereva I.A.<sup>2</sup>  
Yafarova L.V.<sup>2</sup>

*1 – Peoples' Friendship University of Russia (RUDN University), Faculty of Science, Physical and Colloidal Chemistry Department, Moscow, Russian Federation*

*2 – Saint-Petersburg State University, Saint-Petersburg, Russian Federation*  
*shesko-tf@rudn.ru*

Light olefins (ethylene, propylene, butylene) are valuable hydrocarbons, which find their application in the chemical industry as synthetic blocks. In recent years many researches focused on the light olefins synthesis from CO:H<sub>2</sub> gas mixture via Fischer-Tropsch reaction. Meanwhile the required syngas is obtained by methane reforming - an alternative processing method of the huge amount of coal, natural gas and biomass.

In the present work, the catalytic characteristics of the perovskite samples GdFeO<sub>3</sub>, Gd<sub>2</sub>SrFe<sub>2</sub>O<sub>7</sub> and GdSrFeO<sub>4</sub> with a high specific surface area were studied under the conditions of a two-stage process, including the DRM and FTS. The series of the samples were prepared by sol-gel method and characterized by the set of physical-chemical approaches: XRD, BET, TG, SEM+EDX, DLC and <sup>57</sup>Fe Mössbauer spectroscopy. X-ray diffraction patterns of the complex oxides reveal the integration of SrO layer leads to changing of the crystal lattice from orthorhombic to tetragonal. According to SEM micrographs, the presence of SrO into the perovskite structure resulted in a deflection of spherical symmetry and an elongation of crystallites. The surface area, pore volume and average pore diameter of perovskites are BET and DLC results. <sup>57</sup>Fe Mössbauer spectroscopy was performed for precisely determination the degree and location of Fe oxidation. Advanced characterization pointed out the presence of Fe<sup>3+</sup> in three different surroundings and Fe<sup>4+</sup> in ferrites with strontium integration. It is worth noting that the number of SrO layers increase with the Fe<sup>4+</sup> content.

Catalytic activity tests were conducted in a continuous-flow mode during supply of the reaction mixture at a rate of 1,5 and 0,5-1,0 L/h within a temperature range of 523-708K and 773-1223K for FTS and DRM respectively. For analysis of the products was used a chromatographic method.

Experimental data allow us to establish a correlation between the activity and the amount of SrO contained in the catalyst for both processes. It was determined that strontium oxide in the perovskite structure plays an inhibitor role in terms of reactant conversion in the DRM reaction. However, the opposite effect was observed in the carbon monoxide hydrogenation: as the amount of SrO in the ferrite increases, the catalysts become more active (figure 1).

During comparative analysis of target products selectivity was found that the dependence of the values on temperature and the strontium oxide content for two reactions is different. Thus, a downward trend is observed for hydrogen selectivity in DRM, while a significant

## PP-IV-24

increase in light olefins selectivity occurs in the FTS in case of SrO integration and the temperature rise.

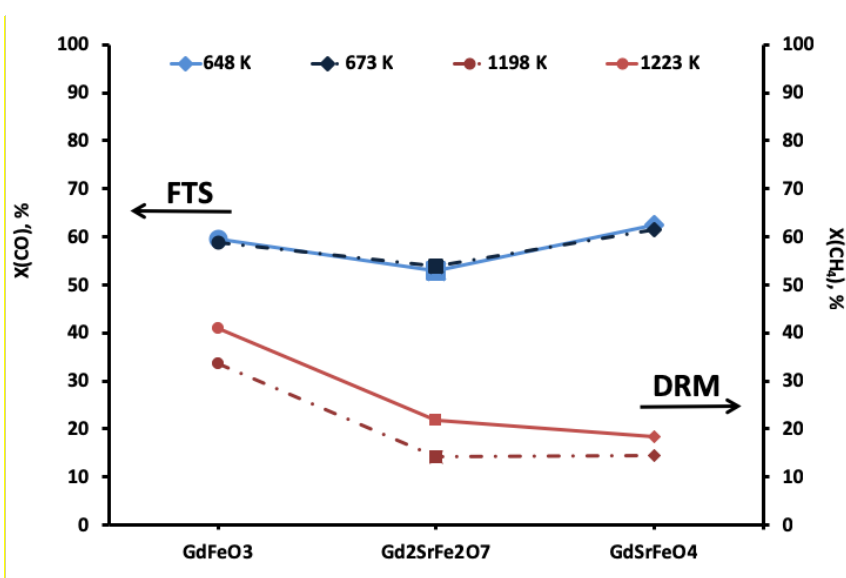


Fig.1. Conversion CO for FTS and conversion CH<sub>4</sub> for DRM processes.

The GdFeO<sub>3</sub> catalysts with SrO prepared by sol-gel technology show higher activity and selectivity in direct synthesis of light olefins from syngas in comparison with unmodified ferrite. This phenomenon can be explained by increased oxygen mobility detected upon addition SrO and responsible for the appearance of oxygen vacancies and formation of additional active sites.

**Acknowledgement.** This work was supported by Russian Foundation for Basic Research, research project No 17-03-00647. The publication has been prepared with the support of the «RUDN University Program 5-100». Diffraction Methods and Nanotechnology, Center for Studies in Surface Science, Center for Thermogravimetric and Calorimetric Research of Research park of St. Petersburg State University.

## Effect of MoVTenbO Catalyst Modification by P on the Selective Oxidative Transformations of Light Alkanes

Kovalev E.P.<sup>1,2</sup>, Lazareva E.V.<sup>1</sup>, Bondareva V.M.<sup>1</sup>, Svintsitskiy D.A.<sup>1</sup>, Kardash T.Yu.<sup>1,2</sup>

1 – Borekov Institute of Catalysis, Novosibirsk, Russia

2 – Novosibirsk State University, Novosibirsk, Russia

*kovalev-e@catalysis.ru*

### Introduction

MoVTenb oxide catalysts are promising systems for selective transformations of C2-C3 alkanes [1]. Their high performance is due to a unique structure of the so-called M1 phase [2,3]. Now, research efforts continue to focus on finding effective promoters in MoVTenb mixed oxides for increasing the efficiency of the catalysts.

The goal of the present work is to study the effect of P additive on the phase composition and catalytic properties of MoVTenbO catalyst in the oxidative dehydrogenation of ethane and selective oxidation of propane.

### Experimental

The  $\text{Mo}_{1.0}\text{V}_{0.3}\text{Te}_{0.23}\text{Nb}_{0.12}\text{P}_{0.001-0.05}$  catalysts were synthesized from aqueous slurry using ammonium heptamolybdate, ammonium metavanadate, telluric acid, orthophosphoric acid and niobium oxalate. The prepared slurry was spray-dried at 220°C and heated in an air flow at 310°C during a short period and in He at 560°C for 2h.

XRD data was measured using CuK $\alpha$ -radiation with Bruker D8 (Germany) diffractometer. Phase analysis and estimation of the quantitative content were performed by the full profile modeling of X-ray patterns by the Rietveld method.

XPS study was performed using a ES-300 photoelectron spectrometer (KRATOS Analytical) with a MgK $\alpha$  ( $h\nu = 1253.6$  eV) X-ray source. The chemical composition of the surface was determined from the integral peak areas using standard atomic sensitivity factors (ASFs).

The catalytic experiments were carried out at atmospheric pressure in a fixed-bed tubular reactor with on-line gas chromatography. The propane oxidation were performed at 380°C using a reaction mixture of 5% C<sub>3</sub>H<sub>8</sub>, 30% H<sub>2</sub>O, 65% air. The ethane oxidative dehydrogenation were carried out at temperature 400°C using feed consisted of a mixture 10% C<sub>2</sub>H<sub>6</sub>, 10% O<sub>2</sub>, 80% N<sub>2</sub>.

### Results and Discussion

Phase composition of P doped catalysts depends substantially of P quantity involved. About 93 % of active phase M1 forms in the samples with small quantity of P ( $\text{P}/\text{Mo} = 0.005-0.01$ ) (Fig 1). Increase of P amount to atomic ratio  $\text{P}/\text{Mo} = 0.1$  leads to formation of significant amount of pseudo-hexagonal phase M2 (~50%).

## PP-IV-25

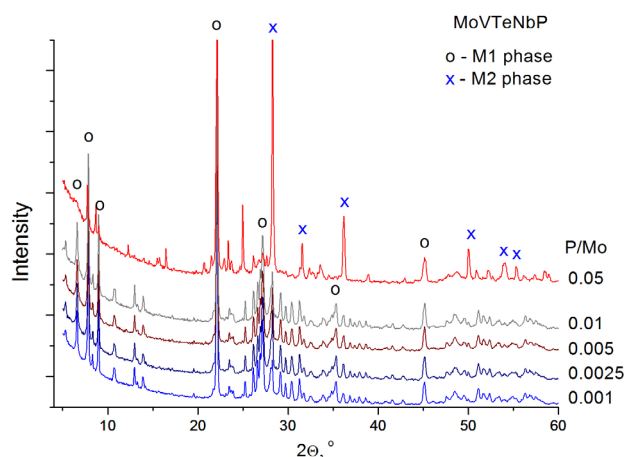


Fig.1. XRD patterns of the MoVTenbP catalysts

Fig. 2 shows the dependence of conversion of propane (2a) and ethane (2b) and selectivity to target products - acrylic acid (2a) and ethylene (2b) on the content of the P additive at a constant contact time.

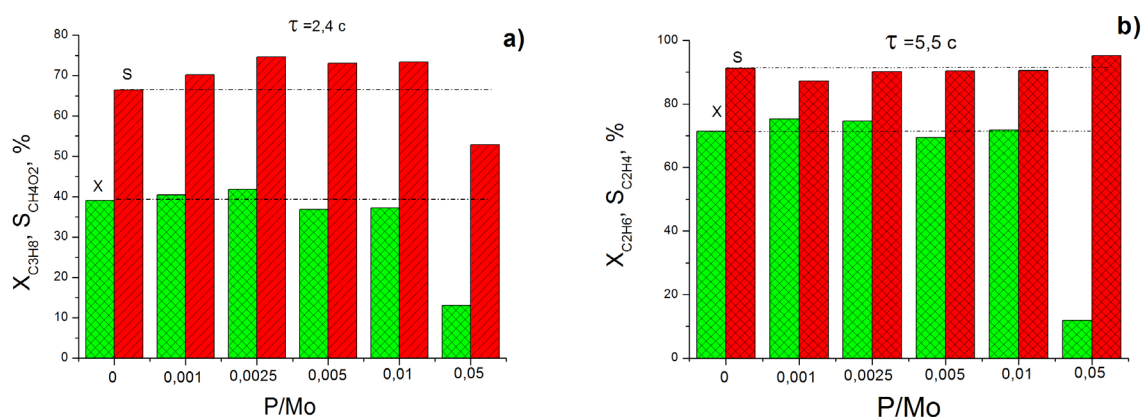


Fig. 2. Catalytic properties of MoVTenbP catalysts in the selective oxidation of propane (a) and oxidative dehydrogenation of ethane (b).

Introduction of P (until P/Mo 0.01) has a little effect on activity in reaction of selective oxidation of propane, meanwhile selectivity increases by 4-8% for acrylic acid. Introduction of P does not have a significant impact on catalytic properties in oxidative dehydrogenation of ethane. Maximum P additive (P/Mo = 0.05) worsens catalytic properties in both reactions, which can be related to the increase of content of low active phase M2.

Positive influence of P in reaction of oxidation of propane can be related to the modification of surface acidity which prevents further oxidation of acrylic acid and promotes it's desorption.

**Acknowledgement.** This work was supported by the Russian Science Foundation, grant 17-73-20073.

### References:

- [1] F. Cavani, N. Ballarini, A. Cericola // *Cat. Today*. 127 (2007) 113.
- [2] H. Murayama, D. Vitry, W. Ueda et al. // *Appl. Catal. A Gen.* 318 (2007) 137.
- [3] R. Grasselli, J. Burrington, D. Buttrey et al. // *Top. Catal.* 23 (2003) 5.

## Mechanisms of Catalytic Degradation of Chloroaromatic Compounds in Presence of CdS/TiO<sub>2</sub> Composite

Kozhevnikova N.S.<sup>1</sup>, Gorbunova T.I.<sup>2</sup>, Pervova M.G.<sup>2</sup>, Enyashin A.N.<sup>1</sup>, Vorokh A.S.<sup>1</sup>

1 – Institute of Solid State Chemistry of UrB RAS, Ekaterinburg, Russia

2 – Postovskii Institute of Organic Synthesis of UrB RAS, Ekaterinburg, Russia

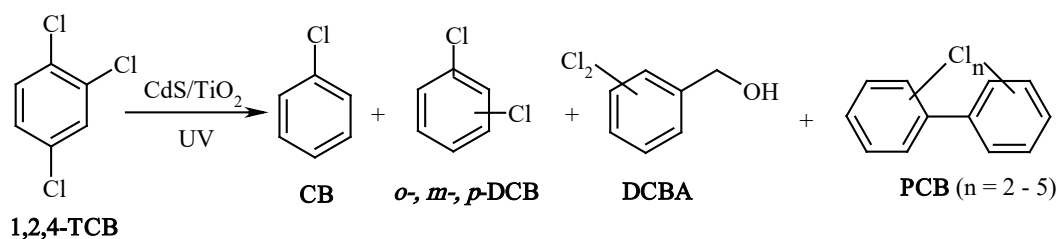
kozhevnikova@ihim.uran.ru

The fate and behavior of chloroaromatic compounds (chloroarenes) have attracted considerable scientific interest. Trichlorobenzenes (**TCBs**) and polychlorinated biphenyls (**PCBs**) relate to toxic organic pollutants and are still under scrutiny by international coordinating, state and municipal organizations due to their toxic properties [1]. These compounds tend to persist in the environment for a long period of time due to their hydrophobic nature, resistance to biodegradation and chemical stability under natural conditions [2,3]. Heterogeneous photocatalysis has become more and more attractive and important since it has a great potential to contribute to degradation of organic contaminants. TiO<sub>2</sub>-based photocatalysts have attracted attention in environmental decontamination due to their availability, high photocatalytic activity, chemical and photochemical stability and biological inertness [4]. A number of recent studies have focused on enhancing the photocatalytic degradation efficiency of TiO<sub>2</sub> using various approaches such as doping with metal chalcogenides [5].

In this study, facile, low-temperature hydrolysis route to *in situ* TiO<sub>2</sub> doping by pre-synthesized CdS for the degradation of chloroaromatic compounds (**1,2,4-TCB** and **PCBs**) is applied [5]. The possible mechanisms of the degradation of 1,2,4-TCB and low-chlorinated mono-, di- and trichlorobiphenyls in MeOH aqueous medium at ambient temperature using UV light ( $\lambda = 240\text{-}320$  nm) is reported. Therefore, the conditions of the simulated photolysis were close to those found in the environment. Since all **TCBs** and **PCBs** congeners are hydrophobic, the aliphatic alcohol facilitates the solubility of chloroaromatic compounds in a water-containing medium. We also described the possible photocatalytic role of nanostructured CdS/TiO<sub>2</sub> composite as heterogeneous (photo)catalyst with extremely low content of the toxic sensitizer (1 at %) in the structure of CdS/TiO<sub>2</sub>.

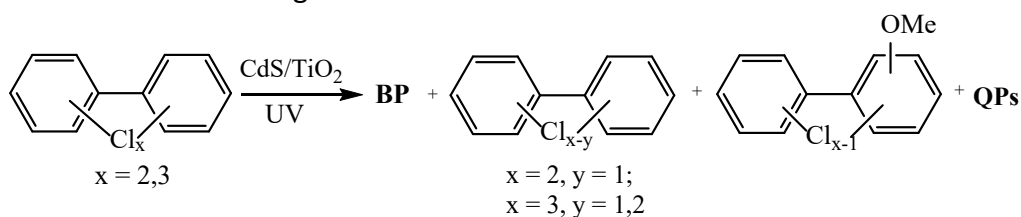
The **1,2,4-TCB** photolysis reaction depth amounted to 97.3 % after 100 hrs of exposure. The main detected products of **1,2,4-TCB** photodegradation were chlorobenzene (**CB**; 9%), *m*-, *p*- and *o*-dichlorobenzenes (**DCB**; 74%), dichlorobenzyl alcohol (**DCBA**; 6%) and **PCB** congeners (2%) (Scheme 1). In control experiment, **CB** was proved to demonstrate extremely low photodegradation ( $\approx 1\%$ ). The role played by the CdS/TiO<sub>2</sub> was suggested to be in the polychlorophenyl radicals' adsorption by the nanoparticles of CdS owing to the surface atoms of Cd having noncompensated bonds.

## PP-IV-26



**Scheme 1.** The main products of **1,2,4-TCB** photodegradation.

The main products of **PCBs** photodegradation are presented in Scheme 2. The **PCBs** photodegradation results showed that chlorobiphenyl **PCB 2** had the lowest conversion depth (13%) compared to di- (**PCB 8**, **PCB 12**, **PCB 13**, **PCB 15**; 32-42%) and trichlorobiphenyls (**PCB 29**, **PCB 31**; 91-98%). After photolysis reaction of **PCBs**, the formation of biphenyl (**BP**, <1-11%), **PCBs** with a smaller amount of chlorine atoms (29-93%), methoxy derivatives of PCBs (**PCBs-OMe**) was detected in all experiments, as a result of the formal exchange of chlorine atom on methoxy group (<1-3%) and quaterphenyls (**QPs**, <1%). The **QPs** were not found in the products after **PCB 31** photolysis. An increase of chlorination favors the conversion of the chlorinated congeners. Low-chlorinated mono- and dichlorobiphenyls make the largest contribution to the photolytic products of **PCBs**. The more chlorine atoms were in the initial **PCBs**, the higher content of lower-chlorinated congeners was.



**Scheme 2.** The main products of **PCBs** photodegradation.

We have assumed that one of the main factors that influenced the photolytic conversion of **PCBs** was the structure of the radicals formed during the primary photochemical process: **PCBs**  $\rightarrow$  **PCBs<sup>•</sup>-Cl**. The obtained results are significant for carrying out monitoring of the environment contaminated with chloroaromatic pollutants.

**Acknowledgement.** This work was supported by the Russian Science Foundation, grant 17-79-20165 and by Ministry of Education and Science of the Russian Federation (No. 075-00578-19-00).

### References:

- [1] M. Nadal, M. Marquès, M. Mari, J.L. Domingo, Environ. Res. 143 (2015) 177.
- [2] P.C.M. van Noort, Chemosphere 74 (2009) 1024.
- [3] J.R. van der Meer, Antonie Van Leeuwenhoek 71 (1997) 159.
- [3] O. Carp, C.L. Huisman, A. Reller, Prog. Solid State Chem., 32 (2004) 33.
- [4] A.S. Vorokh, N.S. Kozhevnikova, T.I. Gorbunova, O.I. Gyrdasova, I.V. Baklanova, L.Yu. Buldakova, M.Yu. Yanchenko, A.M. Murzakaev, E.V. Shalaeva, A.N. Enyashin, J. Alloys. Comp. 706 (2017) 205.

## New Electrochemical Approach to Synthesis of Pd/C Catalysts and Its Electrochemical Performance

Kuriganova A.B.<sup>1</sup>, Faddeev N.A.<sup>1</sup>, Leontyev I.N.<sup>2</sup>, Smirnova N.V.<sup>1</sup>

1 – Platov South-Russian State Polytechnic University (NPI), Novocherkassk, Russia

2 – Southern Federal University, Rostov-on-Don, Russia

*kuriganova\_@mail.ru*

It is well known that platinum is the best catalyst for processes occurring in low-temperature fuel cells and, in particular, in fuel cells with direct oxidation of liquid fuels (methanol, ethanol, formic acid) [1]. An alternative to expensive platinum catalysts may be palladium, which is able to exhibit higher catalytic activity than platinum in the oxidation of alcohols, formic acid, both in acidic and alkaline media [2].

Both Pt-based catalysts and Pd-based catalysts are often obtained by standard methods for such systems.: impregnation-reduction method [3], polyol process [4]. Electrochemical methods for the preparation of Pd-based catalysts based on the electrochemical reduction of palladium ions from a solution of its salt are presented to a lesser extent [5].

In this work, we showed the applicability of the pulse alternating current (PAC) method for the synthesis of a Pd/C catalyst for the proton exchange membrane (PEM) fuel cell application, which was previously successfully applied to the synthesis of Pt/C catalysts [6]. The presence of palladium complexes in the electrolyte after PAC synthesis is demonstrated by UV-vis spectroscopy, which indicates a different mechanism for the formation of Pt and Pd nanoparticles under these conditions. The microstructural characteristics and catalytic activity of synthesized Pd/C catalyst were compared with those of Pt/C catalyst which was prepared under the similar conditions. Pd NPs of Pd/C catalyst exhibited smaller average size and narrower particle size distribution. The electrochemical study highlighted that the electrochemically active surface area of Pd/C catalyst was 1.4 times higher than for Pt/C. The rate of ethanol oxidation on Pd/C catalyst exceeded the rate of ethanol oxidation on Pt/C by 2.6 times, while the rate of oxidation of formic acid was comparable on both catalysts. However, on Pd/C, there was a significant decrease in the overvoltage of the formic acid electrooxidation reaction as compared to the Pt/C sample.

**Acknowledgement.** This work was supported by the Russian Foundation for Basic Research (No 18-33-20064 mol\_a\_ved).

### References:

- [1] B. C. Ong, S. K. Kamarudin, S. Basri, *Int. J. Hydrogen Energy*. 42 (2017) 10142.
- [2] X. Yu, P. G. Pickup, *J. Power Sources*. 182 (2008) 124.
- [3] L. P. R. Moraes, et. al. *Int. J. Hydrogen Energy*. 41 (2016) 6457.
- [4] B. Lesiak, et. al., *Appl. Surf. Sci.* 387 (2016) 929.
- [5] D. Gioia, I. G. Casella, *Sensors and Actuators B: Chemical*. 237 (2016) 400.
- [6] I. Leontyev, A. Kurihnova, Yu. Kudryavtsev, B. Dhill, N. Smirnova, *J. Appl. Catal. A: Gen.* 431-432 (2012) V. 120.

## Benzylic C-H Oxidation of Arylalkanes with Peroxyacetic Acid in the Presence of Palladium-Aminopyridine Complexes

Lubov D.P.<sup>1,2</sup>, Talsi E.P.<sup>1,2</sup>, Bryliakov K.P.<sup>1,2</sup>

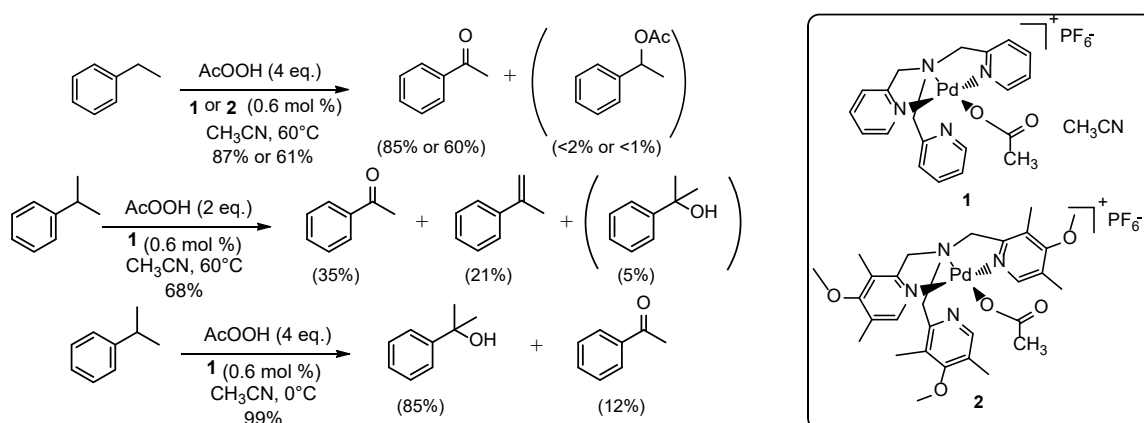
1 – Boreskov Institute of Catalysis, Novosibirsk, Russia

2 – Novosibirsk State University, Novosibirsk, Russia

d.lubov@g.nsu.ru

Designing transition metal based catalysts for the selective oxidation of aliphatic C-H groups has been a challenging task of synthetic chemistry. In the last years, a number of bioinspired iron, ruthenium and manganese complexes with salen and aminopyridine ligands have been reported as effective catalysts of selective aliphatic oxidations [1], mostly relying on safe and environmentally benign oxidants such as molecular oxygen and organic peroxides [2]. Despite unquestionable progress, the area is still lacking large-scale synthetic applications of such catalytic processes, since very few of those meet rigorous practical criteria of high efficiency, selectivity, and sustainability.

In this work, palladium (II) aminopyridine complexes [Pd(tpa)(OAc)](PF<sub>6</sub>)·CH<sub>3</sub>CN (**1**) and [Pd(tpa\*)(OAc)](PF<sub>6</sub>) (**2**) (tpa = tris-(2-pyridylmethyl)amine, tpa\* = tris-(2-(4-methoxy-3,5-dimethylpyridyl)methyl)amine) have been prepared and structurally characterized by <sup>1</sup>H, <sup>13</sup>C, <sup>31</sup>P, <sup>19</sup>F NMR spectroscopy, and single crystal X-ray diffraction. Complexes **1** and **2** have been found to efficiently catalyze the benzylic C-H oxidation of substituted ethylbenzenes with peracetic acid, affording the corresponding ketones with high yield (up to 85 %) and selectivity (up to 98 %) at <1 mol. % catalyst loadings. The oxidation of cumene, depending on the conditions, can be diverted towards either the formation of cumyl alcohol or acetophenone. Kinetic (Hammett, KIE data) and isotopic (<sup>18</sup>O) labelling studies witness rate-limiting benzylic C-H bond breaking by a metal-based electrophilic oxidizing species.



**Acknowledgement.** Financial support from the Russian Science Foundation (project 17-13-01117) is gratefully acknowledged.

### References:

- [1] M. Milan, M. Bietti, M. Costas, Chem. Commun. 54 (2018) 9559.
- [2] A. Shilov, G. Shul'pin, Chem. Rev. 97 (1997) 2879.

## Electrochemical Synthesis of a Novel Me/TiO<sub>2</sub>-CNT Catalyst and Its Performance in the Photocatalytic Reduction of Carbon Dioxide

Maniecki T.P.<sup>1</sup>, Shtyka O.<sup>1</sup>, Sorokina L.<sup>2</sup>, Ciesielski R.<sup>1</sup>, Kędziora A.<sup>1</sup>, Maniukiewicz W.<sup>1</sup>,  
Zakrzewski M.<sup>1</sup>, Dubkov S.<sup>2</sup>, Szyrkowska I.<sup>1</sup>, Gromov D.<sup>2</sup>

1 – Technical University of Lodz, Faculty of Chemistry, Institute of General and Ecological  
Chemistry, Lodz, Poland

2 – Moscow Institute of Electronic technology (MIET), Moscow, Russia  
tmanieck@p.lodz.pl

Solar-driven photocatalytic reduction of carbon dioxide can be considered as a cheap method for producing valuable hydrocarbon products, such as methanol, methane, dimethyl ether and others. The main limitation of this process is low level of CO<sub>2</sub> conversion when the reaction is performed over traditional catalysts. Therefore, lots of efforts have been put into the development of new effective catalysts with enhanced photocatalytic properties, such as nano – and microstructured TiO<sub>2</sub>, metal-decorated TiO<sub>2</sub>, and TiO<sub>2</sub>-based composites. The current research work deals with the investigation of physicochemical and photocatalytic properties of metal (Au, Ag, Cu, Ru) catalysts supported on TiO<sub>2</sub>-CNT composite. Additionally, the influence of preparation conditions of composite on its morphology and photocatalytic activity was evaluated. The TiO<sub>2</sub>-CNT composite was prepared using electrophoretic deposition method (EPD). Stainless steel foil was used as a base of electrodes. The process was carried out on the cathode from the suspension consisting of isopropyl alcohol, nanopowders of titanium dioxide (Degusa P-25), carbon nanotubes (Sigma-Aldrich), and surfactants (lauryl sulfate). The EPD process was performed in potentiostatic regime, using a high voltage power source. The dependence of the deposit mass on the applied voltage regardless of the amount of cycles was experimentally established. The obtained composites (Figure 1) were further used for deposition of metal nanoparticles (0.1, 1, and 2 wt. %) via traditional impregnation method. The photocatalytic activity of prepared samples was studied in a flow photocatalytic microreactor in the temperature range from 25 to 300°C.

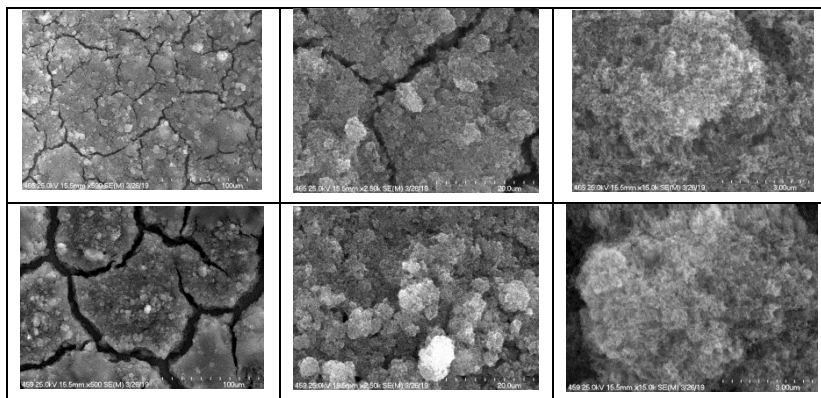


Figure 1. The SEM images of TiO<sub>2</sub> film obtained under different preparation conditions.

## The Effect of Metal in the B-Position of Complex Oxides of Composition $A_2B_2O_7$ on the Process of Propane Dehydrogenation

Markova E.B., Kovtun S.O., Savchenko A.S., Torbeeva A.A., Cherednichenko A.G.  
*Peoples' Friendship University of Russia (RUDN University), Moscow, Russia*  
 ebmarkova@gmail.com

Due to a set of unique physicochemical properties, REE complex oxides are interesting from both scientific and practical points of view and have recently attracted the attention of numerous researchers [1].

The aim of the work was to study the catalytic activity of nanocrystalline powders of Gd complex oxides with different chemical and phase composition  $A_2B_2O_7$  ( $Gd_2B_2O_7$  where B = Ti, Zr, Hf). The original precursors were synthesized from solutions using various techniques (sol-gel, precipitation, reverse co-precipitation). The resulting precursors were isothermally annealed in air at 800-900°C for 1-3 h until the formation of the corresponding oxides.

The crystal structure of the synthesized powders was determined by X-ray diffraction on a Rigaku MiniFlex 600 diffractometer (Rigaku, Japan) ( $CuK\alpha$  - radiation). In order to obtain additional information about the structure of the samples, the method of Raman spectroscopy (Raman scattering) using a confocal Raman microscope inVia (Renishaw, UK) was used. IR spectroscopy of the samples was carried out on a Nicolet iS50 FT-IR FTIR spectrometer (Thermo Fisher Scientific Inc., USA).

The original precursors were found to be X-ray amorphous (or low crystalline in the case of Gd-Mo) powders which annealing led to the formation of nanocrystalline oxides with different types of crystalline structure: cubic in the case of  $Gd_2Ti_2O_7$  (space group  $Fd-3m$ ),  $Gd_2Zr_2O_7$  ( $Fm-3m$ ),  $Gd_2Hf_2O_7$  ( $Fm-3m$ ). The obtained diffraction data correlated well with the results of Raman spectroscopy.

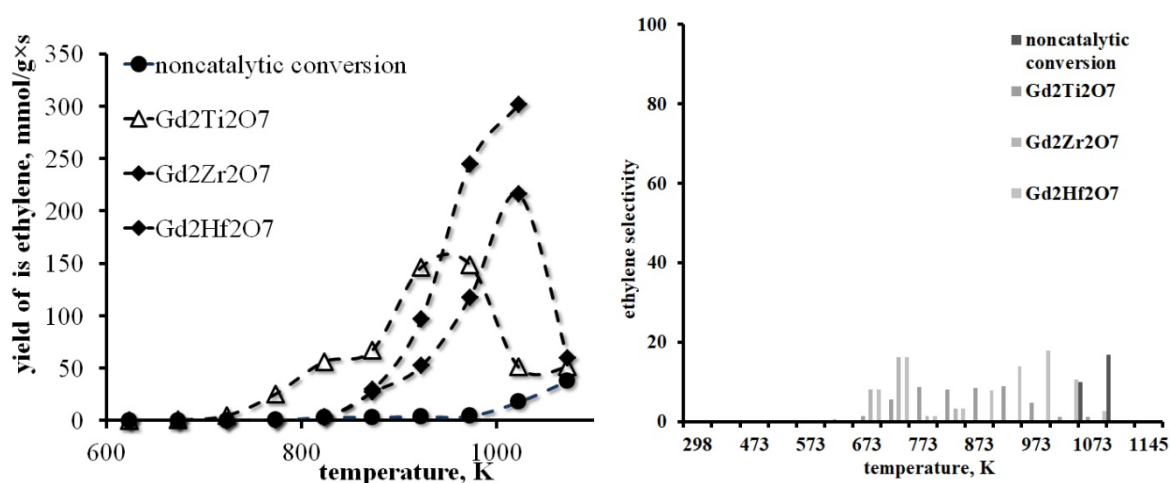


Figure 1. Catalytic indicators for the process of destruction

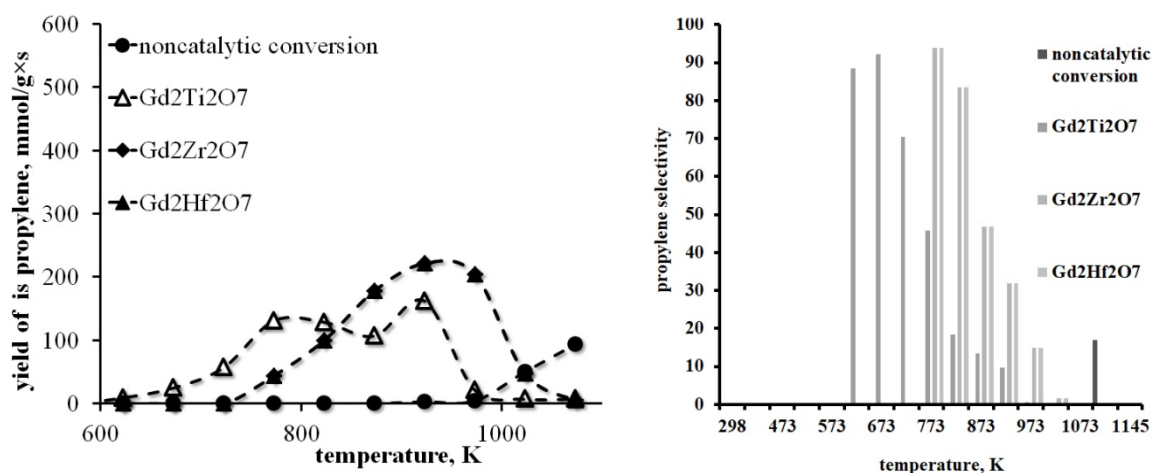


Figure 2. Catalytic performance on the dehydrogenation process

During catalytic experiments, it was found that the formation of a cubic structure promotes an increase of propane conversion degree and a shift of cracking temperatures to a lower region. The formation of this type of nanocrystalline oxides promotes dehydrogenation reaction with propylene selectivity up to 80% at temperatures up to 700K.

In addition to shifting the degree of half-conversion toward lower temperatures, the selectivity with regard to olefin changed with respect to thermal cracking. In the presence of Gd<sub>2</sub>Hf<sub>2</sub>O<sub>7</sub>, the cracking of propane to form ethylene (selectivity 20%) predominates at a temperature of 723 - 973 K (figure 1). Gd<sub>2</sub>Hf<sub>2</sub>O<sub>7</sub> with cubic structure catalyzes the propane cracking process to form ethylene, while dehydrogenation in the presence of the catalyst proceeds slowly.

In contrast, the selectivity toward propylene in the presence of Gd<sub>2</sub>Ti<sub>2</sub>O<sub>7</sub> is 90% at 923 K (figure 2). It is clear that at 100% propane conversion, the yield of targeted products ethylene and propylene was maximal, with only 8% selectivity with respect to methane.

On the Gd<sub>2</sub>Zr<sub>2</sub>O<sub>7</sub> catalyst the cracking process and the dehydrogenation of propane proceed equally (figure 1-2).

**Acknowledgement.** The publication has been prepared with the support of the «RUDN University Program 5-100».

#### References:

[1] E. B. Markova, A. S. Lyadov, and V. V. Kurilkin, J, Physical Chemistry A. 90 (2016) 1754–1759.

## Ru-Fe<sub>3</sub>O<sub>4</sub>-SiO<sub>2</sub> Catalyst for Polysaccharide Conversion

Sulman E.M., Manaenkov O.V., Kislitsa O.V., Ratkevich E.A., Matveeva V.G., Sulman M.G.  
*Tver State Technical University, Tver, Russia*  
*ovman@yandex.ru*

Polyols are an important feedstock; they are commonly used in different branches of modern industry. Ethylene glycol (EG) and propylene glycol (PG) are used in manufacturing medicines, fuels, surfactants, antifreezes, lubricants, and solvents [1]. Propylene glycol is also used for the synthesis of lactic acid, which is used in the production of biodegradable polylactones [2]. Mannitol is used in the pharmaceutical, chemical, and food industries, and in biotechnology [3].

New possibilities in catalysis are offered by the use of magnetically recoverable catalysts. In this work, a Ru-containing catalyst based on Fe<sub>3</sub>O<sub>4</sub>-SiO<sub>2</sub> particles exhibiting magnetic properties is proposed for the hydrogenolysis of cellulose to glycols and the hydrolytic hydrogenation of inulin.

The Ru-Fe<sub>3</sub>O<sub>4</sub>-SiO<sub>2</sub> catalysts were synthesized by incorporation of magnetite nanoparticles (NPs) in mesoporous silica followed by formation of 2 nm Ru NPs. The latter were obtained by thermal decomposition of ruthenium acetylacetonate in the pores. Magnetic properties of Fe<sub>3</sub>O<sub>4</sub>-SiO<sub>2</sub> are typical for superparamagnetic iron oxide NPs of comparable size and allow fast magnetic separation of the catalyst. The results of liquid nitrogen adsorption measurements are typical for mesoporous materials. The BET surface area of catalyst was 280 m<sup>2</sup>/g.

Our tests were conducted in a 50-cm<sup>3</sup> high-pressure steel reactor (Parr Instruments, United States) equipped with a PARR 4843 controller and a propeller stirrer. In a typical test, the polysaccharide, the catalyst, and 30 mL of distilled water were placed into the reactor. The reactor was triply purged with hydrogen at a pressure of 60 bar; heating and stirring (≈100 rpm) were then switched on to prevent the formation of local zones of overheating and the saturation of the catalyst surface with hydrogen. Upon reaching the operational temperature, the speed of the stirrer was increased to 600 rpm. This time was considered to be the starting point of the test. After each test, the catalyst was separated from the reaction mass using a neodymium magnet.

It was shown that magnetically recoverable Ru-containing catalysts can be used in the one-pot conversion of such natural polysaccharides as cellulose and inulin to the high added-value products EG and PG (cellulose) and mannitol (inulin). The effect of the reaction parameters on the selectivity toward the main products was studied.

The main products of cellulose hydrogenolysis are EG (selectivity of 10-19 %, depending on the reaction conditions) and PG (15-23 %). Small amounts of glycerol (up to 5 %), sorbitol (up to 4 %), mannitol (up to 2 %), and xylitol (up to 1 %) also form. In addition,

## PP-IV-31

chromatography-mass spectrometry analysis showed that the liquid phase contained trace amounts of 1,4-sorbitan, hexane-1,2,5,6-tetraol, hexane-1,2,3,4,5-pentanol, and some other products.

In the hydrogenolysis of cellulose, the highest selectivities for EG (19.1 %) and PG (20.9 %) are achieved within 50 min under conditions of 255 °C,  $P(\text{H}_2) = 60$  bar, 0.1167 mmol of Ru in the catalyst composition per gram of cellulose, and 0.195 mol of  $\text{Ca}(\text{OH})_2$  per mole of cellulose. The conversion of cellulose is 100%.

In the hydrolytic hydrogenation of inulin, maximum mannitol selectivity (44.3 %) is reached within 45 min under conditions of 150 °C,  $P(\text{H}_2) = 60$  bar, and 0.1167 mmol of Ru in the catalyst composition per gram of inulin. The conversion of inulin is 100 %. Depending on the test conditions, the liquid phase of the catalysate can contain, in addition to mannitol, sorbitol (selectivity of up to 15 %), glycerol (up to 6.5 %), EG (up to 4 %), PG (up to 5 %), and other polyhydric alcohols in trace amounts. In our studies, we selected the optimum values of the main process parameters: temperature, reaction time, hydrogen partial pressure, and Ru/inulin ratio.

Our results, the stability of the 5 % Ru- $\text{Fe}_3\text{O}_4$ - $\text{SiO}_2$  catalyst under hydrothermal conditions, and the easy way in which the catalyst can be separated from the reaction mixture using an external magnetic field make this catalyst promising for industrial application in the biomass conversion to high added-value chemicals and feedstock for biofuel production.

**Acknowledgement.** The authors thank L.M. Bronstein at the Nesmeyanov Institute of Organoelement Compounds, Russian Academy of Sciences, for her assistance in our research. This work was supported by the Russian Foundation for Basic Research, project nos. 18-08-00404, 18-29-06004, 19-08-00414; and by the Russian Science Foundation, project no. 18-19-00240.

### References:

- [1] H. Yue, Y. Zhao, X. Ma, J. Gong, *Chem. Soc. Rev.* 41(11) (2012) 4218.
- [2] S. Sugiyama, H. Tanaka, T. Bando, K. Nakagawa, K.-I. Sotowa, Y. Katou, T. Mori, T. Yasukawa, W. Ninomiya, *Catal. Today* 203 (2013) 116.
- [3] H.L. Ohrem, E. Schornick, A. Kalivoda, R. Ognibene, *Pharm. Dev. Technol.* 19(3) (2014) 257.

**The Inhibition of Hydrogen and Oxygen Recombination by Halogen Atoms  
and its Effect on Over-All Water Splitting over Pt-TiO<sub>2</sub>**

Gongxuan Lu

*Lanzhou Institute of Chemical Physics, Chinese Academy of Sciences, Lanzhou, China  
gxlu@lzb.ac.cn*

Semiconductor photocatalysts for overall water splitting into H<sub>2</sub> and O<sub>2</sub> require metal cocatalyst, such as Pt, to catalyze H<sub>2</sub> evolution efficiently. However, these metal cocatalysts can also catalyze hydrogen and oxygen recombination to form water. In this work, we found that the pre-adsorbed halogen atom catalyst could inhibit the reverse reaction of water formation from H<sub>2</sub> and O<sub>2</sub> due to the decrease of adsorption energies of H<sub>2</sub> and O<sub>2</sub> on Pt. The adsorption energy decrease of H<sub>2</sub> and O<sub>2</sub> followed the order of F/Pt < Cl/Pt < I/Pt < Br/Pt. H<sub>2</sub>-TPD results exhibited similar dependence. This inhibition was achieved via the occupation of halogen atom on the Pt surface sites, and thereby the adsorption and activation of hydrogen and oxygen molecules were decreased. The occupation difference of halogen atoms are determined by radius of halogen ions, which further leads the different activity for H<sub>2</sub> and O<sub>2</sub> recombination. By inhibition of water formation reverse reaction, the over-all water splitting over various TiO<sub>2</sub> photocatalysts has been achieved. Isotope experiments with D<sub>2</sub>O and H<sub>218</sub>O confirmed the over-all water splitting to H<sub>2</sub> and O<sub>2</sub>. This study may help scientist to develop high-efficient photocatalyst for overall water splitting.

**Acknowledgement.** This work was supported by the NSFC 21433007

## Design of Ag-CeO<sub>2</sub>/SBA-15 Catalysts for Deep Oxidation of Toluene

Mikheeva N.N.<sup>1</sup>, Zaikovskii V.I.<sup>2</sup>, Mamontov G.V.<sup>1</sup>

*1 – Tomsk State University, Tomsk, Russia*

*2 – Boreskov Institute of Catalysis, Novosibirsk, Russia  
natlitv93@yandex.ru*

Volatile organic compounds (VOCs) are among the major air pollutants that cause photochemical smog, ground-level ozone, sick building syndrome, and chemical sensitivity [1]. Toluene is a common and typical VOC [2]. It is used in many industrial processes as a precursor or a solvent. However, it is very dangerous for human health because it is a strong carcinogen. At present, the oxidation of toluene into CO<sub>2</sub> and water over Ag-containing catalysts is one of the most promising ways for toluene abatement.

The aim of this work is to study the effect of the conditions of silver and CeO<sub>2</sub> introduction on their distribution in the porous structure of SBA-15 as well as to study the catalytic activity of the obtained Ag-containing catalysts in deep oxidation of toluene. The main idea of this work is to deposit the active composition Ag-CeO<sub>2</sub> onto the surface of the high-porous silica SBA-15. In our previous work [3] it was shown that the combination of the pore size effect of SBA-15 and effect of citric acid addition allows obtaining ceria particles with the sizes of ~3 nm. In this work the formation and stabilization of silver and ceria particles in the SBA-15 structure is discussed.

Mesoporous ordered silica SBA-15 was synthesized by a template method using Pluronic P123 (triblock copolymer PEO-PPO-PEO) as a soft template [4]. SBA-15-supported Ag and Ag-CeO<sub>2</sub> catalysts were prepared by incipient wetness impregnation technique using aqueous solutions of Ce(NO<sub>3</sub>)<sub>3</sub> (with citric acid [3]) and AgNO<sub>3</sub>. The supports and catalysts were characterized by low-temperature N<sub>2</sub> adsorption, XRD, TEM (including TEM HR and STEM), TPR, TPD toluene, TPSR, UV-visible and Raman spectroscopy. The activity of the catalysts was studied in the deep oxidation of toluene.

The porous structure of the synthesized catalysts was studied by the low-temperature N<sub>2</sub> adsorption (Fig. 1a). The primary support SBA-15 is characterized by an average pore diameter of ~6-8 nm. When the active components are introduced, the pore volume decreases, which indicates the distribution of a part of the component inside the SBA-15 pores.

Fig. 1b shows the curves of the toluene conversion into CO<sub>2</sub> over the synthesized catalysts. The Ag-containing catalysts are active in toluene oxidation at temperatures above 200 °C. The 100 % conversion is achieved at temperatures below 300 °C. The Ag-CeO<sub>2</sub>/SBA-15 catalyst is the most active one (T<sub>98%</sub> = 268 °C). This is due to both small sizes of Ag and CeO<sub>2</sub> particles and the interaction between Ag and CeO<sub>2</sub> in this catalyst that was shown by TPR-H<sub>2</sub> and UV-Vis spectroscopy. A combination of TRD C<sub>7</sub>H<sub>8</sub> and TPSR shows that the adsorption of toluene on the SBA-15 surface occurs due to the weak physical interaction. The presence of silver or ceria

on the SBA-15 surface leads to a decreased amount of weakly bonded toluene and the destruction or oxidation of the chemically bonded toluene that occurs during the heating in He or O<sub>2</sub>-He carrier gas. The presence of both silver and ceria species on the surface of SBA-15 provides its cooperation and the formation of only chemically bonded toluene on the catalyst surface.

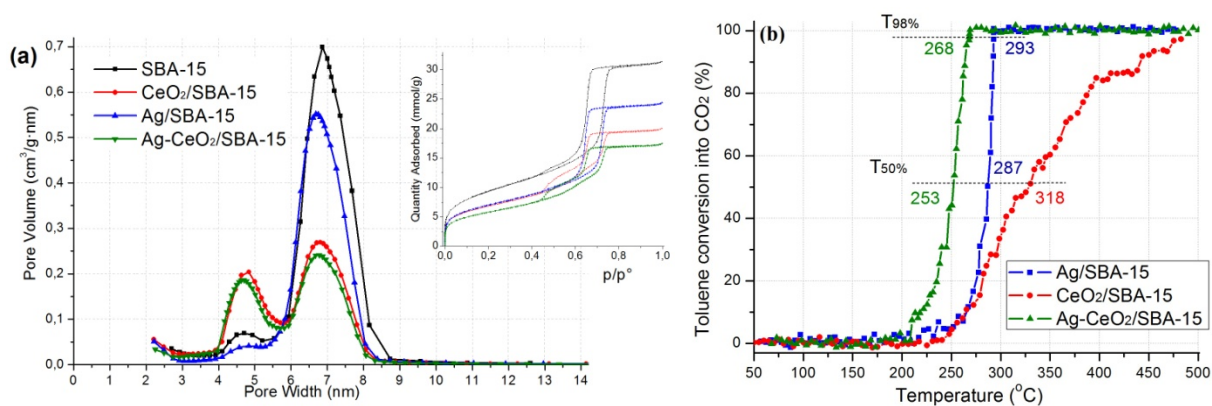


Fig. 1 Isotherms of nitrogen adsorption-desorption and the pore sizes distributions (a) and activity of catalysts in toluene oxidation (b)

Thus, the synthesized Ag-CeO<sub>2</sub> / SBA-15 catalysts are highly effective and promising for deep oxidation of VOC, including toluene oxidation. The use of citric acid to stabilize the cerium precursor and the unique porous structure of SBA-15 as nanoreactors allows synthesizing the Ag-CeO<sub>2</sub>/SBA catalysts that contain fine Ag and CeO<sub>2</sub> particles (<5 nm), providing an enhanced catalytic activity in the deep oxidation of toluene.

**Acknowledgement.** The present work was supported by the Russian Science Foundation (Grant No.18-73-10109).

#### References:

- [1] N. Shimoda et al., Appl. Catal., A General. 507 (2015) 56–64.
- [2] L. Zhang et. al., J. Electrochem. Soc. 164(14)(2017) H1086-H1090.
- [3] Mikheeva N.N., Zaikovskii V.I., Mamontov G.V., Microporous Mesoporous Mater 277 (2019) 10-16.
- [4] D. Zhao, et. al., J. Am. Chem. Soc. 120 (1998) 6024-6036.

## Influence of Borate-Containing Alumina Catalysts on the Conversion of Ethanol-Lignin from Pine Wood in a Supercritical Ethanol

Beregovtsova N.G.<sup>1</sup>, Baryshnikov S.V.<sup>1</sup>, Miroshnikova A.V.<sup>1</sup>, Sharypov V.I.<sup>1</sup>, Lavrenov A.V.<sup>2</sup>,  
Kuznetsov B.N.<sup>1</sup>

*1 – Institute of Chemistry and Chemical Technology SB RAS, FRC KSC SB RAS,  
Krasnoyarsk, Russia*

*2 – Center of New Chemical Technologies BIC, Omsk, Russia  
bnk@icct.ru, inm@icct.ru*

Wood biomass is a promising renewable raw material for obtaining the valuable chemicals and liquid biofuels. The catalytic conversion of lignocellulosic biomass in supercritical ethanol allows to obtain the bio-liquids with a rather high yield. This presentation demonstrates the possibility to increase the yield of low boiling fraction of bio-liquids with the increased content of methoxyphenols by the use of borate-containing alumina catalysts.

Ethanol-lignin was isolated from sawdust of pine-wood (*Pinus sylvestris*) by the extraction of ethanol–water mixture. Samples of borate-containing alumina  $B_2O_3-Al_2O_3$  (BA-20) and nickel-containing  $B_2O_3-Al_2O_3$  (NiO/BA-20) were used as catalysts. Their composition and some characteristics are given in the Table.

Catalyst	Catalyst composition, mas. %	Specific area, m <sup>2</sup> /g	Total volume, cm <sup>3</sup> /g	Micropore volume, cm <sup>3</sup> /g	Pore diameter, nm
BA-20	B <sub>2</sub> O <sub>3</sub> 18.8; Al <sub>2</sub> O <sub>3</sub> 81.2	185	0.44	0.005	9.6
NiO/BA-20	NiO 5.0	167	0.35	0.006	8.5

Thermal conversion of lignin in supercritical ethanol was studied in the reactor Autoclave Engineers (USA) with volume 100 cm<sup>3</sup> in the temperature range 250–400 °C and working pressure from 6.3 MPa to 7.6 MPa.

Thermal behavior of lignin was studied with the use of synchronous analyzer STA-449C Jupiter combined with mass-spectrometer QMS 403C Aëolos. Elemental composition of ethanol-lignin and solid products of lignin thermoconversion was determined with analyzer HCNS-O EA FLASH TM 1112 «Thermo Quest». Gaseous products were analyzed with chromatograph “Kristall-2000” (Russia) supplied by thermal conductivity detector. Liquid products were analyzed by GC-MS with the use of chromatograph Agilent 7890A supplied by the mass selective detector Triple Quad at the registration of full ionic current. Chromatograph was calibrated to quantify the content of phenolic compounds based on the use of standard compounds: phenol, guaiacol, vanillin, syringol, lilac aldehyde.

It was established by thermogravimetry that thermal decomposition of pine wood ethanol-lignin proceeds in the one stage which manifests itself on the different mass loss curve in the form of an intense peak with a maximum at 403.7 °C. The rate of decomposition of lignin

## PP-IV-34

at the point of maximum mass loss is 3.7 mas. %/min, the degree of conversion – 40 mas % at 403.7 °C and 65 mas. % when the temperature is reached to 800 °C.

The influence of temperature on the conversion of ethanol-lignin in supercritical ethanol and on the yield and composition of the products formed was studied. In the absence of catalysts, the highest yield (60 wt.%) of liquid products of thermal conversion of ethanol-lignin was obtained at the temperature of 300 °C. According to GC-MS data, the ethanol-soluble products mainly consist of phenols, methoxyphenols and ethyl esters of carboxylic acids. The increase of the temperature of ethanol-lignin conversion to 400 °C intensifies the transformation of liquid ethanol-soluble products into solid and gaseous substances and leads to a decrease in ethanol-soluble products the content of methoxyphenols by 3 times and of carboxylic acid esters by 2 times.

The use of catalysts, based on borate-containing alumina in the process of ethanol-lignin conversion in a supercritical ethanol at the temperature 300 °C increases the conversion of lignin and the yield of products, boiling up to 180 °C by 3.4-3.6 times. Also these catalysts rise the yield of methoxyphenols by 1.4-1.7 times in comparison with a non-catalytic process.

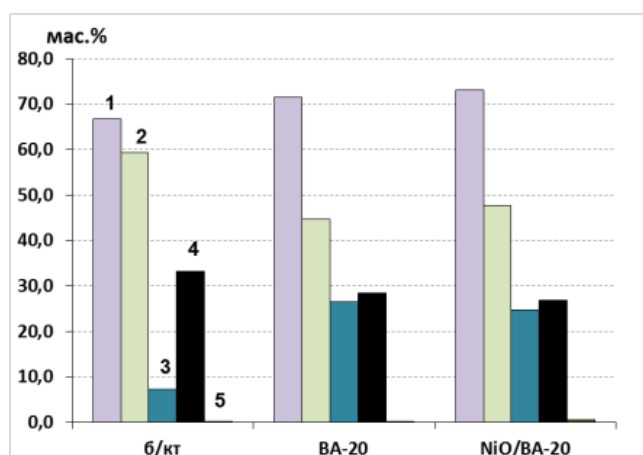


Fig. The influence of the catalysts on the conversion (1) and the yield of the liquid products boiling above 180 °C (2), boiling up to 180 °C (3), solids (4) and gaseous (5) products of the pine ethanol-lignin conversion in supercritical ethanol at 300 °C

The results of the accomplished research show that the catalysts based on affordable and inexpensive borate-containing alumina have the good prospects to the use for obtaining light hydrocarbon fractions from lignin.

**Acknowledgement.** The reported study was supported by the Project RFBR N 18-53-16001.

## Mechanochemical Synthesis – Alternative Effective Technique for the Composite Catalysts Preparation

Morozova O.S.<sup>1</sup>, Firsova A.A.<sup>1</sup>, Tyulenin Yu.P.<sup>1</sup>, Vorobieva G.A.<sup>1</sup>, Leonov A.V.<sup>2</sup>

*1 – Semenov Institute of Chemical Physics RAS, Moscow, Russia*

*2 – Lomonosov Moscow State University, Chemical Department, Moscow, Russia  
om@center.chph.ras.ru*

The main goal of this work is to show ability of ecologically friendly and low-cost mechanochemical synthesis to create nanocomposite catalysts with a reasonable activity and selectivity in CO-PROX and total alkane oxidation reactions from CeO<sub>2</sub> and Cu-containing dopants of different composition and morphology, the typical components, which are widely used for both processes [1-3]. Physico-chemical and catalytic properties of the samples obtained were compared with these of corresponding catalysts prepared by different techniques.

Mechanochemical synthesis in a vibration ball mill was applied to prepare Cu/CuO-CeO<sub>2</sub> catalysts from CeO<sub>2</sub> and following dopants: Cu metal, pure CuO and CuO containing 4 or 16.5 wt% Cu<sub>2</sub>O. A two-fold excess of Cu-containing fractions was used, as compared with optimal concentration in order to control powder phase composition by X-ray diffraction. Original powders consisting of 8 wt% Cu or 10 wt% CuO and CeO<sub>2</sub> were pre-mixed in agate mortar and then ball-milled in air at room temperature under the static conditions. The milling time varied from 30 to 90 min corresponding to energy doses of 1.4, 2.9 and 4.3 kJ, respectively. Reproducibility of mechanochemical synthesis was checked by both catalytic and DSC-DTG experiments.

Mechanically activated mixtures were characterized by XRD, SEM, HRTEM, XPS, CO-, H<sub>2</sub>- and C<sub>2</sub>H<sub>6</sub>- temperature-programmed reduction (TPR). The catalytic activity was tested in CO-PROX reaction and C<sub>2</sub>H<sub>6</sub> oxidation. The following effect of mechanical treatment was observed: (1) preferential dispersion of dopant powder contrary to ceria matrix, whose crystallite size was virtually unchanged; (2) CeO<sub>2</sub> surface modification by Cu ions evidenced by coexisting Cu<sup>2+</sup> and Ce<sup>4+</sup> with Cu<sup>1+</sup> and Ce<sup>3+</sup> on the surface and by increase or decrease in CeO<sub>2</sub> lattice spacing detected in CeO<sub>2</sub> surface nanofragments ( $d_{111} = 310 - 316$  pm instead of  $d_{111} = 313$  pm in the bulk); (3) appearance of the new surface oxygen state (O 1s with a binding energy of 530.6 - 531 eV) different from this in parent oxides. CO-, H<sub>2</sub>- and C<sub>2</sub>H<sub>6</sub> TPR measurements confirmed appearance of the new oxygen state with the low-temperature reactivity towards CO, H<sub>2</sub> and C<sub>2</sub>H<sub>6</sub> in all the nanocomposites synthesized. Both the physical-chemical properties and the catalytic activity of nanocomposites (96-98% of CO conversion at ~160 °C; 98-100% of C<sub>2</sub>H<sub>6</sub> conversion at 450 °C) were comparable with these of the catalysts prepared by a wet-impregnation or co-precipitation techniques. Cu-containing dopant composition and morphology had little effect on the catalytic properties in CO-PROX due to

dominant role of oxygen mobility in newly formed nanocomposites. As for  $C_2H_6$  combustion, the best catalyst is found to be Cu-CeO<sub>2</sub> powder, the worst is pure CuO-CeO<sub>2</sub>. There are two key factors controlling the catalytic properties in this reaction. The first is the surface active center architecture suitable for interaction with  $C_2H_6$  molecule. According to [4] it could be a sigma-type complex with Cu<sup>1+</sup> or other structures. The second one is an ability of lattice oxygen (with low binding energy) to react with such surface complex. As follows from  $C_2H_6$ -TPR measurements, the reactive oxygen fraction is nearly twice larger in the case of Cu-CeO<sub>2</sub>.

Thus, formation of prolonged Cu/Cu-oxide-ceria due to intermixing and high local pressure effect caused by the ball collisions stimulates oxygen mobility in CeO<sub>2</sub> lattice. The milling conditions can govern the catalytic properties through increase in the CeO<sub>2</sub> surface modification by Cu ions. The other effect of ball-milling, which is especially important for CO-PROX, is an averaging different precursor powders: the catalysts with comparable properties can be synthesized from CuO with different Cu<sub>2</sub>O content and even from Cu metal. This fact indicates the universality of the method applied. Mechanism of  $C_2H_6$  catalytic combustion in the presence of mechanochemically synthesized Cu/CuO-CeO<sub>2</sub> nanocomposites is under discussion. Figure 1 shows temperature dependence of CO and  $C_2H_6$  conversion (CO-PROX and  $C_2H_6$  total oxidation, respectively) on Cu/Cu-oxide-ceria composites prepared at a dose of 2.9 kJ (60 min of milling).

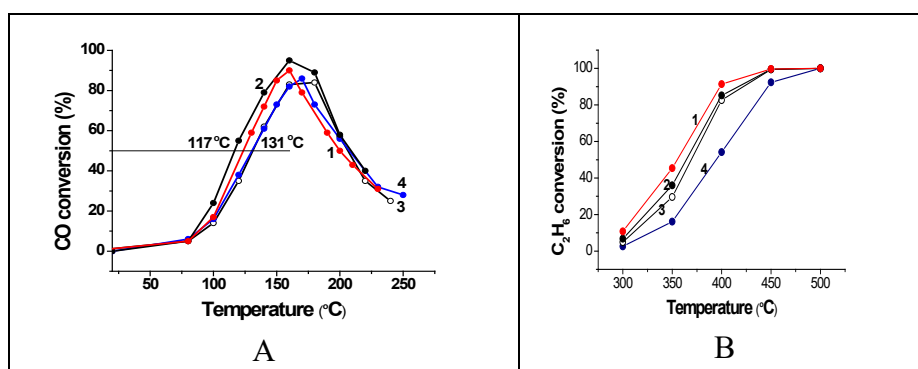


Figure 1. Temperature dependence of (A) CO conversion to CO<sub>2</sub> (CO-PROX) and (B)  $C_2H_6$  conversion to CO<sub>2</sub> on composites of CeO<sub>2</sub> with different additives milled at a dose of 2.9 kJ (60 min): 1 - elemental Cu; 2 - CuO+16.5% Cu<sub>2</sub>O; 3 - CuO+4% Cu<sub>2</sub>O and 4 - CuO. Line points to the temperatures at which CO conversion of 50% was reached.

**Acknowledgement.** This work was supported by the Russian Foundation for Basic Research, grant 19-03-00358.

#### References:

- [1] A. Martínez-Arias, D. Gamarra, A.B. Hungría, M. Fernández-García, G. Munuera, A. Hornés, P. Bera, J.C. Conesa, A.L. Cámara, *Catal.* 3 (2013) 378.
- [2] A.N. Il'ichev, A.A. Firsova, V.N. Korchak, *Kinet. Catal.* 47 (2006) 585.
- [3] W. Yang, D. Li, D. Xu, X. Wang, *J. Nat. Gas. Chem.* 18 (2009) 458.
- [4] E. Pidko, V. Kazansky, *PCCP* 7 (2005) 1939.

## Catalytic Materials Based on Hydrotalcite-Like Hydroxides of Al, Mg, Ni, Co for Partial Oxidation and Dry Reforming of Methane to Synthesis Gas

Dedov A.G.<sup>1,2</sup>, Mukhin I.E.<sup>1</sup>, Loktev A.S.<sup>1,2</sup>, Danilov V.P.<sup>2</sup>, Krasnobaeva O.N.<sup>2</sup>, Nosova T.A.<sup>2</sup>,  
Baranchikov A.E.<sup>2</sup>, Moiseev I.I.<sup>1,2</sup>

1 – Gubkin State University of Oil and Gas (National Research University), Moscow, Russia

2 – Kurnakov Institute of General and Inorganic Chemistry, Russian Academy of Sciences,  
Moscow, Russia

genchem@gubkin.ru, imuhin@mail.ru

Synthesis gas (SG), a valuable intermediate product of petrochemistry, currently produced predominantly by expensive endothermic methane steam reforming process. The SG with the ratio  $H_2/CO > 3$  obtained by methane steam reforming requires further processing for its further use in the synthesis of methanol and Fischer-Tropsch synthesis, and oxo synthesis. The SG with ratio of  $H_2/CO = 2$ , or less and acceptable for above mentioned processes can be obtained using the reactions of partial oxidation of methane (POM) or dry reforming of methane (DRM). Well-known Ni catalysts of POM and DRM are deactivated due to coke deposits formation or the formation of inactive nickel compounds with carriers. So, creation of selective and stable POM and DRM catalysts is actual task.

Partial oxidation of methane and dry methane reforming to synthesis gas in the presence of catalysts based on hydrotalcite-like hydroxo salts  $[AlMg_2Ni_xCo_y(OH)_{6.08}][[(NO_3)_nH_2O]]$ , where  $x = 0, 0.02, 0.04$  and  $y = 0, 0.02, 0.04$  with a total Ni and/or Co content of no more than 2 wt. % have been first studied. It has been shown that the Ni-containing catalysts provide a synthesis gas yield of 90 and 97% in the case of partial oxidation and dry reforming of methane, respectively; in the presence of these catalysts, a trace amount of carbon nanotubes is formed; the catalyst sample containing both nickel and cobalt does not lead to the formation of any carbon nanotubes during dry reforming of methane.

Obtained results can be used to implement new technological process of methane partial oxidation and dry reforming to synthesis gas - a valuable intermediate product of petrochemistry.

**Acknowledgement.** This work has been supported by Russian Science Foundation (project 14-13-01007P), Presidium of RAS, Program No. 33 “Carbon Energy: Chemical Aspects” and the Ministry of Education and Science of the Russian Federation (state task “Leading Researchers on a Permanent Basis”, project 4.6718.2017/6.7, questionnaire No. 1422).

## Highly Dispersed Catalysts Mo<sub>2</sub>C – WC for the Dry Reforming of Methane

Myachina M.A., Gavrilova N.N., Nazarov V.V., Skudin V.V.  
*D. Mendeleev University of Chemical Technology, Moscow, Russia*  
 mmyachina@muctr.ru

The use of new catalytic system is one of the ways to develop chemical technology, including the processing of natural energy. One of these processes is dry reforming of the methane, in which syngas is produced and carbon dioxide is utilized. For implementation of this process in industry, it is necessary to develop a method for producing an active and stable catalyst. Molybdenum carbide is a well-known active catalyst for the dry reforming of the methane. Doping of molybdenum carbide with tungsten carbide probably makes it possible to obtain a catalyst that is more active under the reaction's conditions due to the synergistic effect [1].

In this work, Mo<sub>2</sub>C – WC catalysts were synthesized by the sol-gel method using molybdenum-tungsten blues. The use of molybdenum-tungsten blue hydrosols, synthesized using ascorbic acid, allows to obtain xerogels – precursors of carbides. Heat-treatment of xerogels in an inert medium leads to the formation of highly dispersed molybdenum – tungsten carbides. Catalysts with different Mo and W molar ratios (100; 90:10; 80:20; 35:65) were synthesized at the temperature 900 ° C. The structure of Mo<sub>2</sub>C – WC was identified by XRD – analysis. The Mo<sub>2</sub>C – WC catalysts have mesoporous structure with predominant pore size of 4 nm (Fig. 1,a) and particle size around 100 nm (Fig. 1,b). The surface area of tested catalysts is around 8 m<sup>2</sup>/g.

Mo<sub>2</sub>C - WC catalysts are active in dry reforming of methane at the temperatures 870 – 900 ° C. Among the tested samples Mo<sub>2</sub>C – WC with W content – 10 % showed the highest catalytic activity.

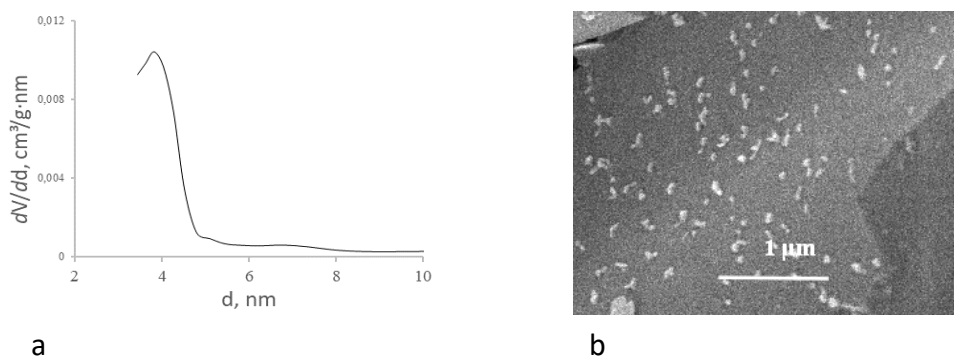


**Fig. 1.** Pore size distribution (a) and SEM – image of Mo<sub>2</sub>C – WC (b)

**Acknowledgement.** The work was carried out with the financial support of the Ministry of Education and Science of the Russian Federation agreement No. 14.583.21.0064 (the unique identifier RFMEFI58317X0064).

### References:

[1] C. Trang, Y. Han, M. Garcia-Perez, S. Kaliaguine, *Catal. Sci. Technol.* (2019) DOI: 10.1039/C8CY02184H.

## Effect of Anodization and Annealing Regimes on the Photocatalytic Properties of Nanostructured Tungsten Oxide Layers

Nazarkina Y.V., Rusakov V.A., Dronov A.A.

*National Research University of Electronic Technology, Zelenograd, Moscow, Russia  
engvel@mail.ru*

Tungsten oxide has relatively narrow band-gap  $\sim 2,6$  eV, and it is physicochemically stable in aggressive environments. These properties determine  $\text{WO}_3$  as a photocatalyst, working under visible light that can be applied as a substitute for  $\text{TiO}_2$  or other metal oxides.

The morphology of the photocatalyst surface is known to be its critical feature. The effective surface area determines the area of the interface between photocatalyst and dissolving reagent and thus photocatalytic efficiency. Moreover, the shape of the nanostructured material itself can affect the differences in the kinetics of photocatalysis.

One of the simplest methods of growing nanostructures  $\text{WO}_3$  films of a big area is the anodic oxidation. However, the routes for the formation of nanostructured  $\text{WO}_3$  layers with uniform and controllable morphology are still the subject of investigation. At this moment there is the lack of information about the effect of anodization parameters on the morphology of the  $\text{WO}_3$  films.

We have investigated anodizing and post-processing conditions at which nanostructured oxide layers could be produced. Several electrolytes for  $\text{WO}_3$  were chosen to form  $\text{WO}_3$  films on the W foils: based on  $\text{H}_3\text{PO}_4$ , ammonium fluorides and nitrates. The effects of anodizing regimes (electrolyte composition, anodization potential, temperature) on their morphology were observed. The samples were annealed for different times, and its crystalline structure was studied by XRD.

The photocatalytic properties of the obtained samples were investigated. The kinetics of methylene blue photodegradation illuminated by a xenon lamp (150 W, Newport, mod. 6255) without and with different  $\text{WO}_3$  photocatalysts were analyzed by spectrophotometer SF-102. The rate constants of the chemical reaction were estimated and generated photocurrents were measured.

Nanostructured  $\text{WO}_3$  films showed higher photocatalytic efficiency than barrier type  $\text{WO}_3$  films and approximately the same efficiency as anodic titanium oxide sample annealed in air. Based on the comparison of photodegradation kinetics and generated photocurrents of samples obtained in different anodization regimes, we defined several anodization regimes as the most appropriate to obtain effective  $\text{WO}_3$  photocatalysts.

**Acknowledgement.** This work was supported by the RFBR grant № 18-29-23038 mk.

## Porous Nitrogen-Doped Carbon Materials as Supports for Catalytically Active Ni Nanoparticles for Hydrogen Production from Gas-Phase Formic Acid

Nishchakova A.D.<sup>1,2</sup>, Asanov I.P.<sup>1,2</sup>, Bulushev D.A.<sup>3</sup>, Bulusheva L.G.<sup>1,2</sup>

1 – Nikolaev Institute of Inorganic Chemistry SB RAS, Novosibirsk, Russia

2 – Novosibirsk State University, Novosibirsk, Russia

3 – Boreskov Institute of Catalysis, Novosibirsk, Russia

*lina.nischakova@gmail.com*

Nowadays, hydrogen is one of the most promising substances that successfully can replace usable sources of energy like natural gas or oil because it is ecologically pure and can be produced from renewable sources. At the same time, hydrogen usage has difficulties associated with its storage and transportation. That is why H<sub>2</sub> production from different organic compounds is a current trend in catalysis. Formic acid is a liquid organic hydrogen carrier containing 4.4 wt% of hydrogen which can be liberated relatively easily using heterogeneous catalysts.

Catalysts' supports may play an important role for catalytic activity. Porous carbon materials are suitable candidates, since they have all the qualities that a support should possess. These materials demonstrate chemical, thermal and mechanical stability and have a developed surface, which can be modified during the synthesis or post-synthetic processing by doping with heteroatoms. They are usually cheap to synthesize and they are easy to handle. Noble metals are widely used as catalysts, but they are expensive and this is a reason why researchers search effective and cheaper analogues. Our earlier results demonstrated a significant promotion of Pd catalysts by N-doping of the carbon support [1]. Hence, the objective of our research is development porous N-doped carbon supports for Ni catalysts of hydrogen production from formic acid.

In the present work, porous N-doped carbon materials were synthesized by CVD from CH<sub>3</sub>CN as a precursor of carbon and nitrogen using Fe@CaCO<sub>3</sub>/CaO nanoparticles as a template [2]. The synthesis was performed at different temperatures (650-900°C) in inert atmosphere. This provided various ratios of four nitrogen forms according to XPS studies: pyridinic (398.3 eV), pyrrolic (399.9 eV), graphitic (401.0 eV) and oxidic (402.7 eV), but the total surface nitrogen content was approximately the same 4.5-5.9 wt%. It is seen in Fig. 1a that the concentration of the pyrrolic N significantly decreases with the synthesis temperature in favor of the graphitic N, but the ratios of pyridinic and oxidized forms of N almost do not change. At the same time, the BET surface area of the support decreases from 866 to 407 m<sup>2</sup>/g with the temperature.

Nickel nanoparticles (in a concentration of 1 wt%) were deposited on the surface of the N-doped carbon supports by impregnation with Ni acetate and subsequent reduction in a 2,5% HCOOH/Ar flow at 350°C. As a result, three catalysts (Ni-CN-700, Ni/CN-800 and Ni/CN-900)

were synthesized and investigated in the catalytic decomposition of formic acid in a fixed-bed reactor. It is seen in Fig. 1b that the catalytic activity only weakly depends on the temperature of the support synthesis and, hence, the ratio of the surface N forms. According to HRTEM studies, the average size of Ni nanoparticles is 6-8 nm. Hence, the observed changes with the N species (Fig. 1b) do not affect the properties of Ni at these particle sizes.

The catalysts supports (without Ni) also showed the decomposition of formic acid, but at higher temperatures ( $>350^{\circ}\text{C}$ ) (Fig. 1b) with apparent activation energies in the range from 125 to 148  $\text{kJ mol}^{-1}$ . The Ni introduction provided a significant decrease of the activation energies by  $\sim 30 \text{ kJ mol}^{-1}$ . Among the studied catalysts, the Ni/CN-900 catalyst showed the highest selectivity to hydrogen production (98% at about  $320^{\circ}\text{C}$ ) and high stability for 5 hours.

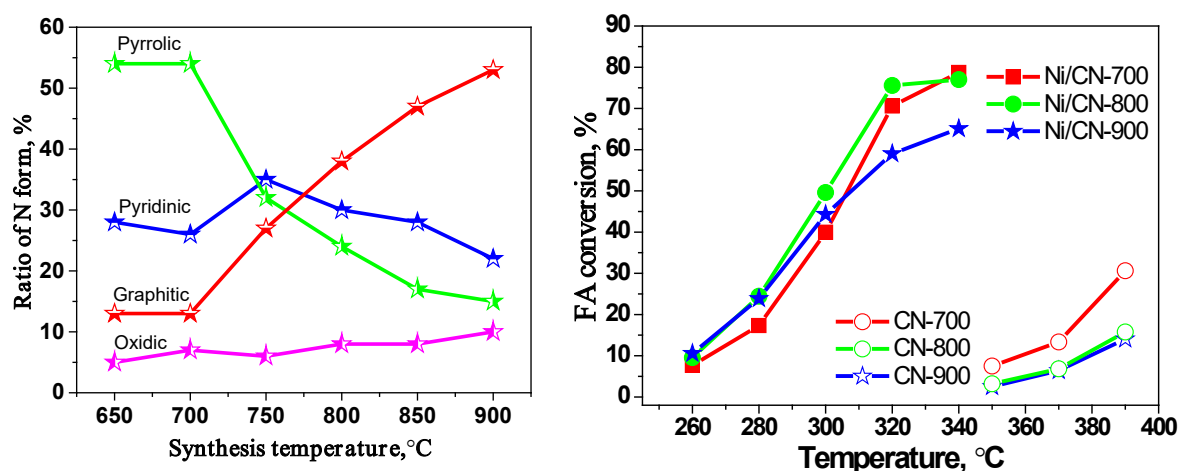


Fig. 1. a) Ratios of N forms in porous carbon depending on the CVD synthesis temperature, b) HCOOH conversion-temperature dependence over Ni/CN catalysts (7 mg) and CN supports (4 mg)

Summarizing, we find that the temperature of CVD synthesis of the porous N-doped carbon supports ( $650\text{--}900^{\circ}\text{C}$ ) strongly affects the ratio of surface pyrrolic and graphitic N; however, these changes do not influence noticeably the catalytic activity of supported Ni particles.

**Acknowledgement.** This work is supported by the Russian Science Foundation (grant 16-13-00016).

#### References:

- [1] Zacharska M., Bulusheva L.G., Lisitsyn A.S., Beloshapkin S., Guo Y., Chuvilin A.L., Shlyakhova E.V., Podyacheva O.Y., Leahy J.J., Okotrub A.V., Bulushev D.A. Factors Influencing the Performance of Pd/C Catalysts in the Green Production of Hydrogen from Formic Acid // *ChemSusChem*. - 2017. - Vol. 10, № 4. - P. 720–730.
- [2] Shlyakhova E.V., Bulusheva L.G., Kanygin M.A., Plyusnin P.E., Kovalenko K.A., Senkovskiy B.V., Okotrub A.V. Synthesis of nitrogen-containing porous carbon using calcium oxide nanoparticles: Synthesis of nitrogen-containing porous carbon // *physica status solidi (b)*. - 2014. - Vol. 251, № 12. - P. 2607–2612.

## Thermodynamic Analysis of Equilibrium Isobutane Yields in the Isomerization of *n*-Butane Fractions of Refinery Gases

Ovchinnikova E.V., Ivanov E.A., Chumachenko V.A.  
*Boreskov Institute of Catalysis, Novosibirsk, Russia*  
*evo@catalysis.ru*

The scaling up in the degree of oil refining and the transition to heavier oil feedstock is inevitably accompanied by an increase in the formation of waste hydrocarbon refinery gases, while light alkanes, in particular the *n*-butane fractions, do not meet an equivalent market and are used mostly as fuel gases. Earlier in [1], we have considered the possibility of utilizing *n*-butane fractions by isomerization, followed by oxidative processing of isobutane into *tertiary*-butyl alcohol based high-octane oxygen-containing components of motor fuels [2]. In this work, we determined the equilibrium yields of isobutane under the conditions of processing the *n*-butane fractions of refinery gases. Thermodynamic calculations consisted in the determining the composition of the reacting gases in the state of chemical equilibrium; the method used was minimization the free Gibbs energy of the initial reactants and the intended products in the pressure range of 0.1-2.5 MPa, temperatures of 20-300°C. Compositions of refinery gases differed in the initial content of isobutane and hydrogen.

In the analysis, we assumed the nomenclature of the reaction products, which is typical for isomerization of *n*-butane on a palladium-promoted sulfated zirconia catalyst Pd-SZ [3]: methane, ethane, propane, isobutane, butenes, pentane, and hexane. For maintaining the stability of the catalyst in the *n*-butane isomerization reaction, a small quantity of hydrogen in the feed is required. Therefore, in these calculations, the equilibrium composition of the products was determined at the ratios  $[H_2] / [nC_4] = 0; 0.1; 0.5; 1.0$ .

We considered the composition of the actual *n*-butane fraction of refinery gases, which contained *ca.* 98.2 mol. percentage of *n*-butane, *ca.* 1.0 mol. percentage of isobutane, and minor impurities as the initial reactant. The equilibrium compositions were calculated for the following variants of the initial composition:

Composition 1 - the original *n*-butane fraction with the addition of hydrogen;

Composition 2 - *n*-butane fraction with the addition of hydrogen and 10% of isobutane;

Composition 3 - *n*-butane fraction with the addition of hydrogen and 20% of isobutane.

In the entire range of conditions studied, the equilibrium concentration of hydrogen was equal to zero.

Thermodynamic analysis showed that in the presence of 1 to 20% isobutane in the original *n*-butane fraction, it does not influence on the equilibrium yield of isobutane and has little effect on the equilibrium composition of the intended products, such as methane, ethane, propane, butenes, pentane, and hexane. It is shown that an increase in the pressure suppresses the formation of by-products, in particular, lower alkanes; this contributes to the

## PP-IV-40

expansion of the range of temperatures at which the equilibrium yield of isobutane is relatively high. In the catalytic isomerization of *n*-butane, as well as of *n*-butane fraction, this fact may contribute to an increase in the selectivity to the target product. It has been established that the small presence of hydrogen in the mixture, which is necessary for the stable operation of the catalyst in the isomerization reaction, slightly increases the equilibrium yield of undesired lower alkanes, but practically does not affect the equilibrium yield of isobutane as the target product.

According to thermodynamic calculations and taking into account the requirements for carrying out a catalytic reaction on a Pd-SZ catalyst, the most favorable conditions for isomerization of *n*-butane, as well as of *n*-butane fraction, can be provided at  $[H_2] / [nC_4] = 0.1$ ,  $P = 2.5$  MPa,  $T = 120 \dots 230^\circ\text{C}$ . Under these conditions, the equilibrium yield of isobutane per *n*-butane will be close to the value determined for individual substances — isobutane and *n*-butane, and the equilibrium yield of by-products, incl. alkanes C1-C6 will be low.

**Acknowledgement.** This work was supported by the Ministry of Science and Higher Education of the Russian Federation, unique project identifier RFMEFI60717X0169.

### References:

- [1] A.S. Kharitonov, K.Yu. Koltunov, V.I. Sobolev, V.A. Chumachenko, A.S. Noskov, S.E. Kuznetsov *Catalysis in Industry*, 10 (2018) 115-117.
- [2] V.M. Kapustin, S.A. Karpov, A.V. Tsarev. *Oxygenates in auto gasolines*, Moscow, KolosS Publ., 2011 (in Russian).
- [3] G.A. Urzhuntsev, E.V. Ovchinnikova, V.A. Chumachenko, S.A. Yashnik, V.I. Zaikovskiy, G.V. Echevsky *Chem. Eng. J.* 238 (2014) 148-156.

## Effect of Cs Content in $\text{Co}_3\text{O}_4$ Deposited on the Ceramic Foam Support Catalyst for $\text{N}_2\text{O}$ Decomposition

Klegova A., Kiška T., Pacultová K., Karásková K., Obalová L.  
*Institute of Environmental Technology, VŠB – Technical University of Ostrava, Ostrava, Czech Republic*  
*katerina.pacultova@vsb.cz*

Nitrous oxide ( $\text{N}_2\text{O}$ ) is considered as an important pollutant contributing to the greenhouse effect. The largest industrial sources of  $\text{N}_2\text{O}$  emissions are waste gases from nitric acid production plants [1]. The low-temperature catalytic decomposition of  $\text{N}_2\text{O}$  (up to 450 °C) to nitrogen and oxygen offers an attractive solution for decrease of  $\text{N}_2\text{O}$  emissions in tail gas from nitric acid production plants. Usage of supported catalysts allows decrease of needed amount of expensive active components in the catalyst, thus lowers their price and can increase mechanical strength of catalyst. Open-cell foams are promising structured supports, which offer remarkable properties such as large external surface area, high mechanical strength, high porosity with resulting low pressure drop.

It is well known that cobalt-based catalysts present excellent catalytic activities for  $\text{N}_2\text{O}$  decomposition [2-4]. Modification of the cobalt spinels with a small amount of alkali metals significantly increases the activity of the catalyst. Alkali promoters present on the catalyst surface lower the work function of the cobalt spinel facilitating redox processes that occur between the catalyst surface and the reaction oxygen intermediates produced during the  $\text{N}_2\text{O}$  decomposition [5].

In this work,  $\text{Co}_3\text{O}_4$  active phase with different loading of Cs (0.3-4 wt. %) was deposited on the  $\text{Al}_2\text{O}_3$  based ceramic foam (manufactured by LANIK Inc., Czech Republic). Prepared catalysts were tested for nitrous oxide decomposition and characterized by AAS, XRD and TPR- $\text{H}_2$ . The aim was to compare effect of Cs content on the catalytic activity in bulk cobalt active phase, with effect of Cs content on the catalytic activity in active phase deposited on the ceramic support and to find optimal Cs loading in the cobalt based catalyst supported on the ceramic foam for  $\text{N}_2\text{O}$  decomposition.

Results of this work confirm that  $\text{Co}_3\text{O}_4$ -Cs deposited on open-cell ceramic foam as catalyst for  $\text{N}_2\text{O}$  decomposition are promising alternative to the conventional fixed bed reactors. Optimal amount of Cs in  $\text{Co}_3\text{O}_4$  deposited on the ceramic foam is about 4 times higher than in the case of bulk  $\text{Co}_3\text{O}_4$ -Cs. This differences could be explained by dispersion of part of Cs species over pure support (places which are not covered by  $\text{Co}_3\text{O}_4$ ), thereby changing the working ratio of Cs :  $\text{Co}_3\text{O}_4$ .

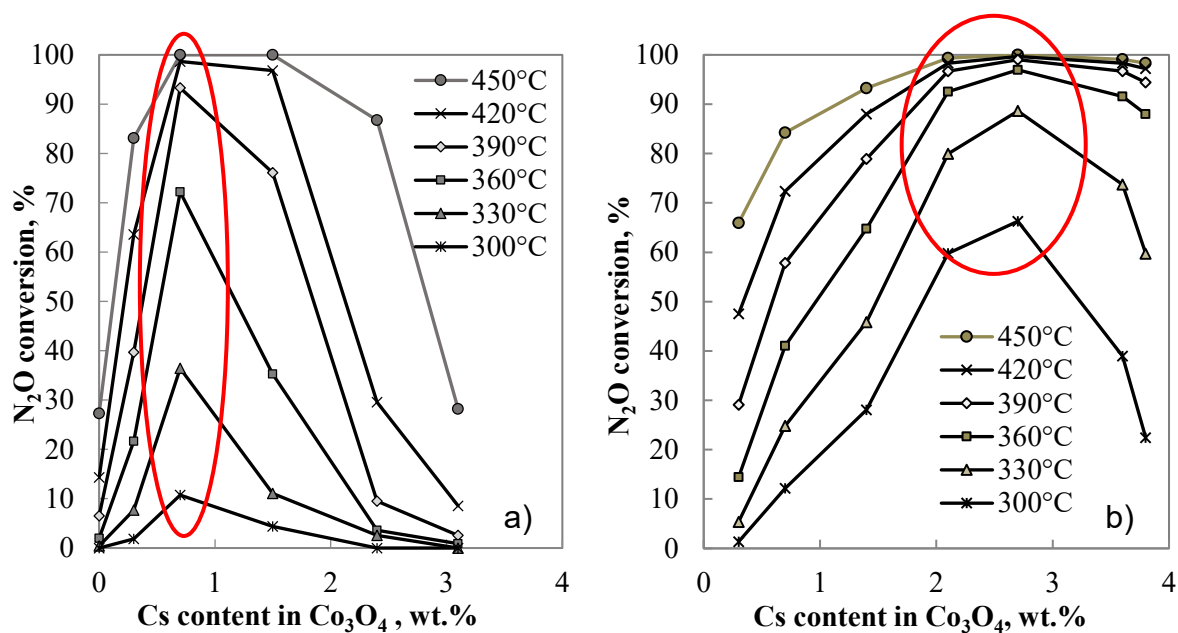


**Fig.1** Dependence of  $N_2O$  conversion on the Cs content in  $Co_3O_4$  over a) bulk active phase and b)  $Co_3O_4$ -Cs deposited on the ceramic foam. Conditions: a) 1000 ppm  $N_2O$  in  $N_2$ , GHSV =  $60 \text{ l g}^{-1} \text{ h}^{-1}$ ; b) 1000 ppm  $N_2O$  in  $N_2$ , GHSV =  $1500 \text{ h}^{-1}$ .

**Acknowledgement.** The work was supported from ERDF "Institute of Environmental Technology – Excellent Research" (No. CZ.02.1.01/0.0/0.0/15\_019/0000853) and by VŠB-TU student project No. SP2019-91. Experimental results were accomplished by using Large Research infrastructure ENREGAT supported by the Ministry of Education, Youth and Sports of the Czech Republic under project No. LM2018098.

#### References:

- [1] J. Pérez-Ramírez, F. Kapteijn, K. Schöffel, J.A. Moulijn, *Appl. Catal. B. Environ.*, 44 (2003) 117-151.
- [2] F. Kapteijn, G. Marbán, J. Rodríguez-Mirasol, J.A. Moulijn, *J. of Catal.*, 167 (1997) 256-265.
- [3] P. Stelmachowski, G. Maniak, A. Kotarba, Z. Sojka, *Catal. Commun.*, 10 (2009) 1062-1065.
- [4] L. Obalová, K. Karásková, K. Jirátová, F. Kovanda, *Appl. Catal. B. Environ.*, 90 (2009) 132-140.
- [5] G. Maniak, P. Stelmachowski, A. Kotarba, Z. Sojka, V. Rico-Pérez, A. Bueno-López, *Appl. Catal. B. Environ.*, 136–137 (2013) 302-307.

## Influence of the Structural Characteristics on the Pt/C Electrocatalysts Stability

Paperzh K.O., Alekseenko A.A.

*Southern Federal University, Faculty of Chemistry, Rostov-on-Don, Russia  
kpaperzh@yandex.ru*

In low-temperature fuel cells the Pt/C electrocatalysts are used as the basis of the catalytic layer, they obtain different structural and electrochemical characteristics: mass fraction, electrochemically active surface area (EASA), aggregation degree, and an average size of crystallites (D). Another essential peculiarity is degradation degree of the Pt/C electrocatalysts, which allows us to conclude about quality of a catalyst.

During the study through methods of liquid-phase synthesis with the usage of different reducing agents the following electrocatalysts with a different average size of crystallites have been produced [1]: sodium borohydride (SB), formic acid (FA), and formaldehyde (F). The further research was aiming at defining structural and electrochemical characteristics of the produced samples with the usage of different methods: gravimetry, radiography, cyclic voltamperometry. Degradation of the Pt/C electrocatalysts was measured with the method of voltamperometrical cycling in the range of potentials 0.6–1.0 V. 0.1 M of HClO<sub>4</sub>, saturated with argon, was used as the electrolyte. The number of cycles was equal to 5000 (watch the Table).

Table – Structural and electrochemical characteristics of the Pt/C electrocatalysts.

Sample	$\omega(\text{Pt}), \%$	D, nm	EASA before the stress-test, m <sup>2</sup> /g(Pt)	EASA after the stress-test, m <sup>2</sup> /g(Pt)	Degradation degree, %	Aggregation degree
SB	20.2±0.6	3.8	63±6	58±6	8	0.4
FA	18±0.5	2.6	66±6	51±5	23	0.4
E-TEK	20±0.6	2.2	73±7	54±5	26	0.3
JM	20±0.6	2	86±9	60±6	30	0.3
F	19±0.6	1.5	97±10	63±6	35	0.5

The produced materials are characterized by mass fracture equal to about 20 % and an average size of crystallites – 1–4 nm. It was defined that the sample F is characterized by the higher EASA, which exceeds commercial Pt/C analogues (E-TEK and JM). Moreover, the sample, produced in formaldehyde, obtains the higher aggregation degree. It is important to note that the samples with the sizes of crystallites equal to 3–4 nm (SB and FA) are characterized by the lower initial area and degradation degree. Perhaps, the connection of

## PP-IV-42

major particles with the carbon carrier is stronger what results in that they move along its surface and detach in lesser degree.

The most promising sample for the further study should be that which is characterized by the higher electrochemically active surface area during the entire research, and this is the sample F. Despite the higher degradation degree, the sample obtains the highest initial and final EASA.

**Acknowledgement.** The work was carried out within the academic advising of Alekseenko A.A. and supported by the Russian Science Foundation (grant № 16–19–10115).

### References:

[1] Alekseenko A.A., Ashihina E.A., Shpanko S.P., Volochaev V.A., Safronenko O.I., Guterman V.E. Application of CO atmosphere in the liquid phase synthesis as a universal way to control the microstructure and electrochemical performance of Pt/C electrocatalysts // Applied Catalysis B: Environmental. 2018. № 226. C. 608–615.

## Hydrogenation of Ethyl Levulinate to $\gamma$ -Valerolactone over Ir Catalysts

Simakova I.L.<sup>1,2</sup>, Demidova Yu.S.<sup>1,2</sup>, Devi N.<sup>3</sup>, Dhepe P.<sup>3</sup>, Bokade V.<sup>3</sup>

1 – Boreskov Institute of Catalysis, Novosibirsk, Russia

2 – Novosibirsk State University, Novosibirsk, Russia

3 – CSIR-National Chemical Laboratory, Pune, India

simakova@catalysis.ru

Lignocellulosic biomass, derived from different plants and waste biomass represents one of the most viable substitutions for fossil fuels [1]. One of the typical chemicals is  $\gamma$ -valerolactone (GVL), which could be used as fuel additive, renewable solvent, and intermediate for the production of chemicals and high-grade alkenes. GVL can be synthesized by hydrogenation of levulinic acid (LA) and its esters, which have already been efficiently produced from lignocellulosic biomass on a large scale [2]. The utilization of ethyl levulinate (EL) is more favorable compared to LA since the strong acidity of LA could affect the support such as zeolites and remove the active metal from the support. In addition, it also heavily corrodes equipment. EL yielded from direct alcoholysis is obviously higher than that of LA from hydrolysis due to substantial suppression of humins formation, and EL is easier to be separated in alcohol medium [3]. In this work catalytic hydrogenation of EL into GVL over Ir catalysts will be studied (Fig. 1).

Ethyl levulinate (97%, Acros Organics, Belgium) in polar aprotic 1,4-dioxane was hydrogenated in a batch reactor at 140-180°C, 20-30 bar of H<sub>2</sub> over Ir supported over SiO<sub>2</sub>, Al<sub>2</sub>O<sub>3</sub> and mesoporous carbon Sibunit. Iridium catalysts were prepared by impregnation with IrCl<sub>3</sub> precursor followed by reduction by hydrogen at TPR conditions and characterized by TEM, XRD, XPS, TPR [4]. Reaction components were analyzed by GLC using BP20 capillary column (60 m/0.25 mm/0.25  $\mu$ m) (Chromos GC-1000).

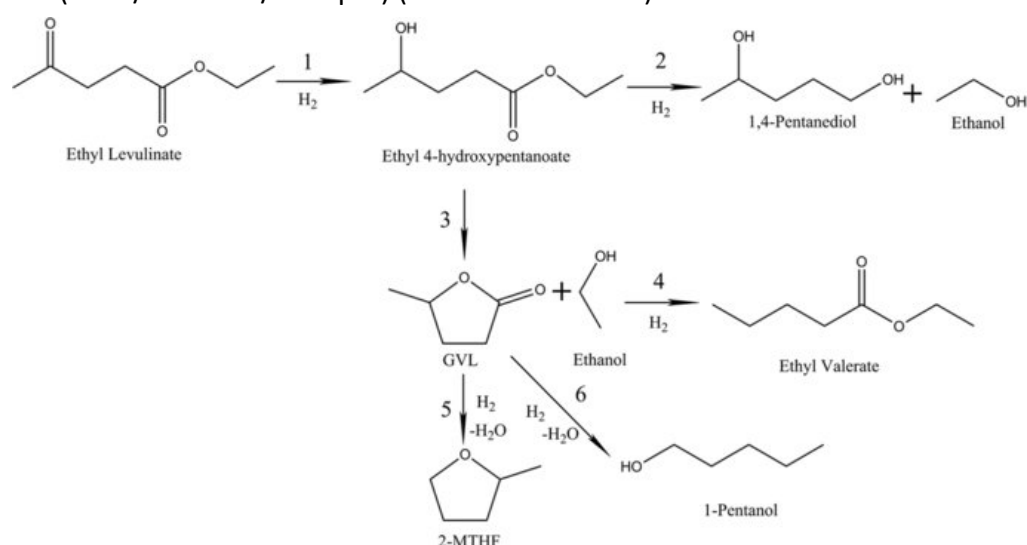


Fig. 1. Ethyl levulinate transformation ways in reductive conditions.

## PP-IV-43

According to GLC analysis the main reaction products were GVL and ethanol. The activity of Ir catalysts varied depending on support nature and was tuned by Ir nanoparticle size and reduction temperature. Samples of Ir catalysts supported on different supports were characterized by TEM, XRD, XRF and N<sub>2</sub> physisorption. The regularities obtained for EL hydrogenation were applied for development of selective GVL synthesis in mild reaction conditions.

**Acknowledgement.** This work was supported by RFBR Grant 18-53-45013 IND\_a.

### References:

- [1] J. Bozell, G. Petersen, *Green Chem.* 12 (2010) 539–554.
- [2] H. Chen, B. Yu, S. Jin, *Bioresour. Technol.* 102 (2011) 3568–3570.
- [3] Y. Cen, S. Zhu, J. Guo, J. Chai, W. Jiao, J. Wang, W. Fan, *RSC Adv.*, 2018, 8, 9152-9160.
- [4] I.L. Simakova, Yu.S. Demidova, S.A. Prikhodko, M.N. Simonov, A.Yu. Shabalin, *J. Siberian Federal University Chemistry* 3 (2015 8) 439-449.

## Low Percent Size-Selected Pd and Pt Catalysts Prepared by Laser Electrodispersion in the CO Oxidation

Golubina E.V.<sup>1</sup>, Shilina M.I.<sup>1</sup>, Lokteva E.S.<sup>1</sup>, Maslakov K.I.<sup>1</sup>, Gurevich S.A.<sup>2</sup>, Kozhevnikov V.M.<sup>2</sup>,  
Yavsin D.A.<sup>2</sup>, Rostovshchikova T.N.<sup>1</sup>

1 – Lomonosov Moscow State University, Moscow, Russia

2 – Ioffe Physico-Technical Institute of RAS, St. Petersburg, Russia

rtn@kinet.chem.msu.ru

Laser ablation is attracting an increasing attention as one step 'green' synthesis of ligand free nanoparticles for catalytic applications [1]. But the conventional laser ablation technique as well as 'wet' chemistry methods is not suitable for the fabrication of densely packed layers of single particles due to their coagulation. Laser electrodispersion (LED) [2] based on melting of a metallic target and cascade fission of liquid metal drops in the laser torch plasma allows producing unusually stable to aggregation amorphous nanoparticles and overcoming this difficulty. The strictly definite particle size is determined only by the electron work function of a metal. In this study the LED method was applied for the fabrication of "core-shell" Pd and Pt catalysts based on size-selected nanoparticles. For these catalysts a high degree of surface coverage (3.5-0.5 ML) is achieved even at low ( $10^{-2}$ - $10^{-3}$  wt.%) percent of metal loading. The catalysts on different supports (ZSM-5, Al<sub>2</sub>O<sub>3</sub>, HOPG and Sibunit) were characterized by TEM, XPS and DRIFT spectroscopy. Their efficiency was compared with traditional supported catalysts in the CO oxidation. In accordance with structural studies in all cases spherical 2 nm particles containing metallic Me<sup>0</sup> and oxidized Me<sup>+2</sup> states were uniformly distributed on the surface of both Pd and Pt catalysts. For each metal the proportion of Me<sup>0</sup>/Me<sup>2+</sup> depends on the support type and surface coverage. The more oxidized particles were formed on Al<sub>2</sub>O<sub>3</sub> at the low surface coverage. All Pd catalysts were more active compared to Pt ones. For both metals the activity increases in the following support order: Sibunit < Al<sub>2</sub>O<sub>3</sub> < ZSM-5. For the most active 0.01%Pd/ZSM-5 catalyst the temperature of 50% conversion of CO was 170°C, that is 50 degrees lower than that for similar catalyst prepared by usual method with the high (0.1%) metal content. The improved activity of LED catalysts is associated with small particle size; the location of metal particles on the outer support surface; purity of particle surface; their high stability against aggregation and electrostatic interactions between closely located particles.

**Acknowledgement.** This work was supported by the Program of Development of MSU.

### References:

[1] Zhang, J., M. Chaker, and D. Ma, J. of Colloid and Interface Science, 449 (2017)138.

[2] Rostovshchikova T.N., Lokteva E.S., Golubina E.V., et al., Advanced Size-Selected Catalysts Prepared by Laser Electrodispersion. In: Advanced Nanomaterials for Catalysis and Energy: synthesis, characterization and application, Ed. V. Sadykov, Elsevier Inc, 2019, p. 61.

## Reduction of Nitrocompounds over Ag-CeO<sub>2</sub> Catalysts

Chernykh M.V., Mikheeva N.N., Mamontov G.V.  
*Tomsk State University, Tomsk, Russia*  
*msadlivskaya@mail.ru*

The reduction of nitrocompounds into corresponding amines is of great importance, since the amines are important precursors for the synthesis of dyes, pesticides and pharmacological agents [1]. At the moment, the reduction of nitrocompounds is carried out by catalytic and non-catalytic methods [2]. Non-catalytic reduction is based on the chemical reaction with Fe and Sn as reducing agents at 130°C. The disadvantages of the non-catalytic methods include the difficulty to control the degree of reduction of the nitrocompound, the difficulty to achieve high selectivity, the excess of reagents and the formation of a large amount of Fe or Sn salts as by-products. In contrast, the catalytic reduction is more efficient and is based on the use of Pd and Pt catalysts. There are difficulty to obtain the catalyst with both high activity and selectivity, and "hard" conditions of the catalytic process (pressure up to 10-20 atm and temperature of 50-180°C).

Currently, the challenge consists in the implementation of such processes under mild conditions (room temperature and atmospheric pressure) using cheap, highly active and selective catalysts, without the formation of the environmentally harmful by-products. The purpose of the present work is to synthesize the Ag-CeO<sub>2</sub> catalysts by varying the preparation method, and study the catalytic properties in selective reduction of nitroaromatic compounds into the corresponding amines in aqueous solution at room temperature and atmospheric pressure.

The series of Ag-CeO<sub>2</sub> catalysts were synthesized by varying the silver content from 1 to 15 wt.% and the preparation method (co-precipitation and incipient wetness impregnation). The synthesis of Ag-CeO<sub>2</sub> catalyst by co-precipitation method was based on the precipitation of AgNO<sub>3</sub> and Ce(NO<sub>3</sub>)<sub>3</sub>·6H<sub>2</sub>O salts in an aqueous solution by the excess of ammonia and the redox reaction between the Ce<sup>3+</sup> and Ag<sup>+</sup> [3]. The impregnation technique was implemented using the aqueous solution of AgNO<sub>3</sub>. The CeO<sub>2</sub> support was synthesized by the precipitation or thermal decomposition of Ce(NO<sub>3</sub>)<sub>3</sub>·6H<sub>2</sub>O at 500 °C. The study of the characteristics of the porous structure of the samples was carried out using the nitrogen adsorption at -196°C on the automatic gas adsorption analyzer TriStar 3020 (Micromeritics, USA). The features of the catalyst reduction were investigated by the temperature-programmed reduction by hydrogen (TPR H<sub>2</sub>) on the ChemiSorb 2750 chemisorption analyzer (Micromeritics, USA).

The catalytic properties of the catalysts were investigated in the p-nitrophenol reduction with sodium borohydride (NaBH<sub>4</sub>) at room temperature and atmospheric pressure. The course of the reaction was monitored by measuring the ultraviolet and visible radiation absorption spectra on a Solar PB 2201 spectrophotometer. The decreasing of the absorption band of the p-nitrophenolate ion at 400 nm was observed (Fig. 1a), and the colour of the reaction mixture changed from bright yellow to colourless during the reaction.

The CeO<sub>2</sub> and Ag-CeO<sub>2</sub> samples are shown to possess a mesoporous structure, and the S<sub>BET</sub> from 5 to 30 m<sup>2</sup>/g. CeO<sub>2</sub> obtained by thermal decomposition has a higher specific surface area (76 m<sup>2</sup>/g). The TEM results show that the agglomerates of strongly bonded Ag and CeO<sub>2</sub> particles are formed for catalyst prepared by co-precipitation method as a result of the redox reaction between Ce<sup>3+</sup> and Ag<sup>+</sup>. The formation of clusters and small silver particles (2-5 nm) homogeneously distributed on the CeO<sub>2</sub> surface was observed for the catalysts prepared by impregnation techniques.

It was shown that the nitrophenol reduction by sodium borohydride does not occur over CeO<sub>2</sub>. The nitrophenol conversion into aminophenol over Ag/CeO<sub>2</sub> catalysts at room temperature occurs for few minutes (5-15 min). The activity increases as the Ag loading rises. The catalysts prepared by the impregnation techniques are more active due to the small size of silver particles and the distribution of silver on the external surface of the catalyst.

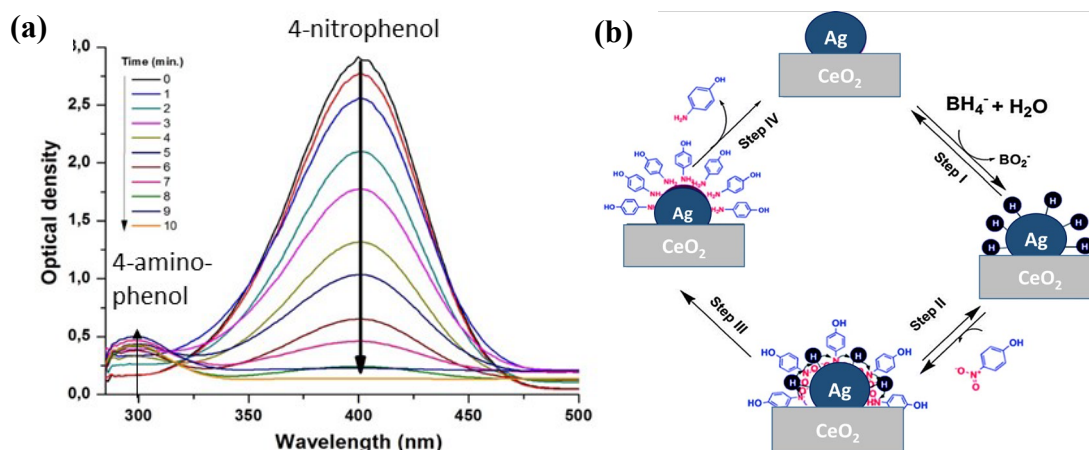


Fig. 1. UV-Vis spectra of 4-nitrophenol reduction over Ag/CeO<sub>2</sub> catalyst (a) and the scheme of 4-nitrophenol reduction according to the Langmuir- Hinshelwood mechanism (b)

The mechanism of nitrophenol reduction to aminophenol is described within the framework of the Langmuir-Hinshelwood theory: atomic hydrogen and 4-nitrophenol are adsorbed on the surface of silver particles and are then chemisorbed on the neighbouring active sites to interact with the formation of the adsorbed reaction product (4-aminophenol), which is then desorbed. The limiting stage of the process is the 4-nitrophenol reduction. This catalytic reaction is a pseudo-first order reaction, because there is an excess of sodium borohydride.

Thus, the selective reduction of 4-aminophenole by sodium borohydride occurs over the Ag/CeO<sub>2</sub> catalysts at room temperature. The method of catalyst preparation and the loading of the silver affect the activity of the Ag/CeO<sub>2</sub> catalysts in the 4-nitrophenol reduction.

**Acknowledgement.** The present work was supported by the Russian Science Foundation (Grant No.18-73-10109).

#### References:

- [1] A.M. Alexander, Chem. Soc. Rev. 39 (2010) 4388–4401.
- [2] J. Song et al., Appl. Catal., B: Environmental. 227 (2018) 386–408.
- [3] X.Deng et al., Chemical Engineering Journal (2016).

## The Use of Dispersed Catalysts in Catalytic Steam Cracking of Vacuum Residue

Saiko A.V.<sup>1</sup>, Zaikina O.O.<sup>1,2</sup>, Sosnin G.A.<sup>1,2</sup>, Yeletsky P.M.<sup>1</sup>, Klimov O.V.<sup>1</sup>,  
Yakovlev V.A.<sup>1</sup>, Noskov A.S.<sup>1</sup>

1 – Boreskov Institute of Catalysis, Novosibirsk, Russia

2 – Novosibirsk State University, Novosibirsk, Russia

saiko@catalysis.ru

One of promising ways of heavy oil feedstocks upgrading, which can be alternative to conventional approaches based on carbon rejection (visbreaking, coking, catalytic cracking) and hydrogen addition (hydrotreatment, hydrocracking) is a catalytic steam cracking. To increase the upgrading efficiency with involving water in the process it is necessary to use catalysts [1].

Seeking of a dispersed catalyst active in the vacuum residue (VR) steam upgrading in a continuous flow mode using slurry-reactor through screening of a series of the dispersed catalysts based on various metals (Mo, Ni, Al, Fe, Co) was carried out in this work. The effect of the catalytic systems on yield and properties of liquid products of the VR upgrading (upgraded oil) was studied, and the most active catalytic compositions was chosen (systems based on Mo and Fe-Co). Table 1 shows yields and composition of products of steam cracking of VR in the presence of 0.5 wt. % catalysts based on various metals (the content is presented in terms of metals), ratio of water to VR = 0.1 : 1, T = 450 °C, P = 20 atm., VR feeding = 0.1 kg/h.

Table 1. Yields and composition of products of catalytic steam cracking of VR.

Characteristic, wt. %	Initial VR	Products obtained using catalysts based on various metals. Metal - the basis of a dispersed catalyst					
		Mo	Ni	Fe	Co	Al	Fe-Co
Conversion C <sub>500+</sub> , %	–	41.7	31.9	46.6	36.8	41.4	50.2
Yield of upgraded oil, including:	–	86.5	81.0	82.6	85.8	82.8	87.1
Gasoline (<200°C)	0	10.3	6.8	13.0	8.6	9.9	12.5
Diesel (200-360°C)	0	12.7	9.6	16.3	12.0	11.9	17.4
VGO (360-500°C)	5	15.6	12.2	11.4	13.7	14.9	16.0
Residue (>500°C)	95	47.9	52.4	41.9	51.5	46.1	41.2
Light fractions	0	23.0	16.4	29.3	20.6	21.8	29.9
Coke	–	3.0	6.1	5.5	3.2	4.7	4.8
Gaseous products	–	6.4	4.9	8.2	5.8	5.2	6.2
Losses		4.1	8.0	3.7	5.2	7.9	1.9
S content in upgraded oil	1.8	1.28	1.32	1.34	1.29	1.35	1.19
O content in upgraded oil	0.5	0.2	0.3	0.2	0.2	0.4	0.3
Density, kg/m <sup>3</sup> (25°C)	960 (60°C)	940	955	915	950	937	920
Viscosity, mm <sup>2</sup> /s (60 °C)	6712,5	62	190	88	128	76	75

## PP-IV-46

Samples of upgraded oil using the most promising catalytic compositions (Mo and Fe-Co) were produced followed by their rectification to obtain gasoline, diesel, VGO and residue fractions. The obtained fractions were analysed by various techniques to determine a wide range of their characteristics: density, kinematic viscosity, H/C ratio; fractional, SARA composition and elemental compositions; CCR, octane number, cetane index, crystallization temperature as well as contents of sulphur, nitrogen, oxygen, metals, olefins, aromatic and C500+ hydrocarbons. The obtained data were compared with the properties of fractions obtained from upgraded oil produced through non-catalytic steam cracking of VR. The perspectivity of application of Fe-Co catalyst for the production of upgraded oil with an increased content of light fractions via VR catalytic steam cracking is shown.

**Acknowledgement.** This work was supported by Ministry of Science and Higher Education of the Russian Federation (project No 14.607.21.0172, identification number RFMEFI60717X0172).

### References:

[1] P.M. Eletskii, G.A. Sosnin, O.O. Zaikina, R.G. Kukushkin, V.A. Yakovlev Journal of Siberian Federal University. Chemistry. 10 (2017) 545.

## Bicomponent Nanocatalysts Based on Bororganic and Platinum Nanoparticles Increasing Ammonia Decomposition Rate

Kharitonov V.A.<sup>1</sup>, Sarvadiy S.Yu.<sup>1</sup>, Ulasevich S.A.<sup>2,3</sup>, Ivashkevich N.M.<sup>2</sup>, Grishin M.V.<sup>1</sup>

1 – *Semenov Institute of Chemical Physics RAS, Moscow, Russia*

2 – *Institute of General and Inorganic Chemistry NASB, Minsk, Belarus*

3 – *ITMO University, St. Petersburg, Russia*

*sarvadiy15@mail.ru*

Ammonia is currently being considered [1] as a promising storage of hydrogen for fuel cells. Indeed, ammonia is easily synthesized in the Haber-Bosch process and is produced on an industrial scale [2], has a high energy density and liquefies under relatively low pressure of nine atmospheres at 293 K [3]. At the same time in the fuel cell hydrogen must be released from ammonia by catalytic decomposition. Ruthenium is the common nanocatalyst for this process, but for relatively high cost and rarity researchers substitute it by similar and more prevalent platinum nanocatalysts [4, 5] modified by other metals, due to the fact of passivation of pure platinum nanoparticles by ammonia decomposition products [6, 7].

The chemical properties of organoboron nanoparticles (OBN) deposited on various substrates during the catalytic decomposition of ammonia [8], the ability to control these properties using the substrate effect and the potential applied to the substrate [9], have been established in our previous studies. OBN-based coatings are not as common as metal NPs in heterogeneous catalysis, though they show metallic type of conductivity. According to our research, coatings made of platinum nanoparticles are among widely used in heterogeneous catalysis of metal nanocatalysts that obtain the properties close to OBN [10]. This makes it interesting to study the properties of bicomponent systems based on platinum and organoboron nanoparticles. Earlier it was shown, that application of OBN over the Pt nanoparticles coating deposited on the high oriented pyrolytic graphite (HOPG) substrate provides more uniform distribution and greater adhesion of OBN than in OBN coatings on pure graphite and prevents the formation of multi-layered agglomerations of OBN. [11] In the present work we investigate the catalytic properties of bicomponent nanocatalysts based on organoboron and platinum nanoparticles towards ammonia decomposition.

Bicomponent coatings were obtained by technique [11]. That provides a coating with a dendritic layered structure: the dendrite from platinum nanoparticles on HOPG is covered with BON monolayer. The interaction with ammonia was conducted in flow mode at a pressure of  $10^{-6}$  Torr and a sample temperature of 700K. Previously, a series of experiments on the decomposition of ammonia with a heated holder without sample were carried out in order to take into account the contribution of the experimental chamber in the decomposition of ammonia. The decomposition of ammonia was found as result of the interaction of ammonia with the bicomponent coatings on HOPG. The data of tunneling spectroscopy

indicate the preservation of the electronic structure of the coating during the experiment. The conversion of ammonia on bicomponent OBN/Pt/HOPG coating is 1.6 times higher than for OBN/HOPG nanocatalyst [8] and is much more stable than for Pt/HOPG [11].

HOPG was used as the model substrate in order to provide the control of the coatings geometric and electronic structure by STM/STS techniques and to compare it with OBN/HOPG nanocatalysts. The substrate-coating interaction can influence the properties of the system, so the jump from the atomically flat HOPG to common in industry substrates may cause a shift in the conversion of ammonia. To take into consideration the effect of the substrate on non-model substrates we tested the TiO<sub>2</sub> and anodized TiO<sub>2</sub> films with and without Pt, OBN and bicomponent coatings on it. The results are in the table.

Table. Ammonia conversion by different samples.

S	TiO <sub>2</sub>	TiO <sub>2</sub> / Pt	TiO <sub>2</sub> / Pt/OBN	TiO <sub>2</sub> / Au	TiO <sub>2</sub> / Au/OBN	TiO <sub>2</sub> (a)	TiO <sub>2</sub> (a) /OBN	HOPG	HOPG/ OBN [8]	HOPG/ Pt [11]	HOPG/ Pt/OBN
C1	6.1	3.8	6.2	4.0	8.0	7.9	10.4	3.6	-	-	7.5
C2	-	-2.3	0.1	-2.1	1.9	-	2.5	-	2.8	→0.0	4.4

*S - sample, C1 – increase in conversion of ammonia gained by the sample (%), C2 – increase in conversion of ammonia gained by the NP coating towards support (%).*

Thus, it is shown that the coverage of the titanium dioxide with metal nanoparticles, no matter Pt or Au, leads to a partial decrease in the yield of products which is higher for pure substrates. The second metal (Au) was used to show that the decrease in ammonia decomposition possibly doesn't depend on metal type and is due blocking active sites of TiO<sub>2</sub> substrate by NPs. The deposition of the OBN coating on the anodized titanium dioxide, as well as on the metal-NPs coatings on titanium dioxide, leads to an increase in the conversion of ammonia. In the latter case of the increase in conversion due to BON compensates and exceeds the drop in conversion after the application of a metal coating on titanium dioxide.

**Acknowledgement.** This work was supported by grant **17-53-04014** RFBR / **X17PM-004** BRFFR.

#### References:

- [1] Choudhary T. V., Sivadinarayana C., Goodman D. W., Catal. Lett. 72 (2001) 197.
- [2] Smil V. Enriching the Earth: Fritz Haber, Carl Bosch and the Transformation of World Food Production. Cambridge MA: MIT Press (2001) 69.
- [3] G. Thomas and G. Parks, Potential Roles of Ammonia in a Hydrogen Economy. Washington DC: U.S. Department of Energy (2006) 7.
- [4] Hansgen D. A., Vlachos D. G., Chen J. G., Nat. Chem. 2 (2011) 484.
- [5] Hansgen D. A., Thomanek L. M., Chen J. G., Vlachos D. G., J. Chem. Phys. 134 (2011) 184701.
- [6] Y.-M. Sun, D. Sloan, H. Ihm, and J. M. White, J. of Vac. Sci. & Tech. A. 14 (1996) 1516.
- [7] Gatin A.K., Grishin M.V., Sarvadii S. Yu. et al., Kinet. Catal. 59 № 2 (2018) 196.
- [8] Grishin M. V., Gatin A. K., Slutskii V. G. et al., Russ. J. Phys. Chem. B. 8 №3 (2014) 416.
- [9] Gatin A. K., Grishin M. V., Sarvadii S. Yu. et al., Nanotechnol. Russ. 11 №1 (2016) 1.
- [10] Grishin M.V., Gatin A.K., Slutskii V.G. et al., Russ. J. Phys. Chem. B. 10 №5 (2016) 760.
- [11] Kharitonov V. A., Grishin M. V., Ulasevich S. A. et al. Russ. J. Phys. Chem. B. 13 №1 (2019) 16.

## Styrene Photocatalytic Oxidation over Me (Au, Pt, Pd)/TiO<sub>2</sub>-NTs Supported Catalysts

Savchuk T.<sup>1,2</sup>, Shtyka O.<sup>2</sup>, Dronov A.<sup>1</sup>, Maniukiewicz W.<sup>2</sup>, Gavrilov S.<sup>1</sup>, Maniecki T.<sup>2</sup>

1 – National Research University of Electronic Technology, Moscow, Russia

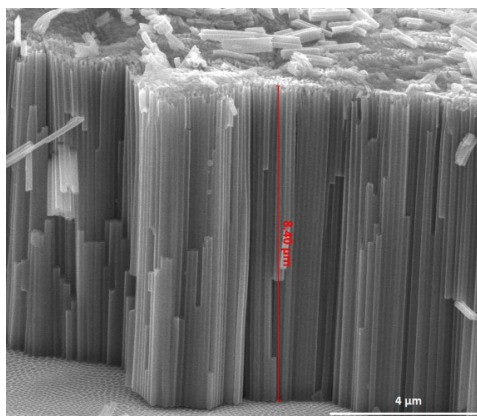
2 – Lodz University of Technology, Lodz, Poland

wewillbe01@gmail.com

Air pollution is currently one of the most important problems of the modern world. Part of this problem is indoor pollution by volatile organic compounds hazardous to people's health. One of the possible solutions is the application of photocatalysts for converting toxic VOC into harmless CO<sub>2</sub> and H<sub>2</sub>O.

Of the many different photocatalysts, titanium dioxide has been the most widely used for this purpose due to its non-toxicity, abundance, chemical stability, and strong oxidizing ability. A great deal of effort has been devoted to the development of new TiO<sub>2</sub>-based materials with enhanced photocatalytic properties, such as nano – and microstructured TiO<sub>2</sub> (sheets, sphere, fibers), metal-decorated TiO<sub>2</sub>, and TiO<sub>2</sub> -based composites.

This paper deals with the investigation of physicochemical and photocatalytic properties of nanotubular titanium dioxide (TiO<sub>2</sub>-NTs) and nanotubular titanium dioxide modified with Au, Pt, and Pd. The nanotubular TiO<sub>2</sub> (Figur 1) was obtained by the method of electrochemical oxidation of titanium foil in fluorine-containing an electrolyte based on ethylene glycol. The deposition of metal nanoparticles on TiO<sub>2</sub> surface was performed using sol-gel method. The photocatalytic activity of obtained materials was evaluated in a model reaction of styrene oxidation under UV and visible light irradiations. The analysis of reaction products was performed by means of on-line gas chromatographs equipped with TCD and FID. The physicochemical properties of catalysts (morphology, phase composition, particle size distribution) were studied using SEM/EDS, XRD, and low-temperature nitrogen adsorption.



Figur 1 – anodic TiO<sub>2</sub>-NTs

**Acknowledgement.** This work was supported by RFBR grant № 18-29-23038 mk.

## Pt and Rh Catalysts Supported on Alumina and Structured Supports for the Reaction of Partial Oxidation of Hydrocarbons

Shefer K.I.<sup>1,2</sup>, Kovtunova L.M.<sup>1,2</sup>, Rogozhnikov V.N.<sup>1</sup>, Chetyrin I.A.<sup>1</sup>, Suprun E.A.<sup>1</sup>,  
Stonkus O.A.<sup>1,2</sup>, Larina T.V.<sup>1</sup>

1 – Boreskov Institute of Catalysis, Novosibirsk, Russia

2 – Novosibirsk State University, Novosibirsk, Russia

shefer@catalysis.ru

The reaction of partial oxidation of hydrocarbons can be used to produce synthesis gas and hydrogen and for burning off waste gases in various technological processes. This exothermic reaction requires the use of catalysts with high thermal stability and effective heat redistribution in the reaction zone. Deposition of thin catalytic coatings onto metallic substrates, such as wire meshes, can be a good decision in this case. Using structured support also allows more efficient and economic use of the catalysts, and it is easy to scale them.

In this project we prepared and characterised catalysts for the reaction of partial oxidation of hydrocarbons based on platinum and rhodium, supported by aluminas of the bayerite series. Aluminum hydroxide and oxide compounds were obtained through the aluminate method. The catalyst samples with various content of active components were prepared by impregnating the support with solutions of different precursors. In addition to granular catalysts, structured catalysts of the same composition, supported by the FeCrAlloy mesh, were prepared. Alumina coating is strongly chemically bounded onto this type of structured support.

Structural characterization is a very important step in understanding catalysts' action, because their structural features determine their properties. Nanosized catalysts require special methods which take into account the specific features of small objects. We investigated the precursors' and resulting catalysts' phase compositions and structural features using X-ray diffraction and other physicochemical methods. The support form's influence, the active component precursor's nature, and the precursor complex's charge on the structure and properties of the resulting catalysts were studied.

**Acknowledgement.** This work was supported by the Russian Foundation of Basic Research, grant 19-03-00595.

## Novel Fe-Containing Catalysts for the Selective Hydrogenation of Aldehydes and Nitro-Compounds

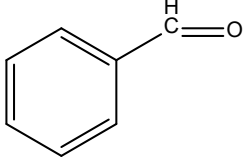
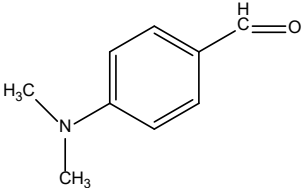
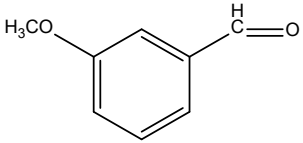
Shesterkina A.A., Strelkova A.A., Kirichenko O.A., Redina E.A., Kustov L.M.  
*N. D. Zelinsky Institute of Organic Chemistry, Russian Academy of Sciences,  
Moscow, Russian Federation  
anastasiia.strelkova@mail.ru*

Hydrogenation reactions are one of the most important types of transformations in synthetic organic chemistry and petrochemistry. Selective hydrogenation of carbonyl compounds makes it possible to obtain alcohols of various structures, including unsaturated ones, which are in the manufacture of medicines, and find wide application as flavourings and fragrances [1]. Hydrogenation of compounds containing nitro groups is used to produce amines, an important class of organic compounds that are used in the drug industry, the production of plastics and dyes, antioxidants and pesticides [2]. Conventional methods for the selective reduction of these compounds are based on the use of stoichiometric reducing agents such as metal hydrides and boranes and homogeneous catalysts, which lead to a large amount of waste and characterized by low atomic efficiency [3]. Heterogeneous catalysts are promising, but existing heterogeneous catalysts for these processes contain large amounts of noble metals (Pt, Pd, Au) are low-selective and require high temperatures and pressures [4].

The objective of our work is to create new heterogeneous catalysts based on supported nanoparticles of non-noble metals (Fe, Cu) for the selective hydrogenation of carbonyl and nitro-compounds under mild reaction conditions. The catalytic properties of Fe-Cu catalysts depend on the composition of the samples, the method of preparation and the carriers. The extent of interaction between Fe and Cu strongly depends on the preparation procedure that affected the catalytic properties of the prepared materials in the reaction of hydrogenation nitroarenes and aldehydes. We studied the Fe-Cu/SiO<sub>2</sub> catalysts prepared by two novel procedures: deposition of Fe and Cu precursors by consecutive incipient wetness impregnation of porous silica beads with ammonium trioxalatoferrate and copper (II) nitrate solutions (CI<sub>m</sub>) and co-deposition of Fe (iron (III) nitrate) and Cu (copper (II) nitrate) precursors on the outer surface of the silica support powder using urea (CoD). Bimetallic Fe-Cu catalysts were characterized by XRD, SEM, TPR-H<sub>2</sub> and DRIFTS-CO techniques. The Fe-Cu/SiO<sub>2</sub> catalysts obtained by co-deposition (CoD) are more active and selective in hydrogenation of nitro-compounds than catalysts obtained by impregnation (CI<sub>m</sub>). The best selectivity towards p-phenylenediamine (89%) at complete conversion of p-dinitrobenzene was obtained on the sample synthesized by co-deposition of metal precursors with urea. We synthesized bimetallic Fe-Cu catalysts deposited on various supports (SiO<sub>2</sub>, CeO<sub>2</sub>-ZrO<sub>2</sub>). The catalytic activity of the catalyst deposited on the CeO<sub>2</sub>-ZrO<sub>2</sub> in hydrogenation of aldehydes is 3 times higher than the catalyst deposited on the carrier SiO<sub>2</sub> (Table 1).

## PP-IV-50

Table 1. Catalytic properties of the 7Fe-3Cu/CeO<sub>2</sub>-ZrO<sub>2</sub> catalysts in hydrogenation of the aromatic aldehyde

Catalyst	Substrate	Conversion, %	Selectivity for alcohol, %
7Fe/CeO <sub>2</sub> -ZrO <sub>2</sub>		2	100
3Cu/ CeO <sub>2</sub> -ZrO <sub>2</sub>		10	100
7Fe-3Cu/ CeO <sub>2</sub> -ZrO <sub>2</sub>		99	100
7Fe-3Cu/SiO <sub>2</sub>		25	100
7Fe-3Cu/CeZr	4- (dimethylamino)benzaldehyde 	95	100
7Fe-3Cu/CeZr	3- methoxybenzaldehyde 	99	100
Reaction conditions: 4 h., 150 ° C, pH <sub>2</sub> -1.2 MPa., 500 rpm, Ethanol, n <sub>sub</sub> :n <sub>Σ</sub> Me = 17.4			

Thus, a new effective catalytic system Fe-Cu was obtained, which allows hydrogenation of aromatic aldehydes and nitro-compounds in the liquid phase under relatively mild conditions with high selectivity for the corresponding alcohols and amines.

**Acknowledgement.** The reported study was funded by RFBR according to the research project № 18-33-00040 and by the Russian Science Foundation № 17-73-20282.

### References:

- [1] Z. Yang, W. Cheng, Z. Li, Catal. Commun. 117 (2018) 38.
- [2] P. N. Sathishkumar, N. Raveendran, N. S. P. Bhuvanesh, R. Karvembu, J. Org. Chem. 876 (2018) 57.
- [3] J. Liu, S. Yang, W. Tang, Z. Yang, J. Xu, Green Chem. 20 (2018) 2118.
- [4] Y. Fujiwara, Y. Iwasaki, T. Maegawa, Y. Monguchi, H. Sajiki, ChemCatChem 3 (2011) 1624.

## Formation Mechanism of Active Phases Based on Mn, Mn-La, Mn-Ce Oxides under Solution Combustion Synthesis

Shikina N.V.<sup>1</sup>, Gavrilova A.A.<sup>1</sup>, Yashnik S.A.<sup>1</sup>, Litvak G.S.<sup>1</sup>, Khairulin S.R.<sup>1</sup>, Ismagilov Z.R.<sup>1,2</sup>

1 – Boreskov Institute of Catalysis, Novosibirsk, Russia

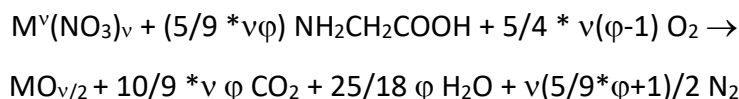
2 – Institute of Coal Chemistry and Chemical Materials Science, Federal Research Center of Coal and Coal Chemistry SB RAS, Kemerovo, Russia

Shikina@catalysis.ru

The use of unconventional synthesis methods, for example the solution-combustion synthesis (SCS), makes it possible to improve the catalytic properties of oxide systems, particularly those supported on ceramic monoliths. The SCS method is a variant of self-propagating high-temperature synthesis. This is an efficient, simple, rapid and inexpensive method for obtaining high-purity and homogeneous nanomaterials [1]. The method is based on the exothermic reaction between oxidant (commonly represented by metal nitrates) and fuel additive (urea, glycine, hydrazine, citric acid, etc.), which proceeds directly on the surface of supports having different origin and geometry.

In this work, Mn, Mn-La, and Mn-Ce SCS catalysts were prepared by impregnation of the silica-alumina ceramic honeycomb monolith (AlSi) with a solution of respective nitrate salts supplemented with glycine, drying at 100°C, and calcination at 550°C. The total content of oxides in the SCS catalysts was 5 wt. %, similar to the case of impregnation catalysts.

According to [2,3], the combustion of nitrate salts with glycine can be described by the following scheme:



where  $v$  is the valence of metal, and  $\phi$  is the ratio of fuel additive to oxidant. At a stoichiometric ratio  $\phi = 1$ , air oxygen is not required for complete oxidation of the fuel additive;  $\phi > 1$  and  $\phi < 1$  testify to an excess (fuel rich condition) or a deficiency (fuel lean condition) of the fuel additive, respectively. In this work, two values of “ $\phi$ ” were considered, namely  $\phi = 0.7$  (fuel lean conditions) and 3.5 (fuel rich conditions).

The formation of Mn oxides in single – and Mn-La, Mn-Ce oxides in two-component monolithic catalysts in the absence of glycine-additive, in fuel lean or fuel rich conditions of the solution combustion synthesis is well illustrated by TGA data (Fig.1). In the course of thermal activation, the impregnated catalysts are formed due to thermal decomposition of nitrate-precursors of active components. Under SCS conditions, an exothermic combustion reaction of nitrates with glycine is added, while the heat wave intensity increases significantly with the amount of fuel additive. At  $\phi < 1$ , the active component is formed as a result of thermal decomposition of nitrates as well as nitrate combustion reaction with glycine. At  $\phi > 1$ , there is

a combination of decomposition and combustion of nitrate, and reduction of metal cations with glycine.

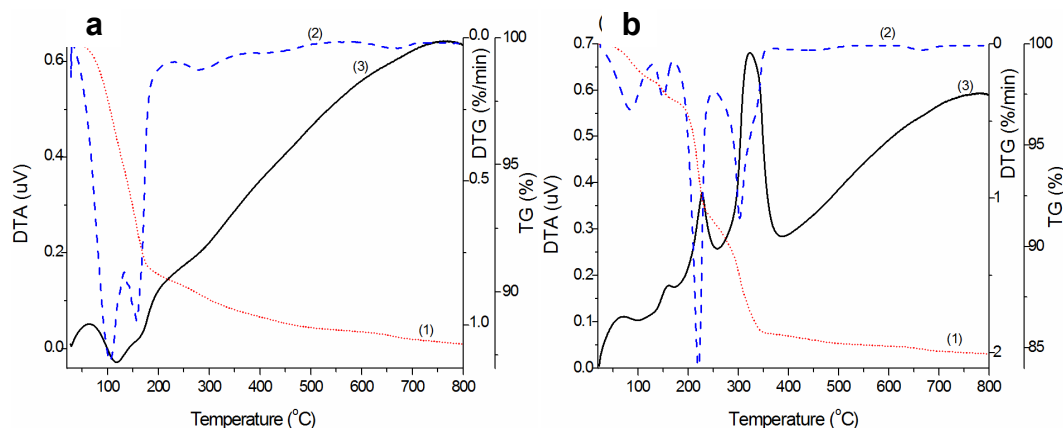


Fig.1 Thermogravimetric (1), differential thermogravimetric (2) and differential thermal analysis (3) curves of the catalysts: (a) Mn-La/AlSi; (b) Mn-La/AlSi ( $\phi=3,5$ )

These reactions are the key factors of phase formation, development of the porous structure, dispersion of the active component, and its localization on the pore surface or in the support volume. Under the conditions of intensive release of gaseous products of the SCS reaction, a more developed porous structure is formed, which ensures the transport of reagents to the active centers. Under SCS conditions, metal oxides are formed in a highly active reduced state, mainly on the surface of the support pores, which also ensures the availability of active centers for reagents and an increase in activity, compared with the impregnated catalysts.

**Acknowledgement.** This work was supported by the Russian Foundation for Basic Research, grant 18-43-540015.

The authors are grateful to researchers from the Boreskov Institute of Catalysis SB RAS V.A. Ushakov, M.S. Melgunov, L.S. Dovitova and A.V. Ishchenko for their assistance with physicochemical studies.

#### References:

- [1] S. L. Gonzalez-Cortes, F. E. Imbert, *Appl. Catal. A: Gen.* 452 (2013) 117–131.
- [2] S. T. Aruna, A. S. Mukasyan, *Curr. Opin. Solid State Mater. Sci.* 12 (2008) 44-50.
- [3] A. S. Mukasyan, P. Dinka, *Intern. J. Self-Prop. High-Temp. Synth.* 16 (2007) 23-35.

## Prospective Ferrite Catalysts for Flue Gases Cleaning from Carbon Monoxide

Shulyaka S.E., Sinitsin S.A., Petrov A.Yu.

*D. Mendeleev University of Chemical Technology of Russia, Moscow, Russia  
ofrolovik@rambler.ru*

Exhaust gases of various composition and origin remain serious ecological threat because some traditional components, such as carbon monoxide (CO), keep activity and toxicity against traditional combustion processes as well as catalytic conversion. Under certain conditions, exhaust gases may consist of up to 50 components, which percentage may vary, many of them require different approach to conversion and detoxication. CO is known poison to living beings, it has compact molecule of linear geometry, possess high reaction activity and high penetrating power, so is objectively hard to bound.

Looking across the market, we have to mention efficient commercial catalysts with active phase containing either platinum group-metals (PGM) or rare-earth metals. Despite of varying design and composition, both contain active monophase or a mechanical mix of active phases, both have limited resource, are aware of catalytic poisons and drastic changes in temperature, humidity and exhaust composition. Moreover, such catalysts are rather expensive, and have known problems with utilization of catalyst or regeneration of valuable metals from within the carrier.

Preliminary studies make us believe that specially treated complex oxides of transient metals have structural premises for catalytic activity against exhausts, including but not limited to CO, comparable to those of PGM and ceria, latter well-known in automotive catalysis. These complex oxides may prove valuable in catalysis because they are cheap, stable and immune both to catalytic poisons and operating conditions change. We also believe that solid solutions may increase catalyst lifecycle and activity, comparing to mechanical mix of active phases, traditional to most catalysts present on the market.

In order to design multi-functional catalyst, based on those transient metal oxides, we performed an excessive SEM and XRD study to describe possible phase and structural changes that samples undergo, paying special attention to the way an investigator may control and maintain those changes.

Both metals and oxides of high purity and dispersity are often synthesized by means of thermolysis, corresponding organic salts are decomposed in vacuum or inert atmosphere. According to XRD, double or more complex oxides are formed almost simultaneously with simple ones, forming a solid solution. Unstable equilibrium between individual phases and solid solution is observed for some time under certain conditions, then it spontaneously shifts, so solid solution decomposes to simple oxides. Aiming on complex oxides formation, we performed thermolysis within reduction atmosphere, that let us keeping the equilibrium and preventing complex oxides from decomposition. We used oxalates of corresponding metals

for thermolysis mixed with flux, containing various organic ammonia salts, including oxalate, in order to maintain atmosphere control.

Transient metal oxides may continuously form and rearrange structural defects within spinel-like ( $AB_2O_4$ ) or perovskite-like ( $ABO_3$ ) structure, that is also valuable for a catalyst, assuming structural stability and self-regeneration possibility. The most promising results were achieved while investigating complex iron oxides (ferrites), structural modification took up to 30% locations of iron oxide, we used Co, Ce, Cu, La, Mn, Ni, Zn oxides as modifiers. Fine crystalline mixture of iron oxalate and modifying metal (s) oxalate(s) mixed 4:1 wt, flux amount and composition varied. Calcination time varied from 1 to 24 hours and temperature varied from 200 to 1250°C. After calcination, the samples were cooled down in the oven for 1 hour and then in a desiccator with a mixture of silica and zeolite filled with high purity nitrogen or argon, where they were naturally cooled down to room temperature. Cooled samples have a regular dispersity of 50-200 nm and are ready-to-use, no need in mechanoactivation or other special measures. Samples were tested for running the catalytic conversion of CO in a flow reactor, or were dispersed into 120 micron particles for the above-mentioned analytical equipment. Analysis of the diffraction data and microscopy allowed to recommend calcination at 900°C for 3 hours, resulting in optimal composition of active phases – ferrite  $MeFe_2O_4$  and magnetite  $Fe_3O_4$ , the whole process is well-described by the modified Wagner model.

According to SEM and XRD studies, samples contain dendrite-like solid solution of magnetite in maghemite ( $\gamma\text{-Fe}_2\text{O}_3$ ) with local ferrite spinel sites. Both aggregate types appear withing the first hour of the calcination process, their composition is also confirmed by elemental analysis. The use of more complex fluxes allowed the authors to control growth and to improve the structure of the product, so that self-arrangement took place, and the target system behaved like an inorganic foam polymer (pore size - 200 nm or less) and looked like HPCM. After 2 more hours of calcination, ferrite grains started to form and local planes began to sprout in one or two directions.

To test conversion productivity the reactor was purged with mixture of carbon monoxide, carbon dioxide and humidified air to simulate the composition and conditions of the flue gases of various origin, including catalytic cracking, CO contents varied 5-20%, gas temperature was 25°C and above. All samples performed well, complete CO conversion occurred at 600°C as gaseous mix flow rate was 1 m<sup>3</sup> per hour. Catalysts show conversion rate, comparable to both ceria-containing and Pt-containing catalysts, some even overcoming them, like Fe-Mn-O system. To ensure catalyst stability, we performed rigorous testing with rapid temperature and composition change, catalysts performed well, according to SEM and XRD, structural and phase shifts took place when needed, resulting in real-time self-regeneration as expected.

## Energy-Effective Fe-Mo Catalyst for the Process of Oxidative Dehydrogenation of Methanol to Formaldehyde

Sinitin S.A.<sup>1</sup>, Polovinkin M.A.<sup>1</sup>, Gavrilov Y.A.<sup>1</sup>, Danilov E.A.<sup>2</sup>, Kostiuchenko V.V.<sup>3</sup>, Vodoleev V.V.<sup>3</sup>

*1 – D.Mendeleev University of Chemical Technology of Russia, Moscow, Russia*

*2 – JSC “Scientific Research Institute of Graphite-Based Structural Materials “Nilgrafit”,  
Moscow, Russia*

*3 – JSC “Tehmetall-2002”, Kirovgrad, Russia  
sergeysinit@rambler.ru*

Formaldehyde production is normally based on oxidative dehydrogenation of methanol in the presence of silver or Fe-Mo-oxide-based catalysts at temperatures below 450 C obtaining concentrated aqueous solutions of CH<sub>2</sub>O containing some methanol which additionally acts as a stabilizer. Said modern production processes have high selectivity, give almost quantitative yield, the catalysts having high stability and long life.

As compared to silver-based catalysts, Fe-Mo-based ones allows for production of formaldehyde with lower content of methanol which is undesirable to most consumers.

In modern catalytic reactors catalyst load can be as high as tens of tons; catalyst grains of various shapes and sizes might be used. As long as the process of oxidative dehydrogenation is carried on in the diffusion region, considerable volume flows of reagents are used, and therefore a lot of energy consumption is due to compensation of catalyst bed-related pressure drop. Energy consumption can be drastically reduced by using so-called energy-effective catalyst grain shapes.

It is well known that conditions of grain formation from catalyst precursor compositions have critical effect on strength and pore structure of the resulting catalysts. For intraparticle diffusion-controlled processes, grain formation conditions should provide for the preservation of relatively big transport pores during the process. Two main routes for formation of catalyst grains are palletization and extrusion. Modern Fe-Mo catalyst production process is based on co-precipitation of the components from aqueous solutions with further drying of the deposit, and pelletization into grain- or ring-shaped particles. Pelletized catalysts possess low strength which leads to high pressure drop along the catalyst bed as a result of pellet fracture at loading and abrasion during reactor operation.

Optimization of shape and size of the catalyst is generally based on several factors: degree of availability of the grain inner surface (e.g. via Tile parameter and/or diffusion inhibition factor), pressure drop-related factors of the catalytic bed (porosity, infusivity) and mechanical strength of the grain. Additionally, for tube-wall reactors ratio between tube diameter and catalyst grain size should also be considered.

Extrusion-based formation is a critical stage for producing energy-effective Fe-Mo catalyst grains. As it is evident, it defines both the product quality and production line output. It should be noted that in the present work the process of formation was studied on an industrially-

## PP-IV-53

scalable extruder used to adequately model the behavior of catalytic pastes on an industrial scale which is confirmed by the consistency of the properties of laboratory and industrial grains. Conditions of catalytic pastes preparation were optimized for stable grain quality extrusion as well as to provide consistent rheological properties.

In the present study, we assessed the following types of energy-effective catalysts: star-shaped (diameter 3, 4 and 5 mm), trifolium-shaped (3 mm), noodle-shaped (2 mm). Such wide variety of shapes and sizes of Fe-Mo catalysts allows optimization selective (throughout the tube height) loading into the reactor, improve heat- and mass-transfer conditions, and, subsequently, provide for advantage over conventional imported ring-shaped (outer diameter 5 mm) pelletized catalysts.

Catalysts manufactured as per our extrusion technique have larger outer surface due to their complex shape which is characterized via form factor, provide more free space in the catalyst bed. Energy-effective types and shapes of catalyst grains were developed based on quantitative modelling as to lower power consumption of gas blowers to compensate for pressure drop in the catalytic bed. These shapes of Fe-Mo catalyst grains also provide for effective use of their inner surface and, consequentially, lower catalyst mass loading.

## The Reasons for Promoting Action of Phosphorus on the Selectivity of Palladium Catalysts for the Synthesis of Hydrogen Peroxide by the Anthraquinone Method

Sterenchuk T.P., Belykh L.B., Skripov N.I., Sanzhieva S.B., Gvozdovskaya K.L., Schmidt F.K.  
*Irkutsk State University, Irkutsk, Russia*  
*belykh@chem.isu.ru*

The report presents the results of studies on the development of selective palladium catalysts for the synthesis of hydrogen peroxide by the anthraquinone method and the determination of the reasons for the phosphorus modifying action.

The main task of the anthraquinone method of producing hydrogen peroxide is the selective hydrogenation of 2-ethyl-9,10-anthraquinone (eAQ) to 2-ethyl-9,10-anthrahydroquinone (eAQH<sub>2</sub>), which is easily oxidized by atmospheric oxygen to H<sub>2</sub>O<sub>2</sub> and the original substrate [1]. However, during the hydrogenation of eAQ, the resulting 2-ethyl-9,10-anthrahydroquinone undergoes further transformations. These include the hydrogenation of aromatic rings and/or the hydrogenolysis of the C-O bond. Using the example of colloidal solutions of palladium, it was found that the contribution of these two side reactions depends on the size of the palladium particles. Small palladium clusters with a diameter of 1.3–2.5 nm, along with eAQ hydrogenation, showed high activity in saturation of the aromatic ring of eAQH<sub>2</sub>. Star-like palladium crystallites with a size of 127±12 nm accelerated, predominantly, the hydrogenolysis of the C-O bond in 2-ethyl-9,10-anthrahydroquinone [2].

The introduction of phosphorus at the stage of palladium catalyst formation increased the yield of hydrogen peroxide from 69% to 94-97%, but reduced the activity in hydrogenation of eAQ by an order of magnitude [2]. The deposition of Pd-P particles on a carbon support contributed to the preparation of active and selective eAQ hydrogenation catalysts.

By a combination of XRD, XPS, HRTEM methods, it was found that Pd-P catalysts are structurally disordered solid solutions. The surface of the catalyst particles is enriched with electron-deficient palladium. The appearance of a partial positive charge on palladium in Pd-P particles, on the one hand, weakens the activation of molecular hydrogen and the H-H bond break, which is necessary for catalytic hydrogenation. On the other hand, in solid solutions of palladium with phosphorus, the solubility of hydrogen (i.e. concentration of "non-selective" hydrogen) decreases in comparison with palladium crystallites. Solutions of palladium with phosphorus contain more tightly bound hydrogen, which is not beneficial for the hydrogenation of the aromatic ring. The combination of these factors allows us to explain the cause of the promoting effect of phosphorus on the selectivity of palladium catalysts for producing hydrogen peroxide by the anthraquinone method.

**Acknowledgement.** This work was supported by the Russian Science Foundation, grant 17-73-10158.

### References:

- [1] R. Ciriminna, L. Albanese, F. Meneguzzo, M. Pagliaro, *ChemSusChem*. 9 (2016) 1.
- [2] T.P. Sterenchuk, L.B. Belykh, N.I. Skripov, S.B. Sanzhieva, K.L. Gvozdovskaya, F.K. Schmidt, *Kinet. Catal.* 59 (2018) 585.

## Benzene Hydrogenation over Ruthenium Catalysts Supported on Aluminosilicate Nanotubes

Smirnova E.M., Shukralieva A.S., Zasyalov G.O., Glotov A.P., Vinokurov V.A.  
*Gubkin Russian State University of Oil and Gas, Moscow, Russia*  
*smirnova.em94@gmail.com*

The hydrogenation of aromatic compounds is one of the most important areas of modern petroleum chemistry. The hydrogenation of benzene yields cyclohexane, which is used in the production of caprolactam, cyclohexanol, and adipinic acid and as a solvent. The reaction is run both in the liquid and gas phases using transition-metal catalysts, with particular attention being paid to ruthenium. Traditionally, alumina, silica, titania, activated carbon, and synthetic and natural aluminosilicates are used as catalyst supports.

In this study halloysite was used as a support. Halloysite represents natural multilayer nanotubes with the outer negatively charged surface composed of silica and the inner positively charged surface composed of alumina. This difference in the chemical compositions and electrochemical charges of the inner and outer surfaces in combination with the mesosized inner space open wide opportunities for the selective modification of halloysite nanotubes (HNTs) to impart the desired properties to them [1].

Ru-containing catalysts based on aluminosilicate (HNTs) are synthesized by preliminary functionalization of the support surface by aminopropyltriethoxysilane (APTES) followed by the microwave-assisted deposition of ruthenium to provide the intercalation of metal nanoparticles into the inner space of nanotubes [2]. The composition and structure of the synthesized catalysts are studied by X-ray fluorescent analysis (XRF), low-temperature nitrogen adsorption/desorption, transmission electron microscopy (TEM), and hydrogen temperature-programmed reduction (TPR-H<sub>2</sub>).

To impart new properties to nanotubes, specifically hydrophobicity, they were modified with APTES, which leads to charge exchange between inner and outer surfaces of nanotubes, as evidenced by a change in the  $\xi$  potential of the outer surface from – 52 to 6 mV. Formation of the active phase is considerably affected not only by the support type but also by the technique of metal deposition. Impregnation of the support with an aqueous solution of ruthenium salt was assisted by microwave radiation. This technique provides a more uniform deposition of the metal on the support surface compared with the standard impregnation method. According to elemental analysis, the content of ruthenium in catalysts Ru/HNT and Ru/HNT-m after their reduction by sodium borohydride ensuring the transition of ruthenium to the zero-valence state is 1.5 and 2.0 wt %, respectively. Reduction in specific surface area and pore volume and diameter upon ruthenium deposition, especially in the case of catalyst Ru/HNT-m, in which the content of the active component is higher than that in the Ru/HNT sample, may be explained by the formation of metal particles on the inner and outer surfaces.

Microwave-assisted impregnation of supports with the aqueous solution of ruthenium salt makes it possible to obtain a fine catalyst with metal nanoparticles uniformly distributed on the support surface, as indicated by the TEM data. The microwaveassisted deposition of

ruthenium on the initial halloysite surface yields a fine phase of ruthenium nanoparticles with a diameter of  $\sim 1.3$  nm, mostly on the outer surface of halloysite nanotubes. Because the inner surface is charged positively, ruthenium cations cannot intercalate into the inner cavity, but they predominantly interact with the negatively charged outer surface.

In the case of the APTES-modified catalyst, ruthenium nanoparticles are intercalated predominantly into the inner space of halloysite. For material Ru/HNT-m, there is a bimodal size distribution of metal particles with maxima at 0.9 and 1.3 nm. A smaller size corresponds to particles adsorbed on the inner surface; a larger size corresponds to particles adsorbed on the outer surface.

The generation of ruthenium nanoparticles both in the inner cavity and on the outer surface of the modified support is also confirmed by the TPR- $H_2$  studies. The TPR- $H_2$  profile obtained for Ru/HNT-m shows peaks at 139 and 161°C corresponding to the reduction of ruthenium oxides  $RuO_x$  and  $RuO_2$  fixed on the material surface and in the inner cavity of HNTs [3]. In the case of Ru/HNT, there is only one peak of hydrogen absorption with a maximum at 139°C assigned to the reduction of  $RuO_2$  to Ru0. This observation suggests that the uniform fine layer of ruthenium nanoparticles is formed on the surface of halloysite and agrees with the TEM data. A wide shoulder in the range of 200–260°C may be attributed to the reduction of ruthenium oxides and oxochloride strongly bound to the support surface.

In accordance with the TPR- $H_2$  data, the content of ruthenium in Ru/HNT and Ru/HNT-m is 1.2 and 1.9 wt %, respectively, in agreement with elemental analysis. Note that for catalyst Ru/HNT-m the most pronounced hydrogen absorption is observed at 161°C (0.220 mmol/g). This finding confirms formation of ruthenium nanoparticles in the inner cavity of nanotubes; their content attains 1.1 wt %.

The activity of the catalysts in benzene hydrogenation at a temperature of 80°C and a hydrogen pressure of 3 MPa both in the hydrocarbon medium and in the twophase system with water is studied. It is shown that, in the presence of water, the hydrogenating activity of the catalyst based on modified halloysite nanotubes is considerably higher than that of the sample prepared using the initial halloysite as a support. For example, in the two-phase system in the presence of water, both catalysts show a fairly high activity during the first 20 min: the conversion of benzene is on the order of 30–40%. In hydrogenation catalyzed by Ru/HNT-m, the substrate conversion attained during 90–150 min is as high as 92%. For Ru/HNT, this parameter does not exceed 40%.

**Acknowledgement.** This work was supported by Ministry of Education and Science of Russian Federation (Grant № 14.Z50.31.0035).

#### References:

- [1] Glotov A., Stavitskaya A., Chudakov Y., Ivanov E., Huang W., Vinokurov V., Zolotukhina A., Maximov A., Karakhanov E., Lvov Y., Bull. Chem. Soc. Jpn., 2019. Vol. 1. P. 61-69.
- [2] Vinokurov V., Glotov A., Chudakov Y. et al., Ind. Eng. Chem. Res. 2017. Vol. 56, no. 47. P. 14043–14052.
- [3] Yang T., Du M., Zhang M., Zhu H., Wang P., Zou M., Nanomater. Nanotechnol. 2015. V.5, P.9.

## From Mechanistic Studies of the Preferential CO Methanation in the Presence of CO<sub>2</sub> to Design of Structured Nickel-Ceria Catalysts

Konishcheva M.V.<sup>1,2</sup>, Potemkin D.I.<sup>1,2</sup>, Snytnikov P.V.<sup>1,2</sup>, Sobyenin V.A.<sup>1,2</sup>

1 – Boreskov Institute of Catalysis, Novosibirsk, Russia

2 – Novosibirsk State University, Novosibirsk, Russia

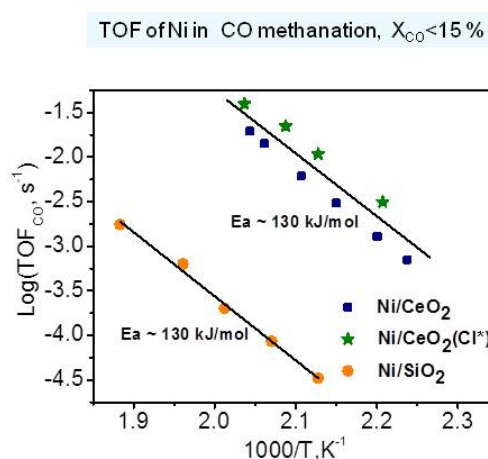
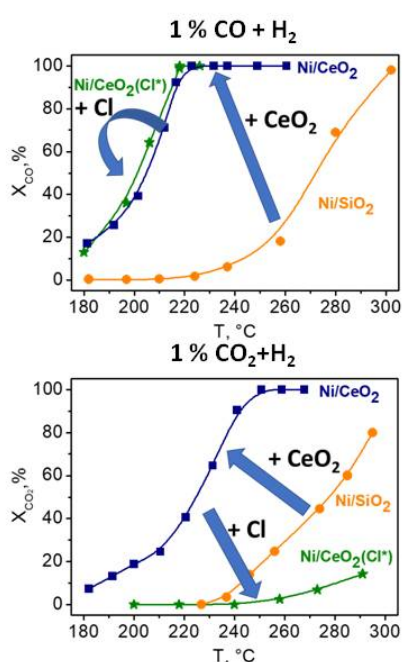
pvsnyt@catalysis.ru

Currently, power units based on low-temperature fuel cells with a polymer proton-exchange membrane (PEM FC) are the most commercially available product. PEM FCs are fueled by hydrogen or hydrogen-rich gas mixtures (reformat). Due to lack of widespread hydrogen-supply infrastructure (production, cleanup, storage) the latest studies are focused on integrating of PEM FC with a unit (reformer) generating hydrogen from gaseous or liquid fuels (hydrocarbons, alcohols, ethers, etc.) with available well developed infrastructure and established logistics. Conventional fuels from gas stations may be converted by steam, partial or autothermal reforming followed by CO water gas shift process into hydrogen –rich gas (reformat). In addition to hydrogen, reformat usually contains (vol.%): 15-25 CO<sub>2</sub>, 5-15 H<sub>2</sub>O and 0.5-2.0 CO. To prevent poisoning of the FC anode catalyst by carbon monoxide, the hydrogen-rich gas must be cleaned up from CO to a level below 10 ppm.

One of the promising methods for CO cleanup from hydrogen-rich gas mixtures is preferential (selective) CO methanation (CO PreMeth). Recently, it was shown that Me (Me= Fe, Co, Ni)/CeO<sub>2</sub>-based systems are promising catalysts for preferential CO methanation [1].

Fig. 1 Preferential CO Methanation over Ni catalysts

Gas mixture composition (vol.%): 1% CO (1 % CO<sub>2</sub>), 65 H<sub>2</sub>, He-balance; 1 atm; GHSV = 29 L/(g·h)



Catalyst	CO Methanation		CO <sub>2</sub> Methanation	
	n <sub>CO</sub>	Ea, kJ/mol	n <sub>CO<sub>2</sub></sub>	Ea, kJ/mol
Ni/CeO <sub>2</sub>	-0,8	130	0	90
Ni/CeO <sub>2</sub> (Cl <sup>*</sup> )	-0,7	140	0,7	100

## PP-IV-56

The effect of halogen (F, Cl, Br) doping was investigated [2]. The positive effect of chlorine additives on Ni/CeO<sub>2</sub> catalyst's selectivity was observed [3]. This work summarizes results on mechanistic study of the influence of chlorine additives on the CO and CO<sub>2</sub> methanation reactions kinetics over Ni/CeO<sub>2</sub> catalysts and compares with CO and CO<sub>2</sub> methanation reactions kinetics over Ni/SiO<sub>2</sub> model catalyst.

The properties of catalysts prepared from different precursors were compared (Fig.1). Catalysts were studied by BET, XRD, TEM, EDX, XPS, FTIR and CO chemisorption techniques. It was shown, that Ni/CeO<sub>2</sub> is active in both CO and CO<sub>2</sub> methanation, exhibiting low selectivity. In contrast to Ni/CeO<sub>2</sub>, Ni(Cl)/CeO<sub>2</sub> is active in CO and inactive in CO<sub>2</sub> methanation at T < 300 °C, providing highly selective operation. Ni/SiO<sub>2</sub> catalyst has lower activity both in CO and CO<sub>2</sub> methanation reactions.

Based on the results obtained the structured Ni(Cl<sub>x</sub>)/CeO<sub>2</sub>/η-Al<sub>2</sub>O<sub>3</sub>/FeCrAl alloy wire mesh catalysts were developed for the reaction of preferential CO methanation in the presence of CO<sub>2</sub>. In hydrogen-rich gas mixture of composition (vol.%): 1.0 CO, 65 H<sub>2</sub>, 10 H<sub>2</sub>O, 20 CO<sub>2</sub>, He - balance, GHSV = 29 L·g<sup>-1</sup>·h<sup>-1</sup>, the catalyst with lower chlorine content and higher nickel dispersion showed better catalytic performance and reduced CO concentration to the level <10 ppm in the temperature interval of 230-300°C with a selectivity >40%.

**Acknowledgement.** Research was conducted within the framework of budget project #AAAA-A17-117041710088-0 for Boreskov Institute of Catalysis

### References:

- [1] M.V. Konishcheva, D.I. Potemkin, P.V. Snytnikov, M.M. Zyryanova, V.P. Pakharukova, P.A. Simonov, V.A. Sobyenin, *Int. J. Hydrogen Energy*. 40 (2015) 14058.
- [2] M. V. Konishcheva, D.I. Potemkin, P. V. Snytnikov, V.P. Pakharukova, V.A. Sobyenin, *Energy Technol.* 5 (2017) 1522.
- [3] M.V. Konishcheva, D.I. Potemkin, P.V. Snytnikov, O.A. Stonkus, V.D. Belyaev, V.A. Sobyenin, *Appl. Catal. B Environ.* 221 (2018) 413.

## Effect of Long-Term Pilot Run on the Properties of Highly Productive Fischer–Tropsch Synthesis Catalyst

Solomonik I.G., Gorshkov A.S., Gryaznov K.O., Zhukova E.A., Ivanov L.A., Perezhogin I.A.,  
Mordkovich V.Z.

*Technological Institute for Superhard and Novel Carbon Materials, Moscow, Russia*  
*igsol@bk.ru*

### Introduction

The results of comparative investigation of a recently developed highly productive Fischer–Tropsch synthesis pelletized catalyst before and after long pilot run are reported. The catalyst is based on cobalt as an active metal, its high productivity is provided by a spatial network of thermally conductive exfoliated graphite as disclosed in [1]. The run duration exceeded 1000 hours. Most of the catalyst bed was under normal operational conditions (temperature under 260°C and GHSV = 4000 1/h) for all the run time. Occasional loss of cooling water in a small area of the 6-meter long reaction tube led to a runaway of up to 530°C that allowed us to compare the catalyst properties before the run, after 1000 hours under normal conditions and after runaway. This comparison provided a good chance to extract data important of understanding of the mechanisms of the processes occurring in a big reactor, where diffusion-burdened Fischer–Tropsch process is realized. Most of interesting features revealed as a result of this research appear due to unusually high thermal conductivity (up to 8 W/m/K as compared to 0.2 W/m/K of conventional catalysts) of this exfoliated graphite-based catalyst.

### Experimental

The run was realized in a 6-meter-high stainless steel tubular reactor provided with a cooling jacket where pressurized boiling water was circulated in order to provide heat removal from the active highly exothermal packed bed of the catalyst. The catalyst was manufactured in the extrudate form with a diameter 1.5 and a length of 1.5 mm after [1]. The pilot unit and activation procedures are described elsewhere [2] although the experiments in [2] were done on a different catalyst. The time on stream was 1,000 hours.

Surface and porosity of the catalyst samples were investigated by low temperature nitrogen adsorption technique and helium pycnometry method (multipurpose sorption meter Autosorb-1, helium pycnometer Ultrapyc 1200e). Electron microscopy was done with a scanning electron microscope JEOL JSM-7600F with Energy-dispersive X-ray spectroscopy set and with a transmission electron microscope JEM 2010. Thermal analysis was used for estimation of changes in surface composition and appearance of new phases by means of NETZSCH STA-449 F1 apparatus. Thermal gravimetric and differential thermal calorimetric

measurements were done both in air and in inert atmosphere. Hedwall method was used for interpretation of fine resolution effects of the thermal analysis chart.

### **Results**

Comparative investigation of three types of the catalyst samples, i.e. pristine catalyst; catalyst after 1,000 hours on stream under normal operational conditions; and after 1,000 hours on stream with 530°C runaways allowed to formulate several interesting conclusions concerning the operational features of this unusual catalyst based on exfoliated graphite, i.e. (a) the high thermal conductivity of the catalyst is responsible for accumulation of high molecular weight products in the core of the catalyst pellets (not at the outside); (b) the runaway does not lead to pellet destruction nor to significant deactivation; (c) the size of active cobalt clusters remains the same under both normal operational conditions and under runaway conditions; (d) runaway leads to formation of carbon nanotube structures inside the pellet and, as a consequence, change in mesopores; (e) it was found that the maximums of fine structure of thermal analysis patterns can be reliably attributed to individual hydrocarbons.

### **References:**

- [1] Rus. Pat. Appl. No 2017118372 of 26.05.2017.
- [2] V.Z. Mordkovich, V.S. Ermolaev, E.B. Mitberg, L.V. Sineva, I.G. Solomonik, I.S. Ermolaev, E.Yu. Asalieva, Composite Pelletized Catalyst for Higher One-Pass Conversion and Productivity in Fischer–Tropsch Process. *Research in Chemical Intermediates*, 2015, vol. 41, No 12, p. 9539-9550.

## Influence of the Silica Sol Addition to the Catalytic Activity of CoMoP Hydrotreating Catalysts

Stolyarova E.A., Klimov O.V., Saiko A.V., Gerasimov E.Y., Chetyrin I.A., Noskov A.S.  
*Boreskov Institute of Catalysis, Novosibirsk, Russia*  
*sea@catalysis.ru*

Nowadays, CoMoP/Al<sub>2</sub>O<sub>3</sub> catalysts are widely used for hydrotreating of diesel fuel. But the addition of acidic compounds is a perspective way to decrease hydrodesulphurization (HDS), hydrodenitrogenation (HDN) and hydrogenation (HYD) activities of the sample [1-3]. Silica is traditional compounds of the hydrotreating catalyst's support [4-5], and silica sol could be potential effective additive to get high-active hydrotreating catalysts.

This work described the effect of the silica sol addition to the physical-chemical properties and catalytic activity of CoMoP hydrotreating catalysts.

Supports with 0-10%wt. of Si were prepared by adding of silica sol and plasticizing agent to the pseudoboehmite with subsequent drying and calcination of the samples. Silica sol (LEIKSIL-15A, "Kompas", Russia) has a pH 9,0, size of the particles 5 nm, surface area 550 m<sup>2</sup>/g. Catalysts were prepared by vacuum impregnation technique. In all instances, concentrations of impregnating solutions were chosen to obtain 12,5 ± 0,2 wt.% of Mo; 3,5 ± 0,1 wt.% of Co; 1,5±0,1 wt.% of P in the final catalysts.

The studying of the supports by HRTEM shown the presence of amorphous silica on the surface of alumina. The particles of SiO<sub>2</sub> marked on the Fig.1 as white circles.

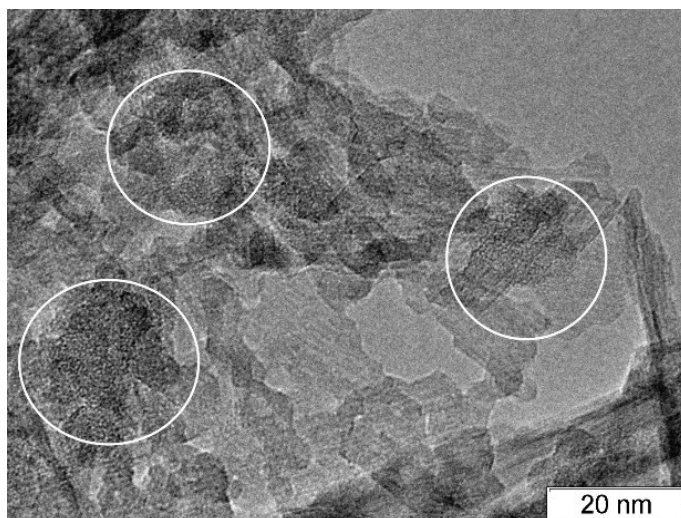


Fig. 1. HRTEM data of supports. White circles are amorphous silica particles.

The particles of SiO<sub>2</sub> is uniformly distributed over the surface of support and have a size distribution from 3 to 20 nm. The presence of amorphous silica in the samples was confirmed by X-ray powder diffraction method. Active component of the catalysts was studied by XPS method. Textural characteristics of supports and catalysts are shown in Table 1. Gradual

## PP-IV-58

increase of surface area (S) and decrease of average pore diameter (D) are observed with increasing of Si-containing in the samples.

Catalysts were tested in the hydrotreating of diesel fuel (3200 ppm S, 193 ppm N), the conditions of the testing were P=38 bar, T=340-370°C, LHSV=2,5 h<sup>-1</sup>, H<sub>2</sub>/feed ratio = 500. The results of testing are presented in Table 1.

Table 1. Textural characteristics of supports and catalysts and hydrotreating activity of the catalysts

Sample	Textural properties of supports/catalysts			Residual containing of S and N, ppm							
				340°C		350°C		360°C		370°C	
	S, m <sup>2</sup> /g	V, cm <sup>3</sup> /g	D, Å	S	N	S	N	S	N	S	N
CoMoP/Al <sub>2</sub> O <sub>3</sub>	245/142	0,65/0,41	105/101	84,3	14,8	53,4	14,0	30,0	9,4	19,3	6,1
CoMoP/Al <sub>2</sub> O <sub>3</sub> +1% Si	250/149	0,58/0,36	98/102	78,0	12,0	49,3	12,9	26,5	8,3	17,0	7,2
CoMoP/Al <sub>2</sub> O <sub>3</sub> +2% Si	250/158	0,59/0,37	98/107	66,4	11,8	41,8	13,7	21,5	9,5	13,6	8,5
CoMoP/Al <sub>2</sub> O <sub>3</sub> +3% Si	255/158	0,61/0,38	96/101	64,5	10,5	33,9	9,6	15,7	6,3	10,4	5,6
CoMoP/Al <sub>2</sub> O <sub>3</sub> +4% Si	256/154	0,61/0,38	99/107	57,5	9,3	40,4	11,1	16,5	7,3	10,6	6,1
CoMoP/Al <sub>2</sub> O <sub>3</sub> +5% Si	260/155	0,61/0,40	97/102	52,6	7,2	37,2	9,7	16,1	7,0	10,5	5,8
CoMoP/Al <sub>2</sub> O <sub>3</sub> +6% Si	262/159	0,63/0,41	97/109	43,4	6,1	34,5	8,4	18,5	6,9	10,5	6,3
<b>CoMoP/Al<sub>2</sub>O<sub>3</sub>+7% Si</b>	<b>264/158</b>	<b>0,62/0,40</b>	<b>96/109</b>	<b>35,9</b>	<b>3,9</b>	<b>26,6</b>	<b>6,2</b>	<b>14,3</b>	<b>5,3</b>	<b>9,0</b>	<b>5,0</b>
CoMoP/Al <sub>2</sub> O <sub>3</sub> +8% Si	266/161	0,62/0,42	94/104	37,0	3,9	26,6	5,8	14,5	5,0	9,7	5,8
CoMoP/Al <sub>2</sub> O <sub>3</sub> +9% Si	266/159	0,64/0,40	96/100	54,7	7,2	36,7	10,3	19,4	7,6	12,4	6,9
CoMoP/Al <sub>2</sub> O <sub>3</sub> +10% Si	267/164	0,61/0,41	94/103	62,2	8,8	39,8	9,8	21,2	8,1	13,3	7,1

Addition silica sol to the support increases the HDS and HDN activities of the catalysts. Catalytic activity of the catalysts increase gradual and has a maximum with a content of 7%w. Si in the support. Catalytic activity in the HDS and HND reaction decrease at addition of 8%w. and more Si to the support. Also, the catalyst with addition of 7%w. Si by silica sol to the support shown the highest activity in the reaction of hydrogenation of aromatic hydrocarbon.

**Acknowledgement.** This work was supported by Ministry of Science and Higher Education of the Russian Federation (project AAAA-A17-117041710077-4).

### References:

- [1] O.V.Klimov et al. / Catalysis Today 307 (2018) 73–83.
- [2] S.K. Maity et al. / Catalysis Today 109 (2005) 42–48.
- [3] F. Rashidi et al. / Journal of Catalysis 299 (2013) 321–335.
- [4] P.Rayo et al. / Fuel 239 (2019) 1293–1303.
- [5] S.K. Maity et al. / Applied Catalysis A: General 250 (2003) 231–238.

## Effect of Composition of $Ce_{1-x}Ni_xO_y$ Catalyst on Their Activity and Stability in Steam/ $CO_2$ Reforming of Methane

Matus E.V.<sup>1,2</sup>, Shlyakhtina A.S.<sup>2</sup>, Sukhova O.B.<sup>1</sup>, Ismagilov I.Z.<sup>1</sup>,  
Kerzhentsev M.A.<sup>1</sup>, Ismagilov Z.R.<sup>1,3</sup>

1 – Boreskov Institute of Catalysis, Novosibirsk, Russia

2 – Novosibirsk State Technical University, Novosibirsk, Russia

3 – Institute of Coal Chemistry and Material Science FRC CCC SB RAS, Kemerovo, Russia  
matus@catalysis.ru

Cerium dioxide is widely used in catalysis as an active component, support or promoter [1]. The strong metal-support interaction has a positive effect on the performance of  $CeO_2$ -based materials. The co-existence and cooperative interplay of small  $Ni^0$  particles and  $Ce^{3+}(OH)_x$  facilitating hydroxyl/oxygen transfer through a strong metal-support interaction mitigates the accumulation of surface carbon which is important for Ni reforming catalysts [2]. In this case, mixed oxides are advantageous to use as catalyst precursors: their activation in a reducing medium leads to the ex-solution of metal from the structure with formation of nanoparticles or clusters with improved characteristics. So in the frame of this work,  $Ce_{1-x}Ni_xO_y$  samples were prepared and the effect of their composition on the activity and stability in steam/ $CO_2$  reforming of methane was studied.

$Ce_{1-x}Ni_xO_y$  ( $x = 0-0.35$ ,  $y = 1.7-2$ ) were synthesized by the polymerizable complex method, characterized by different methods (TA, BET, XRD, HRTEM, SEM, Raman spectroscopy and  $H_2$ -TPR) and tested in steam/ $CO_2$  reforming of methane (1 atm, 600-800°C, molar ratio  $CH_4:CO_2:H_2O:He = 1.0:0.81:0.38:2.8$ ). It was shown that the  $Ce_{1-x}Ni_xO_y$  samples were solid solutions with the fluorite structure and crystallites of 5-8 nm in size. At growth of  $x$  from 0 to 0.35 the increase of the specific surface area ( $85 \rightarrow 115 \text{ m}^2/\text{g}$ ), the ability to reduction ( $H_2/Ni$  ratio) and the defectiveness of the material structure were observed. Under steam/ $CO_2$  reforming of methane the  $Ce_{1-x}Ni_xO_y$  provides a high and stable yield of  $H_2$ , the value of which at 750°C rises from 45 to 80 % at increasing molar ratio of Ni from 0.06 to 0.35. In this case, the conversion of methane changed from 30 to 70 %, while the conversion of  $CO_2$  from 45 to 80 %. The relationships between the compositions, catalyst performance and stability against carbonaceous deposits were established.

**Acknowledgement.** This work was supported by the Russian Foundation for Basic Research (project no. 18-53-45012 IND\_a).

### References:

- [1] Ismagilov Z.R., Kuznetsov V.V., Okhlopko L.B., Tsikoza L.T., Yashnik S.A., Titanium, Cerium, Zirconium, Yttrium, Zluminum Oxides. Properties, Application, and Methods of Synthesis, Novosibirsk: Izdatel'stvo SO RAN, 2010.  
[2] Liu Z., Duchon T., Wang H. et al. // Phys. Chem. Chem. Phys. 18 (2016) 16621–16628.

## Cationic Acetylacetonate Palladium Complexes/Boron Trifluoride Etherate Catalyst Systems for Polymerization of Norbornene Derivatives and Phenylacetylene

Suslov D.S.<sup>1</sup>, Bykov M.V.<sup>1</sup>, Pakhomova M.V.<sup>1</sup>, Ushakov I.A.<sup>2</sup>, Tkach V.S.<sup>1</sup>

1 – Irkutsk State University, Irkutsk, Russia

2 – National Research Irkutsk State Technical University, Irkutsk, Russia

suslov@chem.isu.ru

A simple protocol using cationic acetylacetonate palladium complexes with mono-/bidentate phosphine ligands activated with  $\text{BF}_3 \cdot \text{OEt}_2$  as *in situ*-formed catalyst for polymerization of *endo/exo* mixture of 5-methoxycarbonylnorbornene (activity up to  $1.1 \cdot 10^4 \text{ g} \cdot \text{mol}^{-1} \cdot \text{h}^{-1}$ ) or 5-phenylnorbornene ( $7.2 \cdot 10^5 \text{ g} \cdot \text{mol}^{-1} \cdot \text{h}^{-1}$ ), and norbornene ( $3.3 \cdot 10^8 \text{ g} \cdot \text{mol}^{-1} \cdot \text{h}^{-1}$ ) have been developed [1]. It was observed that the ligands nature strongly influence the catalytic activity. A series of cationic acetylacetonate palladium complexes were also demonstrated to be active for the polymerization and oligomerization of phenylacetylene (PA). Catalyst screening and optimization have determined the superior activity of complex  $[(\text{acac})\text{Pd}(\text{TOMPP})_2]\text{BF}_4$  (TOMPP – *tris*(2-methoxyphenyl)phosphine) for the stereospecific polymerization of phenylacetylene in non-coordinating solvents as well as in aqueous emulsion [2]. Catalyst activities of  $(1-1.6) \cdot 10^4 \text{ g} \cdot \text{mol}^{-1} \cdot \text{h}^{-1}$  were observed in 1,2-dichloroethane as solvent, and obtained polyphenylacetylene (PPA) featured >90% of *cis* double bond content. Complexes with dppf and MeCN ligands also catalyzed PPA formation, but with substantially lower activities. The other studied palladium complexes catalyzed oligomerization of PA. The effect of temperature, solvent nature, addition of cocatalyst,  $\text{BF}_3 \cdot \text{OEt}_2$ , have been studied.

Based on previous studies [3,4] we suggested that a species with a Pd-C bond from monodentate C-bonded acetylacetonate ligand was initially formed, and this started polymerization by the insertion of monomer. The activation hypothesis was further tested by multinuclear ( $^1\text{H}$ ,  $^{19}\text{F}$  and  $^{31}\text{P}$ ) NMR investigations and FTIR.. The reaction of *cis*- $[\text{Pd}(\text{PPh}_3)_2(\kappa^2\text{-O,O'-acac})]\text{BF}_4$  with  $\text{BF}_3 \cdot \text{OEt}_2$  (2 equiv) in  $\text{CH}_2\text{Cl}_2$  in an NMR tube at room temperature led within 1 min to the formation of *cis*- $[\text{Pd}(\text{PPh}_3)_2(\eta^1\text{-C-acac} \cdot \text{BF}_3)]\text{BF}_4$  (12%),  $[\text{Pd}(\text{PPh}_3)_2(\text{F} \cdot \text{BF}_3)_2]$  (anion coordination detected by  $^{19}\text{F}$  NMR,  $J_{\text{P-F}} = 6.8 \text{ Hz}$ , 4%),  $\text{BF}_2(\text{acac})$  (4%) and initial complex (80%). In a reaction of *cis*- $[\text{Pd}(\text{PPh}_3)_2(\kappa^2\text{-O,O'-acac})]\text{BF}_4$  with 4 or 6 equiv of  $\text{BF}_3 \cdot \text{OEt}_2$  similar trend were observed (57% and 39% of *cis*- $[\text{Pd}(\text{PPh}_3)_2(\kappa^2\text{-O,O'-acac})]\text{BF}_4$  were converted to products, respectively). In our opinion, formation of dicationic palladium species suggests catalyst deactivation pathway that occurs in the catalyst systems under study.

Concerning the formation of the active species in case of phenylacetylene polymerization the  $^1\text{H}$  NMR spectrum of PPA showed the presence of weak methyl peaks, indicative of methyl fragment from the acac end group in these products. Surprisingly, FTIR-monitored reaction of

## PP-IV-60

$[(\text{acac})\text{Pd}(\text{TOMPP})_2]\text{BF}_4$  with PA showed only monomer conversion. At the same time intensity of the absorbance bands at 1519, 1562  $\text{cm}^{-1}$  due to stretching vibrations of the C=O and C=C bonds in chelate bonded acac group did not change. This suggests that only a small amount of precursor was transformed into the active species. According to  $^1\text{H}$  NMR investigations during the initial reaction of  $[(\text{acac})\text{Pd}(\text{TOMPP})_2]\text{BF}_4$  with PA (5 equiv) in  $\text{CH}_2\text{Cl}_2$  in an NMR tube at room temperature within 30 min of the reaction 40% of PPA was formed, as indicated by the appearance of signals at 5.7, 6.5 and 6.8 ppm in the  $^1\text{H}$  NMR. New signals appeared between 1.8–2.2 ppm, which potentially correspond to unshielded (by TOMPP aromatic ring current)  $\text{CH}_3$ -protons of  $\gamma$ -bonded acac fragments. After 280 min the monomer was quantitatively consumed as indicated by the disappearance of a  $\equiv\text{CH}$ -proton signal at 2.96 ppm. In addition, the broadened signal at 15.34 ppm appeared presumably from OH acidic proton of 3-substituted-2,4-pentadione fragment of transformed acac ligand. Another explanation of polymer chain initiation is the proton transfer from PA molecule to the acac ligand under the release of acetylacetone and  $\kappa^1\text{-C}$ -coordination of  $\text{C}\equiv\text{CPh}$  ligand to Pd moiety with formation of phenylethynylpalladium complex, similarly to neutral Rh-based catalysts [5], but to the best of our knowledge for cationic palladium complexes such proton transfer have not been reported.

In general, one of the biggest advantages of palladium-based catalysts is its great tolerance toward polar groups [6,7]. Though the present research were limited to the polymerization of phenylacetylene, 5-methoxycarbonylnorbornene, and 5-phenylnorbornene, we assume that developed Pd catalyst can be utilized for the polymerization of substituted arylacetylenes and polar functionalized norbornene-type monomers as well.

**Acknowledgement.** This work was supported by the Government Assignment for Scientific Research from the Ministry of Education and Science of the Russian Federation (No. 4.5183.2017/8.9). Marina V. Pakhomova acknowledges Ministry of Education and Science of the Russian Federation for scholarship (Ord. No. 231 of 3.04.2018).

### References:

- [1] D.S. Suslov, M.V. Bykov, A.V. Kuzmin, et al, *Catal. Commun.* 106 (2018) 30.
- [2] D.S. Suslov, M.V. Pakhomova, M.V. Bykov et al, *Catal. Commun.* 119 (2019) 16.
- [3] D.S. Suslov, M. V. Bykov, P.A. Abramov et al, *RSC Adv.* 5 (2015) 104467.
- [4] D.S. Suslov, M.V. Pakhomova, P.A. Abramov et al, *Catal. Commun.* 67 (2015) 11.
- [5] O. Trhlíková et al, *J. Mol. Catal. A Chem.* 378 (2013) 57.
- [6] C. Chen, *Nat. Rev. Chem.* 2 (2018) 6.
- [7] C. Chen, *ACS Catal.* 8 (2018) 5506.

## Levulinic Acid Hydrogenation into $\gamma$ -Valerolactone over Ru/C Catalysts

Sychev V.V.<sup>1</sup>, Baryshnikov S.V.<sup>1</sup>, Beregovtsova N.G.<sup>1</sup>, Volochaev M.N., Taran O.P.<sup>1,2</sup>

1 – Institute of Chemistry and Chemical Technology SB RAS, FRC KSC SB RAS, Krasnoyarsk, Russia

2 – Kirensky Institute of Physics, SB RAS, FRC KSC SB RAS, Krasnoyarsk, Russia

3 – Borekov Institute of Catalysis, Novosibirsk, Russia

sychev.vv@icct.krasn.ru

$\gamma$ -Valerolactone (GVL) is the one of the platform chemicals which can be derived from lignocellulosic biomass. GVL properties make it a very attractive chemical; it is a non-hazardous, high-boiling-point liquid, which can be used as a building block for polymers, intermediate in fine chemicals and fuels production, a solvent, a flavoring agent and a food additive. [1] There is a growing interest in GVL synthesis in recent years. [2] The main route of GVL synthesis is hydrogenation of levulinic acid (LA) and levulinic acid esters (LAE). Both cellulose and hemicelluloses can be used as a feedstock in GVL production, which is making the economics more attractive and makes finding a wider application easier. [1]

Based on literature analysis, Ru-based catalysts, supported on activated carbon, are providing the best catalytic activities in LA to GVL direct hydrogenation. [3] Microporosity of activated carbons, however, can be a serious drawback in liquid-phase hydrogenation reactions, obstructing substrate and intermediates transfer to catalytic active sites.

This work aims at development of solid catalysts for the processes of LA to GVL direct hydrogenation based on mesoporous graphite-like carbon Sibunit bearing Ru nanoparticles.

In order to prepare 3%Ru-containing catalysts initial Sibunit-4 was oxidized by wet air at 400, 450 and 500°C. Oxidation was followed by deposition of Ru using aqueous solution of Ru(NO)(NO<sub>3</sub>)<sub>3</sub> by incipient wetness impregnation technique described in [4, 5]. Prepared catalysts and supports were characterized by TEM, N<sub>2</sub> adsorption, acid-base titration.

Table 1. Textural properties of Sib-4 supports and 3%Ru/Sib-4 catalysts.

№	Support	SBET m <sup>2</sup> /g		Pore Volume (V <sub>nop</sub> ), cm <sup>3</sup> /g		Average pore width <d pore>, nm	
		support	cat.	support	cat.	support	cat.
1	Sib-4	375	321	0,55	0,43	5,8	5,4
2	Sib-4-Ox-400	332	300	0,42	0,37	5,0	5,0
3	Sib-4-Ox-450	380	341	0,53	0,50	5,6	5,8
4	Sib-4-Ox-500gr	287	233	0,37	0,28	5,1	4,8

## PP-IV-61

Increase of oxidation temperature leads to rise of Sub-4 acidity but reduction of specific surface area, pore volume and average pore width, which can be attributed to a deformation of graphite-like structure of Sibunit.

The hydrogenation of LA to GVL was conducted in autoclave under 160°C and 12 bar H<sub>2</sub> during 3 hours. The products of reaction were determined using developed HPLC technique.

We studied the influence of support acidity and Ru-nanoparticles size on the yields of GVL. The highest GVL yield of 99 mol. % was obtained.

Table 2. LA to GVL hydrogenation over 3%Ru/Sib-4. 160°C, 12 H<sub>2</sub>

No	Solvent	Conv.%	Sel.%	GVL yield mol.%
1	i-PrOH	100,00	99,72	99,72
3	H <sub>2</sub> O	86,74	88,49	76,76
4	H <sub>2</sub> O:C <sub>2</sub> H <sub>5</sub> OH	81,83	56,35	46,11
5	C <sub>2</sub> H <sub>5</sub> OH	59,16	66,42	39,30

Solvents activity row: i-PrOH>H<sub>2</sub>O>H<sub>2</sub>O:C<sub>2</sub>H<sub>5</sub>OH>C<sub>2</sub>H<sub>5</sub>OH.

The use of i-propanol enhanced GVL yield in comparison to water, ethanol and ethanol-water mediums. Superior activity of i-propanol can be attributed to a high hydrogen solubility (in comparison to the other solvents involved) and possible hydrogen donor activity as a solvent. Better performance in aqueous media in comparison to pure ethanol and ethanol-water mixtures can be attributed to co-adsorption of water molecules, which is lowering energy barriers, leading to an easier hydrogenation of carbonyl groups by dissociated hydrogen. Also the dissociation of water increases the surface concentration of hydrogen atoms, thus favoring the hydrogenation process. [6]

**Acknowledgement.** This work was supported by the Russian Foundation for Basic Research, grant 17-53-16027.

### References:

- [1] Alonso, D.M., Wettstein S.G., Dumesic, J.A. Green Chem. 15 (2013) 584.
- [2] Osatiashtiani, A., Lee A.F., Wilson, K. J Chemical Technology & Biotechnol. 92 (2017) 1125.
- [3] Mehdi, H., et al. Topics in Catalysis, 48 (2008) 49.
- [4] Minh, D.P., et al., Applied Catalysis B: Environ. 73 (2007) 236.
- [5] Taran, O.P., et al. Catalysis in Industry. 5 (2013) 164.
- [6] Michel, C. Gallezot, P. *ACS Catalysis* 5 (2015) 4130.

## Catalytic Combustion of Methane over Pd-MeOx-CeO<sub>2</sub>/Al<sub>2</sub>O<sub>3</sub> (Me= Co or Ni) Catalysts

Todorova S.<sup>1</sup>, Naydenov A.<sup>2</sup>, Velinova R.<sup>2</sup>, Karakirova Y.<sup>1</sup>, Kolev H.<sup>1</sup>

<sup>1</sup> – Institute of Catalysis, Bulgarian Acad. of Sciences, Sofia, Bulgaria

<sup>2</sup> – Institute of General and Inorganic Chemistry, Bulgarian Acad. of Sciences, Sofia, Bulgaria  
todorova@ic.bas.bg

Catalytic combustion of methane has been extensively investigated for emission control and power generation during the last decades. The alumina-supported palladium catalyst is widely accepted as the most active catalysts for catalytic combustion of methane. The activity of Pd/Al<sub>2</sub>O<sub>3</sub> decreases during time on stream, especially under water vapor. The following order of activity in the reaction of complete oxidation of methane was established: Co<sub>3</sub>O<sub>4</sub>> CuO>NiO> Mn<sub>2</sub>O<sub>3</sub>> Cr<sub>2</sub>O<sub>3</sub> [1]. It may be expected that the combination between Pd and these oxides could lead to the promising catalysts in reaction of complete methane.

In the present work, we investigate the activity of Pd/Al<sub>2</sub>O<sub>3</sub> catalysts promoted with other metal oxides (MOx; M= Ni, Co, Ce). The Al<sub>2</sub>O<sub>3</sub> was first impregnated with aqueous solutions of Me(NO<sub>3</sub>)<sub>2</sub>.6H<sub>2</sub>O (Me=Co, Ni, Ce, Me = 5 wt. %). After impregnation the samples were dried at 60 °C and calcined for 2 h at 450 °C in air. Palladium (content of about 0.2 %) was introduced on calcined Me/Al<sub>2</sub>O<sub>3</sub> samples by impregnation with aqueous solution of Pd(NO<sub>3</sub>)<sub>2</sub>2H<sub>2</sub>O and then calcined additionally for 2h at 450 C. All samples were characterized by XRD (X-ray diffraction), TPR (temperature-programmed reduction), EPR (electron paramagnetic resonance) and XPS (X-ray photoelectron spectroscopy). An improvement of activity was observed after modification with different oxides.

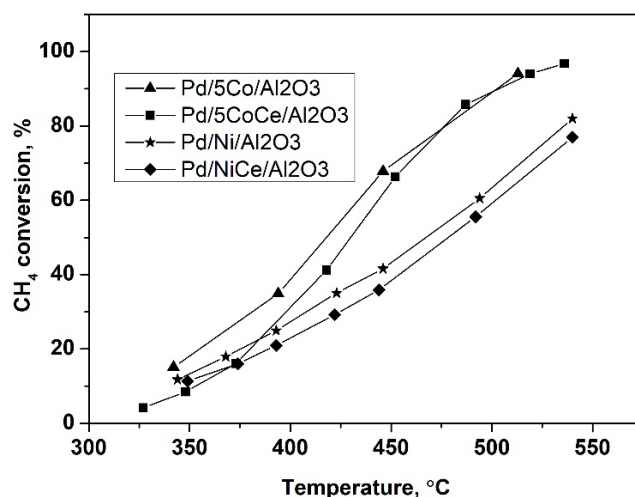


Figure 1. Temperature dependencies of the methane combustion over the different catalysts.

The results demonstrate that the Pd/Al<sub>2</sub>O<sub>3</sub> catalysts modified with Co exhibit the most promising catalytic activity for methane oxidation. Finely dispersed palladium particles were

## PP-IV-62

formed on the surface of all samples. Pd<sup>2+</sup> and Pd<sup>4+</sup> are both present on the surface of the fresh catalysts modified with Co and Ni only, while the modification with Ce before Co or Ni increases the Pd<sup>0</sup> on the surface. The results from different physicochemical characterization indicate the present of cobalt as Co-Al and Ni-Al spinel like phases on the catalyst surface. We suggest that occurrence of Co-Al phase plays a significant role for the stabilization of the palladium as PdO, leading to high activity and stability in the methane combustion.

It is very likely that, when the Ce is deposited before the Co deposition, the formation of cobalt surface phase is hindered as well as the further stabilization of PdO phase. The Pd+CoO<sub>x</sub>/Al<sub>2</sub>O<sub>3</sub> sample demonstrates remarkable stability after ageing.

**Acknowledgement.** The authors are gratefully acknowledged to the National Science Fund of Bulgaria, Grant No DNTS - Russia 01/1.

### References:

[1] J.G. McCarthy, Y.-F. Chang, V.L. Wong, M.E. Johansson, Div. Petrol.Chem. 42 (1997) 158–162.

## Specific Conversion of C<sub>2</sub>-C<sub>4</sub>-Aliphatic Alcohols on Carbon Nanomaterials

Tveritinova E.A., Zhitnev Yu.N., Kulakova I.I., Savilov S.V., Lunin V.V.  
*Lomonosov Moscow State University, Moscow, Russia*  
*eatver@mail.ru*

As opposed to activated carbon, carbon nanomaterials (CNMs) have a strictly defined carbon structure and, due to their nanoscale, they are used in various fields of physics, chemistry, biology, as well as in various technological processes. In catalysis, these materials are used both as carriers for metals and as catalysts. The aim of this work was to identify the effect of the structure of the carbon matrix and the composition of surface groups in the conversion of aliphatic alcohols C<sub>2</sub>-C<sub>4</sub>.

As catalyst carbon nanomaterials with different matrix structure, morphology and composition of surface groups: nanodiamond of detonation synthesis (ND), cylindrical carbon nanotubes (CNT<sub>cyl</sub>) of different degree of oxidation, conical carbon nanotubes (CNT<sub>con</sub>), oxidized and unoxidized lowlayer graphene fragments (LGF) have been selected. Catalytic properties of CNMs were tested in conversion of aliphatic alcohols C<sub>2</sub>-C<sub>4</sub>: ethanol, propanol-1, propanol-2, butanol-1, butanol-2 and t-butanol. Surface and structural properties of CNMs were studied by a set of methods: XRD, XPS, SEM, TEM, BET, DTA.

Oxygen surface atoms in the composition of carbon materials are mainly constituents of carbonyl, carboxyl, anhydride, ester surface groups, which play the role of Lewis acid and basic centers in catalysis [1]. The study of the conversion of C<sub>2</sub>-C<sub>4</sub> alcohols on ND has shown that oxygen-containing surface groups, whose composition is due to the carbon structure of ND (sp<sup>3</sup>-hybridization), play a key role in catalysis. According to the conversion products, carbonyl groups of bridge type are dominated among functional groups on diamond surface. CNMs with mainly graphene carbon structure (sp<sup>2</sup>- hybridization) - CNT<sub>cyl</sub>, CNT<sub>con</sub>, LGF - have different surface composition, which is due to the shape of the carbon matrix: cylindrical and conical in CNTs and flat in LGF. High level of catalytic activity of CNT<sub>cyl</sub> even with a low oxygen content (0.64%) in the conversion of C<sub>2</sub>-C<sub>4</sub> alcohols is explained both by the composition of the surface groups and the presence of defective centers of the carbon structure due to its curvature [2]. With an increase in the degree of oxidation (up to 9.3%) of the surface of CNT<sub>cyl</sub> conversion and selectivity for dehydration products are close to 100% for all alcohols. The conversion of alcohols on oxidized CNT<sub>con</sub> (9.4% O<sub>2</sub>) leads to the formation of dehydration products and dehydrogenation products, which indicates the presence of both carboxyl and aldehyde oxygen-containing surface CNT<sub>con</sub> groups. Unoxidized LGFs (1.8%O<sub>2</sub>) are inert in the conversion of all investigated alcohols due to the absence of structural defects and catalytically active surface groups, while the oxidized LGF (22% O<sub>2</sub>) showed catalytic activity in the conversion of secondary alcohols and t-butanol to form products dehydration. LGF doped with nitrogen, (2.4% O<sub>2</sub>), are inert in the conversion of secondary alcohols and t-

## PP-IV-63

butanol, which suggests that the catalytic centers are nitrogen-containing groups that are not available for alcohols with a branched structure. As an example, Table 1 shows the effect of the structure of the CNM and the conditions of oxidative treatment on the selectivity of the products of propanol-2 conversion.

**Table1**

**The influence of the properties of CNMs on the selectivity of the propanol-2 conversion**

Sample	Nitric acid treatment, processing time (h)	Oxygen content, % by weight	Specific surface, m <sup>2</sup> /g	Selectivity to products, % (270 <sup>o</sup> C)	
				propene	acetone
CNTcyl	-	0.8	192	72	28
CNTcyl	3	1.4	160	77	23
CNTcyl	9	9.4	249	100	0
CNTcon	3	9.4	204	76	24
ND	5	7.4	284	13	87
LGF	-	5.9	326	no conversion	
LGF	4	22.1	-	100	0
LGF-N	-	2.4	456	no conversion	

**Acknowledgement.** This work was supported by the Russian Science Foundation project 18-13-00217.

**References:**

- [1] J. L. Figueiredo, M.F.R. Pereira, *Catalysis Today* 2010, **150**, 2–7.
- [2] Ph. Serp, M. Corrias, Ph. Kalck, *Applied Catalysis A: General* 2003, **253**, 337–358.

## Characterization of Copper-Containing Catalysts in Dehydrogenation of Cyclohexanol into Cyclohexanone

Vanchurin V.I.<sup>1</sup>, Karachenko O.I.<sup>2</sup>, Petrov A.Yu.<sup>3</sup>, Vyatkin Yu.L.<sup>1</sup>

1 – Mendeleev University of Chemical Technology of Russia, Moscow, Russia

2 – GrodnoAzot jsc, Grodno, Belarus

3 – Financial University under the Government of the Russian Federation, Moscow, Russia  
vanchourin@mail.ru

Catalytic dehydrogenation of C-hexanol to C-hexanone on copper-containing catalysts is usually carried out at temperatures not higher than 220–300°C, thus allowing the process to be carried out with high selectivity at satisfactory activity rates, reduce the coking of catalysts and increase their lifecycle. Among domestic industrial catalysts Cu-Mg-catalysts are worth mentioning inline with mixed copper-zinc-alumocalcium catalyst branded K-CO, both widely spread and used. As for imported catalysts that have appeared in recent years in the CIS market, DHC-25 catalyst of "UNICAT" and especially H3-11 catalyst of BASF Corp. are worth mentioning also. The H3-11 catalyst compares favorably with its analogues and has been successfully operated at domestic plants for a number of years. It exhibits high selectivity (~99%) at average cyclohexanol conversion (50-55%). Both domestic and imported copper-containing catalysts have increased sensitivity to temperature effects and overheating that occurs during the reactor start or during their regenerative "burning" (burning coke deposits). As a result, sintering and recrystallization of the active component, reduction of the specific surface area and deterioration of catalytic properties can take place. Researches aimed on higher thermal stability of the catalyst were carried out in MUCTR after D. Mendeleev, the result is original MAK-K catalyst with competitive indicators of selectivity and activity in relation to industrial catalysts, including H3-11, but with higher thermal stability. We have already shown that the use of a hydroxylated form of silicon dioxide, so called "silica white", as a catalyst carrier and the efficient user of ammonia-carbonate technology leads to the formation of fixed nanostructured forms of the active component on the carrier surface. During catalyst recovery stage and in the process of C-hexanol dehydrogenation under the influence of the reaction medium, the formation of new depreciable structural elements of metallic copper and its oxides takes place inside mentioned entities while maintaining the same structure of copper hydroxocarbonate as the precursor of the active component. The strength of the precursor grafting to the carrier actually determines the degree of its aggregate resistance to temperature influences. According to the results of laboratory and industrial tests, it has been found that in terms of activity and selectivity within 200–250°C temperature range and the volume feed rate of 0.5–2.0 h<sup>-1</sup>, the MAK-K and H3-11 catalysts have similar characteristics. In this case, THE MAK-K catalyst is preferably used at lower temperatures and at increased volumetric feed rates. The thermal stability test by holding catalyst samples at a temperature of 350°C in the reaction gas current for 16 h showed that the conversion of C-hexanol over MAK-K reduced by 29 rel.% vs. 49 rel.% over H3-11.

## The Role of Stabilizer in Catalytic Activity in Water Solutions of Ultrasmall Rh, Pd and (Rh + Pd) Nanoparticles Obtained by Mediated Electrosynthesis

Yanilkin V.V.<sup>1</sup>, Nastapova N.V.<sup>1</sup>, Nasretdinova G.R.<sup>1</sup>, Osin Y.N.<sup>2</sup>, Gubaidullin A.T.<sup>1</sup>,  
Ziganshina A.Yu.<sup>1</sup>

1 – *Arbuzov Institute of Organic and Physical Chemistry, FRC Kazan Scientific Center of RAS, Kazan, Russia*

2 – *Kazan Federal University, Interdisciplinary Center “Analytical Microscopy”, Kazan, Russia*  
*yanilkin@iopc.ru*

Efficient electrosynthesis of ultrasmall spherical mono- and bimetallic nanoparticles (NPs) of Rh and Pd stabilized in the shell of cetyltrimethylammonium chloride (CTAC) in the solution bulk was carried out by methylviologen (MV) mediated reduction of equimolar amounts of Pd(II) and Rh(III) (1.5 mM) in the presence of CTAC (10 mM) at controlled potentials<sup>+</sup> of the MV<sup>2+</sup>/MV redox couple in water/ 0.1 M NaCl medium at room temperature. Similar electrosynthesis of RhNPs also effectively proceeds when poly(N-vinylpyrrolidone) (10 mM) is used as a stabilizer. Metal ions are quantitatively converted to NPs upon consumption of the theoretical amount of electricity. Sizes of isolated PdNPs and RhNPs are 4.6±0.9 nm and 1.7±0.3 nm, respectively. Bimetallic (Pd,Rh)NPs were obtained by three procedures: (i) preliminary synthesis of RhNPs followed by reduction of Pd(II) ((Rh/Pd)NPs, 2.2±0.7 nm); (ii) preliminary synthesis of PdNPs followed by reduction of Rh(III) ((Pd/Rh)NPs, 4.9±1.0 nm); (iii) joint reduction of Pd(II) and Rh(III) ((Pd-Rh)NPs, 3.1±0.5 nm). In all cases, a solid-solution alloy (Pd,Rh)NPs are obtained. In an aqueous medium, all the NPs obtained are catalytically active in the hydrogenation of *p*-nitrophenol with sodium borohydride to *p*-aminophenol, but their use in the Suzuki coupling reaction of iodobenzene with phenylboronic acid does not lead to the target product. An increase in the CTAC concentration by 7.5 times leads to an increase in the catalytic activity of PdNPs in both types of reactions.

## Methane Oxidation by H<sub>2</sub>O<sub>2</sub> over Different Cu-Species of Cu-ZSM-5 Catalysts

Yashnik S.A., Taran O.P., Boltenkov V., Parmon V.N.  
*Boriskov Institute of Catalysis, Novosibirsk, Russia*  
*yashnik@catalysis.ru*

The methane functionalization is a sought-after process that simulates the action of natural methane monooxygenase. The kinetics and mechanisms of methane-to-methanol oxidation over Cu-Zeolites activated with gaseous oxygen are studied in details [1], while the use of H<sub>2</sub>O<sub>2</sub> for this purpose is discussed only in some works [2]. Obviously, in both cases, the oxidation of methane to valuable oxygenates are catalyzed by Cu-species, whose oxidative potential is not sufficient for the deep oxidation of oxygenates to CO<sub>2</sub> and H<sub>2</sub>O. Approaches to controlling the redox properties of Cu-substituted zeolites are based on the chemical methods for regulating the structure of Cu-containing species during catalyst synthesis.

The isolated Cu(II) ions, bi- and polynuclear oxo/hydroxo Cu(II) clusters in zeolite channels, as well as nano-dispersed particles of copper oxide/hydroxide on the external surface of zeolite crystallites can be stabilized in the zeolite matrix by targeted selection of the preparation mode (ion exchange, polycondensation in the pores) and conditions (concentration, pH, temperature, etc.) of the postsynthetic modification of the zeolite with Cu(II) ions. Thus, in 0.1 M aqueous solutions of copper salts with a pH below 5 and in their ammonia solutions with a pH above 11.5, ideal conditions of ion exchange mode are realized. As results, the stabilization of the isolated Cu<sup>2+</sup> ions in the cation-exchange sites of the zeolite takes place [3, 4]. Aqueous and ammonia solutions of copper salts with pH 3-6 and 10-11 contain not only the complexes [Cu(H<sub>2</sub>O)<sub>6</sub>]<sup>2+</sup> и [Cu(NH<sub>3</sub>)<sub>4</sub>]<sup>2+</sup>, respectively, but also their hydrolyzed forms ([Cu(OH)]<sup>+</sup>, [Cu<sub>2</sub>(OH)<sub>2</sub>]<sup>2+</sup>, Cu(OH)<sub>2</sub> [5]). Therefore, here Cu<sup>2+</sup> structures with extraframework oxygen are formed during the synthesis of Cu-zeolite [3,4]. Large hydroxide-like nanoparticles Cu<sub>x</sub>(OH)<sub>y</sub> are deposited on the external surface of the zeolite crystallites when medium pH reaches a value below 9 during ion exchange [3]. The action of an alkaline solution on isolated Cu<sup>2+</sup> cations in the zeolite channel results in the formation of the [Cu<sub>2</sub>(OH)<sub>2</sub>]<sup>2+</sup> complexes and other oxo/hydroxo clusters of Cu<sup>2+</sup> ions [6,7]. The various Cu<sup>2+</sup>-structures with extraframework oxygen differ from each other in their redox properties, but they always outperform the isolated ions in the oxidation potential [4].

The choice of optimal reaction conditions, in particular the solution pH, also allows us to control the oxidative properties of Cu-substituted zeolites. In an acidic medium, H<sub>2</sub>O<sub>2</sub> decomposes via a radical mechanism (with the formation of OH· and HO<sub>2</sub>·) catalyzed by Cu<sup>2+</sup> ions, while in an alkaline environment, the decomposition rate of H<sub>2</sub>O<sub>2</sub> decreases 3-4 times and the activation energy increases from 60-62 to 71-75 kJ/mol due to the formation of Cu(II)-peroxocomplexes. UV-Vis DR spectroscopy indicated the terminal peroxocomplexes Cu-OOH (CTB L-M at 36000 cm<sup>-1</sup>) formed from the isolated Cu<sup>2+</sup> ions in the presence of H<sub>2</sub>O<sub>2</sub>. In the

## PP-IV-66

alkaline solution, binuclear Cu(II) peroxocomplexes connected via a terminal OOH-group (CTB L-M at 20700 cm<sup>-1</sup>) or a bridging OO-group (CTB L-M at 26700 cm<sup>-1</sup>) are formed from the Cu<sup>2+</sup>-structures with extraframework oxygen and complexes [Cu(NH<sub>3</sub>)<sub>4</sub>]<sup>2+</sup>.

Cu zeolites catalyze the methane-to-methanol oxidation with hydrogen peroxide, but a thorough analysis of oxygenates shows also the formation of formic acid, formaldehyde, methylhydroperoxide; CO<sub>2</sub> is formed as a deep oxidation by-product. The activity and selectivity of the process is controlled both by the catalyst composition and the structure of its Cu-species, as well as the pH of the reaction medium. For isolated Cu<sup>2+</sup> ions, a slight tendency is observed for the increase in the selectivity of methanol formation. The alkaline medium promotes the formation of methylhydroperoxide, which is further oxidized to formaldehyde. Based on the results obtained, it can be assumed that under acidic conditions, the oxidation of methane (similar to the reactions of deep oxidation of organics [8]) proceeds via a radical mechanism. The formation of Cu-peroxo complexes proceeds in the alkaline medium.

**Acknowledgement.** This work was supported by the Russian Science Foundation, grant 17-73-30032.

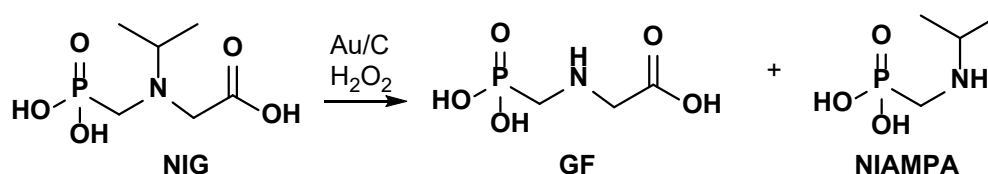
### References:

- [1] K.T. Dinh, M.M. Sullivan, P. Serna, R.J. Meyer, M. Dinca, Y. Roman-Leshkov, *ASC Catal.* 8 (2018) 8306.
- [2] C. Hammond, N. Dimitratos, R.L. Jenkins, J.A. Lopez-Sanchez, S.A. Kondrat, M. Hasbi ab Rahim, M.M. Forde, A. Thetford, S.H. Taylor, H. Hagen, E.E. Stangland, J.H. Kang, J.M. Moulijn, D.J. Willock, G.J. Hutchings, *ACS Catal.* 3 (2013) 689.
- [3] S.A. Yashnik, Z.R. Ismagilov, *Appl. Catal. B* 170-171 (2015) 241.
- [4] S.A. Yashnik, Z.R. Ismagilov, *Kin. & Cat.* 57 (2016) 777.
- [5] C.F. Jr. Baes, R.E. Mesmer, *The Hydrolysis of cations.* - New York: Wiley, Interscience, 1976.
- [6] M. Iwamoto, H. Yahiro, Y. Mine, S. Kagawa, *Chem. Lett.* 2 (1989), 213.
- [7] S.A. Yashnik, A.V. Salnikov, N.T. Vasenin, V.F. Anufrienko, Z.R. Ismagilov, *Catal. Today* 197 (2012) 214.
- [8] O.P. Taran, S.A. Yashnik, A.B. Ayusheev, A.S. Piskun, R.V. Prihod'ko, Z.R. Ismagilov, V.V. Goncharuk, V.N. Parmon, *Appl. Catal. B* 140– 141 (2013) 506.

## Oxidative Dealkylation of Aminophosphoric Acids in the Presence of Nanostructured Au/C Catalysts

Yushchenko D.Yu., Simonov P.A., Khlebnikova T.B., Pai Z.P., Bukhtiyarov V.I.  
Boriskov Institute of Catalysis, Novosibirsk, Russia  
dyy@catalysis.ru

N-(phosphonomethyl)glycine (glyphosate, GF) is one of the largest selling non-selective herbicide worldwide [1]. Among the various manufacturing technology of GF, atom efficient method is described. In this approach, GF is resulted from the oxidative cleavage of an alkyl group of N-substituted GFs, yielding a corresponding ketone as a second major product. For example, in the case of N-isopropyl glyphosate (NIG) oxidation the ketone product is acetone. Atom efficient technology is a low-waste process due to recycling of the by-products - acetone and hydrogen [2]. Our previous work showed that the oxidation of NIG with an aqueous hydrogen peroxide catalyzed by Au nanoparticles (AuNPs) supported on carbon materials [3] resulted in glyphosate and N-(isopropyl)aminomethylphosphonic acid (NIAMPA) formation [4]



The present studies have shown that AuNPs/C catalyze the oxidative dealkylation of NIG with high conversion (up to 100%) of NIG and selectivity to GF up to 79.3% in 2 hours (at 70 °C). It has been found that the catalytic performance strongly depends on the Au particle dispersion, and the best selectivity for glyphosate is achieved using the catalyst with 2 wt% Au deposited on a graphite-like mesoporous carbon material in the form of nanoparticles with a narrow size distribution (2-4 nm).

**Acknowledgement.** This work was supported by the Russian Foundation for Basic Research, grant 16-29-10691.

### References:

- [1] S.O. Duke, *Glyphosate: Pest Manag. Sci.* 74 (2018) 1025–1026.
- [2] D.A. Morgenstern, Y.M. Fobian, D.S. Oburn, *Catal. Org. React.*, CRC Press, New York, 2000: pp. 349–359.
- [3] P.A. Simonov, D.Y. Yushchenko, T.B. Khlebnikova, Z.P. Paj, V.I. Bukhtiyarov, RU2663905, 2018.
- [4] D.Y. Yushchenko, P.A. Simonov, T.B. Khlebnikova, Z.P. Pai, V.I. Bukhtiyarov, *Catal. Commun.* 121 (2019) 57–61.

**Active Sites on Nanorod La<sub>2</sub>O<sub>3</sub> in Oxidative Coupling of Methane.  
In Situ Online MS and XPS Study**

Zhou X., Vovk E.I., Liu Z., Yang Y.  
ShanghaiTech University, Shanghai, China  
zhouxh1@shanghaitech.edu.cn

Catalytic oxidative coupling of methane (OCM) is a process that converts methane directly into valuable C<sub>2</sub> products (C<sub>2</sub>H<sub>6</sub> and C<sub>2</sub>H<sub>4</sub>) by controlled partial oxidation. The main problems in this process development are low C<sub>2</sub> selectivity, low conversion, and the requirement of high temperature (~800 °C). The OCM reaction mechanism and active species are still under discussion [1-4]. In the current work, we have investigated OCM reaction over nanorod lanthanum oxide (n-La<sub>2</sub>O<sub>3</sub>) catalyst using customized micro-reactor with on-line mass spectrometer (MS) and by XPS method after reaction in high pressure gas cell (HPGC) with *in-situ* on-line MS. Online MS analysis of the OCM reaction products vs. temperature indicates that there is a turnover zone in OCM reaction at 600 °C [5], through which the selectivity of the C<sub>2</sub> product vs. CO<sub>x</sub> is significantly increased. The *in situ* XPS analysis indicates that there is a characteristic O 1s peak with bind energy of 531.3 eV consumed after reaction. This oxygen feature is associated with the catalytic active sites. Further elementary step experiments show that this surface enables CH<sub>4</sub> coupling into C<sub>2</sub> products in OCM reaction even without oxygen in the gas phase. The above results provide further insight into the OCM reaction mechanistic study.

**Acknowledgement.** This work was supported by the Shell, grant 2016.10-2020.12.

**References:**

- [1] J.L.G. Fierro, Catal. Letter. 22 (1993) 67-91.
- [2] P. Huang, Y. Zhao, J. Zhang, Y. Zhu, Y. Sun, Nanoscale. 5 (2013) 10844-10848.
- [3] J. Song, Y. Sun, R. Ba, S. Huang, Y. Zhao, J. Zhang, Y. Sun, Y. Zhu, Nanoscale 7 (2015) 2260-2264.
- [4] T. Jiang, J. Song, M. Huo, N. Yang, J. Liu, J. Zhang, Y. Sun, Y. Zhu, RSC Adv. 6 (2016) 34872-34876.
- [5] Z. Liu, J. Li, E. Vovk, Y. Zhu, S. Li, S. Wang, A. Bavel, Y. Yang, ACS Catalysis 8 (2018) 11761-11772.

## Enantioselective Alkynylation of Cyclic Ketones with Phenylacetylene Catalyzed by Lithium Binaphtholate

Ziyadullaev O.E.<sup>1</sup>, Otamukhamedova G.Q.<sup>2</sup>, Samatov S.B.<sup>1</sup>, Abdurakhmanova S.S.<sup>1</sup>,  
Turabdjano S.M.<sup>3</sup>

*1 – Chirchik State Pedagogical Institute, Tashkent region, Uzbekistan*

*2 – National University of Uzbekistan, Tashkent, Uzbekistan*

*3- Tashkent State Technical University, Tashkent, Uzbekistan*  
*bulak2000@yandex.ru*

At present time catalyst – lithium binaphtholat has been obtained on the base of butyllithium and binaphthol (BINOL) and it using for synthesis of different organical compounds including: alcohols, esters of acids, element- organic compounds and at this it is produced in industry [1-2].

In this work new acetylene alcohols: 1-(2-phenylethynil) cyclohexanol (I); 2-methyl-1-(2-phenylethynil) cyclohexanol (II); 2-isopropyl-5- methyl-1-(2-phenylethynil) cyclohexanol (III) and 1,7,7-threemetyl-2-(2-phenylethynyl)bicyclo[2.2.1]heptanol-2 (IV) have been synthesized by reaction of catalytical enantioselective alkylation with using phenylacetylene and cyclical ketones such as cyclohexanon; 2-methylcyclohexanon, mentone and camphora [3-4].

Used catalyst 3,3'-Ph<sub>2</sub>BINOL-2Li orientationally acts on triplet bond of phenylacetylene and has increased mobility of hydrogen atom owing to which it substituted on lithium with formation of lithium phenylacetylene.

On the base of experimental data it was shown that with increasing of number of radicals and their volume in molecules of ketones yield of obtaining aromatical acetylene alcohols has decreased. This is explained by fact that owing to phase difficulties of interaction of substrate of reaction and reaction activity of investigated ketones with phenylacetylene have decreased. Optimal conditions of carrying out of reactions of ketones with phenylacetylene: temperature 0 °C, duration of reaction- 2 h, solvent TGF, mole ratio phenylacetylene: ketone 1:2, catalyst. 3,3'-Ph<sub>2</sub>BINOL-2Li (58,0% by ketone mass.) have been determined. At this optimal yields of acetylene alcohols were equaled correspondently: I-72,1; II-70,4; III-66,0 and IV-53,3%.

By influence of radicals nature on activity of investigated ketones they can be presented by following raw: camphora < mentone < 2-methylcyclohexanon < cyclohexanone.

### References:

- [1]. Shanshan Yu, Lin Pu, Tetrahedron. 71.(2015), 745-772.
- [2]. Dacai Liu, Kunbing, Ouyang, Nianfa Yang Tetrahedron, Vol. 72., 2016, 1018-1023.
- [3]. Ziyadullaev O.E., Abdurakhmanova S.S., Turabdzhanov S.M. / X International conference "Mechanisms of catalytic reactions" Svetlogorsk, (Russia), 2016. 170.
- [4]. Parmanov A.B., Nurmanov S.E., Maniecki Tomash, Ziyadullaev O.E. Inter. J. Research-Granthaalayah, 16/11 (2018) 350-354.

## List of participants

**Agafonov Yury Anatolievich**

N.D. Zelinsky Institute  
of Organic Chemistry RAS  
Moscow, Russia  
[plassey@mail.ru](mailto:plassey@mail.ru)

**Alikin Evgeny**

Ecoalliance LTD  
Novouralsk, Russia  
[alikin@eco-nu.ru](mailto:alikin@eco-nu.ru)

**Ayala Ayala Maria Teresa**

Centro de Investigación  
y de Estudios Avanzados del IPN  
Queretaro, Mexico  
[maria.ayala@cinvestav.mx](mailto:maria.ayala@cinvestav.mx)

**Badmaev Sukhe**

Boreskov Institute of Catalysis  
Novosibirsk, Russia  
[sukhe@catalysis.ru](mailto:sukhe@catalysis.ru)

**Baksheev Evgeny**

Ecoalliance LTD  
Novouralsk, Russia  
[rzmetall102@gmail.com](mailto:rzmetall102@gmail.com)

**Belinskaya Nataliya Sergeevna**

National Research Tomsk  
Polytechnic University  
Tomsk, Russia  
[ns\\_belinskaya@sibmail.com](mailto:ns_belinskaya@sibmail.com)

**Belozertseva Natalia Evgenevna**

National Research  
Tomsk Polytechnic University  
Tomsk, Russia  
[belozertsevanatasha@mail.ru](mailto:belozertsevanatasha@mail.ru)

**Bereskina Polina**

Ural Federal University  
Ekaterinburg, Russia  
[polina.bereskina@urfu.ru](mailto:polina.bereskina@urfu.ru)

**Bluhm Hendrik**

Fritz-Haber Institute  
on the Max Planck Society  
Berlin, Germany  
[hbluhm@lbl.gov](mailto:hbluhm@lbl.gov)

**Bogdanov Ilya**

National Research  
Tomsk Polytechnic University  
Tomsk, Russia  
[boqdanov\\_ilya@mail.ru](mailto:boqdanov_ilya@mail.ru)

**Bryliakov Konstantin**

Novosibirsk State University  
Novosibirsk, Russia  
[bryliako@catalysis.ru](mailto:bryliako@catalysis.ru)

**Bryzhin Alexander**

Lomonosov Moscow State University  
Moscow, Russia  
[alexandrbr93@gmail.com](mailto:alexandrbr93@gmail.com)

**Bugaev Aram**

Southern Federal University  
Rostov-on-Don, Russia  
[arambugaev@gmail.com](mailto:arambugaev@gmail.com)

**Bukhtiyarov Andrei Valerievich**

Boreskov Institute of Catalysis  
Novosibirsk, Russia  
[avb@catalysis.ru](mailto:avb@catalysis.ru)

**Bukhtiyarov Valerii Ivanovich**

Boreskov Institute of Catalysis  
Novosibirsk, Russia  
[vib@catalysis.ru](mailto:vib@catalysis.ru)

**Bukhtiyarova Galina Alexandrovna**

Boreskov Institute of Catalysis  
Novosibirsk, Russia  
[gab@catalysis.ru](mailto:gab@catalysis.ru)

**Bulavchenko Olga Aleksandrovna**

Boreskov Institute of Catalysis  
Novosibirsk, Russia  
[isizy@catalysis.ru](mailto:isizy@catalysis.ru)

**Bychkov Viktor Yurievich**

Semenov Institute of Chemical Physics RAS  
Moscow, Russia  
[bychkov@chph.ras.ru](mailto:bychkov@chph.ras.ru)

**Cao Xiaoming**

East China University of Science and Technology  
Shanghai, China  
[xmcao@ecust.edu.cn](mailto:xmcao@ecust.edu.cn)

**Chernykh Maria Vladimirovna**

Tomsk State University  
Tomsk, Russia  
[msadlivskaya@mail.ru](mailto:msadlivskaya@mail.ru)

**Chernyshev Victor Mikhailovich**

Platov South-Russian State  
Polytechnic University (NPI)  
Novocherkassk, Russia  
[chern13@yandex.ru](mailto:chern13@yandex.ru)

**Chetyrin Igor Anatolievich**  
Boreskov Institute of Catalysis  
Novosibirsk, Russia  
[chia@catalysis.ru](mailto:chia@catalysis.ru)

**Chichkan Aleksandra Sergeevna**  
Boreskov Institute of Catalysis  
Novosibirsk, Russia  
[AlexCsh@yandex.ru](mailto:AlexCsh@yandex.ru)

**Cholach Aleksandr Romanovich**  
Boreskov Institute of Catalysis  
Novosibirsk, Russia  
[cholach@catalysis.ru](mailto:cholach@catalysis.ru)

**Ciesielski Radoslaw**  
Lodz University of Technology  
Lodz, Poland  
[radoslaw.ciesielski@p.lodz.pl](mailto:radoslaw.ciesielski@p.lodz.pl)

**Demidova Yulia Sergeevna**  
Boreskov Institute of Catalysis  
Novosibirsk, Russia  
[demidova@catalysis.ru](mailto:demidova@catalysis.ru)

**Demikhova Nataliya Ruslanovna**  
Gubkin Russian State University  
of Oil and Gas  
Moscow, Russia  
[natashademihova@gmail.com](mailto:natashademihova@gmail.com)

**Dmitrieva Maria**  
Institute of Problems of Chemical Physics RAS  
Chernogolovka, Russia  
[angel.maria@mail.ru](mailto:angel.maria@mail.ru)

**Dolganov Alexandr**  
National Research Ogarev  
Mordovia State University  
Saransk, Russia  
[dolganov\\_sasha@mail.ru](mailto:dolganov_sasha@mail.ru)

**Dronov Alexey Alekseevich**  
National Research University  
of Electronic Technology  
Zelenograd, Russia  
[noiz@mail.ru](mailto:noiz@mail.ru)

**Durakov Sergey Alekseevich**  
Moscow State Academy  
of Fine Chemical Technology  
Moscow, Russia  
[s.a.durakov@mail.ru](mailto:s.a.durakov@mail.ru)

**Dyusembaeva Aiken Amangeldyevna**  
Omsk State University of F.M. Dostoevsky  
Omsk, Russia  
[aykend@mail.ru](mailto:aykend@mail.ru)

**Elimanova Galina Gennadievna**  
Kazan National Research Technological University  
Kazan, Russia  
[yelimanova@mail.ru](mailto:yelimanova@mail.ru)

**Ershova Anna Mikhailovna**  
Boreskov Institute of Catalysis  
Novosibirsk, Russia  
[ershova@catalysis.ru](mailto:ershova@catalysis.ru)

**Fornasiero Paolo**  
University of Trieste  
Trieste, Italy  
[pfornasiero@units.it](mailto:pfornasiero@units.it)

**Gabrienko Anton**  
Boreskov Institute of Catalysis  
Novosibirsk, Russia  
[gabrienko@catalysis.ru](mailto:gabrienko@catalysis.ru)

**Gascon Jorge**  
KAUST Catalysis Research Center  
Thuwal, Saudi Arabia  
[jorge.gascon@kaust.edu.sa](mailto:jorge.gascon@kaust.edu.sa)

**Gavrilov Yurii**  
Semenov Institute of Chemical Physics RAS  
Moscow, Russia  
[yurii.gavrilov@yandex.ru](mailto:yurii.gavrilov@yandex.ru)

**Gavrilova Natalia Nickolaevna**  
D. Mendeleev University  
of Chemical Technology of Russia  
Moscow, Russia  
[ngavrilova@muctr.ru](mailto:ngavrilova@muctr.ru)

**Glukhova Yana**  
Saint-Petersburg State Institute of Technology  
(Technical University)  
Saint-Petersburg, Russia  
[ponyaev2002@mail.ru](mailto:ponyaev2002@mail.ru)

**Glyzdova Daria Vldimirovna**  
Center of New Chemical Technologies BIC  
Omsk, Russia  
[omsk-glyzdova@mail.ru](mailto:omsk-glyzdova@mail.ru)

**Golub Fedor**  
Boreskov Institute of Catalysis  
Novosibirsk, Russia  
[fedorqib@gmail.com](mailto:fedorqib@gmail.com)

**Gongxuan Lu**

Lanzhou Institute of Chemical Physics  
Lanzhou, China  
[gxlu@lzb.ac.cn](mailto:gxlu@lzb.ac.cn)

**Gornostaev Dmitry**

SPECS SURFACE NANO ANALYSIS GmbH  
Moscow, Russia  
[gornostaev@specs-tii.ru](mailto:gornostaev@specs-tii.ru)

**Gorokhova Ekaterina**

Technological Institute  
for Superhard and Novel Carbon Materials  
Troitsk, Russia  
[gorokhova@tisnum.ru](mailto:gorokhova@tisnum.ru)

**Gringolts Maria Leonidovna**

A.V. Topchiev Institute  
of Petrochemical Synthesis RAS  
Moscow, Russia  
[gringol@ips.ac.ru](mailto:gringol@ips.ac.ru)

**Grinvald Iosif Isaevich**

R.E. Alekseev Nizhny Novgorod  
State Technical University  
Nizhniy Novgorod, Russia  
[grinwald@mts-nn.ru](mailto:grinwald@mts-nn.ru)

**Grosheva Ekaterina**

LLC Merck  
Moscow, Russia  
[Ekaterina.Grosheva@merckgroup.com](mailto:Ekaterina.Grosheva@merckgroup.com)

**Hargreaves Justin**

University of Glasgow  
Glasgow, United Kingdom  
[justinh@chem.gla.ac.uk](mailto:justinh@chem.gla.ac.uk)

**Hutchings Graham**

Cardiff Catalysis Institute, Cardiff University  
Cardiff, United Kingdom  
[hutch@cardiff.ac.uk](mailto:hutch@cardiff.ac.uk)

**Ivanchikova Irina Dmitrievna**

Boreskov Institute of Catalysis  
Novosibirsk, Russia  
[idi@catalysis.ru](mailto:idi@catalysis.ru)

**Ivanova Yulia**

Boreskov Institute of Catalysis  
Novosibirsk, Russia  
[ivanova@catalysis.ru](mailto:ivanova@catalysis.ru)

**Jiratova Kveta**

Institute of Chemical Process  
Fundamentals of CAS  
Prague, Czech Republic  
[jiratova@icpf.cas.cz](mailto:jiratova@icpf.cas.cz)

**Kabachkov Evgeny**

Institute of Problems of Chemical Physics RAS  
Chernogolovka, Russia  
[gurov@icp.ac.ru](mailto:gurov@icp.ac.ru)

**Kaichev Vasily**

Boreskov Institute of Catalysis  
Novosibirsk, Russia  
[vvk@catalysis.ru](mailto:vvk@catalysis.ru)

**Kamyshova Elizaveta**

Southern Federal University  
Rostov-on-Don, Russia  
[kamyshova.liza@gmail.com](mailto:kamyshova.liza@gmail.com)

**Kaplin Igor Yurievich**

Lomonosov Moscow State University  
Moscow, Russia  
[kaplinigormsu@gmail.com](mailto:kaplinigormsu@gmail.com)

**Karásková Kateřina**

VSB-Technical University of Ostrava  
Ostrava, Czech Republic  
[katerina.karaskova@vsb.cz](mailto:katerina.karaskova@vsb.cz)

**Keller Sonja**

Leibniz Institute for Catalysis  
Rostock, Germany  
[sonja.keller@catalysis.de](mailto:sonja.keller@catalysis.de)

**Kharlamova Tamara Sergeevna**

Tomsk State University  
Tomsk, Russia  
[kharlamova83@gmail.com](mailto:kharlamova83@gmail.com)

**Kharlampidi Kharlampii Evklidovich**

Kazan National Research Technological University  
Kazan, Russia  
[kharlampidi@kstu.ru](mailto:kharlampidi@kstu.ru)

**Khenkin Alexander**

Weizmann Institute of Science  
Rehovot, Israel  
[alex.khenkin@weizmann.ac.il](mailto:alex.khenkin@weizmann.ac.il)

**Kholdeeva Oxana Anatolievna**

Boreskov Institute of Catalysis  
Novosibirsk, Russia  
[khold@catalysis.ru](mailto:khold@catalysis.ru)

**Kliusa Marina**

Boreskov Institute of Catalysis  
Novosibirsk, Russia  
[kma@catalysis.ru](mailto:kma@catalysis.ru)

**Klokov Sergey Vadimovich**

Lomonosov Moscow State University  
Moscow, Russia  
[servadklokov@gmail.com](mailto:servadklokov@gmail.com)

**Klyushin Alexander**

Helmholtz-Zentrum Berlin  
Berlin, Germany  
[alexander.klyushin@helmholtz-berlin.de](mailto:alexander.klyushin@helmholtz-berlin.de)

**Koklyuhin Aleksandr Sergeevich**

Samara State Technical University  
Samara, Russia  
[koklyuhin@yandex.ru](mailto:koklyuhin@yandex.ru)

**Koledina Kamila Felicsovna**

Institute of Petrochemistry and Catalysis RAS  
Ufa, Russia  
[koledinakamila@mail.ru](mailto:koledinakamila@mail.ru)

**Kolesnikov Ivan Mikhailovich**

Gubkin Russian State University of Oil and Gas  
Moscow, Russia  
[kolesnim@mail.ru](mailto:kolesnim@mail.ru)

**Kondratenko Evgenii**

Leibniz Institute for Catalysis  
Rostock, Germany  
[evgenii.kondratenko@catalysis.de](mailto:evgenii.kondratenko@catalysis.de)

**Kost Veronika**

Peoples' Friendship University of Russia  
(RUDN University)  
Moscow, Russia  
[kost.veronika6@gmail.com](mailto:kost.veronika6@gmail.com)

**Kovalev Evgeny**

Boreskov Institute of Catalysis  
Novosibirsk, Russia  
[kovalev-e@bk.ru](mailto:kovalev-e@bk.ru)

**Kovalevskiy Nikita Sergeevich**

Boreskov Institute of Catalysis  
Novosibirsk, Russia  
[koval701@gmail.com](mailto:koval701@gmail.com)

**Kovtunov Kirill**

International Tomography Center SB RAS  
Novosibirsk, Russia  
[kovtunov@tomo.nsc.ru](mailto:kovtunov@tomo.nsc.ru)

**Kozhevnikova Natalia**

Institute of Solid State Chemistry UrB RAS  
Ekaterinburg, Russia  
[kozhevnikova@ihim.uran.ru](mailto:kozhevnikova@ihim.uran.ru)

**Kozlova Ekaterina**

Boreskov Institute of Catalysis  
Novosibirsk, Russia  
[kozlova@catalysis.nsk.su](mailto:kozlova@catalysis.nsk.su)

**Kryuchkova Tatiana Alekseevna**

Peoples' Friendship University of Russia  
(RUDN University)  
Moscow, Russia  
[kryuchkova\\_ta@list.ru](mailto:kryuchkova_ta@list.ru)

**Kurenkova Anna Yurevna**

Boreskov Institute of Catalysis  
Novosibirsk, Russia  
[kurenkova@catalysis.ru](mailto:kurenkova@catalysis.ru)

**Kuriganova Alexandra**

Platov South-Russian State  
Polytechnic University (NPI)  
Novocherkassk, Russia  
[kuriganova\\_@mail.ru](mailto:kuriganova_@mail.ru)

**Kurokhtina Anna**

Irkutsk State University  
Irkutsk, Russia  
[kurokhtina@chem.isu.ru](mailto:kurokhtina@chem.isu.ru)

**Kuznetsov Boris Nikolaevitch**

Institute of Chemistry and Chemical Technology  
of SB RAS, FRS KSC SB RAS  
Krasnoyarsk, Russia  
[bnk@icct.ru](mailto:bnk@icct.ru)

**Lalayan Svetlana**

Semenov Institute of Chemical Physics RAS  
Moscow, Russia  
[lalayansvetlana@yandex.ru](mailto:lalayansvetlana@yandex.ru)

**Laletina Svetlana**

Institute of Chemistry and Chemical Technology  
of SB RAS, FRS KSC SB RAS  
Krasnoyarsk, Russia  
[shkulepo@rambler.ru](mailto:shkulepo@rambler.ru)

**Larina Elizaveta**

Irkutsk State University  
Irkutsk, Russia  
[tendu90@mail.ru](mailto:tendu90@mail.ru)

**Lashina Elena**

Boreskov Institute of Catalysis  
Novosibirsk, Russia  
[lashina@catalysis.ru](mailto:lashina@catalysis.ru)

**Lermontov Anatoly**

Company Soctrade  
Moscow, Russia  
[asl@soctrade.com](mailto:asl@soctrade.com)

**Li Jun**

Tsinghua University  
Beijing, China  
[unli.thu@gmail.com](mailto:unli.thu@gmail.com)

**Limberg Christian**

Humboldt University of Berlin  
Berlin, Germany  
[christian.limberg@chemie.hu-berlin.de](mailto:christian.limberg@chemie.hu-berlin.de)

**Logunova Svetlana**

Boreskov Institute of Catalysis  
Novosibirsk, Russia  
[logunova@catalysis.ru](mailto:logunova@catalysis.ru)

**Lokteva Ekaterina**

Lomonosov Moscow State University  
Moscow, Russia  
[e.lokteva@rambler.ru](mailto:e.lokteva@rambler.ru)

**Lubov Dmitry**

Boreskov Institute of Catalysis  
Novosibirsk, Russia  
[lubov1dmitriy@gmail.com](mailto:lubov1dmitriy@gmail.com)

**Mammadov Samir**

SPECS SURFACE NANO ANALYSIS GmbH  
Moscow, Russia  
[samir.mammadov@specs.com](mailto:samir.mammadov@specs.com)

**Maniecki Tomasz Przemyslaw**

Lodz University of Technology  
Lodz, Poland  
[tmanieck@p.lodz.pl](mailto:tmanieck@p.lodz.pl)

**Markova Ekaterina Borisovna**

Peoples' Friendship University of Russia  
(RUDN University)  
Moscow, Russia  
[ebmarkova@gmail.com](mailto:ebmarkova@gmail.com)

**Mashkovskii Igor Sergeevich**

N.D. Zelinsky Institute of Organic Chemistry RAS  
Moscow, Russia  
[igormash@gmail.com](mailto:igormash@gmail.com)

**Matveeva Valentina**

Tver State Technical University  
Tver, Russia  
[matveeva@science.tver.ru](mailto:matveeva@science.tver.ru)

**Melnikov Mikhail Olegovich**

Kreator Group of Company  
Moscow, Russia  
[mom@kreator.ru](mailto:mom@kreator.ru)

**Mikhailenko Irina Ivanovna**

RUDN University  
Moscow, Russia  
[imikhailenko@mail.ru](mailto:imikhailenko@mail.ru)

**Mikheeva Natalia Nikolaevna**

Tomsk State University  
Tomsk, Russia  
[natlitv93@yandex.ru](mailto:natlitv93@yandex.ru)

**Miroshnikova Angelina Victorovna**

Institute of Chemistry and Chemical Technology  
of SB RAS, FRS KSC SB RAS  
Krasnoyarsk, Russia  
[miroshnikova35@gmail.com](mailto:miroshnikova35@gmail.com)

**Morozova Olga**

Semenov Institute of Chemical Physics RAS  
Moscow, Russia  
[om@center.chph.ras.ru](mailto:om@center.chph.ras.ru)

**Murzin Vadim**

DESY  
Hamburg, Germany  
[vadim.murzin@desy.de](mailto:vadim.murzin@desy.de)

**Myachina Maria Andreevna**

D. Mendeleev University  
of Chemical Technology of Russia  
Moscow, Russia  
[myachinamary@gmail.com](mailto:myachinamary@gmail.com)

**Mytareva Alina Igorevna**

N.D. Zelinsky Institute of Organic Chemistry RAS  
Moscow, Russia  
[malina1308@yandex.ru](mailto:malina1308@yandex.ru)

**Nasullaev Khikmatullo Abdulazizovich**

Uzbek Scientific Research  
Chemical Pharmaceutical Institute  
Tashkent, Uzbekistan  
[kh.a.nasullaev@gmail.com](mailto:kh.a.nasullaev@gmail.com)

**Nazarkina Yulia Valeryevna**  
National Research University  
of Electronic Technology  
Moscow, Russia  
[enqvel@mail.ru](mailto:enqvel@mail.ru)

**Nedorezova Polina Mikhailovna**  
Semenov Institute of Chemical Physics RAS  
Moscow, Russia  
[polned@mail.ru](mailto:polned@mail.ru)

**Nell Germot**  
Parr Instrument (Deutschland) GmbH  
Berlin, Germany  
[Germont.nell@parrinst.de](mailto:Germont.nell@parrinst.de)

**Neyman Konstantin**  
ICREA and Universitat de Barcelona  
Barcelona, Spain  
[konstantin.neyman@icrea.cat](mailto:konstantin.neyman@icrea.cat)

**Nikitina Nadezhda Anatolievna**  
Lomonosov Moscow State University  
Moscow, Russia  
[nnikitina1719@gmail.com](mailto:nnikitina1719@gmail.com)

**Nishchakova Alina**  
Nikolaev Institute of Inorganic Chemistry SB RAS,  
Novosibirsk, Russia  
[lina.nischakova@gmail.com](mailto:lina.nischakova@gmail.com)

**Nuguid Rob Jeremiah Gotengco**  
École polytechnique fédérale de Lausanne  
Lausanne, Switzerland  
[rob.nuguid@epfl.ch](mailto:rob.nuguid@epfl.ch)

**Nyryllina Natalia Mikhailovna**  
Kazan National Research  
Technological University  
Kazan, Russia  
[nyryllina@mail.ru](mailto:nyryllina@mail.ru)

**Okhlopkova Lyudmila Borisovna**  
Boreskov Institute of Catalysis  
Novosibirsk, Russia  
[mila65@catalysis.ru](mailto:mila65@catalysis.ru)

**Ovchinnikova Elena Victorovna**  
Boreskov Institute of Catalysis  
Novosibirsk, Russia  
[evo@catalysis.ru](mailto:evo@catalysis.ru)

**Pacultová Kateřina**  
VSB-Technical University of Ostrava  
Ostrava, Czech Republic  
[katerina.pacultova@vsb.cz](mailto:katerina.pacultova@vsb.cz)

**Parmon Valentin Nikolaevich**  
Boreskov Institute of Catalysis  
Novosibirsk, Russia  
[parmon@catalysis.ru](mailto:parmon@catalysis.ru)

**Penner Simon**  
University of Innsbruck  
Innsbruck, Austria  
[simon.penner@uibk.ac.at](mailto:simon.penner@uibk.ac.at)

**Pérez-Hernández Raúl**  
Instituto Nacional de Investigaciones Nucleares  
Mexico, Mexico  
[raul.perez@inin.qob.mx](mailto:raul.perez@inin.qob.mx)

**Petukhov Anton Nikolaevich**  
R.E. Alekseev Nizhny Novgorod  
State Technical University  
Nizhniy Novgorod, Russia  
[fox-off@mail.ru](mailto:fox-off@mail.ru)

**Pichugina Daria**  
Lomonosov Moscow State University  
Moscow, Russia  
[dashapi@mail.ru](mailto:dashapi@mail.ru)

**Pimerzin Aleksey**  
Samara State Technical University  
Samara, Russia  
[al.pimerzin@gmail.com](mailto:al.pimerzin@gmail.com)

**Ponomareva Ekaterina**  
Semenov Institute of Chemical Physics RAS  
Moscow, Russia  
[katerinaii@inbox.ru](mailto:katerinaii@inbox.ru)

**Glukhova Yana**  
Saint-Petersburg State Institute of Technology  
(Technical University)  
Saint-Petersburg, Russia  
[ponyaev2002@mail.ru](mailto:ponyaev2002@mail.ru)

**Potapova Natalia**  
Semenov Institute of Chemical Physics RAS  
Moscow, Russia  
[pot.natalia2010@yandex.ru](mailto:pot.natalia2010@yandex.ru)

**Rameshan Raffael**  
Technische Universität Wien  
Vienna, Austria  
[raffael.rameshan@tuwien.ac.at](mailto:raffael.rameshan@tuwien.ac.at)

**Rempel Andrey**  
Institute of metallurgy UrB RAS  
Ekaterinburg, Russia  
[rempel.imet@mail.ru](mailto:rempel.imet@mail.ru)

**Rishina Laura**  
Semenov Institute of Chemical Physics RAS  
Moscow, Russia  
[rishina@yandex.ru](mailto:rishina@yandex.ru)

**Rostovshchikova Tatiana Nikolaevna**  
Lomonosov Moscow State University  
Moscow, Russia  
[rtn@kinet.chem.msu.ru](mailto:rtn@kinet.chem.msu.ru)

**Rupprechter Guenther**  
Technische Universität Wien  
Vienna, Austria  
[guenther.rupprechter@tuwien.ac.at](mailto:guenther.rupprechter@tuwien.ac.at)

**Sadykov Vladislav**  
Boreskov Institute of Catalysis  
Novosibirsk, Russia  
[sadykov@catalysis.ru](mailto:sadykov@catalysis.ru)

**Saiko Anastasiia**  
Boreskov Institute of Catalysis  
Novosibirsk, Russia  
[saiko@catalysis.ru](mailto:saiko@catalysis.ru)

**Salaev Mikhail**  
Tomsk State University  
Tomsk, Russia  
[mihan555@yandex.ru](mailto:mihan555@yandex.ru)

**Salakhov Ildar**  
PJSC Nizhnekamskneftekhim R&D center  
Nizhnekamsk, Russia  
[i.i.salahov@gmail.com](mailto:i.i.salahov@gmail.com)

**Saraev Andrey Aleksandrovich**  
Boreskov Institute of Catalysis  
Novosibirsk, Russia  
[asaraev@catalysis.ru](mailto:asaraev@catalysis.ru)

**Savchuk Timofei**  
National Research University  
of Electronic Technology  
Moscow, Russia  
[wewillbe01@gmail.com](mailto:wewillbe01@gmail.com)

**Sedov Yaroslav**  
Merck LLC  
Moscow, Russia  
[Yaroslav.Sedov@ecternal.merckgroup.com](mailto:Yaroslav.Sedov@ecternal.merckgroup.com)

**Selivanova Aleksandra**  
Boreskov Institute of Catalysis  
Novosibirsk, Russia  
[avselivanova@catalysis.ru](mailto:avselivanova@catalysis.ru)

**Shangareev Dmitriy Rafikovich**  
Yaroslavl State Technical University  
Yaroslavl, Russia  
[antonovt@ystu.ru](mailto:antonovt@ystu.ru)

**Sharaeva Almira**  
Peoples' Friendship University of Russia  
(RUDN University)  
Moscow, Russia  
[alminasharaeva@gmail.com](mailto:alminasharaeva@gmail.com)

**Shemet Darya Borisovna**  
Southern Federal University  
Rostov-on-Don, Russia  
[Shemetdabo@mail.ru](mailto:Shemetdabo@mail.ru)

**Sheshko Tatiana**  
Peoples' Friendship University of Russia  
(RUDN University)  
Moscow, Russia  
[sheshko-tf@rudn.ru](mailto:sheshko-tf@rudn.ru)

**Shesterkina Anastasiya**  
N.D. Zelinsky Institute of Organic Chemistry RAS  
Moscow, Russia  
[anastasiia.strelkova@mail.ru](mailto:anastasiia.strelkova@mail.ru)

**Shikina Nadezhda Vasilievna**  
Boreskov Institute of Catalysis  
Novosibirsk, Russia  
[shikina@catalysis.ru](mailto:shikina@catalysis.ru)

**Shilina Marina**  
Lomonosov Moscow State University  
Moscow, Russia  
[mish@kinet.chem.msu.ru](mailto:mish@kinet.chem.msu.ru)

**Shmakov Alexander Nikolaevich**  
Boreskov Institute of Catalysis  
Novosibirsk, Russia  
[shurka@catalysis.ru](mailto:shurka@catalysis.ru)

**Sigaeva Svetlana**  
Center of New Chemical Technologies BIC  
Omsk, Russia  
[s\\_in\\_cube@mail.ru](mailto:s_in_cube@mail.ru)

**Sinev Mikhail**  
Semenov Institute of Chemical Physics RAS  
Moscow, Russia  
[mysinev@rambler.ru](mailto:mysinev@rambler.ru)

**Sinitsin Sergei Aleksandrovich**  
D. Mendeleev University  
of Chemical Technology of Russia  
Moscow, Russia  
[sergeysinit@rambler.ru](mailto:sergeysinit@rambler.ru)

**Skorb Ekaterina**

ITMO University  
Saint-Petersburg, Russia  
[katjaskorb@mail.ru](mailto:katjaskorb@mail.ru)

**Skorynina Alina**

Southern Federal University  
Rostov-on-Don, Russia  
[alinaskorynina@rambler.ru](mailto:alinaskorynina@rambler.ru)

**Slinko Marina Mikhailovna**

Semenov Institute of Chemical Physics RAS  
Moscow, Russia  
[marinaslinko3@gmail.com](mailto:marinaslinko3@gmail.com)

**Smirnova Ekaterina Maksimovna**

Gubkin Russian State University  
of Oil and Gas  
Moscow, Russia  
[smirnova.em94@gmail.com](mailto:smirnova.em94@gmail.com)

**Solomonik Igor**

Technological institute  
for Superhard and Novel Carbon Materials  
Moscow, Russia  
[igsol@bk.ru](mailto:igsol@bk.ru)

**Soshnikov Igor**

Boreskov Institute of Catalysis  
Novosibirsk, Russia  
[soshnikovster@gmail.com](mailto:soshnikovster@gmail.com)

**Spirin Ivan Alexandrovich**

R.E. Alekseev Nizhny Novgorod  
State Technical University  
Nizhniy Novgorod, Russia  
[ivan.sn.92@mail.ru](mailto:ivan.sn.92@mail.ru)

**Stakheev Alexander**

N.D. Zelinsky Institute of Organic Chemistry RAS  
Moscow, Russia  
[st@ioc.ac.ru](mailto:st@ioc.ac.ru)

**Stepanov Alexander**

Boreskov Institute of Catalysis  
Novosibirsk, Russia  
[stepanov@catalysis.ru](mailto:stepanov@catalysis.ru)

**Stolyarova Elena Aleksandrovna**

Boreskov Institute of Catalysis  
Novosibirsk, Russia  
[anteva93@gmail.com](mailto:anteva93@gmail.com)

**Sukhova Olga Borisovna**

Boreskov Institute of Catalysis  
Novosibirsk, Russia  
[sukhova@catalysis.ru](mailto:sukhova@catalysis.ru)

**Sun Wei**

Lanzhou Institute of Chemical Physics  
Lanzhou, China  
[wsunlz@163.com](mailto:wsunlz@163.com)

**Svintsitskiy Dmitry**

Boreskov Institute of Catalysis  
Novosibirsk, Russia  
[sad@catalysis.ru](mailto:sad@catalysis.ru)

**Sychev Sergey**

LLC "Novomichurinsky catalyst plant"  
Novomichurinsk, Russia  
[nikishina.tatyana@nkz-ooo.ru](mailto:nikishina.tatyana@nkz-ooo.ru)

**Sychev Valentin**

Institute of Chemistry and Chemical Technology  
of SB RAS, FRS KSC SB RAS  
Krasnoyarsk, Russia  
[sychev.vv@icct.krasn.ru](mailto:sychev.vv@icct.krasn.ru)

**Taran Oxana Pavlovna**

Institute of Chemistry and Chemical Technology  
of SB RAS, FRS KSC SB RAS  
Krasnoyarsk, Russia  
[oxanap@bk.ru](mailto:oxanap@bk.ru)

**Todorova Silviya**

Institute of Catalysis  
of Bulgarian Academy of Sciences  
Sophia, Bulgaria  
[todorova@ic.bas.bg](mailto:todorova@ic.bas.bg)

**Tokmachev Dmitry Mikhailovich**

Company Soctrade  
Moscow, Russia  
[dmt@soctrade.com](mailto:dmt@soctrade.com)

**Tregubenko Valentina Yurievna**

Center of New Chemical Technologies BIC  
Omsk, Russia  
[kalinina\\_ihcp1@mail.ru](mailto:kalinina_ihcp1@mail.ru)

**Tsapina Anna**

Boreskov Institute of Catalysis  
Novosibirsk, Russia  
[amtsapina@catalysis.ru](mailto:amtsapina@catalysis.ru)

**Tsyganenko Alexey**

St.-Petersburg State University  
Saint-Petersburg, Russia  
[atsyg@yandex.ru](mailto:atsyg@yandex.ru)

**Usoltsev Oleg**

Southern Federal University  
Rostov-on-Don, Russia  
[oleg-usol@yandex.ru](mailto:oleg-usol@yandex.ru)

**Vasileva Elina**

Kazan National Research  
Technological University  
Kazan, Russia  
[elina.vasiljeva16@gmail.com](mailto:elina.vasiljeva16@gmail.com)

**Vedrov Nikolay Vladimirovich**

LLC "Novomichurinsky catalyst plant"  
Novomichurinsk, Russia  
[nikishina.tatyana@nkz-ooo.ru](mailto:nikishina.tatyana@nkz-ooo.ru)

**Vedrov Vladimir Nikolaevich**

LLC "Novomichurinsky catalyst plant"  
Novomichurinsk, Russia  
[nikishina.tatyana@nkz-ooo.ru](mailto:nikishina.tatyana@nkz-ooo.ru)

**Vedyagin Aleksey**

Boreskov Institute of Catalysis  
Novosibirsk, Russia  
[vedyagin@catalysis.ru](mailto:vedyagin@catalysis.ru)

**Vorotyntsev Andrey**

R.E. Alekseev Nizhny Novgorod  
State Technical University  
Nizhny Novgorod, Russia  
[an.vorotyntsev@gmail.com](mailto:an.vorotyntsev@gmail.com)

**Vovdenko Anna**

Ufa Research Center  
of Russian Academy of Science  
Ufa, Russia  
[vovdenkoann@gmail.com](mailto:vovdenkoann@gmail.com)

**Vovk Evgeny Ivanovich**

ShanghaiTech University  
Shanghai, China  
[evovk@shanghaitech.edu.cn](mailto:evovk@shanghaitech.edu.cn)

**Yanilkin Vitaliy Vasilevich**

Arbuzov Institute of Organic and Physical Chemistry,  
FRC Kazan Scientific Center of RAS  
Kazan, Russia  
[yanilkin@iopc.ru](mailto:yanilkin@iopc.ru)

**Yashnik Svetlana**

Boreskov Institute of Catalysis  
Novosibirsk, Russia  
[yashnik@catalysis.ru](mailto:yashnik@catalysis.ru)

**Yudanov Ilya**

Boreskov Institute of Catalysis  
Novosibirsk, Russia  
[ilya\\_v@ngs.ru](mailto:ilya_v@ngs.ru)

**Yurpalov Vyacheslav**

Center of New Chemical Technologies BIC  
Omsk, Russia  
[yurpalovv@mail.ru](mailto:yurpalovv@mail.ru)

**Yushchenko Dmitry**

Boreskov Institute of Catalysis  
Novosibirsk, Russia  
[dyy@catalysis.ru](mailto:dyy@catalysis.ru)

**Zakharov Vladimir Alexandrovich**

Boreskov Institute of Catalysis  
Novosibirsk, Russia  
[zva@catalysis.ru](mailto:zva@catalysis.ru)

**Zakrzewski Mateusz Łukasz**

Lodz University of Technology  
Lodz, Poland  
[mateusz.zakrzewski@hotmail.com](mailto:mateusz.zakrzewski@hotmail.com)

**Zalomaeva Olga**

Boreskov Institute of Catalysis  
Novosibirsk, Russia  
[zalomaeva@catalysis.ru](mailto:zalomaeva@catalysis.ru)

**Zhou Xiaong**

ShanghaiTech University  
Shanghai, China  
[zhouxh1@shanghaitech.edu.cn](mailto:zhouxh1@shanghaitech.edu.cn)

**Ziyadullaev Odiljon Egamberdiyevich**

Chirchik State Pedagogical Institute  
Tashkent, Uzbekistan  
[Bulak2000@yandex.ru](mailto:Bulak2000@yandex.ru)

**Zubkevich Sergey Vadimovich**

Lomonosov Moscow State University  
Moscow, Russia  
[zubkevich.serqey@gmail.com](mailto:zubkevich.serqey@gmail.com)

## Content

<b>PLENARY LECTURES</b> .....	<b>5</b>
<b>PL-2</b> Kholdeeva O.A. <b>Mechanisms of Hydrogen Peroxide Activation over Ti(IV) and Nb(V) Single Sites</b> .....	<b>7</b>
<b>PL-3</b> Hutchings G.J. <b>Catalysis Using Nanomaterials</b> .....	<b>8</b>
<b>PL-4</b> Fornasiero P. <b>Smart Catalysts and Today's Energy and Environmental Challenges</b> .....	<b>9</b>
<b>PL-5</b> Bluhm H. <b>Heterogeneous Chemistry at Liquid/Vapor Interfaces Investigated with Photoelectron Spectroscopy</b> .....	<b>10</b>
<b>PL-6</b> Li J. <b>Nano-Catalysis vs. Dynamic Single-Atom Catalysis: Insights from Computational Modelling</b> .....	<b>11</b>
<b>KEYNOTE LECTURES</b> .....	<b>13</b>
<b>KL-1</b> Lokare K.S., Frank N., Manicke N., Pinkert D., Braun-Cula B., Goikoetxea I., Jorewitz M., Kelly J.T., Herwig C., Leach S., Baldauf C., Asmis K., Sauer J., <u>Limberg C.</u> <b>Molecular Aluminium and Iron Siloxide Compounds as Models for Active Sites in the Pores of Zeolites</b> .....	<b>15</b>
<b>KL-2</b> Rupprechter G. <b>In Situ Surface Spectroscopy and Microscopy of Reactions on Zirconia Based Model Catalysts</b> .....	<b>17</b>
<b>KL-3</b> Ottenbacher R.V., Talsi E.P., <u>Bryliakov K.P.</u> <b>Dynamic Nonlinear Effects in Asymmetric Catalysis</b> .....	<b>18</b>
<b>KL-4</b> Hargreaves J.S.J. <b>Mechanistic Considerations Related to Ammonia Synthesis</b> .....	<b>19</b>
<b>KLS-1</b> Gascon J. <b>Multi-Scale Engineering of Catalytic Systems for the Hydrogenation of Carbon Dioxide</b> .....	<b>20</b>

<b>ORAL PRESENTATIONS .....</b>	<b>21</b>
<b>Section I. Basic concepts, theory and modeling in catalysis</b>	
<b>IOP-I-1</b>	
<u>Kovtunov K.V., Koptuyug I.V.</u>	
<b>Robust In Situ Investigation of Heterogeneous Hydrogenation Mechanisms with Parahydrogen .....</b>	<b>23</b>
<b>OP-I-2</b>	
<u>Xiao-Ming Cao, Wende Hu, P. Hu</u>	
<b>Synergistic Effect of Multi Active Sites with Low-Coordination Lattice Oxygen on Catalytic Combustion of Methane over Co<sub>3</sub>O<sub>4</sub>(110) .....</b>	<b>24</b>
<b>OP-I-3</b>	
<u>Sinev M.Yu.</u>	
<b>Interrelations between Apparent Kinetics and Mechanism in Catalytic Processes of Redox Type: Oxygen Activation and Pathways in Light Alkane Oxidation .....</b>	<b>26</b>
<b>OP-I-4</b>	
<u>Cholach A.R., Bryliakova A.A.</u>	
<b>Resonance-Coordinated Active Sites in the Catalytic Synthesis of Ammonia .....</b>	<b>27</b>
<b>OP-I-5</b>	
<u>Chernyshev V.M., Astakhov A.V., Chikunov I.E., Tyurin R.V., Eremin D.B., Ranny G.S., Khrustalev V.N., Ananikov V.P.</u>	
<b>“Mercury Test” and Fundamental Problems of Catalyst Poisoning in the Studies of Reaction Mechanisms .....</b>	<b>28</b>
<b>OP-I-6</b>	
<u>Sun W., Du J.Y., Sun Q.S.</u>	
<b>Mechanistic Insights into the Enantioselective Oxidation Reactions Catalyzed by Chiral Manganese Catalysts .....</b>	<b>30</b>
<b>OP-I-7</b>	
<u>Neyman K.M.</u>	
<b>Metal/Metal-Oxide Interface Effects in Catalytic Materials: Theory Versus Experiment .....</b>	<b>31</b>
<b>OP-I-8</b>	
<u>Mamatkulov M., Yudanov I., Neyman K.</u>	
<b>Theoretical Study of Chemical Ordering in Pd-Au Nanoparticles and Palladium Surface Segregation in Reactive Environment .....</b>	<b>33</b>
<b>OP-I-9</b>	
<u>Pichugina D.A., Nikitina N.A., Kuz'menko N.E.</u>	
<b>Structure, Stability and Catalytic Properties of Gold Protected Nanoclusters from DFT Calculation .....</b>	<b>35</b>

**OP-I-10**

Lashina E.A., Chumakova N.A., Chumakov G.A., Kaichev V.V.

**Self-Sustained Oscillations in Oxidation of CH<sub>4</sub>, C<sub>2</sub>H<sub>6</sub> and C<sub>3</sub>H<sub>8</sub> over Metallic Catalysts: Mathematical Modelling Using the Quasi-Steady-State Approximations** ..... 36

**OP-I-11**

Makeev A.G., Peskov N.V., Slinko M.M., Bychkov V.Yu.,  
Haritonov V.A., Korchak V.N.

**Spatial and Temporal Self-Organization during CO Oxidation over Ni** ..... 38

**Section II. Physical methods, including in situ and operando techniques, in catalysis****IOP-II-1**

Zhang Ya., Otroshchenko T., Han Sh., Rodemerck U., Linke D., Jiang G., Kondratenko E.V.

**The Potential of Time-Resolved Operando UV-Vis Spectroscopy for Deriving Insights into Coke Formation and Removal in Propane Dehydrogenation**..... 40

**OP-II-2**

Keller S., Rabeah J., Bentrup U., Brückner A.

**Impact of V and M on Mechanism and Performance of V/Ce<sub>1-x</sub>M<sub>x</sub>O<sub>2-δ</sub> (M=Fe, Bi, Sb) Catalysts in NH<sub>3</sub>-SCR of NO<sub>x</sub> Assessed by Operando Spectroscopy**..... 41

**OP-II-3**

Kaichev V.V., Chesalov Yu.A., Saraev A.A., Tsapina A.M.

**Dehydrogenation of Propane over Vanadia-Titania Catalysts: Active Sites and Reaction Mechanism**..... 43

**OP-II-4**

Rameshan R., Lindenthal L., Ruh T., Raschhofer, Nenning A.,  
Opitz A., Rameshan C.

**Enhancing Catalytic Activity of Perovskites by Tailored Exsolution**..... 44

**OP-II-5**

Svintsitskiy D.A., Kardash T.Yu., Lazareva E.V., Saraev A.A.,  
Derevyannikova E.A., Vorokhta M., Šmíd B., Bondareva V.M.

**Bi-Modified MoVNbTeO Catalysts for Oxidative Dehydrogenation of Ethane: NAP-XPS and In Situ XRD Study** ..... 45

**OP-II-6**

Bugaev A.L., Guda A.A., Lomachenko K.A., Usoltsev O.A., Skorynina A.A.,  
Groppo E., Safonova O., van Bokhoven J.

**Determination of Active Species in Pd Catalysts by Time-Resolved X-Ray Absorption Spectroscopy** ..... 46

**OP-II-7**

Murzin V., Caliebe W., Welter E.

**X-ray Absorption Spectroscopy Studies of Catalysts at P64/P65 Beamlines** ..... 48

**OP-II-8**

Saraev A.A., Tsapina A.M., Fedorov A.V., Trigub A.L.,  
Murzin V.Yu., Kaichev V.V.

**CuFeAl Nanocomposite Catalysts of CO Oxidation: *Operando* XAS Study** ..... 49

**OP-II-9**

Klyushin A.Yu., Jones T., Li X., Timpe O., Huang X., Lunkenbein T., Bukhtiyarov A.V.,  
Prosvirin I.P., Bukhtiyarov V.I., Hävecker M., Knop-Gericke A., Schlögl R.

**Au Activation via Strong Metal Support Interaction in CO oxidation** ..... 51

**OP-II-10**

Bukhtiyarov A.V., Prosvirin I.P., Mamatkulov M., Yudanov I.V., Klyushin A.Yu.,  
Knop-Gericke A., Neyman K.M., Bukhtiyarov V.I.

**CO Oxidation on the Model Pd-Au/HOPG Catalysts: NAP XPS and MS Study** ..... 53

**OP-II-11**

Bulavchenko O.A., Vinokurov Z.S., Afonasenkov T.N., Tsyrl'nikov P.G.,  
Ivanchikova A.V., Gerasimov E.Y., Saraev A.A., Kaichev V.V., Tsybulya S.V.

**In Situ XRD and XPS Study of the Reduction of Mixed Mn-Zr and Mn-Co Oxide Catalysts of CO Oxidation** ..... 55

**OP-II-12**

Yurpalov V.L., Drozdov V.A., Nepomnyashchiy A.A., Buluchevskiy E.A.,  
Lavrenov A.V.

**Deactivation Study of Pt/WO<sub>3</sub>-Al<sub>2</sub>O<sub>3</sub> Catalysts for Vegetable Oil Hydrodeoxygenation by EPR Spectroscopy and Thermal Analysis** ..... 56

**OP-II-13**

Vorotyntsev A.V., Petukhov A.N., Markov A.N.

**Tandem Operando FTIR with GCMS Analysis for Evaluation Chlorosilanes Disproportionation Mechanism on the Supported Ionic Liquids Like Phase (SILLPs) Catalysts** ..... 58

**OP-II-14**

Tsyganenko A.A.

**Application of Isotopic Substitution in the IR Studies of Catalysts** ..... 61

**Section III. Kinetics and mechanisms of catalyzed processes****IOP-III-1**

Bonmassar N., Schlicker L., Gili A., Gurlo A., Heggen M., Yunxua G.,  
Doran A., Bernardi J., Penner S.

***In situ* - Determined Structural Dynamics as a Mechanistic Key Parameter in the Reactivity of LaNiO<sub>3</sub>-based Methane Dry Reforming Catalysts** ..... 62

**OP-III-2**

Sadykov V.A., Ereemeev N.F., Rogov V.A., Sadovskaya E.M., Bobin A.S., Avdeev V.I.,  
Chesalov Yu.A., Smal E.A., Lukashevich A.I., Krasnov A.V., Simonov M.N., Roger A.-C.

**Detailed Mechanism of Ethanol Transformation into Syngas on Nanocomposite Catalysts** ..... 64

**OP-III-3**

Kuznetsov B.N., Sudakova I.G., Garyntseva N.V., Tarabanko V.E.,  
Djakovitch L., Rataboul F.

**Kinetic Studies and Optimization of Heterogeneous Catalytic Oxidation Processes  
for the Green Biorefinery of Wood..... 66**

**OP-III-4**

Vedyagin A.A., Kenzhin R.M., Tashlanov M.Y., Stoyanovskii V.O.,  
Plyusnin P.E., Shubin Y.V., Slavinskaya E.M., Mishakov I.V.

**Impact of Metal Ratio in the Bimetallic Three-Way Catalyst on Mechanism  
of the Catalysed Reactions..... 68**

**OP-III-5**

Vlasova E.N., Shamanaev I.V., Aleksandrov P.V., Nuzhdin A.L., Bukhtiyarova G.A.

**The Benefit of Catalytic Materials Cooperation in the Hydrodeoxygenation  
of Aliphatic Oxygenates ..... 70**

**OP-III-6**

Yashnik S.A., Ismagilov Z.R.

**Some Regularity and Peculiarity of SCR NO-NH<sub>3</sub> Behaviour of Cu-ZSM-5  
with Different Copper Electronic State ..... 72**

**OP-III-7**

Khenkin A.M.

**Mechanism of Activation of Molecular Oxygen by Homogeneous Vanadium  
Substituted Polyoxometalates..... 74**

**OP-III-8**

Zalomaeva O.V., Evtushok V.Yu., Glazneva T.S., Kholdeeva O.A.

**Mechanistic Study on the Oxidation of Organic Sulfides and Sulfoxides with H<sub>2</sub>O<sub>2</sub>  
over Zr-Based Metal-Organic Frameworks..... 75**

**OP-III-9**

Gabrienko A.A., Yashnik S.A., Stepanov A.G.

**Methane Activation on Cu/H-ZSM-5 Zeolites: A Spectroscopic Investigation  
of Methane Interaction with Different Cu-Sites ..... 76**

**OP-III-10**

Kurokhtina A.A., Larina E.V., Yarosh E.V., Lagoda N.A., Schmidt A.F.

**Differential Selectivity Patterns of Mizoroki-Heck Reaction: Novel Data on the Reaction  
Mechanism and Active Species Nature ..... 78**

**OP-III-11**

Morontsev A.A., Denisova Yu.I., Gringolts M.L., Peregudov A.S., Kudryavtsev Y.V.,  
Finkelshtein E.Sh.

**New Macromolecular Cross-Metathesis Reaction in the Mixtures of Polynorbornene  
with Polydienes Mediated by Grubbs' Catalysts: A Kinetic Study..... 79**

<b>OP-III-12</b> Arzumanov S.S., Gabrienko A.A., Toktarev A.V., <u>Stepanov A.G.</u> <b>Different Efficiency of Zn<sup>2+</sup> Cations and ZnO Species in Activation of Propane on Zn-Modified Zeolite BEA</b> .....	<b>81</b>
<b>OP-III-13</b> <u>Sigaeva S.S.</u> , Anoshkina E.V., Temerev V.L., Shlyapin D.A. <b>Interaction of Ethylene with Methane and its Pyrolysis Products on a Resistive FeCrAl Alloy Catalyst</b> .....	<b>83</b>
<b>OP-III-14</b> <u>Matveeva V.G.</u> , Protsenko I.I., Nikoshvili L.Zh., Sulman E.M. <b>Kinetics of Levulinic Acid Hydrogenation to Gamma-Valerolactone Using Ru-Containing Polymeric Catalysis</b> .....	<b>85</b>
<b>OP-III-15</b> <u>Zakharov V.A.</u> , Nikolaeva M.I., Matsko M.A., Barabanov A.A., Sukulova V.V. <b>Stereospecific Propylene Polymerization over Supported Titanium-Magnesium Catalysts: Study of the Effect of Catalyst Composition on the Distribution of Active Sites According to Stereospecificity</b> .....	<b>86</b>
<b>OP-III-16</b> Salakhov I.I. <b>Olefins and Dienes Polymerization over Ziegler-Natta Catalysts Modified with Various Chlorohydrocarbons</b> .....	<b>87</b>
<b>OP-III-17</b> <u>Bychkov V.Yu.</u> , Tulenin Yu.P., Slinko M.M., Korchak V.N. <b>Effect of Surface Oxidation Degree on Catalytic Activity of Metallic Ni and Co</b> .....	<b>89</b>
<b>OP-III-18</b> <u>Mammadov S.</u> , Socaciu-Siebert L., Meyer M., Dietrich P., Schaff O., Thissen A. <b>Near Ambient Pressure XPS: New Horizons</b> .....	<b>91</b>
 <b>Section IV. Advanced catalyst systems addressing current challenges: energy, materials, sustainability</b>	
<b>IOP-IV-1</b> Ryzhkov N.V., Nesterov P., Nikolaev K., Yurchenko S.O., <u>Skorb E.V.</u> <b>Coupling Multilayers Regulated by pH with Photocatalytically Active Surface for Bionic Devices and Infochemistry</b> .....	<b>92</b>
<b>OP-IV-2</b> <u>Rempel A.A.</u> , Valeeva A.A., Weinstein I.A., Kozlova E.A., Dorosheva I.B., Kuznetsova Yu.V., Selishchev D.S. <b>Organic Molecules Oxidation on Hybrid Titania – Cadmium Sulfide Photocatalyst Active under Visible Light</b> .....	<b>94</b>

**OP-IV-3**Pylinina A.I., Mikhaleenko I.I.**Isobutanol Dehydration over Ag-ZP Catalysts Obtained by Sol-Gel Method..... 95****OP-IV-4**Kozlova E.A., Lyulyukin M.N., Markovskaya D.V., Kozlov D.V.**Photocatalytic CO<sub>2</sub> Reduction over Cd<sub>1-x</sub>Zn<sub>x</sub>S-Based Photocatalysts: Effect of the Phase Composition on the Reaction Rate and Product Distribution..... 96****OP-IV-5**Demidova Yu.S., Suslov E.V., Mozhajcev E.S., Simakova O.A., Volcho K.P., Salakhutdinov N.F., Simakova I.L., Murzin D.Yu.**Hydrogenation of Monoterpenoids Catalyzed by Gold and Platinum Catalysts ..... 97****OP-IV-6**Lokteva E.S., Kaplin I.Yu., Golubina E.V., Maslakov K.I., Zhilyaev K., Shishova V.V., Tikhonov A.V.**The Effect of Template Nature and the Composition of Double and Triple Oxide Catalysts Based on CeO<sub>2</sub> in CO Oxidation..... 99****OP-IV-7**Maniecki T.P., Shtyka O., Ciesielski R., Kędziora A., Maniukiewicz W., Zakrzewski M., Dubkov S., Gromov D.**Photocatalytic Reduction of CO<sub>2</sub> over Me (Pt, Ru, Pd, Au)/TiO<sub>2</sub> Catalysts..... 101****OP-IV-8**Mondragón-Galicia G., Gutierrez-Wing C., Carrera Nuñez O., Vega Hernandez M., Gutierrez Martinez A., Perez Hernandez R.**Carbon Dioxide Methanation over Ni Catalysts Supported on TiO<sub>2</sub> Nanotubes ..... 102****OP-IV-9**Pimerzin A.I.A., Martynenko E.A., Savinov A.A., Verevkin S.P., Pimerzin A.A.**The Features of the Decalin Dehydrogenation over Platinum Catalysts Supported over Various Silica-Alumina Carriers ..... 104****OP-IV-10**Badmaev S.D., Pechenkin A.A., Paukshtis E.A., Belyaev V.D., Sobyanin V.A.**Catalytic Chemistry of Dimethoxymethane: Carbonylation, Steam Reforming and Partial Oxidation ..... 105****OP-IV-11**Vovk E.I., Zhou X., Liu Z., Guan C., Yang Y., Kong W., Si R.**Why Ni/Silicalite-1 Catalyst Shows High Stability and Reactivity in Dry Reforming of Methane? ..... 106****OP-IV-12**Taran O.P., Yashnik S.A., Boltenkov V.V., Parkhomchuk E.V., Sashkina K.A., Babushkin D.E., Parmon V.N.**Formic Acid Production via Methane Peroxide Oxidation over Oxalic Acid Activated Fe-MFI Catalysts. Mechanistic Insights..... 108**

**OP-IV-13**

Ciesielski R., Zakrzewski M., Kubicki J., Maniukiewicz W., Kedziora A., Maniecki T.P.

**Mechanistic Studies of Methanol Synthesis Reaction over Cu and Pd-Cu Catalysts ..... 110**

**OP-IV-14**

Kharlamova T., Timofeev K., Vodyankina O.

**The Role of Structural, Redox and Acid-Base Properties of Monolayer**

**MgVO<sub>x</sub>/Al<sub>2</sub>O<sub>3</sub> Catalysts in Oxidative Dehydrogenation of Propane ..... 111**

**OP-IV-15**

Okhlopova L.B., Kerzhentsev M.A., Ismagilov Z.R.

**Titania-Zirconia Coatings of a Capillary Microreactor for the Selective**

**Hydrogenation of 2-Methyl-3-Butyn-2-OL Using a PdZn/Ti<sub>x</sub>Zr<sub>1-x</sub>O<sub>2</sub> Catalyst:**

**Stability, Effect of the Catalyst's Activation Conditions and a Kinetic Study ..... 112**

**School-Conference for young scientists "CATALYSIS FOR ENERGY, FUELS, RENEWABLES" ..... 115**

**OPS-1**

Stolyarova E.A., Saiko A.V., Zaikina O.O., Sosnin G.A., Yeletsky P.M.,

Klimov O.V., Yakovlev V.A., Noskov A.S.

**NiMoP Catalyst in the Hydroprocessing of Mixture of Straight-Run Diesel Fuel and**

**Secondary Light Fractions Obtained by Catalytic Steam Cracking of Vacuum Residue..... 117**

**OPS-2**

Zakrzewski M., Shtyka O., Ciesielski R., Kedziora A., Maniecki T.

**Determination of the Type and Reactivity of Carbon Deposits in the Mixed**

**Reforming of Methane ..... 119**

**OPS-3**

Chetyrin I.A., Bukhtiyarov A.V., Prosvirin I.P., Bukhtiyarov V.I.

**In situ XPS and MS Study of Methane Oxidation over Bimetallic Pt-Pd/Al<sub>2</sub>O<sub>3</sub> Catalysts ..... 122**

**OPS-4**

Tsapina A.M., Selivanova A.V., Saraev A.A., Fedorov A.V., Vorokhta M.,

Šmíd B., Kaichev V.V.

**In situ NAP-XPS Study of Cu-Fe-Al-Based Nanocomposite Catalysts of CO Oxidation ..... 124**

**OPS-5**

Selivanova A.V., Tsapina A.M., Medvedeva Yu.I., Saraev A.A.,

Kaichev V.V., Bukhtiyarov V.I.

**In situ Study of Methanol Adsorption on Pt(111) and Pd(111) at Low**

**Temperatures by Polarization Modulation infrared Reflection Absorption Spectroscopy ..... 126**

**OPS-6**

Glyzdova D.V., Afonassenko T.N., Domanina T.P., Leont'eva N.N.,

Prosvirin I.P., Bukhtiyarov A.V., Shlyapin D.A.

**Study of the Zinc Addition Influence on the Pd/Sibunit Catalyst of Selective Acetylene**

**Hydrogenation..... 128**

<b>OPS-7</b> <u>Zubkevich S.V., Tuskaev V.A., Gagieva S.Ch., Pavlov A.A., Bulychev B.M.</u> <b>The Formation of Precatalysts for Selective Ethylene Dimerization in System NiBr<sub>2</sub>[bis(3,5-Dimethylpyrazol-1-yl)Methane]/PPh<sub>3</sub>.....</b>	<b>130</b>
<b>OPS-8</b> <u>Nuguid R.J.G., Nachtegaal M., Ferri D., Kröcher O.</u> <b>Mechanistic Insights into the Selective Catalytic Reduction of NO Revealed by Modulated-Excitation Raman Spectroscopy .....</b>	<b>132</b>
<b>OPS-9</b> <u>Nikitina N.A., Pichugina D.A., Kuz'menko N.E.</u> <b>DFT Simulation of the Molecular Structure of VO<sub>x</sub>/TiO<sub>2</sub> Catalysts.....</b>	<b>134</b>
<b>OPS-10</b> <u>Salaev M.A., Salaeva A.A., Vodyankina O.V.</u> <b>A Theoretical Study of the Effects of Promoters of Silver Catalysts for Ethylene Epoxidation.....</b>	<b>135</b>
<b>OPS-11</b> <u>Skorynina A.A., Olsbye U., Lillerud K.P., Lamberti C., Soldatov A.V., Bugaev A.L.</u> <b>Theoretical Investigation of Active Metal Sites in Pt- and Pd-Functionalized Metal-Organic Frameworks .....</b>	<b>136</b>
<b>OPS-12</b> <u>Ayala-Ayala M.T., Bahnemann D., Muñoz-Saldaña J.</u> <b>Structural, Microstructural and Optical Characterization of Bi<sub>2</sub>O<sub>3</sub>-Cu<sub>2</sub>O Heterojunctions for Photocatalytic Applications.....</b>	<b>138</b>
<b>OPS-13</b> <u>Kurenkova A.Yu., Markovskaya D.V., Kozlova E.A.</u> <b>Photocatalytic Hydrogen Evolution from Glucose Aqueous Solutions under Visible Light Irradiation .....</b>	<b>139</b>
<b>OPS-14</b> <u>Dmitrieva M.V., Zolotukhina E.V., Gerasimova E.V., Dobrovolskiy Yu.A.</u> <b>Kinetic Features of Mediator Bioelectrocatalytic Oxidation of Glucose by «Crude» Bacterial Extracts.....</b>	<b>141</b>
<b>OPS-15</b> <u>Kovalevskiy N.S., Selishchev D.S., Svintsitskiy D.A., Selishcheva S.A., Kozlov D.V.</u> <b>Synergetic Effect of Polychromatic Irradiation in the Reactions of Photocatalytic Oxidation on the Surface of N-Doped Titanium Dioxide .....</b>	<b>143</b>

<b>POSTER PRESENTATIONS .....</b>	<b>145</b>
<b>Section I. Basic concepts, theory and modeling in catalysis</b>	
<b>PP-I-1</b>	
<u>Belozertseva N.E., Belinskaya N.S.</u>	
<b>Computer Simulation System for the Catalytic Dewaxing Process .....</b>	<b>147</b>
<b>PP-I-2</b>	
<u>Dohlikova N.V., Gatin A.K., Sarvadii S.Y., Haritonov V.A., Rudenko E.I., Grishin M.V., Shub B.R.</u>	
<b>The Interface Effect of Gold Nanoparticles and Pyrolytic Graphite on Hydrogen Adsorption .....</b>	<b>149</b>
<b>PP-I-3</b>	
<u>Dyusembaeva A.A., Vershinin V.I.</u>	
<b>Computer Simulation of the Kinetics of a Multistage Process as a Method of Studying the Mechanism of Catalytic Naphtha Reforming .....</b>	<b>151</b>
<b>PP-I-4</b>	
<u>Grinvald I.I., Kalagaev I.Yu., Spirin I.A., Kapustin R.V., Petukhov A.N.</u>	
<b>Catalysis of Hydrogen Atom Transfer in Water Complexes with Organic Compounds .....</b>	<b>153</b>
<b>PP-I-5</b>	
<u>Ivchenko P.V., Nifant'ev I.E., Vinogradov A.A.</u>	
<b>Breaking the Rules in Zirconocene-Catalyzed <math>\alpha</math>-Olefin Oligomerization: DFT Visualization of Zr-Al and Zr-Al<sub>2</sub> Mechanistic Concepts .....</b>	<b>154</b>
<b>PP-I-6</b>	
<u>Kolesnikov I.M.</u>	
<b>Generalized Quantum-Chemical Principle and the Theory of Catalysis by Polyedres as a Basis Formulating the Mechanisms of Chemical and Catalytic Processes .....</b>	<b>156</b>
<b>PP-I-7</b>	
<u>Koltover V.K.</u>	
<b>Nuclear Spin Catalysis: From Chemical Physics to Living Cells .....</b>	<b>157</b>
<b>PP-I-8</b>	
<u>Laletina S.S., Shor A.M., Nasluzov V.A., Ivanova-Shor E.A.</u>	
<b>DFT Study of Adsorption of Au-Au, Au-Re and Au-Mn Dimers at Ceria Nanoparticle.....</b>	<b>159</b>
<b>PP-I-9</b>	
<u>Mashkovsky I.S., Rassolov A.V., Smirnova N.S., Baeva G.N., Bragina G.O., Stakheev A.Yu.</u>	
<b>Tuning the Structure of Active Sites and Catalytic Performance of Pd-Ag/Al<sub>2</sub>O<sub>3</sub> Selective Hydrogenation Catalyst by CO and O<sub>2</sub> Adsorption-Induced Segregation.....</b>	<b>160</b>

**PP-I-10**

Mashkovsky I.S., Smirnova N.S., Markov P.V., Baeva G.N., Bragina G.O.,  
Bukhtiyarov A.V., Prosvirin I.P., Bukhtiyarov V.I., Stakheev A.Yu.

**Mild Oxidative-Reductive Treatments as an Effective Way to Tune the Surface Structure and Catalytic Properties of PdIn Catalyst in Liquid-Phase Hydrogenation of Substituted Alkynes** ..... 162

**PP-I-11**

Mel'gunov M.S.

**Catalysis in Adsorbed Domens and Layers** ..... 164

**PP-I-12**

Mytareva A.I., Bokarev D.A., Baeva G.N., Belyankin A.Yu., Stakheev A.Yu.

**Dual-Zone Zeolite Catalyst for Complex Abatement of Power Plant and Automotive Emissions** ..... 165

**PP-I-13**

Sarvadiy S.Yu., Kharitonov V.A., Dokhlikova N.V.

**Synthesis of Titanium Oxide Coatings with a Given Band Gap Value** ..... 167

**PP-I-14**

Gatin A.K., Grishin M.V., Sarvadiy S.Yu., Shub B.R.

**Influence of Size Effect on the Hydrogen Adsorption on the Surface of Supported Gold Nanoparticles** ..... 168

**PP-I-15**

Troitskii S.Yu., Prosvirin I.P.

**Pt, Pd, Ru on Sibunit: Synergistic Effect in Hydrogenation Reactions** ..... 170

**PP-I-16**

Vovdenko A.G., Vovdenko M.K., Koledina K.F., Gubaydullin I.M.

**Mathematical Modeling of Reaction Benzylbutyl Ethersynthesis** ..... 172

## Section II. Physical methods, including in situ and operando techniques, in catalysis

**PP-II-1**

Vinokurov Z.S.<sup>1,2</sup>, Bulavchenko O.A.<sup>1,2</sup>, Afonasenko T.N.<sup>3</sup>, Tsybulya S.V.<sup>1,2</sup>

**Influence of CO Oxidation Conditions on the MnOx-ZrOx Catalyst Structure: In Situ XRD and MS Study** ..... 174

**PP-II-2**

Parfenov M.V., Ivanov D.P., Dubkov K.A., Kharitonov A.S.

**Gas-Phase Selective Oxidation of Propane-Propylene Mixture with Nitrous Oxide** ..... 176

**PP-II-3**

Gabrienko A.A., Danilova I.G., Stepanov A.G.

**Zeolite Brønsted Acidity: Direct Quantitative Characterization by Joint FTIR Spectroscopy and Solid-State <sup>1</sup>H MAS NMR Approach** ..... 178

**PP-II-4**

Kamyshova E., Skorynina A., Bugaev A., Soldatov A.

**X-ray Absorption Spectroscopy Study of Metal-Organic Frameworks Functionalized by Pd for Catalytic Hydrogenation of CO<sub>2</sub> ..... 180**

**PP-II-5**

Klokov S.V., Lokteva E.S., Golubina E.V., Maslakov K.I., Isaikina O.Y., Trenikhin M.V.

**The Nature of Active Sites in PdCo/C Catalysts Prepared by Pyrolysis of Wood Sawdust Impregnated with Pd(NO<sub>3</sub>)<sub>2</sub> and Co(NO<sub>3</sub>)<sub>2</sub> in Hydrodechlorination of Chlorobenzene ..... 182**

**PP-II-6**

Mel'gunova E.A., Krapivina E.A., Mel'gunov M.S.

**Advances in Characterization of Aluminum Oxides Porous Structure ..... 184**

**PP-II-7**

Köpfle N., Götsch T., Grünbacher M., Carbonio E. A., Hävecker M., Knop-Gericke A., Schlicker L., Doran A., Kober D., Gurlo A., Penner S., Klötzer B.

**Zirconium-Assisted Activation of Palladium to Boost Syngas Production by Methane Dry Reforming ..... 186**

**PP-II-8**

Selivanova A.V., Kurenkova A.Y., Tsapina A.M., Saraev A.A., Kozlova E.A., Kaichev V.V.

**Photocatalytic Hydrogen Production over Titania-Based Photocatalyst ..... 188**

**PP-II-9**

Shemet D.B., Pryadchenko V.V., Menshikov V.S., Nevelskaya A.K., Guterman V.E., Bugaev L.A.

**Atomic Structure and Catalytic Properties of Bimetallic Nanoparticles PtM (M = Ni, Co, Cu) in Metall-Carbon PtM/C Electrocatalysts for Low-Temperature Fuel Cells ..... 189**

**PP-II-10**

Shilina M.I., Gloriov I.P., Zhidomirov G.M.

**Adsorption and Oxidation of Carbon Monoxide on Co - ZSM-5 Zeolites ..... 190**

**PP-II-11**

Shmakov A.N., Nesterov N.S., Yakushkin S.S., Martyanov O.N.

**In Situ High Energy XRD Study of Reduction Process of Transition Metal Oxides in Supercritical Isopropanol ..... 191**

**PP-II-12**

Spirin I.A., Grinvald I.I., Kalagaev I.Yu., Kapustin R.V.

**IR Study of Hydrogen Atom Transfer in Hydrates of Alkali Metal Halides ..... 192**

**PP-II-13**

Usoltsev O.A., Bugaev A.L., Skorynina A.A., Tereshchenko A.A., Lomachenko K.A., Guda A.A., Groppo E., Pellegrini R., Lamberti C., Soldatov A.V.

**Dynamics of the Atomic and Electronic Structure of Nanoparticles of Noble Metals during Catalytic Reactions ..... 193**

**PP-II-14**

Vinokurov Z.S., Saraev A.A., Zaguzova V.V., Lashina E.A., Kaichev V.V.

***Operando* XRD Study of the Self-Sustained Reaction Rate Oscillations in the Oxidation of Methane over Palladium ..... 195**

**Section III. Kinetics and mechanisms of catalyzed processes****PP-III-1**

Agafonov Yu.A., Gaidai N.A., Botavina M.A., Lapidus A.L.

**Specifics of Propane Dehydrogenation over Silica Supported Gallium Catalysts ..... 197**

**PP-III-2**

Luu Cam Loc, Dao Thi Kim Thoa, Nguyen Tri, Ha Cam Anh, Gaidai N.A., Agafonov Yu.A., Lapidus A.L.

**HZSM-5 Supported Pt- and Pd-Catalysts Doped by Ni for Hydro-Isomerisation of n-Hexane ..... 199**

**PP-III-3**

Badyrova N.M., Nindakova L.O.

**Hydrogenation of Dimethyl Itaconate over Rhodium Nanoparticles, Modified by Optically Active Quarternary Ammonium Salts ..... 201**

**PP-III-4**

Boeva O.A., Vorakso I.A., Kudinova E.S., Paniukova N.S., Nesterova N.I., Zhavoronkova K.N.

**The Mechanism of Ortho-Para Conversion of Protium on the Nanoparticles of Silver and Gold in the Field of Low Temperatures ..... 202**

**PP-III-5**

Bogdanov I.A., Altynov A.A., Kirgina M.V.

**Investigation the Transformations Regularities of Stable Gas Condensate Hydrocarbons during Their Processing on Zeolite Catalysts ..... 203**

**PP-III-6**

Boretskaya A.V., Il'yasov I.R., Lamberov A.A.

**Butadiene-1,3 Hydrogenation on Palladium Nanoparticles Supported on Modified Alumina ..... 205**

**PP-III-7**

Ottenbacher R.V., Sun W., Sun, Q., Bryliakov K. P.

**Benzylic C-H Hydroxylations in the Presence of Bioinspired Mn Complexes: the Origin of Acetate Products ..... 207**

**PP-III-8**

Bykov M.V., Suslov D.S., Pakhomova M.V., Tkach V.S., Schmidt A.F.

**On the Role of Nanoscale Particles Formed on the Basis of Nickel (II) Complexes and Aluminum Alkyl Halides in Catalysis of Propene Oligomerization ..... 208**

<b>PP-III-9</b> <u>Bykova L.N., Vitkovskaya R.F., Rumynskaya I.G., Novoselov N.P.</u> <b>Study of the Properties of Bimetallic Polymer Catalysts .....</b>	<b>209</b>
<b>PP-III-10</b> <u>Cherepanov I.S.</u> <b> Pyrrole Ring Formation Mechanisms in Carbohydrate – Aryl Amine Condensations .....</b>	<b>211</b>
<b>PP-III-11</b> <u>Chernyshev D.O., Dubrovsky V.S., Varlamova E.V., Suchkov Y.P., Kozlovskiy R.A.</u> <b>The Dehydration Mechanism of Methyl Lactate over Phosphates .....</b>	<b>212</b>
<b>PP-III-12</b> <u>Chichkan A.S., Chesnokov V.V.</u> <b>Catalytic Coking of High Molecular Hydrocarbons.....</b>	<b>214</b>
<b>PP-III-13</b> <u>Durakov S.A., Flid V.R., Shamsiev R.S.</u> <b>Palladium-Catalyzed Allylation and Hydroallylation of Norbornadiene: Key Intermediates and Mechanism .....</b>	<b>215</b>
<b>PP-III-14</b> <u>Elimanova G.G., Batyrshin N.N., Kharlampidi Kh.E.</u> <b>The Mechanism of Decomposition and Stabilization of Molybdenum Epoxidation Catalysts for Olefinic Hydrocarbons .....</b>	<b>216</b>
<b>PP-III-15</b> <u>Faingol'd E.E., Zharkov I.V., Bravaya N.M., Panin A.N., Saratovskikh S.L., Babkina O.N., Shilov G.V.</u> <b>Sterically Crowded Dimeric Diisobutylaluminum Aryloxides: Synthesis, Characteristics, and Application as Activators in Homo- and Copolymerization of Olefins.....</b>	<b>218</b>
<b>PP-III-16</b> <u>Fedushchak T.A., Uyimin M.A., Maykov V.V., Mikubaeva E.V., Zhuravkov S.P., Vosmerikov A.V., Stasieva L.A., Prosvirin I.P., Zaykovsky V.I., Kogan V.M.</u> <b>Molybdenite-Based Hydrodesulfurization Catalysts Prepared under the Conditions of Cryo-Mechanical Activation.....</b>	<b>219</b>
<b>PP-III-17</b> <u>Gavrilova N.N., Osipenko N.N., Nazarov V.V., Sapunov V.N., Skudin V.V.</u> <b>Kinetic Experiment of Dry Reforming of Methane on Mo<sub>2</sub>C/CeZrO<sub>2</sub> Catalysts.....</b>	<b>221</b>
<b>PP-III-18</b> <u>Golub F.S., Beloshapkin S.A., Bolotov V.A., Parmon V.N., Bulushev D.A.</u> <b>Hydrogen Production from Formic Acid Decomposition over Pd/C Catalysts: Effect of Deposition of N-Containing Precursors on Carbon Support .....</b>	<b>222</b>

<b>PP-III-19</b> <u>Gorokhova E.O., Kulchakovskaya E.V., Asalieva E.Yu., Sineva L.V., Mordkovich V.Z.</u> <b>Catalytic Transformations of 1-Heptene and n-Heptane over Selected Zeolites at 170–260 °C</b> .....	<b>224</b>
<b>PP-III-20</b> <u>Grishin M.V., Gatin A.K., Dohlikova N.V., Kulak A.I., Sarvadii S.Yu., Shub B.R.</u> <b>Interaction of Hydrogen, Carbon Monoxide and Oxygen with Films Consisting of Gold and Copper Nanoparticles</b> .....	<b>226</b>
<b>PP-III-21</b> <u>Mannanova G.I., Koledina K.F., Gubaydullin I.M.</u> <b>Kinetic Model of Sonochemiluminescence Process of Aqueous Solution of Ruthenium Tris-Bipyridyl Chloride (II)</b> .....	<b>227</b>
<b>PP-III-22</b> <u>Mannanova G.I., Gubaydullin I.M.</u> <b>Models of the Reaction Unit of Catalytic Cracking</b> .....	<b>229</b>
<b>PP-III-23</b> <u>Ivanchikova I.D., Evtushok V.Yu., Suboch A.N., Podyacheva O.Yu., Kholdeeva O.A.</u> <b>Polyoxotungstate Supported on Carbon Nanotubes (CNT) as Effective Heterogeneous Catalyst for Epoxidation of Olefins</b> .....	<b>232</b>
<b>PP-III-24</b> <u>Kaichev V.V., Maksimov G.M., Fedorov A.V., Gerasimov E.Yu., Tsapina A.M., Selivanova A.V., Saraev A.A.</u> <b>Size Effect in the Oxidation of CO and Methane on Pd/TiO<sub>2</sub> Catalysts</b> .....	<b>233</b>
<b>PP-III-25</b> <u>Koledina K.F., Koledin S.N., Gubaydullin I.M.</u> <b>Kinetic Model of the Reaction of Dimethylcarbonate with Alcohols in the Presence Metal Complex Catalysts</b> .....	<b>234</b>
<b>PP-III-26</b> <u>Larina E.V., Lagoda N.A., Yarosh E.V., Kurokhtina A.A, Schmidt A.F.</u> <b>Differential Selectivity Measurements of Phosphine-Containing and Phosphine-Free Catalytic Systems of Mizoroki-Heck Reaction with Aromatic Carboxylic Anhydrides</b> .....	<b>236</b>
<b>PP-III-27</b> <u>Lokteva E.S., Golubina E.V., Gurbanova U.D., Kharlanov A.N.</u> <b>The Effect of Pd/Al<sub>2</sub>O<sub>3</sub> Modification with Si,W-Heteropolyacid on the Mechanism of 1,3,5-Trichlorobenzene Multi-Phase Hydrodechlorination</b> .....	<b>237</b>
<b>PP-III-28</b> <u>Nikoshvili L.Zh., Matveeva V.G., Sulman E.M., Kiwi-Minsker L.</u> <b>Influence of the Affinity of Metal Precursor to Polymeric Support on Activity of Ligandless Catalysts of Suzuki Cross-Coupling</b> .....	<b>238</b>

<b>PP-III-29</b>	
<u>Mukhamediarova A.N.</u> , Boretsky K.S., Egorova S.R., Ermolaev R.V., Lamberov A.A.	
<b>Influence of a Hydrothermal Treatment of the Amorphous Aluminum Compounds on the Properties of the Obtained Aluminum Hydroxides</b> .....	<b>239</b>
<b>PP-III-30</b>	
Palaznik O.M., <u>Nedorezova P.M.</u> , Polshikov S.V., Klyamkina A.N.	
<b>Polymerization of Propylene on Metal-Complex Catalysts in the Presence of Carbon Nanoparticles</b> .....	<b>241</b>
<b>PP-III-31</b>	
<u>Nurullina N.M.</u> , Batyrshin N.N., Kharlampidi Kh.E.	
<b>Catalysis of Hydroperoxide Decomposition Reactions in the Presence of Group I Metal Compounds</b> .....	<b>243</b>
<b>PP-III-32</b>	
<u>Parfenova L.V.</u> , Kovyazin P.V., Bikmeeva A.Kh., Islamov D.N., Tyumkina T.V.	
<b>Bimetallic Zr,Al- Hydrides as Active Intermediates in Alkene Di- and Oligomerization</b> .....	<b>245</b>
<b>PP-III-33</b>	
Makarov D.A., Vorotyntsev A.V., <u>Petukhov A.N.</u> , Markov A.N.	
<b>Investigation of the Mechanism of Triethoxysilane Dismutation over Ion-Exchange Resin in a Free Base Form via Operando FTIR Technique</b> .....	<b>247</b>
<b>PP-III-34</b>	
Lomonosov V.I., Gordienko Yu.A., <u>Ponomareva E.A.</u> , Sinev M.Yu.	
<b>Alternation in Kinetics of C<sub>1</sub>-C<sub>2</sub> Hydrocarbon Oxidation in the Presence of Model OCM Catalysts</b> .....	<b>249</b>
<b>PP-III-35</b>	
Ponyaev A.I., <u>Glukhova Y.S.</u> , Frolov A.N.	
<b>Photocatalysis of Hydrogen Evolution from Water by Systems Based on Boron Chelates with Diheterylamine</b> .....	<b>251</b>
<b>PP-III-36</b>	
<u>Potapenko O.V.</u> , Plekhova K.S., Altinkovitch E.O., Krol O.V., Sorokina T.P., Doronin V.P.	
<b>Catalytic Cracking of Deuterated Hydrocarbons as Method for Investigation of Hydrogen Transfer on Zeolite-Containing Catalyst</b> .....	<b>253</b>
<b>PP-III-37</b>	
<u>Potapova N.V.</u> , Kasaikina O.T.	
<b>Catalytic Generation of Radicals in Mixed Micelles {Acetylcholine – Hydroperoxide}</b> .....	<b>255</b>
<b>PP-III-38</b>	
<u>Rishina L.A.</u> , Kissin Y.V., Gagieva S.Ch., Lalayan S.S.	
<b>New Cocatalyst for Alkene Polymerization Reactions with Transition Metal Catalysts</b> .....	<b>256</b>

<b>PP-III-39</b>	
<u>Shangareev D.R., Antonova T.N., Sivova T.S., Abramov I.G.</u>	
<b>The Mechanism of Cyclooctene Epoxide Formation in the Process of Catalytic Liquid-Phase Oxidation of Cyclooctene by Molecular Oxygen</b> .....	<b>258</b>
<b>PP-III-40</b>	
<u>Shorayeva K.A., Massalimova B.K., Sadykov V.A., Nauryzkulova S.M., Altynbekova D.T., Jetpisbayeva G.D.</u>	
<b>Polyoxide Catalysts Based on Pillared Clays for the Oxidative Dehydrogenation of Ethane to Ethylene</b> .....	<b>259</b>
<b>PP-III-41</b>	
<u>Sil'chenkova O.N., Bychkov V.Yu., Matyshak V.A.</u>	
<b>Copper Containing Catalysts Based on CeO<sub>2</sub>- ZrO<sub>2</sub> Supports for Ethanol Conversion</b> .....	<b>260</b>
<b>PP-III-42</b>	
<u>Simakova I.L., Demidova Yu.S., Devi N., Dhepe P., Bokade V.</u>	
<b>Improvement of Selectivity to <math>\gamma</math>-Valerolactone in Hydrodeoxygenation of Lignocellulose Derived Levulinic Acid by Ir Catalyst Modification</b> .....	<b>262</b>
<b>PP-III-43</b>	
<u>Gavrilova N.N., Sapunov V.N., Skudin V.V.</u>	
<b>Reactor with Membrane Catalyst: Experimental Evaluation and Intensification Hypothesis</b> .....	<b>264</b>
<b>PP-III-44</b>	
<u>Soshnikov I.E., Semikolenova N.V., Antonov A.A., Bryliakov K.P., Talsi E.P.</u>	
<b>On the Nature of Active Sites of Ethylene Polymerization in the Presence of Nickel(II)-<math>\alpha</math>-Diimine Complexes</b> .....	<b>265</b>
<b>PP-III-45</b>	
<u>Startsev A.N.</u>	
<b>The Key Role of Catalysts in the Low Temperature Process of H<sub>2</sub>S Decomposition: Non-Equilibrium Thermodynamics of Open Systems</b> .....	<b>267</b>
<b>PP-III-46</b>	
<u>Goryunova V.D., Strakhov V.O., Nindakova L.O.</u>	
<b>Catalytic Transfer Hydrogenation of Acetophenone over Rhodium Nanoparticles</b> .....	<b>269</b>
<b>PP-III-47</b>	
<u>Tregubenko V.Yu., Vinichenko N.V., Belopukhov E.A., Paukshtis E.A., Belyi A.S.</u>	
<b>Trimetallic Naphtha Reforming Catalysts. Properties of the Metal and Acid Functions of Pt-Re-Zr/<math>\gamma</math>-Al<sub>2</sub>O<sub>3</sub>-Cl</b> .....	<b>270</b>
<b>PP-III-48</b>	
<u>Troitskii S.Yu., Zavarukhin S.G.</u>	
<b>Low-Temperature Sintering of the Active Components of Pd/C Catalysts</b> .....	<b>272</b>

<b>PP-III-49</b>	
<u>Vasileva E.A.</u> , Mukhamedzyanov R.R., Sitmuratov T.S., Petukhov A.A., Akhmedyanova R.A.	
<b>Features of the Oxidation of Light Saturated Hydrocarbons under Heterogeneous Catalysis</b> .....	<b>274</b>
<b>PP-III-50</b>	
<u>Vovdenko M.K.</u> , Vovdenko A.G., Koledina K.F., Gubaydullin I.M.	
<b>Isopropylbenzene Oxidation Kinetic Model</b> .....	<b>276</b>
<b>PP-III-51</b>	
<u>Vyatkin Yu.L.</u> <sup>1</sup> , Balaev A.V. <sup>2</sup> , Savenkov A.C. <sup>3</sup> , Vanchurin V.I. <sup>1</sup>	
<b>Mechanism of Chemical Evaporation of a Platinum Catalyst in an Ammonia Oxidation Reaction</b> .....	<b>278</b>
<b>PP-III-52</b>	
<u>Yushchenko D.Yu.</u> , Pai Z.P., Khlebnikova T.B.	
<b>Oxidation of N-(Phosphonomethyl)Iminodiacetic Acid with Hydrogen Peroxide in Phase-Transfer Conditions</b> .....	<b>279</b>
<b>PP-III-53</b>	
<u>Zabalov M.V.</u> , Levina M.A., Tiger R.P.	
<b>Kinetics and Quantum Chemical Study of Mechanism of TBD Catalyzed Aminolysis of Cyclocarbonates in DMSO</b> .....	<b>280</b>
<b>PP-III-54</b>	
<u>Zima A.M.</u> , Lyakin O.Y., Bryliakov K.P., Talsi E.P.	
<b>Aromatic C–H Bond Oxidation by Catalytic Systems Based on an Iron Complex with Ligand TPA Family</b> .....	<b>281</b>
 <b>Section IV. Advanced catalyst systems addressing current challenges: energy, materials, sustainability</b>	
<b>PP-IV-1</b>	
<u>Alikin E.A.</u> , Denisov S.P., Baksheev E.O., Kenzhin R.M., Vedyagin A.A.	
<b>The Effect of Barium on Behaviour of the OSC-Material in the Composition of Three-Way Catalysts</b> .....	<b>282</b>
<b>PP-IV-2</b>	
<u>Antonov A.A.</u> , Semikolenova N.V., Bryliakov K.P., Talsi E.P.	
<b>Ethylene Dimerization into 1-Butene and 2-Butene Using Homogeneous and Supported Nickel(II) 2–Iminopyridine Catalysts</b> .....	<b>284</b>
<b>PP-IV-3</b>	
<u>Bereskina P.A.</u> , Mashkovtsev M.A., Guryanova A.A., Osolihina A.Y.	
<b>The Influence of Synthesis Parameters on Surface Characteristics of Alumina</b> .....	<b>286</b>

**PP-IV-4**Bryzhin A., Gantman M., Buryak A., Tarkhanova I.**Oxidative Desulfurization of Diesel Fuel Catalysed by Brønsted Acidic Ionic Liquids with Heteropolyacids Immobilized on  $\gamma$ -Al<sub>2</sub>O<sub>3</sub> and Silica.....288****PP-IV-5**Bulanova A.V., Shafigulin R.V., Filippova E.O., Shmelev A.A., Tokranov A.A.**Hydrogenation of Aromatic Hydrocarbons on Mesoporous Silica Doped with Dy and Modified with Ni and Cu.....289****PP-IV-6**Buzaev A.A., Rogacheva A.O., Paukshtis E.A., Kozik V.V.**Production of Composite Materials Based on TiO<sub>2</sub> Modified Particles SiO<sub>2</sub> and Ag.....291****PP-IV-7**Chislova I.V., Yafarova L.V., Chislov M.V., Zvereva I.A., Borodina E.M., Sheshko T.F.**The Thermal Stability Study of Iron and Cobalts-Containing Catalysts with Layered Perovskite-Like Structure.....292****PP-IV-8**Demikhova N.R., Artemova M.I., Nedolivko V.V., Glotov A.P., Vinokurov V.A.**Investigation of New Functional Micro-Mesoporous Platinum Containing Catalysts Based on Halloysite Nanotubes and ZSM-5 Type Zeolite for Xylene Isomerization.....293****PP-IV-9**Dolganov A.V., Tanaseychuk B.S., Chernyaeva O.Yu. , Selivanova Yu.M., Yudina A.Yu., Grigorian K.A., Yurova V.Yu.**2,4,6-Triphenylpyridine as “Metal-Free” Electrocatalyst of Hydrogen Evolution Reaction (HER) .....295****PP-IV-10**Dronov A.A., Pinchuk O.V., Zheleznyakova A.V., Savchuk T.P., Kamaleev M.F., Dronova D.A., Gavrilin I.M.**Formation and Characterization of Photocatalytic Heterostructures Based on TiO<sub>2</sub> NTs/CuO NPs .....296****PP-IV-11**Dossumov K., Ergazieva G.E., Mironenko A.V., Ermagambet B.T., Telbayeva M.M., Myltykbayeva L.K., Kassenova Zh.M.**Oxide Catalysts for Production of Synthesis Gas and its Conversion to Liquid Hydrocarbons.....298****PP-IV-12**Gavrilov Yu.A., Pletneva I.V., Nefedov S.E.**Homogeneous Catalysts of Oxidation of Thiols by Oxygen in Hydrocarbon Media .....300****PP-IV-13**Gogin L.L., Zhizhina E.G.**One-Pot Processes of Quinones Syntheses in the Presence of Heteropoly Acid Solutions as Bifunctional Catalysts.....302**

<b>PP-IV-14</b>	
<u>Golubina E.V., Lokteva E.S., Kavalerskaya N.E., Kharlanov A.N., Maslakov K.I.</u>	
<b>Influence of Ni Deposition Method on Catalytic Properties of Ni/Al<sub>2</sub>O<sub>3</sub> in Hydrodechlorination of Chlorobenzenes .....</b>	<b>304</b>
<b>PP-IV-15</b>	
<u>Sutormina E.F., Isupova L.A., Rogov V.A., Ivanova Y.A., Vovk E.I.</u>	
<b>The Effect of Sr Substitution in Bulk and Supported La<sub>1-x</sub>Sr<sub>x</sub>FeO<sub>3</sub> Perovskites on the Catalytic Activity in NH<sub>3</sub> Oxidation and N<sub>2</sub>O Decomposition Reactions .....</b>	<b>306</b>
<b>PP-IV-16</b>	
<u>Ivanova Y.A., Sutormina E.F., Nartova A.V., Isupova L.A.</u>	
<b>Oxidative Coupling of Methane over Different Sr<sub>2</sub>TiO<sub>4</sub> Catalysts .....</b>	<b>307</b>
<b>PP-IV-17</b>	
<u>Jirátová K., Pacultová K., Balabánová J., Karásková K., Klegová A., Bílková T., Jandová V., Koštejn M., Obalová L.</u>	
<b>Precipitated K-Promoted Co-Mn-Al Mixed Oxides for Direct NO Decomposition: Preparation and Properties .....</b>	<b>309</b>
<b>PP-IV-18</b>	
<u>Kabachkov E.N., Balikhin I.L., Vershinin N.N., Efimov O.N., Kurkin E.N.</u>	
<b>Synthesis and Properties of Catalyst Based on Titanium Dioxide Modified by Nanomaterials and Catalytic Metals (Pt, Pd) Used in Air Purifiers.....</b>	<b>311</b>
<b>PP-IV-19</b>	
<u>Kaplin I.Yu., Lokteva E.S., Golubina E.V., Maslakov K.I., Shishova V.V., Fionov A.V.</u>	
<b>Effect of the Nature of Manganese Species in Mn-Ce-Zr Mixed Oxide Systems on Catalytic Properties in CO Oxidation .....</b>	<b>312</b>
<b>PP-IV-20</b>	
<u>Karásková K., Pacultová K., Klegova A., Fridrichová D., Kiška T., Jiratová K., Obalová L.</u>	
<b>K/Co-Mg-Mn-Al Mixed Oxide Catalyst System for Direct NO Decomposition .....</b>	<b>314</b>
<b>PP-IV-21</b>	
<u>Kirgizov A.J., Ilyasov I.R., Laskin A.I. Lamberov A.A.</u>	
<b>Supported Palladium Catalysts of Selective Hydrogenation on the Basis of High-Porous Cellular Materials.....</b>	<b>316</b>
<b>PP-IV-22</b>	
<u>Kokliukhin A.S., Ishutenko D.I., Mozhaev A.V., Pimerzin A.A., Nikulshin P.A.</u>	
<b>The Influence of the Nature of the Support on the Inhibitory Effect of Oxygen-Containing Compounds in the Process of co-Hydrotreatment of Model Compounds of Petroleum and Renewable Raw Materials.....</b>	<b>318</b>
<b>PP-IV-23</b>	
<u>Koskin A.P., Vedyagin A.A.</u>	
<b>Novel Lanthanide-Grafted Catalytic Systems for Alcohols Acylation and Carboxylic Esters Hydrolysis .....</b>	<b>320</b>

**PP-IV-24**

Sheshko T.F., Sharaeva A.A., Kost V.V., Kryuchkova T.A., Chislova I.V.,  
Zvereva I.A. Yafarova L.V.

**SrO Integration Effect on Structure and Activity of Perovskite-Type  
Oxides GdFeO<sub>3</sub> for DRM and FTS .....322**

**PP-IV-25**

Kovalev E.P., Lazareva E.V., Bondareva V.M., Svintsitskiy D.A., Kardash T.Yu.

**Effect of MoVTeNbO Catalyst Modification by P on the Selective Oxidative  
Transformations of Light Alkanes .....324**

**PP-IV-26**

Kozhevnikova N.S., Gorbunova T.I., Pervova M.G., Enyashin A.N., Vorokh A.S.

**Mechanisms of Catalytic Degradation of Chloroaromatic Compounds in Presence  
of CdS/TiO<sub>2</sub> Composite.....326**

**PP-IV-27**

Kuriganova A.B., Faddeev N.A., Leontyev I.N., Smirnova N.V.

**New Electrochemical Approach to Synthesis of Pd/C Catalysts and  
Its Electrochemical Performance .....328**

**PP-IV-28**

Lubov D.P., Talsi E.P., Bryliakov K.P.

**Benzylic C-H Oxidation of Arylalkanes with Peroxyacetic Acid in the  
Presence of Palladium-Aminopyridine Complexes .....329**

**PP-IV-29**

Maniecki T.P., Shtyka O., Sorokina L., Ciesielski R., Kędziora A., Maniukiewicz W.,  
Zakrzewski M., Dubkov S., Szyrkowska I., Gromov D.

**Electrochemical Synthesis of a Novel Me/TiO<sub>2</sub>-CNT Catalyst and Its Performance  
in the Photocatalytic Reduction of Carbon Dioxide .....330**

**PP-IV-30**

Markova E.B., Kovtun S.O., Savchenko A.S., Torbeeva A.A., Cherednichenko A.G.

**The Effect of Metal in the B-Position of Complex Oxides of Composition A<sub>2</sub>B<sub>2</sub>O<sub>7</sub>  
on the Process of Propane Dehydrogenation .....331**

**PP-IV-31**

Sulman E.M., Manaenkov O.V., Kislitsa O.V., Ratkevich E.A.,  
Matveeva V.G., Sulman M.G.

**Ru-Fe<sub>3</sub>O<sub>4</sub>-SiO<sub>2</sub> Catalyst for Polysaccharide Conversion.....333**

**PP-IV-32**

Gongxuan Lu

**The Inhibition of Hydrogen and Oxygen Recombination by Halogen Atoms and  
its Effect on Over-All Water Splitting over Pt-TiO<sub>2</sub> .....335**

**PP-IV-33**

Mikheeva N.N., Zaikovskii V.I., Mamontov G.V.

**Design of Ag-CeO<sub>2</sub>/SBA-15 Catalysts for Deep Oxidation of Toluene .....336**

<b>PP-IV-34</b>	
Beregovtsova N.G., Baryshnikov S.V., Miroshnikova A.V., Sharypov V.I., Lavrenov A.V., <u>Kuznetsov B.N.</u>	
<b>Influence of Borate-Containing Alumina Catalysts on the Conversion of Ethanol-Lignin from Pine Wood in a Supercritical Ethanol .....</b>	<b>338</b>
<b>PP-IV-35</b>	
<u>Morozova O.S.</u> , Firsova A.A., Tyulenin Yu.P., Vorobieva G.A., Leonov A.V.	
<b>Mechanochemical Synthesis – Alternative Effective Technique for the Composite Catalysts Preparation .....</b>	<b>340</b>
<b>PP-IV-36</b>	
Dedov A.G., <u>Mukhin I.E.</u> , Loktev A.S., Danilov V.P., Krasnobaeva O.N., Nosova T.A., Baranchikov A.E., Moiseev I.I.	
<b>Catalytic Materials Based on Hydrotalcite-Like Hydroxides of Al, Mg, Ni, Co for Partial Oxidation and Dry Reforming of Methane to Synthesis Gas .....</b>	<b>342</b>
<b>PP-IV-37</b>	
<u>Myachina M.A.</u> , Gavrilova N.N., Nazarov V.V., Skudin V.V.	
<b>Highly Dispersed Catalysts Mo<sub>2</sub>C – WC for the Dry Reforming of Methane .....</b>	<b>343</b>
<b>PP-IV-38</b>	
<u>Nazarkina Y.V.</u> , Rusakov V.A., Dronov A.A.	
<b>Effect of Anodization and Annealing Regimes on the Photocatalytic Properties of Nanostructured Tungsten Oxide Layers.....</b>	<b>344</b>
<b>PP-IV-39</b>	
<u>Nishchakova A.D.</u> , Asanov I.P., Bulushev D.A., Bulusheva L.G.	
<b>Porous Nitrogen-Doped Carbon Materials as Supports for Catalytically Active Ni Nanoparticles for Hydrogen Production from Gas-Phase Formic Acid .....</b>	<b>345</b>
<b>PP-IV-40</b>	
<u>Ovchinnikova E.V.</u> , Ivanov E.A., Chumachenko V.A.	
<b>Thermodynamic Analysis of Equilibrium Isobutane Yields in the Isomerization of n-Butane Fractions of Refinery Gases .....</b>	<b>347</b>
<b>PP-IV-41</b>	
Klegova A., Kiška T., <u>Pacultová K.</u> , Karásková K., Obalová L.	
<b>Effect of Cs Content in Co<sub>3</sub>O<sub>4</sub> Deposited on the Ceramic Foam Support Catalyst for N<sub>2</sub>O Decomposition .....</b>	<b>349</b>
<b>PP-IV-42</b>	
<u>Paperzh K.O.</u> , Alekseenko A.A.	
<b>Influence of the Structural Characteristics on the Pt/C Electrocatalysts Stability.....</b>	<b>351</b>
<b>PP-IV-43</b>	
Simakova I.L., <u>Demidova Yu.S.</u> , Devi N., Dhepe P., Bokade V.	
<b>Hydrogenation of Ethyl Levulinate to g-Valerolactone over Ir Catalysts .....</b>	<b>353</b>

<b>P-IV-44</b>	
Golubina E.V., Shilina M.I., Lokteva E.S., Maslakov K.I., Gurevich S.A., Kozhevnikov V.M., Yavsin D.A., <u>Rostovshchikova T.N.</u>	
<b>Low Percent Size-Selected Pd and Pt Catalysts Prepared by Laser Electrodispersion in the CO Oxidation .....</b>	<b>355</b>
<b>PP-IV-45</b>	
<u>Chernykh M.V.</u> , Mikheeva N.N., Mamontov G.V.	
<b>Reduction of Nitrocompounds over Ag-CeO<sub>2</sub> Catalysts .....</b>	<b>356</b>
<b>PP-IV-46</b>	
<u>Saiko A.V.</u> , Zaikina O.O., Sosnin G.A., Yeletsky P.M., Klimov O.V., Yakovlev V.A., Noskov A.S.	
<b>The Use of Dispersed Catalysts in Catalytic Steam Cracking of Vacuum Residue.....</b>	<b>358</b>
<b>PP-IV-47</b>	
Kharitonov V.A. <sup>1</sup> , <u>Sarvadiy S.Yu.</u> <sup>1</sup> , Ulasevich S.A. <sup>2,3</sup> , Ivashkevich N.M. <sup>2</sup> , Grishin M.V.	
<b>Bicomponent Nanocatalysts Based on Bororganic and Platinum Nanoparticles Increasing Ammonia Decomposition Rate .....</b>	<b>360</b>
<b>PP-IV-48</b>	
<u>Savchuk T.</u> , Shtyka O., Dronov A., Maniukiewicz W., Gavrilov S., Maniecki T.	
<b>Styrene Photocatalytic Oxidation over Me (Au, Pt, Pd)/TiO<sub>2</sub>-NTs Supported Catalysts .....</b>	<b>362</b>
<b>PP-IV-49</b>	
Shefer K.I., Kovtunova L.M., Rogozhnikov V.N., Chetyrin I.A., Suprun E.A., Stonkus O.A., Larina T.V.	
<b>Pt and Rh Catalysts Supported on Alumina and Structured Supports for the Reaction of Partial Oxidation of Hydrocarbons.....</b>	<b>363</b>
<b>PP-IV-50</b>	
<u>Shesterkina A.A.</u> , Strelakova A.A., Kirichenko O.A., Redina E.A., Kustov L.M.	
<b>Novel Fe-Containing Catalysts for the Selective Hydrogenation of Aldehydes and Nitro-Compounds.....</b>	<b>364</b>
<b>PP-IV-51</b>	
<u>Shikina N.V.</u> , Gavrilova A.A., Yashnik S.A., Litvak G.S., Khairulin S.R., Ismagilov Z.R.	
<b>Formation Mechanism of Active Phases Based on Mn, Mn-La, Mn-Ce Oxides under Solution Combustion Synthesis .....</b>	<b>366</b>
<b>PP-IV-52</b>	
<u>Shulyaka S.E.</u> , Sinitsin S.A., Petrov A.Yu.	
<b>Prospective Ferrite Catalysts for Flue Gases Cleaning from Carbon Monoxide.....</b>	<b>368</b>
<b>PP-IV-53</b>	
<u>Sinitsin S.A.</u> , Polovinkin M.A., Gavrilov Y.A., Danilov E.A., Kostiuchenko V.V., Vodoleev V.V.	
<b>Energy-Effective Fe-Mo Catalyst for the Process of Oxidative Dehydrogenation of Methanol to Formaldehyde.....</b>	<b>370</b>

<b>PP-IV-54</b>	
Sterenchuk T.P., Belykh L.B., <u>Skripov N.I.</u> , Sanzhieva S.B., Gvozdozskaya K.L., Schmidt F.K.	
<b>The Reasons for Promoting Action of Phosphorus on the Selectivity of Palladium Catalysts for the Synthesis of Hydrogen Peroxide by the Anthraquinone Method .....</b>	<b>372</b>
<b>PP-IV-55</b>	
<u>Smirnova E.M.</u> , Shukralieva A.S., Zasyalov G.O., Glotov A.P., Vinokurov V.A.	
<b>Benzene Hydrogenation over Ruthenium Catalysts Supported on Aluminosilicate Nanotubes .....</b>	<b>373</b>
<b>PP-IV-56</b>	
Konishcheva M.V., Potemkin D.I., <u>Snytnikov P.V.</u> , Sobyenin V.A.	
<b>From Mechanistic Studies of the Preferential CO Methanation in the Presence of CO<sub>2</sub> to Design of Structured Nickel-Ceria Catalysts .....</b>	<b>375</b>
<b>PP-IV-57</b>	
<u>Solomonik I.G.</u> , Gorshkov A.S., Gryaznov K.O., Zhukova E.A., Ivanov L.A., Perezhogin I.A., Mordkovich V.Z.	
<b>Effect of Long-Term Pilot Run on the Properties of Highly Productive Fischer–Tropsch Synthesis Catalyst .....</b>	<b>377</b>
<b>PP-IV-58</b>	
<u>Stolyarova E.A.</u> , Klimov O.V., Saiko A.V., Gerasimov E.Y., Chetyrin I.A., Noskov A.S.	
<b>Influence of the Silica Sol Addition to the Catalytic Activity of CoMoP Hydrotreating Catalysts .....</b>	<b>379</b>
<b>PP-IV-59</b>	
Matus E.V., Shlyakhtina A.S., <u>Sukhova O.B.</u> , Ismagilov I.Z., Kerzhentsev M.A., Ismagilov Z.R.	
<b>Effect of Composition of Ce<sub>1-x</sub>Ni<sub>x</sub>O<sub>y</sub> Catalyst on Their Activity and Stability in Steam/CO<sub>2</sub> Reforming of Methane.....</b>	<b>381</b>
<b>PP-IV-60</b>	
<u>Suslov D.S.</u> , Bykov M.V., Pakhomova M.V., Ushakov I.A., Tkach V.S.	
<b>Cationic Acetylacetonate Palladium Complexes/Boron Trifluoride Etherate Catalyst Systems for Polymerization of Norbornene Derivatives and Phenylacetylene .....</b>	<b>382</b>
<b>PP-IV-61</b>	
<u>Sychev V.V.</u> , Baryshnikov S.V., Beregovtsova N.G., Volochaev M.N., Taran O.P.	
<b>Levulinic Acid Hydrogenation into <math>\gamma</math>-Valerolactone over Ru/C Catalysts .....</b>	<b>384</b>
<b>PP-IV-62</b>	
<u>Todorova S.</u> , Naydenov A., Velinova R., Karakirova Y., Kolev H.	
<b>Catalytic Combustion of Methane over Pd-MeOx-CeO<sub>2</sub>/Al<sub>2</sub>O<sub>3</sub> (Me= Co or Ni) Catalysts.....</b>	<b>386</b>
<b>PP-IV-63</b>	
<u>Tveritina E.A.</u> , Zhitnev Yu.N., Kulakova I.I., Savilov S.V., Lunin V.V.	
<b>Specific Conversion of C<sub>2</sub>-C<sub>4</sub>-Aliphatic Alcohols on Carbon Nanomaterials .....</b>	<b>388</b>

<b>PP-IV-64</b>	
<u>Vanchurin V.I., Karachenko O.I., Petrov A.Yu., Vyatkin Yu.L.</u>	
<b>Characterization of Copper-Containing Catalysts in Dehydrogenation of Cyclohexanol into Cyclohexanone</b> .....	<b>390</b>
<b>PP-IV-65</b>	
<u>Yanilkin V.V., Nastapova N.V., Nasretdinova G.R., Osin Y.N., Gubaidullin A.T., Ziganshina A.Yu.</u>	
<b>The Role of Stabilizer in Catalytic Activity in Water Solutions of Ultrasmall Rh, Pd and (Rh + Pd) Nanoparticles Obtained by Mediated Electrosynthesis</b> .....	<b>391</b>
<b>PP-IV-66</b>	
<u>Yashnik S.A., Taran O.P., Boltenkov V., Parmon V.N.</u>	
<b>Methane Oxidation by H<sub>2</sub>O<sub>2</sub> over Different Cu-Species of Cu-ZSM-5 Catalysts</b> .....	<b>392</b>
<b>PP-IV-67</b>	
<u>Yushchenko D.Yu., Simonov P.A., Khlebnikova T.B., Pai Z.P., Bukhtiyarov V.I.</u>	
<b>Oxidative Dealkylation of Aminophosphoric Acids in the Presence of Nanostructured Au/C Catalysts</b> .....	<b>394</b>
<b>PP-IV-68</b>	
<u>Zhou X., Vovk E.I., Liu Z., Yang Y.</u>	
<b>Active Sites on Nanorod La<sub>2</sub>O<sub>3</sub> in Oxidative Coupling of Methane. <i>In Situ</i> Online MS and XPS Study</b> .....	<b>395</b>
<b>PP-IV-69</b>	
<u>Ziyadullaev O.E., Otamukhamedova G.Q., Samatov S.B., Abdurakhmanova S.S., Turabdjanov S.M.</u>	
<b>Enantioselective Alkynylation of Cyclic Ketones with Phenylacetylene Catalyzed by Lithium Banaphtolate</b> .....	<b>396</b>
<b>List of participants</b> .....	<b>397</b>
<b>Content</b> .....	<b>406</b>

## **Scientific edition**

XI International Conference “Mechanisms of Catalytic Reactions”  
October 7-11, 2019 Sochi, Krasnodar region, Russia

### **Abstracts Editors:**

Prof. V.I. Bukhtiyarov, Prof. Bryliakov K.P., Prof. Kozlova E.A., Dr. Kaichev V.V.

Compiled by: Marina Suvorova, Marina Klyusa  
Computer processing of text: Yulia Klimova, Aleksey Spiridonov

## **Научное издание**

XI Международная конференция “Механизмы каталитических  
реакций” (МКР-XI), 7-11 октября 2019 года, Сочи, Краснодарский край,  
Россия Сборник тезисов докладов

Под общей редакцией: акад. В.И. Бухтиярова, д.х.н. К.П. Брылякова,  
д.х.н. Е.А. Козловой, к.ф.-м.н. В.В. Каичева

Составители: М.С. Суворова, М.А. Ключа  
Компьютерная обработка: Ю.В. Климова, А.А. Спиридонов

### **Издатель:**

Федеральное государственное бюджетное учреждение науки  
«Федеральный исследовательский центр «Институт катализа им. Г.К. Борескова  
Сибирского отделения Российской академии наук»  
630090, Новосибирск, пр-т Академика Лаврентьева, 5, ИК СО РАН  
<http://catalysis.ru> E-mail: [bic@catalysis.ru](mailto:bic@catalysis.ru) Тел.: +7 383 330-67-71

### **Электронная версия:**

Издательский отдел Института катализа СО РАН  
E-mail: [pub@catalysis.ru](mailto:pub@catalysis.ru) Тел.: +7 383 326-97-15

Объём: 22 МБ. Подписано к размещению: 23.09.2019

Адрес размещения:

[http://catalysis.ru/resources/institute/Publishing/Report/2019/Abstracts-MCR-XI\\_2019.pdf](http://catalysis.ru/resources/institute/Publishing/Report/2019/Abstracts-MCR-XI_2019.pdf)

Системные требования: i486; Adobe® Reader® (чтение формата PDF)

ISBN 978-5-906376-25-1



[http://catalysis.ru/resources/institute/Publishing/Report/2019/ABSTRACTS\\_MCR-XI\\_on\\_Catalysis2019.pdf](http://catalysis.ru/resources/institute/Publishing/Report/2019/ABSTRACTS_MCR-XI_on_Catalysis2019.pdf)